

Strength Assessment of Soil Cement Base in Alabama

By

Matthew Connor Scales

A thesis submitted to the Graduate Faculty of
Auburn University
in partial fulfillment of the
requirements for the Degree of
Master of Science

Auburn, Alabama
August 8, 2020

Keywords: compressive strength, molded cylinders, dynamic cone penetrometer

Copyright 2020 by Matthew Connor Scales

Approved by

Anton K. Schindler, Chair, Professor of Civil Engineering
J. Brian Anderson, Co-Chair, Associate Professor of Civil Engineering
Benjamin F. Bowers, Assistant Professor of Civil Engineering

Abstract

Soil cement is a mixture of soil, portland cement, and water that is compacted and cured to form a strong, durable pavement base. Variances among construction practices and core strength data have led to questions concerning proper quality control practices and strength testing protocol for soil cement base. The major objective of this research is to develop means to reliably assess the strength of soil cement base.

In order to develop a method to reliably assess soil cement, a laboratory testing program and a field testing program were developed to evaluate the suitability of using the dynamic cone penetrometer based upon ASTM D6951 (2018) and the plastic mold method to prepare cylinders for compressive strength testing. In the laboratory, molded cylinder strength and the dynamic cone penetrometer results were well correlated between 100 to 930 psi. The effectiveness of the dynamic cone penetrometer was evaluated during an ongoing Alabama Department of Transportation (ALDOT) soil cement project. The results from this research are aimed at providing guidance to the ALDOT when specifying strength assessment parameters of soil cement base.

Based on the results of this research, the plastic mold method should be used to produce molded cylinders on-site for compressive strength testing for quality assurance of the soil cement mixture. If the plastic mold compressive strength is less than or greater than the ALDOT requirement for soil cement base, then the dynamic cone penetrometer should be used to determine the in-place strength of soil cement base.

Acknowledgments

First, I would like to thank my advisors Dr. Anton Schindler and Dr. J. Brian Anderson for their guidance, knowledge, and all around support during this research project and throughout my college career. Without their instruction, this thesis would not have been completed. I would also like to thank Dr. Benjamin Bowers for time and participation as one of my committee members and for help he has given me for some extracurricular activities.

I would also like to thank my research partner Emily Mueller for her hard work and diligence throughout the project. To Rob Crosby, the laboratory manager, who helped during all of the laboratory and field testing, thank you. To all of the laboratory assistants, Hongyang Wu, William Bloodworth, and Melanie Monaghan, who have helped throughout the research project, thank you. My appreciation goes to ALDOT and the Highway Research Center (HRC) at Auburn University for their financial support on this research project. I would also like to thank Kevin Jones of ALDOT for his assistance and collaboration on this project.

Finally, I would like to thank my mother, father, and sister for their love, encouragement, and amazing support throughout my life and especially over these last few years. I certainly would not have been able to accomplish this milestone without any of you.

Table of Contents

Abstract.....	ii
Acknowledgments.....	iii
List of Tables.....	xii
List of Figures.....	xiv
Chapter 1: Introduction.....	1
1.1 Background.....	1
1.2 Research Objectives.....	5
1.3 Research Approach.....	6
1.4 Thesis Outline.....	7
Chapter 2: Literature Review.....	9
2.1 Introduction.....	9
2.2 Materials.....	9
2.2.1 Soil.....	9
2.2.1.1 Particle Size.....	10
2.2.2 Portland Cement.....	11
2.2.3 Water.....	12
2.3 Soil Cement Properties.....	13
2.3.1 Density and Moisture Content.....	13
2.3.2 Compressive Strength.....	16
2.3.3 Shrinkage and Reflective Cracking.....	20

2.3.4 Durability.....	22
2.4 Overview of Soil Cement Base Construction.....	24
2.4.1 Soil Cement Base Construction.....	24
2.4.1.1 Mixed-In-Place Method.....	25
2.4.1.2 Central Mixing Plant Method.....	28
2.4.1.3 Compaction of Soil Cement Base.....	31
2.4.1.4 Curing.....	33
2.4.2 Quality Control and Assurance Testing.....	34
2.4.2.1 Cement Content.....	35
2.4.2.2 Moisture Content.....	37
2.4.2.3 Mixing Uniformity.....	38
2.4.2.4 Compaction.....	38
2.4.2.5 Lift Thickness and Surface Tolerance.....	39
2.5 Strength Evaluation.....	40
2.5.1 Overview of Alabama Department of Transportation Practice.....	40
2.5.2 Overview of Georgia Department of Transportation Practice.....	42
2.5.3 Overview of North Carolina Department of Transportation Practice.....	44
2.5.4 Core Testing.....	46
2.5.5 Dynamic Cone Penetrometer.....	49
2.5.5.1 Configuration of DCP Strength Evaluation in Laboratory.....	54
2.5.5.2 Configuration of DCP Strength Evaluation in the Field.....	58
2.5.5.3 Correlation between DCP and Unconfined Compressive Strength.....	59

2.5.6 Molded Cylinder Strength.....	65
2.5.6.1 Strength Correction Factors for Length-to-Diameter Ratios.....	65
2.5.6.2 Proctor Molded Specimens.....	66
2.4.6.3 Plastic-Mold (PM) Method.....	67
2.4.6.3.1 MDOT PM Configuration.....	69
2.4.6.3.2 ALDOT PM Modification.....	70
2.5.6.4 Steel-Mold (SM) Method.....	72
Chapter 3: Experimental Plan.....	77
3.1 Introduction.....	77
3.1.1 Laboratory Testing Phase.....	77
3.1.2 Field Testing Phase.....	77
3.2 Laboratory Testing Program.....	78
3.2.1 Correlation between Molded Cylinder Strength and DCP.....	80
3.2.2 Suitability of the Dynamic Cone Penetrometer (DCP).....	80
3.2.3 Laboratory Mixtures Evaluated.....	81
3.2.3.1 Waugh Clay and Waugh Sand.....	81
3.2.3.2 Waugh Soil.....	82
3.2.3.3 Elba Soil.....	82
3.2.3.4 Coarse Soil.....	83
3.2.4 Material Classification.....	84
3.2.5 Soil Classification Impact.....	84
3.3 Laboratory Testing Phase Procedures.....	85
3.3.1 Laboratory Mixing of Soil Cement.....	85

3.3.1.1	Moisture-Density Curve.....	85
3.3.1.2	Batching.....	85
3.3.1.3	Mixing.....	86
3.3.1.4	Plastic-Mold Cylinder Production	87
3.3.1.5	DCP Specimen Production.....	89
3.3.2	Initial Curing.....	89
3.3.2.1	Plastic-Mold Cylinders.....	89
3.3.2.2	DCP Specimens.....	90
3.3.3	Final Curing.....	91
3.3.3.1	Plastic-Mold Cylinders.....	91
3.3.3.2	DCP Specimens.....	91
3.3.4	Testing.....	92
3.3.4.1	Plastic-Mold Cylinder Testing.....	92
3.3.4.1.1	Moisture Content and Density.....	92
3.3.4.1.2	PM Cylinder Compressive Strength.....	93
3.3.4.2	DCP Testing.....	96
3.3.4.2.1	Moisture Content and Density.....	96
3.3.4.2.2	DCP Strength.....	97
3.4	Field Testing Program.....	99
3.4.1	Field Mixture.....	100
3.4.2	Location of Project Site.....	101
3.4.3	Testing Strategy within a Section.....	102
3.5	Field Testing Phase Procedures.....	104

3.5.1 In-Place Sampling of Mixed Soil Cement.....	104
3.5.2 Plastic-Mold Cylinder Production.....	105
3.5.3 Initial Curing.....	106
3.5.4 Plastic-Mold Extrusion.....	107
3.5.5 Final Curing.....	107
3.5.6 Testing.....	107
3.5.6.1 PM Cylinder Testing.....	107
3.5.6.1.1 Moisture Content and Density.....	107
3.5.6.1.2 PM Cylinder Compressive Strength.....	108
3.5.6.2 DCP Testing.....	108
3.5.6.2.1 Moisture Content and Density.....	108
3.5.6.2.2 DCP Strength.....	109
3.5.6.3 Core Testing.....	111
Chapter 4: Presentation and Analysis of Laboratory Testing Phase Results.....	114
4.1 Introduction.....	114
4.2 Material Classification.....	114
4.3 Mixture Properties.....	114
4.4 DCP Initial Curing Study.....	116
4.5 Soil Classification Impact.....	116
4.6 Suitability of Dynamic Cone Penetrometer.....	118
4.6.1 DCP Penetration Depth Analysis.....	119
4.6.1.1 Twenty-five Millimeter Penetration Depth Analysis.....	121
4.6.1.2 Fifty Millimeter Penetration Depth Analysis.....	121

4.6.1.3 Seventy-five Millimeter Penetration Depth Analysis.....	122
4.6.1.4 One-hundred Millimeter Penetration Depth Analysis.....	123
4.6.1.5 Full-depth Analysis.....	124
4.6.2 Conclusion of Penetration Depth Analysis.....	125
4.7 DCP to Unconfined Compressive Strength Correlation.....	127
4.7.1 Introduction.....	127
4.7.2 Logarithmic Function for DCP to MCS Correlation.....	127
4.7.3 Correlation Analysis.....	129
4.7.4 Comparison to Other Published Correlations.....	130
Chapter 5: Presentation and Analysis of Field Testing Phase Results.....	132
5.1 Introduction.....	132
5.2 Dynamic Cone Penetrometer Analysis.....	132
5.2.1 Reasons for Analyzing DCP Results for Outliers.....	132
5.2.2 Protocol for Analyzing DCP Results.....	135
5.2.2.1 Converting Data to Standard of Blows to Penetrate	
Five Millimeters.....	135
5.2.2.2 Identification of Outliers.....	137
5.2.3 DCP Penetration Depth Analysis.....	138
5.2.4 Results of Penetration Depth Analysis.....	139
5.3 Plastic-Mold Method Results.....	143
5.4 Dynamic Cone Penetrometer Results.....	145
5.5 Core Results.....	147
5.6 In-Place Density Results.....	148

5.7 Comparison of the Test Methods Evaluated.....	149
5.7.1 Variability of Each Test Method.....	150
5.7.2 Subsection Comparison.....	151
5.7.3 Location Comparison.....	152
Chapter 6: Summary, Conclusions, and Recommendations.....	154
5.1 Summary.....	154
5.2 Conclusions.....	154
5.3 Recommendations.....	156
References.....	159
Appendix A: Design Curves and Gradations.....	168
Appendix B: DCP Initial Curing Study.....	177
Appendix C: Soil Classification Impact Data.....	180
Appendix D: 25 Millimeter Penetration Depth Data.....	182
Appendix E: 50 Millimeter Penetration Depth Data.....	201
Appendix F: 75 Millimeter Penetration Depth Data.....	220
Appendix G: 100 Millimeter Penetration Depth Data.....	239
Appendix H: Full Depth Penetration Data.....	258
Appendix I: Summary of All Field Strengths Obtained from Different Test Methods.....	277
Appendix J: 25 Millimeter Penetration Field Data.....	280
Appendix K: 50 Millimeter Penetration Field Data.....	320
Appendix L: 75 Millimeter Penetration Field Data.....	360
Appendix M: 100 Millimeter Penetration Field Data.....	400
Appendix N: Full Depth Penetration Field Data.....	440

Appendix O: Summary of Sections, Subsections, and Locations 480

List of Tables

Table 1.1 ALDOT (2014) compressive strength specifications.....	3
Table 2.1 Typical cement requirements for various soil types (ACI 230 2009).....	12
Table 2.2 Maximum limit for impurities in water used for soil cement applications (adapted from ALDOT 2012).....	13
Table 2.3 Ranges of unconfined compressive strength of soil cement (ACI 230 2009).....	17
Table 2.4 PCA criteria for wet-dry and freeze-thaw soil cement durability tests (PCA 1971).....	23
Table 2.5 ALDOT compressive strength requirements.....	42
Table 3.1 Multiplier of Standard Deviation or Coefficient of Variation (adapted from ASTM C670 2015).....	96
Table 3.2 Mixture properties of field mixture.....	101
Table 4.1 Summary of soil classifications.....	114
Table 4.2 Mixture properties of Waugh laboratory mixtures.....	115
Table 4.3 Mixture properties of Elba laboratory mixtures.....	115
Table 4.4 Mixture properties of Coarse laboratory mixtures.....	115
Table 4.5 DCP Initial Curing Study Results.....	116
Table 4.6 Summary of the penetration versus strength investigation.....	119
Table 4.7 Summary of blow counts needed to reach each penetration depth.....	127
Table C.1 Data for soil classification impact for Elba soil.....	180
Table C.2 Data for soil classification impact for Waugh soil.....	180
Table C.3 Data for soil classification impact for Coarse soil.....	181

Table I.1 Tests conducted on locations 1 through 8.....	277
Table I.2 Tests conducted on locations 9 through 16.....	277
Table I.3 Tests conducted on locations 17 through 24.....	277
Table I.4 Tests conducted on locations 25 through 32.....	278
Table I.5 Tests conducted on locations 33 through 40.....	278
Table I.6 Tests conducted on locations 41 through 48.....	278
Table I.7 Tests conducted on locations 49 through 57.....	279

List of Figures

Figure 1.1 Compressive strengths of cores from ALDOT project STPAA-0052 (504).....	4
Figure 2.1 Aggregate gradation band for minimum cement requirements (Halsted et al. 2006)...	11
Figure 2.2 Maximum dry density and optimum moisture content (Halsted et al. 2006).....	14
Figure 2.3 Relationship between dry density and moisture content when cement is added (adapted from Yoon and Abu-Farsakh 2008).....	15
Figure 2.4 Effect of a water reducing admixture on moist-density curve (Jin et al. 2017).....	16
Figure 2.5 Effects of curing time and different soils on unconfined compressive strength (FHWA 1979).....	18
Figure 2.6 Relationship between dry density and unconfined compressive strength (adapted from Yoon and Abu-Farsakh 2008).....	19
Figure 2.7 Relationship between water-to-cement ratio and unconfined compressive strength (adapted from Yoon and Abu-Farsakh 2008).....	19
Figure 2.8 Shrinkage cracks in soil cement (McLaughlin 2017).....	20
Figure 2.9 Relationship between compressive strength and the durability of soil cement (PCA 1971).....	24
Figure 2.10 Transverse single-shaft mixer.....	25
Figure 2.11 Cement being spread by mechanical spreader.....	26
Figure 2.12 Cement dusting into the air.....	27
Figure 2.13 Water truck applying water to soil cement.....	28
Figure 2.14 A typical continuous-flow pug mill plant (adapted from ACI 230 2009).....	29

Figure 2.15 Motor grader spreading soil cement.....	30
Figure 2.16 Sheepsfoot roller.....	32
Figure 2.17 Vibratory steel-wheeled roller.....	32
Figure 2.18 Emulsified asphalt coating the compacted soil cement.....	34
Figure 2.19 Cement content being checked (ACI 230 2009).....	36
Figure 2.20 Nuclear gauge method right after rolling.....	39
Figure 2.21 Nuclear gauge.....	41
Figure 2.22 NCDOT DCP test pattern (NCDOT Field Manual 2015).....	46
Figure 2.23 Core removal process.....	47
Figure 2.24 A sampled core that is too small.....	48
Figure 2.25 Compressive strength from ALDOT project STPAA-0052 (504) (McLaughlin 2017).....	49
Figure 2.26 ASTM-Standard DCP schematic (ASTM D6951 2018).....	51
Figure 2.27 Replaceable point tip (ASTM D6951 2018).....	52
Figure 2.28 Disposable cone tip (ASTM D6951 2018).....	52
Figure 2.29 DCP equipped with a magnetic ruler used for testing.....	53
Figure 2.30 Designed reinforced concrete confinement block schematic (Nemiroff 2016).....	55
Figure 2.31 Reinforced concrete confinement block with and without a DCP specimen (Nemiroff 2016).....	56
Figure 2.32 Vibrating compaction hammer with circular steel plate.....	57
Figure 2.33 DCP specimen compaction pattern (ASTM D1557 2012).....	57
Figure 2.34 Field testing locations (McLaughlin 2017).....	58
Figure 2.35 DCP testing pattern (McLaughlin 2017).....	59

Figure 2.36 Correlation between unconfined compressive strength and DCP results (adapted from McElvaney and Djatnika 1991).....	61
Figure 2.37 Correlation between unconfined compressive strength and DCP results (Patel and Patel 2012).....	62
Figure 2.38 Comparison between predicted and experimental results (Enayatpour et al. 2006)...	63
Figure 2.39 Correlation between molded cylinder strength and DCP slope results (Nemiroff 2016).....	65
Figure 2.40 Proctor mold specifications diagram (ASTM D698 2012).....	66
Figure 2.41 Proctor mold and 5.5-pound hammer.....	67
Figure 2.42 Plastic-Mold preparation apparatus.....	68
Figure 2.43 Plastic-Mold modification (Sullivan et al. 2014).....	69
Figure 2.44 Plastic-Mold specimen damaged by extrusion process (McLaughlin 2017).....	70
Figure 2.45 Plastic-Mold modification process (McLaughlin 2017).....	71
Figure 2.46 Steel-Mold equipment dimensions (ASTM D1632 2017).....	73
Figure 2.47 Steel-Mold equipment (Nemiroff 2016).....	73
Figure 2.48 SM cylinder compacted with drop-weight machine.....	75
Figure 2.49 SM cylinders during initial curing period.....	75
Figure 3.1 Summary of Laboratory Testing Program.....	78
Figure 3.2 Summary of materials and variables considered.....	79
Figure 3.3 Soils used during testing.....	81
Figure 3.4 Location of the Waugh Borrow Pit (Google Maps).....	82
Figure 3.5 Map of project site where Elba soil was collected (Google Maps).....	83
Figure 3.6 Coarse soil sample location (Google Maps).....	84

Figure 3.7 Mixing of soil prior to batching.....	86
Figure 3.8 12 cubic foot mortar mixer for soil cement mixing.....	87
Figure 3.9 McLaughlin (2017) tape arrangement.....	88
Figure 3.10 New PM tape arrangement.....	88
Figure 3.11 Straightedge used to trim the soil cement to the top of the mold.....	89
Figure 3.12 Specimen removal from plastic-mold.....	90
Figure 3.13 Initial curing of DCP specimen.....	90
Figure 3.14 Final curing of the PM cylinders.....	91
Figure 3.15 Measurements of the soil cement cylinder using a caliper.....	92
Figure 3.16 Dry soil cement samples about to be weighed.....	93
Figure 3.17 Forney 100-kip compression testing machine.....	94
Figure 3.18 Specimen being tested in the 100-kip compression testing machine.....	95
Figure 3.19 Height measurement of DCP specimen.....	97
Figure 3.20 Kessler Magnetic Ruler.....	98
Figure 3.21 DCP testing arrangement in the specimen.....	99
Figure 3.22 Summary of Field Testing Plan.....	100
Figure 3.23 U.S. Highway 84 bypass project location (Google Maps).....	101
Figure 3.24 Field testing plan.....	103
Figure 3.25 DCP testing pattern.....	104
Figure 3.26 Material ready to be sampled for PM cylinder production.....	105
Figure 3.27 Soil cement cylinder being compacted at the jobsite house.....	106
Figure 3.28 PM specimens during initial curing on site.....	107
Figure 3.29 Use of nuclear gauge on test section.....	108

Figure 3.30 Replaceable DCP tip.....	109
Figure 3.31 Testing pattern for each DCP testing location.....	110
Figure 3.32 Magnetic ruler and manual ruler used for DCP testing.....	111
Figure 3.33 Core being cut from the section.....	112
Figure 3.34 Core being placed in plastic bag.....	113
Figure 3.35 Multiple attempts at retrieving a valid core sample.....	113
Figure 4.1 Effect of soil classification on PM cylinder strength.....	117
Figure 4.2 Effect of soil classification on DCP slope.....	118
Figure 4.3 Penetration depth summary.....	120
Figure 4.4 Twenty-five millimeter depth penetration relationship.....	121
Figure 4.5 Fifty millimeter depth penetration relationship.....	122
Figure 4.6 Seventy-five millimeter depth penetration relationship.....	123
Figure 4.7 One-hundred millimeter depth penetration relationship.....	124
Figure 4.8 Full-depth penetration relationship between 0 and 175 millimeters.....	125
Figure 4.9 Coefficient of determination for all DCP data collected on penetration depth.....	126
Figure 4.10 Semi-logarithmic relationship between DCP slope and MCS of the different soils.....	128
Figure 4.11 Best-fit semi-logarithmic equation for all data collected.....	129
Figure 4.12 Comparison of Equation 4.1 to other published correlations.....	131
Figure 5.1 First example of highly variable DCP test results on US Highway 84 bypass.....	133
Figure 5.2 Second example of highly variable DCP test results on US Highway 84 bypass.....	134
Figure 5.3 Third example of highly variable DCP test results on US Highway 84 bypass.....	135
Figure 5.4 DCP test conducted on soil cement layer.....	136
Figure 5.5 Example of test when it reaches point of refusal.....	137

Figure 5.6 Coefficient of determination for all DCP test results collected.....	140
Figure 5.7 Coefficient of determination for DCP test results collected (McLaughlin 2017).....	141
Figure 5.8 Coefficient of determination for DCP tests conducted in laboratory (Nemiroff 2016).....	142
Figure 5.9 Seven-day compressive strength results for the plastic-mold method.....	144
Figure 5.10 Plastic-mold method average density values at each testing subsection.....	145
Figure 5.11 Seven-day compressive strength results from DCP results.....	146
Figure 5.12 Seven-day compressive strength results of cores taken along US Highway 84 bypass.....	147
Figure 5.13 Core results collected along US Highway 84 bypass.....	148
Figure 5.14 In-place density of soil cement base along US Highway 84 bypass.....	149
Figure 5.15 Adjusted coefficient of variation of strength using each test method.....	150
Figure 5.16 PM cylinder strength versus other test methods averaged per subsection.....	152
Figure 5.17 Left: Field results of PM cylinder strength versus the 75 mm DCP result per location; Right: Laboratory results of PM cylinder strength versus the 75 mm DCP result per testing day.....	153
Figure A.1 Design curve for Waugh soil with 4 percent cement content.....	168
Figure A.2 Design curve for Waugh soil with 5 percent cement content.....	168
Figure A.3 Design curve for Waugh soil with 6 percent cement content.....	169
Figure A.4 Design curve for Waugh soil with 8 percent cement content.....	169
Figure A.5 Design curve for Waugh soil with 10 percent cement content.....	170
Figure A.6 Design curve for Elba soil with 5 percent cement content.....	170
Figure A.7 Design curve for Elba soil with 6.5 percent cement content.....	171

Figure A.8 Design curve for Elba soil with 8 percent cement content.....	171
Figure A.9 Design curve for Elba soil with 10 percent cement content.....	172
Figure A.10 Design curve for Coarse soil with 4 percent cement content.....	172
Figure A.11 Design curve for Coarse soil with 6 percent cement content.....	173
Figure A.12 Design curve for Coarse soil with 8 percent cement content.....	173
Figure A.13 Design curve for Coarse soil with 9 percent cement content.....	174
Figure A.14 Design curve for Coarse soil with 10 percent cement content.....	174
Figure A.15 Gradation for Waugh soil.....	175
Figure A.16 Gradation for Elba soil.....	175
Figure A.17 Gradation for Coarse soil.....	176
Figure B.1 Plastic lid method at 4 percent cement.....	177
Figure B.2 Plastic sheet and clip method at 4 percent cement.....	177
Figure B.3 Plastic lid method at 6 percent cement.....	178
Figure B.4 Plastic sheet and clip method at 6 percent cement.....	178
Figure B.5 Plastic lid method at 8 percent cement.....	179
Figure B.6 Plastic sheet and clip method at 8 percent cement.....	179
Figure D.1 Waugh 4% No.1 3 day.....	182
Figure D.2 Waugh 4% No. 1 7 day.....	182
Figure D.3 Waugh 4% No. 2 3 day.....	183
Figure D.4 Waugh 4% No. 2 7 day.....	183
Figure D.5 Waugh 5% No. 1 3 days (Third specimen was removed due to error).....	184
Figure D.6 Waugh 5% No. 1 7 days.....	184
Figure D.7 Waugh 5% No. 2 3 days.....	185

Figure D.8 Waugh 5% No. 2 7 days.....	185
Figure D.9 Waugh 6% 3 day.....	186
Figure D.10 Waugh 6% 7 day.....	186
Figure D.11 Waugh 8% No. 1 3 days.....	187
Figure D.12 Waugh 8% No. 1 7 days.....	187
Figure D.13 Waugh 8% No. 2 3 days.....	188
Figure D.14 Waugh 8% No. 2 7 days.....	188
Figure D.15 Waugh 10% 3 days.....	189
Figure D.16 Waugh 10% 7 days.....	189
Figure D.17 Elba 5% 3 days.....	190
Figure D.18 Elba 5% 7 days.....	190
Figure D.19 Elba 6.5% No. 1 3 days.....	191
Figure D.20 Elba 6.5% No. 1 7 days.....	191
Figure D.21 Elba 6.5% No. 2 3 days.....	192
Figure D.22 Elba 6.5% No. 2 7 days.....	192
Figure D.23 Elba 8% 3 days.....	193
Figure D.24 Elba 8% 7 days.....	193
Figure D.25 Coarse 4% No. 1 3 days.....	194
Figure D.26 Coarse 4% No. 1 7 days.....	194
Figure D.27 Coarse 4% No. 2 3 days.....	195
Figure D.28 Coarse 4% No. 2 7 days.....	195
Figure D.29 Coarse 6% No. 1 3 days.....	196
Figure D.30 Coarse 6% No. 1 7 days.....	196

Figure D.31 Coarse 6% No. 2 3 days.....	197
Figure D.32 Coarse 6% No. 2 7 days.....	197
Figure D.33 Coarse 8% No. 1 3 days.....	198
Figure D.34 Coarse 8% No. 1 7 days.....	198
Figure D.35 Coarse 8% No. 2 3 days.....	199
Figure D.36 Coarse 8% No. 2 7 days.....	199
Figure D.37 Coarse 9% 3 days.....	200
Figure D.38 Coarse 9% 7 days.....	200
Figure E.1 Waugh 4% No. 1 3 days.....	201
Figure E.2 Waugh 4% No. 1 7 days.....	201
Figure E.3 Waugh 4% No. 2 3 days.....	202
Figure E.4 Waugh 4% No. 2 7 days.....	202
Figure E.5 Waugh 5% No. 1 3 days (Third specimen was removed due to error).....	203
Figure E.6 Waugh 5% No. 1 7 days.....	203
Figure E.7 Waugh 5% No. 2 3 days.....	204
Figure E.8 Waugh 5% No. 2 7 days.....	204
Figure E.9 Waugh 6% 3 day.....	205
Figure E.10 Waugh 6% 7 day.....	205
Figure E.11 Waugh 8% No. 1 3 days.....	206
Figure E.12 Waugh 8% No. 1 7 days.....	206
Figure E.13 Waugh 8% No. 2 3 days.....	207
Figure E.14 Waugh 8% No. 2 7 days.....	207
Figure E.15 Waugh 10% 3 days.....	208

Figure E.16 Waugh 10% 7 days.....	208
Figure E.17 Elba 5% 3 days.....	209
Figure E.18 Elba 5% 7 days.....	209
Figure E.19 Elba 6.5% No. 1 3 days.....	210
Figure E.20 Elba 6.5% No. 1 7 days.....	210
Figure E.21 Elba 6.5% No. 2 3 days.....	211
Figure E.22 Elba 6.5% No. 2 7 days.....	211
Figure E.23 Elba 8% 3 days.....	212
Figure E.24 Elba 8% 7 days.....	212
Figure E.25 Coarse 4% No. 1 3 days.....	213
Figure E.26 Coarse 4% No. 1 7 days.....	213
Figure E.27 Coarse 4% No. 2 3 days.....	214
Figure E.28 Coarse 4% No. 2 7 days.....	214
Figure E.29 Coarse 6% No. 1 3 days.....	215
Figure E.30 Coarse 6% No. 1 7 days.....	215
Figure E.31 Coarse 6% No. 2 3 days.....	216
Figure E.32 Coarse 6% No. 2 7 days.....	216
Figure E.33 Coarse 8% No. 1 3 days.....	217
Figure E.34 Coarse 8% No. 1 7 days.....	217
Figure E.35 Coarse 8% No. 2 3 days.....	218
Figure E.36 Coarse 8% No. 2 7 days.....	218
Figure E.37 Coarse 9% 3 days.....	219
Figure E.38 Coarse 9% 7 days.....	219

Figure F.1 Waugh 4% No. 1 3 days.....	220
Figure F.2 Waugh 4% No. 1 7 days.....	220
Figure F.3 Waugh 4% No. 2 3 days.....	221
Figure F.4 Waugh 4% No. 2 7 days.....	221
Figure F.5 Waugh 5% No. 1 3 days (Third specimen was removed due to error).....	222
Figure F.6 Waugh 5% No. 1 7 days.....	222
Figure F.7 Waugh 5% No. 2 3 days.....	223
Figure F.8 Waugh 5% No. 2 7 days.....	223
Figure F.9 Waugh 6% 3 day.....	224
Figure F.10 Waugh 6% 7 day.....	224
Figure F.11 Waugh 8% No. 1 3 days.....	225
Figure F.12 Waugh 8% No. 1 7 days.....	225
Figure F.13 Waugh 8% No. 2 3 days.....	226
Figure F.14 Waugh 8% No. 2 7 days.....	226
Figure F.15 Waugh 10% 3 days.....	227
Figure F.16 Waugh 10% 7 days.....	227
Figure F.17 Elba 5% 3 days.....	228
Figure F.18 Elba 5% 7 days.....	228
Figure F.19 Elba 6.5% No. 1 3 days.....	229
Figure F.20 Elba 6.5% No. 1 7 days.....	229
Figure F.21 Elba 6.5% No. 2 3 days.....	230
Figure F.22 Elba 6.5% No. 2 7 days.....	230
Figure F.23 Elba 8% 3 days.....	231

Figure F.24 Elba 8% 7 days.....	231
Figure F.25 Coarse 4% No. 1 3 days.....	232
Figure F.26 Coarse 4% No. 1 7 days.....	232
Figure F.27 Coarse 4% No. 2 3 days.....	233
Figure F.28 Coarse 4% No. 2 7 days.....	233
Figure F.29 Coarse 6% No. 1 3 days.....	234
Figure F.30 Coarse 6% No. 1 7 days.....	234
Figure F.31 Coarse 6% No. 2 3 days.....	235
Figure F.32 Coarse 6% No. 2 7 days.....	235
Figure F.33 Coarse 8% No. 1 3 days.....	236
Figure F.34 Coarse 8% No. 1 7 days.....	236
Figure F.35 Coarse 8% No. 2 3 days.....	237
Figure F.36 Coarse 8% No. 2 7 days.....	237
Figure F.37 Coarse 9% 3 days.....	238
Figure F.38 Coarse 9% 7 days.....	238
Figure G.1 Waugh 4% No. 1 3 days.....	239
Figure G.2 Waugh 4% No. 1 7 days.....	239
Figure G.3 Waugh 4% No. 2 3 days.....	240
Figure G.4 Waugh 4% No. 2 7 days.....	240
Figure G.5 Waugh 5% No. 1 3 days (Third specimen was removed due to error).....	241
Figure G.6 Waugh 5% No. 1 7 days.....	241
Figure G.7 Waugh 5% No. 2 3 days.....	242
Figure G.8 Waugh 5% No. 2 7 days.....	242

Figure G.9 Waugh 6% 3 day.....	243
Figure G.10 Waugh 6% 7 day.....	243
Figure G.11 Waugh 8% No. 1 3 days.....	244
Figure G.12 Waugh 8% No. 1 7 days.....	244
Figure G.13 Waugh 8% No. 2 3 days.....	245
Figure G.14 Waugh 8% No. 2 7 days.....	245
Figure G.15 Waugh 10% 3 days.....	246
Figure G.16 Waugh 10% 7 days.....	246
Figure G.17 Elba 5% 3 days.....	247
Figure G.18 Elba 5% 7 days.....	247
Figure G.19 Elba 6.5% No. 1 3 days.....	248
Figure G.20 Elba 6.5% No. 1 7 days.....	248
Figure G.21 Elba 6.5% No. 2 3 days.....	249
Figure G.22 Elba 6.5% No. 2 7 days.....	249
Figure G.23 Elba 8% 3 days.....	250
Figure G.24 Elba 8% 7 days.....	250
Figure G.25 Coarse 4% No. 1 3 days.....	251
Figure G.26 Coarse 4% No. 1 7 days.....	251
Figure G.27 Coarse 4% No. 2 3 days.....	252
Figure G.28 Coarse 4% No. 2 7 days.....	252
Figure G.29 Coarse 6% No. 1 3 days.....	253
Figure G.30 Coarse 6% No. 1 7 days.....	253
Figure G.31 Coarse 6% No. 2 3 days.....	254

Figure G.32 Coarse 6% No. 2 7 days.....	254
Figure G.33 Coarse 8% No. 1 3 days.....	255
Figure G.34 Coarse 8% No. 1 7 days.....	255
Figure G.35 Coarse 8% No. 2 3 days.....	256
Figure G.36 Coarse 8% No. 2 7 days.....	256
Figure G.37 Coarse 9% 3 days.....	257
Figure G.38 Coarse 9% 7 days.....	257
Figure H.1 Waugh 4% No. 1 3 days.....	258
Figure H.2 Waugh 4% No. 1 7 days.....	258
Figure H.3 Waugh 4% No. 2 3 days.....	259
Figure H.4 Waugh 4% No. 2 7 days.....	259
Figure H.5 Waugh 5% No. 1 3 days (Third specimen was removed due to error).....	260
Figure H.6 Waugh 5% No. 1 7 days.....	260
Figure H.7 Waugh 5% No. 2 3 days.....	261
Figure H.8 Waugh 5% No. 2 7 days.....	261
Figure H.9 Waugh 6% 3 day.....	262
Figure H.10 Waugh 6% 7 day.....	262
Figure H.11 Waugh 8% No. 1 3 days.....	263
Figure H.12 Waugh 8% No. 1 7 days.....	263
Figure H.13 Waugh 8% No. 2 3 days.....	264
Figure H.14 Waugh 8% No. 2 7 days.....	264
Figure H.15 Waugh 10% 3 days.....	265
Figure H.16 Waugh 10% 7 days.....	265

Figure H.17 Elba 5% 3 days.....	266
Figure H.18 Elba 5% 7 days.....	266
Figure H.19 Elba 6.5% No. 1 3 days.....	267
Figure H.20 Elba 6.5% No. 1 7 days.....	267
Figure H.21 Elba 6.5% No. 2 3 days.....	268
Figure H.22 Elba 6.5% No. 2 7 days.....	268
Figure H.23 Elba 8% 3 days.....	269
Figure H.24 Elba 8% 7 days.....	269
Figure H.25 Coarse 4% No. 1 3 days.....	270
Figure H.26 Coarse 4% No. 1 7 days.....	270
Figure H.27 Coarse 4% No. 2 3 days.....	271
Figure H.28 Coarse 4% No. 2 7 days.....	271
Figure H.29 Coarse 6% No. 1 3 days.....	272
Figure H.30 Coarse 6% No. 1 7 days.....	272
Figure H.31 Coarse 6% No. 2 3 days.....	273
Figure H.32 Coarse 6% No. 2 7 days.....	273
Figure H.33 Coarse 8% No. 1 3 days.....	274
Figure H.34 Coarse 8% No. 1 7 days.....	274
Figure H.35 Coarse 8% No. 2 3 days.....	275
Figure H.36 Coarse 8% No. 2 7 days.....	275
Figure H.37 Coarse 9% 3 days.....	276
Figure H.38 Coarse 9% 7 days.....	276
Figure J.1 Test performed on July 9, 2019, Location 1 (top left = 5 tests,	

top right = 4 tests, bottom = 3 tests).....	280
Figure J.2 Test performed on July 10, 2019, Location 4 (top left = 5 tests, top right = 4 tests, bottom = 3 tests).....	281
Figure J.3 Test performed on July 10, 2019, Location 5 (top left = 5 tests, top right = 4 tests, bottom = 3 tests).....	282
Figure J.4 Test performed on July 10, 2019, Location 6 (top left = 5 tests, top right = 4 tests, bottom = 3 tests).....	283
Figure J.5 Test performed on July 16, 2019, Location 7 (top left = 5 tests, top right = 4 tests, bottom = 3 tests).....	284
Figure J.6 Test performed on July 16, 2019, Location 8 (top left = 5 tests, top right = 4 tests, bottom = 3 tests).....	285
Figure J.7 Test performed on July 16, 2019, Location 9 (top left = 5 tests, top right = 4 tests, bottom = 3 tests).....	286
Figure J.8 Test performed on July 16, 2019, Location 10 (top left = 5 tests, top right = 4 tests, bottom = 3 tests).....	287
Figure J.9 Test performed on July 16, 2019, Location 11 (top left = 5 tests, top right = 4 tests, bottom = 3 tests).....	288
Figure J.10 Test performed on July 16, 2019, Location 12 (top left = 5 tests, top right = 4 tests, bottom = 3 tests).....	289
Figure J.11 Test performed on July 16, 2019, Location 13 (top left = 5 tests, top right = 4 tests, bottom = 3 tests).....	290
Figure J.12 Test performed on July 16, 2019, Location 15 (only 2 tests completed).....	290

Figure J.13 Test performed on July 17, 2019, Location 17 (top left = 5 tests, top right = 4 tests, bottom = 3 tests).....	291
Figure J.14 Test performed on July 17, 2019, Location 18 (left = 4 tests, right = 3 tests).....	292
Figure J.15 Test performed on July 17, 2019, Location 19 (top left = 5 tests, top right = 4 tests, bottom = 3 tests).....	292
Figure J.16 Test performed on July 17, 2019, Location 20 (top left = 5 tests, top right = 4 tests, bottom = 3 tests).....	293
Figure J.17 Test performed on July 17, 2019, Location 21 (top left = 5 tests, top right = 4 tests, bottom = 3 tests).....	294
Figure J.18 Test performed on July 17, 2019, Location 22 (top left = 5 tests, top right = 4 tests, bottom = 3 tests).....	295
Figure J.19 Test performed on July 18, 2019, Location 23 (top left = 5 tests, top right = 4 tests, bottom = 3 tests).....	296
Figure J.20 Test performed on July 18, 2019, Location 24 (top left = 5 tests, top right = 4 tests, bottom = 3 tests).....	297
Figure J.21 Test performed on July 18, 2019, Location 25 (top left = 5 tests, top right = 4 tests, bottom = 3 tests).....	298
Figure J.22 Test performed on July 18, 2019, Location 28 (top left = 5 tests, top right = 4 tests, bottom = 3 tests).....	299
Figure J.23 Test performed on July 19, 2019, Location 30 (top left = 5 tests, top right = 4 tests, bottom = 3 tests).....	300
Figure J.24 Test performed on July 19, 2019, Location 31 (top left = 5 tests, top right = 4 tests, bottom = 3 tests).....	301

Figure J.25 Test performed on July 19, 2019, Location 32 (top left = 5 tests, top right = 4 tests, bottom = 3 tests).....	302
Figure J.26 Test performed on July 19, 2019, Location 33 (top left = 5 tests, top right = 4 tests, bottom = 3 tests).....	303
Figure J.27 Test performed on July 19, 2019, Location 34 (top left = 5 tests, top right = 4 tests, bottom = 3 tests).....	304
Figure J.28 Test performed on July 19, 2019, Location 35 (top left = 5 tests, top right = 4 tests, bottom = 3 tests).....	305
Figure J.29 Test performed on July 19, 2019, Location 36 (top left = 5 tests, top right = 4 tests, bottom = 3 tests).....	306
Figure J.30 Test performed on July 23, 2019, Location 37 (top left = 5 tests, top right = 4 tests, bottom = 3 tests).....	307
Figure J.31 Test performed on July 23, 2019, Location 38 (top left = 5 tests, top right = 4 tests, bottom = 3 tests).....	308
Figure J.32 Test performed on July 23, 2019, Location 39 (top left = 5 tests, top right = 4 tests, bottom = 3 tests).....	309
Figure J.33 Test performed on July 23, 2019, Location 40 (top left = 5 tests, top right = 4 tests, bottom = 3 tests).....	310
Figure J.34 Test performed on July 23, 2019, Location 41 (only 3 tests completed).....	310
Figure J.35 Test performed on July 23, 2019, Location 42 (top left = 5 tests, top right = 4 tests, bottom = 3 tests).....	311
Figure J.36 Test performed on July 23, 2019, Location 43 (top left = 5 tests, top right = 4 tests, bottom = 3 tests).....	312

Figure J.37 Test performed on July 24, 2019, Location 44 (top left = 5 tests, top right = 4 tests, bottom = 3 tests).....	313
Figure J.38 Test performed on July 24, 2019, Location 45 (top left = 5 tests, top right = 4 tests, bottom = 3 tests).....	314
Figure J.39 Test performed on July 24, 2019, Location 46 (top left = 5 tests, top right = 4 tests, bottom = 3 tests).....	315
Figure J.40 Test performed on July 24, 2019, Location 47 (top left = 5 tests, top right = 4 tests, bottom = 3 tests).....	316
Figure J.41 Test performed on July 24, 2019, Location 48 (top left = 5 tests, top right = 4 tests, bottom = 3 tests).....	317
Figure J.42 Test performed on July 24, 2019, Location 49 (top left = 5 tests, top right = 4 tests, bottom = 3 tests).....	318
Figure J.43 Test performed on July 24, 2019, Location 50 (top left = 5 tests, top right = 4 tests, bottom = 3 tests).....	319
Figure K.1 Test performed on July 9, 2019, Location 1 (top left = 5 tests, top right = 4 tests, bottom = 3 tests).....	320
Figure K.2 Test performed on July 10, 2019, Location 4 (top left = 5 tests, top right = 4 tests, bottom = 3 tests).....	321
Figure J.3 Test performed on July 10, 2019, Location 5 (top left = 5 tests, top right = 4 tests, bottom = 3 tests).....	322
Figure J.4 Test performed on July 10, 2019, Location 6 (top left = 5 tests, top right = 4 tests, bottom = 3 tests).....	323
Figure J.5 Test performed on July 16, 2019, Location 7 (top left = 5 tests, top right = 4 tests, bottom = 3 tests).....	324

top right = 4 tests, bottom = 3 tests).....	324
Figure J.6 Test performed on July 16, 2019, Location 8 (top left = 5 tests, top right = 4 tests, bottom = 3 tests).....	325
Figure J.7 Test performed on July 16, 2019, Location 9 (top left = 5 tests, top right = 4 tests, bottom = 3 tests).....	326
Figure J.8 Test performed on July 16, 2019, Location 10 (top left = 5 tests, top right = 4 tests, bottom = 3 tests).....	327
Figure J.9 Test performed on July 16, 2019, Location 11 (top left = 5 tests, top right = 4 tests, bottom = 3 tests).....	328
Figure J.10 Test performed on July 16, 2019, Location 12 (top left = 5 tests, top right = 4 tests, bottom = 3 tests).....	329
Figure J.11 Test performed on July 16, 2019, Location 13 (top left = 5 tests, top right = 4 tests, bottom = 3 tests).....	330
Figure J.12 Test performed on July 16, 2019, Location 15 (only 2 tests completed).....	330
Figure J.13 Test performed on July 17, 2019, Location 17 (top left = 5 tests, top right = 4 tests, bottom = 3 tests).....	331
Figure J.14 Test performed on July 17, 2019, Location 18 (left = 4 tests, right = 3 tests).....	332
Figure J.15 Test performed on July 17, 2019, Location 19 (top left = 5 tests, top right = 4 tests, bottom = 3 tests).....	332
Figure J.16 Test performed on July 17, 2019, Location 20 (top left = 5 tests, top right = 4 tests, bottom = 3 tests).....	333
Figure J.17 Test performed on July 17, 2019, Location 21 (top left = 5 tests,	

top right = 4 tests, bottom = 3 tests).....	334
Figure J.18 Test performed on July 17, 2019, Location 22 (top left = 5 tests, top right = 4 tests, bottom = 3 tests).....	335
Figure J.19 Test performed on July 18, 2019, Location 23 (top left = 5 tests, top right = 4 tests, bottom = 3 tests).....	336
Figure J.20 Test performed on July 18, 2019, Location 24 (top left = 5 tests, top right = 4 tests, bottom = 3 tests).....	337
Figure J.21 Test performed on July 18, 2019, Location 25 (top left = 5 tests, top right = 4 tests, bottom = 3 tests).....	338
Figure J.22 Test performed on July 18, 2019, Location 28 (top left = 5 tests, top right = 4 tests, bottom = 3 tests).....	339
Figure J.23 Test performed on July 19, 2019, Location 30 (top left = 5 tests, top right = 4 tests, bottom = 3 tests).....	340
Figure J.24 Test performed on July 19, 2019, Location 31 (top left = 5 tests, top right = 4 tests, bottom = 3 tests).....	341
Figure J.25 Test performed on July 19, 2019, Location 32 (top left = 5 tests, top right = 4 tests, bottom = 3 tests).....	342
Figure J.26 Test performed on July 19, 2019, Location 33 (top left = 5 tests, top right = 4 tests, bottom = 3 tests).....	343
Figure J.27 Test performed on July 19, 2019, Location 34 (top left = 5 tests, top right = 4 tests, bottom = 3 tests).....	344
Figure J.28 Test performed on July 19, 2019, Location 35 (top left = 5 tests,	

top right = 4 tests, bottom = 3 tests).....	345
Figure J.29 Test performed on July 19, 2019, Location 36 (top left = 5 tests, top right = 4 tests, bottom = 3 tests).....	346
Figure J.30 Test performed on July 23, 2019, Location 37 (top left = 5 tests, top right = 4 tests, bottom = 3 tests).....	347
Figure J.31 Test performed on July 23, 2019, Location 38 (top left = 5 tests, top right = 4 tests, bottom = 3 tests).....	348
Figure J.32 Test performed on July 23, 2019, Location 39 (top left = 5 tests, top right = 4 tests, bottom = 3 tests).....	349
Figure J.33 Test performed on July 23, 2019, Location 40 (top left = 5 tests, top right = 4 tests, bottom = 3 tests).....	350
Figure J.34 Test performed on July 23, 2019, Location 41 (only 3 tests completed).....	350
Figure J.35 Test performed on July 23, 2019, Location 42 (top left = 5 tests, top right = 4 tests, bottom = 3 tests).....	351
Figure J.36 Test performed on July 23, 2019, Location 43 (top left = 5 tests, top right = 4 tests, bottom = 3 tests).....	352
Figure J.37 Test performed on July 24, 2019, Location 44 (top left = 5 tests, top right = 4 tests, bottom = 3 tests).....	353
Figure J.38 Test performed on July 24, 2019, Location 45 (top left = 5 tests, top right = 4 tests, bottom = 3 tests).....	354
Figure J.39 Test performed on July 24, 2019, Location 46 (top left = 5 tests, top right = 4 tests, bottom = 3 tests).....	355

Figure J.40 Test performed on July 24, 2019, Location 47 (top left = 5 tests, top right = 4 tests, bottom = 3 tests).....	356
Figure J.41 Test performed on July 24, 2019, Location 48 (top left = 5 tests, top right = 4 tests, bottom = 3 tests).....	357
Figure J.42 Test performed on July 24, 2019, Location 49 (top left = 5 tests, top right = 4 tests, bottom = 3 tests).....	358
Figure J.43 Test performed on July 24, 2019, Location 50 (top left = 5 tests, top right = 4 tests, bottom = 3 tests).....	359
Figure L.1 Test performed on July 9, 2019, Location 1 (top left = 5 tests, top right = 4 tests, bottom = 3 tests).....	360
Figure L.2 Test performed on July 10, 2019, Location 4 (top left = 5 tests, top right = 4 tests, bottom = 3 tests).....	361
Figure L.3 Test performed on July 10, 2019, Location 5 (top left = 5 tests, top right = 4 tests, bottom = 3 tests).....	362
Figure L.4 Test performed on July 10, 2019, Location 6 (top left = 5 tests, top right = 4 tests, bottom = 3 tests).....	363
Figure L.5 Test performed on July 16, 2019, Location 7 (top left = 5 tests, top right = 4 tests, bottom = 3 tests).....	364
Figure L.6 Test performed on July 16, 2019, Location 8 (top left = 5 tests, top right = 4 tests, bottom = 3 tests).....	365
Figure L.7 Test performed on July 16, 2019, Location 9 (top left = 5 tests, top right = 4 tests, bottom = 3 tests).....	366
Figure L.8 Test performed on July 16, 2019, Location 10 (top left = 5 tests,	

top right = 4 tests, bottom = 3 tests).....	367
Figure L.9 Test performed on July 16, 2019, Location 11 (top left = 5 tests, top right = 4 tests, bottom = 3 tests).....	368
Figure L.10 Test performed on July 16, 2019, Location 12 (top left = 5 tests, top right = 4 tests, bottom = 3 tests).....	369
Figure L.11 Test performed on July 16, 2019, Location 13 (top left = 5 tests, top right = 4 tests, bottom = 3 tests).....	370
Figure L.12 Test performed on July 16, 2019, Location 15 (only 2 tests completed).....	370
Figure L.13 Test performed on July 17, 2019, Location 17 (top left = 5 tests, top right = 4 tests, bottom = 3 tests).....	371
Figure L.14 Test performed on July 17, 2019, Location 18 (left = 4 tests, right = 3 tests).....	372
Figure L.15 Test performed on July 17, 2019, Location 19 (top left = 5 tests, top right = 4 tests, bottom = 3 tests).....	372
Figure L.16 Test performed on July 17, 2019, Location 20 (top left = 5 tests, top right = 4 tests, bottom = 3 tests).....	373
Figure L.17 Test performed on July 17, 2019, Location 21 (top left = 5 tests, top right = 4 tests, bottom = 3 tests).....	374
Figure L.18 Test performed on July 17, 2019, Location 22 (top left = 5 tests, top right = 4 tests, bottom = 3 tests).....	375
Figure L.19 Test performed on July 18, 2019, Location 23 (top left = 5 tests, top right = 4 tests, bottom = 3 tests).....	376
Figure L.20 Test performed on July 18, 2019, Location 24 (top left = 5 tests,	

top right = 4 tests, bottom = 3 tests).....	377
Figure L.21 Test performed on July 18, 2019, Location 25 (top left = 5 tests, top right = 4 tests, bottom = 3 tests).....	378
Figure L.22 Test performed on July 18, 2019, Location 28 (top left = 5 tests, top right = 4 tests, bottom = 3 tests).....	379
Figure L.23 Test performed on July 19, 2019, Location 30 (top left = 5 tests, top right = 4 tests, bottom = 3 tests).....	380
Figure L.24 Test performed on July 19, 2019, Location 31 (top left = 5 tests, top right = 4 tests, bottom = 3 tests).....	381
Figure L.25 Test performed on July 19, 2019, Location 32 (top left = 5 tests, top right = 4 tests, bottom = 3 tests).....	382
Figure L.26 Test performed on July 19, 2019, Location 33 (top left = 5 tests, top right = 4 tests, bottom = 3 tests).....	383
Figure L.27 Test performed on July 19, 2019, Location 34 (top left = 5 tests, top right = 4 tests, bottom = 3 tests).....	384
Figure L.28 Test performed on July 19, 2019, Location 35 (top left = 5 tests, top right = 4 tests, bottom = 3 tests).....	385
Figure L.29 Test performed on July 19, 2019, Location 36 (top left = 5 tests, top right = 4 tests, bottom = 3 tests).....	386
Figure L.30 Test performed on July 23, 2019, Location 37 (top left = 5 tests, top right = 4 tests, bottom = 3 tests).....	387
Figure L.31 Test performed on July 23, 2019, Location 38 (top left = 5 tests,	

top right = 4 tests, bottom = 3 tests).....	388
Figure L.32 Test performed on July 23, 2019, Location 39 (top left = 5 tests, top right = 4 tests, bottom = 3 tests).....	389
Figure L.33 Test performed on July 23, 2019, Location 40 (top left = 5 tests, top right = 4 tests, bottom = 3 tests).....	390
Figure L.34 Test performed on July 23, 2019, Location 41 (only 3 tests completed).....	390
Figure L.35 Test performed on July 23, 2019, Location 42 (top left = 5 tests, top right = 4 tests, bottom = 3 tests).....	391
Figure L.36 Test performed on July 23, 2019, Location 43 (top left = 5 tests, top right = 4 tests, bottom = 3 tests).....	392
Figure L.37 Test performed on July 24, 2019, Location 44 (top left = 5 tests, top right = 4 tests, bottom = 3 tests).....	393
Figure L.38 Test performed on July 24, 2019, Location 45 (top left = 5 tests, top right = 4 tests, bottom = 3 tests).....	394
Figure L.39 Test performed on July 24, 2019, Location 46 (top left = 5 tests, top right = 4 tests, bottom = 3 tests).....	395
Figure L.40 Test performed on July 24, 2019, Location 47 (top left = 5 tests, top right = 4 tests, bottom = 3 tests).....	396
Figure L.41 Test performed on July 24, 2019, Location 48 (top left = 5 tests, top right = 4 tests, bottom = 3 tests).....	397
Figure L.42 Test performed on July 24, 2019, Location 49 (top left = 5 tests, top right = 4 tests, bottom = 3 tests).....	398

Figure L.43 Test performed on July 24, 2019, Location 50 (top left = 5 tests, top right = 4 tests, bottom = 3 tests).....	399
Figure M.1 Test performed on July 9, 2019, Location 1 (top left = 5 tests, top right = 4 tests, bottom = 3 tests).....	400
Figure M.2 Test performed on July 10, 2019, Location 4 (top left = 5 tests, top right = 4 tests, bottom = 3 tests).....	401
Figure M.3 Test performed on July 10, 2019, Location 5 (top left = 5 tests, top right = 4 tests, bottom = 3 tests).....	402
Figure M.4 Test performed on July 10, 2019, Location 6 (top left = 5 tests, top right = 4 tests, bottom = 3 tests).....	403
Figure M.5 Test performed on July 16, 2019, Location 7 (top left = 5 tests, top right = 4 tests, bottom = 3 tests).....	404
Figure M.6 Test performed on July 16, 2019, Location 8 (top left = 5 tests, top right = 4 tests, bottom = 3 tests).....	405
Figure M.7 Test performed on July 16, 2019, Location 9 (top left = 5 tests, top right = 4 tests, bottom = 3 tests).....	406
Figure M.8 Test performed on July 16, 2019, Location 10 (top left = 5 tests, top right = 4 tests, bottom = 3 tests).....	407
Figure M.9 Test performed on July 16, 2019, Location 11 (top left = 5 tests, top right = 4 tests, bottom = 3 tests).....	408
Figure M.10 Test performed on July 16, 2019, Location 12 (top left = 5 tests, top right = 4 tests, bottom = 3 tests).....	409
Figure M.11 Test performed on July 16, 2019, Location 13 (top left = 5 tests, top right = 4 tests, bottom = 3 tests).....	409

top right = 4 tests, bottom = 3 tests).....	410
Figure M.12 Test performed on July 16, 2019, Location 15 (only 2 tests completed).....	410
Figure M.13 Test performed on July 17, 2019, Location 17 (top left = 5 tests, top right = 4 tests, bottom = 3 tests).....	411
Figure M.14 Test performed on July 17, 2019, Location 18 (left = 4 tests, right = 3 tests).....	412
Figure M.15 Test performed on July 17, 2019, Location 19 (top left = 5 tests, top right = 4 tests, bottom = 3 tests).....	412
Figure M.16 Test performed on July 17, 2019, Location 20 (top left = 5 tests, top right = 4 tests, bottom = 3 tests).....	413
Figure M.17 Test performed on July 17, 2019, Location 21 (top left = 5 tests, top right = 4 tests, bottom = 3 tests).....	414
Figure M.18 Test performed on July 17, 2019, Location 22 (top left = 5 tests, top right = 4 tests, bottom = 3 tests).....	415
Figure M.19 Test performed on July 18, 2019, Location 23 (top left = 5 tests, top right = 4 tests, bottom = 3 tests).....	416
Figure M.20 Test performed on July 18, 2019, Location 24 (top left = 5 tests, top right = 4 tests, bottom = 3 tests).....	417
Figure M.21 Test performed on July 18, 2019, Location 25 (top left = 5 tests, top right = 4 tests, bottom = 3 tests).....	418
Figure M.22 Test performed on July 18, 2019, Location 28 (top left = 5 tests, top right = 4 tests, bottom = 3 tests).....	419
Figure M.23 Test performed on July 19, 2019, Location 30 (top left = 5 tests, top right = 4 tests, bottom = 3 tests).....	420

Figure M.24 Test performed on July 19, 2019, Location 31 (top left = 5 tests, top right = 4 tests, bottom = 3 tests).....	421
Figure M.25 Test performed on July 19, 2019, Location 32 (top left = 5 tests, top right = 4 tests, bottom = 3 tests).....	422
Figure M.26 Test performed on July 19, 2019, Location 33 (top left = 5 tests, top right = 4 tests, bottom = 3 tests).....	423
Figure M.27 Test performed on July 19, 2019, Location 34 (top left = 5 tests, top right = 4 tests, bottom = 3 tests).....	424
Figure M.28 Test performed on July 19, 2019, Location 35 (top left = 5 tests, top right = 4 tests, bottom = 3 tests).....	425
Figure M.29 Test performed on July 19, 2019, Location 36 (top left = 5 tests, top right = 4 tests, bottom = 3 tests).....	426
Figure M.30 Test performed on July 23, 2019, Location 37 (top left = 5 tests, top right = 4 tests, bottom = 3 tests).....	427
Figure M.31 Test performed on July 23, 2019, Location 38 (top left = 5 tests, top right = 4 tests, bottom = 3 tests).....	428
Figure M.32 Test performed on July 23, 2019, Location 39 (top left = 5 tests, top right = 4 tests, bottom = 3 tests).....	429
Figure M.33 Test performed on July 23, 2019, Location 40 (top left = 5 tests, top right = 4 tests, bottom = 3 tests).....	430
Figure M.34 Test performed on July 23, 2019, Location 41 (only 3 tests completed).....	430
Figure M.35 Test performed on July 23, 2019, Location 42 (top left = 5 tests, top right = 4 tests, bottom = 3 tests).....	431

Figure M.36 Test performed on July 23, 2019, Location 43 (top left = 5 tests, top right = 4 tests, bottom = 3 tests).....	432
Figure M.37 Test performed on July 24, 2019, Location 44 (top left = 5 tests, top right = 4 tests, bottom = 3 tests).....	433
Figure M.38 Test performed on July 24, 2019, Location 45 (top left = 5 tests, top right = 4 tests, bottom = 3 tests).....	434
Figure M.39 Test performed on July 24, 2019, Location 46 (top left = 5 tests, top right = 4 tests, bottom = 3 tests).....	435
Figure M.40 Test performed on July 24, 2019, Location 47 (top left = 5 tests, top right = 4 tests, bottom = 3 tests).....	436
Figure M.41 Test performed on July 24, 2019, Location 48 (top left = 5 tests, top right = 4 tests, bottom = 3 tests).....	437
Figure M.42 Test performed on July 24, 2019, Location 49 (top left = 5 tests, top right = 4 tests, bottom = 3 tests).....	438
Figure M.43 Test performed on July 24, 2019, Location 50 (top left = 5 tests, top right = 4 tests, bottom = 3 tests).....	439
Figure N.1 Test performed on July 9, 2019, Location 1 (top left = 5 tests, top right = 4 tests, bottom = 3 tests).....	440
Figure N.2 Test performed on July 10, 2019, Location 4 (top left = 5 tests, top right = 4 tests, bottom = 3 tests).....	441
Figure N.3 Test performed on July 10, 2019, Location 5 (top left = 5 tests, top right = 4 tests, bottom = 3 tests).....	442
Figure N.4 Test performed on July 10, 2019, Location 6 (top left = 5 tests,	

top right = 4 tests, bottom = 3 tests).....	443
Figure N.5 Test performed on July 16, 2019, Location 7 (top left = 5 tests, top right = 4 tests, bottom = 3 tests).....	444
Figure N.6 Test performed on July 16, 2019, Location 8 (top left = 5 tests, top right = 4 tests, bottom = 3 tests).....	445
Figure N.7 Test performed on July 16, 2019, Location 9 (top left = 5 tests, top right = 4 tests, bottom = 3 tests).....	446
Figure N.8 Test performed on July 16, 2019, Location 10 (top left = 5 tests, top right = 4 tests, bottom = 3 tests).....	447
Figure N.9 Test performed on July 16, 2019, Location 11 (top left = 5 tests, top right = 4 tests, bottom = 3 tests).....	448
Figure N.10 Test performed on July 16, 2019, Location 12 (top left = 5 tests, top right = 4 tests, bottom = 3 tests).....	449
Figure N.11 Test performed on July 16, 2019, Location 13 (top left = 5 tests, top right = 4 tests, bottom = 3 tests).....	450
Figure N.12 Test performed on July 16, 2019, Location 15 (only 2 tests completed).....	450
Figure N.13 Test performed on July 17, 2019, Location 17 (top left = 5 tests, top right = 4 tests, bottom = 3 tests).....	451
Figure N.14 Test performed on July 17, 2019, Location 18 (left = 4 tests, right = 3 tests).....	452
Figure N.15 Test performed on July 17, 2019, Location 19 (top left = 5 tests, top right = 4 tests, bottom = 3 tests).....	452
Figure N.16 Test performed on July 17, 2019, Location 20 (top left = 5 tests,	

top right = 4 tests, bottom = 3 tests).....	453
Figure N.17 Test performed on July 17, 2019, Location 21 (top left = 5 tests, top right = 4 tests, bottom = 3 tests).....	454
Figure N.18 Test performed on July 17, 2019, Location 22 (top left = 5 tests, top right = 4 tests, bottom = 3 tests).....	455
Figure N.19 Test performed on July 18, 2019, Location 23 (top left = 5 tests, top right = 4 tests, bottom = 3 tests).....	456
Figure N.20 Test performed on July 18, 2019, Location 24 (top left = 5 tests, top right = 4 tests, bottom = 3 tests).....	457
Figure N.21 Test performed on July 18, 2019, Location 25 (top left = 5 tests, top right = 4 tests, bottom = 3 tests).....	458
Figure N.22 Test performed on July 18, 2019, Location 28 (top left = 5 tests, top right = 4 tests, bottom = 3 tests).....	459
Figure N.23 Test performed on July 19, 2019, Location 30 (top left = 5 tests, top right = 4 tests, bottom = 3 tests).....	460
Figure N.24 Test performed on July 19, 2019, Location 31 (top left = 5 tests, top right = 4 tests, bottom = 3 tests).....	461
Figure N.25 Test performed on July 19, 2019, Location 32 (top left = 5 tests, top right = 4 tests, bottom = 3 tests).....	462
Figure N.26 Test performed on July 19, 2019, Location 33 (top left = 5 tests, top right = 4 tests, bottom = 3 tests).....	463
Figure N.27 Test performed on July 19, 2019, Location 34 (top left = 5 tests, top right = 4 tests, bottom = 3 tests).....	464

Figure N.28 Test performed on July 19, 2019, Location 35 (top left = 5 tests, top right = 4 tests, bottom = 3 tests).....	465
Figure N.29 Test performed on July 19, 2019, Location 36 (top left = 5 tests, top right = 4 tests, bottom = 3 tests).....	466
Figure N.30 Test performed on July 23, 2019, Location 37 (top left = 5 tests, top right = 4 tests, bottom = 3 tests).....	467
Figure N.31 Test performed on July 23, 2019, Location 38 (top left = 5 tests, top right = 4 tests, bottom = 3 tests).....	468
Figure N.32 Test performed on July 23, 2019, Location 39 (top left = 5 tests, top right = 4 tests, bottom = 3 tests).....	469
Figure N.33 Test performed on July 23, 2019, Location 40 (top left = 5 tests, top right = 4 tests, bottom = 3 tests).....	470
Figure N.34 Test performed on July 23, 2019, Location 41 (only 3 tests completed).....	470
Figure N.35 Test performed on July 23, 2019, Location 42 (top left = 5 tests, top right = 4 tests, bottom = 3 tests).....	471
Figure N.36 Test performed on July 23, 2019, Location 43 (top left = 5 tests, top right = 4 tests, bottom = 3 tests).....	472
Figure N.37 Test performed on July 24, 2019, Location 44 (top left = 5 tests, top right = 4 tests, bottom = 3 tests).....	473
Figure N.38 Test performed on July 24, 2019, Location 45 (top left = 5 tests, top right = 4 tests, bottom = 3 tests).....	474
Figure N.39 Test performed on July 24, 2019, Location 46 (top left = 5 tests, top right = 4 tests, bottom = 3 tests).....	475

Figure N.40 Test performed on July 24, 2019, Location 47 (top left = 5 tests, top right = 4 tests, bottom = 3 tests).....	476
Figure N.41 Test performed on July 24, 2019, Location 48 (top left = 5 tests, top right = 4 tests, bottom = 3 tests).....	477
Figure N.42 Test performed on July 24, 2019, Location 49 (top left = 5 tests, top right = 4 tests, bottom = 3 tests).....	478
Figure N.43 Test performed on July 24, 2019, Location 50 (top left = 5 tests, top right = 4 tests, bottom = 3 tests).....	479
Figure O.1 Subsection layout for Station 423+45 to Station 409+58.....	480
Figure O.2 Subsection layout for Station 409+58 to Station 395+84.....	481
Figure O.3 Subsection layout for Station 395+84 to Station 382+22.....	482
Figure O.4 Subsection layout for Station 382+22 to Station 376+65.....	483

Chapter 1

Introduction

1.1 Background

Soil cement is a mixture of native soils with a measured amount of portland cement and water that hardens after compaction and curing to form a strong, durable, frost-resistant paving material (Halsted et al. 2006). Soil cement can be mixed in place using on site materials or mixed in a central plant using selected materials (Halsted et al. 2006). It is used throughout the industry as a pavement base for highways, roads, streets, parking areas, airports, industrial facilities, and materials handling and storage areas (Halsted et al. 2006). The Alabama Department of Transportation (ALDOT) uses soil cement as a base where crushed stone is unavailable or transportation to site is too costly.

Advantages of using soil-cement bases include (Halsted et al 2006):

- Provides a stronger, stiffer base that reduces deflections due to traffic loads, delaying the onset of surfaces distress such as fatigue cracking and extended pavement life,
- Thickness of the base are less than those required for granular bases carrying the same traffic load because the loads are distributed over a large area,
- A wide variety of in-situ soils can be used, eliminating the need to haul in expensive select granular aggregates,
- The construction operation progresses quickly with little disruption of the traveling public,
- Rutting is reduced due to the resistance of consolidation and movement of the cement stabilized base,

- Forms a moisture-resistant base that keeps water out and maintains higher levels of strength, even when saturated, thus reducing the potential for pumping of subgrade soils,
- Provides a durable, long-lasting base in all types of climates, designed to resist damaged caused by cycles of wetting and drying and freeze-thaw conditions, and
- Continues to gain strength with age.

While there are many advantages to using soil cement, there are some reasons why it may not be used. Research has shown that a soil cement base requires an upper and lower bound on the required strength so that a quality product can be obtained. Strengths that are too low are undesirable because the base will not provide adequate support for traffic, resulting in rutting and large deflections (George 2002). Strengths that are too high are undesirable since excessive cement content may lead to wide shrinkage cracks (George 2002). These wide cracks can cause reflective cracking in the hot mix asphalt surface (George 2002).

Due to strength restrictions placed on soil cement, ALDOT 304 (2014) requires seven-day compressive strengths of cores to be between 250 and 600 psi to receive full payment for the construction of the roadbed. If the compressive strength is less than 250 psi, a price reduction will be imposed following Equation 1.1 (ALDOT 304 2014). If the compressive strength of the core is greater than 600 psi, a price reduction will be imposed following Equation 1.2 (ALDOT 304 2014). For compressive strengths less than 200 psi or greater than 650 psi, the soil-cement layer shall be removed and replaced by the contractor without addition compensation (ALDOT 304 2014). A summary of these ALDOT requirements is presented in Table 1.1.

$$\textit{Price Reduction} = (0.4\% \textit{ per psi}) * (250 \textit{ psi} - f_c) \quad (\textit{Equation 1.1})$$

$$\textit{Price Reduction} = 20\% - (0.4\% \textit{ per psi}) * (650 \textit{ psi} - f_c) \quad (\textit{Equation 1.2})$$

Where:

Price Reduction = reduction in pay (%), and

f_c = 7-day compressive strength of cores (psi).

Table 1.1: ALDOT (2014) compressive strength specifications

Average 7-day Strength (f_c)	Action
$f_c < 200$ psi	Remove and Replace
$200 \text{ psi} \leq f_c < 250$ psi	Price Reduction
$250 \text{ psi} \leq f_c \leq 600$ psi	No Price Reduction
$600 \text{ psi} < f_c \leq 650$ psi	Price Reduction
$f_c > 650$ psi	Remove and Replace

Certain construction practices and high variability of core strength data have led to questions concerning the proper quality control practices and testing protocol. ALDOT 304 (2014) states the current practice for the state that consists of recovering cores on the sixth day and the testing then on the seventh to determine the compressive strength. Results from past ALDOT projects have shown high variability in core strength values and has led to an increase in concern of the in-place strength and the use of cores as a pay item. Figure 1.1 shows 7-day core strengths from ALDOT project STPAA-0052 (504) in Houston and Geneva Counties in Alabama. Cores taken just a few feet apart show strengths that differ by over 200 percent. Strength limits are shown on the graph showing the pay scale that ALDOT uses.

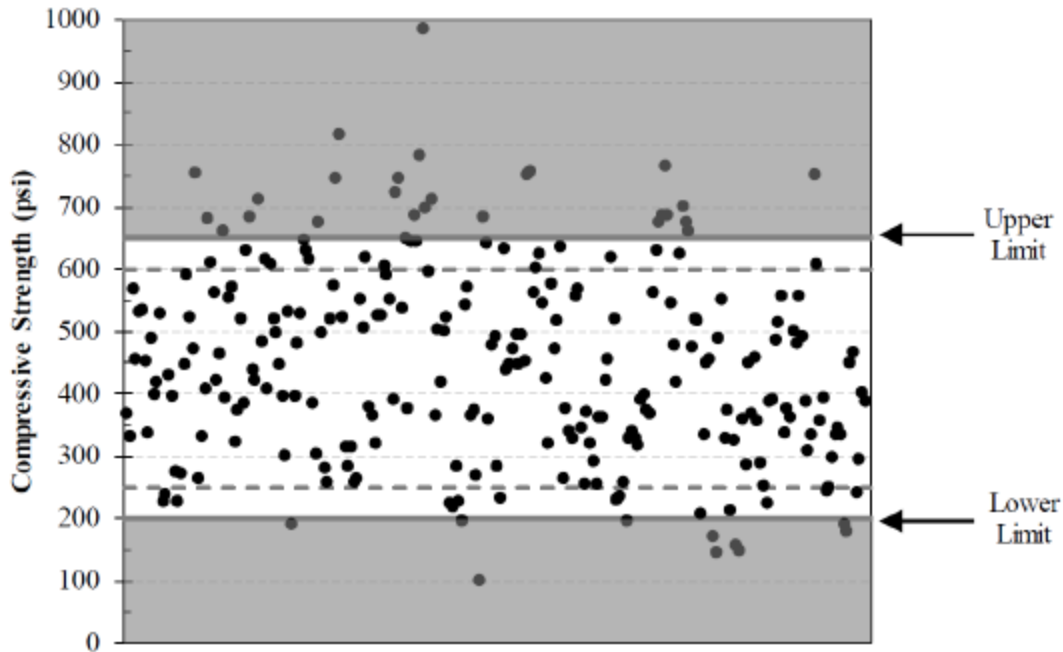


Figure 1.1: Compressive strengths of cores from ALDOT project STPAA-0052 (504)

(McLaughlin 2017)

Due to the high variability of core strengths in past ALDOT projects, other techniques have been researched and developed to create a reliable method to assess the strength of soil cement. The latest method evaluated on an Alabama soil cement project was the one developed by Nemiroff (2016) and McLaughlin (2017). Nemiroff (2016) determined a relationship between using molded cylinders made in accordance with ASTM D1632 (2017), *Standard Practice for Making and Curing Soil Cement Compressive and Flexure Test Specimens in the Laboratory*, and the dynamic cone penetrometer results of penetration depth over the amount of blows used using ASTM D6951, *Standard Test Method for Use of the Dynamic Cone Penetrometer in Shallow Pavement Applications*. Molded cylinder method used by Nemiroff (2016) will be referred to herein as the steel-mold method. McLaughlin (2017) modified the plastic-mold method introduced by Sullivan et al. (2014) with the dynamic cone penetrometer in the field to determine how well

the relationship Nemiroff (2016) determined worked in the field when compared to strengths determined by core testing.

The dynamic cone penetrometer has been evaluated by McElvaney and Djatnika (1991), Enayatpour et al. (2006), Patel and Patel (2012), and Nemiroff (2016), to name a few, in order to determine compressive strength of soil cement; however, few have evaluated it at the high strengths that ALDOT uses for soil cement. The dynamic cone penetrometer has also been correlated to other engineering properties such as soil classification (Huntley 1990) and California Bearing Ratio. As mentioned before, McLaughlin (2017) sampled material on-site and used the steel-mold and plastic-mold cylinder methods to prepare molded cylinders that were then tested in compression and compared to the dynamic cone penetrometer and core strength results at seven days.

1.2 Research Objectives

The main objective of this research was to further investigate and finalize the method to assess soil cement base that was developed by McLaughlin (2017). To do this, the following objectives were set:

- Evaluate the suitability of using plastic-mold cylindrical samples based on Sullivan et al. (2014) and McLaughlin (2017) to assess the strength of soil cement,
- Establish the correlation between the 7-day unconfined compressive strength and dynamic cone penetrometer results of 150 to 800 psi soil cement,
- Evaluate different gradations of soils to assess if there is a difference between different AASHTO classified soils in the strength of soil cement,

- Continue the evaluation of McLaughlin (2017) to determine the suitability of using the plastic-mold method in the field as the quality assurance test method to assess the strength of soil cement,
- Continue the evaluation of McLaughlin (2017) to determine the suitability of using the dynamic cone penetrometer in the field to assess the in-place strength of soil cement,
- Recommend a testing protocol that the Alabama Department of Transportation (ALDOT) should implement to assess the strength of soil cement to replace coring.

1.3 Research Approach

At the beginning of this research project, there was no soil cement base being constructed in Alabama. Further research in the laboratory was done by collecting different soils with different AASHTO classifications and experimenting with different cement contents. The PM Method developed by Sullivan et al. (2014) with modifications used by McLaughlin (2017) was used to create molded soil cement cylinders. DCP specimens were created using the method from Nemiroff (2016) and tested using ASTM D6957 (2009). Data collected to depths of 25, 50, 75, 100, and 175 millimeters was analyzed, and the best fit correlation established between the DCP results and cylinder compressive strength.

Next, field work was started on an ALDOT soil cement base project that started on U.S. Highway 84 bypass East of Elba, Alabama. One method evaluated was the PM Method developed by Sullivan et al. (2014) with same modifications proposed by McLaughlin (2017). The second method used was the DCP as per ASTM D6957 (2009) with the DCP to strength correlation as established by the earlier laboratory work. Both these methods were conducted in the field on U.S. Highway 84 and these results were compared to the seven-day core results obtained from ALDOT for each section.

After these results were available, the suitability of the DCP for determining the in-place strength of soil cement base was evaluated. DCP tests were conducted over the whole eight-inch deep layer at certain locations with the number of DCP tests at a location being evaluated as well as the most effective testing depth evaluated.

Based on the findings of this research, an updated strength testing method was developed for ALDOT using the PM method to produce molded cylinder on-site for compressive strength testing for quality assurance. If the plastic-mold cylinder compressive strength is less than or greater than the ALDOT requirement for on soil cement base outlined previously, then the DCP shall be used to determine the in-place strength of soil cement base.

1.4 Thesis Outline

Chapter 2 of this thesis presents an overview of previous research and literature that pertains to all aspects of this research project. This begins with the discussion of the materials that are used to produce soil cement. Next, the importance of engineering properties such as density, compressive strength, cracking, and durability are presented and discussed. Then, an overview of soil cement base construction is presented with mixing, compaction, curing, and quality control methods being discussed. The last section covers the different ways to evaluate strength of soil cement that are used in different states and those that were used during this research such as coring, molded cylinders, and the dynamic cone penetrometer.

Chapter 3 presents the experimental plan for both the laboratory and field testing phases. The laboratory testing phase is presented first where it evaluates the laboratory mixtures and introduces the soil classification study. Detailed descriptions of the equipment and testing procedures are then outlined and discussed. The field testing phase is then presented beginning with where the location of the field project. The purpose of doing the field phase is then discussed.

A detailed description of the testing procedures that were used for this phase are then presented. The last section of this chapter describes how the testing was performed through the different apparatuses and methods.

The results from the laboratory testing phase are presented in Chapter 4. Results of the soil classification are discussed. Then a correlation between the dynamic cone penetrometer results and plastic-mold cylinder strength is presented along with how it compares to previous correlations determined by other researchers.

The results from the field testing phase are presented in Chapter 5. Results obtained from the dynamic cone penetrometer analysis are discussed. Then, results of the plastic-mold method, dynamic cone penetrometer, cores, and in-place densities are presented. The last section presents a comparison of the results obtained from all the test methods by evaluating the variability and the results by each testing location.

A summary of all the research performed is presented in Chapter 6. All conclusions and recommendations determined from this research are presented in Chapter 6 as well.

Chapter 6 is followed by Appendices A through O. Appendix A contains Proctor density curves and gradations for all mixtures used in making soil cement in the laboratory. Appendix B contains the results from the initial curing method study. Appendix C contains the results from the soil classification study of the three different soils. Appendices D through H contain all of the DCP penetration results from the laboratory experiments, with the penetration is plotted against the blow count. Appendix I contains a summary of all strengths determined at each of the locations tested in the field testing phase. Appendices J through N contain all of the DCP penetration results collected at each of the locations in the field testing phase. Finally, Appendix O summarizes the location and subsection layout used over the entirety of the field testing phase.

Chapter 2

Literature Review

2.1 Introduction

First in this chapter, a literature review of the materials used to produce soil cement base is presented. Next, soil cement properties such as densities, compressive strengths, and its durability are discussed. An overview of the process and quality control of soil cement base construction are then explained. Lastly, the evaluation of strength of soil cement base using different test methods such as dynamic cone penetrometer, steel molded cylinders, plastic-mold method, and coring are discussed along with how different Departments of Transportation evaluate soil cement projects.

2.2 Materials

2.2.1 Soil

Soil is defined as the relatively loose agglomerate of minerals, organic materials and sediments found above the bedrock (Holtz and Kovacs 1981). ACI 230 (2009) states that almost all soil types can be used in the construction of soil cement except for organic soils, highly plastic clays, and poorly reacting sandy soils. However, granular soils are preferred because they pulverize and mix easier than fine grained soils. According to ACI 230 (2009), the most commonly used soils are silty sand, processed crushed or uncrushed sand and gravel, and crushed stone.

Poorly reacting sandy soils are not used in soil cement because the cement can react and have an adverse effect on the final soil cement product. A study conducted by Robbins and Mueller (1960) found that a sandy soil with an organic content greater than 2 percent or having a pH lower than 5.3 will probably not react normally with cement. Robbins and Mueller (1960) also showed

that acidic organic material often had adverse effects of strength development in soil cement mixtures.

2.2.1.1 Particle Size

AASHTO terminology was used to clarify the boundary between coarse- and fine-grained soils for this research. Coarse-grained soils are soils with more than 35 percent retained on or above the No. 200 sieve and fine-grained soils are soils with 35 percent or more passing the No. 200 sieve (McCarthy 2007).

The most preferred choice of grain size for use in soil cement are coarse-grained soils because of their ability to pulverize and mix more easily (PCA 1995; ACI 230 2009). All types and sizes of soil can be hardened with portland cement because its stability is formed through the hydration of the cement and not by the cohesion and internal structure of the material (PCA 1995). ACI 230 (2009) recommends well graded sandy and gravelly materials with about 10 to 35 percent of non-plastic fines as they have the most favorable characteristics and generally require the least amount of cement. Silty and clayey soils with high clay contents are harder to pulverize and need higher cement content to harden it adequately so these soils are not very economic (ACI 230 2009).

Halsted et al. (2006) states that an increase in the quantity of coarse material will reduce the cement requirement because the finer particles requiring cement to bind them together are replaced by coarser particles. Figure 2.1 shows a band of gradation sizes that would use the least amount of cement that would produce a quality base that meets density and strength requirements. Gradations outside of this range will require more cement due to the material being too fine or too coarse as the particles would not interlock with one another on their own to a sufficient strength.

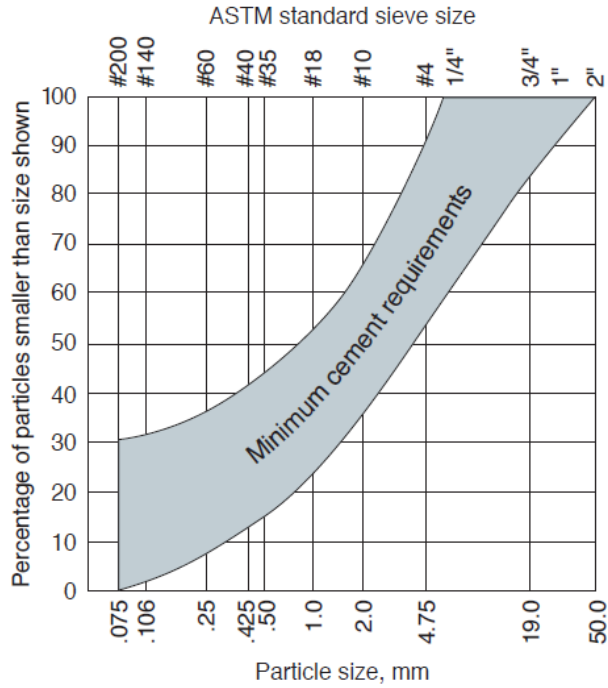


Figure 2.1: Aggregate gradation band for minimum cement requirements (Halsted et al. 2006)

2.2.2 Portland Cement

The cement that is typically used for soil cement construction are Type I or Type II portland cement that meet the requirements of ASTM C150 (2016). Cement contents may range from as low as 2 percent to as high as 16 percent by dry weight of the soil (ACI 230 2009). Table 2.1, adapted from ACI 230 (2009), shows a variety of AASHTO soils and ASTM classified soils with their typical range of cement required. This table shows estimated cement contents that would be required for each of the different soil types. Table 2.1 should not be taken as a requirement as the values could be lower or higher as the required amount of cement varies depending upon the desired properties and the soil type (ACI 230 2009).

Table 2.1: Typical cement requirements for various soil types (ACI 230 2009)

AASHTO Soil Classification	ASTM Soil Classification	Typical Cement Range, * percent by weight	Typical Cement for moisture-density test (ASTM D558), percent by weight	Typical Cement for durability tests (ASTM D559 and D560, percent by weight)
A-1-a	GW, GP, GM, SW, SP, SM	3 to 5	5	3-5-7
A-1-b	GM, GP, SM, SP	5 to 8	6	4-6-8
A-2	GM, GC, SM, SC	5 to 9	7	5-7-9
A-3	SP	7 to 11	9	7-9-11
A-4	CL, ML	7 to 12	10	8-10-12
A-5	ML, MH, CH	8 to 13	10	8-10-12
A-6	CL, CH	9 to 15	12	10-12-14
A-7	MH, CH	10 to 16	13	11-13-15
*Does not include organic or poorly reacting soils. Also, additional cement may be required for severe exposure conditions such as slope protection				

Other cementitious materials have also been proven to work in soil cement applications. Slag cement should meet the requirements of ASTM C989, and the allowed Grades 80, 100, and 120 specified (ACI 230 2009). If slag cement is blended with portland cement then the combinations should meet the requirements of ASTM C595 or C1157 (ACI 230 2009). Class F fly ashes have been the predominant fly ash used in soil cement as a filler or as a cementitious component (ACI 230 2009). Fly ash should conform to ASTM C618 (ACI 230 2009). Lime has also been used for highly plastic clay soils to reduce plasticity and make the soil more friable and susceptible to pulverization before mixing with cement (ACI 230 2009).

2.2.3 Water

Water is necessary in soil cement to help obtain maximum compaction and for hydration of the portland cement (ACI 230 2009). Moisture contents of soil cement are usually in the range of 5 to 13 percent by weight of oven-dry soil cement (ACI 230 2009). ACI 230 (2009) states that

potable water or other relatively clean water that are free from harmful amounts of alkalis, acids, or organic matter may be used. ACI 230 (2009) also states that seawater has been used satisfactorily as the chlorides in the seawater may increase early age strengths. Typically, water from the city is acceptable and used in soil cement applications without being tested (ALDOT 2012). Table 2.2 is a table adapted from ALDOT (2012) Section 807 that requires that water used shall be fresh, free from oil, and shall contain impurities in excess of the limits given.

Table 2.2: Maximum limit for impurities in water used for soil cement applications (adapted from ALDOT 2012)

Item	Limit
Acidity or alkalinity in terms of calcium carbonate	500 mg/L AASHTO T26
Total organic solids	500 mg/L AASHTO T26
Total inorganic solids	500 mg/L AASHTO T26
Chloride ion concentration	250 mg/L AASHTO T26
Sulfate ion concentration	250 mg/L AASHTO T26
pH	6.0 to 8.0 ASTM D1293

2.3 Soil Cement Properties

2.3.1 Density and Moisture Content

AASHTO T134 (2013) and ASTM D558 (2019) outline the Proctor test that is used to determine the optimum moisture content and the maximum dry density. Figure 2.2 shows a typical moisture-density curve developed from a Proctor test. ACI 230 (2009) states that the density of soil should be defined in terms of dry density.

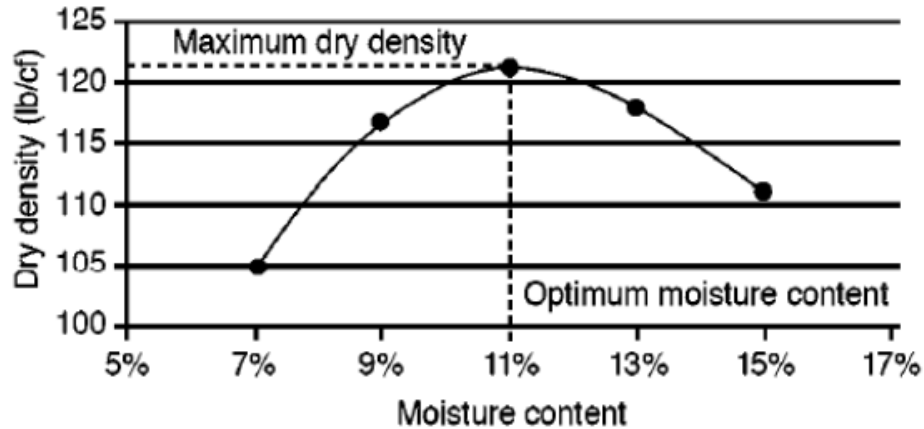


Figure 2.2: Maximum dry density and optimum moisture content (Halsted et al. 2006)

Adding cement to a soil usually alters the optimum moisture content and maximum dry density; however, it is difficult to determine whether these properties will increase or decrease (ACI 230 2009). The flocculating action of cement tends to increase the optimum moisture content and decrease the maximum dry density (ACI 230 2009). However, the high specific gravity of cement compared to the soils tend to produce a higher density (ACI 230 2009).

Given a cement content, the higher the density of the specimen, the higher the compressive strength of the cohesionless soil cement mixture (Shen and Mitchell 1966). West (1959) showed that letting a soil cement mixture sit for more than 2 hours before compaction would result in a significant decrease in both density and compressive strength. Felt (1955) also found similar findings to West (1959); however, the effect could be minimized if the mixture was mixed several times over the delay between initial mixing and the compaction if the moisture content at the time of compaction was at or slightly above optimum moisture.

Figure 2.3 shows the relationship between dry density and moisture content when cement is added into soil at different percentages. The figure from Yoon and Abu-Farsakh (2008) shows that the dry density increases with an increase in the cement content while the optimum moisture

content remains fairly similar to other cement contents, but the optimum moisture content decreases slightly when the test is performed only on soil.

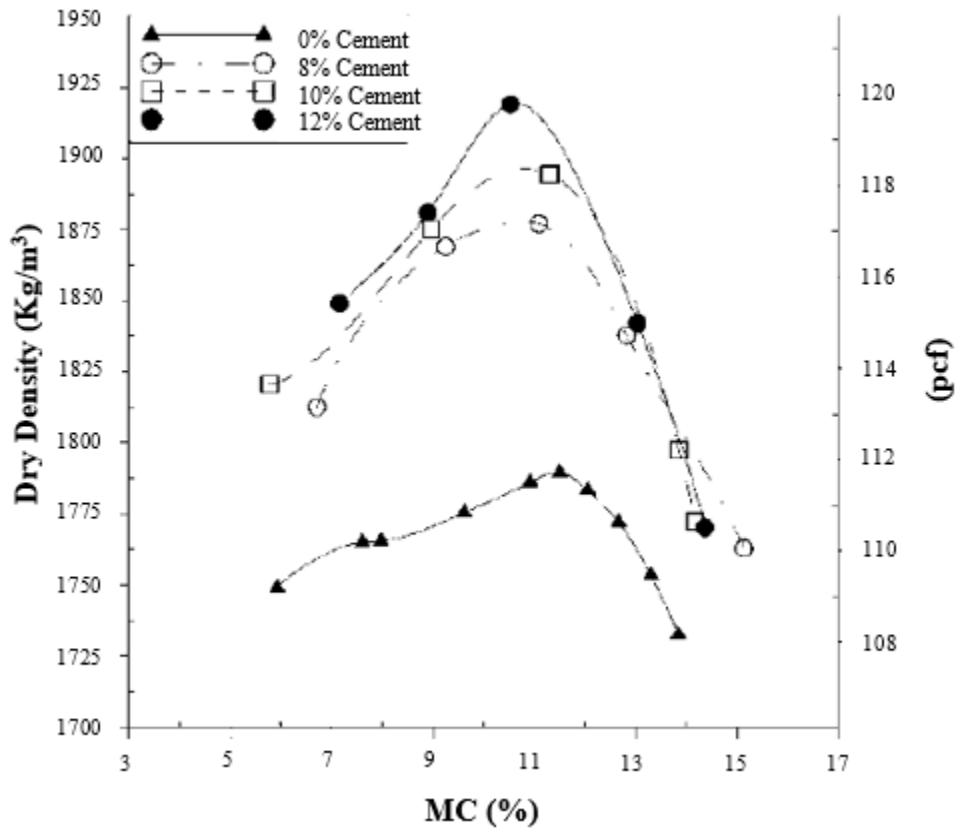


Figure 2.3: Relationship between dry density and moisture content when cement is added
(adapted from Yoon and Abu-Farsakh 2008)

At optimum moisture content, water serves as a lubricating agent among soil particles to reduce the friction resistance between them, thus improving the compaction quality to achieve the maximum dry density (Jin et al. 2017). Jin et al. (2017) determined that water reducers could be used in cement treated soils. These water-reducing admixtures, while decreasing the optimum moisture content, would increase the maximum dry density and the unconfined compressive strength, reduce weight loss in wet-dry cycles and reduce the permeability (Jin et al. 2017). Figure 2.4 from Jin et al. (2017) shows how adding cement and water reducers would affect the moist-

density curve with “Shelby” being the soil name, “C” being portland cement, and “WR” being a water-reducing admixture.

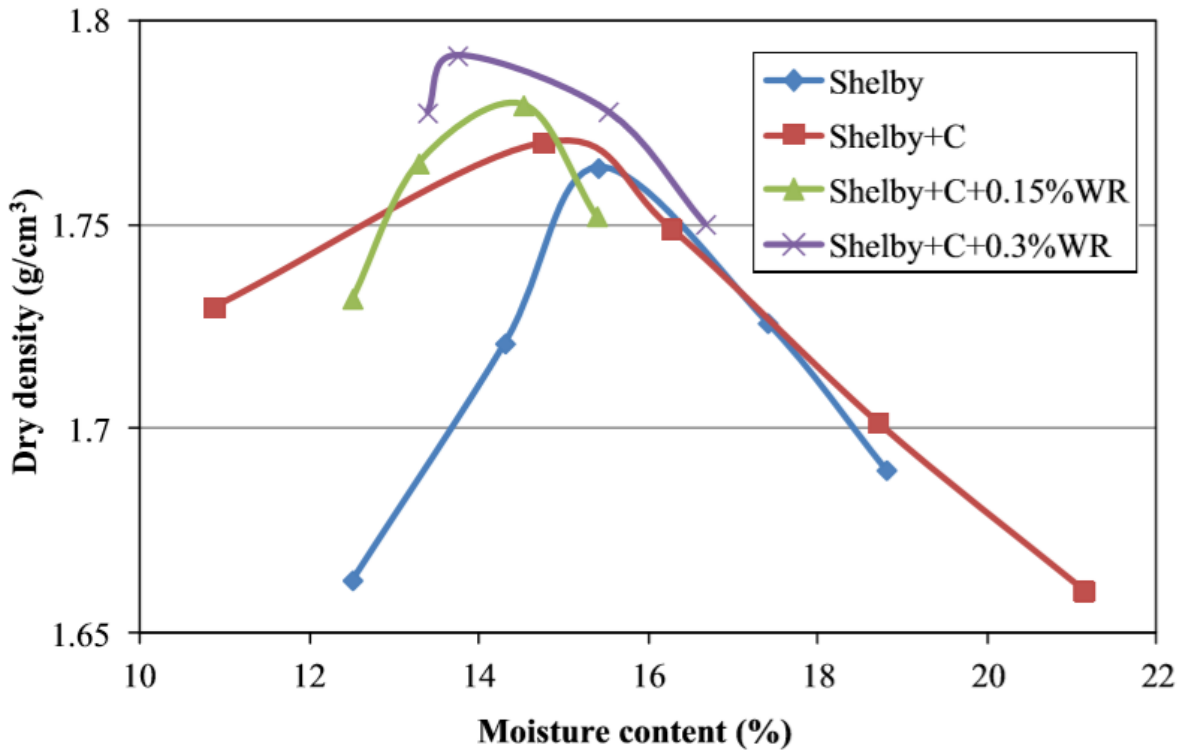


Figure 2.4: Effect of a water-reducing admixture on moist-density curve (Jin et al. 2017)

2.3.2 Compressive Strength

The unconfined compressive strength, f_c , is the most widely referenced property of soil cement (ACI 230 2009). The unconfined compressive strength for soil cement mixtures is measured using ASTM D1633 (2007). This strength indicates the degree of reaction of the soil cement-water mixture and the rate of hardening (ACI 230 2009). Compressive strength can also be used as a criterion to determine how much cement needs to be added to the mixture (ACI 230 2009). ACI 230 (2009) has examples of 7-day and 28-day unconfined compressive strengths for soaked soil cement specimens of different soil types and are shown in Table 2.3. The soils listed

in Table 2.3 represent a majority of soils used in the United States for soil cement construction (ACI 230 2009).

Table 2.3: Ranges of unconfined compressive strength of soil cement (ACI 230 2009)

Soil type	Soaked compressive strength, * psi	
	7-day	28-day
Sandy and gravelly soils: AASHTO Groups A-1, A-2, A-3 Unified Groups GW, GC, GP, GM, SW, SC, SP, SM	300 to 600	400 to 1000
Silty soils: AASHTO Groups A-4 and A-5 Unified Groups ML and CL	250 to 500	300 to 900
Clayey soils: AASHTO Groups A-6 and A-7 Unified Groups MH and CH	200 to 400	250 to 600

* Specimens moist-cured 7 or 28 days, then soaked in water before strength testing.
Note: 1 psi = 0.0069 MPa.

Figure 2.5 from the Federal Highway Administration (FHWA) (1979) shows that with fine-grained soils, the unconfined compressive strength is less than that of coarse-grained soils, which is also shown in Table 2.3. Figure 2.5 also shows the effect that curing time has on the strength of a soil cement mixture. A coarse-grained soil shows a greater increase in strength over a longer curing time but both fine-grained and coarse-grained soils follow the trend of having a gain in strength.

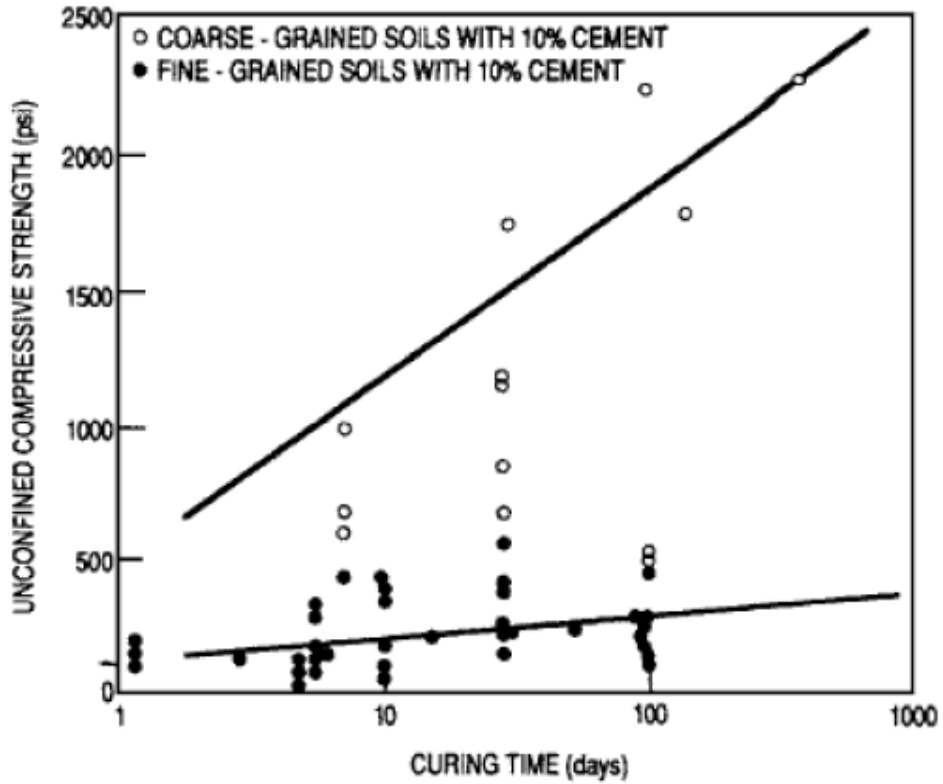


Figure 2.5: Effects of curing time and different soils on unconfined compressive strength (FHWA 1979)

Generally, strength increases with the increase in dry density (Yoon and Abu-Farsakh 2008). The highest strength does not occur at the highest dry density due to the factor that the water-to-cement ratio is one of the major controlling factors that affects strength (Yoon and Abu-Farsakh 2008). Figure 2.6 shows the relationship between dry density and unconfined compressive strength. Figure 2.7 shows the relationship between the water-to-cement ratio by weight and the unconfined compressive strength.

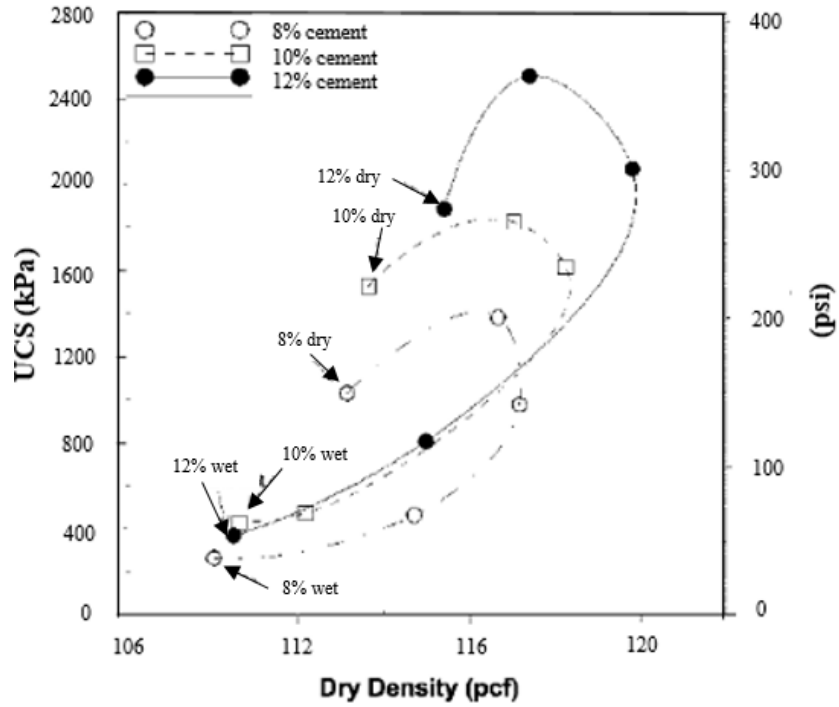


Figure 2.6: Relationship between dry density and unconfined compressive strength
(adapted from Yoon and Abu-Farsakh 2008)

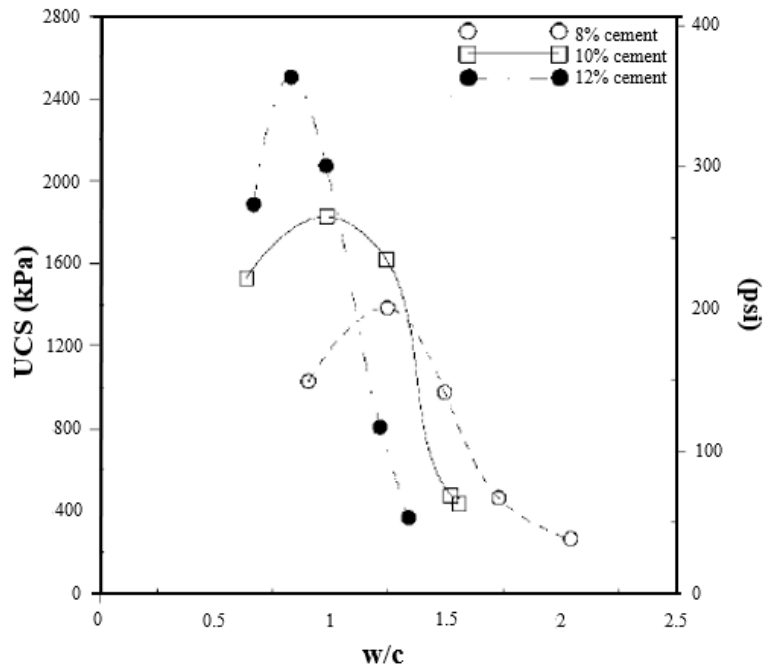


Figure 2.7: Relationship between water-to-cement ratio and unconfined compressive strength
(adapted from Yoon and Abu-Farsakh 2008)

2.3.3 Shrinkage and Reflective Cracking

Shrinkage cracks may develop in the soil cement base over time and result in reflective cracking in the upper asphalt surface layer. Soon after construction of a soil cement base, shrinkage will develop over time (Kuhlman 1994). The shrinkage and subsequent cracking are dependent upon the cement content, soil type, water content, degree of compaction, and allowed curing time (ACI 230 2009). Each soil type used in a soil cement mixture produces a different crack pattern (ACI 230 2009). Soil cement made with clay tends to have higher total shrinkage, but crack widths are smaller and individual cracks are more closely spaced, about 2 to 10 feet apart (ACI 230 2009). ACI 230 (2009) states that soil cement made with more granular soils produce less shrinkage, but larger cracks spaced at greater intervals, about 10 to 20 feet apart. Figure 2.8 shows shrinkage cracks in the soil cement along US Highway 84 project in Elba, Alabama.



Figure 2.8: Shrinkage cracks in soil cement (McLaughlin 2017)

Kuhlman (1994) stated that cracking in the soil cement base can cause reflective cracks in the bituminous riding surface that may be about 0.03 to 0.05 inches in width. Kuhlman (1994) also

stated that the least cracking will occur in those soil cements having the lowest moisture content at the time of compaction while compacted to a high density. Therefore, clays and silts have the highest moisture requirement to achieve maximum density and will have the greatest tendency for dry shrinkage as compared to more granular soils. George (2002) found that soil cement cracking is highly correlated to the following:

1. Volume change resulting from drying, temperature change, or both,
2. Tensile strength of the stabilized material,
3. Stiffness and creep of stabilized materials, and
4. Subgrade restraint.

These soil cement base cracks sometimes become reflective cracks in the asphalt pavements. Alligator cracking in the wheel paths would be an indication of inadequate design and structural failure rather than just a few expansive or shrinkage cracks spread throughout a typical two-lane roadway (Kuhlman 1994). Kuhlman (1994) and George (2002) indicate that good construction and quality control procedures such as proper moisture, density, mixing, and curing, are essential to minimize cracking. Desirable cracking occurs when cracks are closely spaced and narrow so that load transfer continues across the crack and that little water can seep into the opening (ACI 230 2009). ACI 230 (2009) states that large cracks will cause raveling, loss of subgrade material, pavement faulting, surface deterioration, and poor ride quality.

Expansive forces can also cause cracking. Wet-dry and freeze-thaw cycles cause expansion and shrinking throughout the soil cement base. As the soil cement base freezes or gains water, the soil cement base will expand. When the thawing or drying of the soil cement base happens, the soil cement will then begin to shrink and lead to shrinkage cracks. These cracks can lead to reflective cracking in the asphalt pavements above the soil cement base.

Methods of controlling cracking to achieve the desirable cracking include proportioning to minimize shrinkage, following quality construction procedures, and controlling the cracking through the bituminous surface (ACI 230 2009). Allowing the soil cement to dry too quickly will ensure that shrinkage occurs early where tensile stresses will lead to more cracking (Kuhlman 1994). ACI 230 (2009) has more specific techniques that would help to prevent the shrinkage such as compacting at a slightly less than optimum moisture content, limiting the fines content, using interlayers, using a thicker base slab with reduced cement content, and quick placement of asphalt pavement on the soil cement base. Another technique would be to delay surfacing and prolong the curing for 14 to 28 days to allow initial cracks to form which will allow for the asphalt to bridge the cracks and reduce their reflectivity and size (ACI 230 2009).

Scullion (2002) recommends a microcracking process where a vibratory roller passes over the soil cement base 24 to 72 hours after being laid in order to create microcracks in the base. This substantially reduced the amount of surface cracking in the asphalt layer as well as the base, while also maintaining a very high stiffness (Scullion 2002).

2.3.4 Durability

For a hardened soil cement mixture to have a satisfactory service life, adequate strength and durability are essential. ASTM D559 (2015), *Standard Test Methods for Wetting and Drying Compacted Soil-Cement Mixtures*, and ASTM D560 (2016), *Standard Test Methods for Freezing and Thawing Compacted Soil-Cement Mixtures*, are standard test methods that are conducted to determine the amount of cement needed to hold the mass together permanently and to maintain stability under the shrinkage and expansive forces that develop after placement (ACI 230 2009). The Portland Cement Association (PCA) (1971) criteria for wet-dry and freeze-thaw durability are shown in Table 2.4. Cement contents sufficient to prevent weight losses greater than the values

indicated after 12 cycles of wetting, drying, thawing, and freezing are considered adequate to produce a durable soil cement.

Table 2.4: PCA criteria for wet-dry and freeze-thaw soil cement durability tests (PCA 1971)

AASHTO Soil Group	Unified Soil Group	Maximum Allowable Weight Loss, %
A-1-a	GW, GP, GM, SW, SP, SM	14
A-1-b	GM, GP, SM, SP	14
A-2	GM, GC, SM, SC	14*
A-3	SP	14
A-4	CL, ML	10
A-5	ML, MH, CH	10
A-6	CL, CH	7
A-7	OH, MH, CH	7

*Ten percent is maximum allowable weight loss for A-2-6 and A-2-7 soils.

Additional criteria:

1. Maximum volume changes during durability test should be less than 2% of initial volume.
2. Maximum water content during test should be less than quantity required to saturate sample at time of molding.
3. Compressive strength should increase with age of specimen.
4. Cement content determined as adequate for pavement, using the aforementioned PCA criteria, will be adequate for soil cement slope protection that is 5 ft (1.5 m) or more below the minimum water elevation. For soil cement that is higher than that elevation, cement content should be increased two percentage points.

Some agencies use the results of the standard test methods, ASTM D559 (2015) and ASTM D560 (2016), to determine a compressive strength to determine the minimum cement content. Figure 2.9 shows the relationship between the compressive strength at 7 days and durability of soil cement based on PCA durability criteria. The curves show that a compressive strength of 800 psi would be adequate for all soils, but this strength would be too conservative and too costly for most soil cement designs (ACI 230 2009). When a specific gradation or soil type is used, some agencies have determined a compressive strength requirement for that particular type of material and is generally based off of the wet-dry and freeze-thaw testing methods.

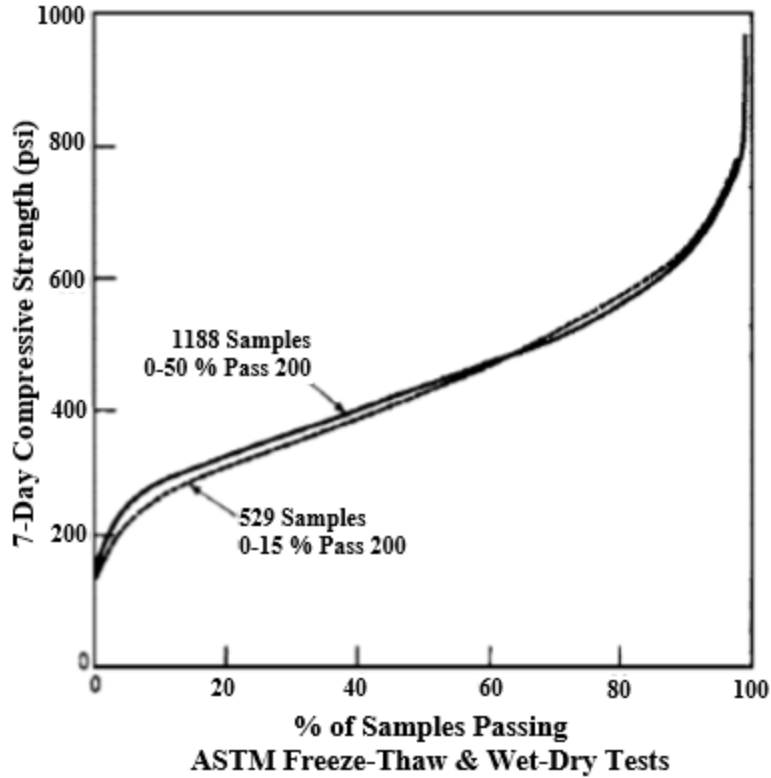


Figure 2.9: Relationship between compressive strength and the durability of soil cement
(PCA 1971)

2.4 Overview of Soil Cement Base Construction

2.4.1 Soil Cement Base Construction

The objective when constructing soil cement is to obtain a thoroughly mixed, adequately compacted, and cured material with sufficient strength (ACI 230 2009). ACI 230 (2009) states that soil cement should not be mixed or placed when the soil or subgrade is frozen or when the temperature is below 45 degrees Fahrenheit. Common practice is to construct soil cement when the air temperature is at least 40 degrees Fahrenheit and rising (ACI 230 2009). Soil cement shall be protected from freezing for at least 7 days if freezing temperatures are expected to be reached (ACI 230 2009). If there is heavy rainfall during construction, it can be detrimental, especially if the optimum moisture had already been added to the mixture or if the cement is still being spread

(ACI 230 2009). Rain will not normally harm the soil cement mixture if it has been compacted (ACI 230 2009). The methods of mixed-in-place, central mixing plant, compaction, and curing will be discussed in the remainder of this section.

2.4.1.1 Mixed-In-Place Method

Almost all types of soil, from granular to fine-grained, can be pulverized and mixed to produce soil cement in the field (ACI 230 2009). These soils can consist of material already in-place or obtained from a borrow pit. Mixing operations can be performed with transverse single-shaft-type mixers (ACI 230 2009). Figure 2.10 shows a transverse single-shaft mixer that was used on a soil cement project on US Highway 84 near New Brockton, AL.



Figure 2.10: Transverse single-shaft mixer

During construction, some soils may require multiple passes of the mixer to achieve adequate pulverization and uniformity (ACI 230 2009). As the gradation of the material may change, material taken from a borrow pit should be monitored for purposes of quality control for cement requirements, optimum moisture content, and density (ACI 230 2009).

The Mixed-In-Place method begins with preparation of the soil. All soft or wet subgrade areas are located and corrected. All deleterious materials such as stumps, roots, organic soils, and aggregates greater than 3 inches should be removed (ACI 230 2009). The soil is then shaped to

approximate final lines and grades before mixing using a single-shaft mixer (ACI 230 2009). For coarse-grained soils, mixing at less than optimum moisture content minimizes the chances for cement balls to form, while for fine-grained soils, keeping the moisture content near optimum may be necessary for effective for pulverization (ACI 230 2009).

After the soil is prepared, the cement is generally distributed over the soil in bulk using a mechanical spreader or in a slurry form by using a distributor truck equipped with an agitation system (Halsted 2008). The use of a mechanical spreader to spread cement on a project on US Highway 84 near New Brockton, AL is shown in Figure 2.11. If there is a concern of major dusting of the cement into the air, cement can be applied as a slurry (ACI 230 2009). Dusting of the cement can be seen in Figure 2.12 where a slurry was not used.



Figure 2.11: Cement being spread by mechanical spreader



Figure 2.12: Cement dusting into the air

The primary objective of the cement-spreading operation is to achieve uniform distribution of the cement in the proper proportions across the width of the roadway (ACI 230 2009). To obtain a uniform spread, the mechanical spreader should be operated at a uniform speed with a constant level of cement in the hopper (ACI 230 2009). Cement is moved pneumatically from the truck through an air-separator cyclone, which removes the air pressure, before the cement falls into the hopper of the spreader (ACI 230 2009). For slurry applications, a 50/50 by weight of water and cement is mixed in a slurry pump thoroughly that is then pumped into a liquid tanker truck (ACI 230 2009). This truck is equipped with internal agitation devices or recirculation pumps to keep the cement in suspension (ACI 230 2009). The amount of cement required is specified as a percentage by weight of oven-dry soil or in pounds of cement per cubic foot of compacted soil (ACI 230 2009).

Once all the cement has been evenly placed on the soil, a single-shaft mixer like the one shown in Figure 2.10 is used to mix the cement in with the soil. Agricultural-type equipment is not recommended due to the relatively poor mixing uniformity (ACI 230 2009). Soils with higher fines

content and plasticity tend to create more difficulties when pulverizing and mixing. Once the cement has been mixed into the soil, a water truck is used to apply the specified amount of water onto the surface of the mixture to obtain the desired moisture content. A water truck spraying water onto the surface can be seen in Figure 2.13. The single shaft mixer then passes over all of the material again to mix the water into the soil cement. In-place mixing efficiency, as measured by the strength of the soil cement, is usually less than that found in the laboratory and can be compensated by adding one or two percentage points to the cement content that was determined in the laboratory testing (ACI 230 2009).



Figure 2.13: Water truck applying water to soil cement

2.4.1.2 Central-Plant-Mixed Method

Central mixing plants tend to be used for projects that need borrow materials. Granular borrow materials are generally used because of their ease in handling and mixing while clayey soils should be avoided because they are difficult to pulverize (ACI 230 2009). The two basic type of central plant mixers are the rotary-drum mixers and the pug mill mixers. Typically, pug mill mixers consist of two types: continuous flow and batch. The most common one used is the

continuous-flow pug mill mixer with production rates varying between 200 and 800 tons per hour (ACI 230 2009).

Just like any soil cement mixing operation, the objective of the central plant mixers is to produce a thorough and intimate mixture of the soil, cement, and water in the correct proportions (ACI 230 2009). A typical continuous-flow pug mill plant can be seen in Figure 2.14. This plant typically consists of at least one soil bin, a cement silo with surge hopper, a conveyor belt to deliver the soil and cement to the mixing chamber, a mixing chamber, a water-storage tank for adding water during mixing, and a holding or gob hopper to temporarily store the mixed soil cement before loading (ACI 230 2009). Most plants will also screen the soil with 1 to 1-1/2 inch mesh to remove larger materials or organics that may not have been removed from the borrow material prior. The mixing chamber consists of two parallel shafts equipped with paddles along each shaft that rotate in opposite directions (ACI 230 2009). Thorough mixing is very important and is specified to about 15 to 30 seconds depending on the efficiency of the mixer (ACI 230 2009).

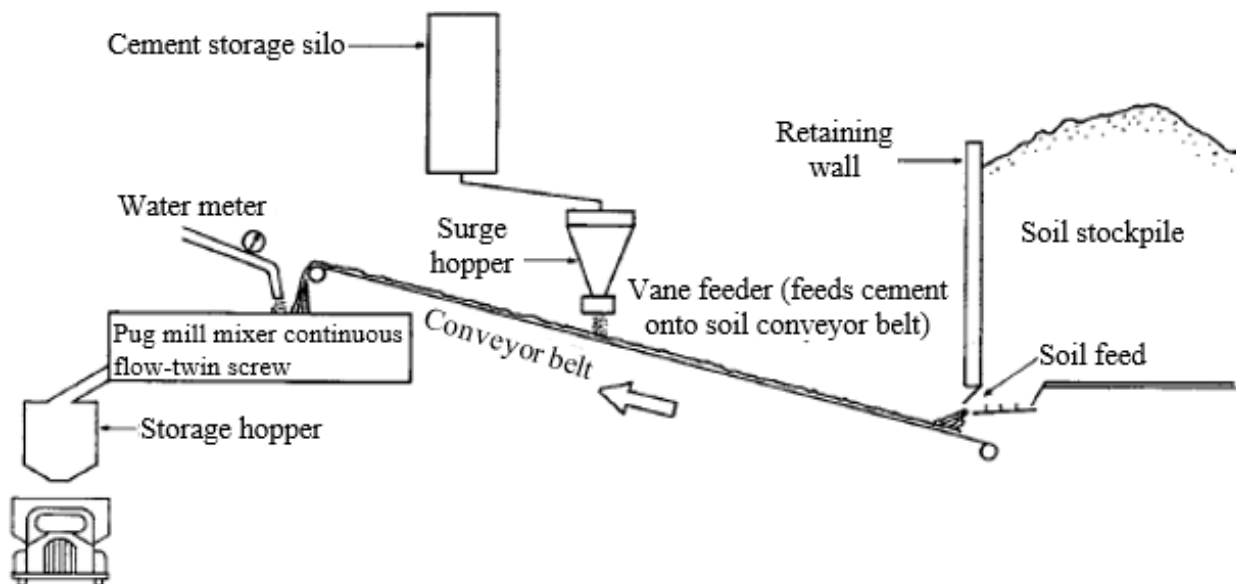


Figure 2.14: A typical continuous-flow pug mill plant (adapted from ACI 230 2009)

Once the soil cement has finished mixing and is being held in the storage hopper, it must be transported to the site and start being compacted within 60 minutes (ACI 230 2009). To reduce evaporation losses during hot, windy conditions and to protect from sudden showers, rear and bottom dump trucks are equipped with protective covers (ACI 230 2009). Haul time in these trucks is usually limited to 30 minutes as that would leave 30 minutes to place and spread the soil cement before starting compaction (ACI 230 2009).

Before placing the mixed soil cement, all adjacent surfaces and the subgrade should be moistened (ACI 230 2009). The most common way to spread the soil cement is by using a motor grader or spreader box attached to a dozer or by using asphalt-type pavers (ACI 230 2009). Figure 2.15 shows a motor grader spreading soil cement. Asphalt-type pavers sometimes place one or more tamping bars on the back to initiate the compaction process (ACI 230 2009). Soil cement is typically placed in a layer about 10 to 30 percent thicker than the desired final compacted thickness (ACI 230 2009). This percentage is determined by trial-and-error methods or by contractor experience. Compaction, finishing, and curing follow the same procedures of that of the mixed in-place method.



Figure 2.15: Motor grader spreading soil cement

2.4.1.3 Compaction of Soil Cement

West (1959) and ACI 230 (2009) state that compaction should begin as soon as possible and should be completed within 2 hours of initial mixing. The effect of having delayed compaction on density and strength were covered in sections 2.3.1 and 2.3.2. Sections should not be left unworked for longer than 30 minutes during compaction (ACI 230 2009). In order to obtain maximum density, the soil cement mixture should be at or near optimum moisture content as determined by ASTM D558. Standard practice requires that the soil cement base be compacted to a minimum of 95 to 98 percent depending on the state's requirements. North Carolina, Georgia, and Alabama's requirements for percent compaction are covered in section 2.5.

As soon as all of the soil cement has been placed or mixed along the section, the compaction process should begin. The main types of rollers used for soil cement compaction are sheepfoot roller, multiple-wheel rubber-tired roller, vibratory steel-wheeled roller, and heavy rubber-tired roller. Initial compaction may be combined with the placement of the soil cement with a tamping bar as mentioned in section 2.4.1.2. If the tamping bar is not used, a sheepfoot roller, seen in Figure 2.16, is then used to initiate compaction. A vibratory steel-wheeled roller, seen in Figure 2.17, follows the initial compaction.



Figure 2.16: Sheepfoot roller



Figure 2.17: Vibratory steel-wheeled roller

When finishing the soil cement base layer, a multiple-wheel rubber-tired roller is used for fine-grained soils. A vibratory steel-wheeled roller, without vibration, or a heavy rubber-tired roller is used for more granular soils (ACI 230 2009). To obtain adequate compaction, it is sometimes necessary to operate the rollers with ballast to produce greater contact pressure (ACI 230 2009). The general rule is to use the greatest contact pressure that will not exceed the bearing

capacity of the soil cement mixture (ACI 230 2009). A finished compacted layer tends to range from 6 to 9 inches in depth (ACI 230 2009).

2.4.1.4 Curing

Curing begins as soon as the compaction and finishing process has been completed. Strength gain of soil cement is dependent upon time, temperature, and the presence of water (ACI 230 2009). Proper curing is very important in order for continued hydration of the cement and strong bonds are able to form between the cement and soil particles. The process generally takes 3 to 7 days, during which heavier equipment is not allowed on the soil cement section (ACI 230 2009). Lighter traffic is allowed on the completed soil cement immediately after construction provided that the method of curing is not impacted (ACI 230 2009).

The two most popular methods of curing soil cement are water-sprinkling and bituminous coating (ACI 230 2009). Sprinkling the surface with water until a bituminous cure coat or the 3- to 7-day curing period is complete has proven successful (ACI 230 2009). Soil cement is commonly sealed with emulsified asphalt in bituminous coating where the rate of application is dependent upon the particular emulsion (ACI 230 2009). The rate typically varies from 0.15 to 0.30 gallons per square yard (ACI 230 2009). Before this bituminous coat can be applied, the soil cement should be moist and free of dry, loose material (ACI 230 2009). Figure 2.18 shows a bituminous coat applied to the compacted soil cement for curing.



Figure 2.18: Emulsified asphalt coating the compacted soil cement

Concrete curing compounds can be used to cure soil cement as well but should be applied at a rate of 1-1/2 times its normal application rate for concrete (ACI 230 2009). Soil cement curing can also be accomplished by covering it with wet burlap, plastic tarps, or moist earth (ACI 230 2009). If temperature were to drop below freezing during the curing period, insulation blanket, straw, or soil cover would commonly be used to protect the soil cement (ACI 230 2009).

2.4.2 Quality Control and Assurance Testing

Quality control is testing of the soil cement base as it is being produced in order to make sure the base is meeting the proper requirements and specifications. Quality assurance is testing of a final product that the contractor has constructed to establish if it is adequate for its intended use and in accordance with the plans and specifications. Field inspection and testing of soil cement construction involves controlling the following factors:

- Cement content,
- Mixing uniformity,
- Moisture content,

- Compaction,
- Compressive strength, and
- Lift thickness and surface tolerance.

The quality assurance of soil cement base as it pertains to compressive strength is covered in section 2.5. Each of the other field testing and inspection method are discussed over the rest of this section.

2.4.2.1 Cement Content

For mixing soil cement in-place where cement is spread by bulk cement spreaders, a check on the accuracy of the cement spread is necessary to ensure that the proper quantity is being applied (ACI 230 2009). This check is made in two ways: spot check and overall check. A spot check is done by placing a sheet of canvas or tarp that is one square yard in area ahead of the cement spreader. Once the spreader has passed, this sheet is carefully picked up and weighed, seen in Figure 2.19. If necessary, the spreader is adjusted, and the procedure is repeated until the correct coverage per square yard is obtained (ACI 230 2009). For slurry applications, the sheet is replaced with a metal pan that would capture the liquid and then be weighed, as the cement content can be determined by knowing the water-to-cement ratio of the slurry (ACI 230 2009). The overall check takes the known weight of cement in the truckload and compares it to the area in which the truckload placed the cement over and then compares that area to the theoretical area that the truckload should have covered (ACI 230 2009). It is important to keep a continuous check on cement-spreading operations as continuous adjustments may need to be made throughout construction (ACI 230 2009).



Figure 2.19: Cement content being checked (ACI 230 2009)

For a central mixing plant operation, proper proportions of cement and soil need to be checked before they enter the mixing chamber (ACI 230 2009). Mixing soil cement in a batch-type pug mill or rotary-drum mixing plant, proper quantities of soil, cement, and water for each batch are weighed on scales prior to being transferred to the mixer (ACI 230 2009). These plants are calibrated simply by checking the accuracy of the scales (ACI 230 2009). For a continuous-flow mixing plant, there are two methods of calibration that can be used. The first is while the plant is operating, soil passing through the plant during a specific time period is collected in a truck and the same is done for the cement directly from the cement feeder. Both the soil and the cement are then weighed. The cement feeder is adjusted as necessary until the correct amount of cement is discharged (ACI 230 2009). The second is when the plant is operated with only soil feeding onto the main conveyor belt. Soil is collected along a selected length of the conveyor belt and its dry weight is determined. The same procedure is then repeated with cement only being feed onto the main conveyor belt until the correct amount of cement is discharged onto the belt. Plants are

typically calibrated daily at the project's beginning and then periodically thereafter to assure no changes have occurred in the operation (ACI 230 2009).

Determining the cement content of freshly mixed soil cement can be done using ASTM D5982 (2015). This test can be conducted in the field and can provide accurate results in about 15 minutes to within 1 percent of the actual cement (ACI 230 2009). Some limitations of using ASTM D5982 (2015) include: must contain 3 to 15% cement content, maximum particle size of the soil cement can only be 3 inches, and at least 50 percent of the material must pass through the No. 4 sieve size.

The cement content of a hardened soil cement mixture can also be determined using ASTM D806 (2019). ASTM D806 (2019) is based on the determination by chemical analysis of the calcium oxide content of the sample. So, a limitation of using this test method is it should not be used on soil cement material that contain soil or aggregate that yield significant amounts of dissolved calcium oxide as it would affect the results of this test (ASTM D806 2019).

2.4.2.2 Moisture Content

As mentioned in previous sections, moisture is necessary to reach adequate compaction and for hydration of the portland cement. The optimum moisture content is determined through the moisture-density test, ASTM D558 (2019). Additional moisture may be added to account for evaporation that normally occurs during construction (ACI 230 2009).

For quality control, an estimate of the moisture content of a soil cement mixture can be made by feel or by observation (ACI 230 2009). A mixture near or at optimum moisture content is just moist enough to dampen the hands when it is squeezed in a tight ball (ACI 230 2009). Mixtures that are above optimum moisture content will leave excess water on the hands, while mixtures below optimum will tend to crumble easy (ACI 230 2009). Checks of actual moisture

content can be made daily by taking a sample, placing it in an oven-safe tin, and placing it in a conventional oven until dry.

If the surface of the soil cement mixture becomes dry during the compaction and finishing process, a very light spray of water can bring the moisture content back to optimum (ACI 230 2009). Proper moisture content of the compacted soil cement is evidenced by a smooth, moist, tightly knit, compacted surface that is free of cracks and surface dusting (ACI 230 2009).

2.4.2.3 Mixing Uniformity

A thorough mixture of pulverized soil, cement, and water is necessary to make high-quality soil cement (ACI 230 2009). For quality control purposes, mixing uniformity can be determined by the look of the soil cement after mixing has been completed for the mixed in-place method. A series of holes at regular intervals for the full depth of the treatment can be dug to inspect the color (ACI 230 2009). If the mixture has uniform color from top to bottom, the mixture is satisfactory but if there are streaks, then more mixing needs to be done (ACI 230 2009).

For central mixing plant operations, the uniformity is normally checked visually at the mixing plant (ACI 230 2009). Once the soil cement mixture has been transported and placed on-site, the same method as the mixed in-place method can be used to check the uniformity. The mixing time necessary to achieve a uniform mixture will depend on the soil gradation and the plant used (ACI 230 2009). With this method, the average mixing time varies between 20 to 30 seconds (ACI 230 2009).

2.4.2.4 Compaction

The density requirement required by various owners ranges from 95 to 100 percent of the maximum density as determined by the moisture-density test, ASTM D558 (2019). To determine the in-place density, the most common methods include the nuclear gauge method (ASTM D6938

2017), the Sand-Cone method (ASTM D1556 2015), and the balloon method (ASTM D2167 2015). The densities are determined daily at frequencies that vary per the states' Department of Transportation and on the application of the soil cement (ACI 230 2009). Density tests are taken immediately after rolling to determine if adjustments need to be made for the rest of the soil cement compaction process to ensure compliance with job specifications (ACI 230 2009). Figure 2.20 shows the nuclear gauge method being done immediately after the rolling of a small portion of the soil cement section. ALDOT (2012) specifies that measurements of in-place density be taken using the nuclear gauge method. Most states prefer to use the nuclear gauge method because of how quickly results can be obtained on-site even though the equipment may be relatively expensive.



Figure 2.20: Nuclear gauge method right after rolling

2.4.2.5 Lift Thickness and Surface Tolerance

The lift thickness of soil cement is checked when performing field density tests if using the sand-cone or balloon method (ACI 230 2009). If using the nuclear gauge method, small holes must be dug in the fresh soil cement to determine the thickness prior to density test on the compacted soil cement. A two percent solution of phenolphthalein can be squirted down the side of a freshly cut face of compacted soil cement. The soil cement will turn a pinkish-red, while the subgrade will

remain its natural color, unless it is calcium-rich soil (ACI 230 2009). Lift thickness can also be checked by coring the hardened soil cement. ALDOT (2012) requires coring to check for the strength of soil cement, so the lift thickness is normally checked during the coring process. Lift thickness is more critical for pavements than for embankment applications (ACI 230 2009).

Surface tolerances are usually specified for soil cement pavement applications (ACI 230 2009). Smoothness is usually measured with a 10-foot or 12-foot straightedge, or with surveying equipment. The U.S. Army Corps of Engineers (USACE) and most states typically require that deviations from the plane of a soil cement base cannot exceed 3/8 inch over 12 feet (ACI 230 2009).

2.5 Strength Evaluation

2.5.1 Overview of Alabama Department of Transportation Practice

The Alabama Department of Transportation (ALDOT) specifications for the construction of soil cement follow Section 304 of the ALDOT Standard Specifications for Highway Construction (2014). ALDOT 304 (2014) provides the specifications to construct soil cement for a base, subbase, shoulder, or other structures. ALDOT specifies that soil cement shall be produced using one of two methods, Mixed-In-Place or Central-Plant-Mixed method (ALDOT 304 2014). The time allowed from the initial mixing of the soil cement until compaction is completed is two hours (ALDOT 304 2014). Soil cement construction shall not take place if the air temperature is below 40°F in the shade, when the soil temperature is below 50°F, or during rain or if rain is imminent (ALDOT 304 2014). Once compaction is completed and the surface is finished, a prime coat of “Bituminous Treatment, Type A, MC 30 or MC 70” shall be applied to the completed soil cement structure (ALDOT 304 2014).

The type of soil that must be used in the construction of soil cement according to ALDOT must meet a certain gradation. The gradation of the soil must meet the following requirements: 100 percent passing the 1.5 inch sieve, at least 80 percent passing the No. 4 sieve, between 15 and 65 percent passing the No. 50 sieve, and zero to 25 percent passing the No. 200 sieve (ALDOT 304 2014). The gradation must also contain 4 to 25 percent clay (ALDOT 304 2014). Chemical properties of the soil must also meet the following requirements: zero to 25 percent liquid limit, zero to 10 percent plasticity index, dry density must be 95 pounds per cubic foot or more, the pH of the soil must be 4 or more, and the sulfate content must be no more than 4,000 parts per million (ALDOT 304 2014).

During compaction, the moisture content must be 100 percent of the optimum moisture content and not exceed 120 percent of the optimum moisture content (ALDOT 304 2014). The required density shall be at least 98 percent of the theoretical dry density (ALDOT 304 2014). ALDOT checks these values using a nuclear gauge over each section that can be no more than 528 feet (ALDOT 304 2014). Figure 2.21 shows a nuclear gauge used on an ALDOT soil cement project.



Figure 2.21: Nuclear gauge

ALDOT 304 (2014) states that the soil cement compressive strength needs to meet the requirements stated in Table 2.5. At least two cores shall be taken to evaluate the in-place compressive strength of the soil cement per each 528 ft section (ALDOT 304 2014). For a soil cement base greater than or equal to 7 inches in depth, the core must be 6 inches in diameter and for a soil cement base less than 7 inches in depth, the core must be 4 inches in diameter. Table 2.5 also defines the actions to take depending on the 7-day core strength result.

Table 2.5: ALDOT Compressive Strength Requirements

7-Day Compressive Strength (X)	Specification Action
X < 200 psi	Remove and Replace
200 psi < X < 250 psi	Price Reduction
250 psi < X < 600 psi	No Price Reduction
600 psi < X < 650 psi	Price Reduction
X > 650 psi	Remove and Replace

The thickness is checked where the cores are taken (ALDOT 304 2014). The compacted layer shall not be more than one half of an inch less or one inch more than the required thickness (ALDOT 304 2014). When all of the quality assurance checks of density, strength, and thickness have passed inspection, the contractor may then get paid.

2.5.2 Overview of Georgia Department of Transportation Practice

The Georgia Department of Transportation (GDOT) specifications for the construction of soil cement follow Section 301 of the GDOT General Specifications for Base and Subbase Courses (2019). GDOT uses Section 301 (2013) to construct soil cement as a base, subbase, and shoulders. Section 301 (2013) specifies that soil cement must be constructed using the Mixed-In-Place or Central-Plant-Mix methods. Soil cement should not be constructed if the air temperature is below 40°F and if the soil temperature is below 50°F. If construction of the soil cement is interrupted for

more than two hours after cement has been added, or if rain increases the moisture content outside of the limits, the section must be removed and replaced (GDOT 301 2013).

GDOT specifies that the soil used in soil cement construction shall all pass through the 1.5 inch sieve and at least 80 percent of the soil pass through the No. 4 sieve (GDOT 301 2013). This applies for both methods of soil cement construction. All organics and rocks that exceed 3 inches must also be removed (GDOT 301 2013). The maximum thickness allowed to compact is 8 inches (GDOT 301 2013). Compaction of the soil cement mixture must begin within 45 minutes of water being added to the mixture and must be done in 2 hours (GDOT 301 2013).

GDOT 301 (2013) requirements for quality control and assurance include compaction, finishing, thickness, and strength. For compaction, a density of at least 98 percent of the maximum dry density must be achieved. For finishing, the variation of slope and grade from the plans must not exceed a quarter of an inch. Thickness shall not exceed more than half an inch absolute difference from the specified plan thickness. And for strength, GDOT uses cores to test the unconfined compressive strength. If the compressive strength falls below 300 psi and the density is less than 98 percent, then more cores are taken and retested from the area. If the compressive strength still falls below 300 psi then 135 pounds per square yard of asphaltic concrete needs to be added to the area. If the compressive strength is less than 200 psi then the area needs to be reconstructed. GDOT 301 (2013) does not specify what to do if the compressive strengths are too strong.

GDOT 301 (2013) and ALDOT 304 (2014) have similar requirements for the soil cement. Both states allow for either mixing method to be used. The time allowed to mix is the same. The quality control and assurance tests are the same except for the compressive strength requirement.

GDOT 301 (2013) does not specify an upper bound strength that is unacceptable while ALDOT 304 (2014) does at 650 psi.

2.5.3 Overview of North Carolina Department of Transportation Practice

North Carolina Department of Transportation (NCDOT) follows the *NCDOT Standard Specifications for Roads and Structures (Standard Specifications)* when constructing soil cement as a subgrade or base. For quality assurance testing of soil cement, NCDOT uses the *Chemical Stabilization Subgrade/Base QA Field Manual (2015)*. The field manual (2015) states that NCDOT can use two types of chemical stabilization, cement or lime. Lime is generally used when the soil contains a high clay content and cement typically reacts well with sandy or silty soils (NCDOT Field Manual 2015).

The soil requirements are the same for both the lime and cement stabilization operations. Before beginning to mix, each soil must be pulverized and mixed until all the material will pass a one-half inch sieve and at least 80 percent passes the No. 4 sieve (NCDOT Field Manual 2015). For the addition of cement, the moisture content of the mixture must stay in the range of plus or minus two percent of the optimum moisture content. Any soil that has been treated with cement has a maximum amount of time to be compacted and finished of 30 minutes (NCDOT Field Manual 2015). For both lime and cement operations, the density that must be achieved is at least 97 percent along with maintaining their specific moisture content ranges (NCDOT Field Manual 2015).

The quality assurance procedures for NCDOT are to accept the density and the strength performance. Density is measured using a nuclear gauge and shall be compared immediately to the laboratory tested optimum moisture content and maximum dry density (NCDOT Field Manual 2015). The NCDOT Field Manual (2015) states that if this test is failed, the contractor may

continue to compact until the allotted 30 minutes has run out to try and reach the 97 percent. If the density is not achieved, more lime or cement shall be added, and density shall be tested again 24 hours later (NCDOT Field Manual 2015). Failure again may lead to the removal and replacement of the material after the engineer inspects the section (NCDOT Field Manual 2015).

For strength, the NCDOT Field Manual (2015) states that one soil sample shall be collected every 440 feet and compacted in a “split” Proctor Mold in accordance to ASTM test D698. The cylinder must then cure for a seven-day period in a humidity room without being directly in contact with water (NCDOT Field Manual 2015). An unconfined compression test following ASTM D1633 procedures is then performed to make sure lime treated soils reach an average strength of 60 psi and cement treated soils reach an average strength of 200 psi (NCDOT Field Manual 2015). The NCDOT Field Manual (2015) also states that cement treated specimens may not exceed 600 psi as soils this strong can create problems for flexible pavement structures.

If the contractor prefers not to do the compression tests, the NCDOT Field Manual (2015) requires DCP tests to be conducted. NCDOT Field Manual (2015) suggests that the DCP is normally only used for lime-treated subgrades, although it can also be used on soil cement subgrades as well only if little curing time has elapsed. The NCDOT Field Manual (2015) requires the DCP depth penetrated to be read in centimeters and plugged into the CBR equation shown as Equation 2.1. It can then be converted to pounds per square inch using Equation 2.2.

$$CBR = 10^{[1.53 - (\text{Log}X) * 1.066]} \quad (\text{Equation 2.1})$$

Where;

CBR = California Bearing Ratio, and

X = penetration in centimeters.

$$psi = \left(\frac{CBR}{.070}\right)^{.658} * 1.171 \quad (\text{Equation 2.2})$$

Where;

psi = compressive strength in pounds per square inch, and

CBR = California Bearing Ratio.

The NCDOT Field Manual (2015) randomizes the test locations but the number of locations depends on the length of the soil cement section divided by 440 feet. The resulting number is rounded up to give a total number of DCP test locations (NCDOT Field Manual 2015). Each test location requires five DCP tests to be performed in the pattern shown in Figure 2.22 (NCDOT Field Manual 2015). The five tests are averaged together to gain a single CBR value to plug into Equations 2.1 and 2.2 to determine the strength of the chemically treated subgrade (NCDOT Field Manual 2015). The NCDOT Field Manual (2015) states that if the strength is not reached, it needs to be reevaluated in order to determine if removal and replacement is needed.

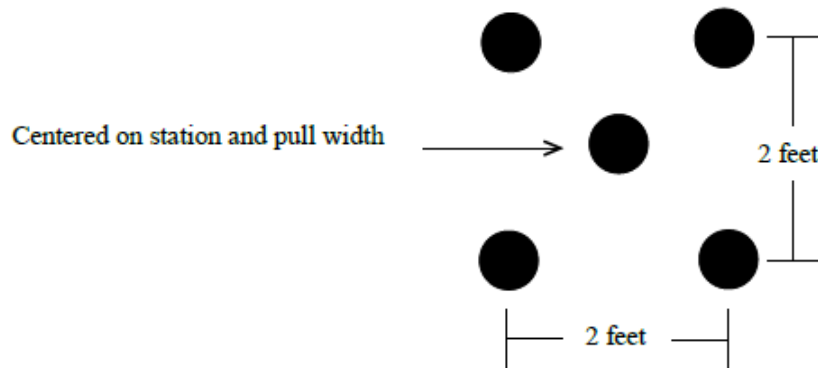


Figure 2.22: NCDOT DCP test pattern (NCDOT Field Manual 2015)

2.5.4 Core Testing

Coring is a destructive test method done in order to obtain a sample of material for strength tests to determine the in-place strength of the material. Coring is currently ALDOT's quality

assurance method of determining the in-place strength of soil cement as mentioned in section 2.5.1.

Figure 2.23 shows a core being removed on an ALDOT project.



Figure 2.23: Core removal process

There are several methods used to cut cores from the soil cement and condition them until the time of testing. For the state of Alabama, ALDOT 304 (2014) states that the locations of cores taken are to be randomly selected by the Engineer. ALDOT 419 (2008) specifies the requirements for the coring operation and states that the coring equipment shall follow the specifications in AASTHO T24. ALDOT 304 (2014) states that cores shall be 6 inches in diameter for soil cement layers greater than 7 inches in thickness. If the core is not greater than 6 inches in height, then the core must be taken again. Figure 2.24 shows a core that was taken that was too small because it fell apart while being pulled out. Coring should be done dry but can be performed with a minimum amount of water at a low flow as shown in Figure 2.23.



Figure 2.24: A sampled core that is too small

All cores taken from the in-place soil cement base shall be placed in a plastic bag to minimize moisture loss on site and during transportation to the lab (ALDOT 419 2008). If water was used during the operation, the core shall be let to air dry in the shade for 30 minutes before placing them in the plastic bag (ALDOT 419 2008). Once in the bags, the cores are to be placed horizontally with at least half of their diameter embedded in a pre-dampened bed of sand in a covered wooden box or cooler provided by the contractor and transported to the testing location as soon as all cores have been removed (ALDOT 419 2008). The sample is removed from the plastic bag and dry-sawn down to remove any irregularities to the surfaces upon arrival at the testing location. ALDOT 419 (2008) states that both ends of the cores should be capped per AASHTO T231 specifications using sulfur mortar only. Cores should only be tested when the sulfur mortar has hardened (ALDOT 419 2008). Testing equipment shall meet AASTHO T22 guidelines and the person performing the test shall be an ACI certified Concrete Strength Testing Technician (ALDOT 419 2008). Since the length-to-diameter ratio is less than 2, a correction factor specified in AASHTO T22 shall be applied to the unconfined compressive strength results

(ALDOT 419 2008). Once the cores have been extracted, the contractor shall fill the holes with either the same mixture of soil cement or by other repair methods approved by the State Materials and Tests Engineer (ALDOT 419 2008). If repaired with the soil cement mixture, it shall be placed in increments of 3-inch thick layers at a time and consolidated by tamping (ALDOT 419 2008).

Core strength results from past ALDOT projects have been found to be highly variable. A sample of these unconfined compressive strength results taken from ALDOT project STPAA-0052 (504) over the length of the roadway are shown in Figure 2.25. These results indicate that core strengths are highly variable.

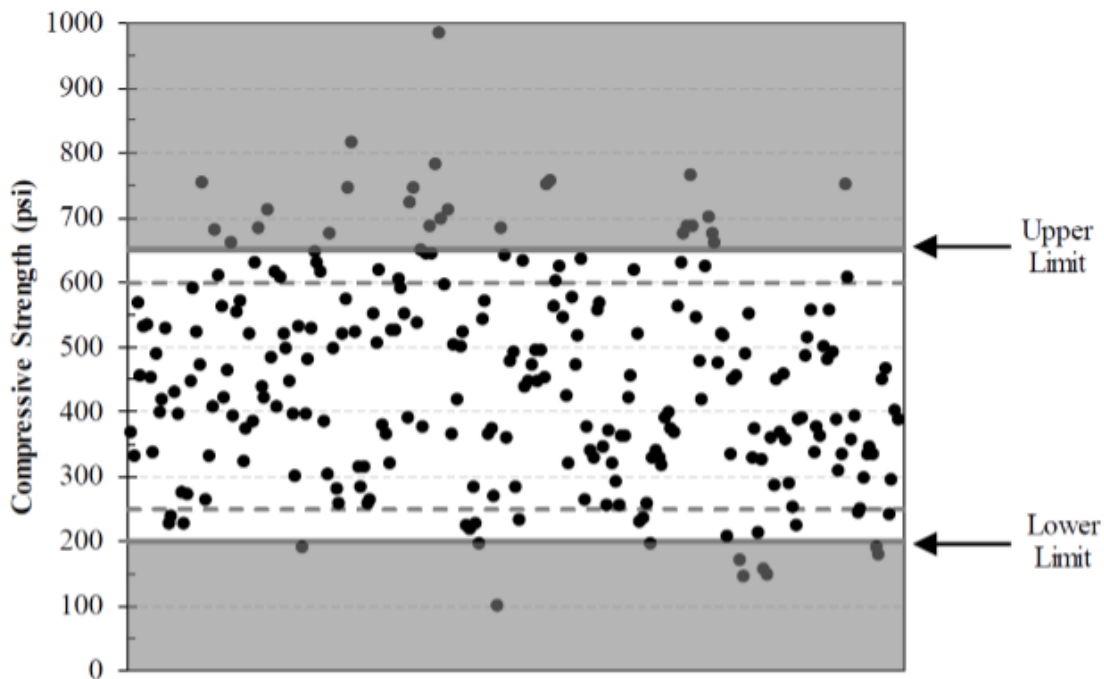


Figure 2.25: Compressive strength from ALDOT project STPAA-0052 (504)

(McLaughlin 2017)

2.5.5 Dynamic Cone Penetrometer

The dynamic cone penetrometer (DCP) is an in-situ testing device used in field exploration, and for quality control and quality assurance of compacted soils during construction. It is easy to operate while being relatively inexpensive. The DCP was originally developed in South Africa for

in-situ evaluation of pavement layer strength (Scala 1956). Ahsan (2014) states that the DCP has been used in South Africa, the United Kingdom, Australia, New Zealand, and in few states in the United States such as California, Florida, Minnesota, Mississippi, Texas, and North Carolina. The DCP has been correlated to engineering properties such as the California Bearing Ratio (Mohammadi et al. 2008), soil classification (Huntley 1990), and unconfined compressive strength (McElavaney and Djatnika 1991; Patel and Patel 2012; Nemiroff 2016).

By changing the weight and or the drop height a dynamic cone penetrometer can be configured for its intended use. ASTM D6951 (2018) is for DCP used in shallow pavement applications and this DCP configuration consists of a 17.6 pound (8 kg) or a 10.1 pound (4.6 kg) hammer with a drop height of 22.6 inches (575 mm). A schematic of this ASTM-standard DCP is shown in Figure 2.26.

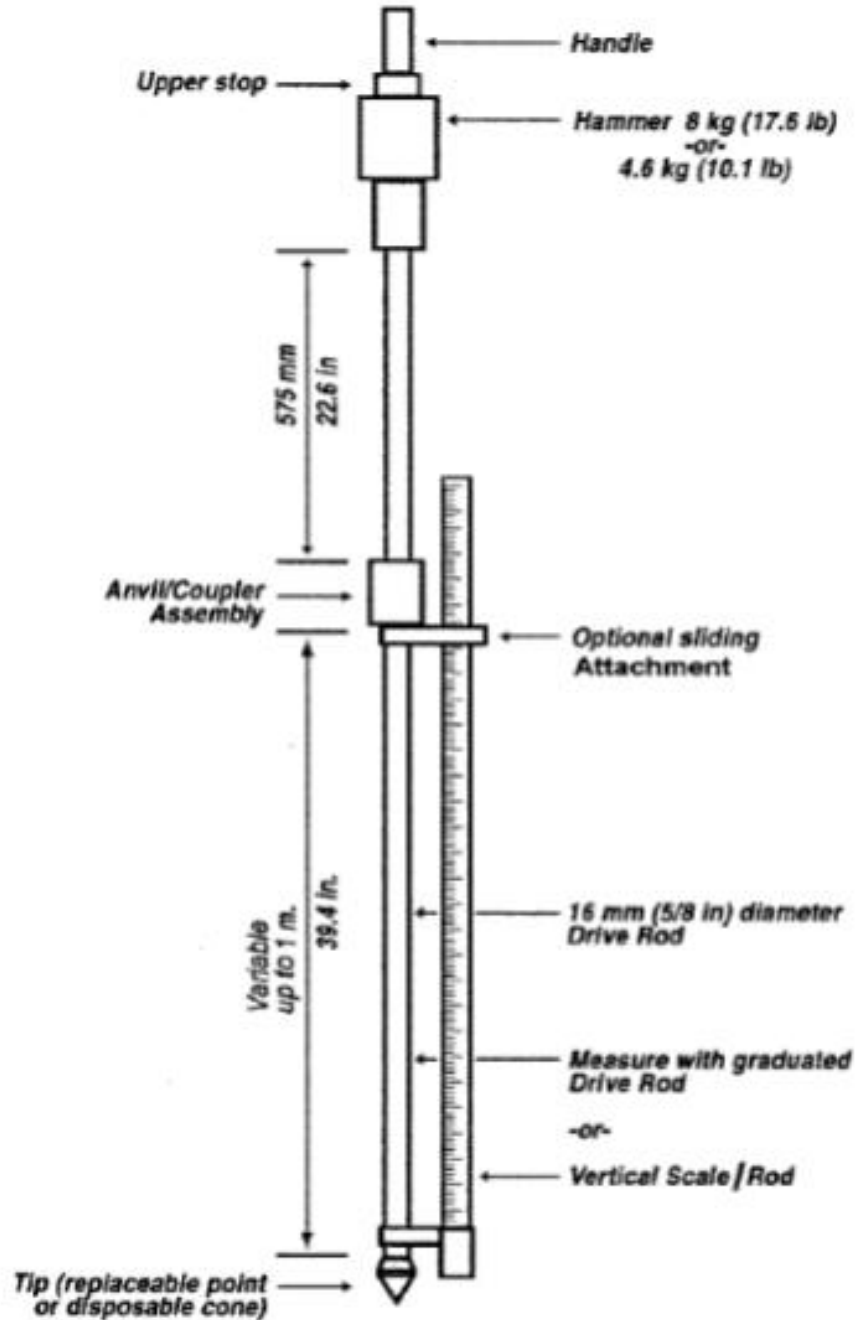


Figure 2.26: ASTM-Standard DCP schematic (ASTM D6951 2018)

The ASTM-Standard DCP consists of a 5/8 inch (16 mm) diameter steel drive rod with a replaceable point or disposable cone tip, a coupler, a handle, and a vertical scale (ASTM D6951 2018). Schematic drawings of a replaceable point tip and a disposable cone tip are shown in Figure 2.27 and Figure 2.28, respectively. The tip has an included angle of 60 degrees and a diameter at

the base of 20 mm (ASTM D6951 2018). Figure 2.29 shows the use of a DCP with a magnetic ruler for testing.

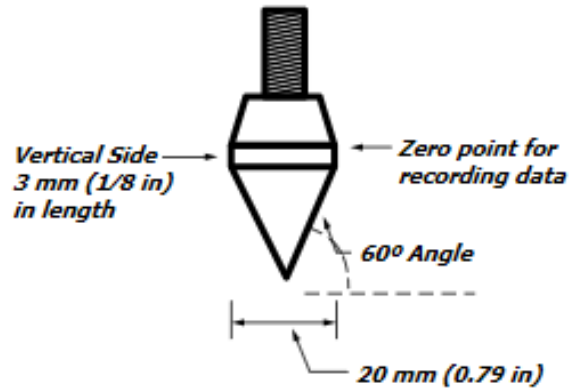


Figure 2.27: Replaceable point tip (ASTM D6951 2018)

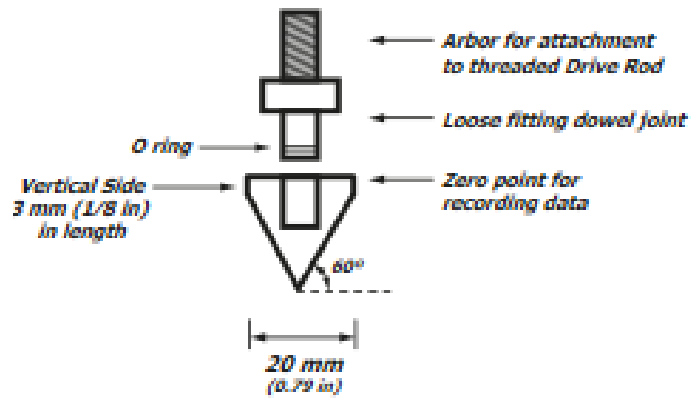


Figure 2.28: Disposable cone tip (ASTM D6951 2018)



Figure 2.29: DCP equipped with a magnetic ruler used for testing

To use the DCP, the device is to be held plumb and the hammer raised to the maximum height and then dropped. The penetration distance is read on the scale and recorded. There are two methods to recording the distance after it has been dropped, using a magnetic ruler or manually on a millimeter scale. A magnetic ruler will read it automatically after every drop, while a reading is typically manually taken after every five drops on a millimeter scale. The readings obtained are then used to calculate various parameters, one of which is the dynamic cone penetration index (DCPI) using Equation 2.3 from Enayatpour et al. (2006).

$$DCPI = \frac{PR_2 - PR_1}{BC_2 - BC_1} \quad (\text{Equation 2.3})$$

Where:

PR = the penetration reading (mm),

BC = the blow count,

$PR_2 - PR_1$ = the difference between two consecutive readings at different depths (mm),
and

$BC_2 - BC_1$ = the difference between two consecutive blow counts

The DCPI can be calculated after every five drops or can be calculated based on the total penetration depth and blow count. The unconventional use of millimeters as units for penetration was chosen as it is more accurate and easier to record penetration data in millimeters than in inches. This unit convention has also been used previously by Ahsan (2014), Nemiroff (2016), and McLaughlin (2017) during their investigations into using the DCP to determine strength of stabilized soils.

Extensive research has been performed on soils that have not been stabilized on factors that can affect the measurements. Plasticity, density, moisture content, and gradation affect the measurements of the DCP (Kleyn and Savage 1982). Hassan (1996) concluded that moisture content, AASHTO soil classification, confining pressures and dry density of fine-grained soils affect the measurements. George and Uddin (2000) concluded that the maximum aggregate size and the coefficient of uniformity could affect the DCP results.

Also, researchers have found that the DCP penetration slope, in penetration depth per blow, is inversely related to the strength of the specimen being tested (McElvaney and Djatnika 1991; Patel and Patel 2012; Nemiroff 2016). Therefore, a specimen that has a high strength will take many more blows to reach a certain depth compared to a low strength specimen reaching the same depth.

2.5.5.1 Configuration of DCP Strength Evaluation in Laboratory

Research pertaining to how to evaluate DCP strength results have been done in the laboratory and in the field. Nemiroff (2016) evaluated the use of the DCP to estimate cylinder

strengths in the laboratory. NCDOT (2013) has a field manual, mentioned in section 2.5.3, that shows how the DCP was used and evaluated. McLaughlin (2017) used the DCP to assess the in-place strength of soil cement base.

Nemiroff (2016) designed a concrete block that confines a cylindrical, plastic five-gallon bucket with a 12-inch diameter and a 14-inch height. The buckets were chosen based on research performed by Enayatpour et al. (2006) as the bucket allowed for a 10-inch tall specimen to be produced and a large enough diameter for the DCP to collect representative data (Nemiroff 2016). A schematic of the confinement block is shown in Figure 2.30. Figure 2.31 shows the reinforced concrete confinement block with and without a DCP specimen inside. The confinement block was necessary to replicate the confinement present in field conditions when testing an in-situ base (Nemiroff 2016).

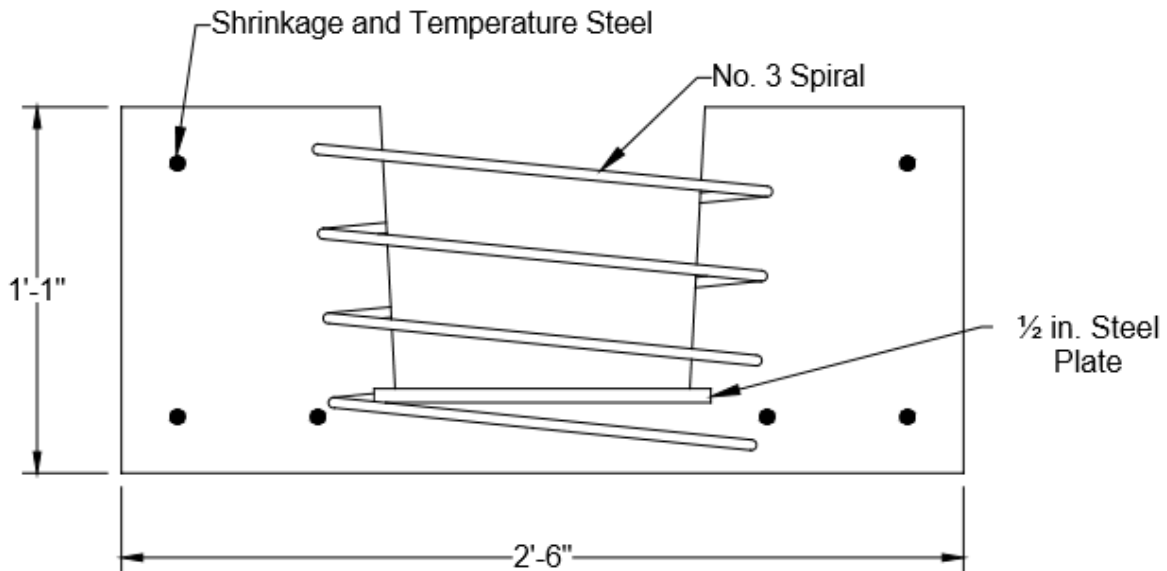


Figure 2.30: Designed reinforced concrete confinement block schematic (Nemiroff 2016)

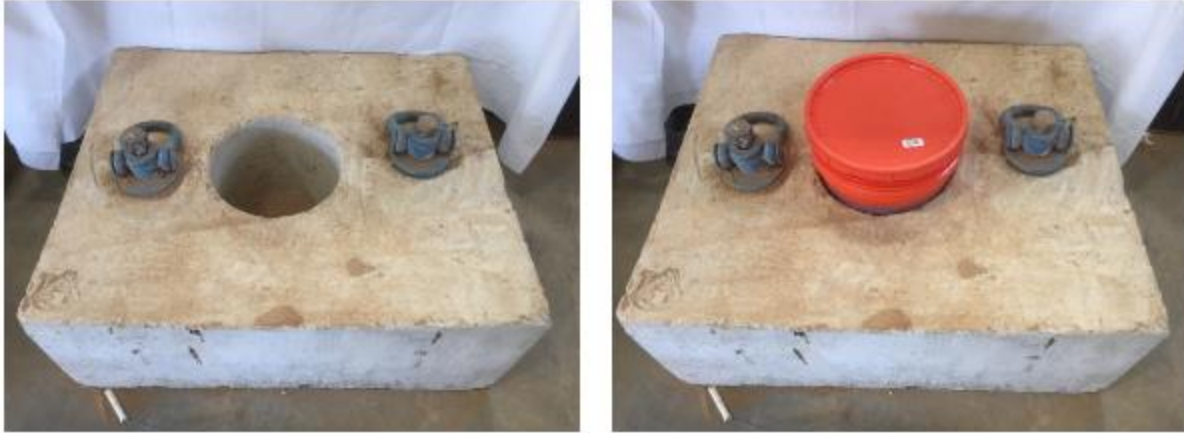


Figure 2.31: Reinforced concrete confinement block with and without a DCP Specimen

(Nemiroff 2016)

Nemiroff (2016) compacted the soil cement in the mold using a Kango 900B $\frac{3}{4}$ in. Hex Demolition Hammer based on recommendations from ASTM C1435 (2014). A circular steel tamping plate welded to a steel shaft was attached to the compaction hammer to simulate the vibrating roller used to compact soil cement in field construction as seen in Figure 2.32 (Nemiroff 2016). The production of the specimens started immediately after the soil cement mixing was completed (Nemiroff 2016). An empty five-gallon bucket was placed inside the concrete block with marks at 4.5 inches, 7.5 inches, and 11.5 inches from the bottom for where the soil cement would be compacted into three equal lifts to ensure the entire specimen would be compacted equally, similar to the compaction method used in ASTM D1557 (2012) (Nemiroff 2016). The DCP compaction pattern followed ASTM D1557 (2012) for each compaction layer as shown in Figure 2.33. For positions 1 through 4, the vibrating hammer was run for 3 seconds each. The hammer then moved in a circular pattern making one revolution every 14 seconds. Three complete revolutions were made before stopping the vibratory compactor and the next layer was filled. This was done until three DCP specimens were made using the same soil cement mixture.



Figure 2.32: Vibrating compaction hammer with circular steel plate

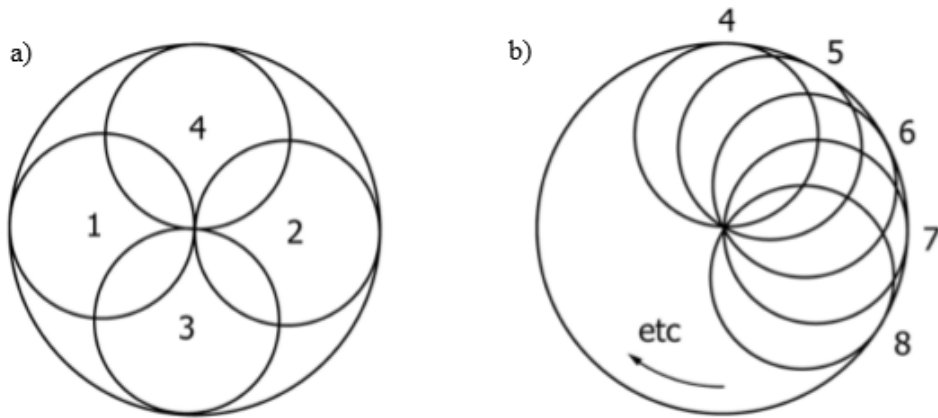


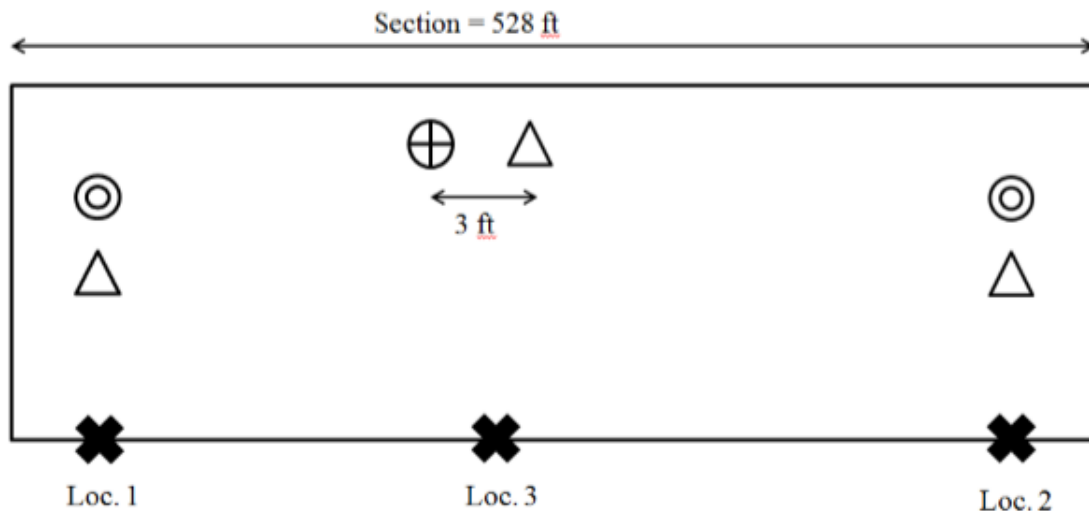
Figure 2.33: DCP specimen compaction pattern (ASTM D1557 2012)

Curing of these laboratory DCP specimens began as soon as the compaction process was completed. The buckets were covered with a lid and moved to a moist-cure room. Once in the moist-curing room, the lids were removed for a few minutes to allow moist air to enter the bucket

and the lid was then placed back on the bucket (Nemiroff 2016). After 12 to 48 hours, the lid was removed and replaced with a plastic sheet and attached using plastic clips to prevent water from entering the specimen (Nemiroff 2016). After the specified amount of time was spent in the cure room, DCP tests were performed at three and seven days. The DCP specimens were moved back to the concrete confinement block where the DCP was seated in the center of the specimen and run to a depth of 8 inches. The three DCP specimens tested were then combined for a single DCP penetration slope result (Nemiroff 2016).

2.5.5.2 Configuration of DCP Strength Evaluation in Field Construction

McLaughlin (2017) followed a similar configuration pattern as NCDOT field manual (2013) discussed in section 2.5.3. A schematic of the testing locations in the field are shown in Figure 2.34. The DCP was tested at each sampling location for the molded cylinders and at the core testing locations in the pattern shown in Figure 2.35.



Where:

- ⊙ Sample location of cylinder material
- △ Location where 3 dynamic cone penetrometer tests will be performed
- ⊕ Coring location performed by Newell and tested by ALDOT

Figure 2.34: Field testing locations (McLaughlin 2017)

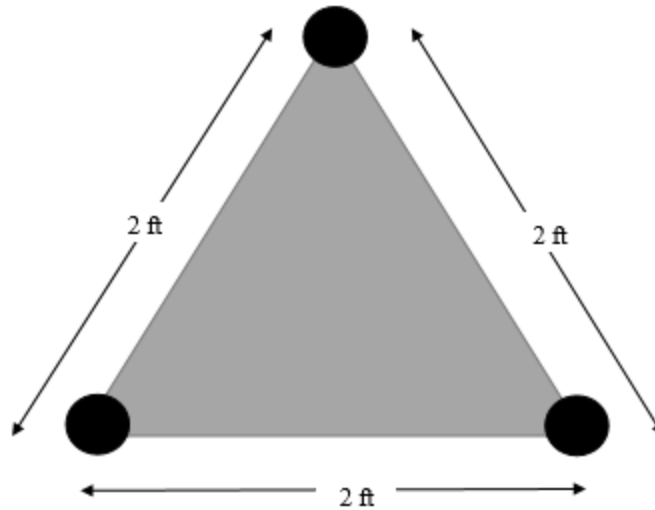


Figure 2.35: DCP testing pattern (McLaughlin 2017)

The number of DCP tests were reduced to three in a triangular pattern from the NCDOT field manual (2013) to reduce the number of DCP blows and thus technician effort (McLaughlin 2017). Each of the tests were conducted two feet apart from each other so that the tests would not be impacted by the previous ones, yet the tests are close enough to each other so that an average would characterize the in-place strength at the location. The average DCP result would be inserted into the Nemiroff (2016) equation that is covered in section 2.5.5.3. The tests were run to a depth of 8 inches.

2.5.5.3 Correlation between DCP and Unconfined Compressive Strength

Research has been completed on various soil types to determine a relationship between the dynamic cone penetration index and the unconfined compressive strength. The first were laboratory studies performed by McElvaney and Djatnika (1991) on silty clay, clay, and sandy clay with and without the addition of lime. McElvaney and Djatnika (1991) performed DCP tests using an ASTM-standard DCP hammer of 17.6 pounds on specimens that were 5.98 inches (152 mm) in diameter and 4.57 inches (152 mm) tall. The test specimens were penetrated a total of 50 millimeters. The unconfined compressive strength tests were conducted using BS 1924 (1990) on

specimens with a L/D ratio of 2.0 (McElvaney and Djatnika 1991). McElvaney and Djatnika (1991) concluded that the DCP can be used to provide an estimate of the unconfined compressive strength of lime-stabilized soil mixtures. It was also concluded that since the inclusion of data for material with zero lime content had negligible effects, the correlation is a function of strength and not the way the strength is obtained (McElvaney and Djatnika 1991). McElvaney and Djatnika (1991) developed three correlations shown in Equations 2.4 to 2.6 but cautioned these might only apply to lower strength values.

50 percent probability of underestimation:

$$\log(UCS) = 3.56 - 0.807\log(DN) \quad (\text{Equation 2.4})$$

95 percent confident that probability of underestimation will not exceed 15 percent:

$$\log(UCS) = 3.29 - 0.809\log(DN) \quad (\text{Equation 2.5})$$

99 percent confident that probability of underestimation will not exceed 15 percent:

$$\log(UCS) = 3.21 - 0.809\log(DN) \quad (\text{Equation 2.6})$$

Where:

UCS = the unconfined compressive strength (kPa)

DN = the DCP reading (mm/blow)

McElvaney and Djatnika (1991) plotted the results shown in Figure 2.36 of both stabilized and non-stabilized material versus the results of the DCP.

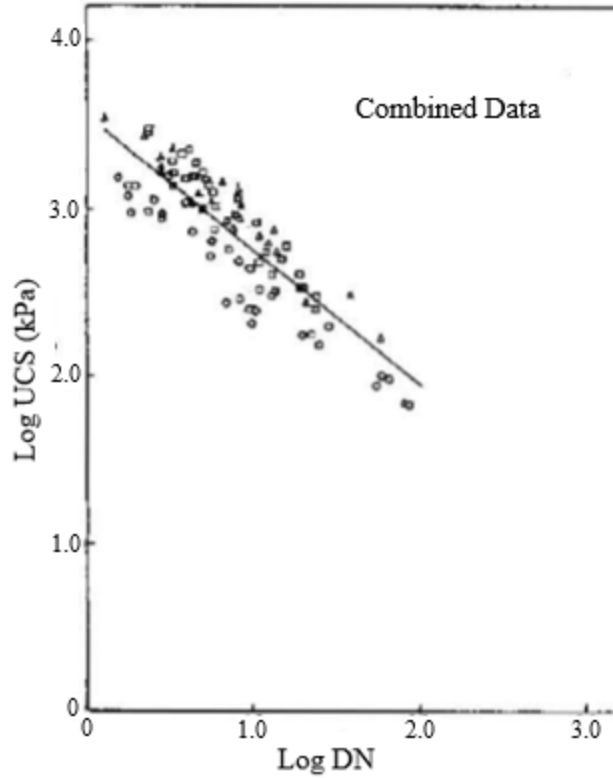


Figure 2.36: Correlation between unconfined compressive strength and DCP results
(adapted from McElvaney and Djatnika 1991)

Next, Patel and Patel (2012) conducted tests on in-situ conditions simulated in the laboratory on ASTM classified soils of CH, CI, CL, CL-ML, MI, SC, and SM-SC. These soils were also tested while being stabilized with cement, lime, and fly ash. The DCP tests were performed using an ASTM-standard, 17.6-pound hammer on soaked and unsoaked specimens using an automated DCP device (Patel and Patel 2012). The penetration was recorded up to 300 millimeters. Unconfined compressive strength was tested in accordance with Indian Standard 2720 (1980), using a L/D ratio of 2.0. Patel and Patel (2012) obtained the following equation for stabilized and non-stabilized soils:

$$UCS = 3.1237 * DCPI^{-0.865} \quad (\text{Equation 2.7})$$

Where:

UCS = the unconfined compressive strength (N/mm^2), and

$DCPI$ = the dynamic cone penetration index (mm/blow).

Patel and Patel (2012) concluded that the correlation between the unconfined compressive strength and DCPI were independent of soil type and the use of cement, lime, or fly ash. Figure 2.37 shows the correlation Patel and Patel (2012) found between the unconfined compressive strength and the dynamic cone penetrometer index for a wide variety of soils that were stabilized using cement, lime, and fly ash and non-stabilized soils.

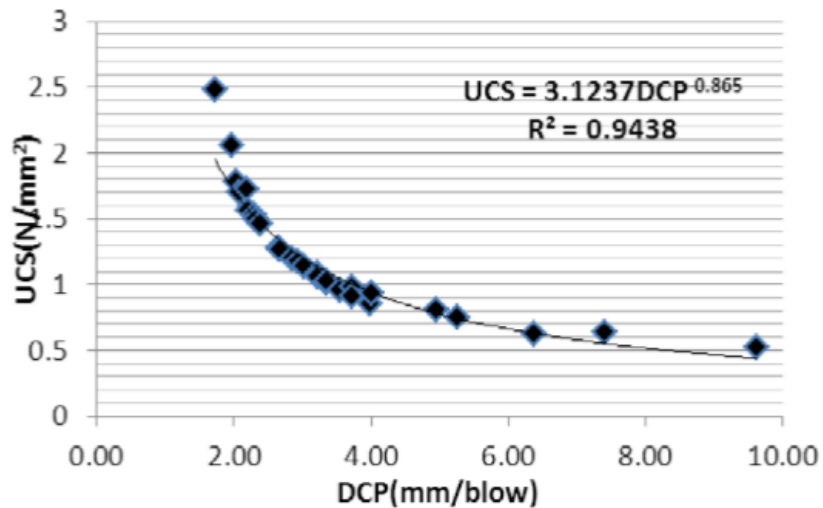


Figure 2.37: Correlation between unconfined compressive strength and DCP results

(Patel and Patel 2012)

Enayatpour et al. (2006) performed a series of laboratory tests on cement and lime stabilized soils to correlate the unconfined compressive strength with the DCP. Enayatpour et al. (2006) related percent content of cement and lime with the DCP index to estimate the unconfined compressive strength. The coefficient of determination for both equations below, cement and lime, are 0.97 and 0.91 respectively. Figure 2.38 shows the results of the predicted strengths of the specimens using the equations versus the measured strength of the specimens. The equations for cement and lime are shown in Equations 2.8 and 2.9 (Enayatpour et al. 2006).

For soils treated with cement:

$$q_c = 470.0 + 104.3 * CC + 201.0 * t - 4052.7 * DPI \quad (\text{Equation 2.8})$$

For soils treated with lime:

$$q_c = 341.2 - 26.2 * LC + 21.6 * t + 335.7 * DPI \quad (\text{Equation 2.9})$$

Where:

q_c = unconfined compressive strength (kPa),

CC = cement content (%),

LC = lime content (%),

t = curing time (days), and

DPI = dynamic cone penetrometer index (mm/blow).

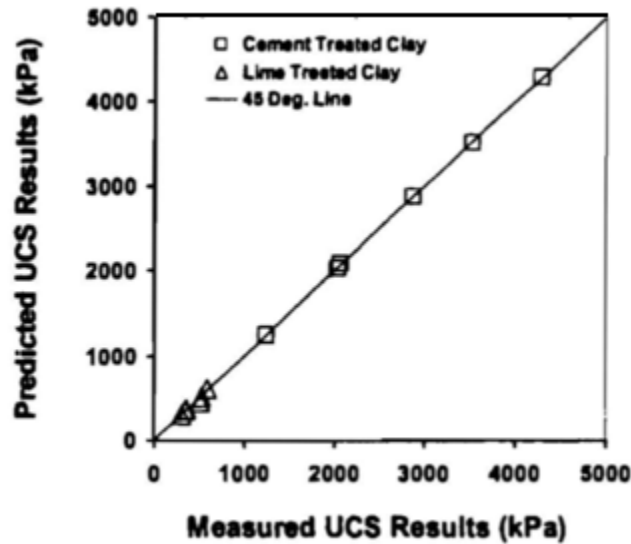


Figure 2.38: Comparison between predicted and experimental results

(Enayatpour et al. 2006)

Nemiroff (2016) conducted tests on in-situ conditions simulated in the laboratory on ASTM classified soils of SC, SP, and SP-SC stabilized with cement. The tests were performed with an ASTM-standard DCP hammer of 17.6 pounds on 3- and 7-day cured soil cement specimens. The specimens made in a five-gallon bucket were made to simulate the 8-inch lift thickness of constructed soil cement. The first inch (25 mm) of penetration was discarded as per

ASTM D6951 (2018) to allow the DCP to be seated and the next 7 inches (160 mm) were recorded. Nemiroff (2016) determined that a 75-millimeter (3-inch) penetration depth was the ideal penetration depth because it produced the best results with the least amount of technician effort. This depth of penetration was also recommended by McLaughlin (2017). McLaughlin (2017) concluded that the 75 millimeter depth produces the most efficient results in the field which matches the laboratory results of Nemiroff (2016). Unconfined compressive strengths were determined following the modified ASTM D1632 (2017) method that Wilson (2013) created using a L/D of 2.0 (Nemiroff 2016). Nemiroff (2016) recommended Equation 2.10 for soil cement applications. Nemiroff (2016) used a total of 185 cylinders and 57 DCP specimens to determine the relationship. The equation is valid for a strength range between 100 and 800 psi, which causes ALDOT's range for soil cement.

$$MCS = 926 * e^{-0.615DCP} \quad \text{(Equation 2.10)}$$

Where:

MCS = molded cylinder strength (psi), and

DCP = dynamic cone penetrometer slope (mm/blow).

Nemiroff (2016) determined the best way to show the correlation between the unconfined compressive strength and the DCP slope for typical soils used for soil-cement applications was a logarithmic relationship. Figure 2.39 shows the relationship recommended by Nemiroff (2016). It was concluded that the correlation between unconfined compressive strength and the DCP was independent of soil type and the amount of cement that was used to stabilize the material.

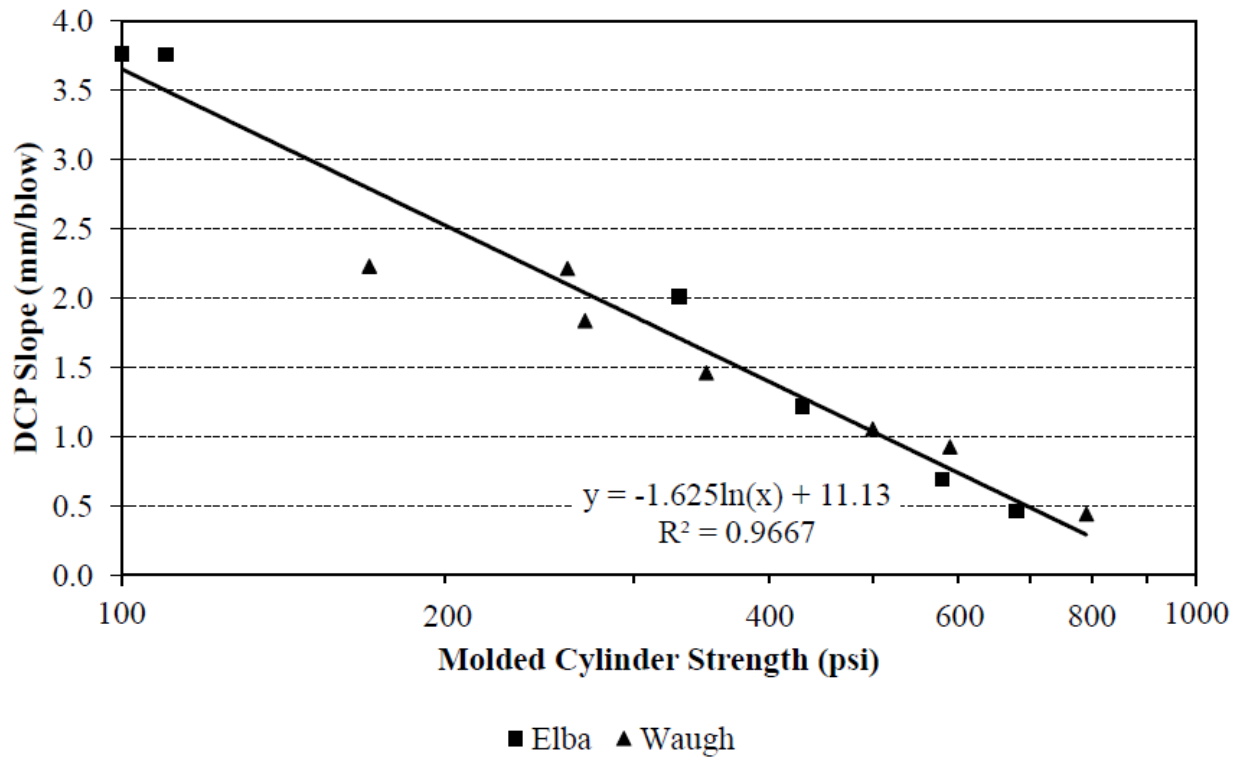


Figure 2.39: Correlation between molded cylinder strength and DCP slope results

(Nemiroff 2016)

2.5.6 Molded Cylinder Strength

2.5.6.1 Strength Correction Factors for Length-to-Diameter Ratios

ASTM C39 (2020) states that if a cylindrical specimen's length-to-diameter ratio (L/D) is 1.75 or less, the compressive strength needs to be multiplied by the appropriate strength correction factor. ASTM D1633 (2017) suggests the use of the same strength correction factors be used for soil cement specimens. Wilson (2013) performed a study on L/D strength correction factors for correcting unconfined compressive strength of soil cement cylinders. Wilson (2013) showed that the ASTM C39 (2020) L/D strength correction factors were not applicable to soil cement cylinders when made using ASTM D1632 (2017). The unbiased estimate of the standard deviation for the error of using ASTM C39 (2020) correction factor was six times greater than that of using no

correction factors (Wilson 2013). Wilson (2013) recommended that no L/D strength correction factor be applied for L/D ratios of soil cement that ranged between 1.0 and 2.0.

2.5.6.2 Proctor Molded Specimens

Soil cement compressive strength was first conducted using a specimen size of 4.0 inches in diameter and 4.58 inches in height with a L/D ratio of 1.15 (ASTM D559 2015). Figure 2.40 shows the geometry of the Proctor mold. ASTM D1633 (2017) states that using a specimen of this size gives a “relative measure of the strength rather than a rigorous determination of compressive strength”. As most soil testing laboratories have this equipment on hand, it is often used because of its availability.

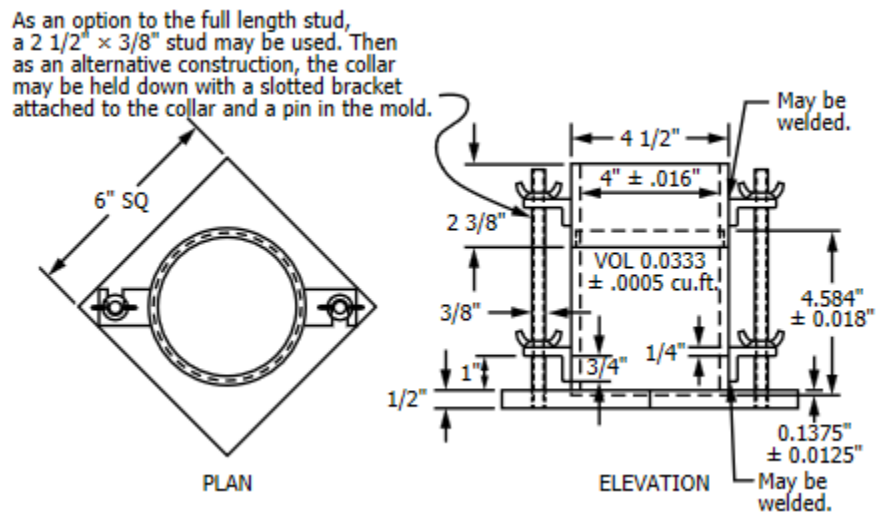


Figure 2.40: Proctor mold specifications diagram (ASTM D698 2012)

ASTM D1633 (2017) states that to use this method, at least 70 percent of the material must be able to pass the 19.0 millimeter (¾ inch) sieve. To produce a soil cement specimen, ASTM D698 (2012) outlines a specific technique and procedure. The method utilizes a Proctor mold and a 5.5-pound hammer as shown in Figure 2.41. A soil cement mixture is placed in the mold in three equal lifts and the hammer is dropped 25 times per lift around the specimen. Once three lifts are

completed, the top portion of the mold is removed, and the surface is trimmed to the top edge of the bottom mold.



Figure 2.41: Proctor mold and 5.5-pound hammer

ASTM D1632 (2017) specifies how the specimen should be handled once the specimen has been made. The molded specimen shall remain in the Proctor mold in a moist room for 12 hours or longer, and once it is removed, the specimen shall be extruded from the mold (ASTM D1632 2017). The soil cement specimen should then be placed back into the continuous moist-curing room (ASTM D1632 2017). Before the unconfined compression strength testing, the specimen shall be immersed in water for four hours and then tested immediately.

2.5.6.3 Plastic-Mold (PM) Method

Sullivan et al. (2014) developed a method using plastic molds similar to concrete to produce and cure soil cement specimens in the laboratory and in the field. The method uses a standard 3-inch by 6-inch plastic mold, which meets the single use concrete mold requirements based on ASTM C470 (2015). Both Alabama and Mississippi have been doing research into using the plastic mold method as quality assurance soil cement base. Sullivan et al. (2014) developed the device for Mississippi and later, McLaughlin (2017) used it for research on Alabama soil

cement projects. The methods have the same principle in determining the unconfined compressive strength of a soil cement mixture in the laboratory and field settings. Sullivan et al. (2014) and McLaughlin (2017) found that using the plastic-mold method was much easier and took less time to create specimens than using the steel-mold method.

Most of the plastic-mold method equipment to create the specimen are still the same between the two states. A steel mold was designed to allow a 3-inch diameter by 5.9-inch tall specimen to be compacted while preventing the mold from distorting. The mold is mounted to a 11.4- by 9.5- by 0.5-inch steel plate. Figure 2.42 shows the PM specimen preparation apparatus. The split-mold inner diameter is the same as the outer diameter of the plastic mold because it helps facilitate alignment and prevents the plastic mold from distorting during compaction. The opening of the split mold is held together with a vise-grip. The collar helps to temporarily contain soil during the compaction process. Compaction is done by a modified Proctor hammer (10 pounds dropped 18 inches) and is also shown in Figure 2.42.



Figure 2.42: Plastic-Mold preparation apparatus

2.5.6.3.1 MDOT PM Configuration

The Mississippi Department of Transportation (MDOT) uses soil cement extensively as quality base aggregates are in short supply (Sullivan and Howard 2017). Sullivan et al. (2014) developed the PM method as a way to produce a feasible device that would produce reasonable soil cement specimens that were not as variable as core testing. MDOT uses the same method that was developed by Sullivan et al. (2014). This method uses a standard 3-inch by 6-inch mold, with the bottom plastic ridge sanded away to provide a flush surface. A drill-press was used to create a 1.4-inch diameter hole through the center of the mold's bottom. This hole is created to allow for the specimen to be extruded without any damage. An aluminum plate that is 3 inches in diameter and 0.06 inches thick is inserted into the bottom of the mold to cover the hole and provide a rigid surface for extrusion. The plastic cut-outs from the drilling process are placed back over the bottom of the mold and held in place with tape to provide a solid compaction surface. The modification process is shown in Figure 2.43.



Figure 2.43: Plastic mold modification (Sullivan et al. 2014)

Sullivan et al. (2014) produce the soil cement specimens using three pre-weighed lifts. Each lift is compacted using five blows with the modified Proctor hammer and each lift is scarified before adding the rest of the material. After the last lift, the collar is removed, and the material is trimmed flush with the top of the mold with a straightedge. The mold is capped and Sullivan et al.

(2014) found that this method produced between 92 to 100 percent of the target maximum dry density. Equation 2.11 shows how the weight of each lift is determined (Sullivan et al. 2014).

$$W_{s-c} = 3.8 * \gamma_d * \left(\frac{100 + OMC}{100} \right) \quad (\text{Equation 2.11})$$

Where:

W_{s-c} = Weight of soil cement material per lift (grams),

γ_d = Maximum dry density of soil cement mixture (lb/ft³), and

OMC = Optimum moisture content of soil cement mixture (%).

The specimens were demolded using a vertical extruder after 24 hours. Measurements for diameter and height are collected before placing inside of the moist-cure room. Curing of the specimens followed the procedures of ASTM D1633 (2017) until strength testing was done on the seventh day. The specimens are not soaked prior to compressive testing (Sullivan et al. 2014).

2.5.6.3.2 ALDOT PM Modification

ALDOT and McLaughlin (2017) collaborated to develop adjustments to the Sullivan et al. (2014) method. ALDOT and McLaughlin (2017) modified the method because of the specimens were coming out damaged during the extrusion process as seen in Figure 2.44.



Figure 2.44: Plastic-mold specimen damaged by the extrusion process (McLaughlin 2017)

Instead of drilling a hole in the bottom, McLaughlin (2017) cut down the side of the plastic mold with a box blade. The mold was sealed together with aluminum tape to remain closed during the compaction process. The modification process of the plastic mold can be seen in Figure 2.45.



Figure 2.45: Plastic mold modification process (McLaughlin 2017)

Compaction of the soil cement specimens consisted of three equal lifts, not pre-weighed. As the PM method is not dependent upon the water content, the specimens were able to be made immediately after mixing. McLaughlin (2017) determined that using seven blows creates enough energy for this size of a cylinder to compact the soil cement to a 98 percent density better than using five blows that was set forth by Sullivan et al. (2014). After the last lift, the collar was removed, and the material was trimmed down flush with the top of the mold with a straightedge. A piece of aluminum tape was applied to the split of the mold to help avoid moisture loss after the specimen was covered with a plastic cap.

The plastic-mold specimens were transported back to the lab and demolded after 24 hours. To demold, the tape along the side was removed and the mold was pulled apart. The cylinder would then just slide out. The specimens were then weighed, and the height and diameter measurements were taken. Curing followed the method Nemiroff (2016) used for the steel-mold cylinders where the specimens were placed in sealed plastic bags and put in the cure room until the time of testing. Testing followed ASTM D1633 (2017) on the seventh day of curing with a few

changes created by Wilson (2013) and McLaughlin (2017). First, the specimens were not soaked four hours prior to compression testing. The loading rate was changed to 10 ± 5 psi/second. The specimens were also not capped.

2.5.6.4 Steel-Mold (SM) Method

The Steel-Mold (SM) method pertains to the procedures of ASTM D1632 (2017). Wilson (2013) studied the SM method to determine how best to produce and cure soil cement specimens. ASTM D1632 (2017) procedures produce a soil cement cylinder that has a diameter of 2.8 inches and a height of 5.6 inches that results in a L/D of 2.0; however, it is a laboratory procedure. The specimen size gives a better measure of the compressive strength since it reduces the complex stress that may occur during the shearing of the smaller L/D ratio specimens (ASTM D1633 2017).

The cylindrical steel molds used had an inside diameter of 2.8 ± 0.01 inches and a height of 9 inches. A machined steel top and bottom pistons having a diameter of 0.005 inches less than the mold, a 6-inch long mold extension, a spacer clip, two aluminum separating disks 1/16 inches thick by 2.78 inches in diameter, and two ultra-high molecular weight polyethylene (UHMW) plugs with a diameter 0.005 inches less than the mold are also necessary with the cylindrical steel molds (ASTM D1632 2017). The dimensions of the equipment as well as the equipment are shown in Figures 2.46 and 2.47.

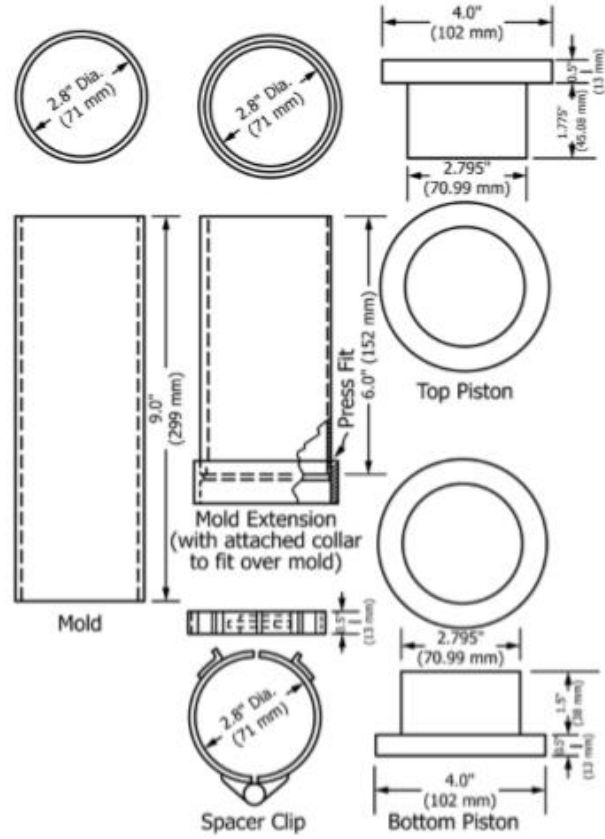


Figure 2.46: Steel-Mold equipment dimensions (ASTM D1632 2017)

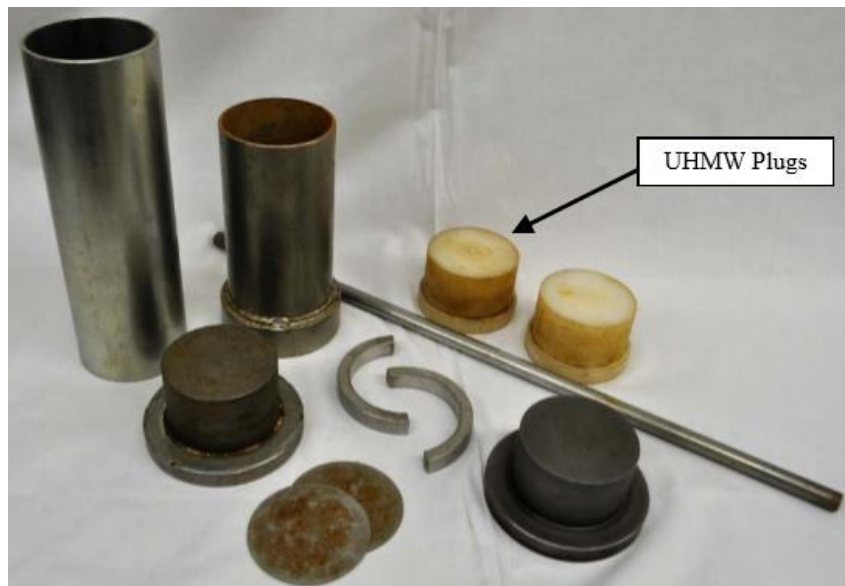


Figure 2.47: Steel-Mold equipment (Nemiroff 2016)

To produce a specimen, a freshly mixed soil cement sample is tested to determine its moisture content. Based on the moisture content and the moisture-density curve of the mixture, a target mass is determined using Equation 2.12 to create a soil cement cylinder with a density of at least 98 percent. The coefficient takes the volume of the cylinder and converts the weight from pounds to grams.

$$M_{SC} = 9.056 * \gamma_{dry} \frac{lb}{ft^3} \quad (\text{Equation 2.12})$$

Where:

M_{SC} = mass of soil cement (grams), and

γ_{dry} = dry unit weight corresponding to composite sample moisture content, lb/ft³.

The mold and separating disks are lightly coated with a low-viscosity oil and placed on the bottom piston. Once assembled, the extension is placed on top of the mold. The predetermined amount of soil cement is then transferred into the mold where the smooth steel rod is used to tamp the soil cement below the extension sleeve. The extension sleeve is removed, and a separating disk and the top piston placed on top of the mold. The specimen is compacted until the top piston touches the mold using a compacting drop-weight machine as shown in Figure 2.48. Once compaction is completed, the pistons are replaced with the UHMW plugs to limit moisture loss. Metal foil tape is wrapped around the plugs to add an extra layer of moisture loss prevention during the initial stages of curing. Figure 2.49 shows the SM cylinders once they have been completed.



Figure 2.48: SM cylinder compacted with drop-weight machine



Figure 2.49: SM cylinders during initial curing period

The steel-molds are then transferred out of the sun or to a location in the laboratory where they had limited exposure to the elements to eliminate chances of rapid evaporation for at least 12 hours. The specimens are then transported to the laboratory where the specimens are extruded from the mold using a vertical specimen extruder. Nemiroff (2016) adjusted the curing method by

immediately placing the SM specimens into sealed plastic bags and then placed the bagged specimens inside a moist-cure room. This method was used as specimens placed without bags in the moist-cure room became soft and did not gain strength from three to seven days (Nemiroff 2016).

Chapter 3

Experimental Plan

3.1 Introduction

3.1.1 Laboratory Testing Phase

The main objective of this laboratory testing phase is to establish a method to reliably assess the strength of soil cement base. To accomplish this, a laboratory experimental testing program is developed similar to that of Nemiroff (2016). This chapter provides an overview of the laboratory testing program. For the laboratory testing program, an outline of the soil cement mixtures from each pit location is defined with details of all testing procedures. The preparation and curing methods for soil cement cylinders and DCP specimens are also discussed in detail along with the equipment used.

3.1.2 Field Testing Phase

At the time of this research project, the U.S. Highway 84 bypass East of Elba, Alabama was being constructed with soil cement as the base of the roadway. Numerous trips were made to Elba to assess the strength of the soil cement base being placed by S.A. Graham Company out of Brundidge, Alabama as the contractor for ALDOT. This chapter provides an overview of the field testing program. For the field testing program, the soil cement mixture used on site is described and its mixture proportions defined. The reason for selecting the specific sampling and testing locations for all test types is discussed. The procedures for procuring the soil cement specimens and performing DCP tests in the field are explained. How the compressive strength of the cylinders are compared to the DCP results is explained. The preparation and curing methods for soil cement cylinders are also discussed in detail along with the equipment used.

3.2 Laboratory Testing Program

In order to more accurately assess the strength of soil cement base in the field, more laboratory work was done following a similar laboratory testing program as Nemiroff (2016). Figure 3.1 shows a summary of the laboratory testing program that was developed. Two strength testing methods were used: Plastic-Mold Method (AASHTO Method PP 92) with adjusted modifications from McLaughlin (2017) for soil cement cylinders and ASTM D6951 (2018) for DCP testing. The plastic-mold cylinders were tested for their unconfined compressive strengths at ages of 3 days and 7 days. The DCP specimens were tested at the same ages of 3 days and 7 days.

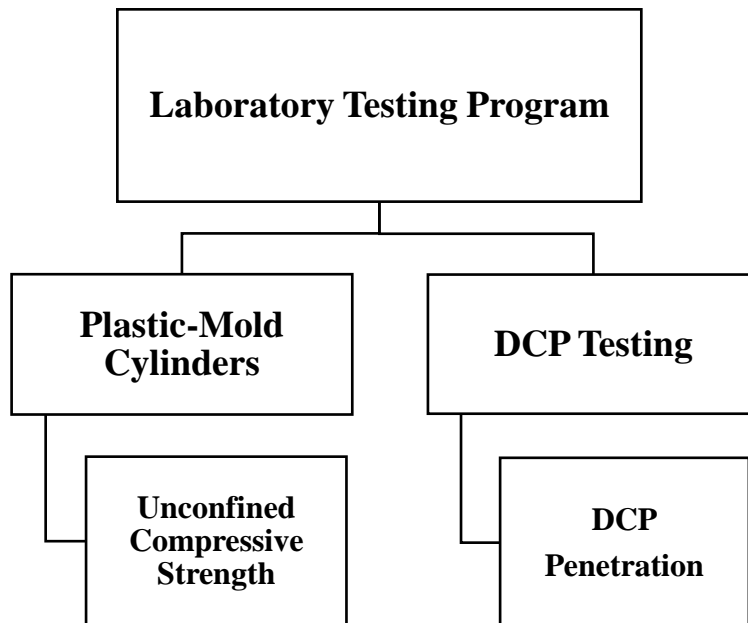


Figure 3.1: Summary of Laboratory Testing Program

Different soils were tested at different cement contents and because of that, different strength ranges were achieved. Figure 3.2 provides a summary of the materials and variables considered. The soils are first described by their respective AASHTO soil classifications. Next, shows the strength range that will try and be reached while differing the cement contents. Lastly, the age of determining the unconfined compression strength of each specimen is shown.

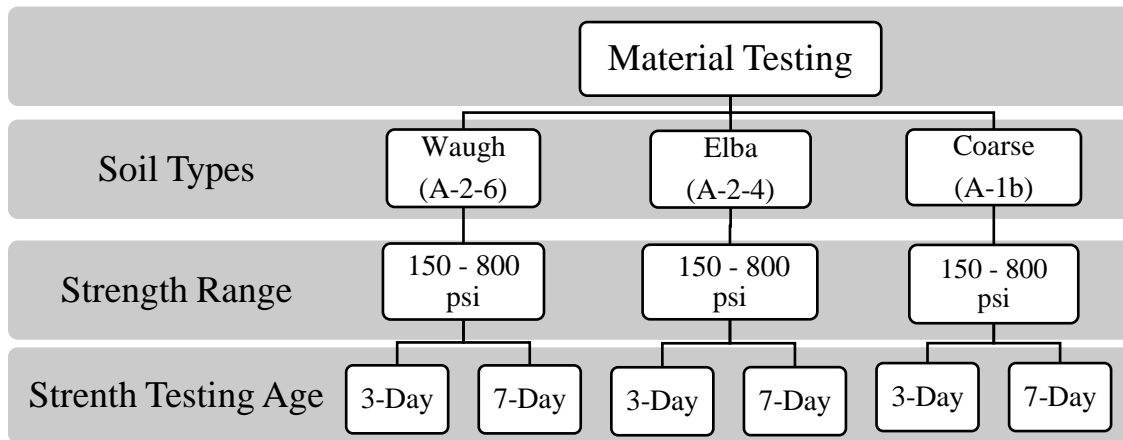


Figure 3.2: Summary of materials and variables considered

All soils used in the soil cement mixtures were collected from borrow pits that have been used for soil cement base projects or collected from a soil cement base project site that was ongoing during this research. This ensures the best representation for comparison between DCP and cylinder strength in the laboratory mixtures to the field mixtures. Each soil was tested to determine the USCS and AASHTO soil classification. Each soil was mixed with a range of cement contents. Using a proctor test, the optimum moisture content and maximum dry unit weight that corresponded to a specific cement content was found. The percentage of cement used was determined to target three strength ranges: low (100 to 250 psi), moderate (250 to 600 psi), and high (600 to 800 psi). The moderate range corresponds with the acceptable values specified by ALDOT 304 (2014).

Like Nemiroff (2016), an evaluation of whether soil classification had an impact on soil cement strength or cement content will be conducted. From Nemiroff (2016), the curing method used consisted of placing the cylindrical specimens into a sealed bag and then placing them in a moist-cure room. With ALDOT’s acceptable range of placement strength being 200 psi to 650 psi, the suitability of the DCP to penetrate strengths from 150 psi to 800 psi will be evaluated. The depth of penetration that would be the most feasible and give the most accurate results will be

determined. A logarithmic expression based on the findings of Nemiroff (2016) and new points found through these experiments will then be used to find the best expression that provides the best fit correlation between the plastic-mold cylinder strengths and the DCP tests.

3.2.1 Correlation between Molded Cylinder Strength and DCP

Nemiroff (2016) proposed an expression to correlate the different DCP results to the cylinder strengths obtained by the cylinders created by using the modified ASTM D1632 method (Wilson 2013). Using the PM device to create cylinders, data points will be added to the data that Nemiroff (2016) had collected. The study consists of testing various mixtures of soil cement with different soil types and varying amounts of cement that will produce a range of strengths. The unconfined compressive strength of the soil cement cylinders will then be compared to the depth penetrated to blow count ratio of the DCP tests. The correlations will then be compared and added to the logarithmic expression that Nemiroff (2016) recommended.

3.2.2 Suitability of the Dynamic Cone Penetrometer (DCP)

Nemiroff (2016) and McLaughlin (2017) evaluated the suitability of the DCP to determine the strength of soil cement base. The DCP will be tested at unconfined compressive strengths ranging from 100 psi to about 1,000 psi to evaluate its suitability to test material with this high strength. This is necessary, as most other researchers (NCDOT Field Manual 2014; Patel and Patel 2012; McElvaney and Djatnika 1991; Enayatpour et al. 2004) have used the DCP on lower strength subgrade and subbase material. During the evaluation, testing will be performed to find the most efficient DCP penetration depth while also considering technician effort. The most efficient depth will be determined by analyzing penetration depths from 1 inch to a full depth.

3.2.3 Laboratory Mixtures Evaluated

Three different classifications of soils will be sampled from Central and South Alabama. Figure 3.3 labels each soil as they are referred to throughout the research. The soil types are further introduced in the next sections.



Figure 3.3: Soils used during testing

3.2.3.1 Waugh Clay and Waugh Sand

Waugh Clay and Waugh Sand will be used as it is the same soil from the same pit used by Nemiroff (2016). Samples will be collected from a pit owned by Newell Construction in Waugh, Alabama. The location of this borrow pit is shown in Figure 3.4 and the coordinates are N 32.366983, W -86.042014. The sand and clay samples will be mixed to create what will be called Waugh soil.

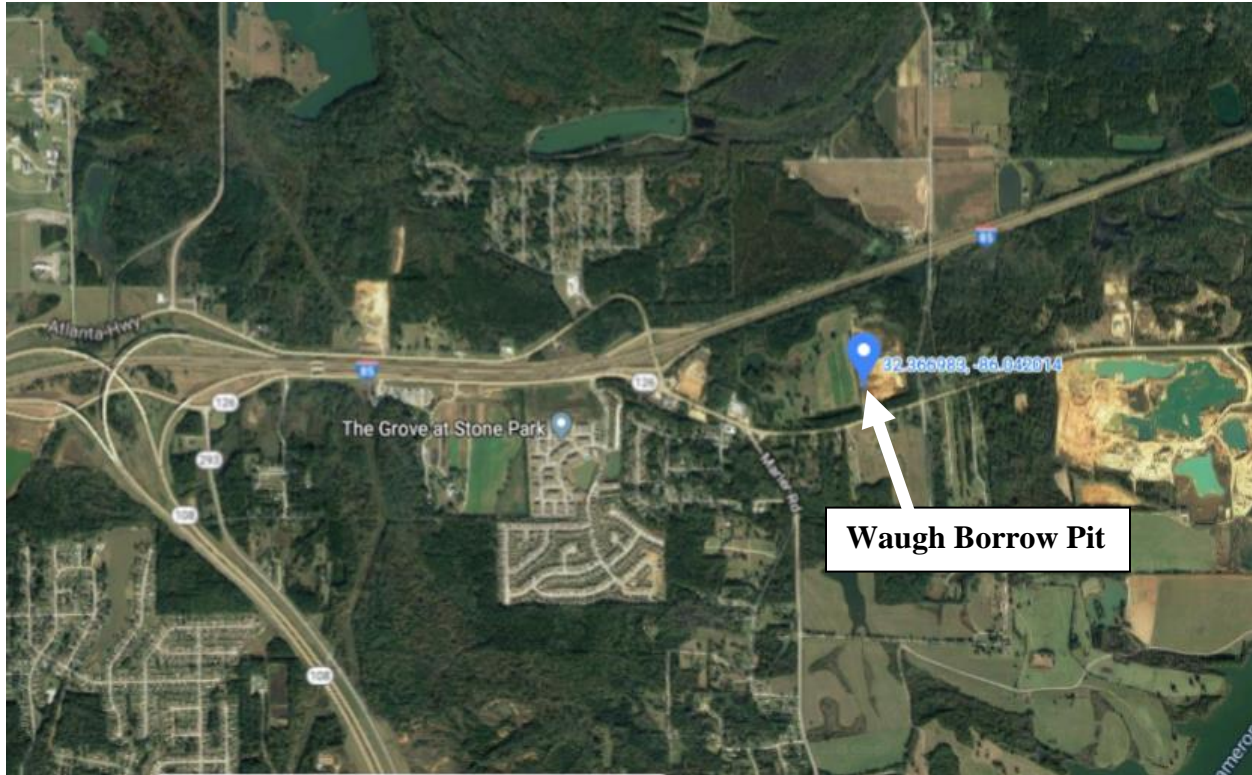


Figure 3.4: Location of the Waugh borrow pit (Google Maps)

3.2.3.2 Waugh Soil

According to ALDOT 304 (2014), a soil cement mixture needs to have a fines content of 5% to 35%. To create this, the Waugh Clay and Waugh Sand were mixed at a 20% to 80% ratio respectively (Nemiroff 2016). This mixture will be referred to as Waugh soil throughout the rest of the research. To create a wide range of strengths, from about 150 psi to 800 psi, the cement contents mixed with the dry Waugh soil will be 4, 5, 6, 8, and 10 percent cement by weight of dry soil.

3.2.3.3 Elba Soil

Elba soil was collected from a soil cement base project that was ongoing during the time of this research project. The contractor on site was S.A. Graham. The project was along Eastbound

U.S. Highway 84 to the East of Elba. The location where soil was sampled for the project is shown in Figure 3.5 and the coordinates were N 31.400602, W -86.006807.

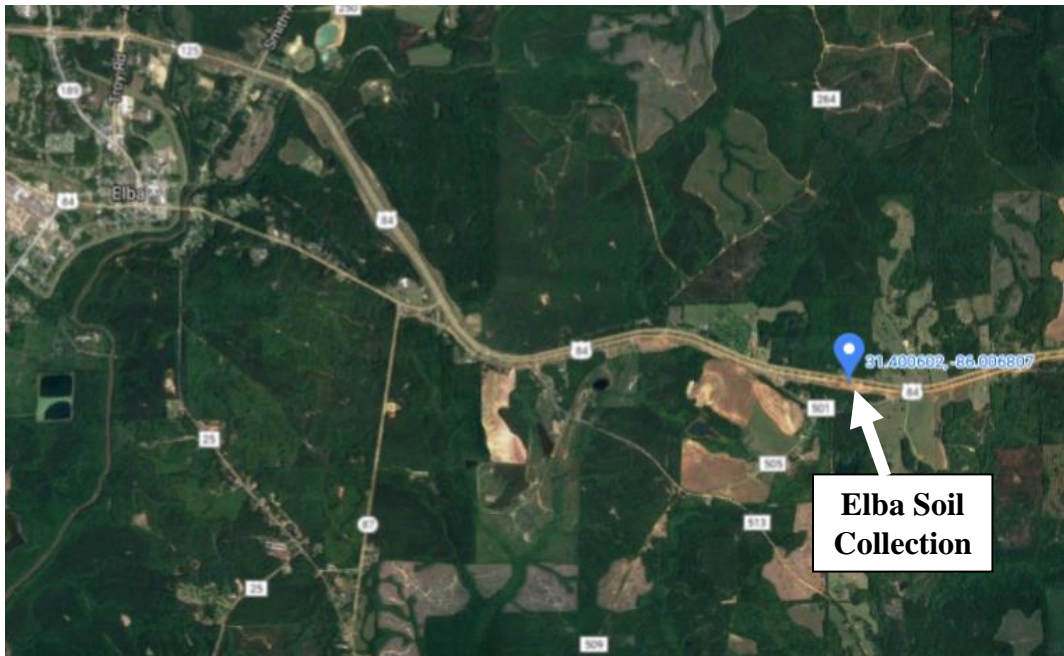


Figure 3.5: Map of Project Site where Elba soil was collected (Google Maps)

To create a range of strengths from 150 psi to 800 psi like the Waugh soil, the cement contents were changed to be 5, 6.5, and 8 percent to the dry Elba soil. The 6.5 percent was also prepared to allow for comparison to the results of the field testing.

3.2.3.4 Coarse Soil

Coarse sand will be collected from a borrow pit located in Emerald Mountain, Alabama owned by Foley Materials. This coarse sand is normally used as a fine aggregate while mixing concrete so it has a larger fineness modulus than the other soils. In order to create a soil cement mixture, this coarse sand will be mixed with Waugh clay at a ratio of four to one, or 80 percent coarse sand to 20 percent Waugh clay. This mixture of soils will be known as Coarse soil through the rest of this report. The location of this borrow pit is shown in Figure 3.4 and the coordinates

were N 32.415318, W -86.179164. To create a range of strengths from 150 psi to 800 psi, the cement contents will be 4, 6, 8, 9, and 10 percent by weight of dry Coarse soil.



Figure 3.6: Coarse soil sample location (Google Maps)

3.2.4 Material Classification

The geotechnical properties of each soil will be determined to allow their soil classification to be determined. First, ASTM D422 (2007) will be used to determine the soil's grain size distribution. The soils will then be classified using both the American Association of State Highway and Transportation Officials (AASHTO) method and the Unified Soil Classification System (USCS) method. ASTM D698 (2012) was then used to run proctor tests to determine the optimum moisture content and maximum dry density of the mixture of soil, cement, and water.

3.2.5 Soil Classification Impact

The effects of different soil types will be evaluated to determine its impact on strength of the soil cement and the correlation between DCP output and molded cylinder strength. Different soils were selected to compare the results of laboratory mixtures with low fines content to those

made with a high fines content. The soils will also be tested to determine the cement content needed to obtain the strength to meet ALDOT specifications.

3.3 Laboratory Testing Phase Procedures

3.3.1 Laboratory Mixing of Soil Cement

The soils collected from the borrow pits will be stored in five-gallon drums with a plastic lining. The portland cement used for mixes will be Type I/II. The water used in the mixes will be collected from the City of Auburn's public water supply.

3.3.1.1 Moisture-Density Curve

Before producing soil cement, a proctor test from which a moisture-density curve can be obtained will be performed for each mixture with different cement contents. The optimum moisture content and maximum dry density were determined using ASTM D698 (2012). This information is very important when weighing out all the material before production. Method A is used which uses a four-inch diameter mold. For this method, the specimen is compacted in three equal lifts using 25 blows per lift. The weight of the mold and soil cement was weighed once completely compacted. A sample from the soil cement is taken to determine the moisture content. The results from each sample are then plotted to create the moisture-density curve. A curve is added and the optimum moisture content and maximum dry density scaled off at the peak of the curve as shown in Figure 2.2.

3.3.1.2 Batching

Before batching, the material that will be used is poured out on a plastic sheet and mixed to make sure the moisture content is equal throughout the soil. This can be seen in Figure 3.7. A moisture content of the soil was then sampled using ASTM D2216 (2010). Based on the optimum moisture content and maximum dry density obtained from the moisture-density curve, the weight

of the soil, cement, and water is weighed to achieve 100 percent density. The components will be weighed out in five-gallon buckets to the nearest one hundredth of a pound and covered to minimize moisture loss until the mixing has started.



Figure 3.7: Mixing of soil prior to batching

3.3.1.3 Mixing

A 2.5 cubic foot batch is needed to produce enough material to create the five plastic-mold cylinders and three DCP specimens. A mortar mixer with a capacity of 12 cubic feet is powerful enough to uniformly mix the full batch of material. The mixing will be performed by a Multiquip/Whiteman WM120PHD mortar mixer as shown in Figure 3.8. Once mixing has been completed, samples will be collected to determine the moisture content of the material.



Figure 3.8: 12-cubic foot mortar mixer for soil cement mixing

3.3.1.4 Plastic-Mold Cylinder Production

The 3-inch by 6-inch plastic-mold cylinder production closely follows the method of McLaughlin (2017) who changed the method slightly from the method that Sullivan et al. (2014) from Mississippi State University created. The mold is to be cut down the side with a box blade, same as McLaughlin (2017). After cutting, the mold is taped together with aluminum foil tape to allow the cut to remain sealed during production of the specimen. The way the mold is taped is changed from the McLaughlin (2017) method. McLaughlin (2017) used a single, vertical strip of aluminum tape to seal the side as seen in Figure 3.9. The change to this added two strips of tape from the top that wrap around one third of the circumference of the mold, centered on the cut, as seen in Figure 3.10. This method will greatly reduce the chance of the taped mold splitting while being compacted.



Figure 3.9: McLaughlin (2017) tape arrangement



Figure 3.10: New PM tape arrangement

The plastic-mold cylinders are compacted using 7 blows per lift in accordance to McLaughlin (2017) in order to obtain the 98 percent density required by ALDOT. Once compaction is completed, the mold will be removed from the testing apparatus and the soil cement

will be trimmed level with the top of the plastic-mold shown in Figure 3.11. A plastic cap will then be placed on the top to prevent moisture loss.



Figure 3.11: Straightedge used to trim the soil cement to the top of the mold

3.3.1.5 DCP Specimen Production

The dynamic cone penetrometer specimens will be created using the method developed by Nemiroff (2016) as previously presented in Section 2.5.5.1. Once complete, the buckets will be removed from the concrete confinement block by grabbing the top edge of the bucket as to not deform the bucket and fracture or disturb the freshly compacted DCP specimen that could happen while removing with the handle.

3.3.2 Initial Curing

3.3.2.1 Plastic-Mold Cylinders

Sullivan et al. (2014) suggested plastic-mold cylinders be stored on site for one day before moving to laboratory. This is used in the laboratory as well. The specimens shall be stored exposed to laboratory air conditions in the mold for initial curing overnight. This was typically between 12 and 48 hours.

The next day, the soil cement cylinders are removed from the plastic mold by removing the cap and all of the tape. With the split being down the side, the mold is slightly pulled apart until the cylinder would slide out. Removal of the cylinder from mold can be seen in Figure 3.12. At this point, the weight, diameter, and height of the cylinder will be measured in order to calculate the density of the specimen, described in Section 3.3.4.1.1. This is done to make sure the specimens achieved the 98 percent of maximum dry density requirement.



Figure 3.12: Specimen removal from plastic-mold

3.3.2.2 DCP Specimens

The DCP specimens will be immediately covered with a piece of plastic and attached with plastic clips around the edges, as seen in Figure 3.13. The specimens will be kept undisturbed in the laboratory similar to the plastic-mold specimens overnight for 12 to 48 hours.



Figure 3.13: Initial curing of DCP specimen

A study will be done on if the initial curing of the DCP specimens has an effect on the strength. The second half of the study will switch the initial curing to the same done by Nemiroff (2016). After compaction, the DCP specimens will be covered using a plastic lid and moved to the moist-cure room. The plastic lid will be removed to allow the moisture to enter the top of the specimen for about one minute, and then the lid will be placed back on and kept undisturbed in the moist-cure room for 24 hours.

3.3.3 Final Curing

3.3.3.1 Plastic-Mold Cylinders

Final curing began as soon as the specimens were removed from the mold. The plastic-mold cylinders were removed from the plastic-mold and sealed in a plastic bag. All air was removed prior to sealing it shut and wrapping a rubber band around it. The cylinders were then placed on their sides in the moist curing room which was kept at a temperature of $73\text{ }^{\circ}\text{F} \pm 3\text{ }^{\circ}\text{F}$. The specimens remained there until it was time for compression testing. Figure 3.14 shows the final curing.



Figure 3.14: Final curing of the PM cylinders

3.3.3.2 DCP Specimens

The final curing for the plastic-mold specimens and DCP specimens occur at the same time. The DCP specimens are moved from the laboratory to the moist curing room 12 to 48 hours after compaction. The specimens are moved at the same time as the PM specimens described in section 3.3.3.1. These specimens are kept in the moist-cure room until time for testing.

3.3.4 Testing

3.3.4.1 Plastic-Mold Cylinder Testing

3.3.4.1.1 Moisture Content and Density

When the soil cement cylinder is removed from the plastic-mold, measurements of the diameter, length, and weight are taken. A caliper is used to read the values of the diameter and length of the soil cement cylinder. A measurement is taken at the top, middle, and bottom of the cylinder with the caliper to obtain an average diameter of the soil cement cylinder. Two readings are taken of the length of the cylinder to determine its average. Figure 3.15 shows how the diameter and length of the cylinder are measured with the caliper.



Figure 3.15: Measurements of the soil cement cylinder using a caliper

After the unconfined compressive strength test, described in Section 3.3.4.1.2, has been completed, a sample of the soil cement is taken and put into an oven to determine a moisture content of the cylinder. This sample serves as the moisture content used to find the dry density of

the sample. The weights of the samples and equipment used are determined in accordance with ASTM D2216 (2010). Figure 3.16 shows samples about to be weighed to the nearest hundredth after having dried in the oven.



Figure 3.16: Dry soil cement samples about to be weighed

The dry density is determined by using Equation 3.1. The specimen's dry density is then compared to the maximum dry density to ensure the percent compaction has exceeded 98%.

$$\gamma_{dry} = \frac{W_{sample}}{V * (1 + w)} \quad (\text{Equation 3.1})$$

Where;

γ_{dry} = dry density,

W_{sample} = weight of sample,

V = volume of sample, and

w = water content.

3.3.4.1.2 PM Cylinder Compressive Strength

Compression testing of the plastic-mold cylinders followed the changes that McLaughlin (2017) made to the Wilson (2013) method that had modified ASTM D1633 (2007). A detailed summary of the changes are in Section 2.5.6.3.2.

For precise control of the loading rate, a 100-kip compression testing machine from Forney was used and can be seen in Figure 3.17. The specimens were removed from the moist curing room and taken out of the plastic bags one at a time. The specimens were tested in the machine. As seen in Figure 3.18, the vertical axis of the specimen was aligned with the center of thrust from the upper plate to avoid any load eccentricity that may impact the measured strength.



Figure 3.17: Forney 100-kip compression testing machine



Figure 3.18: Specimen being tested in the 100-kip compression testing machine

The load applied to the specimens will be kept at a constant rate of 10 ± 5 psi/s until failure occurs. Failure load will be recorded to the nearest 5 pounds. The compressive strength will then be calculated by dividing the total failure load by the cross-sectional area of the specimen. The average of the 5 specimens is then taken and rounded to the nearest 5 psi. As concrete tensile strength relates to the strength of soil cement, ASTM C496 (2017) will be used for precision.

To determine if any outliers exist, the same method used by McLaughlin (2017) is used. The coefficient of variation for compressive strength found in Wilson (2013) of 7.1 percent for no capping of the specimen is used. Based on the number of test results, the multiplier of the coefficient of variation from ASTM C670 (2015) shown in Table 3.1 is used to obtain an acceptable range of results. The range is determined by taking the difference between the maximum and minimum strengths and dividing by the average strength of the cylinders (ASTM C670 2015). Since five cylinders were made for each testing day, the multiplier used will be 3.9 that yields an acceptable range of 27.7 percent. This method of identifying outliers is consistent with the way Wilson (2013) and McLaughlin (2017) identified outliers.

Table 3.1: Multiplier of Standard Deviation or Coefficient of Variation (Adapted from ASTM C670 2015)

Number of Test Results	Multiplier of Standard Deviation or Coefficient of Variation
2	2.8
3	3.3
4	3.6
5	3.9
6	4.0
7	4.2
8	4.3
9	4.4
10	4.5

3.3.4.2 DCP Testing

3.3.4.2.1 Moisture Content and Density

For consistency, each DCP soil cement specimen is created in a five-gallon bucket. Measuring of the volume of the DCP specimens is done prior to curing. The diameter around the bottom and top of the bucket are measured, as well as the full height of the bucket. Once the soil cement has been compacted in the bucket, five measurements are read with a ruler from top of the bucket to the top of the soil cement. These are measured to the nearest 1/16 of an inch. Four of the measurements were taken around the edge of the bucket and one was taken from the center to average the full height of the soil cement specimen and is shown in Figure 3.19. This height was subtracted from the total height of the bucket. This height is also used to interpolate the diameter between the top and bottom of the bucket. The diameter of the top of the soil cement specimen was averaged with the bottom diameter. The volume is then calculated using the volume equation of a cylinder, height multiplied by pi and the radius squared.



Figure 3.19: Height measurement of DCP specimen

The total weight of the soil cement specimen is measured just before DCP testing. At an age of either three or seven days, the DCP test is run and the moisture sample is recorded. The weights of the samples and equipment used were determined in accordance with ASTM D2216 (2010). The dry density is determined using Equation 3.1.

3.3.4.2.2 DCP Strength

Testing the dynamic cone penetrometer specimens follows the procedure of ASTM D6951 (2018). A 17.6-pound hammer with a 5/8-inch diameter steel rod with a 22.6-inch drop height met the requirements of ASTM D6951 (2018) and was used. All tests were completed using a replaceable 60-degree point tip that was replaced at maximum of 100 tests. The testing procedure follows the same as Nemiroff (2016) with the exception of using a Kessler Magnetic Ruler instead of manually recording readings. Figure 3.20 shows a picture of the Kessler Magnetic Ruler. The Kessler Magnetic Ruler recorded penetration readings after every blow in millimeters. This information is transferred directly from the magnetic ruler to a computer using a flash drive.



Figure 3.20: Kessler Magnetic Ruler

The DCP specimens were taken out of the cure room and transported back to the concrete block in which they were produced. The tip of the DCP is seated 1 inch (25 mm) to ensure the widest part of the tip is flush with the surface of the soil cement specimen. Figure 3.21 shows the arrangement of the DCP testing in the bucket. In accordance with ASTM D6951 (2018), if the penetration is less than 2 millimeters after 5 blows or the handle deflects more than 3 inches from the vertical position, the test is stopped and assumed to have reached refusal. The DCP is removed from the specimen by driving the hammer upwards against the top handle.



Figure 3.21: DCP testing arrangement in the specimen

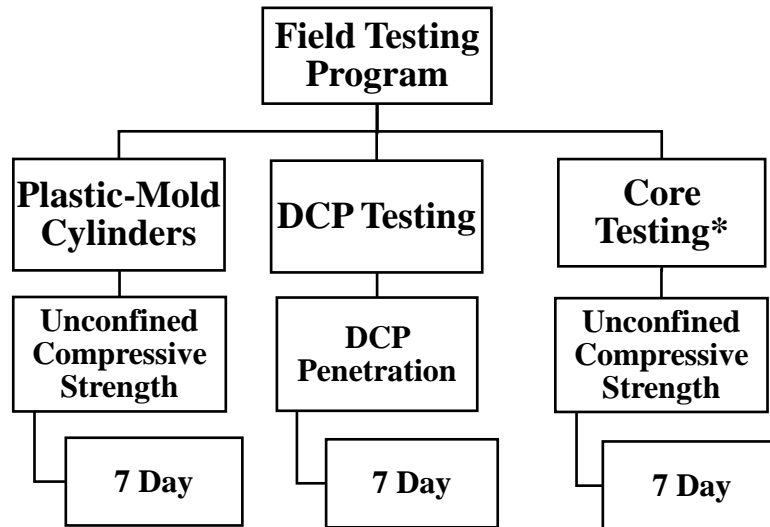
When the tests are completed and all the data has been collected, the penetration depth versus the blow count is plotted. To determine if there are any outliers, McLaughlin (2017) suggested an acceptable range between the DCP results of 50 percent. The procedure outlined in ASTM C670 (2015) is used to determine the percent range of the three slopes. If the maximum slope minus the minimum slope divided by the average slope of the tests multiplied by 100 is greater than 50 percent, an outlier existed. Any outliers are removed from the data. A trend line is produced from the three DCP tests in order to determine the slope of all of the tests. This slope is then plotted against the cylinder strengths to produce a relationship between DCP slop and PM cylinder compressive strength.

3.4 Field Testing Program

In order to evaluate the various strength testing methods of soil cement in the field, a testing program was developed for an ongoing ALDOT project. Figure 3.22 shows a summary of the field testing plan. Three different soil cement testing methods will be evaluated: a modified version of

the Plastic-Mold method (McLaughlin 2017) for molded cylinder strength, Dynamic Cone Penetrometer Method (ASTM D6951 2018), and core testing (ALDOT 419 2008). All molded cylinders will be tested at seven days to determine their unconfined compressive strength. The cores will be removed on the sixth day and tested on the seventh day for their unconfined compressive strength in accordance with ALDOT 419 (2008). The DCP tests will be run on the seventh day on the constructed soil cement base.

The results from the DCP tests will be converted into strength from the best-fit relationship determined from the data collected by Nemiroff (2016) and the results of the before mentioned laboratory study described in Sections 3.2 and 3.3. By converting the output from the DCP from the strength, the DCP results can then be compared to the unconfined compressive strengths found from testing cores and PM cylinders.



***Note: All core testing done by ALDOT**

Figure 3.22: Summary of Field Testing Program

3.4.1 Field Mixture

The field mixture evaluated for this research is shown in Table 3.2 and was developed by the Contractor, SA Graham Company, Inc. These data were obtained from testing performed by

Carmichael Engineering, Inc. This information was available at the time of making field molded specimens at the jobsite and was used during the production of the specimens. According to AASHTO Soil Classification, the soil used during the project was A-2-4 (0).

Table 3.2: Mixture properties of field mixture

Project Location	AASHTO Classification	Mixture Properties of Field Mixture		
		Cement Content, %	Optimum Moisture Content, %	Maximum Dry Density, lb/ft ³
Elba, AL	A-2-4 (0)	6	13.0	116.9

3.4.2 Location of Project Site

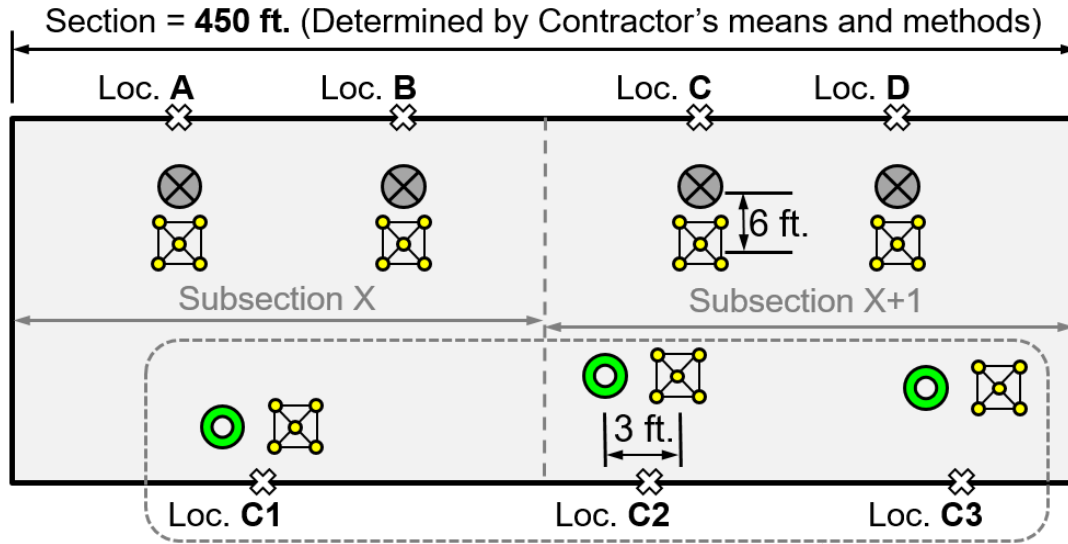
The field testing will take place along U.S. Highway 84 bypass between Elba and New Brockton, AL. The ALDOT project number was RPF-NHF-0012(507). The project’s objective is to construct two new westbound lanes. The project location is shown in Figure 3.23 with beginning coordinates of 31.401416 N, -86.010603 W and ending coordinates of 31.399468 N, -85.972982 W.



Figure 3.23: U.S. Highway 84 bypass project location (Google Maps)

3.4.3 Testing Strategy within a Section

Through previous field testing of McLaughlin (2017), testing of a soil cement section is considered. After further evaluating McLaughlin's results and the Contractor's practices, it was decided to use more testing locations within a section. This includes four testing locations for the PM cylinders and seven DCP testing locations. Figure 3.24 shows a schematic of the field testing plan. A section for the U.S. Highway 84 bypass project is considered to be about 450 feet in length which is the most the Contractor placed per day. The contractor planned to mix and compact half of the total section with one cement truck, and then plans to move on to the second half of the section in one day. Each of two parts within a section is labeled as a subsection. A more in depth description of what each subsection was throughout the length of the field work phase is detailed in Appendix N. Soil will be sampled at one-third and two-thirds the length of each subsection for a total of four locations per section in order to make a total of twenty PM cylinders, or five per sample location. The DCP will be tested at each sampling location for PM cylinders as well as at each of the three core locations in the section. A DCP test will be performed within three feet of the coring locations and within six feet of where the molded cylinder samples are taken. The core locations will not be known until the soil cement has been in place for six days when the core locations will then randomly be generated, so no PM samples will be compared directly to where the cores will be taken from. The DCP tests at the core locations will occur on the same day of the core being tested for its compressive strength, so mostly on the seventh day, or eighth day if the seventh day falls on a Monday as the staff does not core on a Sunday.



Where:



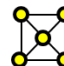
-  Sample location of PM cylinder material
-  Coring location performed by the contractor and tested by ALDOT
-  Location where 5 DCP tests are performed

Figure 3.24: Field testing plan

At each testing location, five DCP tests will be conducted. This is two more than that tested by McLaughlin (2017). NCDOT (2013) conducts five tests at each testing location as well. The number will be increased to five in order to determine the number of tests needed to test material with this variability while also being practical for a technician to conduct. The five DCP tests are arranged in a square pattern with a location at the center as shown in Figure 3.25. The points at the corners of the square are measured two feet apart from each other. The center location is one foot down and one foot across from the corner. The tests are conducted close enough so that they can be averaged together to represent the in-place strength at a location, yet not too close to be affected by another adjacent test. The order of the tests are important to keep consistency through all tests and be able to determine the number of DCP tests needed. The order was as follows: top left of

square (UL), top right of square (UR), center (CE), bottom left of square (BL), and then bottom right of square (BR).

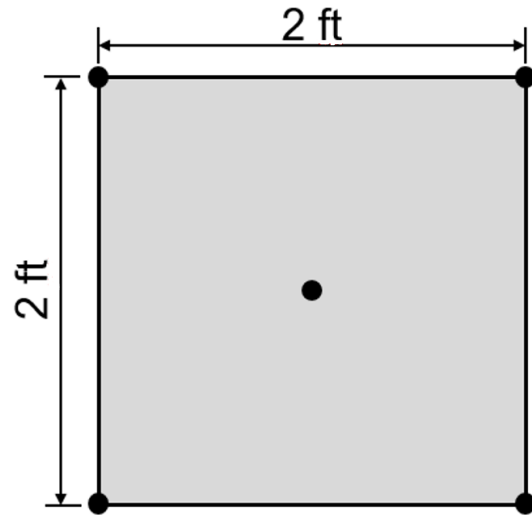


Figure 3.25: DCP testing pattern

3.5 Field Experimental Procedures

3.5.1 In-Place Sampling of Mixed Soil Cement

To make the plastic-mold cylinders, material samples will be taken after mixing of the soil cement mixture is finished in place. Samples will be taken twice from each subsection, for a total of four per section, as shown in Figure 3.24. Figure 3.26 shows material that has been mixed and is ready to be sampled.



Figure 3.26: Material ready to be sampled for PM cylinder production

Each location will have its own five-gallon bucket where the material is collected and covered by a lid immediately to reduce the loss of moisture. The sample buckets will then be transported to the jobsite house where the plastic-mold cylinders will be made. The buckets will be kept out of direct sunlight and protected from other sources of evaporation, such as wind, and contaminations during the preparation of the PM cylinders.

3.5.2 Plastic-Mold Cylinder Production

Figure 3.24 shows that on each day, four locations will be sampled to make soil cement cylinders, described in Section 3.5.1. The samples will be taken to the jobsite house located about five miles east of the project, along the US Highway 84 bypass. The samples will be stored on the porch that was roofed to keep the exterior conditions such as sun, wind, or rain from affecting the moisture content of the sample while the cylinders are being made.

Just as in the laboratory, 3-inch by 6-inch plastic-mold soil cement cylinders will be made. The plastic molds were cut and then taped together just like it is specified in Section 3.3.1.4 and

shown in Figure 3.10. Figure 3.27 shows the soil cement cylinder being compacted. Five cylinders will be made per sample bucket so a total of 20 cylinders will be made in a single day. The specimens will then be capped with plastic caps immediately after completing the compaction process.



Figure 3.27: Soil cement cylinder being compacted at jobsite house

3.5.3 Initial Curing

Sullivan et al. (2014) suggested that plastic-mold cylinders be stored on site until the following day before being transported. This was also the process that McLaughlin (2017) followed when creating field specimens. The specimens for this field portion will follow the same guidelines. Specimens will be kept safe in the shade on the porch next to where the cylinders were made as can be seen in Figure 3.28. The specimens will be kept on site for about 24 hours and then transported back to the laboratory at Auburn University. The specimens are to be placed in a bin and wrapped with soft towels to prevent damage during transport.



Figure 3.28: PM specimens during initial curing on site

3.5.4 Plastic-Mold Extrusion

Once the PM specimens have safely been returned to the laboratory, the same extrusion process used for the laboratory PM cylinders as described in Section 3.3.2.1. The tape is removed, then the mold is split, and the cylinder is removed as shown in Figure 3.12. The cylinders will be weighed and measurements will be taken of the diameter and height as can be seen in Figure 3.15. These values will be used to calculate the density of each specimen. Each specimen will then be placed into a plastic bag, sealed, wrapped with a rubber band, and placed in the moist-cure room as described in Section 3.3.3.1.

3.5.5 Final Curing

The final curing of the plastic-mold cylinders will follow the same procedure as the laboratory PM specimens. A detailed procedure is given in Section 3.3.3.1.

3.5.6 Testing

3.5.6.1 Plastic-Mold Cylinder Testing

3.5.6.1.1 Moisture Content and Density

Volume measurements, such as length, diameter, and weight, were determined before the soil cement cylinders were sealed in plastic bags, as described in Section 3.3.4.1.1. Density is then

determined by using Equation 3.1. Moisture contents will be taken using the same method used for the laboratory specimens by following ASTM D2216 (2010). The compaction percentage will then be determined by taking the dry density and comparing it to the maximum dry density as stated in Table 3.2.

3.5.6.1.2 PM Cylinder Compressive Strength

Compression strength testing will follow the same testing practices described in Section 3.3.4.1.2 for the laboratory-produced soil cement cylinders. ASTM C670 (2015) will also be used to determine if there are any outliers while using the same coefficient of variation for molded cylinders of 7.1% that Wilson (2013) recommended. Five cylinders were made at each location, same as in the laboratory, the same multiplier of 3.9 from Table 3.1 will be used.

3.5.6.2 DCP Testing

3.5.6.2.1 Moisture Content and Density

The moisture content and density of the in-place soil cement will be determined through the use of a nuclear gauge, shown in Figure 3.29. The nuclear gauge will be run one time on each subsection, as shown in Figure 3.24. Although the DCP tests will not be run directly where the nuclear gauge test is run, the result of this singular nuclear gauge test per subsection is related to all of the DCP tests run in that subsection.



Figure 3.29: Use of nuclear gauge on test section

3.5.6.2.2 DCP Strength

The dynamic cone penetrometer testing will follow the procedure of ASTM D6951 (2018) as discussed in Section 3.3.4.2. The tests will be completed using a replaceable point tip with a 60 degree angle which is shown in Figure 3.30. This tip is to be replaced after every 100 tests or when it is visible that the tip has been damaged which may impact results.



Figure 3.30: Replaceable DCP tip

Before the tests are run, the DCP will be assembled and inspected for any damaged parts. Testing will begin once all pieces making up the DCP pass inspection. The testing locations are explained in Section 3.4.3 and are shown in Figure 3.24. Five tests will be conducted at each location as specified by the pattern shown in Figure 3.25 and an example shown in Figure 3.31.

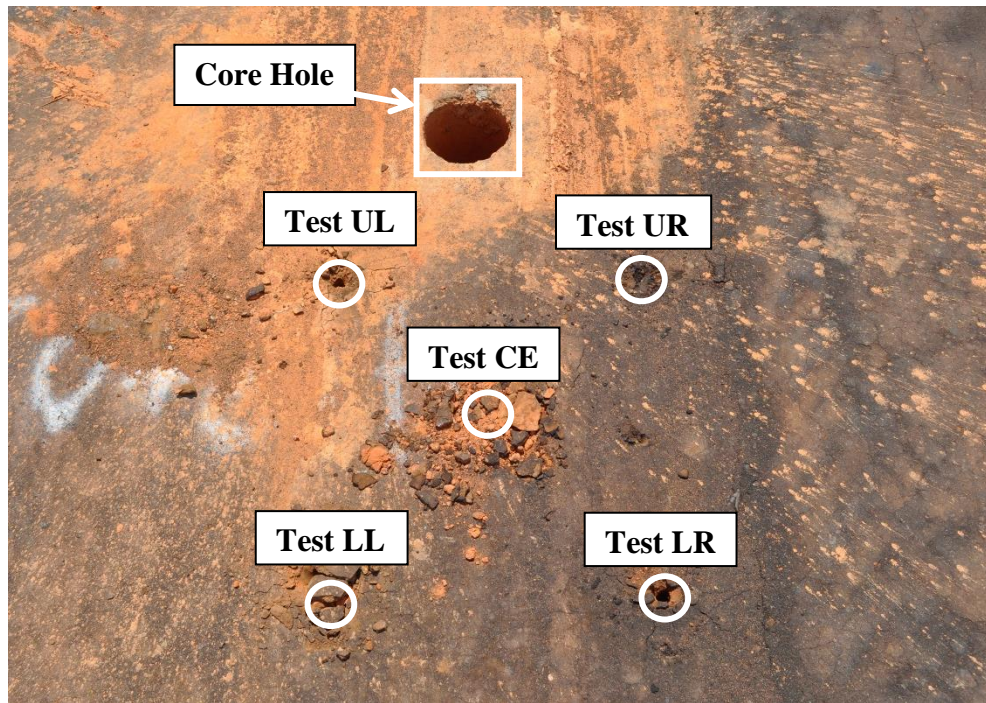


Figure 3.31: Testing pattern for each DCP testing location

Before starting to record penetration depth readings, the DCP will be held vertically and seated a depth of 1 inch (25 mm) into the soil cement base so that the widest part of the tip is level with the surface of the soil cement. A Kessler Magnetic Ruler will be used to record data for the DCP testing which allows for an easier one-person operation. The Magnetic Ruler and manual ruler can be seen in Figure 3.32. The operator of the DCP will hold it up vertically, raise the hammer until it makes light contact with the top handle, and will then release the hammer to initiate a blow. The Kessler Magnetic Ruler specifications were covered in Section 3.3.4.2.2. When reading the ruler manually, the penetration is recorded using the millimeter scale after every five blows. This process continues until 175 millimeters of total penetration is reached, after seating. If at any point the penetration is 2 millimeters or less after 5 blows or if the handle deflects 3 inches from the vertical position, the test is deemed to reach the refusal limit and will be stopped in accordance with ASTM D6951 (2018). After testing, the DCP is removed from the soil cement

base by striking the hammer upwards against the bottom of the handle. When all five tests have been completed at each location, the penetration depth versus the blow count will be plotted to determine the average strength of this test location. To determine any outliers from the five tests, the process used for the laboratory outlined in Section 3.3.4.2.2 will be used.



Figure 3.32: Magnetic ruler and manual ruler used for DCP testing

3.5.6.3 Core Testing

ALDOT Section 304 (2016) states that the Contractor must recover and test at least two cores from random locations within each sampling interval. As mentioned earlier, this project consists of 450-foot long sections. The Contractor decided to have three cores removed over each section where two will then be chosen and averaged together. If the sixth day is on a Sunday, the cores will be extracted on Monday and tested on Tuesday. The Contractor only placed soil cement during the week so no testing occurred on the weekends. The three core locations per section will be picked at random by the Engineer and then Carmichael Engineering will recover them for SA Graham. Cores being recovered are shown in Figure 3.33.



Figure 3.33: Core being recovered from the section

After removal, each core will be measured to make sure it meets the criteria. If the core meets the height requirement as specified by ALDOT Section 304 (2016), it shall be placed in a plastic bag to minimize moisture loss seen in Figure 3.34. The core will then be placed in a cooler while being transported by ALDOT to their testing facility in Troy, Alabama. If the core does not meet the height requirement, another core will be recovered from a nearby location. Multiple core holes for a single location are shown in Figure 3.35. ALDOT's 7th Division will perform all the compressive strength testing on the cores obtained for this project.



Figure 3.34: Core being placed in plastic bag



Figure 3.35: Multiple attempts at retrieving a valid core sample

Chapter 4

Presentation and Analysis of Laboratory Testing Phase Results

4.1 Introduction

In this chapter, results of the laboratory testing phase described in Chapter 3 are presented and discussed. An in-depth analysis of the dynamic cone penetrometer results with respect compared to the plastic-mold cylinder strength results is presented. The correlation between the two are then established and discussed with comparisons to other similar correlations. A summary of all data collected are presented in Appendices A through H.

4.2 Material Classification

Section 3.2.4 described the methods to determine the AASHTO and USCS classification of the different soils used in this project. Table 4.1 summarizes the results and classifications of each of the soils. Gradation curves of the soils can be found in Appendix A. No liquid limit (LL) or plasticity index (PI) was tested for the Coarse soil.

Table 4.1: Summary of soil properties and classifications

Soil Name	Percent Passing #200 Sieve	LL	PI	USCS	AASHTO
Waugh Clay	38.9%	21*	18*	SC	A-6b
Waugh Sand	1.2%	N/A	N/A	SP	A-1b
Waugh	8.3%	14*	12*	SP-SC	A-2-6
Elba	0.9%	N/A	N/A	SM	A-2-4
Coarse	8.2%	N/A	N/A	SW-SC	A-1b

*Completed by Matt Barr (Nemiroff 2016)

4.3 Mixture Properties

Section 3.2.2 describes the laboratory test performed to collect the mixture properties of each of the soils. Tables 4.2 through 4.4 show the cement contents, optimum dry densities, and

maximum dry densities for Waugh soil, Elba soil, and Coarse soil, respectively. The Proctor moisture-density curves for these mixtures can be found in Appendix A.

Table 4.2: Mixture properties of Waugh laboratory mixtures

Mixture Properties of Waugh Laboratory Mixtures		
Cement Content, %	Optimum Moisture Content, %	Maximum Dry Density, lb/ft ³
4	12.0	119.4
5	10.7	120.0
6	12.0	120.5
8	11.4	123.8
10	11.5	124.0

Table 4.3: Mixture properties of Elba laboratory mixtures

Mixture Properties of Elba Laboratory Mixtures		
Cement Content, %	Optimum Moisture Content, %	Maximum Dry Density, lb/ft ³
5	12.4	115.0
6.5	13.8	115.1
8	12.2	116.9

Table 4.4: Mixture properties of Coarse laboratory mixtures

Mixture Properties of Coarse Laboratory Mixtures		
Cement Content, %	Optimum Moisture Content, %	Maximum Dry Density, lb/ft ³
4	11.7	120.5
6	11.2	123.8
8	10.8	125.2
9	11.0	125.3
10	10.2	126.2

4.4 DCP Initial Curing Study

Section 3.3.2.2 describes the two different types of initial curing methods used throughout the laboratory testing phase. A total of three soil cement mixtures were made. A total of four DCP specimens were compacted. Two DCP specimens using the plastic clip and plastic lid methods were produced. Then a DCP test was run that compared the DCP slopes at a depth of 75 millimeter on the seventh day. The results of this study are shown in Table 4.5. Using the plastic lid method tends to have a slightly lower slope value than the plastic sheet and clips. There is minimal effect on strength with how similar the slopes are while using these different initial curing methods for the DCP specimens; therefore, with both curing methods showing similar results, all DCP specimens produced using either method are combined in the final results. The 75 millimeter penetration analysis of all initial curing study specimens can be found in Appendix B.

Table 4.5: DCP Initial Curing Study Results

Cement Content (%)	Plastic Lid Method Slope (mm/blow)	Plastic Sheet and Clip Method Slope (mm/blow)	Percent Difference
4	2.6432	2.8156	6.3%
6	2.0018	2.1116	5.3%
8	1.7364	1.9735	12.8%

4.5 Soil Classification Impact

Nemiroff (2016) found that soils containing less particles that pass through the No. 200 sieve, tend to need more cement content to reach higher molded cylinder compressive strengths. This is also seen in the DCP results of Nemiroff (2016) that showed that more particles passing through the No. 200 sieve needed more blows to penetrate further into the soil. However, both the cylinder strength and DCP blow count increase, Nemiroff (2016) concluded that the best-fit correlation between DCP output and compressive strength is unimpacted by soil type.

Figure 4.1 shows a comparison of the plastic-mold cylinder strength results versus cement content for the different soil classifications. Figure 4.2 shows a similar comparison, except using the DCP slope results at 75 mm penetration depth versus the cement content of the soil cement mixture. The DCP slope was obtained by penetrating the soil cement specimen at a penetration depth of 75 millimeters. The data pertaining to this study can be found in Appendix C. These slopes are further evaluated and discussed in Section 4.5.1. These results are similar to the literature from ACI 230 (2009) that states “soils containing between 5% and 35% fines passing a No. 200 sieve produce the most economical soil cement” as well as results found in Nemiroff (2016).

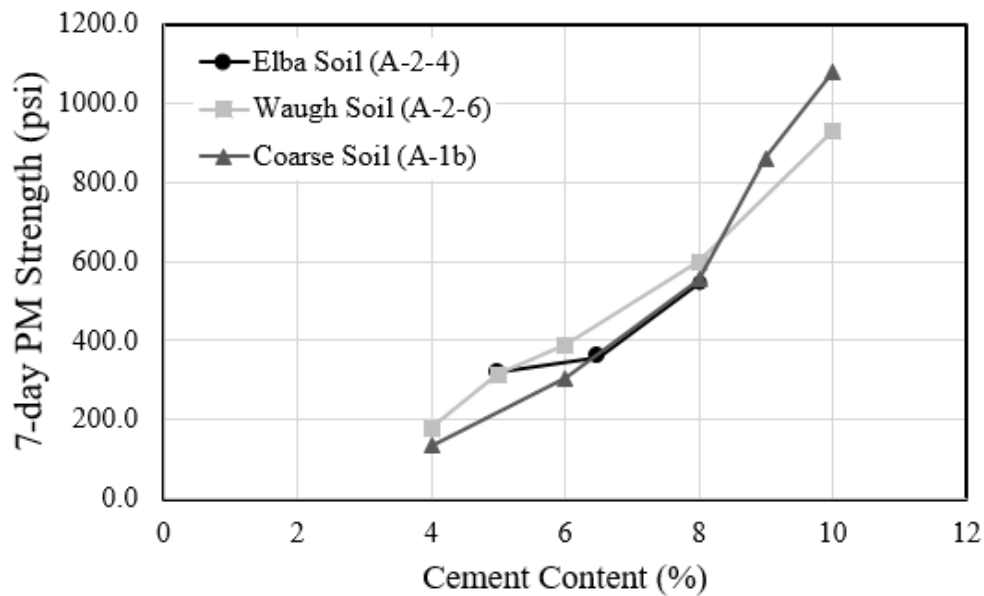


Figure 4.1: Effect of soil classification on PM cylinder strength

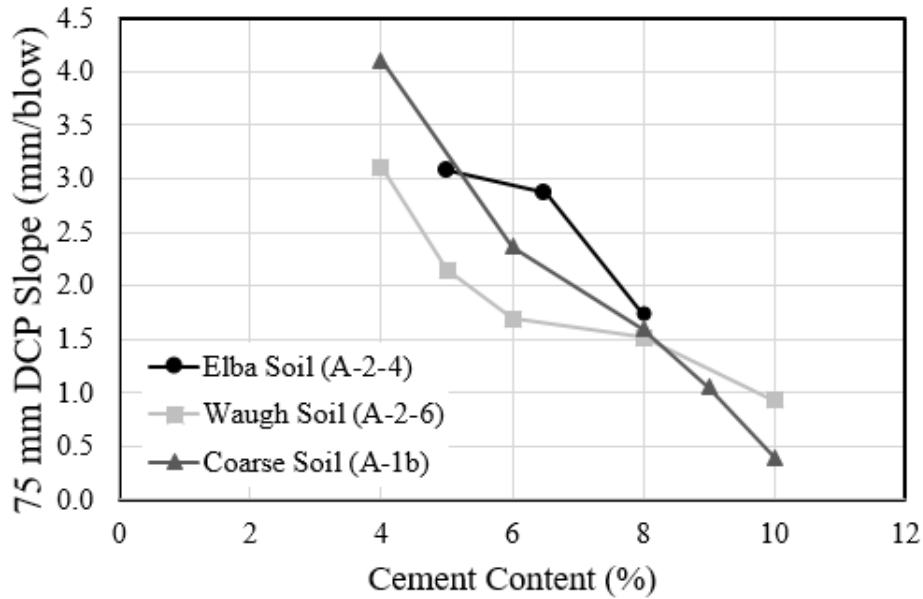


Figure 4.2: Effect of soil classification on DCP slope

4.6 Suitability of Dynamic Cone Penetrometer

The suitability of the dynamic cone penetrometer was assessed to make sure that it would penetrate the soil cement after curing. In accordance with ASTM D6951 (2018), if a penetration of 2 mm was not reached over 5 blows, then the test was stopped as it had reached refusal by the 75 mm depth. Nemiroff (2016) ran tests of soil cement with a strength range from 100 psi to 1,000 psi and found that refusal was reached at 800 psi. Using different soils and cement contents, the DCP was assessed again over the strength range of 100 psi to 1,080 psi. Table 4.5 provides a summary of the penetration versus strength results obtained from this study.

Table 4.6: Summary of the penetration versus strength investigation

Strength (psi)	Refusal (Yes/No)
100	No
205	No
340	No
465	No
545	No
635	No
740	No
860	No
930	No
965	Yes
1080	Yes

The point of refusal was not obtained through the soil cement specimens at 75 mm until a compressive strength of 965 psi was reached. At 965 psi, the DCP was unable to create any penetration in the soil. The DCP was able to still penetrate in strengths well above 650 psi, the maximum strength allowed by ALDOT, so no changes of the standard DCP as defined in ASTM D6951 (2018) were needed.

4.6.1 DCP Penetration Depth Analysis

An analysis was performed on all of the retrieved DCP data. The figures presented in 4.5.1.1 through 4.5.1.5 are shown as a demonstration of the process used to analyze each soil cement mixture. All graphs that are shown are from the same soil cement mixture; however, overall conclusions are based on all the tests that were performed.

For each mixture design, the three DCP specimens that were created were tested. The penetration data obtained were plotted on the x-axis against the DCP penetration in millimeters on the y-axis. A linear-regression analysis was used on each set of data to determine the slope of the best-fit line across different depths of analysis. The y-intercept was restricted to zero, as it is a fact that all results started at zero. The penetration depths that were evaluated were 25, 50, 75, 100, and

175 millimeters. All data recovered from the DCP test was processed to provide a data point at every 5 millimeters of penetration. With the magnetic ruler pulling depth of penetration readings after every blow, linear interpolation of the surrounding data was used to achieve a data point at every 5 millimeters in depth. This was also deemed necessary as some weaker soils would have too few data points for reliable regression analysis. A summary of the different penetration depths is shown in Figure 4.3.

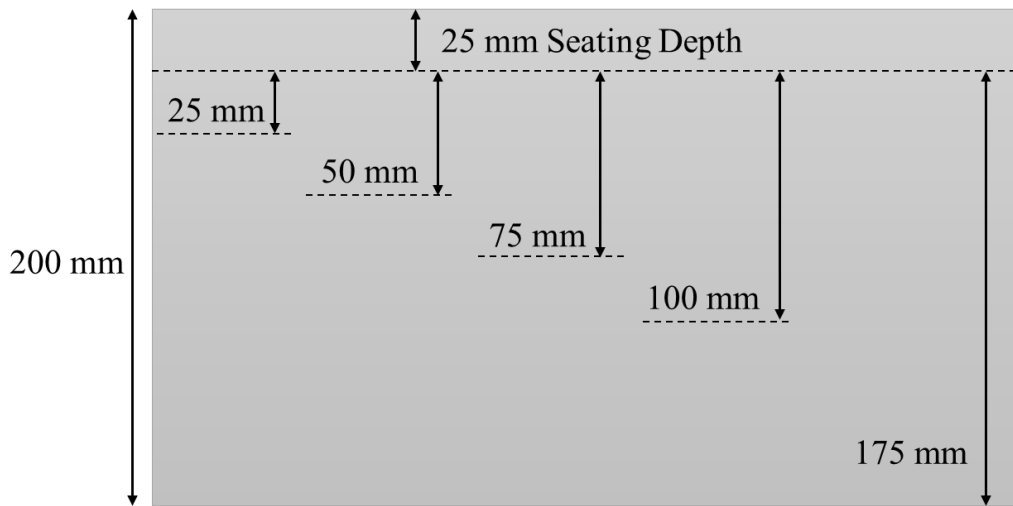


Figure 4.3: Penetration depth summary

Nemiroff (2016) concluded that a 75 millimeter (3 inches) was the most ideal penetration depth as it produced the best results with the least amount of technician effort. McElvaney and Djatnika (1991) used penetration depths of only 2 inches. These penetration depths were analyzed and compared to determine which penetration depth produced the most accurate results while using the least amount of effort when performing a DCP test. A summary of all the data from each mixture design can be found in Appendices D through H.

Outliers were determined through the same method used by McLaughlin (2017). Any data that exhibited a range greater than 50 percent were deemed to contain an outlier test (McLaughlin 2017). The range was evaluated following ASTM C670 (2015). Once all three slopes of the three

laboratory tests were determined, the percent range was determined by taking the maximum slope minus the minimum slope divided by the average of all three slopes. In the laboratory phase, outliers were only found for the 25 millimeter depth analysis.

4.6.1.1 Twenty-five Millimeter Penetration Depth Analysis

An analysis was performed on only 25 millimeters (1 inch) of penetration. This depth is about 15 percent of the full penetration depth, not including the seating depth. Example results based on 25 millimeters of penetration are shown in Figure 4.4. The coefficient of determination is as high as with some of the other analysis depths. There were also two outliers found in this analysis while the other laboratory depths had zero. Based upon the results from Nemiroff (2016), a one-inch depth was not the best at characterizing the results of the entire depth.

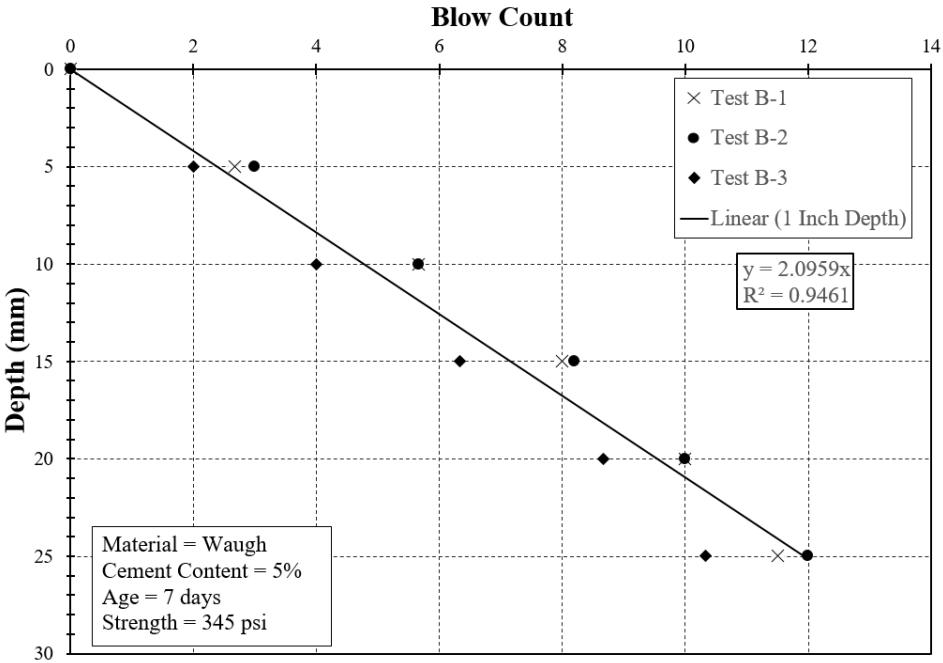


Figure 4.4: Twenty-five millimeter depth penetration to blow count relationship

4.6.1.2 Fifty Millimeter Penetration Depth Analysis

Example results from this depth analysis can be found in Figure 4.5 for one of the mixtures. The slope of this line compared to the 25 millimeter analysis decreased and the coefficient of

determination increased leading to better results. This indicates a better linear relationship at this depth than that of the 25 millimeter depth. Research performed by Nemiroff (2016) and McLaughlin (2017) showed that the results from the DCP at 50 millimeters in depth would not be much different than that of the 75 millimeter depth.

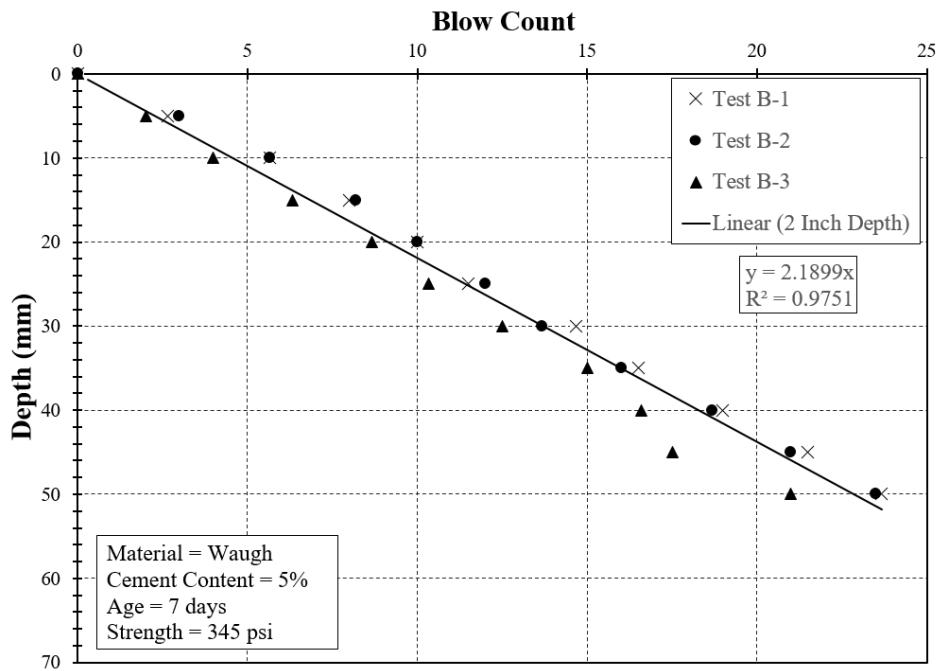


Figure 4.5: Fifty millimeter penetration depth to blow count relationship

4.6.1.3 Seventy-five Millimeter Penetration Depth Analysis

Next, a penetration depth of 75 millimeters was analyzed to determine if this depth would continue to produce the most accurate results with the least amount of technician effort, as concluded by Nemiroff (2016) and McLaughlin (2017). An example of the relationship at an analysis depth of 75 millimeters is shown in Figure 4.6. In this one example, the penetration slope decreased from the 50 millimeter depth and the coefficient of determination increased. In this case, this indicates that the soil cement gets a little stronger with depth while keeping a strong linear relationship.

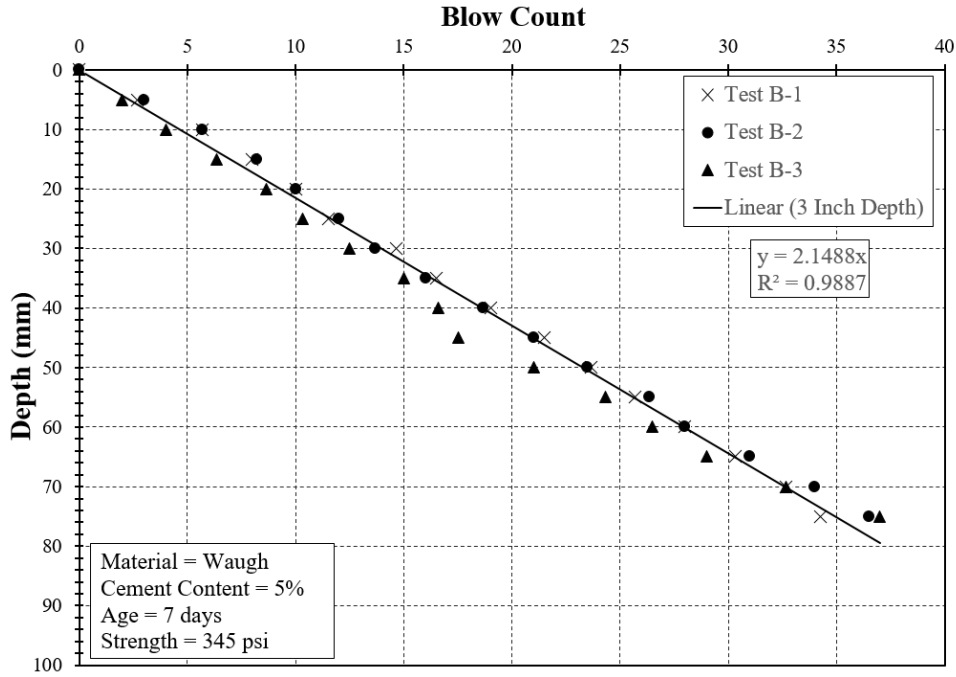


Figure 4.6: Seventy-five millimeter penetration depth to blow count relationship

4.6.1.4 One-hundred Millimeter Penetration Depth Analysis

A penetration depth of 100 millimeters was then analyzed to determine if this depth would show different results when compared to the 75 millimeter penetration analysis. This depth had been seen to show very similar results to the 75 millimeter depth according to Nemiroff (2016) analysis. This depth was checked to make sure the accuracy was still similar. An example of the relationship at an analysis depth of 100 millimeters is shown in Figure 4.7. The penetration slope decreased only a little from the 75 millimeter depth, but the coefficient of determination decreased in this case.

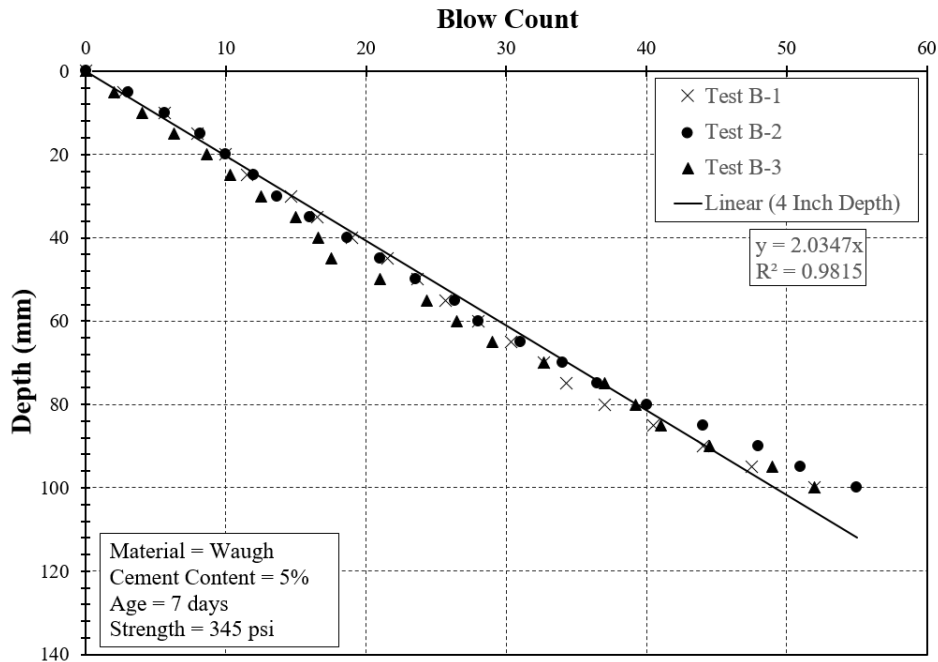


Figure 4.7: One-hundred millimeter penetration depth to blow count relationship

4.6.1.5 Full-depth Analysis

The full set of data collected over a penetration ranging from 0 to about 175 millimeters was analyzed to determine if the strong linear relationship continued throughout the entirety of the sample. An example of full-depth penetration data of the dynamic cone penetrometer is presented in Figure 4.8. As shown, the strong linear relationship between blow count and penetration is continued from the 100 to 175 millimeter depth analyses. The relationship follows the laboratory research done by Nemiroff (2016) using uniformly mixed soil cement as well as the research performed on soil cement and lime-stabilized soils by Enayatpour et al. (2006).

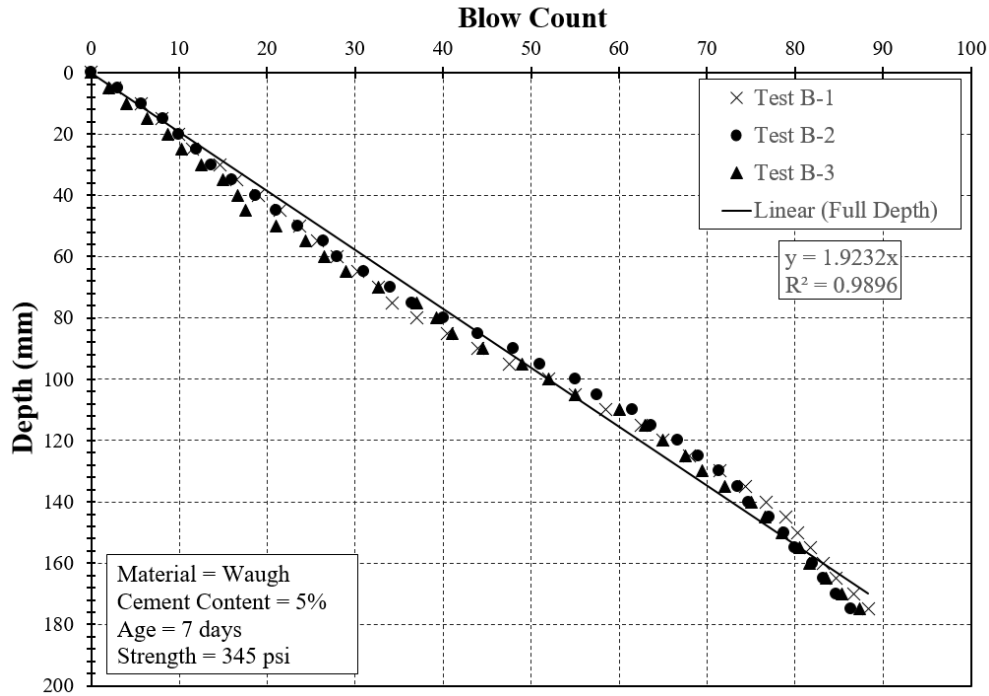


Figure 4.8: Full-depth penetration relationship between 0 and 175 millimeters to blow count

4.6.2 Conclusions of the Penetration Depth Analysis

The average coefficient of determination for each penetration depth for all data analyzed for this laboratory testing phase is shown in Figure 4.9. Range bars were added to the plot to show the minimum and maximum coefficient of determination obtained for each depth analysis. The penetration depth with the highest average value was 75 mm penetration depth. It is noticeable in Figure 4.9 that the range of coefficient of determination decreases as the analysis depth is increased, with a significant improvement observed between the 50 millimeter to 75 millimeter analysis depths.

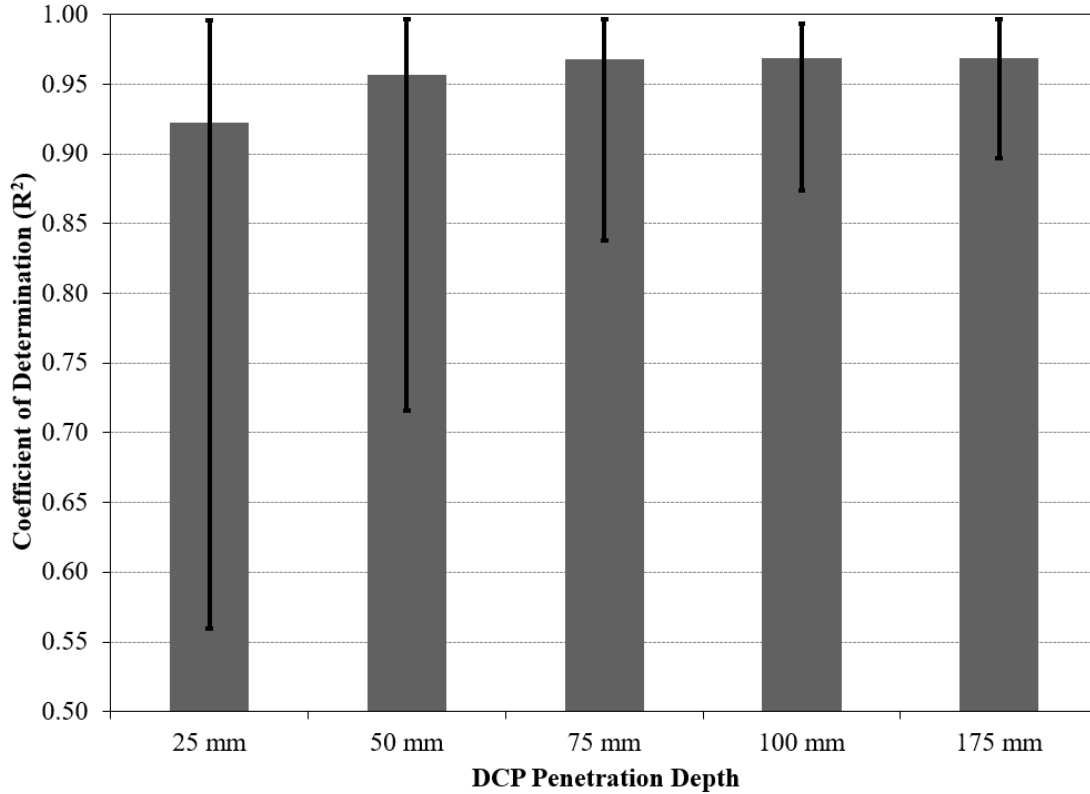


Figure 4.9: Coefficient of determination for all DCP data collected on penetration depth

Using the data analyzed, Table 4.6 was created to estimate the quantity of DCP blows needed to penetrate a certain depth dependent upon the strength of the soil cement. The strength range was chosen based on the ALDOT 304 (2014) specification requirements for in-place strength of the soil cement. As expected, with an increase in soil cement strength and penetration depth, there is an increase in how many blows are required leading to more technician time and effort. Based on the average coefficient of determination of each of the penetration depths and the required effort, it is recommended that 75 millimeters (3 inches) of penetration depth be used by ALDOT which is in agreement with the findings of Nemiroff (2016) and McLaughlin (2017).

Table 4.7: Summary of blow counts needed to reach each penetration depth

Penetration Depth	Blow Count		
	250 psi	425 psi	600 psi
25 mm	9	13	20
50 mm	18	26	39
75 mm	26	40	59
100 mm	35	53	79

4.7 DCP to Unconfined Compressive Strength Correlation

4.7.1 Introduction

As determined by Nemiroff (2016), McLaughlin (2017), and the data before, the DCP was able to penetrate throughout the desired strength range required by ALDOT 304 (2014) of 250 psi to 650 psi. This research made sure the DCP was still a viable option regardless of the soil type. Nemiroff (2016) determined that a logarithmic function had the best correlation between the DCP slope and the molded cylinder strength (MCS). Section 2.5.5.3 covers some DCP to unconfined compressive strength correlation equations that were determined from McElvaney and Djatnika (1991), Patel and Patel (2012), Enayatpour et al. (2006), and Nemiroff (2016). Based on the results from the penetration depth analysis discussed in Section 4.5.2, a penetration depth of 75 millimeters will be used. The results collected in this study were combined with those developed by Nemiroff (2016) at a penetration depth of 75 millimeters. The dataset consists of 435 cylinders and 207 DCP specimens were produced and tested at 3 days and 7 days.

4.7.2 Logarithmic Function for DCP to MCS Correlation

The logarithmic function and coefficient of determination developed for the collected data are presented in Figure 4.10 for the results of different soil types. The function is developed from the new data collected during the laboratory testing phase of this study.

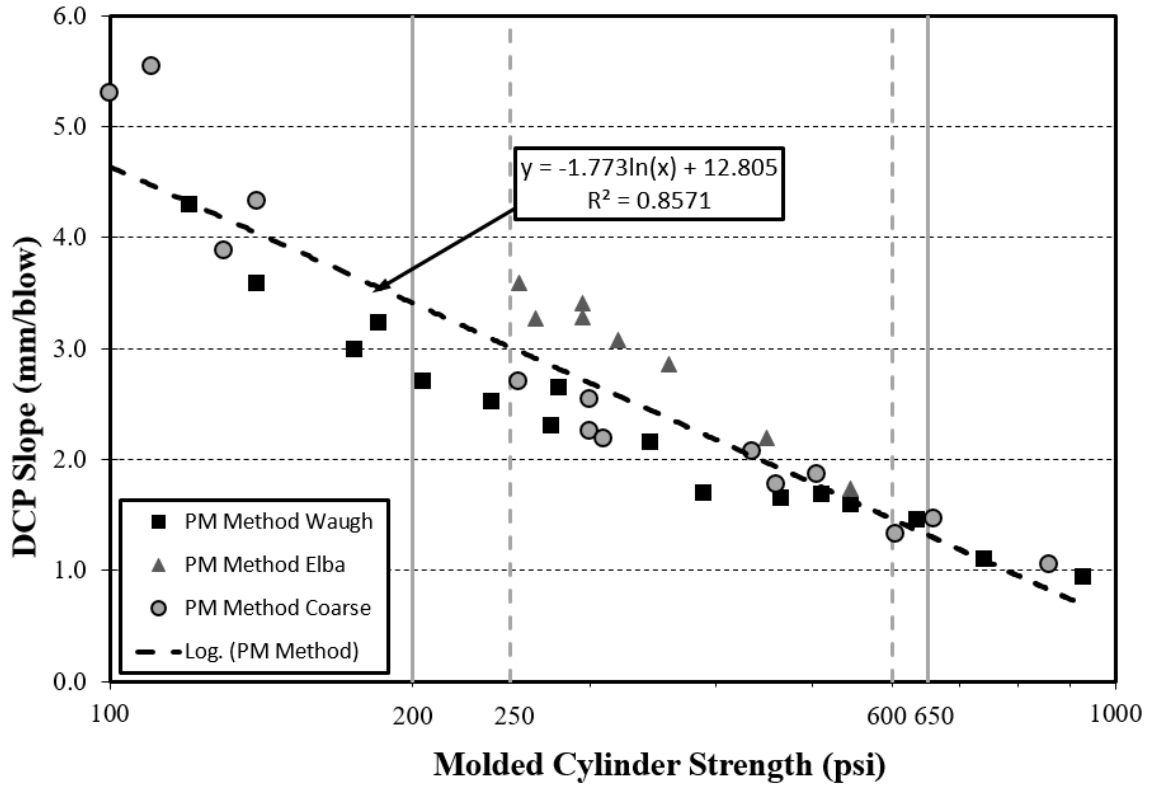


Figure 4.10: Logarithmic relationship between DCP slope and MCS of the different soils

Figure 4.11 shows all of the data points combined as one data set to obtain the best-fit logarithmic relationship. This relationship is based on a variety of soils and provides a strong correlation which would be able to better estimate the strength of more types of soils used to create soil cements.

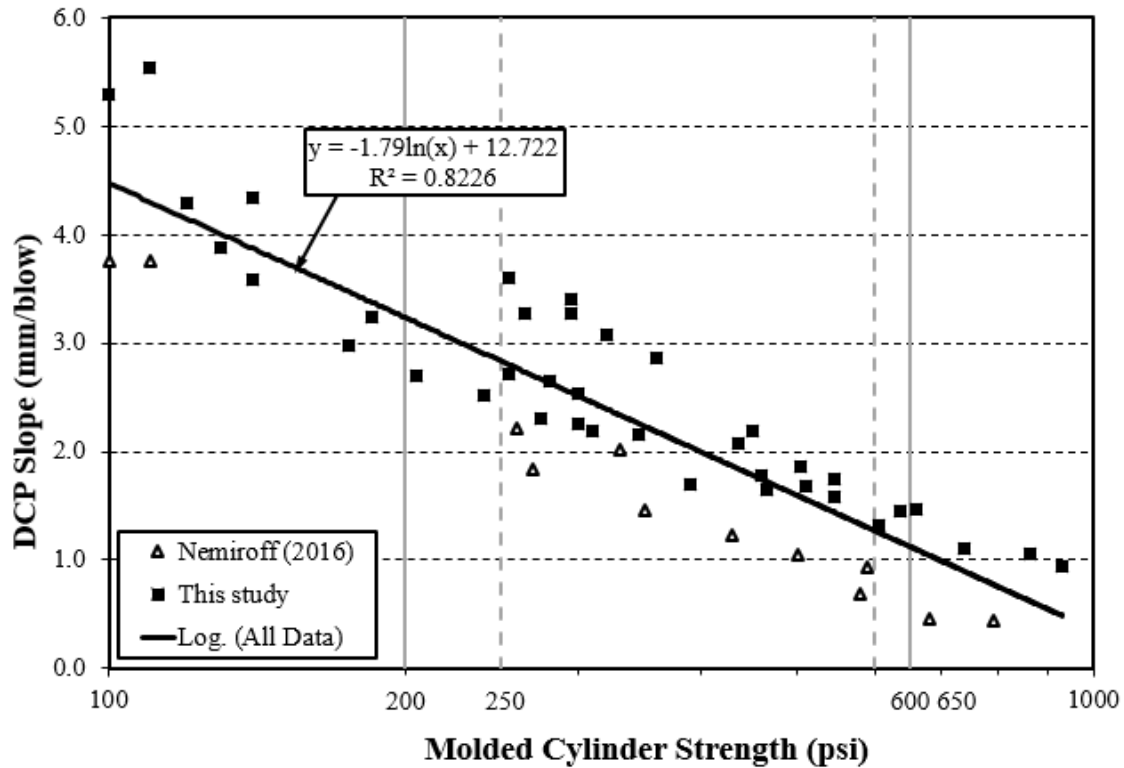


Figure 4.11: Best-fit logarithmic equation for all data collected

4.7.3 Correlation Analysis

Based on the data collected in this study and by Nemiroff (2016), it was determined that the best relationship between the DCP slope and cylinder strengths was obtained with the function displayed in Figure 4.11. The relationship between the DCP output and molded cylinder strength have a high coefficient of determination of 0.8226 which indicates strong linear relationship between molded cylinder strength and DCP slope. The strong relationship agrees with the results from Patel and Patel (2012) who tested a variety of soil classifications and concluded that a single equation is all that is necessary to relate all soil types.

For ease of calculation, the best-fit logarithmic function shown in Figure 4.11 was rearranged and is presented as Equation 4.1. This equation is valid for a strength range between 100 and 930 psi.

$$MCS = 1220e^{-0.559DCP} \quad (\text{Equation 4.1})$$

Where:

MCS = molded cylinder strength (psi), and

DCP = dynamic cone penetrometer slope (mm/blow).

As previously discussed, the unconventional units in this equation were chosen for several reasons. When collecting data with the dynamic cone penetrometer, it is more accurate and easier to record in millimeters. The magnetic dynamic cone penetrometer also outputs its data in millimeters. McElvaney and Djatnika (1991), Patel and Patel (2012), and Nemiroff (2016) all utilized millimeters to collect DCP results. ASTM D6951 (2017) recommends recording DCP penetration in millimeters.

4.7.4 Comparison to Other Published Correlations

In order to compare the correlations, each of the correlations developed by the researchers was plotted on a single graph. Each correlation is plotted using the range of strengths tested. The comparison of these functions can be seen in Figure 4.12. The McElvaney and Djatnika (1991) function was a correlation created for lime-stabilized soils. Patel and Patel (2012) created a function using a variety of stabilized soils that reasonably predicted strength between the 200 and 360 psi range. Nemiroff (2016) created the logarithmic function estimating the range of 100 to 800 psi. The relationship proposed in Equation 4.1 is within range of the other functions, and when considering it was developed for a wide strength range and different soil types it is recommended for ALDOT to implement.

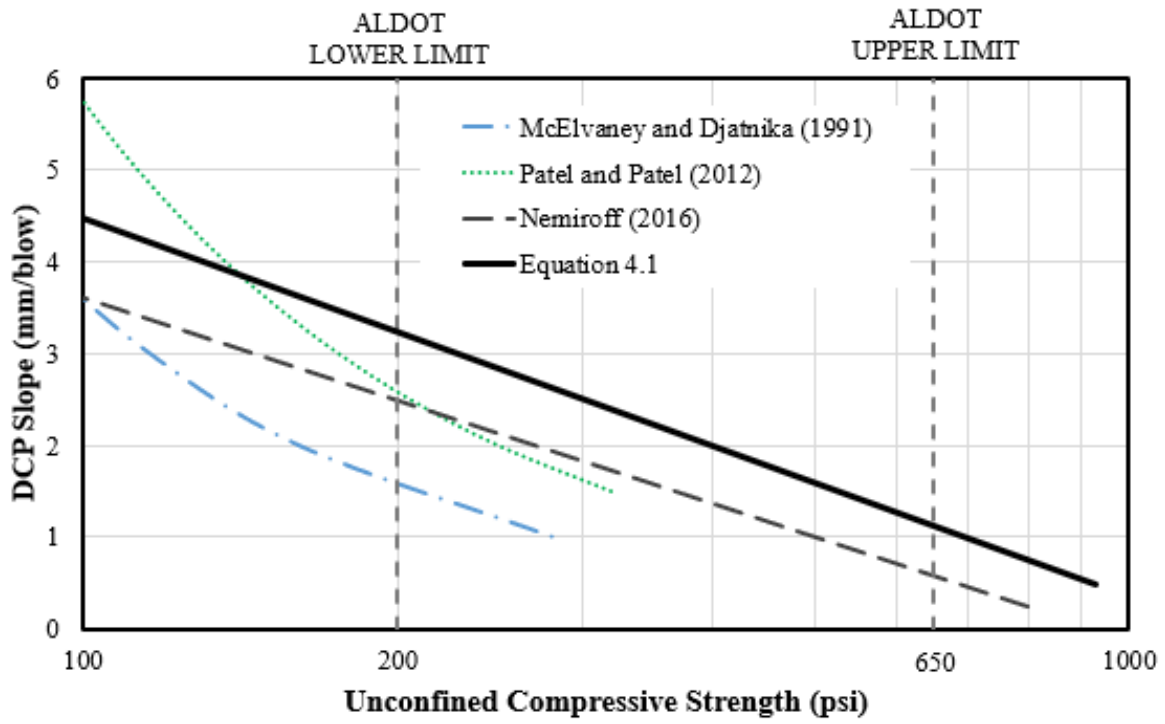


Figure 4.12: Comparison of Equation 4.1 to other published correlations

Chapter 5

Presentation and Analysis of Field Testing Phase Results

5.1 Introduction

In this chapter, results from the experimental field testing phase covered in sections 3.4 and 3.5 are presented and discussed. An in-depth analysis of the DCP results is presented. Analysis is presented to determine the most efficient number of tests and penetration analysis depth to obtain sufficiently accurate results. The compressive strength results from the plastic-mold cylinders and core strengths are presented and evaluated. All the data collected from the ALDOT's US Highway 84 bypass soil cement base project can be found in Appendices I through O.

5.2 Dynamic Cone Penetrometer Analysis

This section is used to discuss the reason for performing an extensive analysis on the DCP. Following that is how the data were analyzed to produce the results. Then a discussion on how the most efficient penetration depth and number of tests needed was chosen is presented.

5.2.1 Reasons for Analyzing DCP Results for Outliers

The main reason for analyzing the DCP results is similar to the laboratory phase, to have a consistent method that obtains reliable results. When tests were conducted in the laboratory, the mixtures were reasonably uniform as they were produced under controlled conditions. When conducted in the field, each individual DCP test showed a strong correlation between blow count and penetration depth. However, in some instances when five DCP tests were plotted from a single location, the correlation began to show some variation. These findings were similar to that of McLaughlin (2017). There were a few different types of variability in the results. Figure 5.1 shows an example of variability caused by a change of slope throughout the test. This example starts with

all tests being very close together and being reasonably linear for the first 50 millimeters of penetration, then the linear relationship changes as the slope flattens. Then again after about 140 millimeters, the test curves begin to follow the same slope it began with.

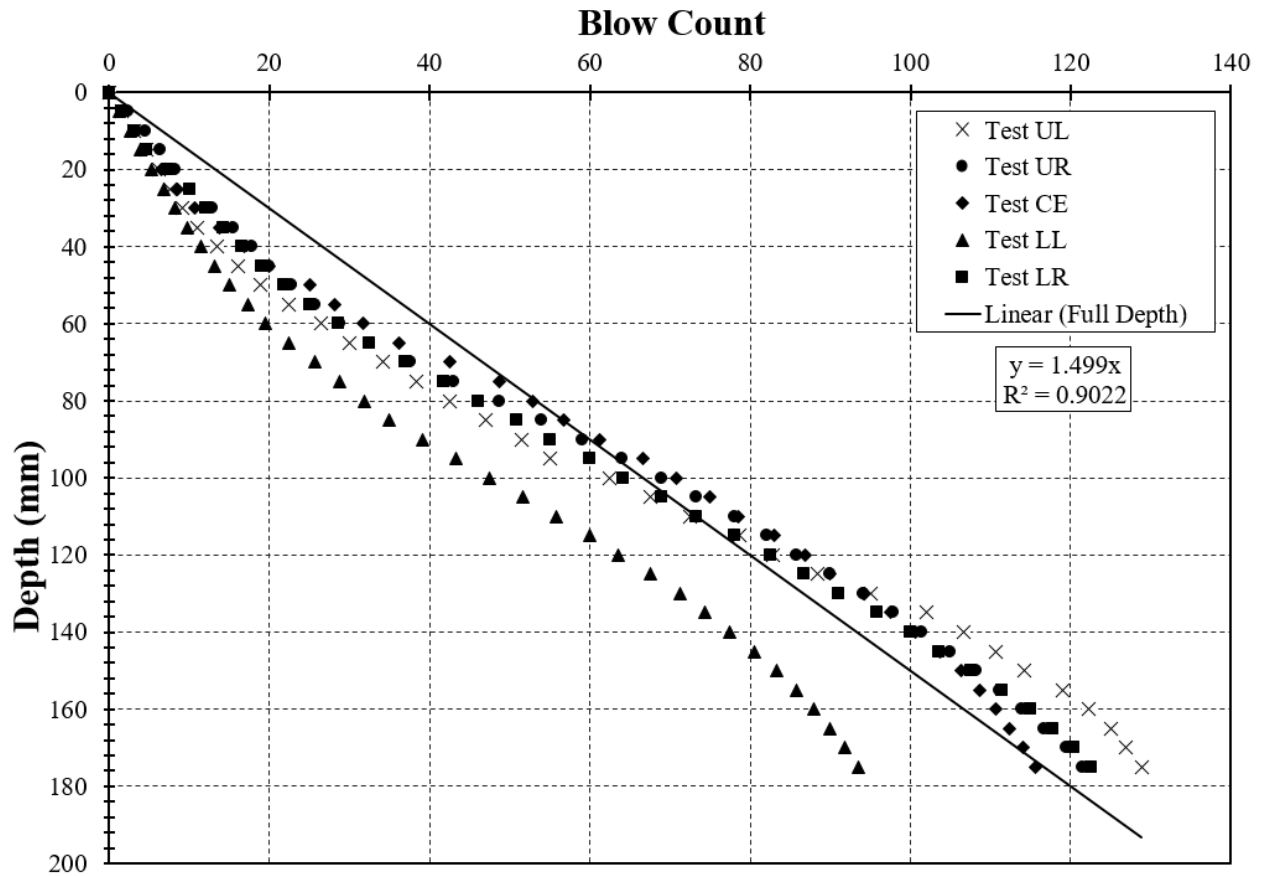


Figure 5.1: First example of highly variable DCP test results on US Highway 84 bypass

Figure 5.2 shows an example of refusal where all the tests have similar slopes for the first 50 millimeters of penetration; however, the one test reaches refusal in accordance with ASTM D6951 and the slope of two millimeters per five blows is assigned to it. A second test begins to show a stronger soil cement as it is taking more blows per penetration depth while the other three tests having similar DCP slope results.

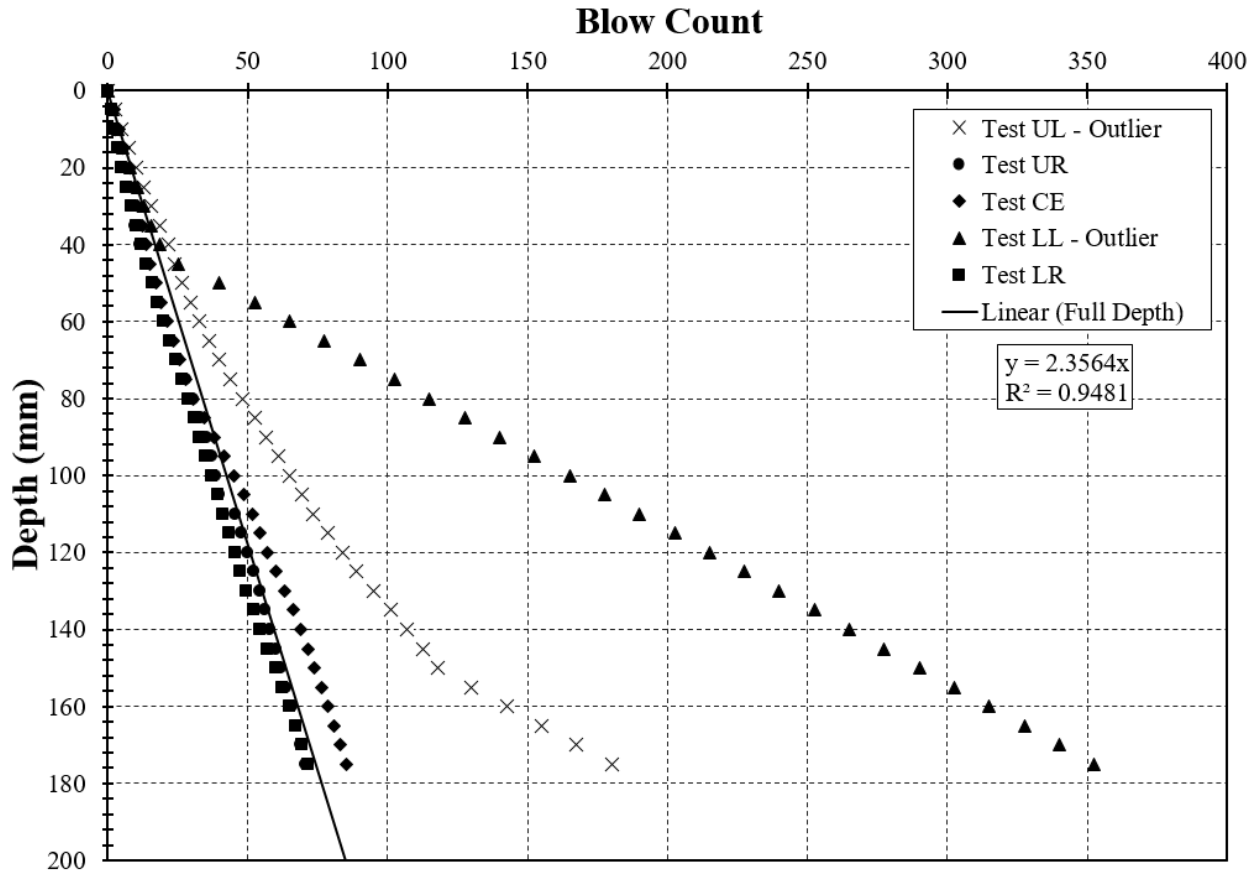


Figure 5.2: Second example of highly variable DCP test results on US Highway 84 bypass

Figure 5.3 shows the variability when most of the tests have different rates of penetration. All the tests are linear; however, only two are similar with the other three having much different slopes. These examples of irregularities that were seen in the DCP results help to justify the need for a systematic approach to analyze the data and identify outliers.

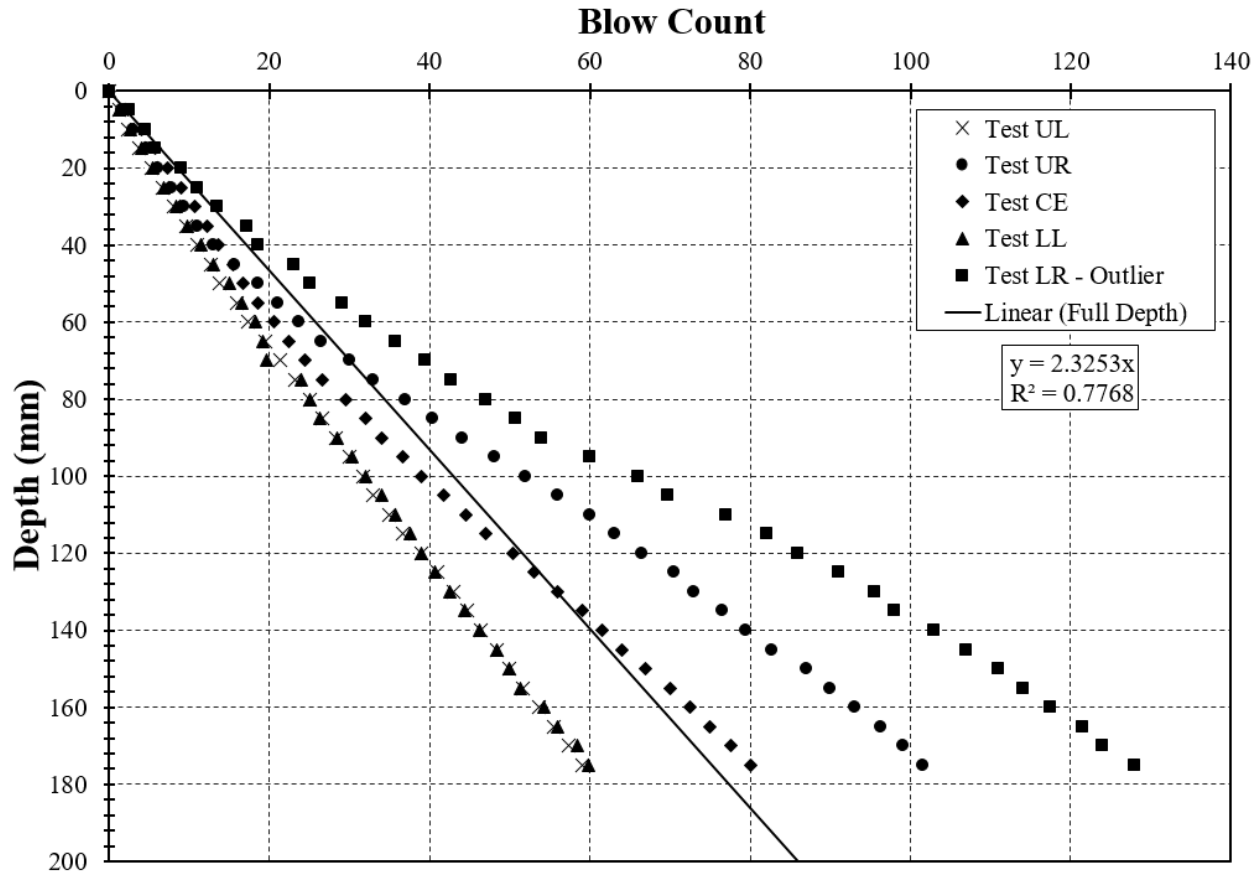


Figure 5.3: Third example of highly variable DCP test results on US Highway 84 bypass

5.2.2 Protocol for Analyzing DCP Results

The section covers the systematic approach used to analyze the DCP results. The first step was to take all of the DCP readings from the magnetic or manual ruler and convert the data to obtain results at every five millimeters of penetration. The second step was to determine if there were any outliers among the five different tests run at a single location.

5.2.2.1 Converting Data to Standard of Blows to Penetrate Five Millimeters

Five dynamic cone penetrometer tests were conducted at each testing location. After completion of the tests, the results were entered into a spreadsheet for analysis in terms of blow count and penetration depth in millimeters. The blow count was then linearly interpolated to obtain the blow count at every five millimeters of penetration. The field analysis of obtaining data points

was performed the same way as the laboratory testing phase and discussed in section 4.5.1. Once all five tests were linearly interpolated, the slope of each individual DCP test was determined using the least squares method to calculate a straight line. The linest function within Excel was used. The five slopes were then averaged together to produce a single DCP slope for that location. Figure 5.4 shows an example of five tests that were completed at a location.

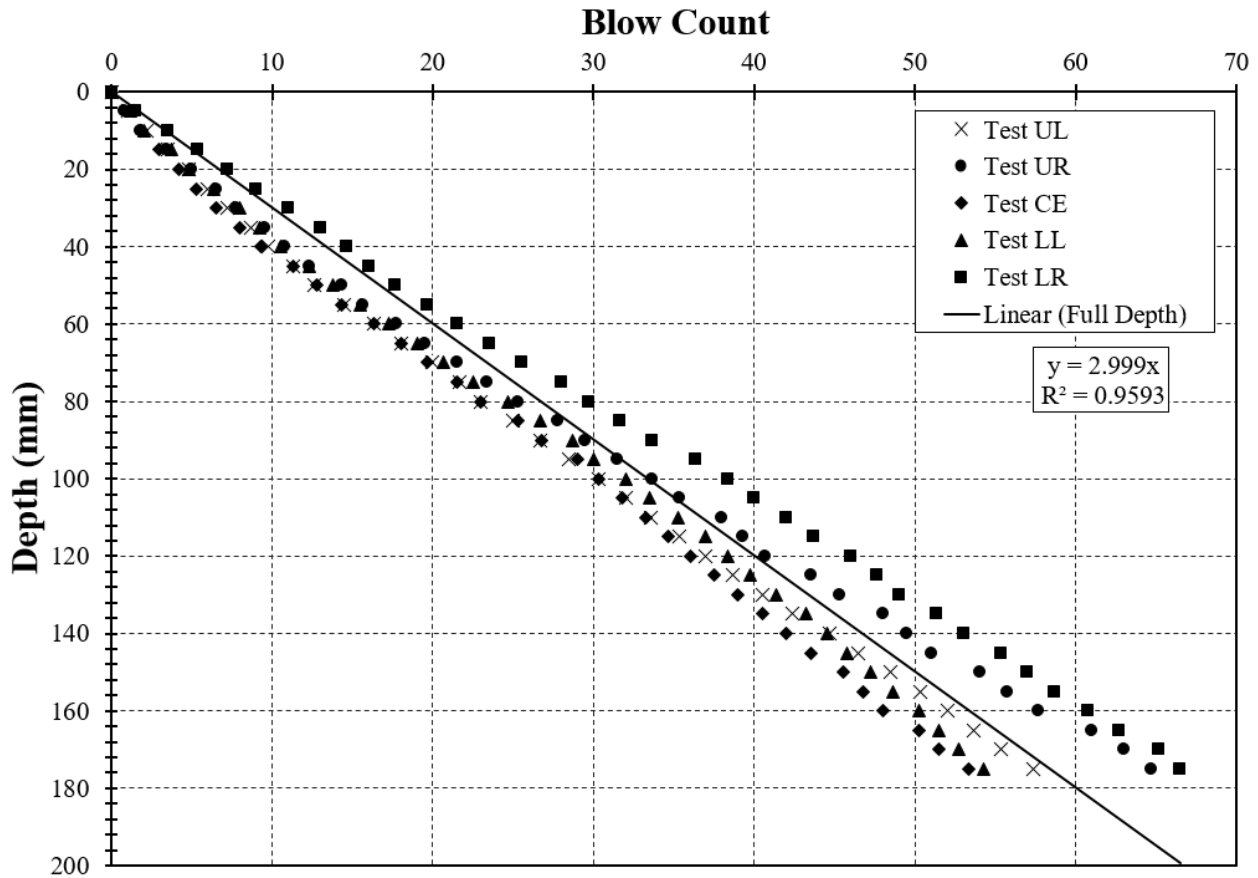


Figure 5.4: DCP test conducted on soil cement layer

If a test reached refusal, the test would still be considered in analysis. Refusal may occur due to the presence of larger aggregates, roots, or some other hard object. Once the test was entered into the spreadsheet, the rest of the test was assumed to have a slope of 2 millimeter per 5 blows, which is defined in ASTM D6951 (2018) as refusal. Figure 5.5 shows an example of

when two tests, Test UL and Test LL, reach refusal and follows the slope of 2 millimeters per 5 blows to get to full depth.

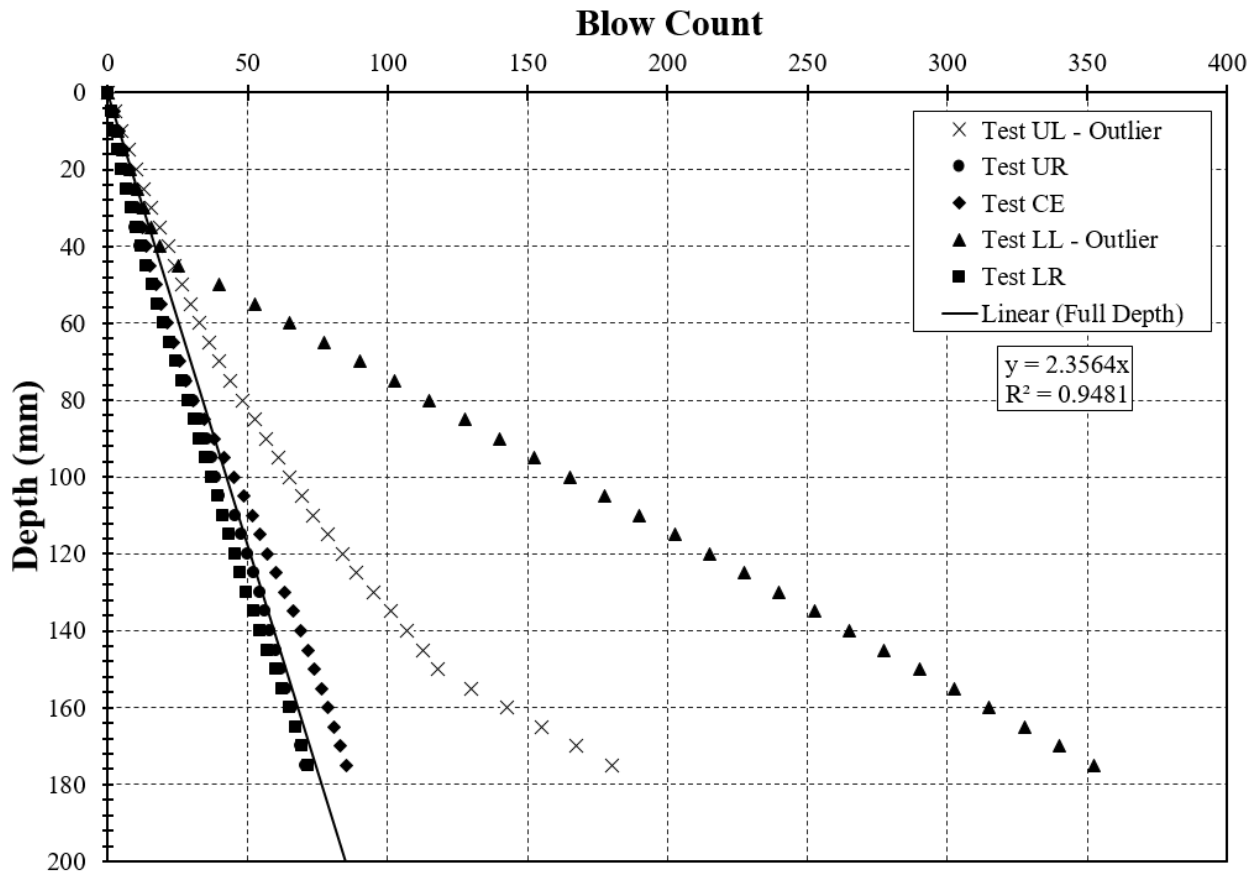


Figure 5.5: Example of test when it reaches point of refusal

5.2.2.2 Identification of Outliers

The next step of analysis was to determine if there were any outliers causing a significant change to the slope. McLaughlin (2017) developed a way to determine outliers using ASTM C670 (2015) using the acceptable range of data being 50 percent. In doing this, the maximum slope of the five tests was subtracted by the minimum slope and divided by the average of all five tests times 100 percent. This value indicates the range of the five tests. If the range was less than 50 percent then no outlier existed and all tests were analyzed together.

If the range was greater than the 50 percent, an outlier existed in the dataset. The next step was to determine the absolute value of the difference between the slopes of each of the five tests conducted with the average slope of the dataset. The test with the largest difference was deemed the outlier and was removed from the dataset. The next step was to recalculate the average slope of the four remaining tests and identify the new maximum and minimum slopes. The same process was repeated until there were no outliers remaining in the dataset. The DCP tests would be disregarded if more than three of the five tests were identified as outliers.

5.2.3 DCP Penetration Depth Analysis

This section covers further investigation into determining if a penetration depth of 75 millimeters would be the most efficient considering the data collected during the field testing phase. For each testing location, data from the five (assuming no outliers were found) DCP tests were plotted using the procedure outlined in Section 5.2.2. The plots were labeled with blow count on the x-axis and the depth of penetration on the y-axis in millimeters. The soil cement layer in the field was placed at a thickness of 8 inches, or 200 millimeters.

Just like in the laboratory, the DCP was seated the first 25 millimeters and five different penetration depths were evaluated: 25, 50, 75, 100, and 175 millimeters. A summary of this can be seen in Figure 4.3. The results obtained from these penetration depths were analyzed and compared to each other to determine which penetration depth produced the most accurate results.

At each testing location, the number of tests used was also evaluated to determine how many would be needed to produce accurate results while considering the technician effort required to perform the testing. Each location was tested in the exact same order: upper left (UL), upper right (UR), center (CE), lower left (LL), and lower right (LR). To evaluate only four tests, the lower right test was removed. To evaluate 3 tests, the lower left and lower right tests were removed

from the data set. A summary of all the DCP data from the testing locations can be found in Appendices J through N.

5.2.4 Results of Penetration Depth Analysis

The results of the analysis that were performed over each penetration depth, similar to that of laboratory testing phase discussed in Sections 4.5.1.1 through 4.5.1.5, are covered in this section. The average coefficient of determination (R^2) for each penetration analysis depth was determined for all the data gathered during the field testing phase and is shown in Figure 5.6. Range bars that indicate the minimum and maximum coefficient of determination were added to Figure 5.11. The number of tests needed at each location was also a factor of this research. For three tests, four tests, and five tests, the coefficient of determination for each penetration depth are also shown in Figure 5.6. All outliers were removed by the method stated in Section 5.2.2.2 before producing Figure 5.6.

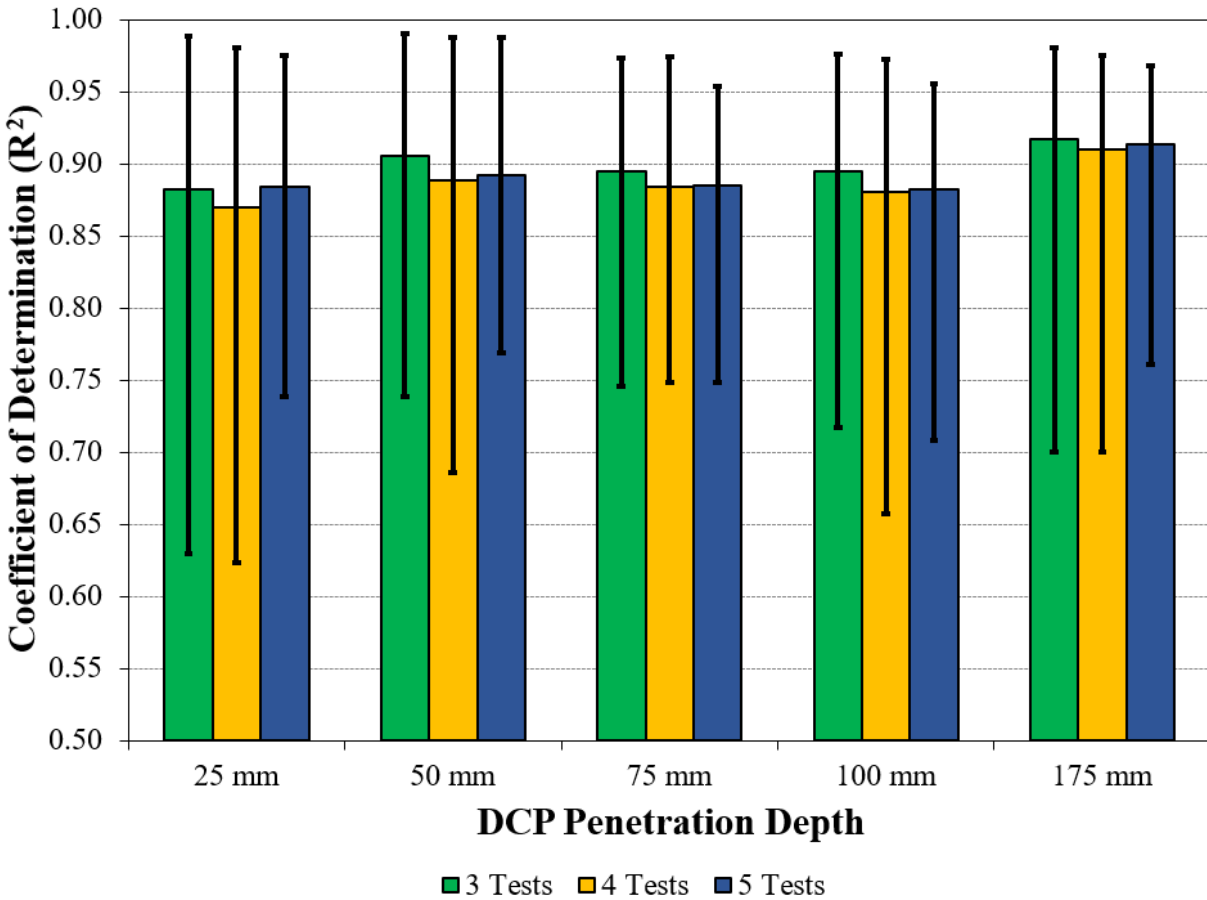


Figure 5.6: Coefficient of determination for all DCP test results collected

The results of the all the penetration data shown in Figure 5.6 show a high coefficient of determination for a linear relationship, meaning that the DCP penetration rate is linear with the depth. Penetration depth of 25 millimeters has a wide variability in part due to not having as many data points as the other depths, and it also has the lowest average coefficient of determination while using three, four, and five tests. Penetration depth of 175 millimeters has the greatest average coefficient of determination compared to the other depths, but it also has greater range of variability compared to the 75 millimeter analysis depth. Out of all the depths, 75 millimeters shows the least amount of variability whether three, four, or five tests were being analyzed. The two analysis depths that needed the least amount of technician effort but showed high coefficients of determination were 50 millimeters and 75 millimeters.

When evaluating how many tests should be used at each DCP test location, the coefficient of determination is actually the greatest with three tests performed, regardless of the analysis depth. This may be because of less data points; however, the variability between its maximum and minimums is also less showing that there is no need to perform more than three DCP tests at a location. The extra data points will only serve as more effort for the technician needs to put forth. A sufficiently accurate test of the soil cement base can be determined with the use of only three DCP tests. The field penetration depth analysis of McLaughlin (2017) is shown in Figure 5.7 and the laboratory penetration depth analysis of Nemiroff (2016) is presented in Figure 5.8.

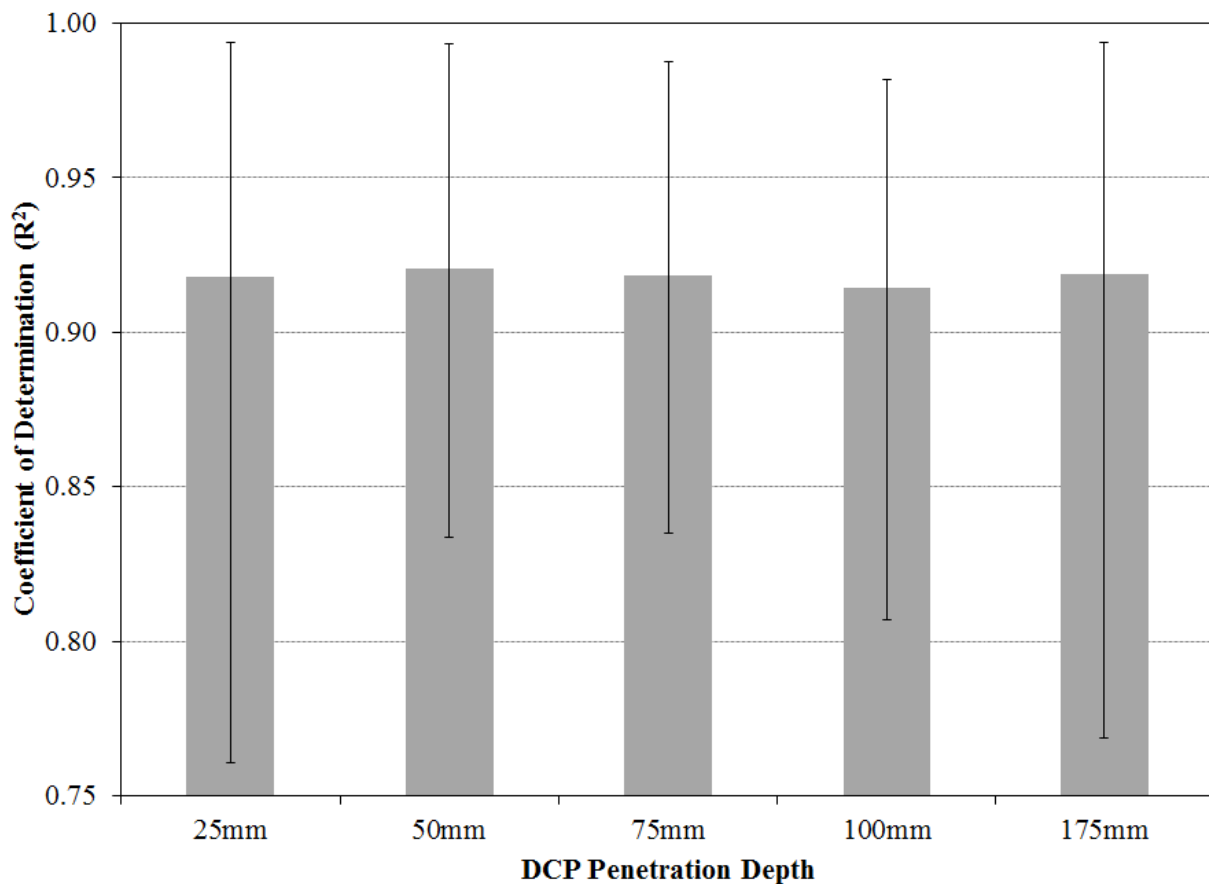


Figure 5.7: Coefficient of determination for DCP test results collected
(McLaughlin 2017)

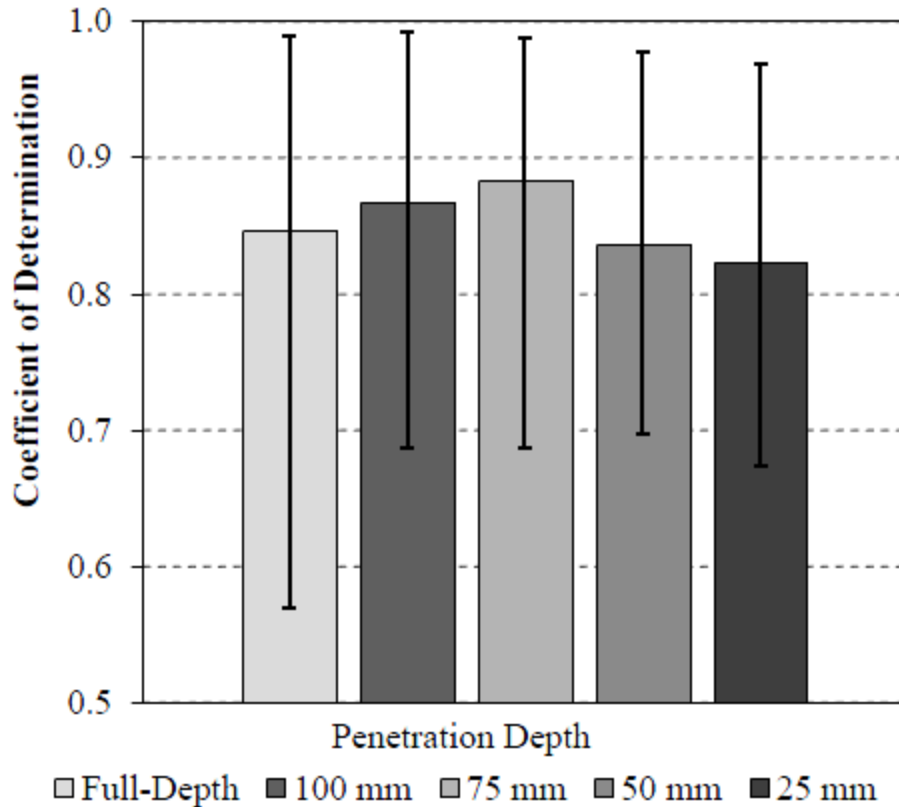


Figure 5.8: Coefficient of determination for DCP tests conducted in laboratory
(Nemiroff 2016)

Based on the laboratory results presented in Section 4.5.2, the coefficients of determination from the laboratory analysis presented in Figure 4.9, with the above two figures, it can be concluded that a penetration depth of 75 millimeters should be used by ALDOT. This depth was chosen for three reasons:

1. Laboratory results show it to be the most efficient penetration depth when conducting laboratory tests on soil cement.
2. The technician performing the test would penetrate exactly half of the 8-inch thick soil cement layer, once the DCP has been seated as shown in Figure 4.3.
3. The results from a 3-inch analysis depth has been recommended by Nemiroff (2016) and McLaughlin (2017) with the results of this study following the same trend.

5.3 Plastic-Mold Method Results

McLaughlin (2017) used the plastic-mold method to make cylinders for compression strength testing on a project in Elba. This same plastic-mold method was used again on the US Highway 84 bypass near New Brockton, Alabama. Figure 5.9 shows the average seven-day compressive strength test results for each testing location obtained for the plastic-mold method. No test data were collected for the first six subsections shown in Figure 5.9. In a subsection, material at two locations was obtained and used to create five plastic-mold cylinders as stated in Section 3.4.3. The values presented are the averages of 10 plastic-mold cylinder results made in each testing subsection. A detailed outline of the subsections and locations can be found in Appendix N. Any outliers were removed from the data set by the method stated in Section 3.3.4.1.2. Figure 5.14 also shows the ALDOT 304 (2014) strength requirements for soil cement. Specimens testing below 200 psi and above 650 psi shall have those sections be removed and replaced without compensation. Specimens testing between 200 to 250 psi and 600 to 650 psi indicate sections that are subject to pay reduction. All strength results between 250 and 600 psi would result in full pay.

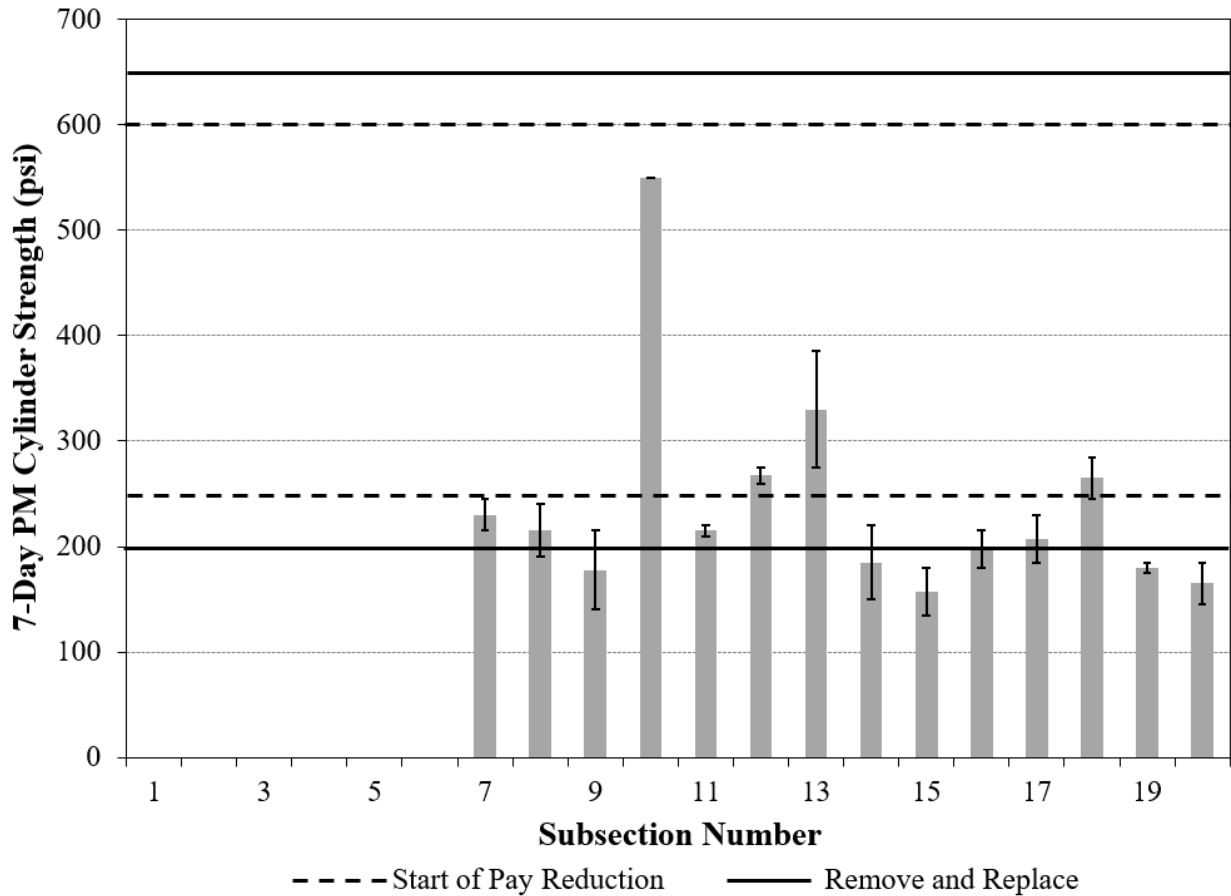


Figure 5.9: Seven-day compressive strength results for the plastic-mold method

Density was determined for each plastic-mold cylinder made during this field project. Figure 5.10 shows the density of the plastic-mold cylinders for each subsection. ALDOT 304 (2014) requires density to reach 98 percent. Figure 5.15 also shows the deviations from optimum moisture content range on the secondary y-axis. The density used for comparison was the laboratory proctor test run with the Elba soil at 6.5 percent cement content.

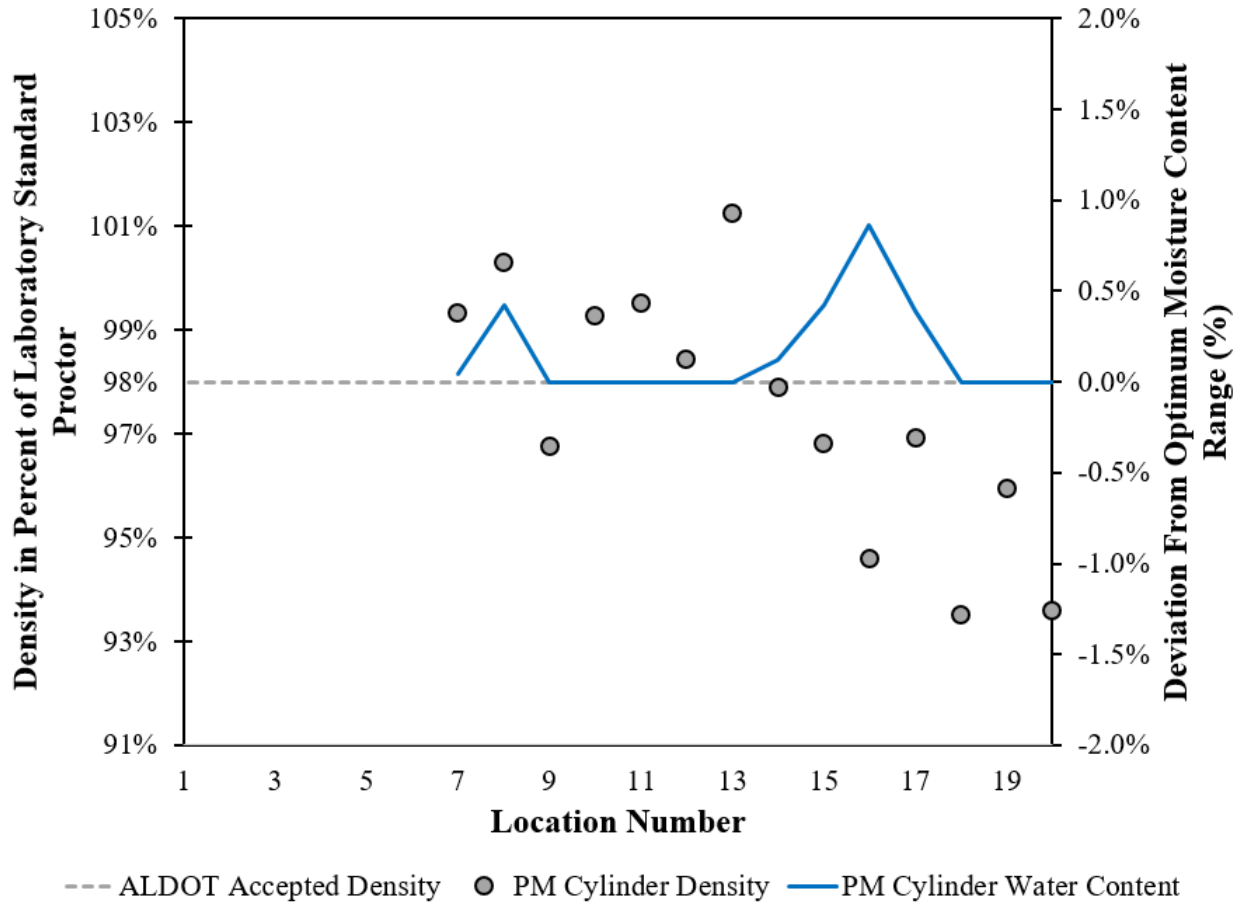


Figure 5.10: Plastic-mold method average density values at each testing subsection

Figure 5.10 shows that the density started to drop below the ALDOT threshold of 98 percent for many of the tests, where this coincided in some cases when the water was seen to be greater than the optimum moisture content range. The majority of the plastic-mold cylinders did reach a density of 98 percent or more when the optimum moisture content fell within the range.

5.4 Dynamic Cone Penetrometer Results

The second method used to evaluate the strength of the soil cement base was the DCP used in accordance with ASTM D6951 and the correlation between strength and DCP slope developed in Chapter 4. Figure 5.11 shows the compressive strength of the soil cement base using Equation 4.1. The strength estimates shown in Figure 5.11 are the average of three DCP tests conducted at each location that were then averaged with the other DCP results from the same subsection to

characterize the average strength of the subsection. The maximum and minimum strength estimated in each subsection are shown with range bars. Outliers were removed before the data were plotted. DCP subsection results shown in Figure 5.11 can range from one location (three DCP tests) up to four locations (twelve DCP tests) dependent upon on weather that day and if each location was able to be tested with the DCP. For location 2, no DCP tests were able to be completed due to weather. For subsections 19 and 20, the Contractor had the asphalt paved on the section before DCP tests were able to be completed.

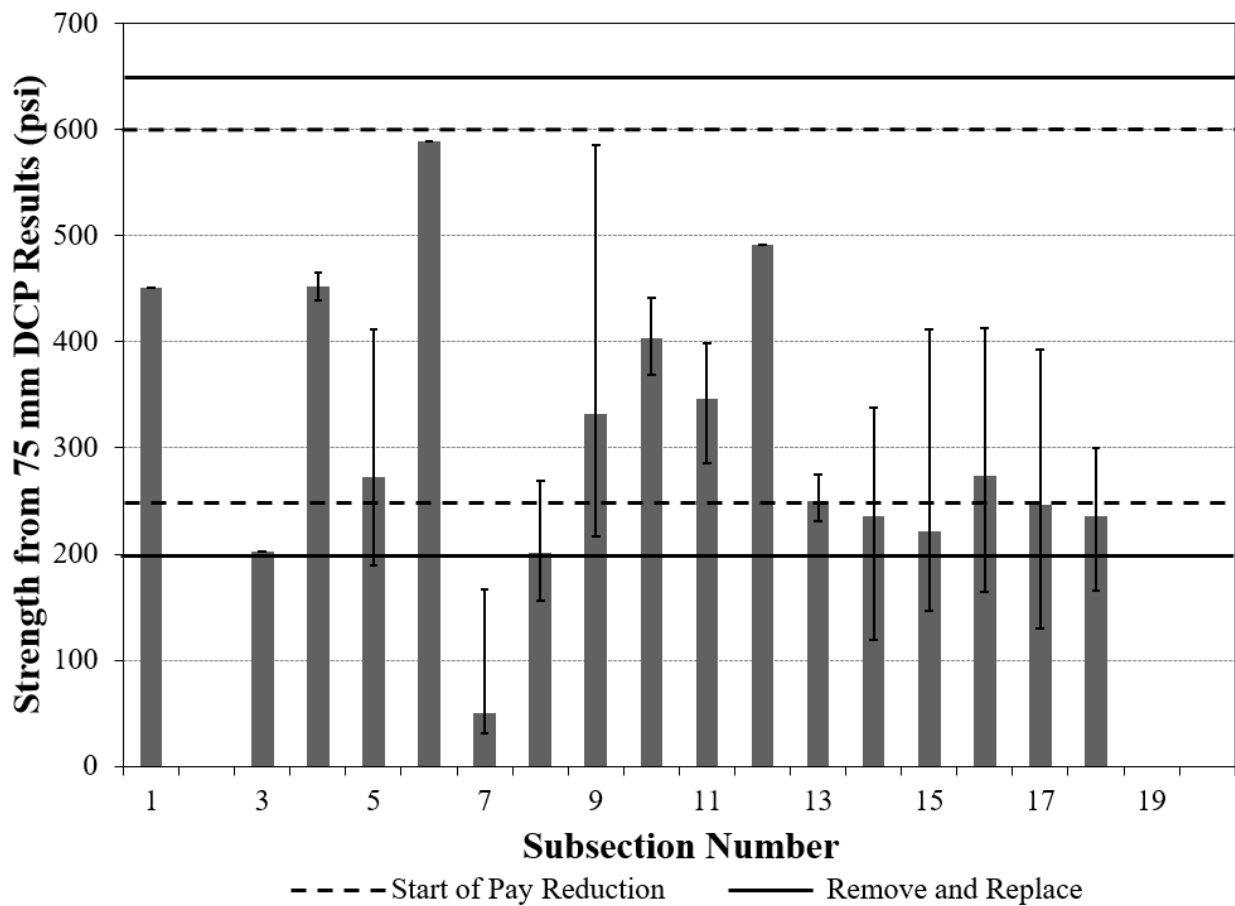


Figure 5.11: Seven-day compressive strength results from DCP results

The DCP shows the strength of the in-place soil cement, whereas the plastic-mold cylinders were made of samples of the soil cement mixed at the job site and compacted by a technician. Note

that it was expected that the variability of in-place strengths will be greater than those of the cylinders that were made and cured under controlled-laboratory conditions.

5.5 Core Results

Cores were extracted by SA Graham Construction and tested by ALDOT on the seventh day. As shown in Figure 3.24, three cores were extracted from each section of about 450 feet that was constructed per day. The values shown in Figure 5.12 are the average of the cores recovered from each subsection. Some subsections only had one as the random selection of locations had one fall on the first subsection, while the other two were on the other subsection constructed that day. The range bars in Figure 5.12 show the maximum and minimum core strength obtained for each subsection. Each subsection without range bars had only one core tested.

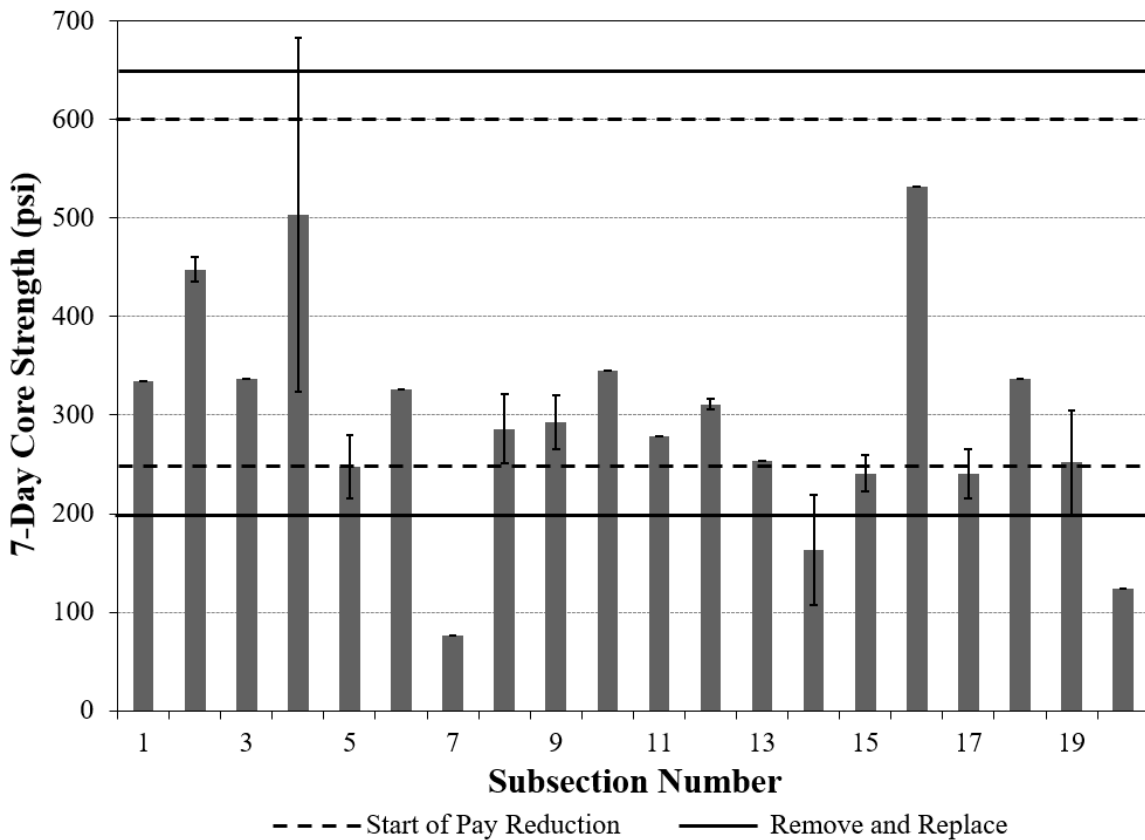


Figure 5.12: Seven-day compressive strength results of cores taken along US Highway 84

bypass

Figure 5.12 indicates that some sections did not meet ALDOT’s strength requirements. A graph of all the individual core strength results taken during the US Highway 84 bypass can be seen in Figure 5.13.

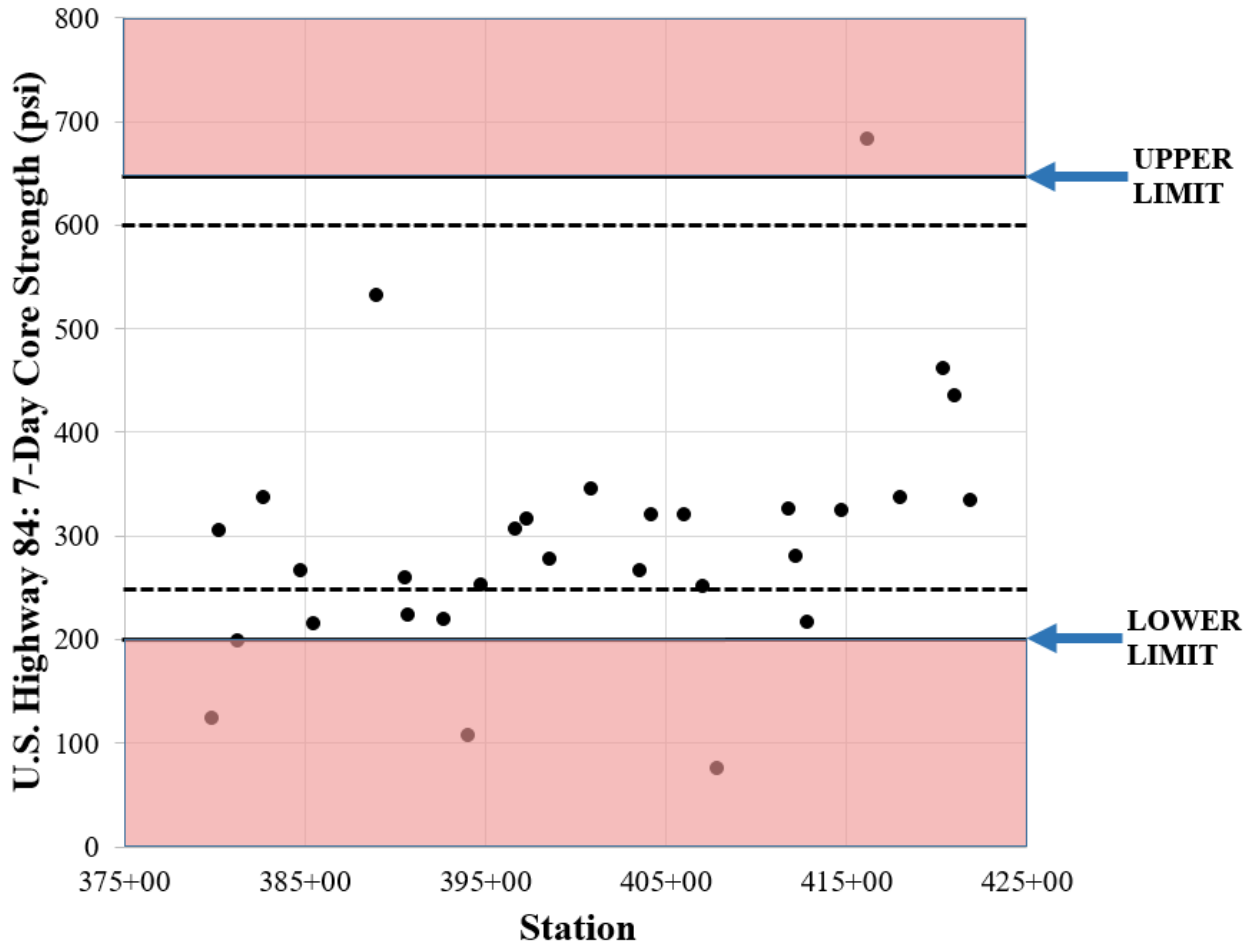


Figure 5.13: Core results collected along US Highway 84 bypass

5.6 In-Place Density Results

The in-place density of the tested sections was measured by using a nuclear density gauge by ALDOT. Figure 5.14 shows the density obtained at each testing subsection during the soil cement project. Figure 5.14 shows the in-place density of the soil cement after the first strip and initial density testing of the subsection was completed. If the nuclear density gauge showed values that did not meet either the density or water content, the Contractor added more water or applied

more compaction to the soil cement layer by rolling it over a few more times. This practice ensured that each section met ALDOT’s density and moisture content requirements, which is evident from Figure 5.14.

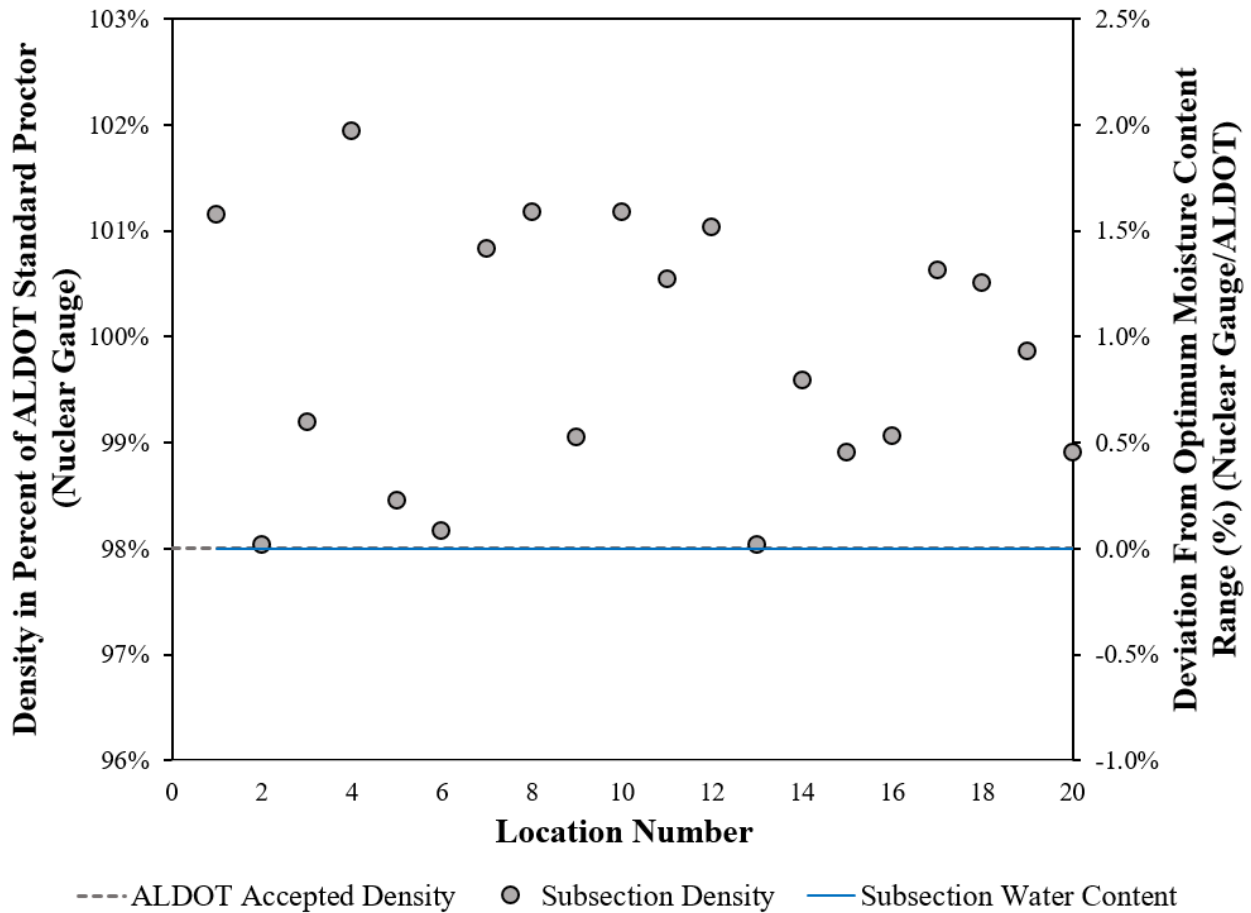


Figure 5.14: In-place density of soil cement base along US Highway 84 bypass

5.7 Comparison of the Test Methods Evaluated

In this section, the results of each of the test methods used in this study are compared to each other. First, the variability of each test method is compared against the variability of the other test methods. Then, an evaluation of the strength of the soil cement base in a subsection calculated using each of the test methods is presented and discussed. As shown in Figure 3.24, a subsection could consist of up to twelve DCP tests (from up to four DCP test locations), two cores, and ten

plastic-mold cylinder strength tests. And finally, a location comparison of strength of each test method is presented and discussed.

5.7.1 Variability of Each Test Method

The variability of each test method was analyzed to determine which methods had the least variability. Figure 5.15 shows the average variation in strength obtained from each test method as determined for the field testing phase of this project. All outliers were included in the plot in order to fairly compare the variability of all the test methods. Three different test methods were analyzed during this research project for their variability. The adjusted coefficient of variation was determined by dividing the coefficient of variation using a statistical coefficient that is determined to account for the number of tests performed (ASTM C670 2015; Harter 1969).

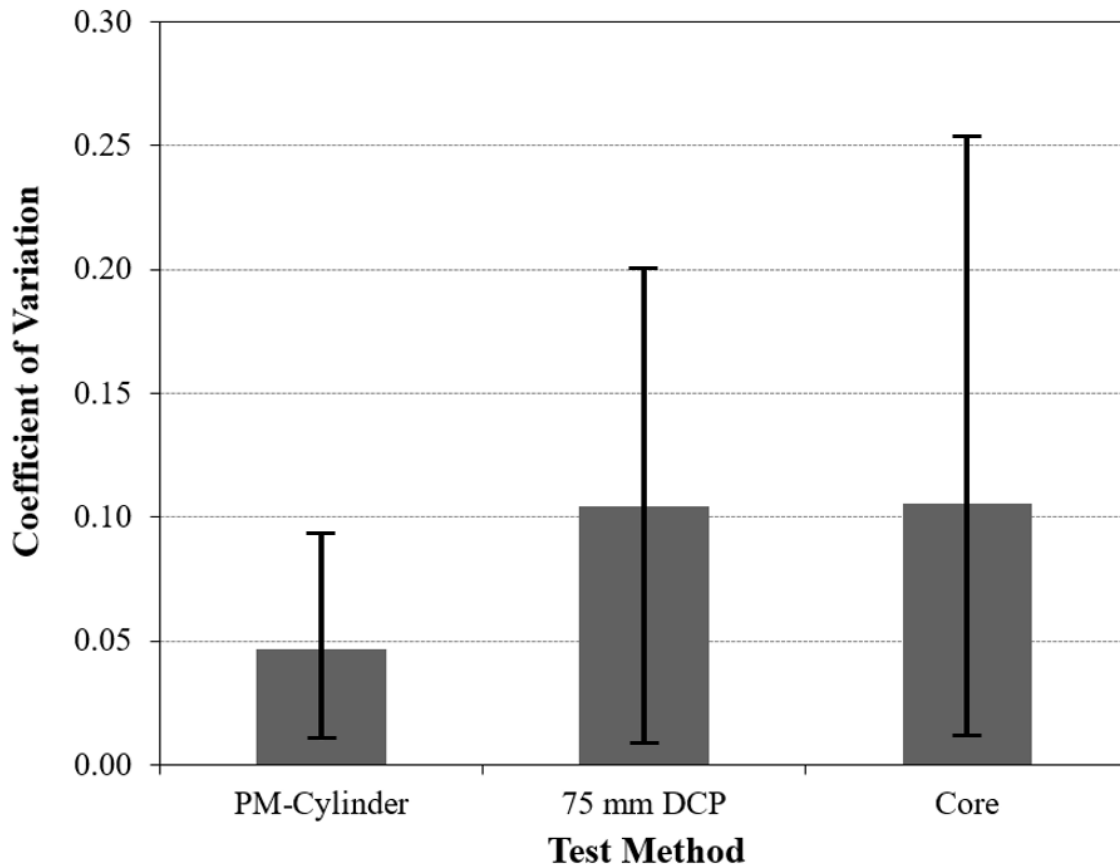


Figure 5.15: Adjusted coefficient of variation of strength using each test method

The coefficient of variation, shown in Figure 5.15, was calculated by using the average of the strength results at each testing location and identifying the maximum and minimum values. Specimens made from the plastic-mold (PM) method were made from material sampled at the project site during placement of the soil cement base, whereas the DCP test and cores tested in-place strengths. The test method with the least amount of variability is seen to be the plastic-mold cylinders. The DCP test method produced the least amount of variability when comparing the in-place strengths following the findings of McLaughlin (2017). Variability that was encountered during the compressive testing of the specimens cored from the soil cement layer was large.

5.7.2 Subsection Comparison

ALDOT uses seven-day core strengths for each section that is about 1/10 of a mile according to ALDOT 304 (2014). The Contractor on site for this US Highway 84 bypass project mixed two subsections at about 225 feet each as described in Section 3.4.3. These subsections consisted of up to two core results, up to twelve DCP results, and ten plastic mold tests. Figure 5.16 shows the relationship of the core strengths versus the DCP test method and plastic-mold compressive strength results.

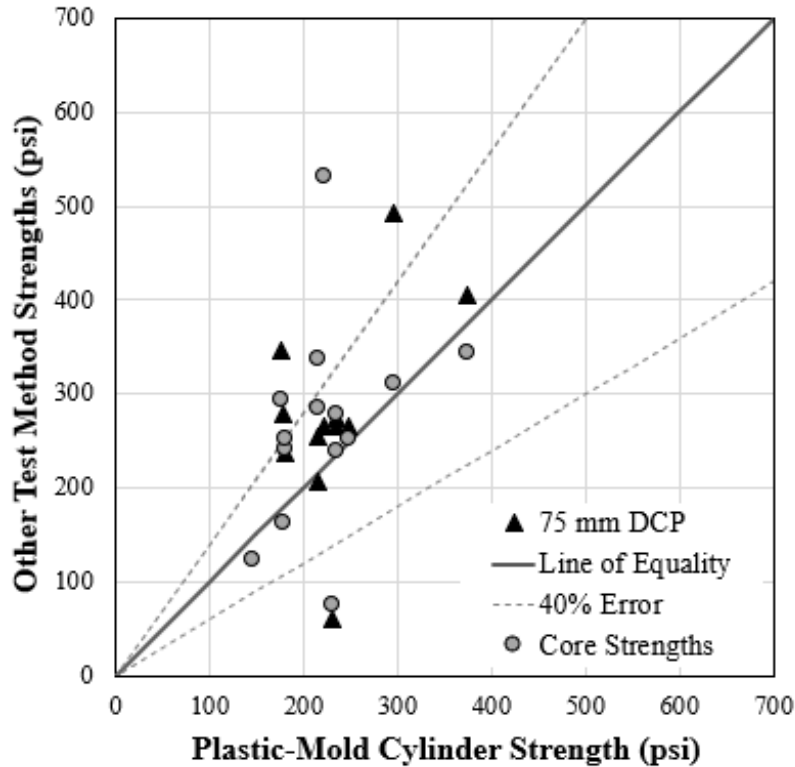


Figure 5.16: PM cylinder strength versus other test methods averaged per subsection

Figure 5.16 shows that most of the data fall above the line of equality. This indicates the plastic-mold cylinder strength values were found to be slightly less than the other two methods. However, the majority of the data points fall inside of the ± 40 percent error lines, with eight points falling outside this error margin.

5.7.3 Location Comparison

The plastic-mold method and DCP tests were performed at two locations within a subsection. Since they were done very close to each other, they can be compared based on their matching locations. At each location, there were five plastic-mold cylinder tests and five DCP tests conducted. As mentioned earlier, only three DCP tests analyzed to a depth of 75 millimeters are needed for accurate and efficient data collection. Figure 5.17 shows the DCP strengths versus the plastic-mold strengths.

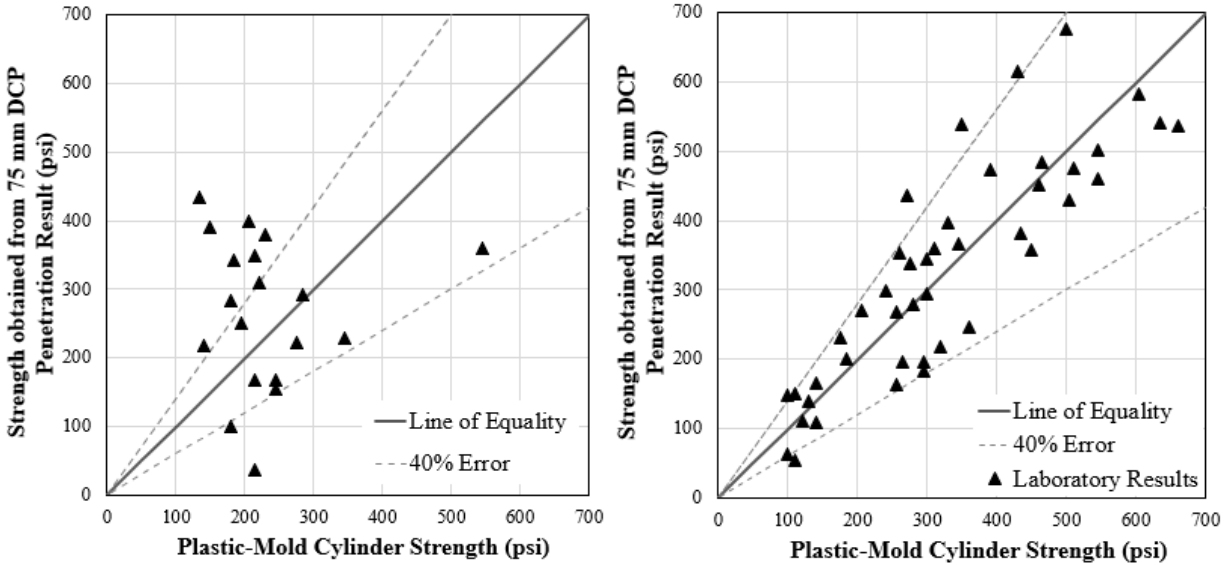


Figure 5.17: Left: Field results of PM cylinder strength versus the 75 mm DCP result per location; Right: Laboratory results of PM cylinder strength versus the 75 mm DCP result per testing day

On the left, the majority of points fall within the 40 percent error margin, which show that the plastic-mold strength results on average agree with the strengths obtained from using the DCP. When comparing the results in Figure 5.17, the plastic-mold cylinders were created using the soil cement mixture and taken to a laboratory for curing, whereas the DCP tested the strength of the in-place soil cement base. In the right figure of Figure 5.17, the laboratory results show the best outcome of using Equation 4.1 when comparing the 75 millimeter DCP result to the PM cylinder strength. The laboratory results have a few points falling outside of the 40 percent error margin even under the most controlled conditions. Based on this, the average plastic-mold strengths showed similar comparisons to that of the average DCP strengths.

Chapter 6

Summary, Conclusions, and Recommendations

6.1 Summary

Soil cement is a mixture of soil, portland cement, and water that creates a strong, durable, frost-resistant pavement base layer once it is properly compacted and cured. During the laboratory testing phase, soil classification was tested to determine its impact on soil cement strength. The suitability of the DCP for use to determine the strength of soil cement was evaluated. Finally, a correlation between the DCP and cylinder strength was established over a compressive strength range of 100 to 930 psi. Approximately 435 cylinders and 207 DCP specimens were created and tested over the course of the laboratory testing phase of this research project.

During the field testing phase, several test methods were evaluated to assess the strength of soil cement base. The plastic-mold method modified from McLaughlin (2017) was evaluated as a quality assurance test method to determine the strength of the soil cement mixtures on the job site. The DCP method used in the laboratory testing phase and the standard ALDOT method of testing the core's compressive strength were also evaluated to measure the strength of soil cement base. The number of DCP tests needed to approximate the in-place strength most efficiently of the soil cement base was also evaluated. Approximately 135 plastic-mold cylinders were made, 30 core compressive strengths tested, and 189 DCP tests evaluated over the course of the field testing phase of this research.

6.2 Conclusions

The laboratory testing phase yielded the following key conclusions:

- As cement content is increased, the maximum dry density will also increase regardless of the soil classification,
- The addition of two pieces of aluminum foil tape placed horizontally across the slit on the plastic mold, as seen in Figure 3.10, greatly reduces the chance of the cylinder splitting while being compacted,
- The DCP is able to efficiently penetrate laboratory mixed soil cement bases with strengths up to 930 psi,
- After seating to a depth of 25 millimeters (1 inch), the recommended penetration depth of the DCP is 75 millimeters (3 inches), because this depth produces reliable results with the least amount of technician effort,
- Different soil types do not have a strong enough impact on the relationship between DCP and unconfined compressive strength; therefore, one relationship can be used,
- The most practical molded cylinder strength to DCP slope correlation based on ease of use for field applications and best-fit is the logarithmic function equation that is presented in Equation 5.1. This equation is valid for a strength range between 100 and 930 psi.

$$MCS = 1220e^{-0.559DCP} \quad \text{(Equation 5.1)}$$

Where:

MCS = molded cylinder strength (psi), and

DCP = dynamic cone penetrometer slope (mm/blow).

The field testing phase yielded the following key conclusions:

- The DCP is able to efficiently penetrate mixed-in-place soil cement bases,

- After seating to a depth of 25 millimeters (1 inch), the most efficient penetration depth of the dynamic cone penetrometer is 75 millimeters (3 inches). This depth produces the lowest variability, highest coefficient of determination, and matches the findings of the laboratory testing phase, Nemiroff (2016), and McLaughlin (2017). This depth also provides less technician effort than full-depth penetration, and penetrates exactly half of the soil cement layer after accounting for the DCP seating depth,
- A sufficiently accurate assessment of the soil cement base strength can be determined with the use of only three DCP tests at a single location,
- The DCP versus strength equation recommended by the laboratory testing phase, Equation 5.1, should be used to evaluate the strength of soil-cement base with 75 millimeters (3 inches) of DCP penetration,
- The dynamic cone penetrometer is a more reliable test method to determine the in-place strength of soil-cement base compared to compression testing of cores, which is the standard practice that ALDOT currently uses to determine strength.

6.3 Recommendations

It is recommended that ALDOT implement a new testing procedure to assess the strength of soil cement base. The recommendation from the laboratory and field testing phases would be to use the plastic-mold method for mixture qualification in soil cement base applications. The plastic-mold method be used as quality assurance test in the field to assess the soil cement strength. Sections will still be passed or failed on a 1/10 of a mile stretch of soil cement. The process would include picking two random sampling locations along the section and making three specimens at each using the plastic-mold method during the placement of the soil cement base. Before compaction, the plastic-mold cylinder shall prepared by cutting a slit down the side, one piece of

aluminum tape covering the slit, and then two pieces of aluminum tape wrap about one-third the circumference around the top and middle of the cylinder. Compaction of the plastic-mold cylinders shall be completed by using three equal lifts at seven blows per lift, scarifying after each layer has been compacted. The cylinders shall be capped and then be placed in a shady area, protected from wind and rain, to allow for initial curing on-site of the specimens for 24 hours before being transported to the laboratory for final curing and testing. Final curing would include demolding the cylinders from the plastic mold, placing them in a sealed plastic bag, and placing them in a moist-curing room until the seventh day when the cylinders will be tested to determine their compression strength. The average strength of the two locations will then be averaged together to obtain a single value which shall be used as the indicator of strength of the soil cement base. Passing or failing will be based upon whether the average plastic-mold cylinder strengths fall within ALDOT's acceptable range. Full pay will be awarded for cylinder strengths between 250 and 600 psi. If plastic-mold cylinder strengths fall outside of this range, the DCP shall be conducted on the soil cement base section. Three DCP test locations shall be randomly selected by the Engineer. Three DCP tests shall be conducted at each of the three random locations, penetrating 75 millimeters (3 inches) into the soil cement layer once the DCP is properly seated 25 millimeter (1 inch). The data should be processed as discussed in Section 5.2.2 to check for outliers among the three DCP tests performed at a location. Once this is done, the average DCP strength of the three locations shall be taken as the strength of the soil cement base using Equation 5.1. If the strength falls with 250 psi to 600 psi full pay shall be awarded. If the strength falls with 200 to 250 psi or 600 to 650 psi pay reduction shall be incorporated following Equations 1.1 and 1.2. If the strength is below 200 psi or is above 650 psi, the section of soil cement base shall be removed and replaced at the expense of the Contractor.

A recommendation for future work would be to confirm that the plastic-mold compressive strength test results compares closely to the steel-molded cylinder compressive strength test results that follows ASTM D1633 (2017). A strong correlation between laboratory made molded cylinders and the DCP was found by Nemiroff (2016) and added to the results of the laboratory testing phase. A correlation between the steel-mold cylinder method and the plastic-mold method can be done by making both types of cylinders in the laboratory from the same uniformly mixed soil cement and tested for strength on the same day. Another recommendation would be to create software that is user friendly to make DCP results easy to obtain soon after the DCP penetration testing. A final recommendation would be to develop a draft ALDOT Special Provision to incorporate these findings into a quality assurance protocol for soil cement base strength testing.

References

AASHTO T 22. 2010. Standard Test Method for Compressive Strength of Cylindrical Concrete Specimens. AASHTO - *Standard Specifications for Transportation Materials and Methods of Sampling and Testing*, American Association of State Highway and Transportation Officials, Washington, DC.

AASHTO T 134. 2013. Standard Method of Test for Moisture-Density Relations of Solid-Cement Mixtures. AASHTO - *Standard Specifications for Transportation Materials and Methods of Sampling and Testing*, American Association of State Highway and Transportation Officials, Washington, DC.

ACI 230. 2009. *Report on Soil Cement*. (ACI 230.1R-09), American Concrete Institute, Farmington Hills, MI.

Ashan, Ahmed. 2014. "Pavement Performance Monitoring Using Dynamic Cone Penetrometer and Geogauge During Construction." Master's Thesis, The University of Texas at Arlington.

Alabama Department of Transportation. 2012. *Standard Specifications for Highway Construction*. Alabama Department of Transportation.

ALDOT 304. 2014. *Soil-Cement*. Alabama Department of Transportation, Special Provision No. 12-1167.

ALDOT 419. 2008. *Extracting, Transporting, and Testing Core Samples from Soil-Cement*, Alabama Department of Transportation.

ASTM C39. 2020. *Standard Test Method for Compressive Strength of Cylindrical Concrete Specimens*. ASTM International. West Conshohocken, PA.

ASTM C150. 2016. *Standard Specification for Portland Cement*. ASTM International. West Conshohocken, PA.

ASTM C470. 2015. *Standard Specification for Molds for Forming Concrete Test Cylinders Vertically*. ASTM International. West Conshohocken, PA.

ASTM C670. 2015. *Standard Practice for Preparing Precision and Bias Statements for Test Methods for Construction Materials*. ASTM International. West Conshohocken, PA.

ASTM C1435. 2014. *Standard Practice for Molding Roller-Compacted Concrete in Cylinder Molds Using a Vibrating Hammer*. ASTM International. West Conshohocken, PA.

ASTM D422. 2007. *Standard Test Method for Particle-Size Analysis of Soils*. ASTM International. West Conshohocken, PA.

ASTM D558. 2019. *Standard Test Methods for Moisture-Density (Unit Weight) Relations of Soil-Cement Mixtures*. ASTM International. West Conshohocken, PA.

ASTM D559. 2015. *Standard Test Method for Wetting and Drying Compacted Soil-Cement Mixtures*. ASTM International. West Conshohocken, PA.

ASTM D560. 2016. *Standard Test Methods for Freezing and Thawing Compacted Soil-Cement Mixtures*. ASTM International. West Conshohocken, PA.

ASTM D698. 2012. *Standard Test Methods for Laboratory Compaction Characteristics of Soil Using Standard Effort (12,400 ft-lbf/ft³ (600 kN-m/m³))*. ASTM International. West Conshohocken, PA.

ASTM D806. 2019. *Standard Test Method for Cement Content of Hardened Soil-Cement Mixtures*. ASTM International. West Conshohocken, PA.

ASTM D1556. 2015. *Standard Test Method for Density and Unity Weight of Soil in Place by Sand-Cone Method*. ASTM International. West Conshohocken, PA.

ASTM D1557. 2012. *Standard Test Methods for Laboratory Compaction Characteristics of Soil Using Modified Effort (56,000 ft-lbf/ft³ (2,700 kN-m/m³))*. ASTM International. West Conshohocken, PA.

ASTM D1632. 2017. *Standard Practice for Making and Curing Soil-Cement Compression and Flexure Test Specimens in the Laboratory*. ASTM International. West Conshohocken, PA.

ASTM D1633. 2017. *Standard Test Methods for Compressive Strength of Molded Soil-Cement Cylinders*. ASTM International. West Conshohocken, PA.

ASTM D2167. 2015. *Standard Test Method for Density and Unit Weight of Soil in Place by the Rubber Balloon Method*. ASM International. West Conshohocken, PA.

ASTM D5982. 2015. *Standard Test Methods for Determining Cement Content of Fresh Soil-Cement (Heat of Neutralization Method)*. ASTM International. West Conshohocken, PA.

ASTM D6938. 2005. *Standard Test Methods for In-Place Density and Water Content of Soil and Soil-Aggregate in Place by Nuclear Methods (Shallow Depth)*. ASTM International. West Conshohocken, PA.

ASTM D6951. 2018. *Standard Test Methods for Use of the Dynamic Cone Penetrometer in Shallow Pavement Applications*. ASTM International. West Conshohocken, PA.

Enayatpour, S., A. J. Puppala, and H. Vasudevan. 2006. "Dynamic Cone Penetrometer to Evaluate Unconfined Compressive Strength of Stabilized Soils." *Geotechnical Special Publication*, American Society of Civil Engineers, pp.285-292.

Federal Highway Administration (FHWA). 1979. *Soil Stabilization in Pavement Structures: A User's Manual*, V.2. Report No. FHWA-IP-80-2, Washington, DC.

Felt, E. J. 1955. "Factors Influencing Physical Properties of Soil-Cement Mixtures." *Bulletin No. 108*, Highway Research Board, Washington, D.C., pp. 138-162.

GDOT Section 301. 2013. *Soil-Cement Construction*. Georgia Department of Transportation.

George, K.P. and W. Uddin. 2000. *Subgrade Characterization for Highway Pavement Design Final Report*, Mississippi Department of Transportation, Jackson, MS.

George, K.P. 2002. "Minimizing Cracking in Cement-Treated Material for Improved Performance." *Research and Development Bulletin RD123*, Portland Cement Association. Skokie, IL.

Google Maps. 2020. <https://www.google.com/maps/>

Halsted, G.E., D.R. Luhr, and W.S. Adaska. 2006. *Guide to Cement-Treated Base (CTB)*. Portland Cement Association. Skokie, IL.

Halsted, G.E., W.S. Adaska, and W.T. McConnell. 2008. *Guide to Cement-Modified Soil (CMS)*. Portland Cement Association. Skokie, IL.

- Harter, H. L. 1969. *Order statistics and their use in testing and estimation, Vol. 1: Tests based on range and studentized range of samples from a normal population*. Aerospace Research Laboratories, Office of Aerospace Research, United States Air Force, Wright-Patterson Air Force Base, Ohio.
- Hassan, A.B. 1996. “The Effects of Material Parameters on Dynamic Cone Penetrometer Results for Fine-Grained Soils and Granular Materials.” PhD diss., Oklahoma State University.
- Holtz, R.D., and W.D. Kovacs. 1981. *An Introduction to Geotechnical Engineering*. 1st Edition, Englewood Cliffs, NJ: Prentice Hall.
- Huntley, S.L. 1990. “Use of a dynamic penetrometer as a ground investigation and design tool in Hertfordshire.” *Field Testing in Engineering Geology*. Geological Society Engineering Geology Special Publications No. 6.
- Jin, L., W. Song, X. Shu, and B. Huang. 2018. “Use of Water Reducer to Enhance the Mechanical and Durability Properties of Cement-Treated Soil.” *Construction and Building Materials* 159, pp. 690-694.
- Kleyn, E. G. 1975. *The Use of the Dynamic Cone Penetrometer (DCP)*. Report 2/74. Transvaal Roads Department, Pretoria.

- Kleyn, E.G. and P.E. Savage. 1982. "The Application of the Pavement DCP to Determine the Bearing Properties and Performance of the Road Pavements". *International Symposium on Bearing Capacity of Roads and Airfields*, Trondheim, Norway.
- Kuhlman, R.H. 1994. "Cracking in Soil Cement – Cause, Effect, Control." *Concrete International* 16, n. 8:56-59.
- McCarthy, D. 2007. *Essentials of Soil Mechanics and Foundations: Basic Geotechnics*. Seventh Edition. New Jersey: Pearson.
- McElvaney, J. and IR. Bunadi Djatnika. 1991. "Strength Evaluation of Lime-Stabilized Pavement Foundations Using the Dynamic Cone Penetrometer." *Australian Road Research*, v. 21, no. 1: 40-52.
- McLaughlin, Justin Blake. 2017. Evaluation of Methods to Assess the Strength of Soil Cement Base. Master's Thesis, Auburn University.
- Nemiroff, Jordan Michelle. 2016. Strength Assessment of Soil Cement. Master's Thesis, Auburn University.
- North Carolina Department of Transportation. 2013. *Chemical Stabilization QA Subgrade/Base Field Testing*. North Carolina Department of Transportation.

- Patel, Mukesh A. and H.S. Patel. 2012. "Experimental Study to Correlate the Test Results of PBT, UCS, and CBR with DCP on Various Soils in Soaked Condition." *International Journal of Engineering*, v. 6, no. 5: 244-261.
- Portland Cement Association (PCA). 1971. "Soil Cement Laboratory Handbook." *Engineering Bulletin*, Portland Cement Association. Skokie, IL.
- Portland Cement Association (PCA). 1995. "Soil-Cement Construction Handbook." *Engineering Bulletin*, *Portland Cement Association*. Skokie, IL.
- Robbins, E.G., and P.E. Mueller. 1960. "Development of a Test for Identifying Poorly Reacting Sandy Soils Encountered in Soil-Cement Applications." Highway Research Board, *Bulletin 267*, pp: 46-49.
- Scala, A.J. 1956. "Simple Methods of Flexible Pavement Design Using Cone Penetrometer." *N.Z. Eng.* 11 (2).
- Scullion, T. 2002. "Precracking of Soil-Cement Bases to Reduce Reflection Cracking." *Transportation Research Record*, n. 1787:22-32.
- Shen, C.K. and J.K. Mitchell. 1966. "Behavior of Soil-Cement in Repeated Compression and Flexure." Highway Research Board, *Highway Research Record*, No. 128. Washington, DC., pp. 68-100.

Sullivan, W., I. Howard, and B. Anderson. 2014. "Development of Equipment for Compacting Soil-Cement into Plastic Molds for Design and Quality Control Purposes." 94th Annual Meeting of the Transportation Research Board.

Sullivan, W. G., and I. L. Howard. 2017. "Piloted Quality Control Techniques Using the Plastic Mold Compaction Device for Cement Stabilized Materials," *Advances in Civil Engineering Materials* 6, no. 1: 385–403.

Webster, S., R. Grau, and T. Williams. 1992. *Description and Application of Dual Mass Dynamic Cone Penetrometer*. Project AT40. US Army Corps of Engineers, Washington, DC.

West, G. 1959. "A Laboratory Investigation into the Effect of Elapsed Time After Mixing on the Compaction and Strength of Soil-Cement." *Geotechnique*, v. 9, no. 1:22-28.

Wilson, William Herbert Jr. 2013. Strength Assessment of Soil Cement. Master's Thesis, Auburn University.

Yoon, S., and M. Abu-Farsakh. 2008. Laboratory Investigation on the Strength Characteristics of Cement-Sand as Base Material. *KSCCE Journal of Civil Engineering* 13, no. 1:15-22.

Appendix A

Design Curves and Gradations

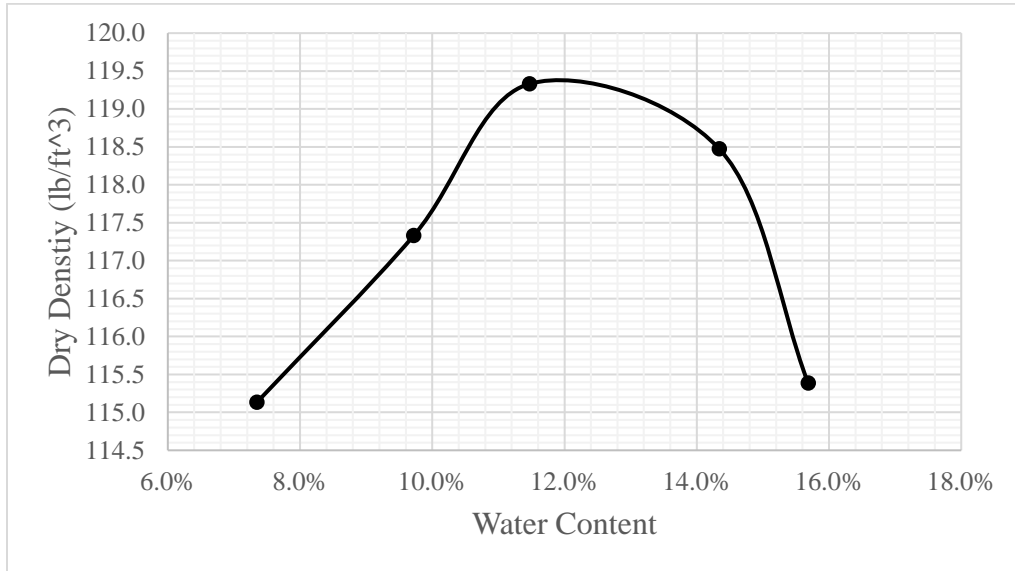


Figure A.1: Design curve for Waugh soil with 4 percent cement content

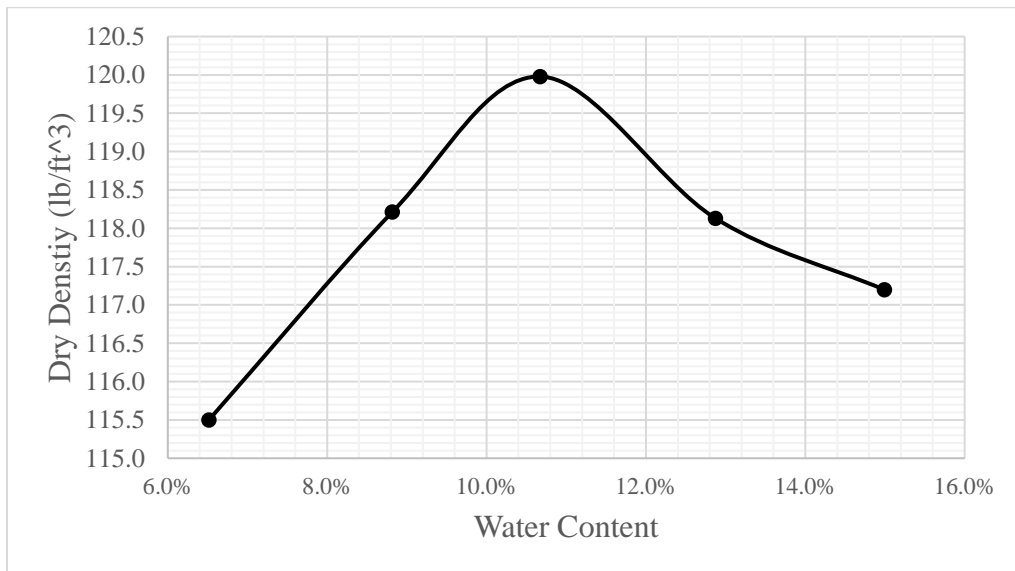


Figure A.2: Design curve for Waugh soil with 5 percent cement content

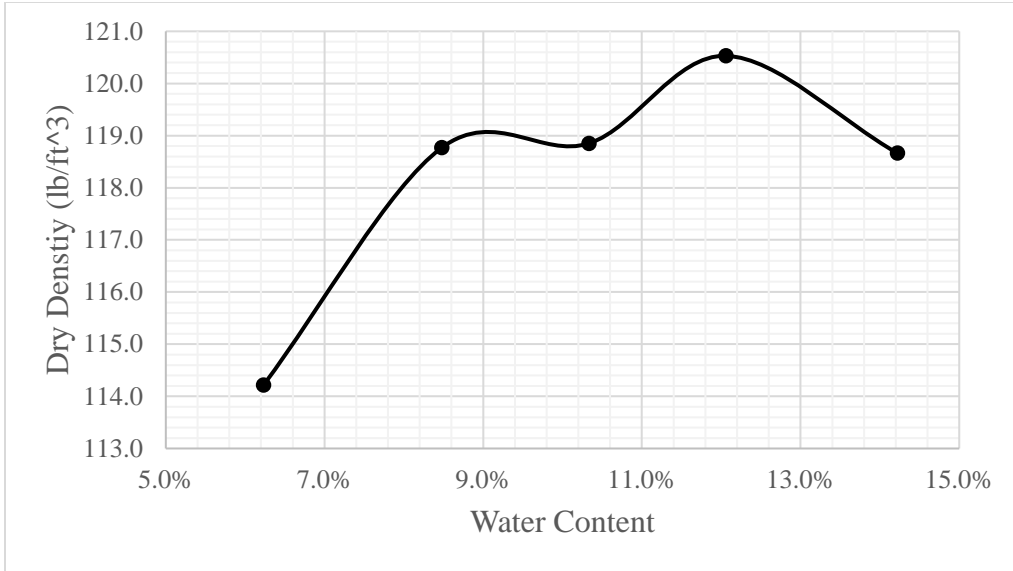


Figure A.3: Design curve for Waugh soil with 6 percent cement content

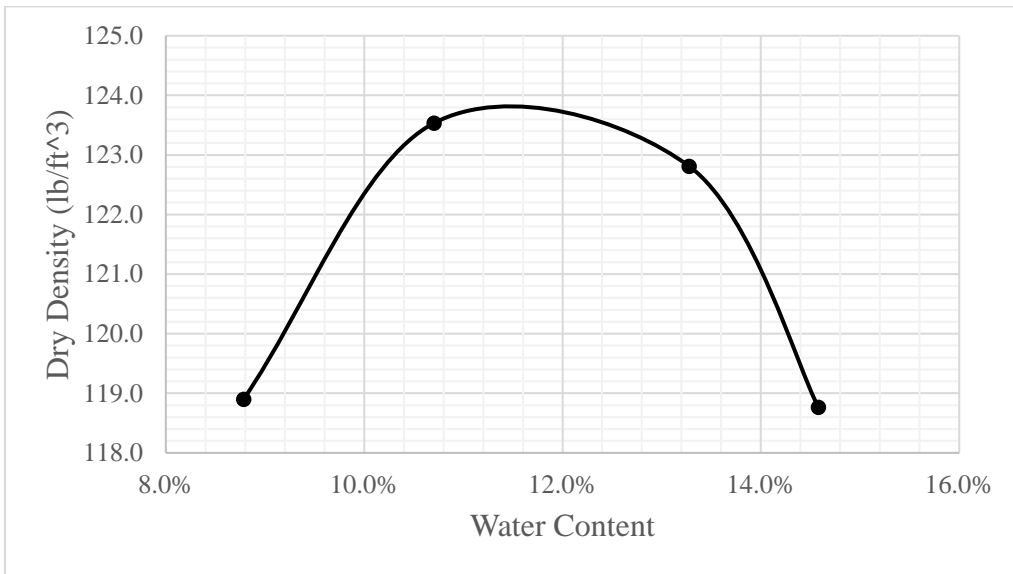


Figure A.4: Design curve for Waugh soil with 8 percent cement content

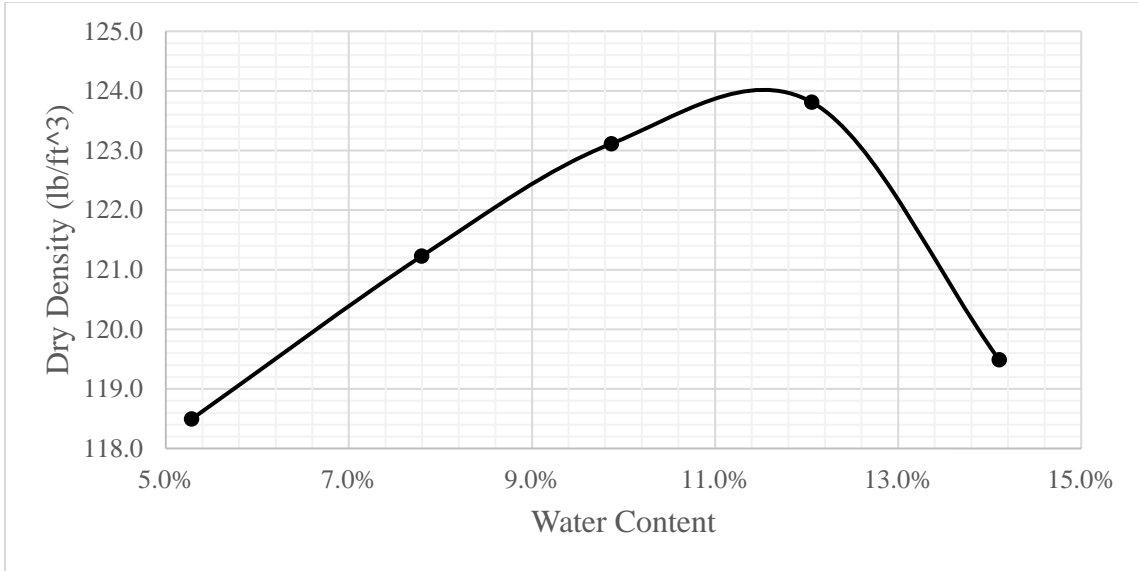


Figure A.5: Design curve for Waugh soil with 10 percent cement content

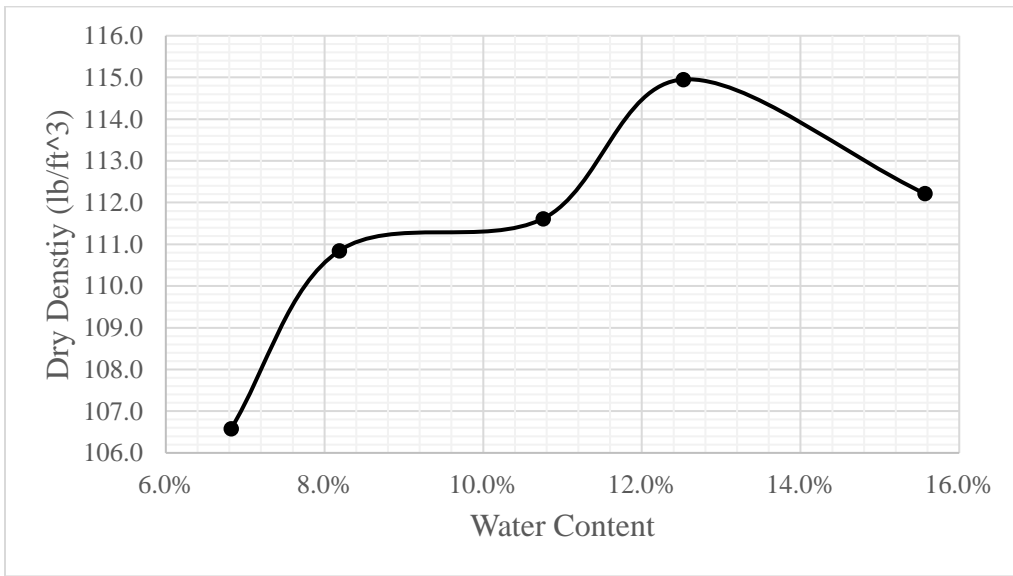


Figure A.6: Design curve for Elba soil with 5 percent cement content

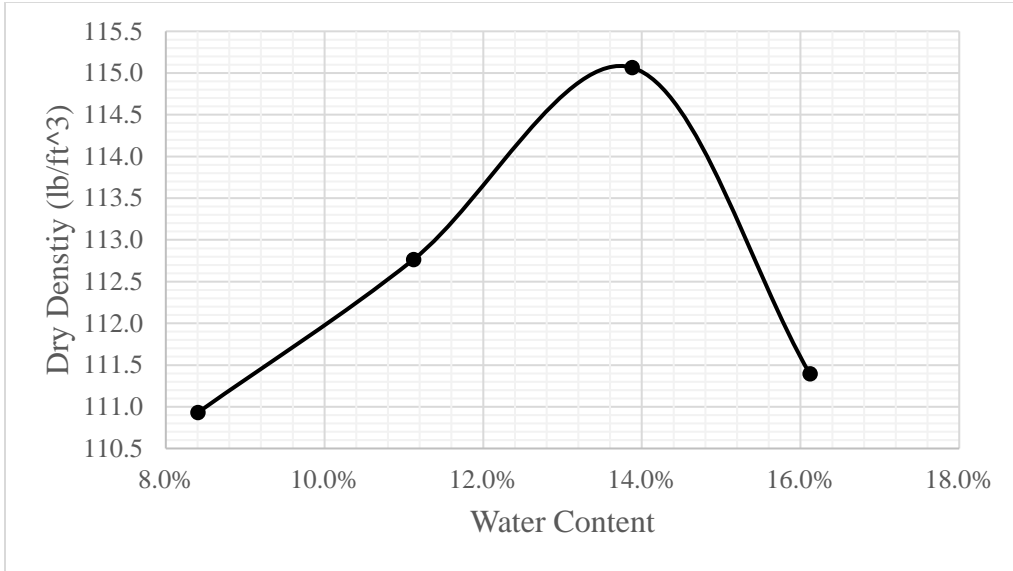


Figure A.7: Design curve for Elba soil with 6.5 percent cement content

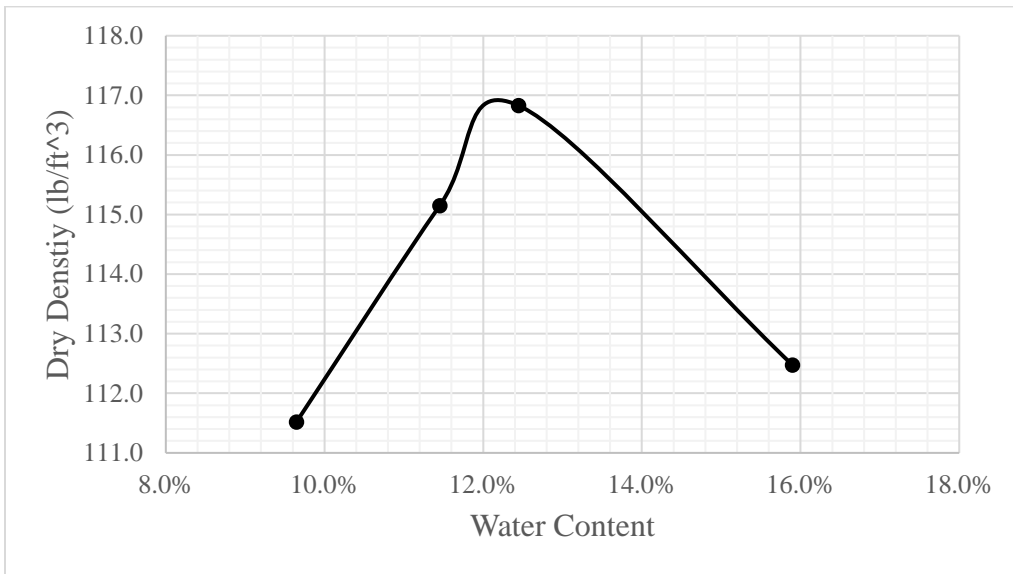


Figure A.8: Design curve for Elba soil with 8 percent cement content

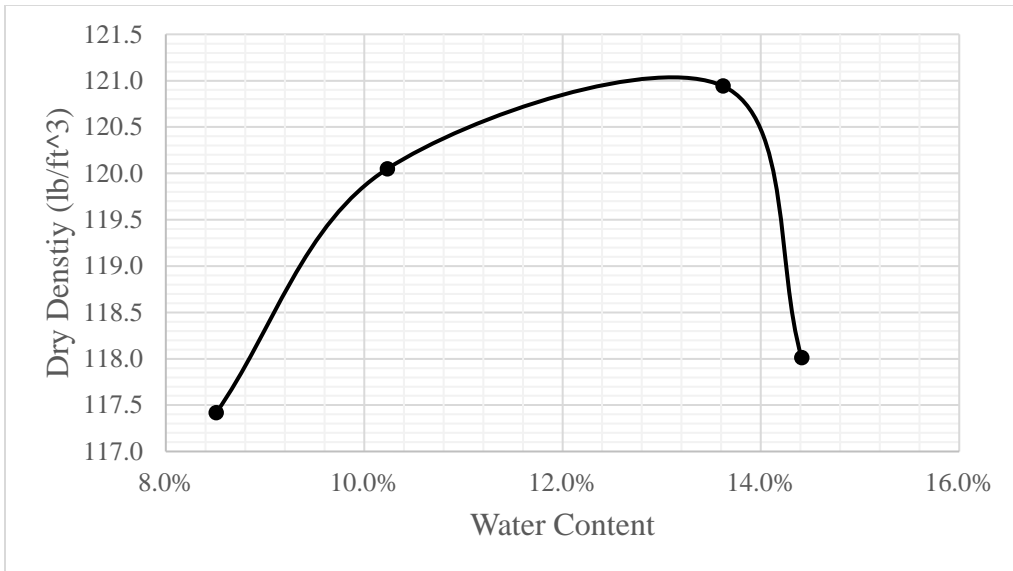


Figure A.9: Design curve for Elba soil with 10 percent cement content

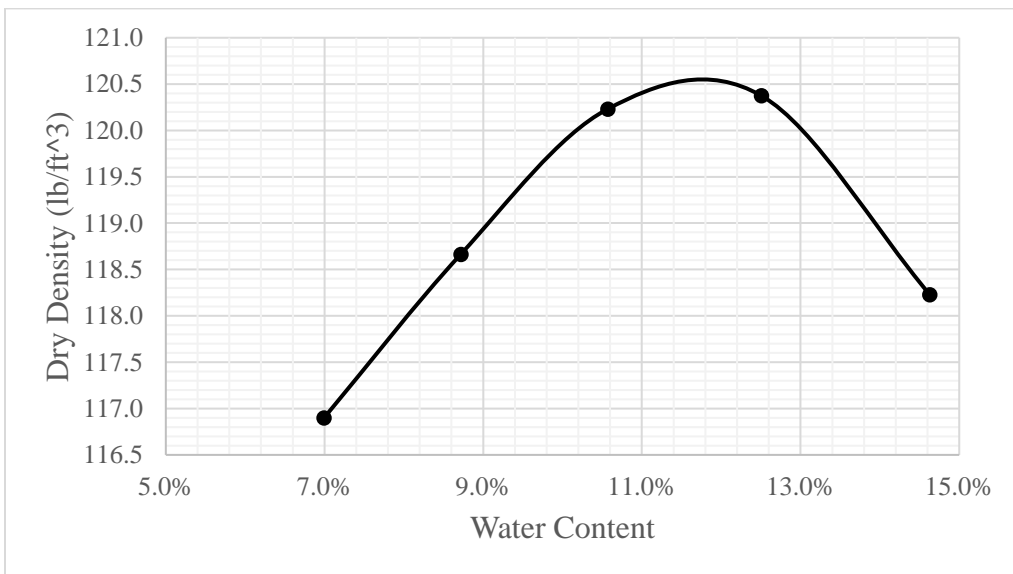


Figure A.10: Design curve for Coarse soil with 4 percent cement content

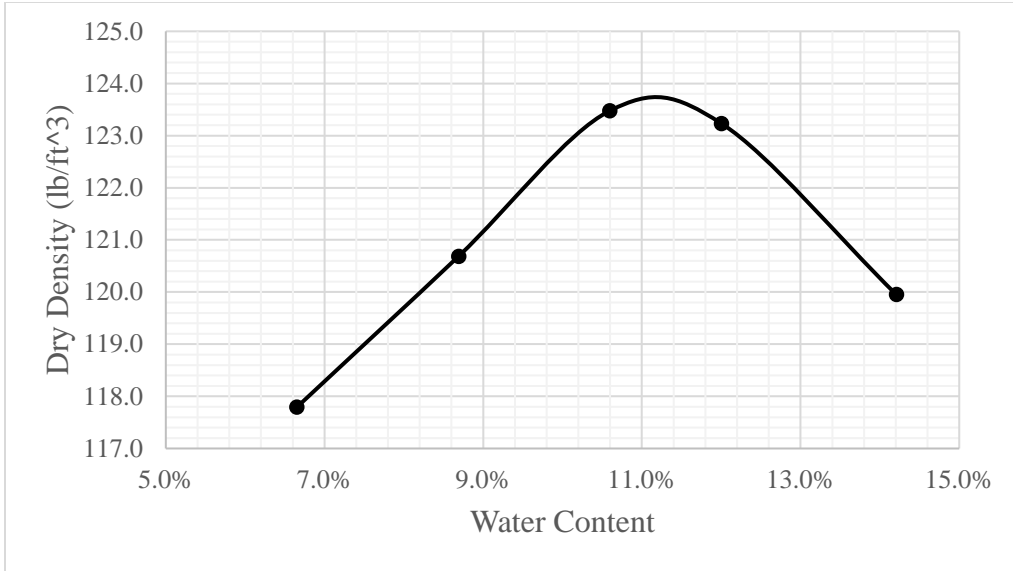


Figure A.11: Design curve for Coarse soil with 6 percent cement content

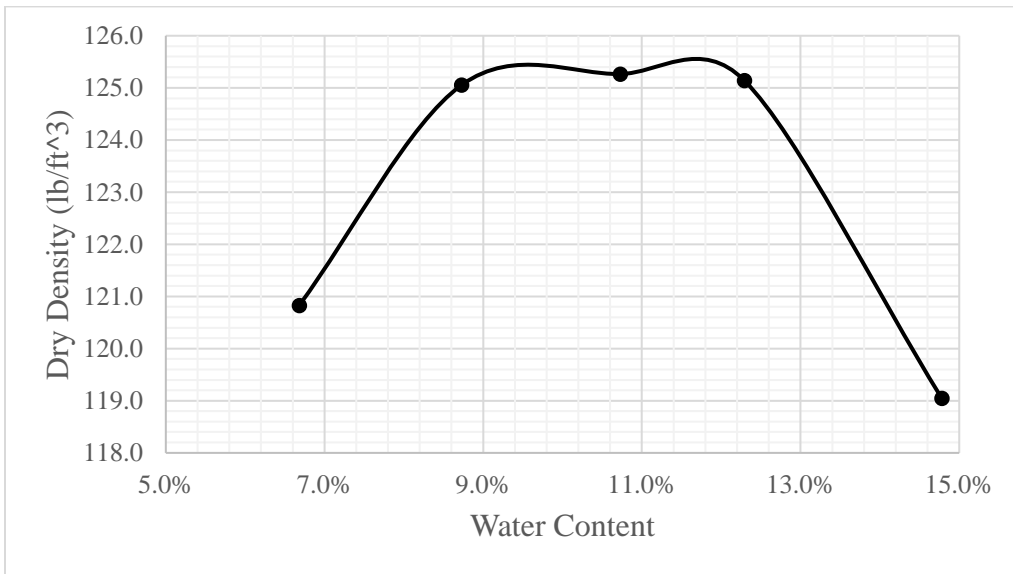


Figure A.12: Design curve for Coarse soil with 8 percent cement content

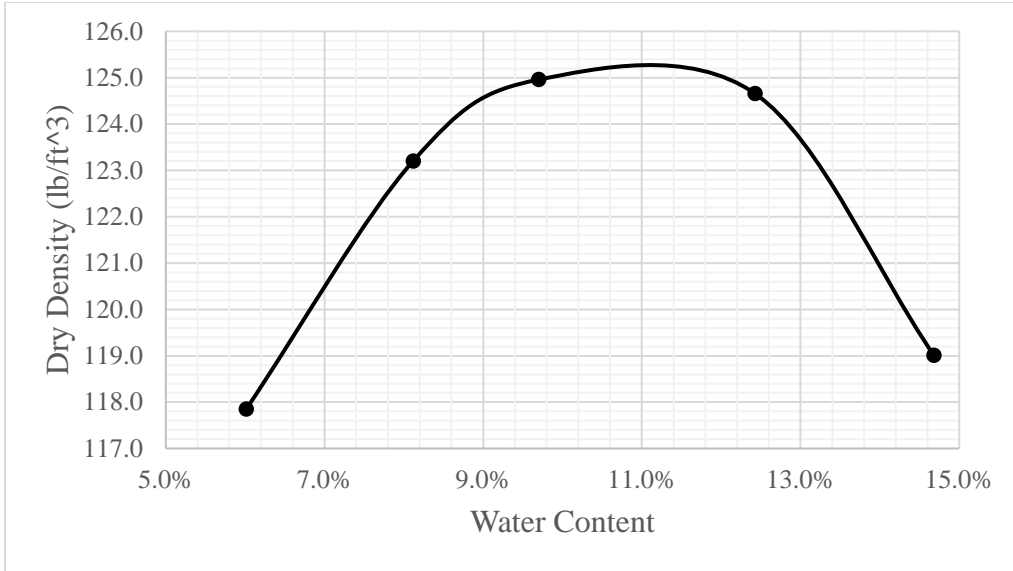


Figure A.13: Design curve for Coarse soil with 9 percent cement content

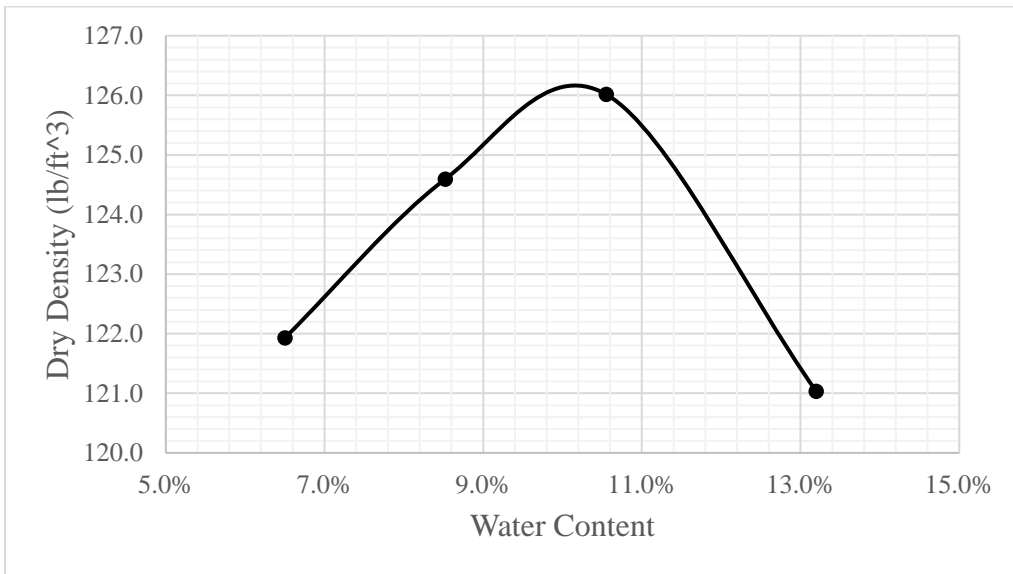


Figure A.14: Design curve for Coarse soil with 10 percent cement content

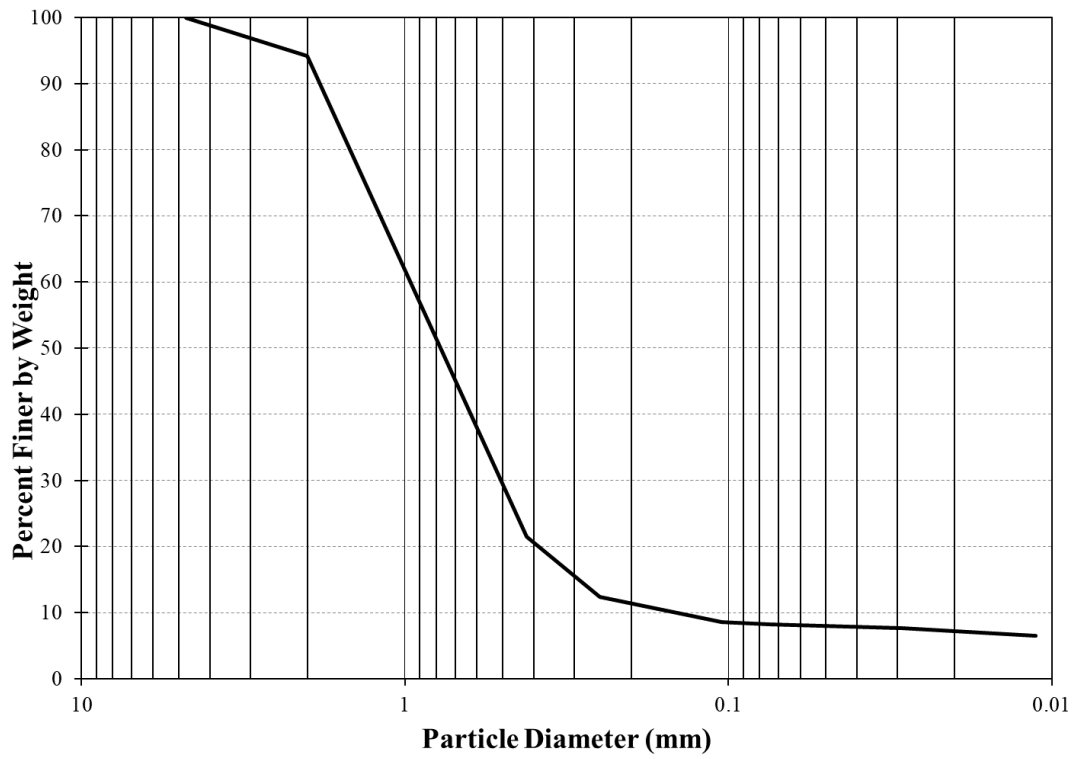


Figure A.15: Gradation for Waugh soil

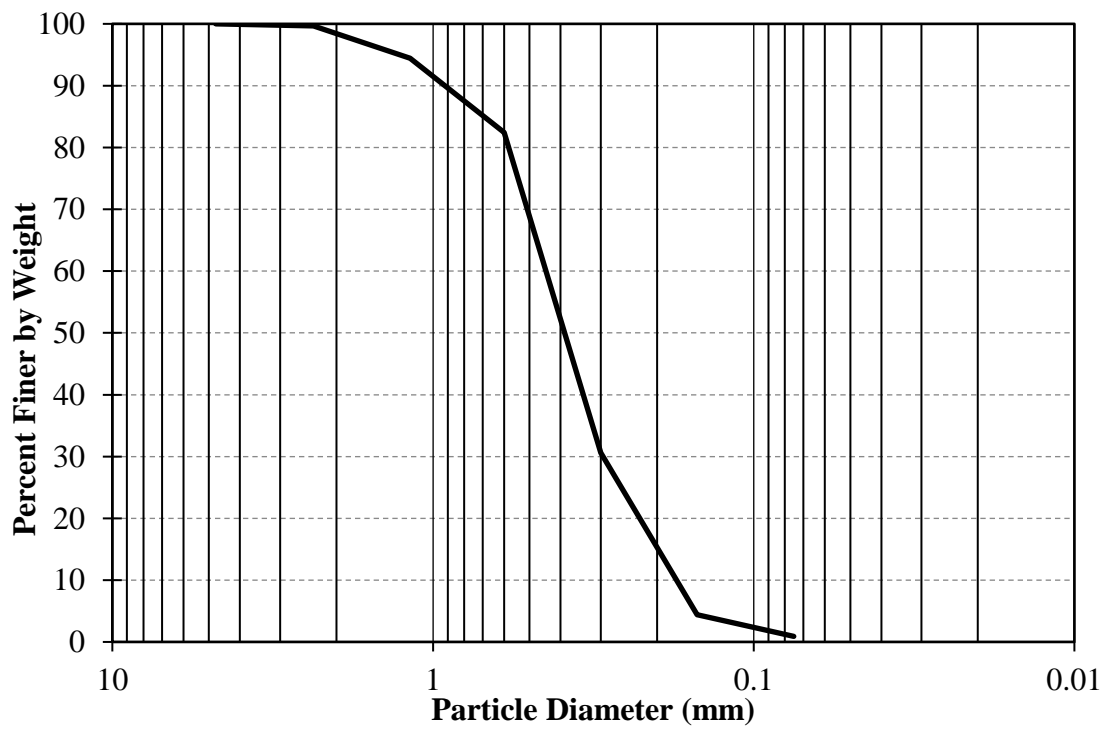


Figure A.16: Gradation for Elba soil

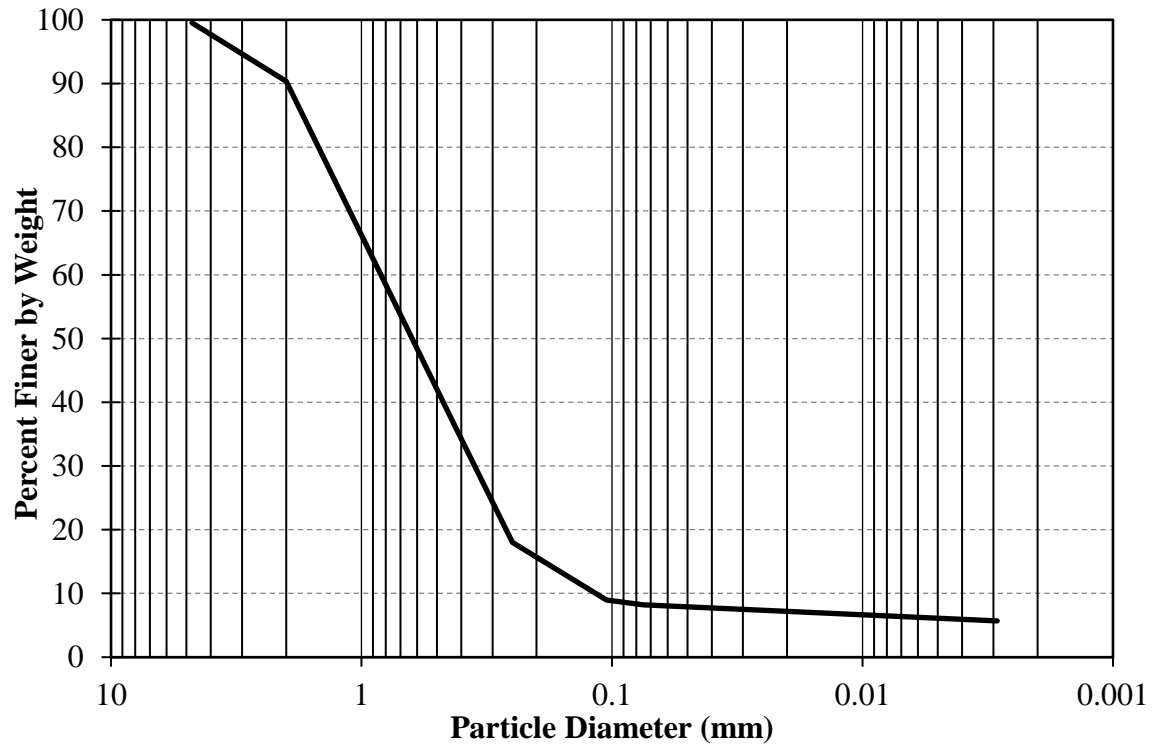


Figure A.17: Gradation for Coarse soil

Appendix B

DCP Initial Curing Study

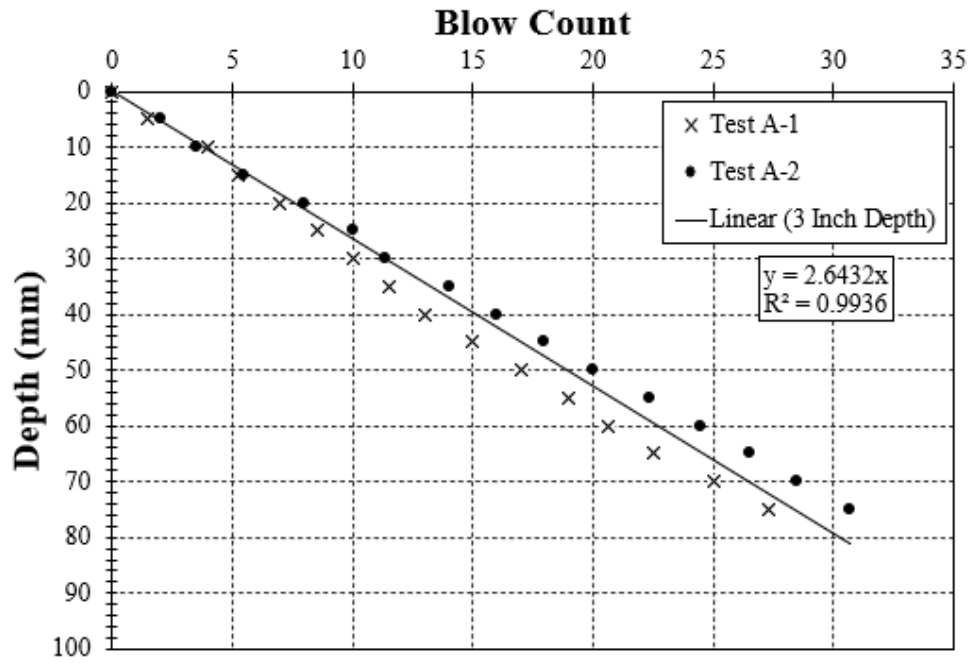


Figure B.1: Plastic lid method at 4 percent cement

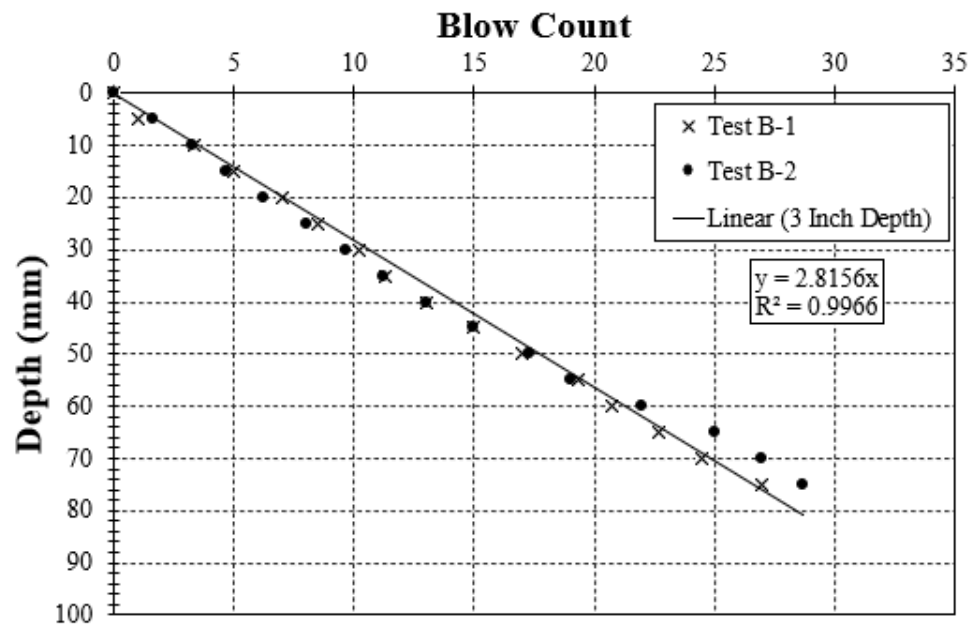


Figure B.2: Plastic sheet and clip method at 4 percent cement

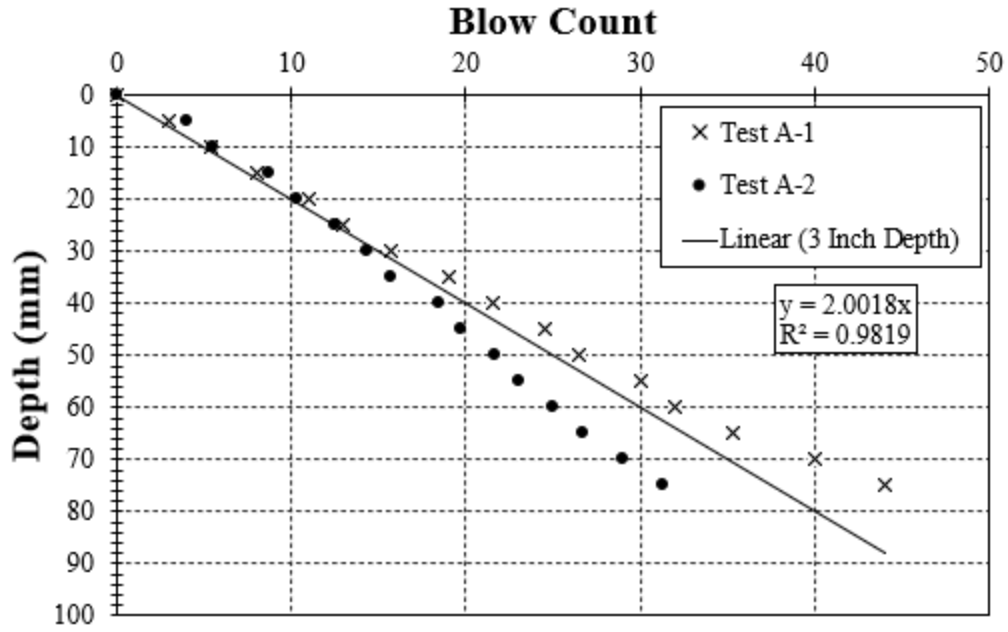


Figure B.3: Plastic lid method at 6 percent cement

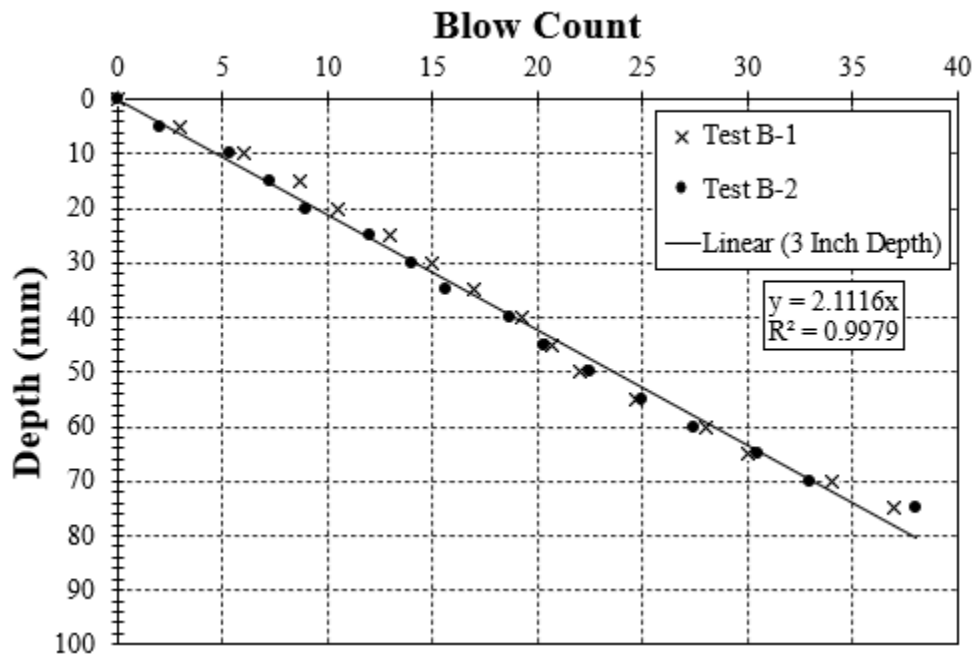


Figure B.4: Plastic sheet and clip method at 6 percent cement

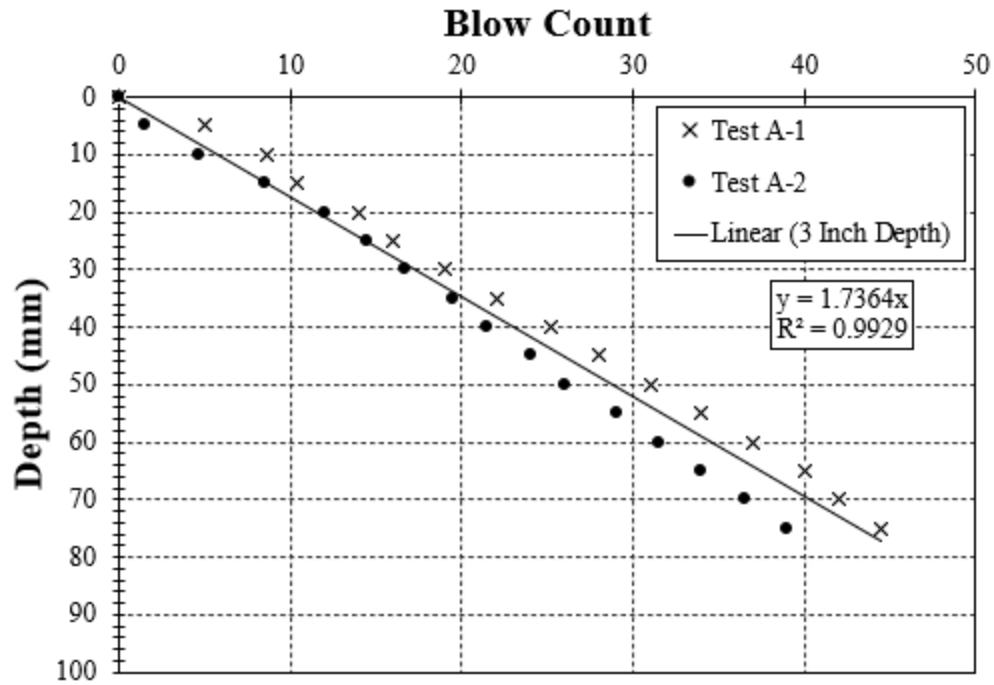


Figure B.5: Plastic lid method at 8 percent cement

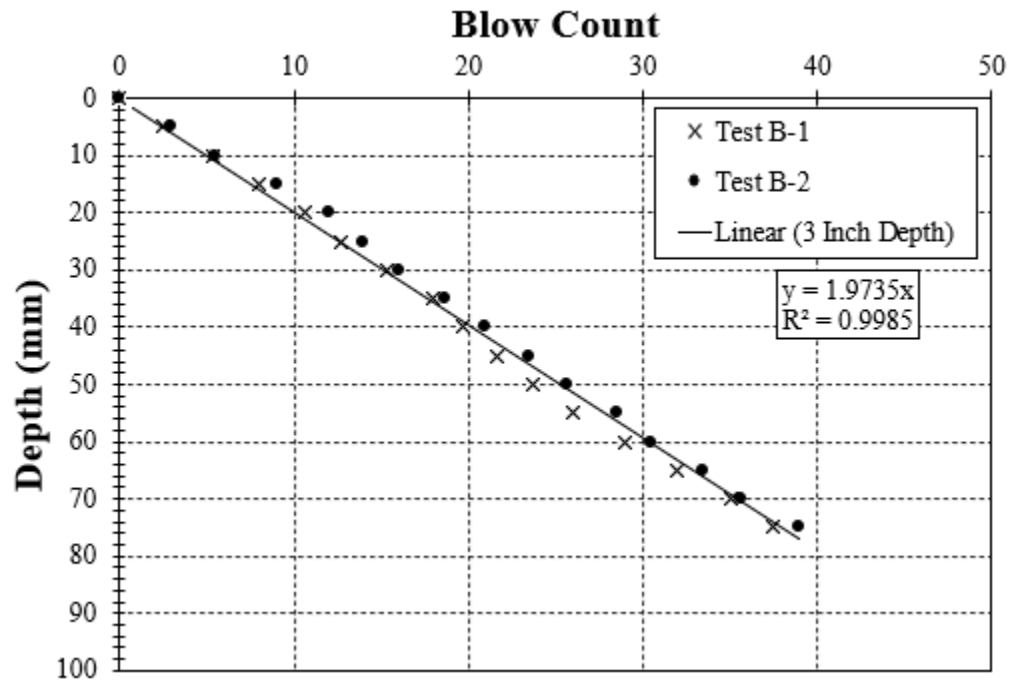


Figure B.6: Plastic sheet and clip method at 8 percent cement

Appendix C

Soil Classification Impact Data

Table C.1: Data for soil classification impact for Elba soil

Elba Soil		
AASHTO Soil Classification		A-2-4
USCS		SM
Cement Content, %	75 mm 7-day DCP Slope	7-day PM Strength (psi)
5	3.075	320
6.5	2.863	360
8	1.740	545

Table C.2: Data for soil classification impact for Waugh soil

Waugh Soil		
AASHTO Soil Classification		A-2-6
USCS		SP-SC
Cement Content, %	75 mm 7-day DCP Slope	7-day PM Strength (psi)
4*	3.109	180
5*	2.149	315
6	1.691	390
8*	1.520	600
10	0.936	930

*Multiple tests completed so average slope and strength was taken

Table C.3: Data for soil classification impact for Coarse soil

Coarse Soil		
AASHTO Soil Classification		A-1b
USCS		SW-SC
Cement Content, %	75 mm 7-day DCP Slope	7-day PM Strength (psi)
4*	4.106	135
6*	2.363	305
8*	1.596	555
9	1.057	860
10**	0.400	1080

*Multiple tests completed so average slope and strength was taken

**Soil was in-penetrable using DCP so slope is taken as refusal (2 mm/5 blows)

Appendix D

25 Millimeter Penetration Depth Data

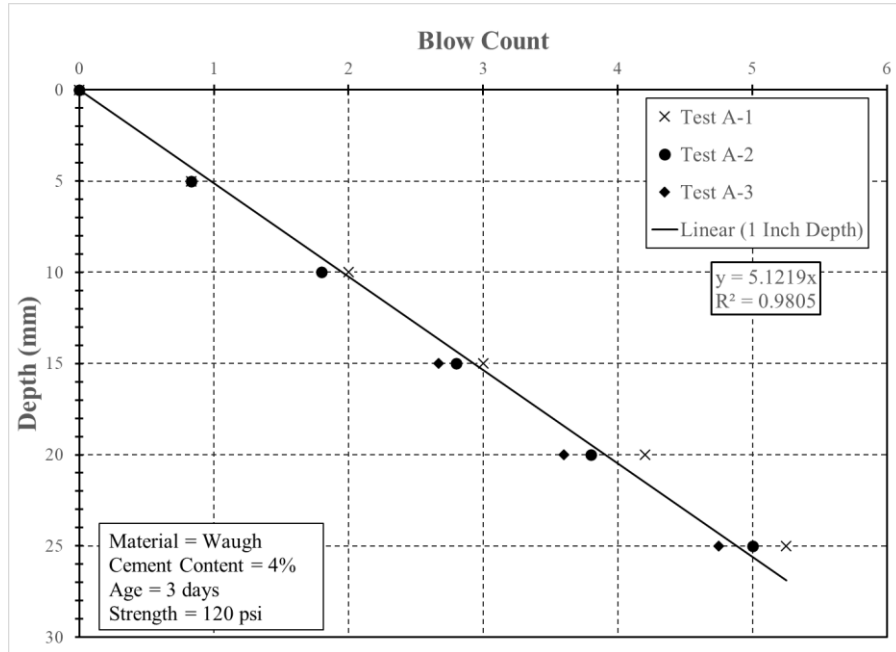


Figure D.1: Waugh 4% No. 1 3 day

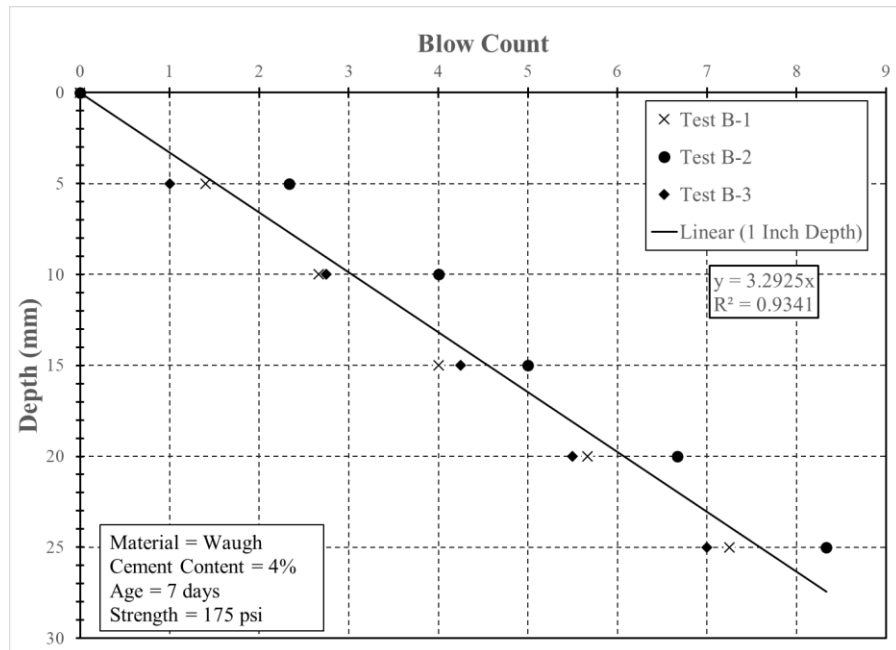


Figure D.2: Waugh 4% No. 1 7 day

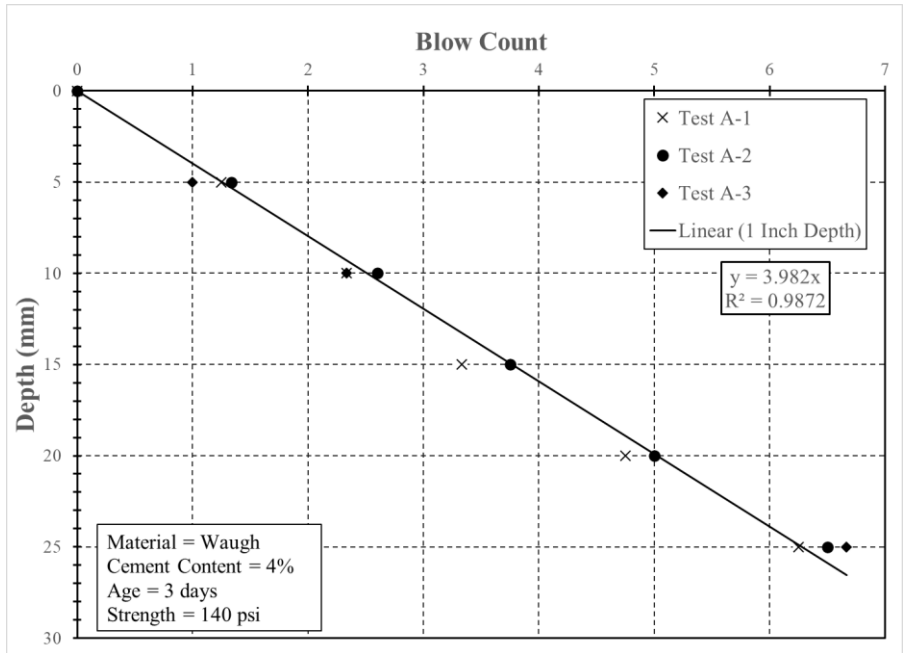


Figure D.3: Waugh 4% No. 2 3 day

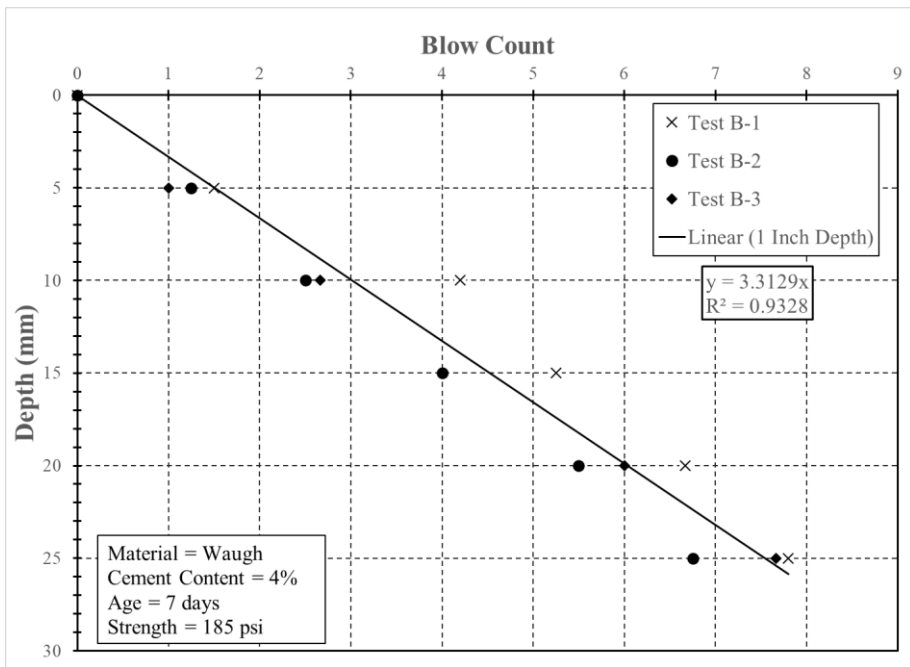


Figure D.4: Waugh 4% No. 2 7 day

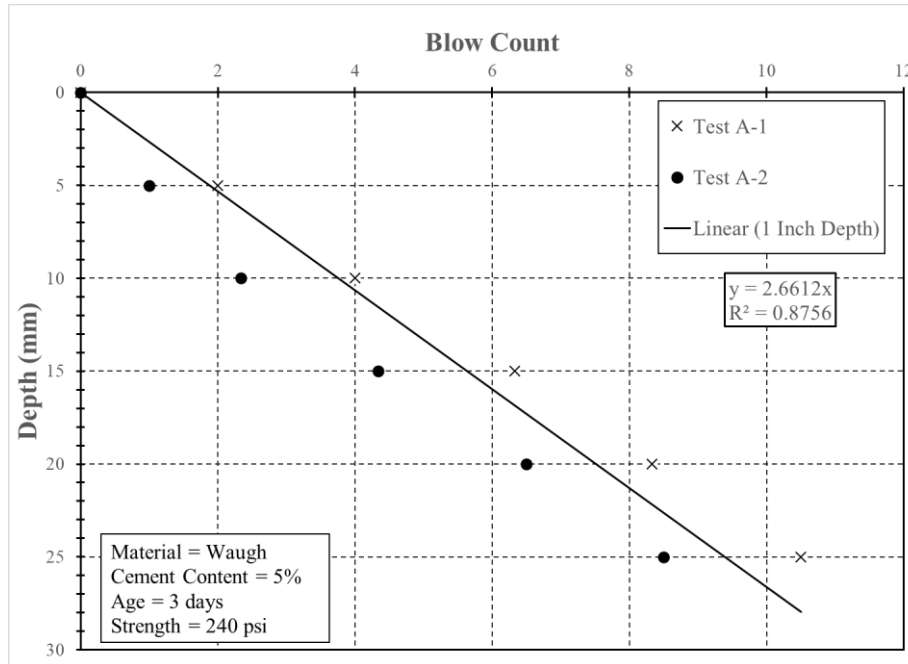


Figure D.5: Waugh 5% No. 1 3 days (Third specimen was removed due to error)

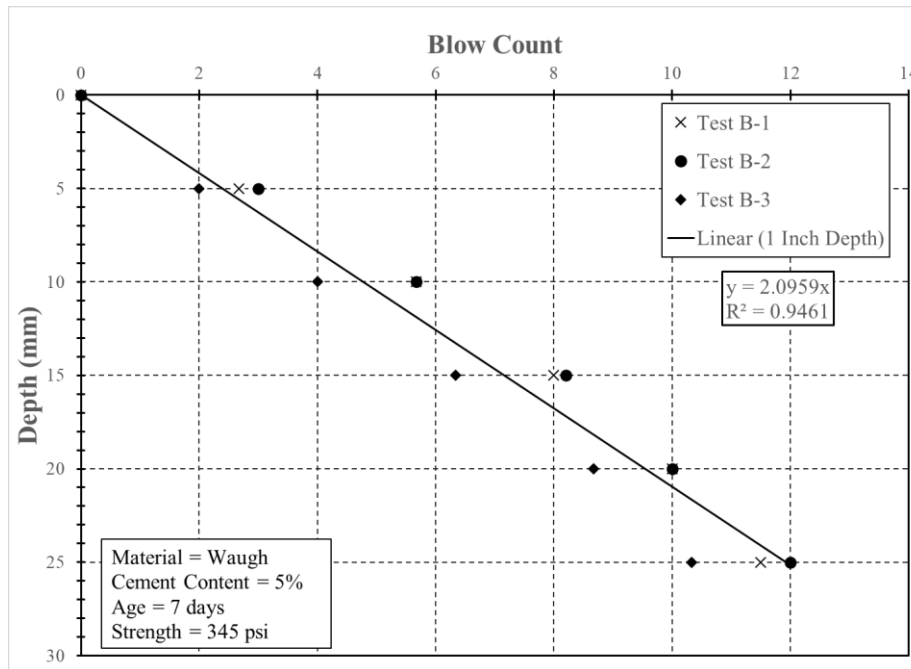


Figure D.6: Waugh 5% No. 1 7 days

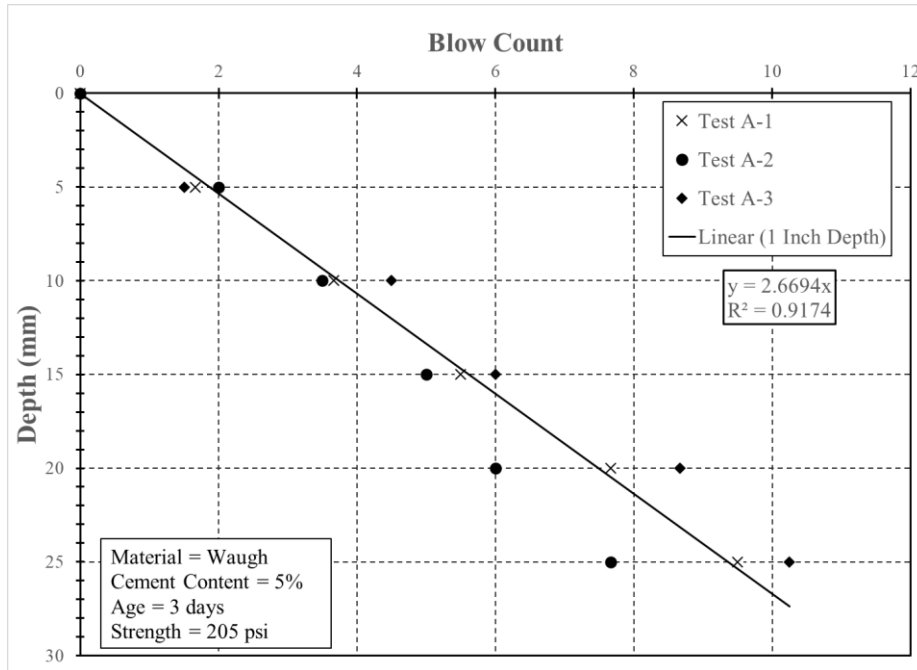


Figure D.7: Waugh 5% No. 2 3 days

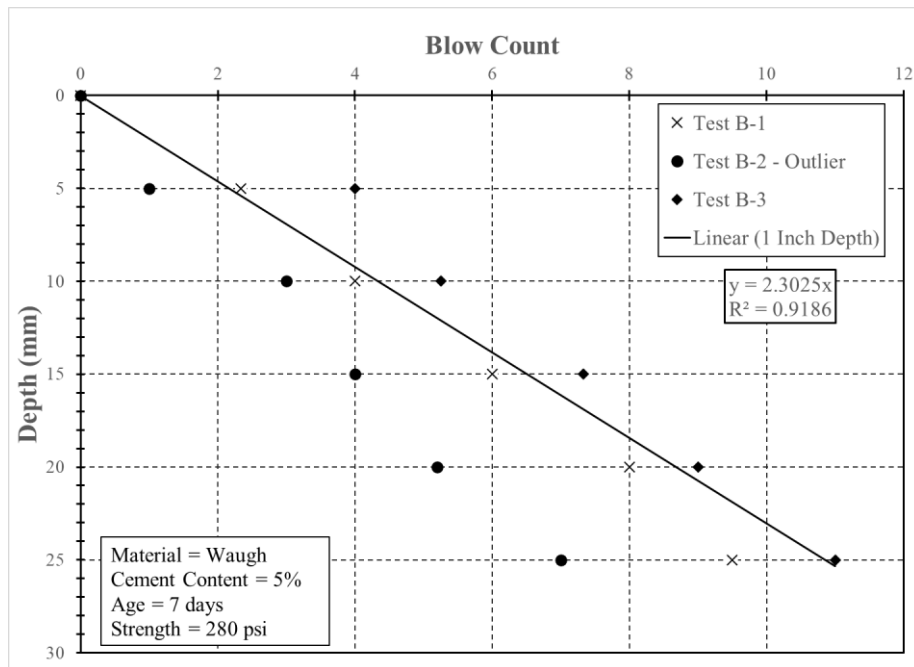


Figure D.8: Waugh 5% No. 2 7 days

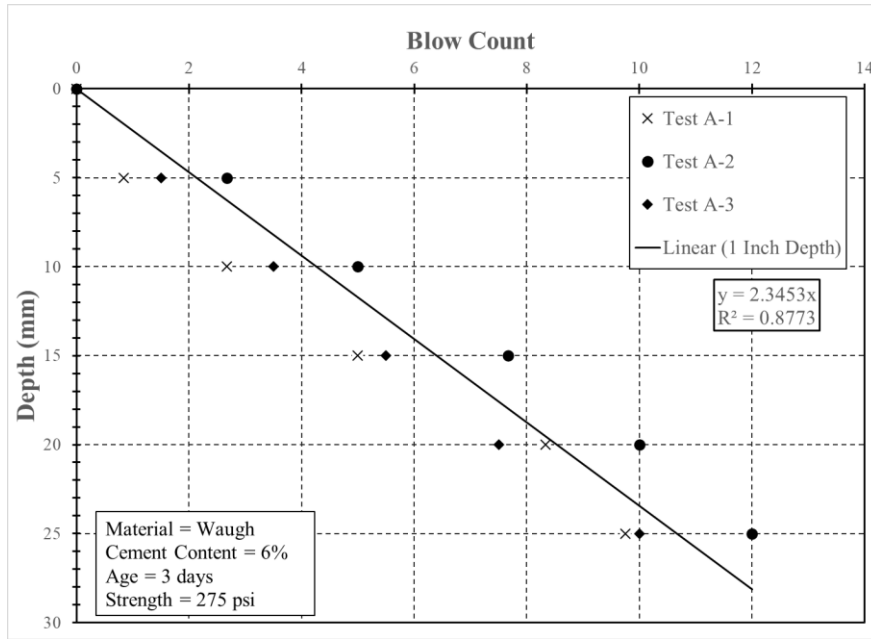


Figure D.9: Waugh 6% 3 day

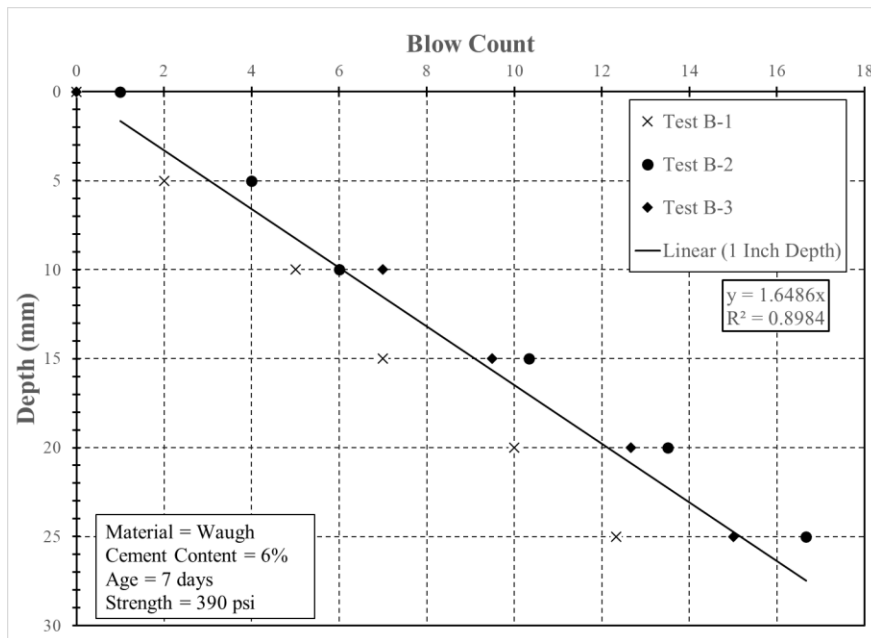


Figure D.10: Waugh 6% 7 day

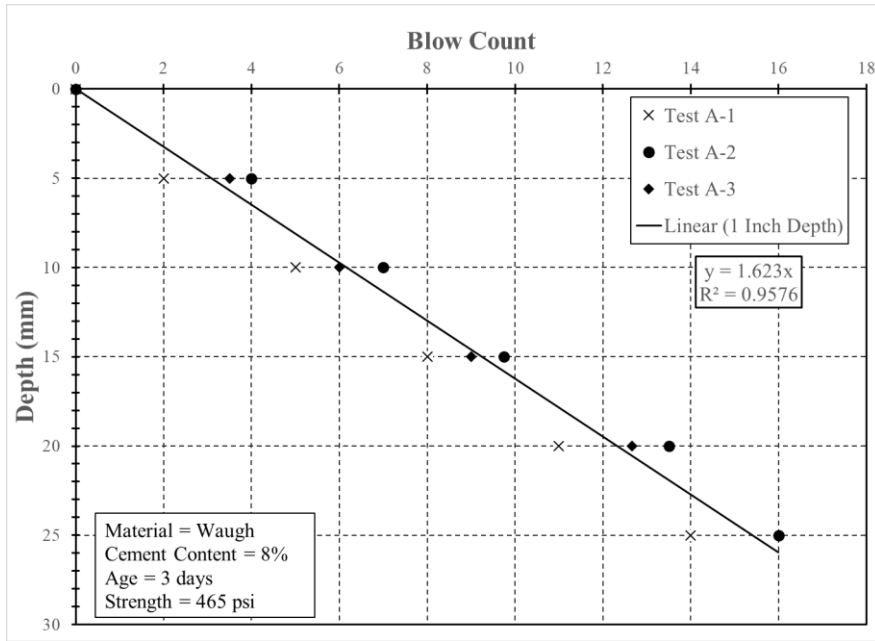


Figure D.11: Waugh 8% No. 1 3 days

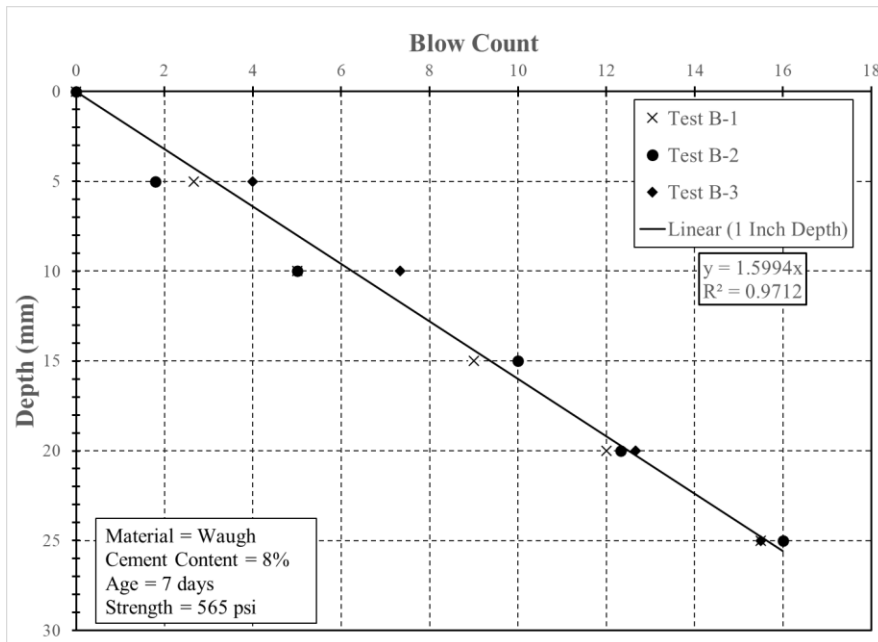


Figure D.12: Waugh 8% No. 1 7 days

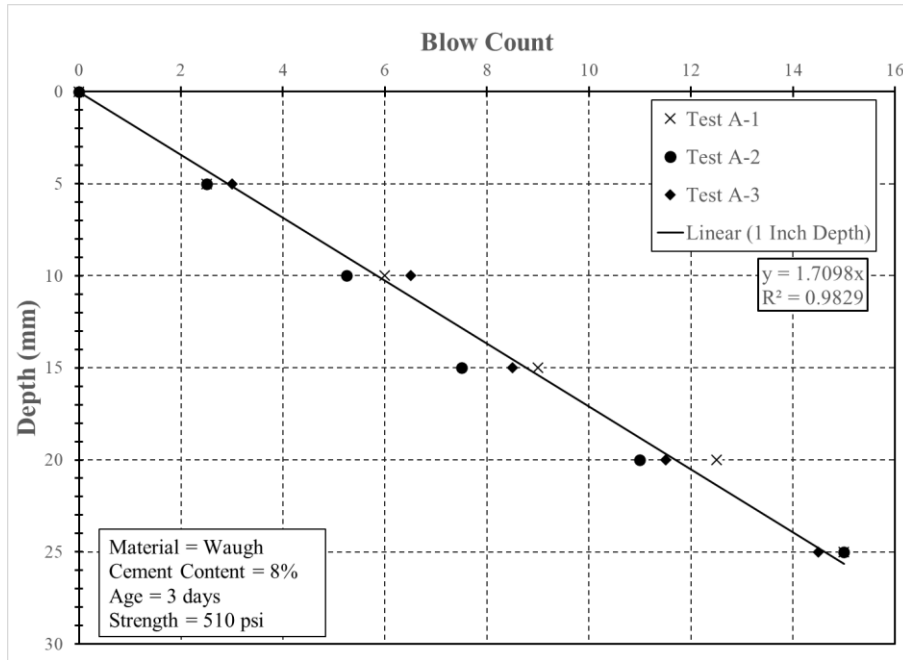


Figure D.13: Waugh 8% No. 2 3 days

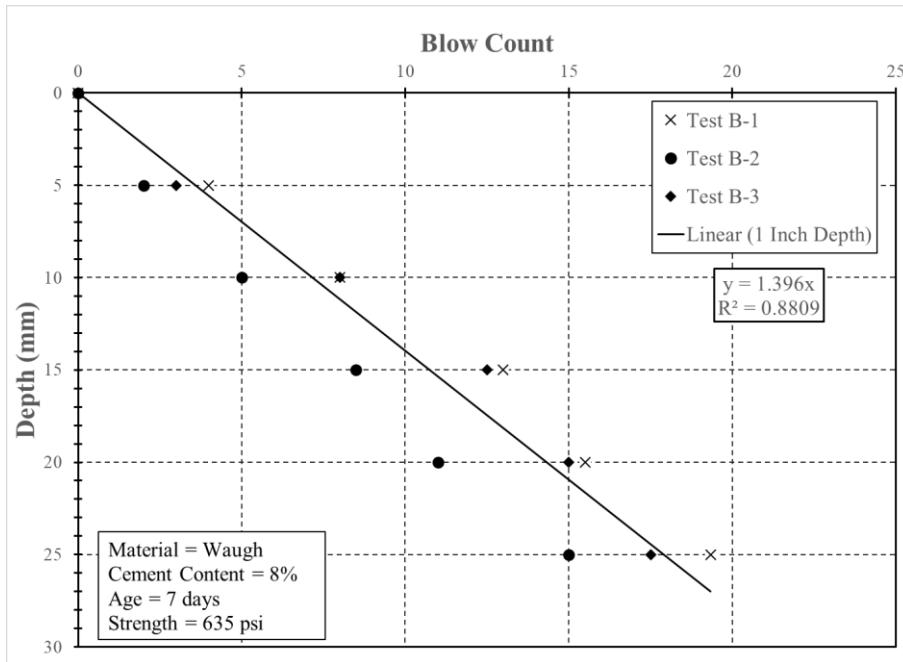


Figure D.14: Waugh 8% No. 2 7 days

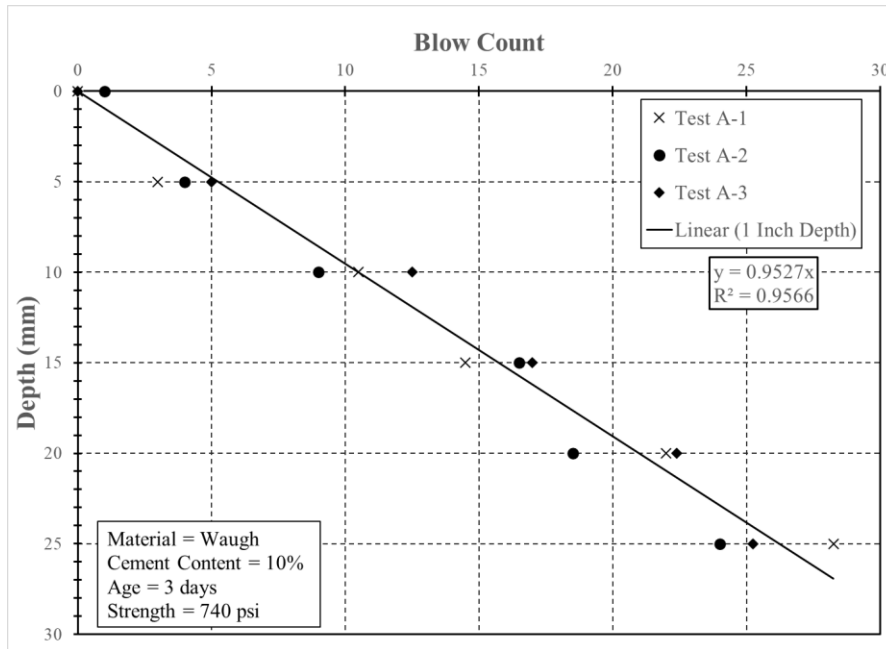


Figure D.15: Waugh 10% 3 days

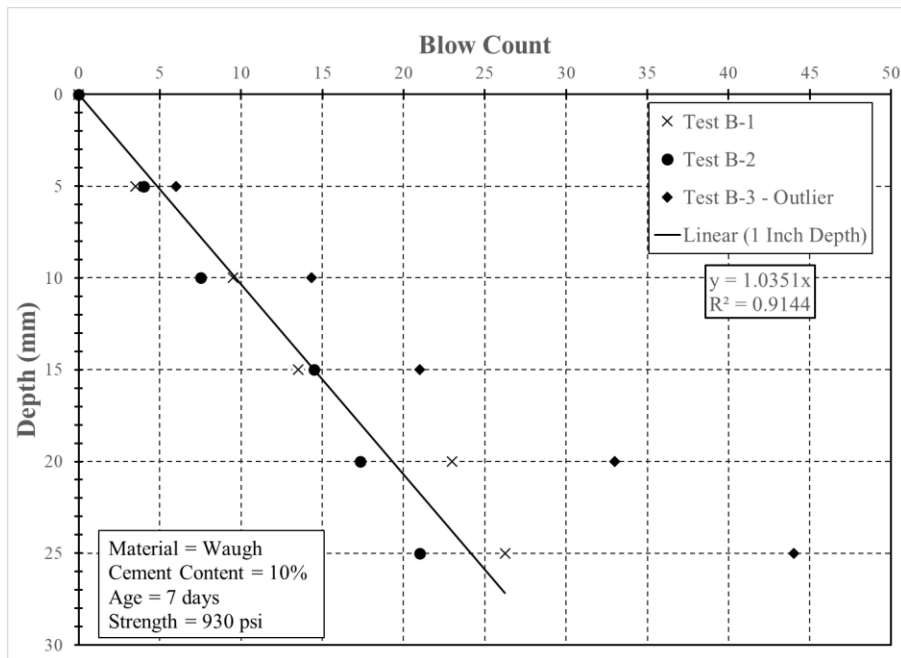


Figure D.16: Waugh 10% 7 days

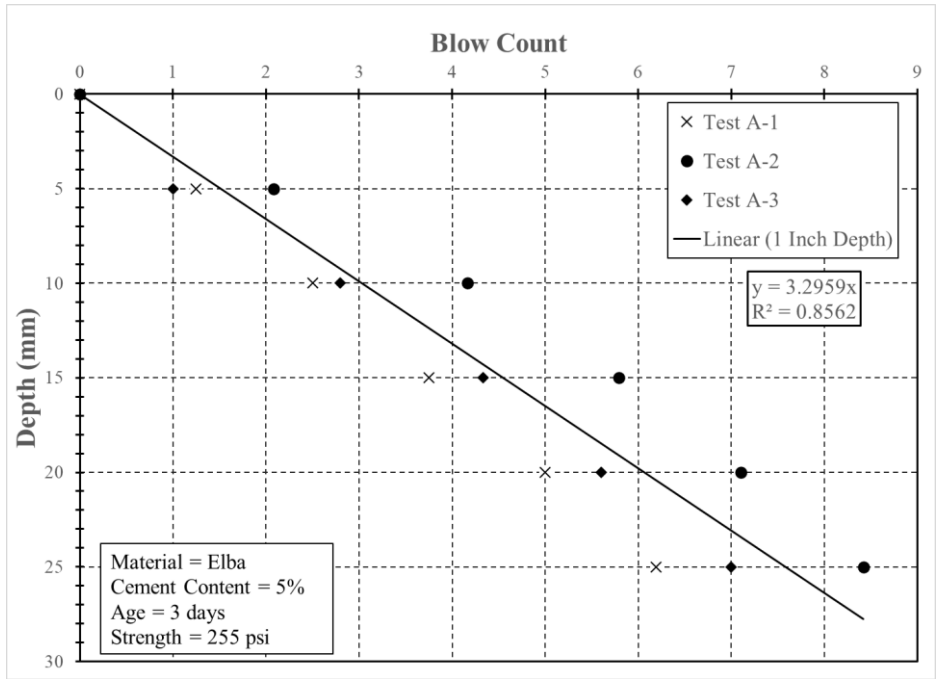


Figure D.17: Elba 5% 3 days

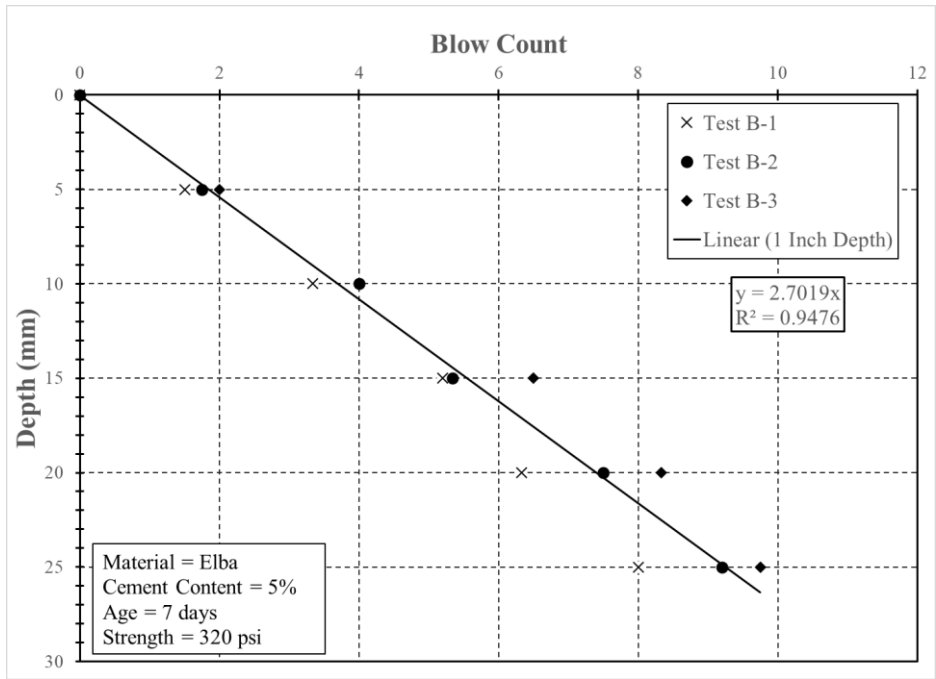


Figure D.18: Elba 5% 7 days

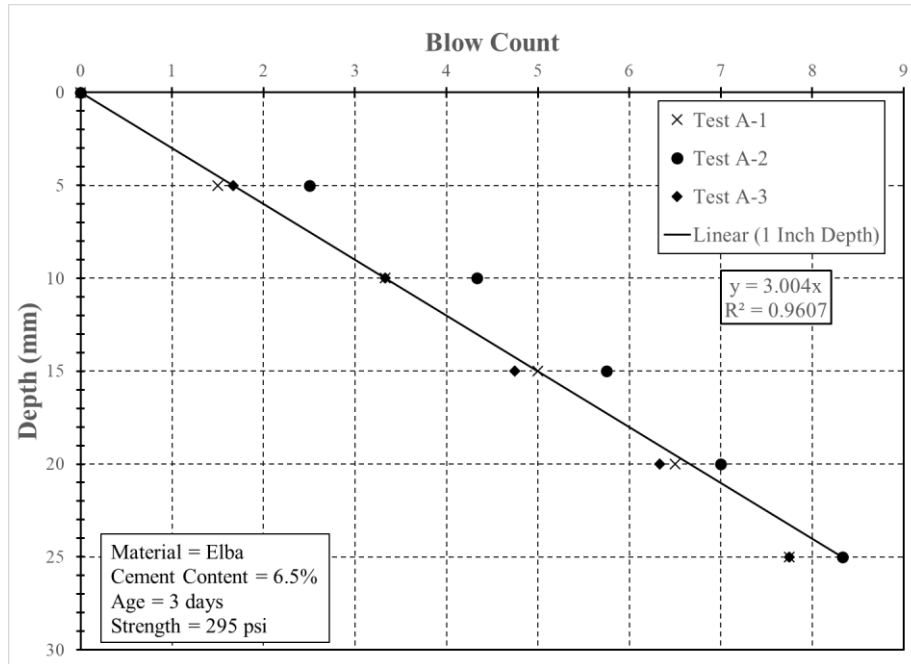


Figure D.19: Elba 6.5% No. 1 3 days

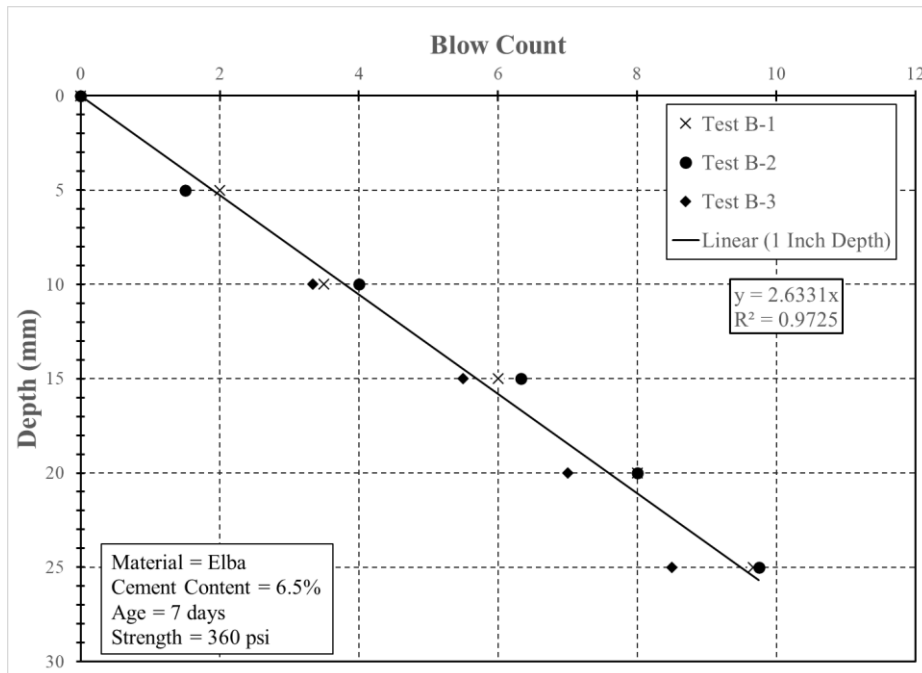


Figure D.20: Elba 6.5% No. 1 7 days

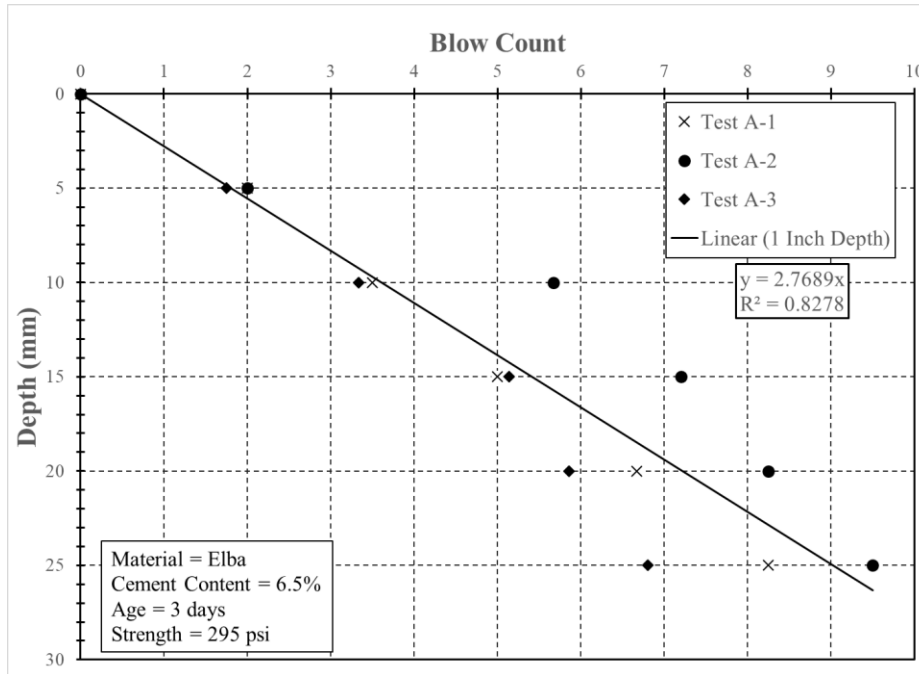


Figure D.21: Elba 6.5% No. 2 3 days

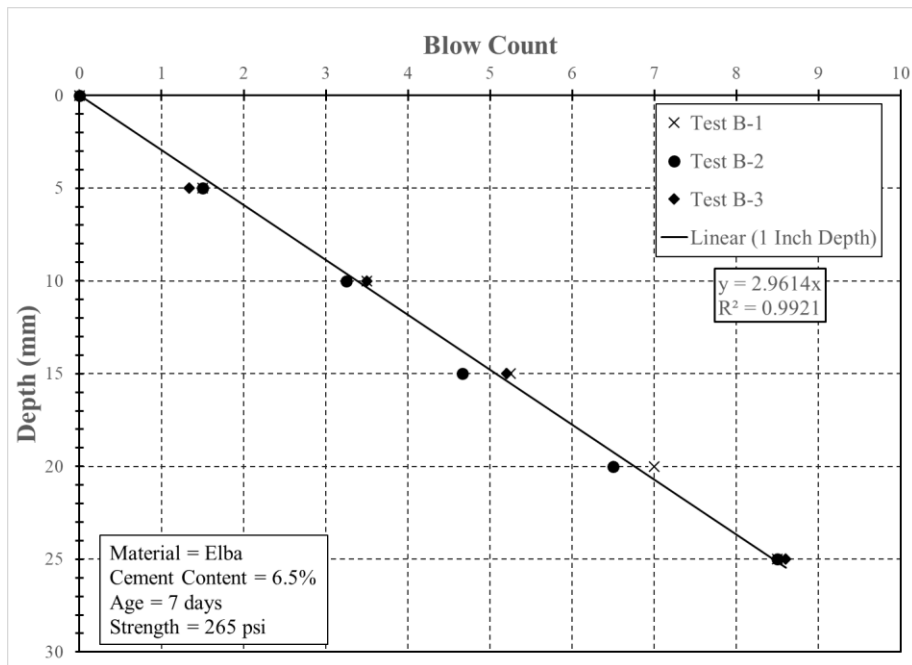


Figure D.22: Elba 6.5% No. 2 7 days

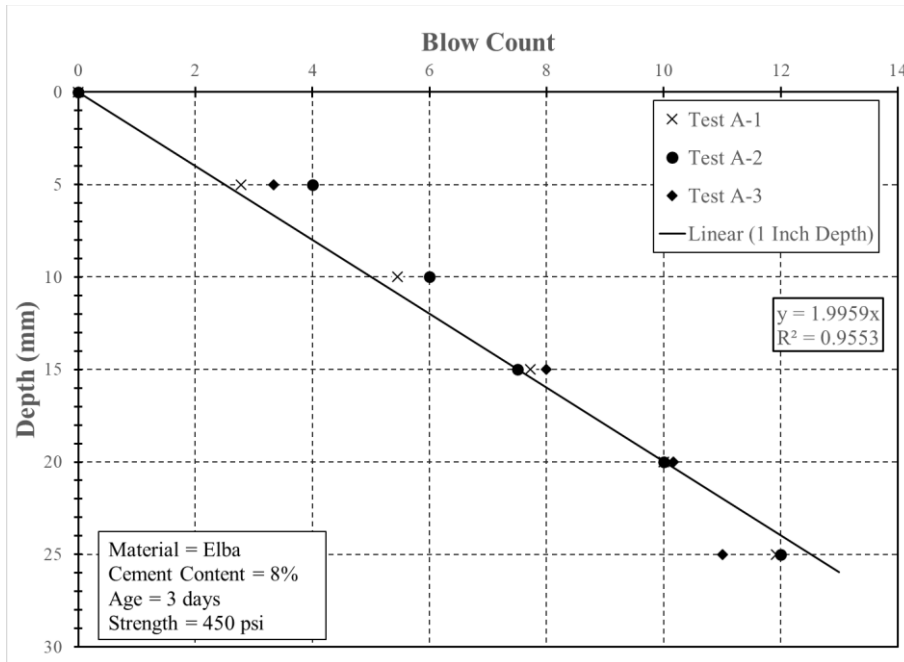


Figure D.23: Elba 8% 3 days

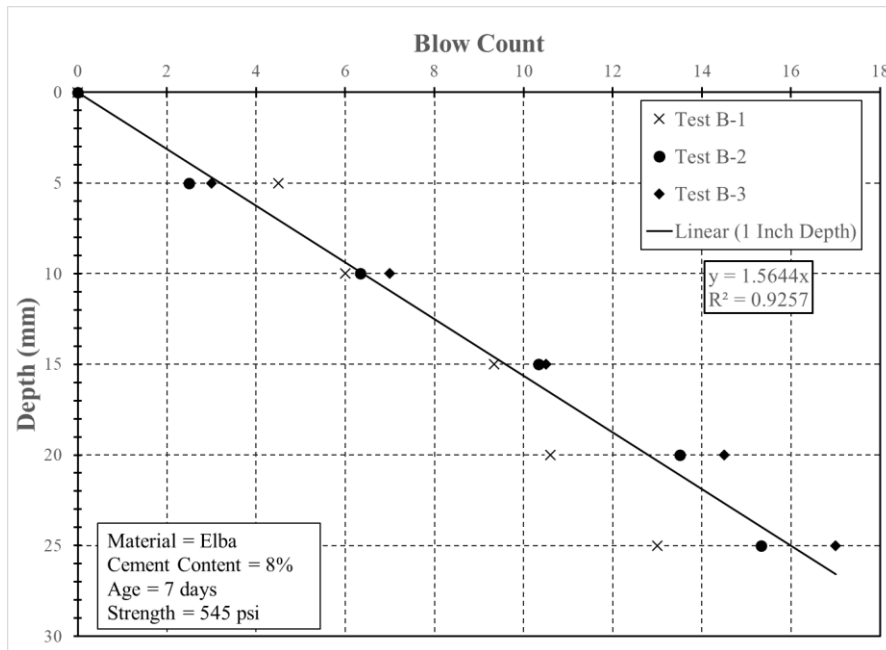


Figure D.24: Elba 8% 7 days

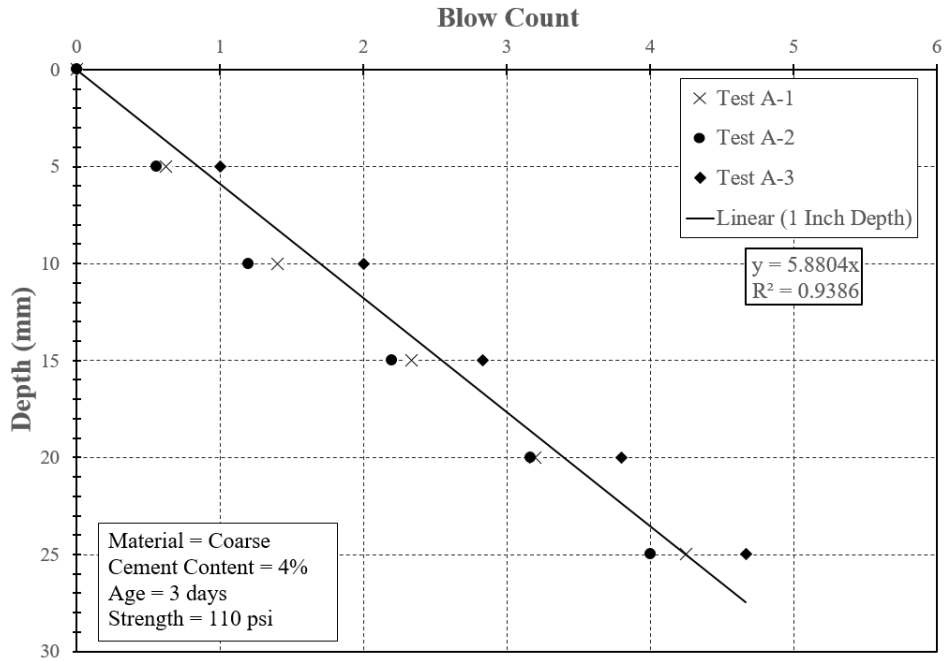


Figure D.25: Coarse 4% No. 1 3 days

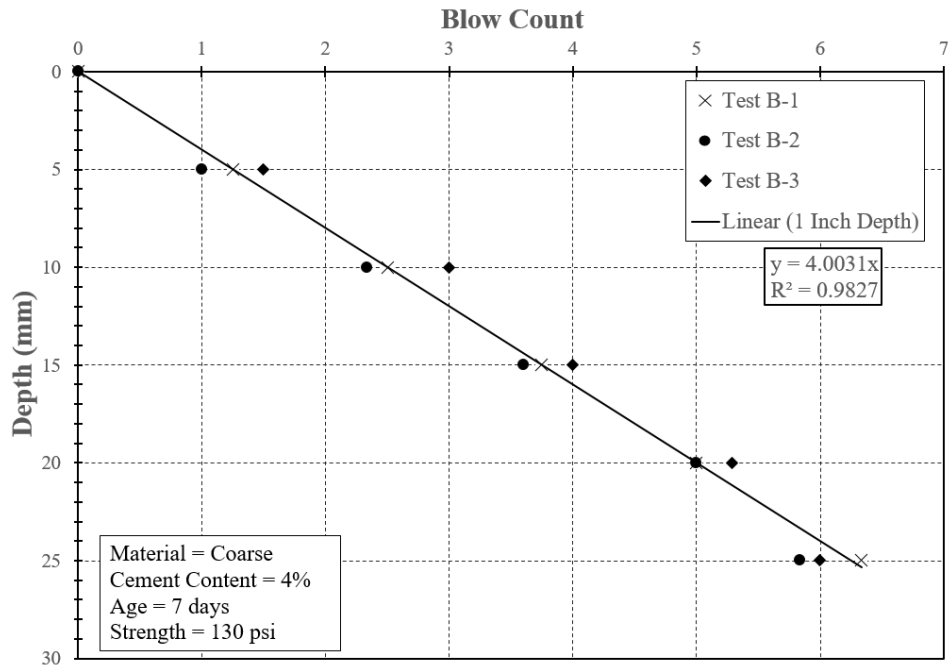


Figure D.26: Coarse 4% No. 1 7 days

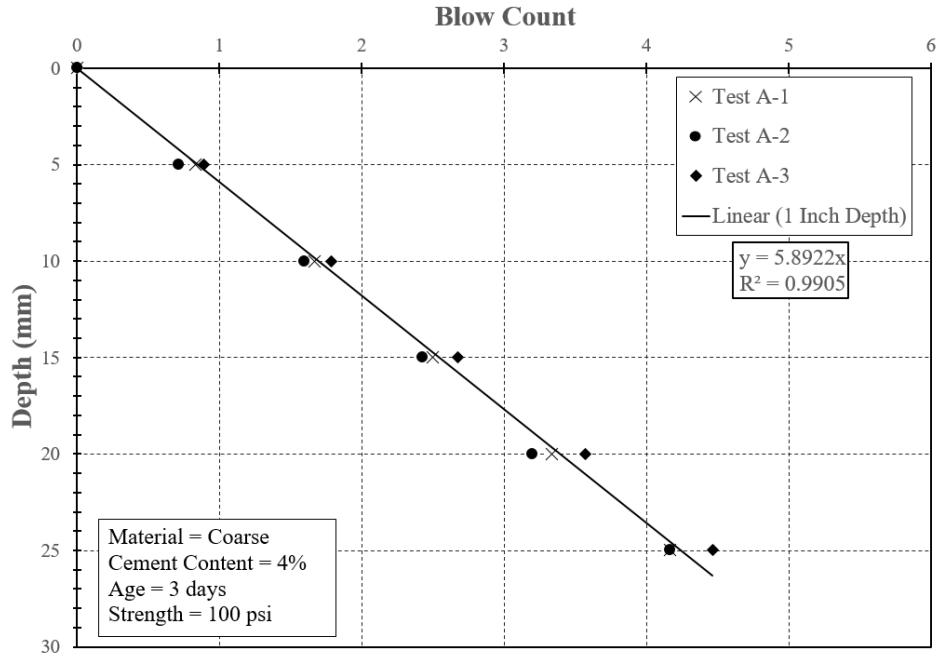


Figure D.27: Coarse 4% No. 2 3 days

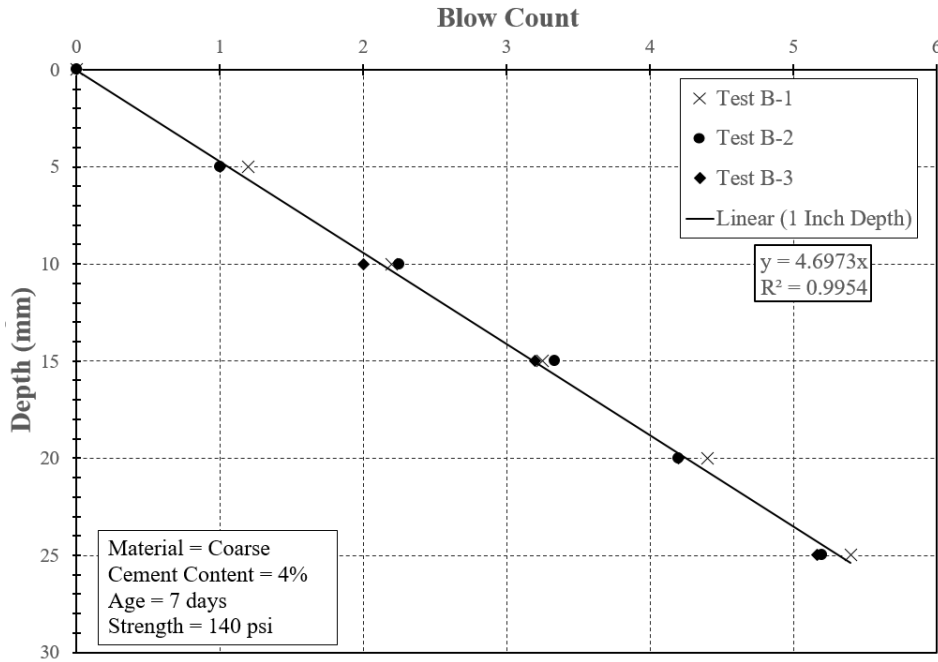


Figure D.28: Coarse 4% No. 2 7 days

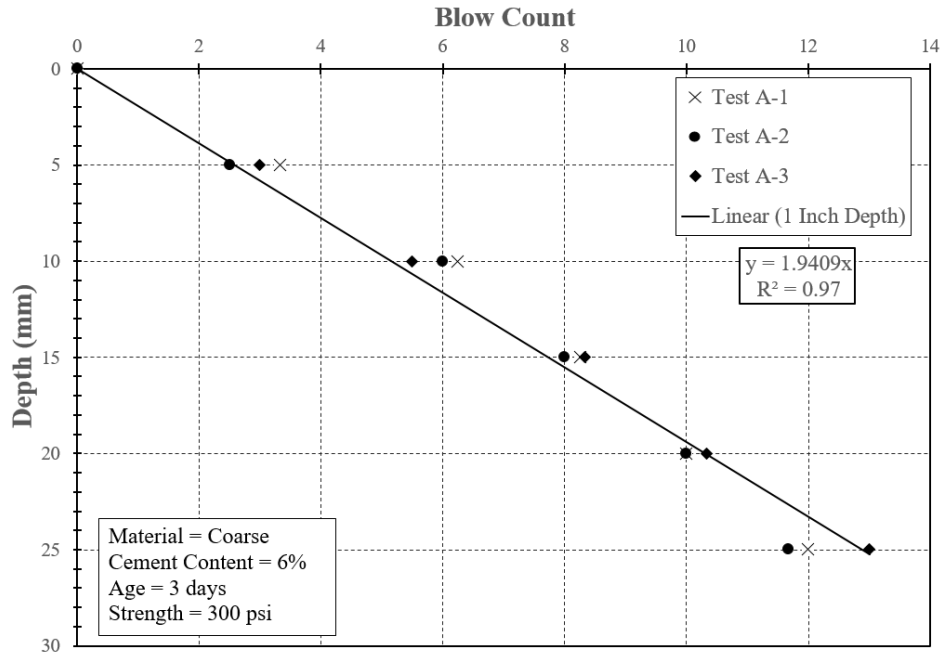


Figure D.29: Coarse 6% No. 1 3 days

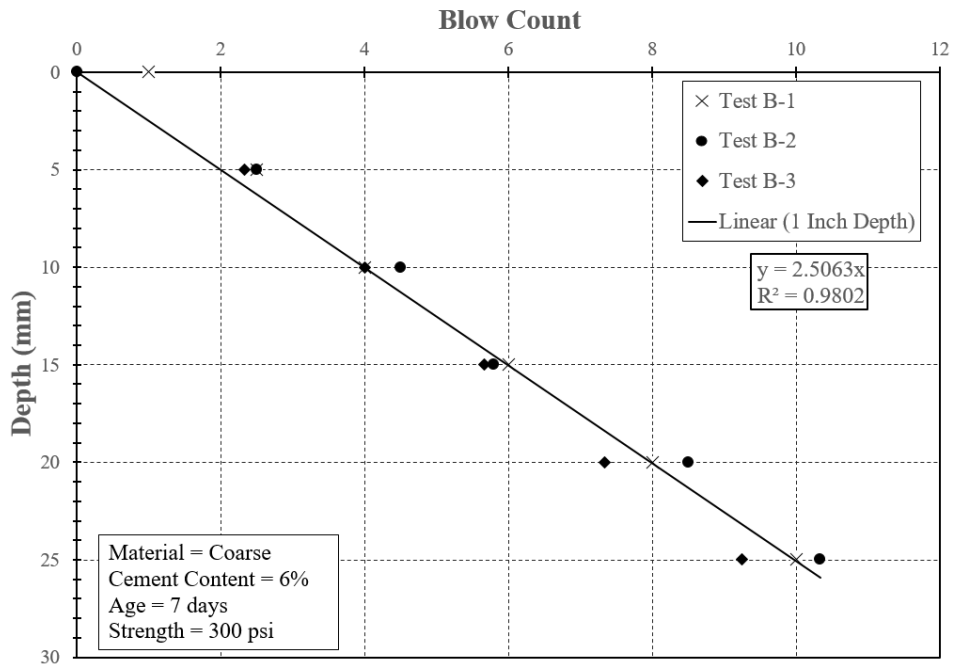


Figure D.30: Coarse 6% No. 1 7 days

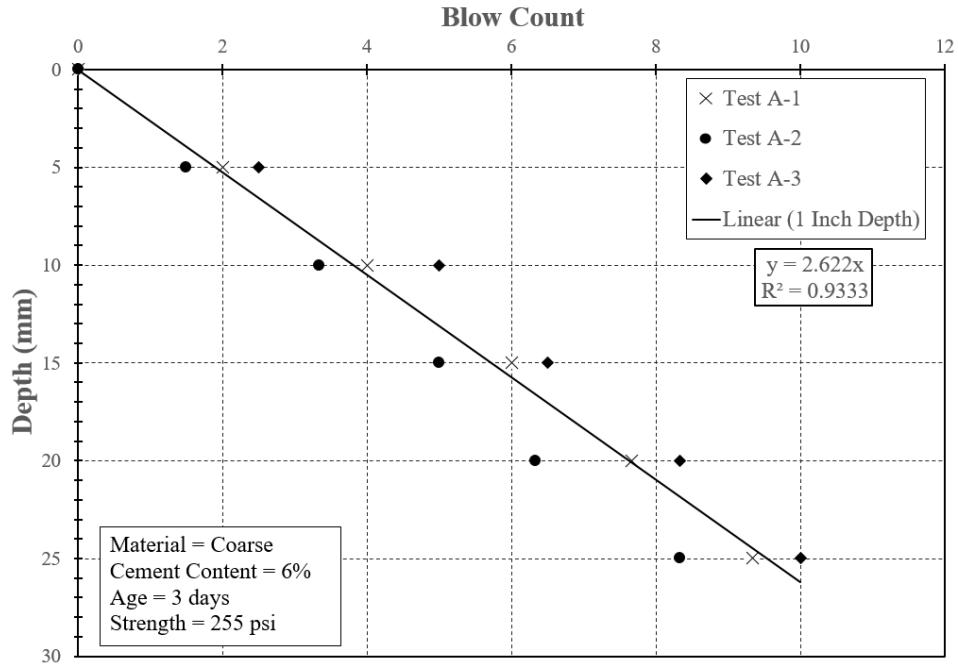


Figure D.31: Coarse 6% No. 2 3 days

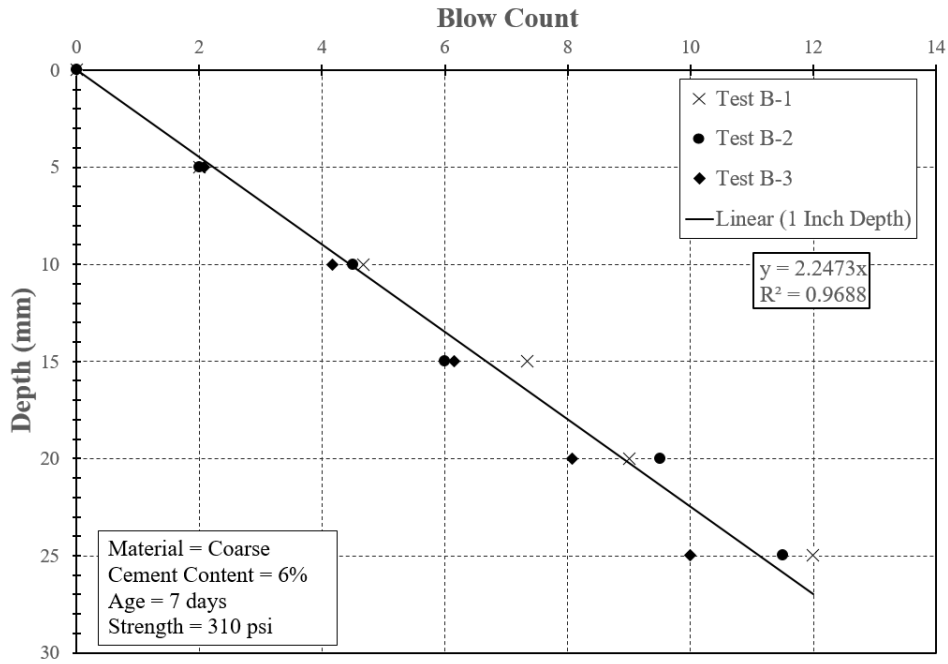


Figure D.32: Coarse 6% No. 2 7 days

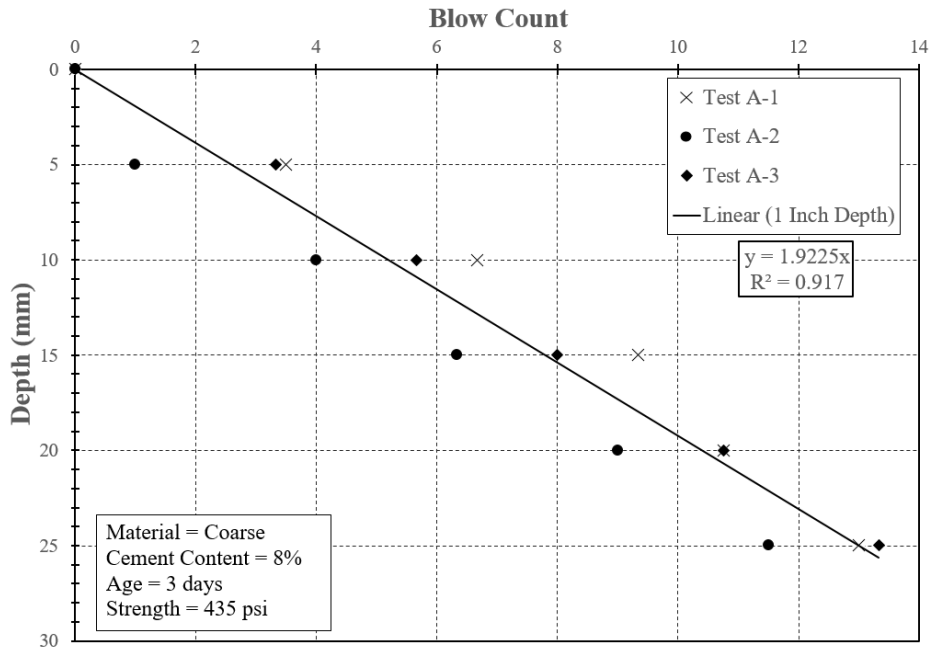


Figure D.33: Coarse 8% No. 1 3 days

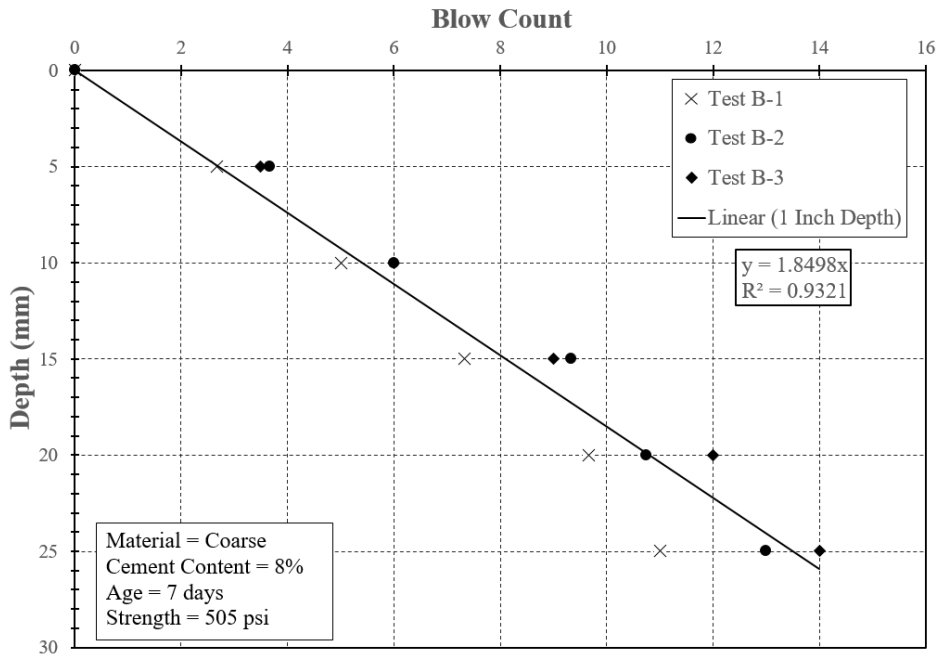


Figure D.34: Coarse 8% No. 1 7 days

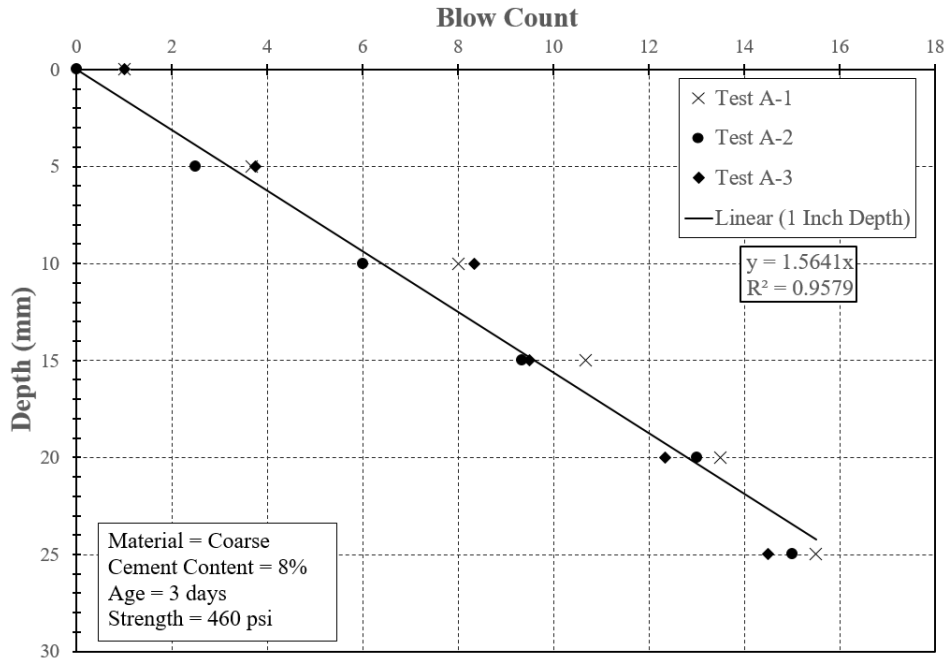


Figure D.35: Coarse 8% No. 2 3 days

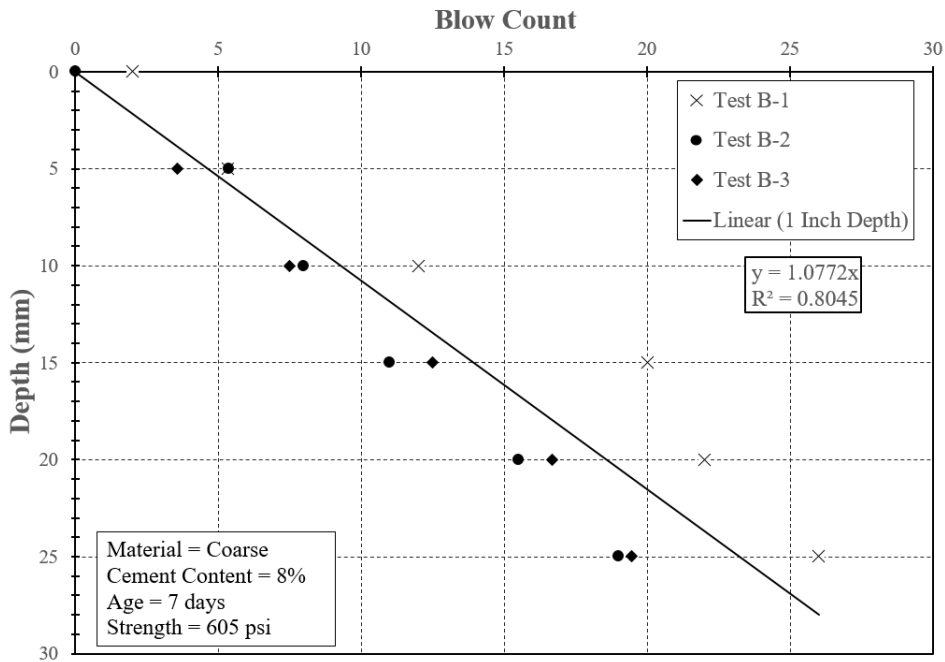


Figure D.36: Coarse 8% No. 2 7 days

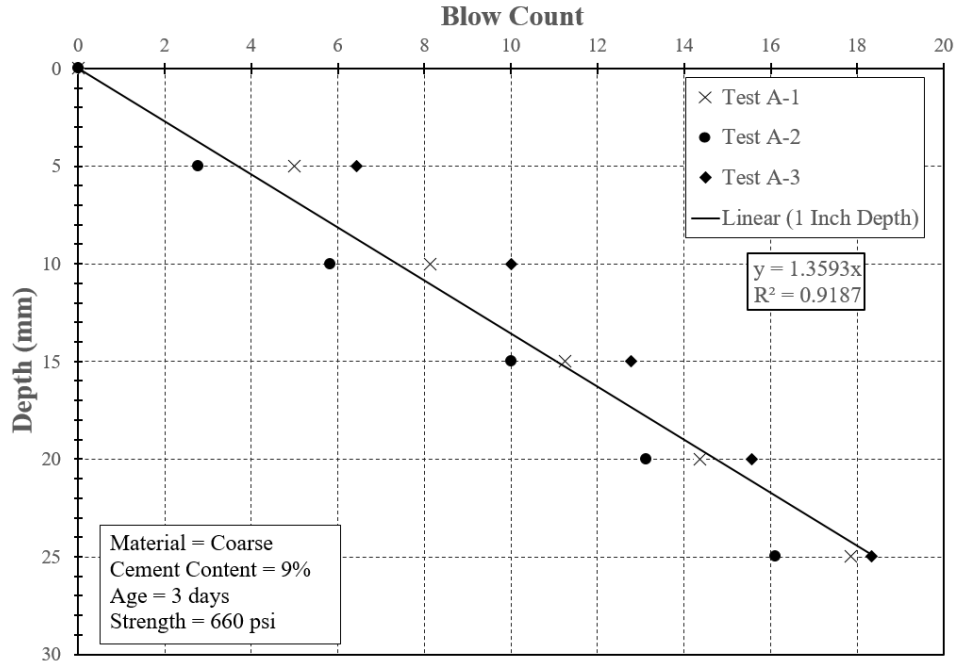


Figure D.37: Coarse 9% 3 days

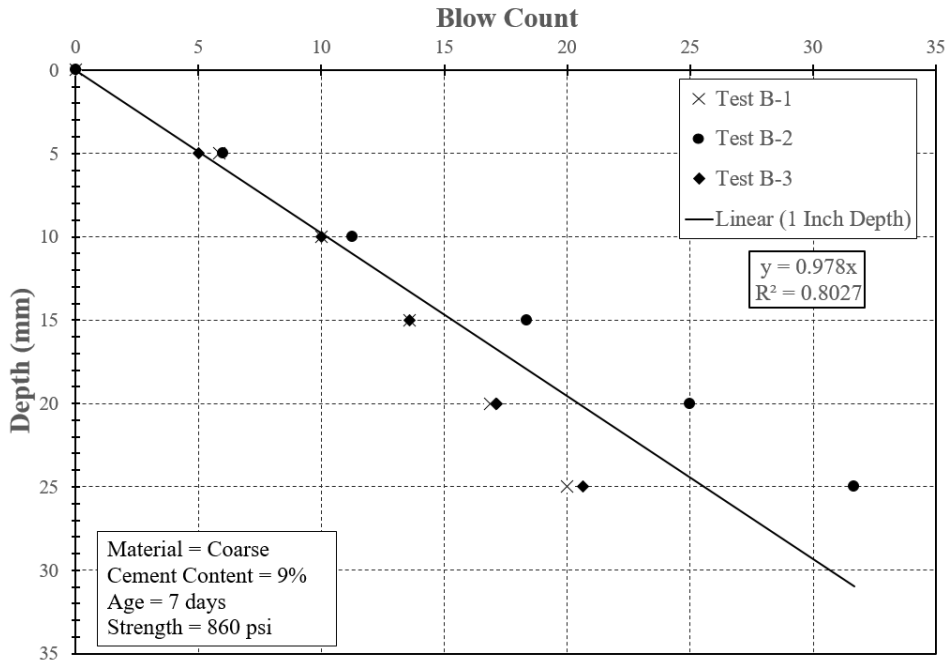


Figure D.38: Coarse 9% 7 days

Appendix E

50 Millimeter Penetration Depth Data

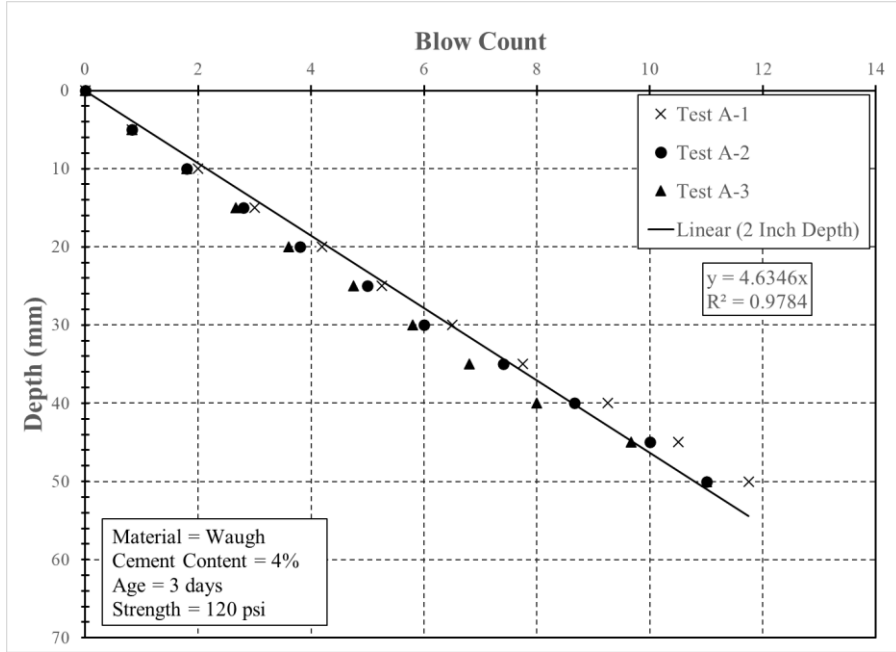


Figure E.1: Waugh 4% No. 1 3 days

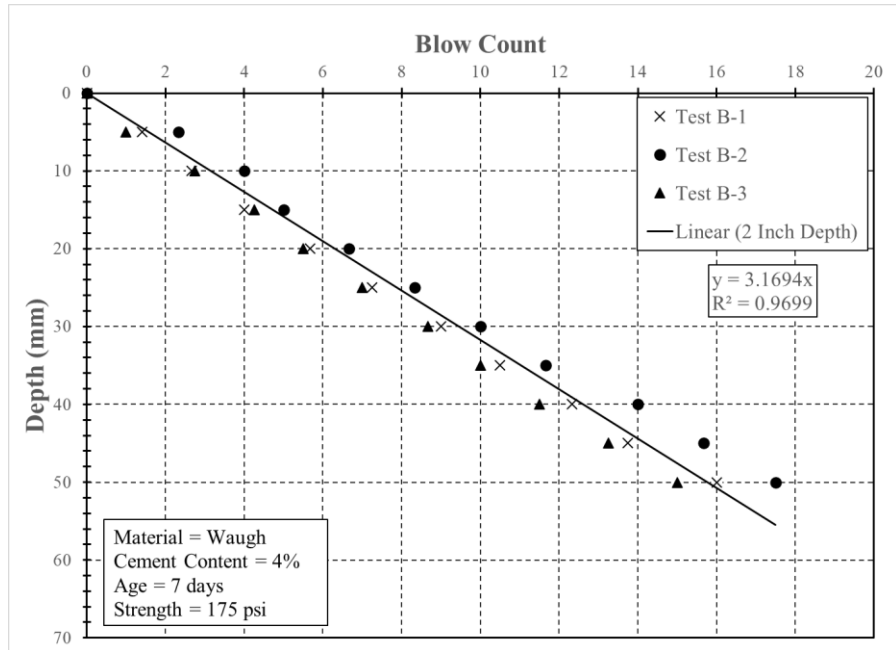


Figure E.2: Waugh 4% No. 1 7 days

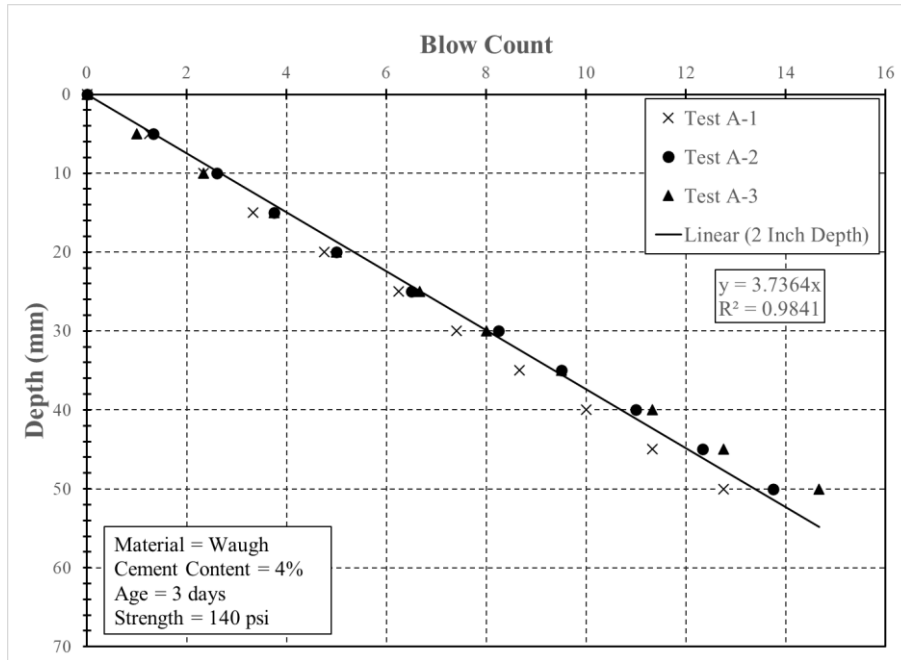


Figure E.3: Waugh 4% No. 2 3 days

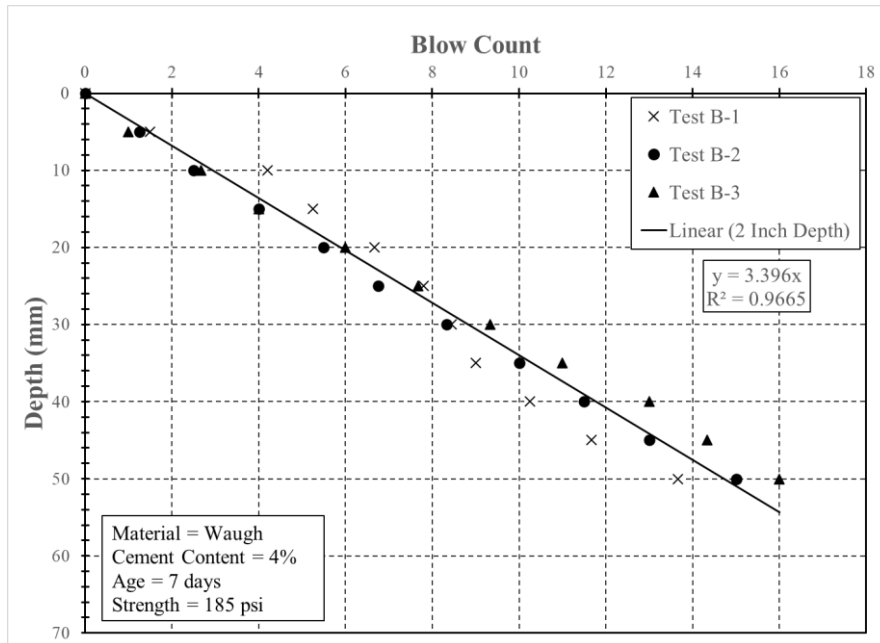


Figure E.4: Waugh 4% No. 2 7 days

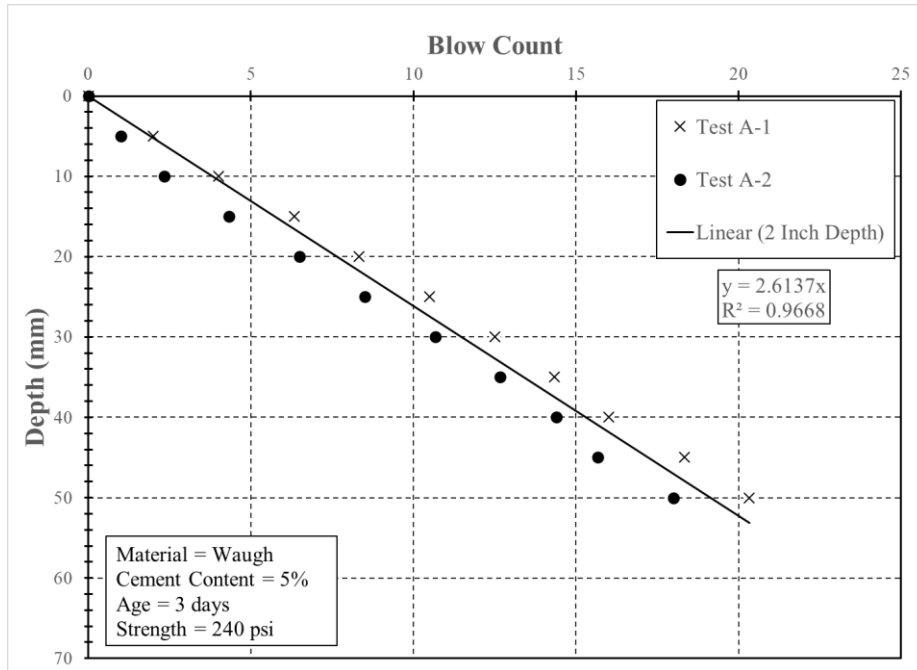


Figure E.5: Waugh 5% No. 1 3 days (Third specimen was removed due to error)

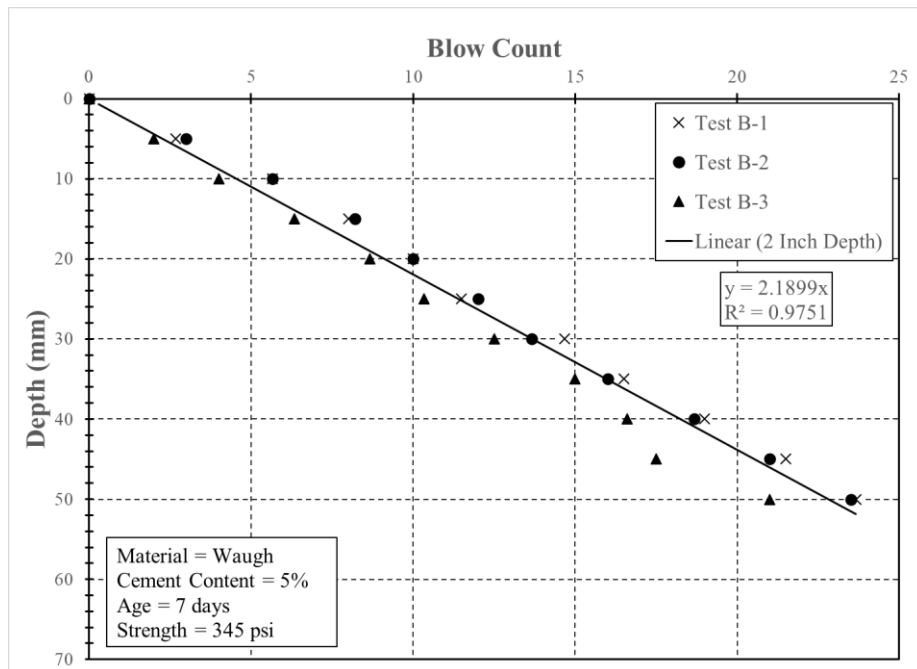


Figure E.6: Waugh 5% No. 1 7 days

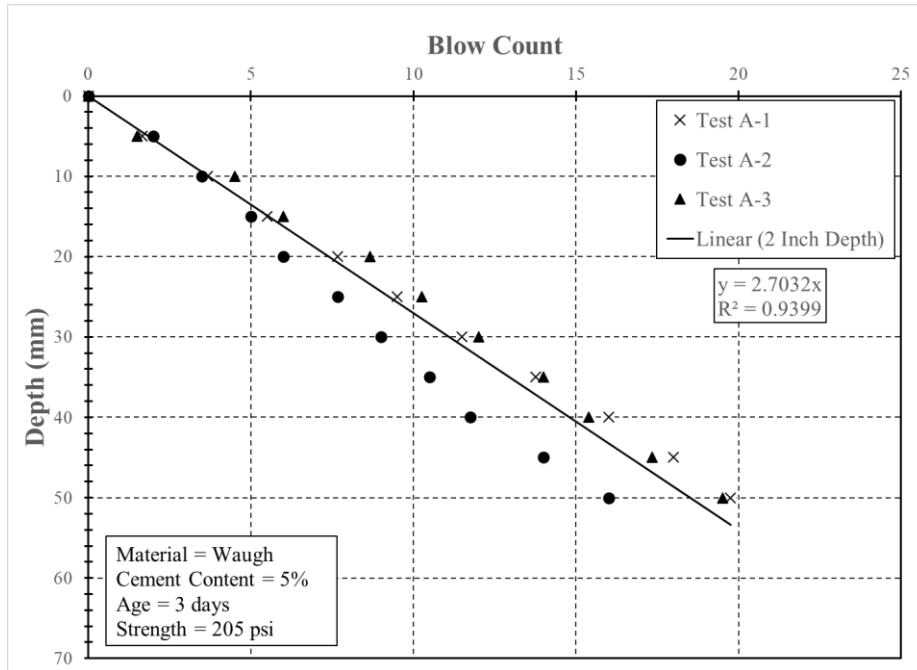


Figure E.7: Waugh 5% No. 2 3 days

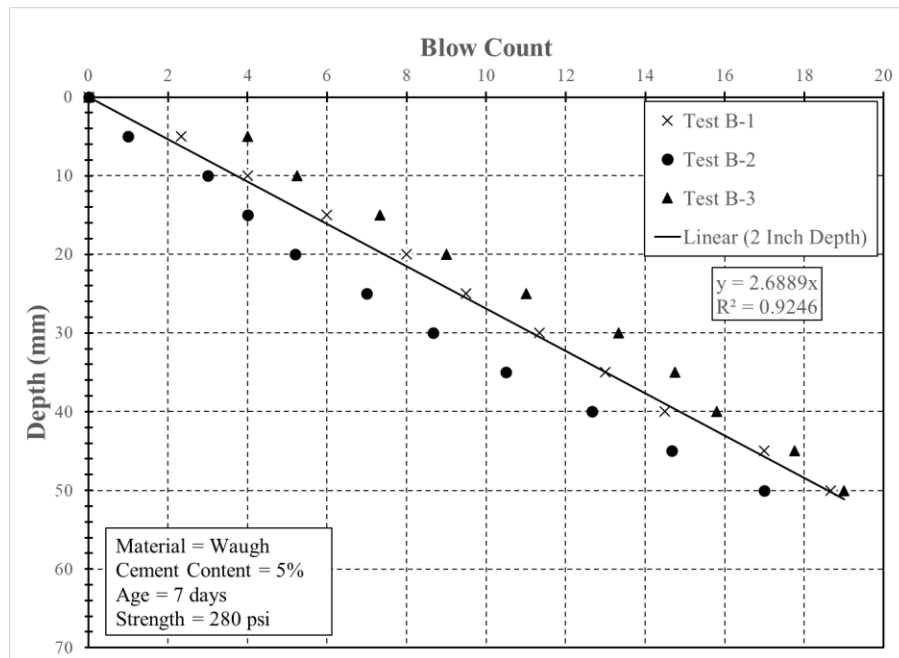


Figure E.8: Waugh 5% No. 2 7 days

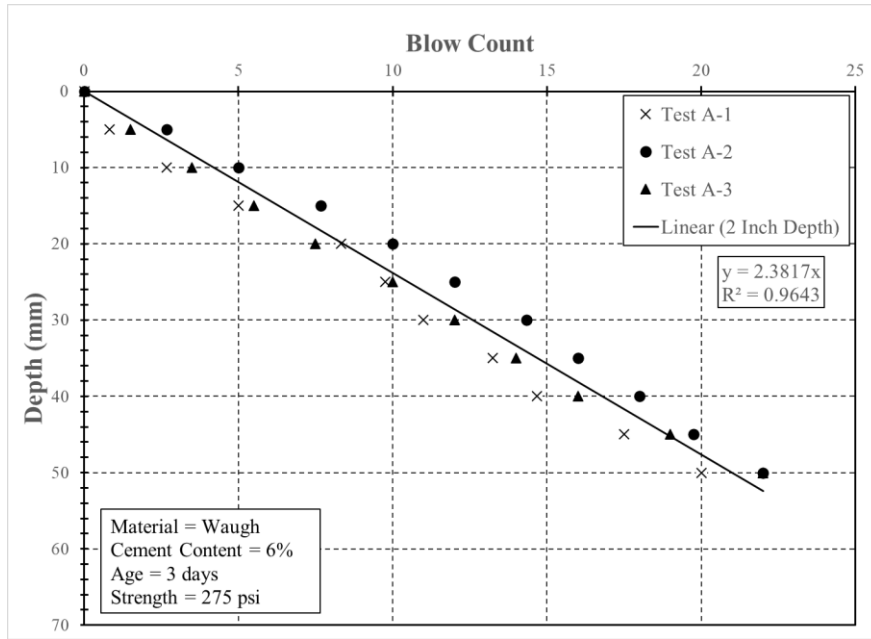


Figure E.9: Waugh 6% 3 days

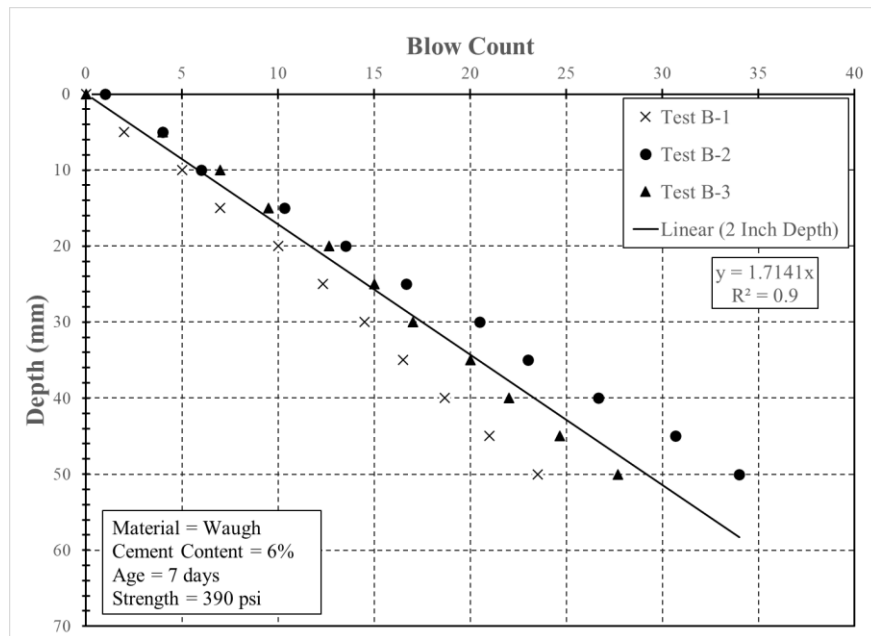


Figure E.10: Waugh 6% 7 days

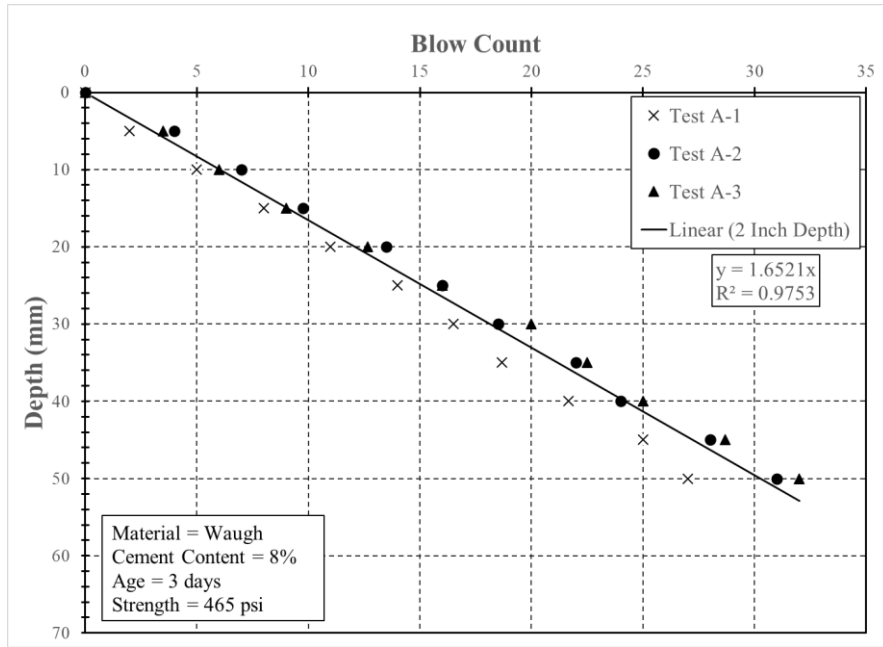


Figure E.11: Waugh 8% No. 1 3 days

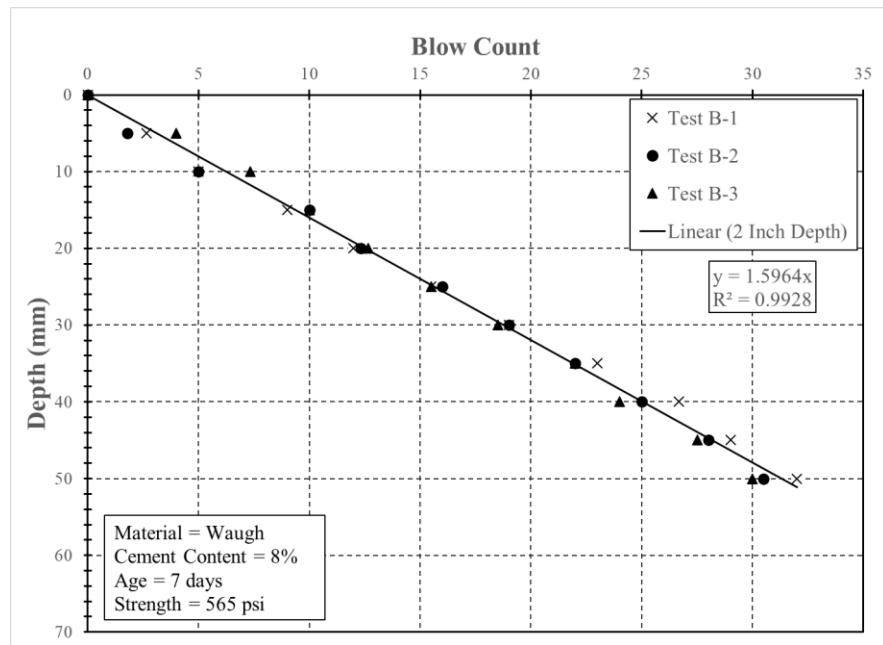


Figure E.12: Waugh 8% No. 1 7 days

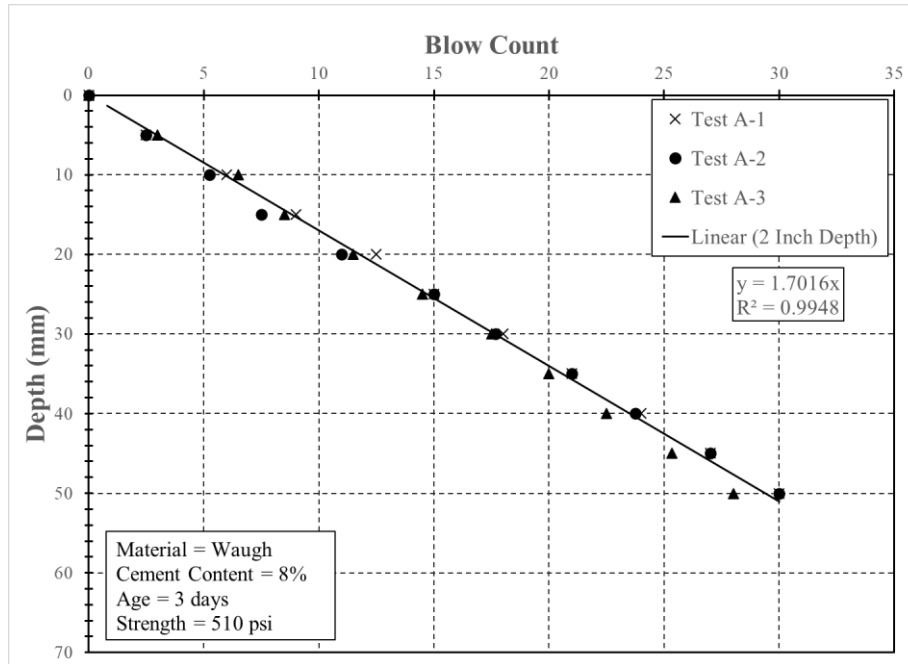


Figure E.13: Waugh 8% No. 2 3 days

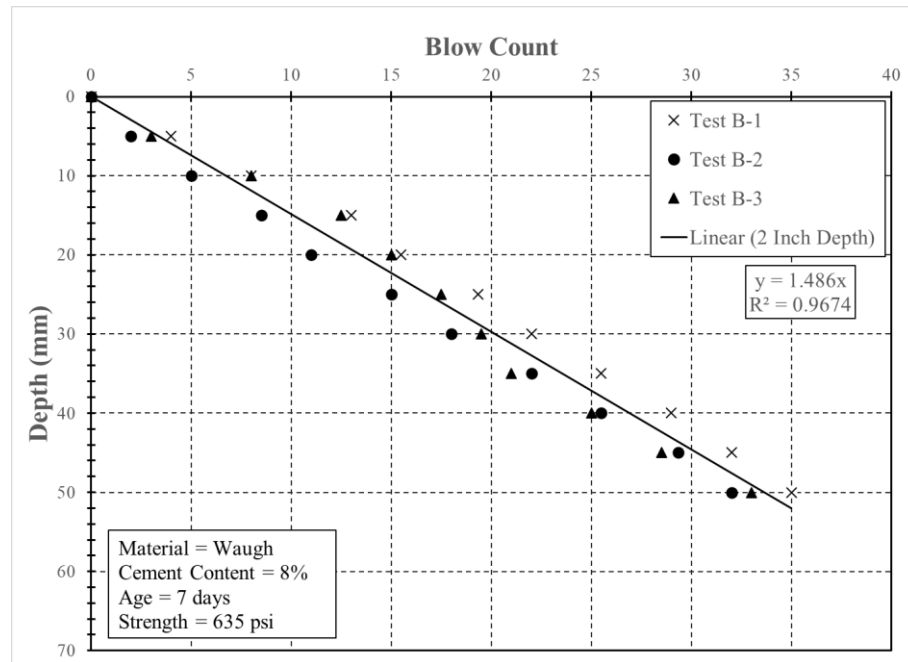


Figure E.14: Waugh 8% No. 2 7 days

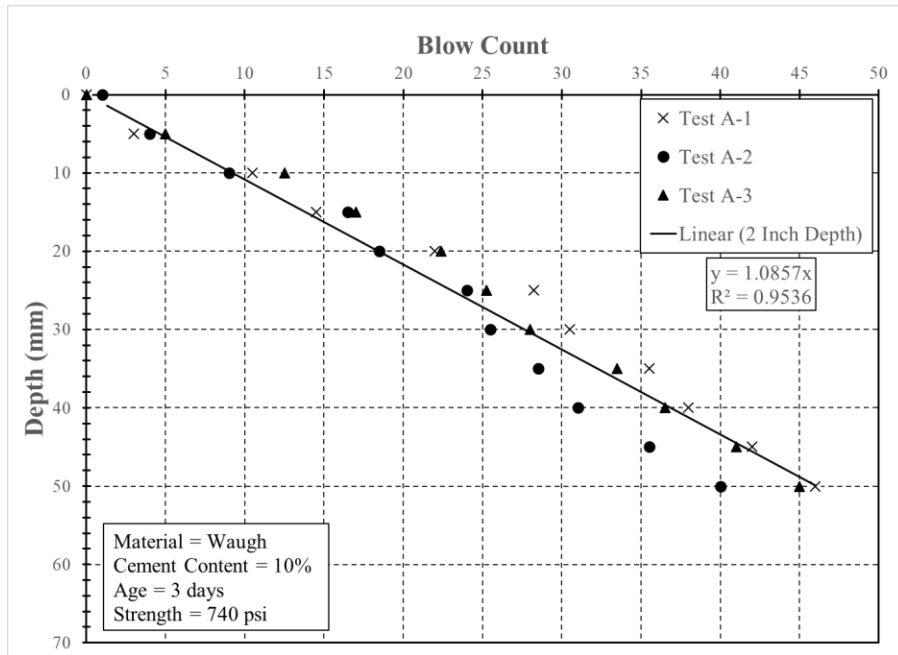


Figure E.15: Waugh 10% 3 days

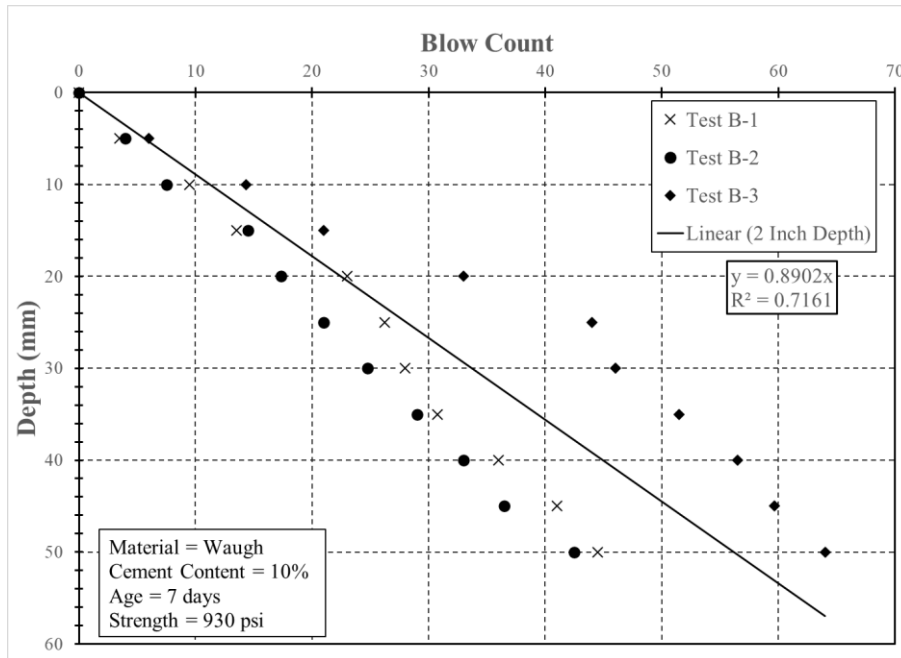


Figure E.16: Waugh 10% 7 days

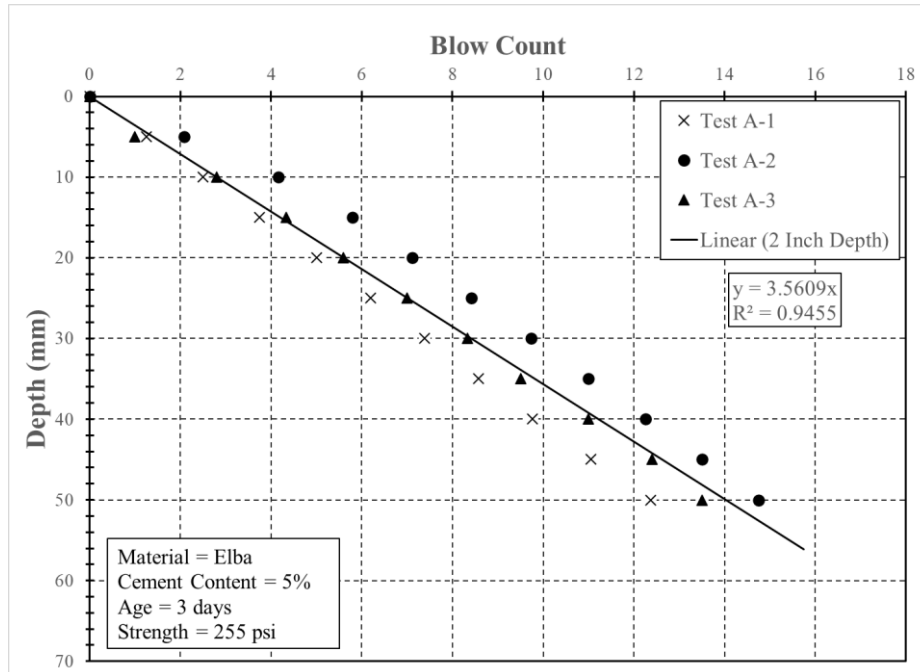


Figure E.17: Elba 5% 3 days

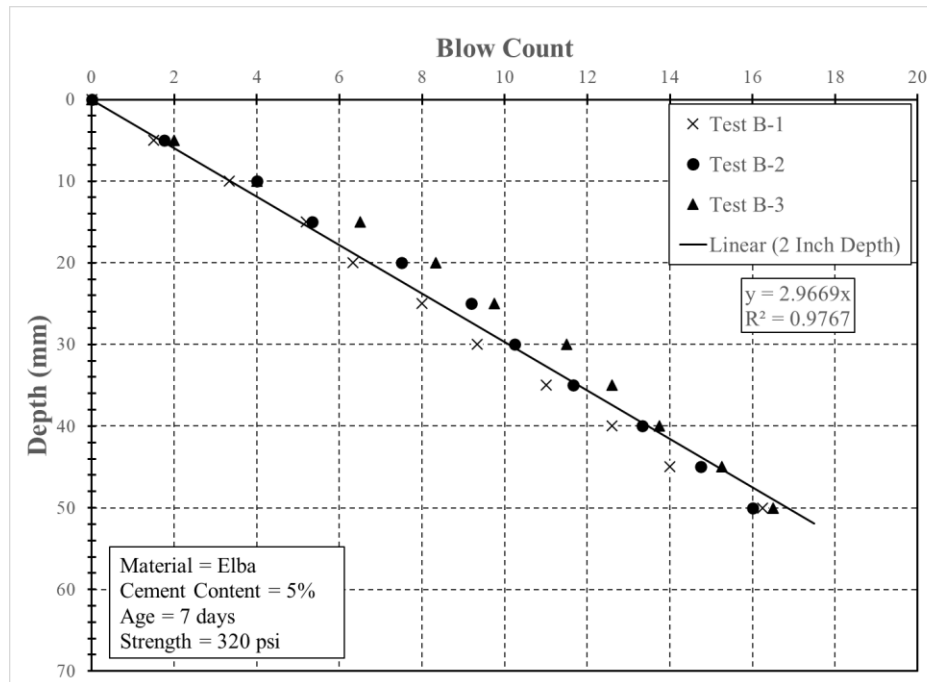


Figure E.18: Elba 5% 7 days

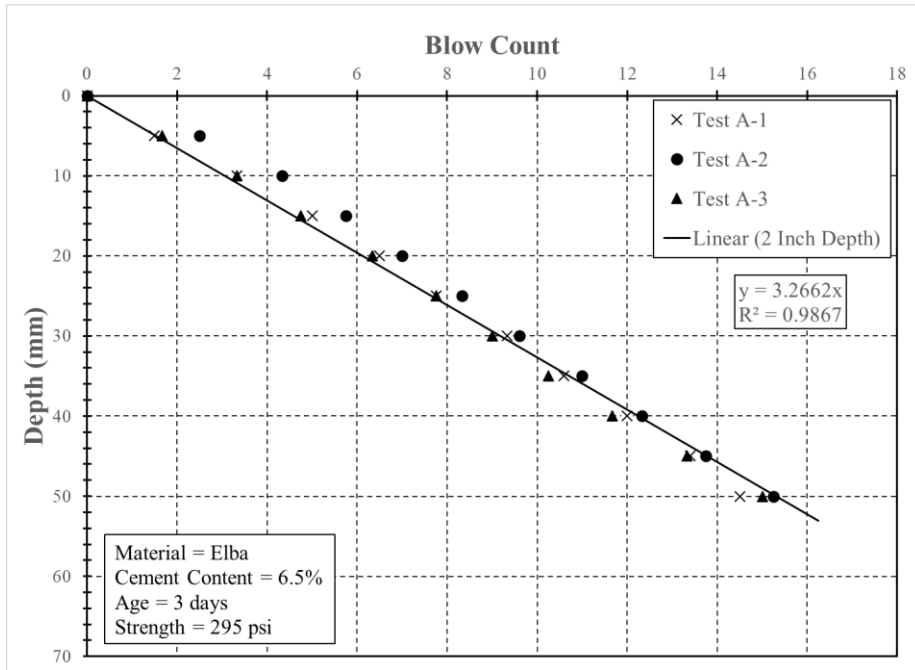


Figure E.19: Elba 6.5% No. 1 3 days

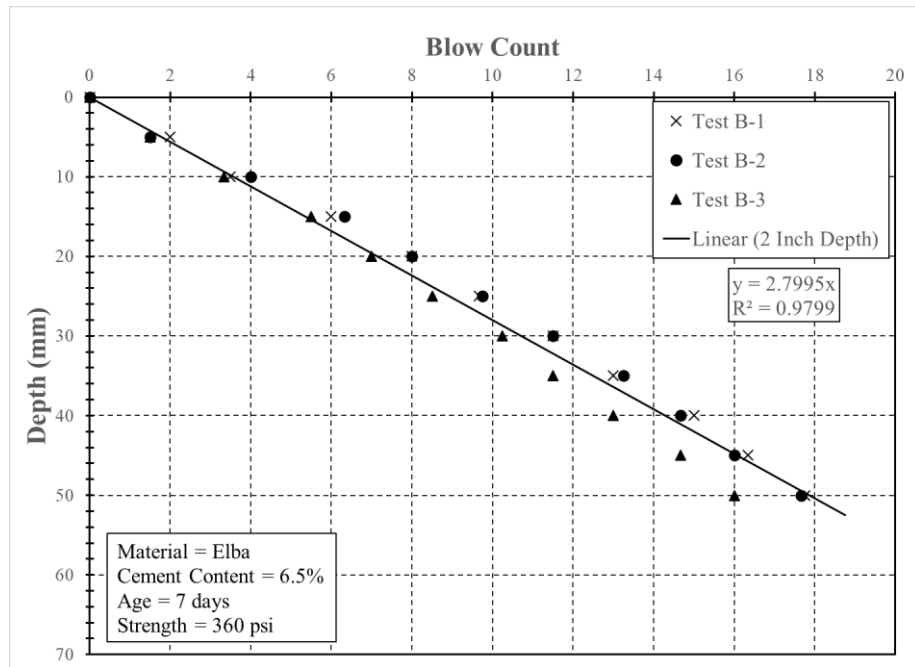


Figure E.20: Elba 6.5% No. 1 7 days

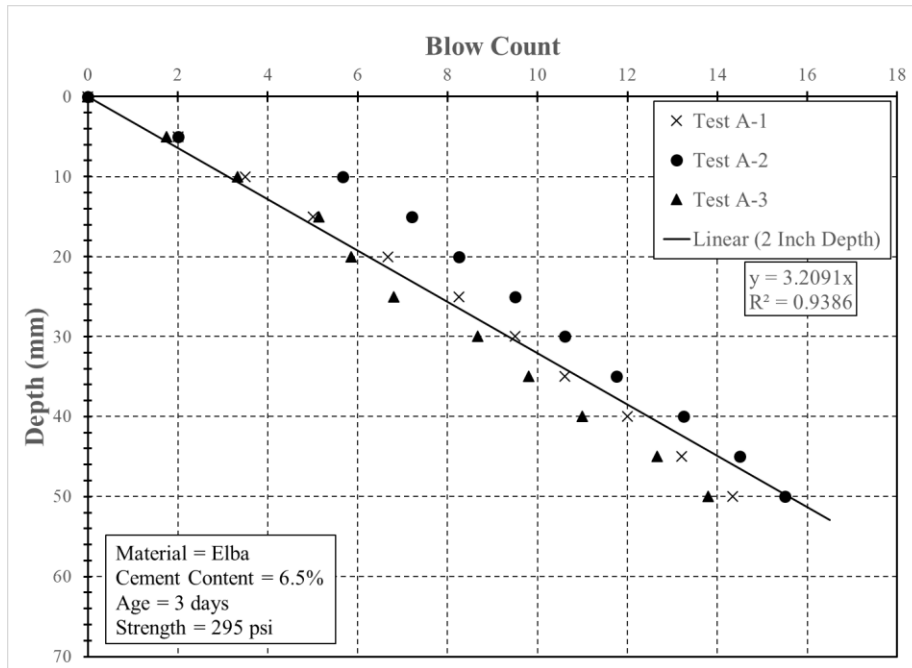


Figure E.21: Elba 6.5% No. 2 3 days

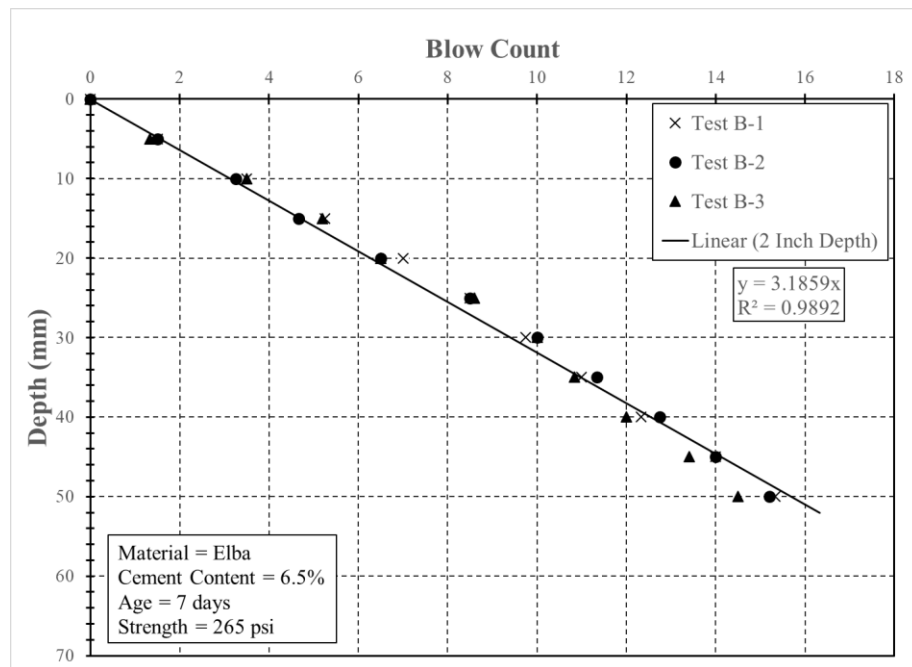


Figure E.22: Elba 6.5% No. 2 7 days

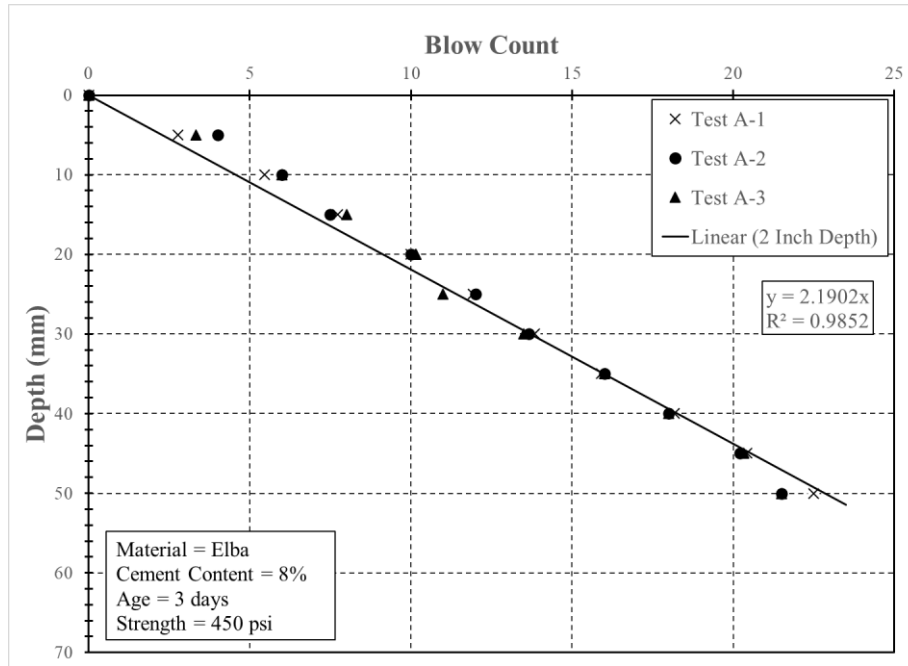


Figure E.23: Elba 8% 3 days

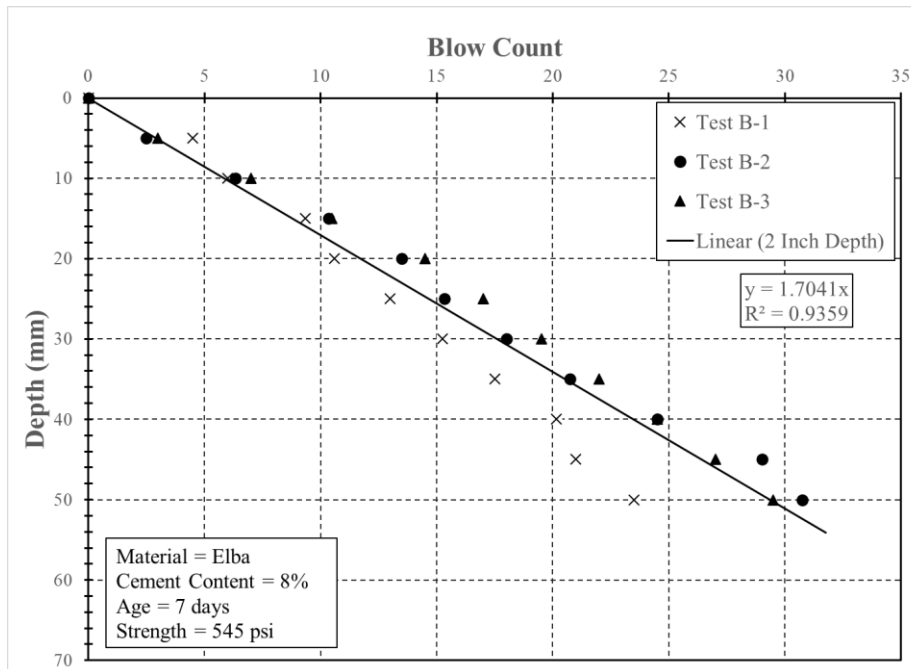


Figure E.24: Elba 8% 7 days

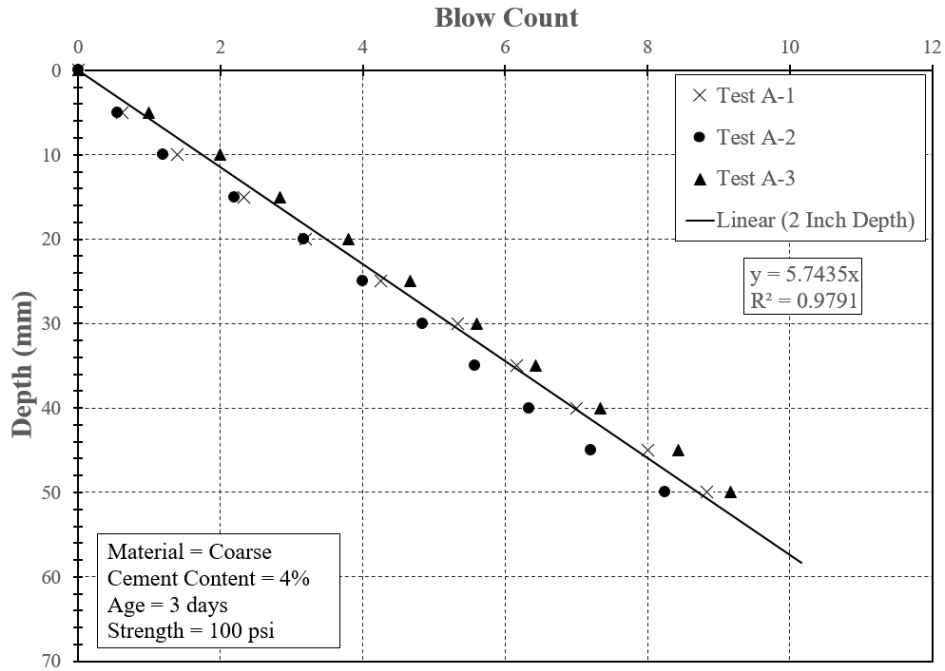


Figure E.25: Coarse 4% No. 1 3 days

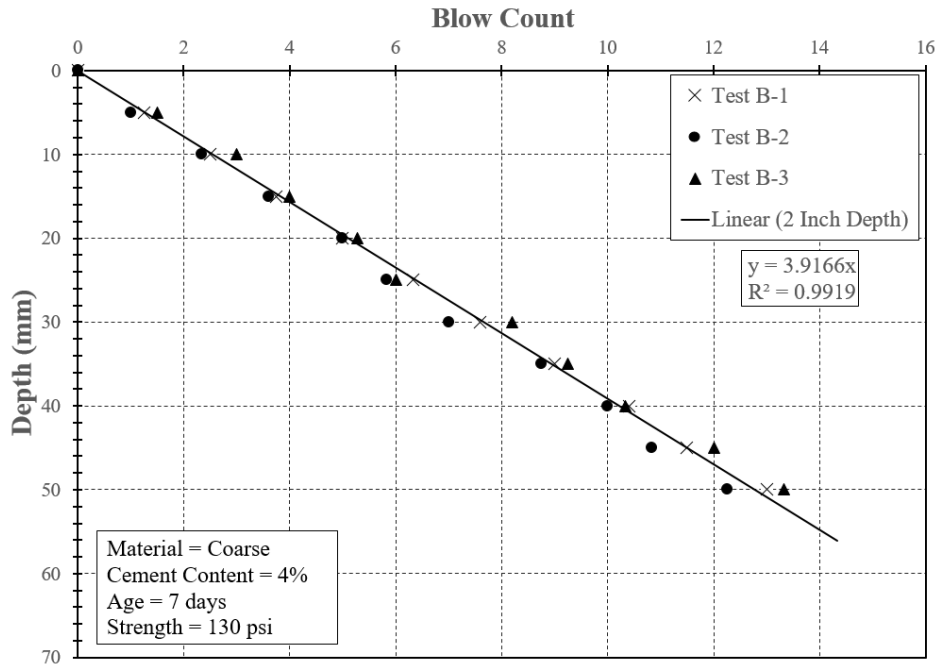


Figure E.26: Coarse 4% No. 1 7 days

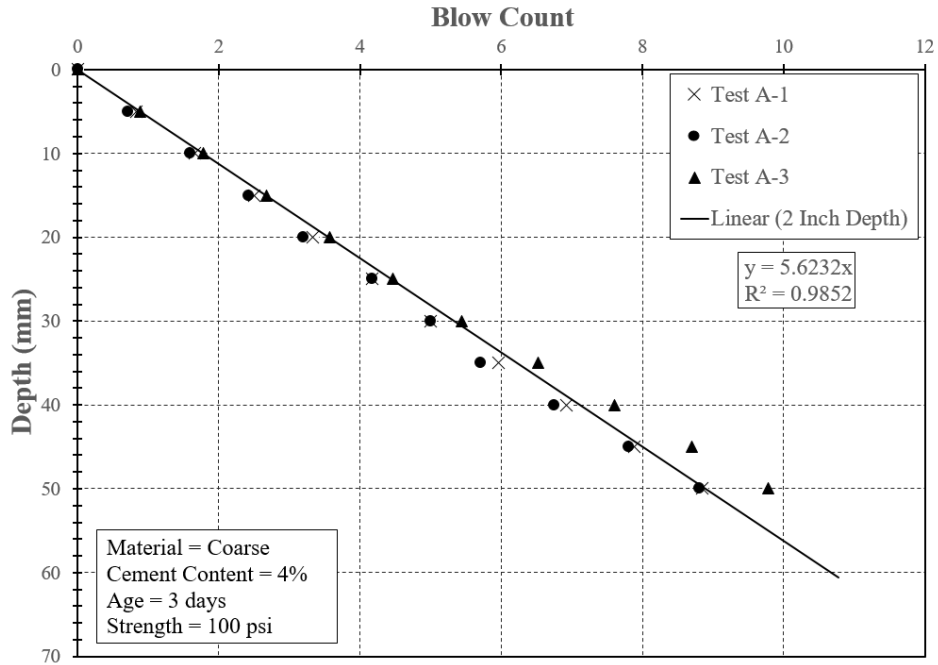


Figure E.27: Coarse 4% No. 2 3 days

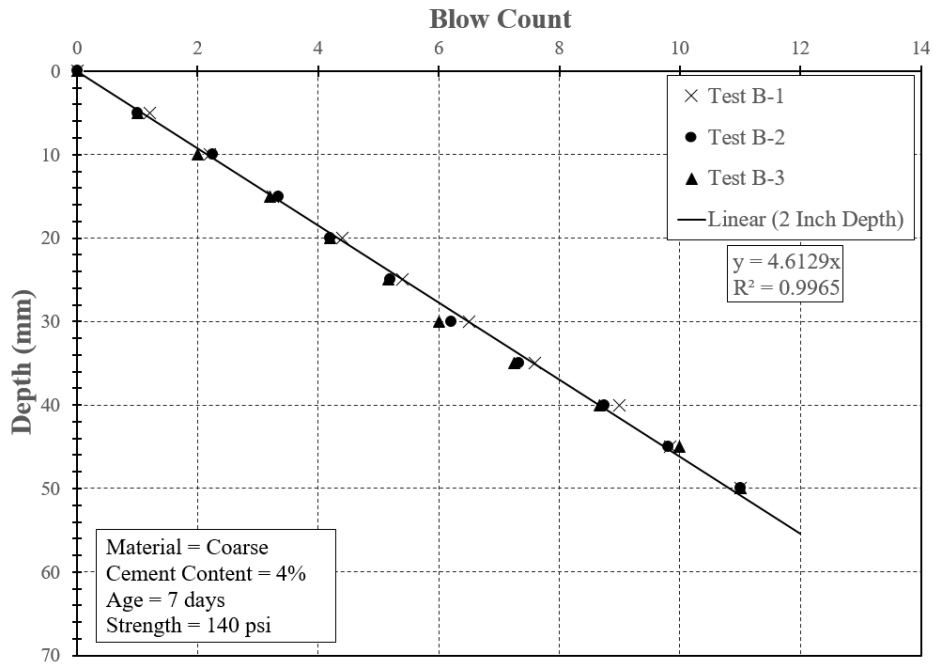


Figure E.28: Coarse 4% No. 2 7 days

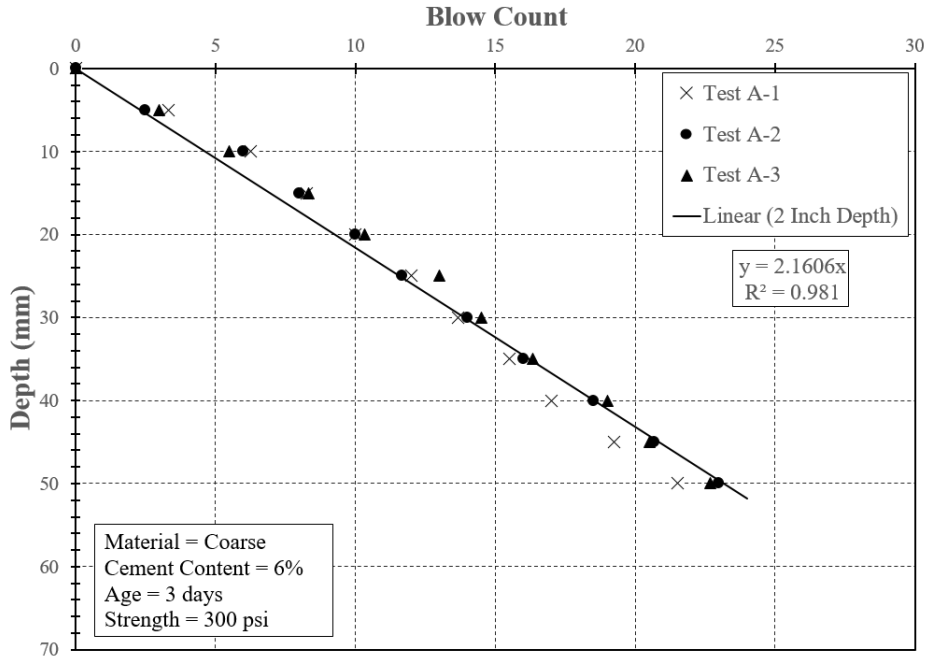


Figure E.29: Coarse 6% No. 1 3 days

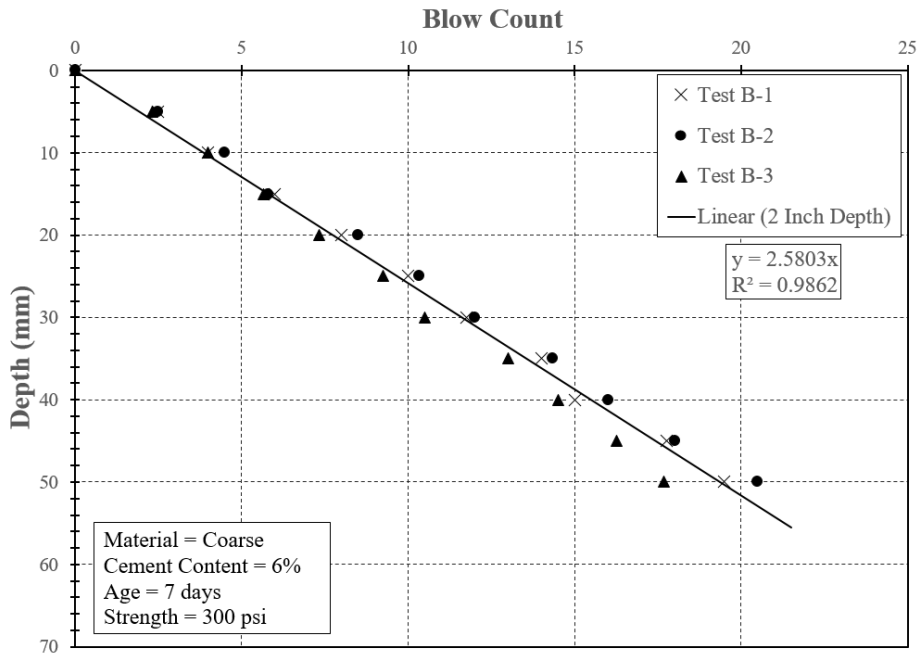


Figure E.30: Coarse 6% No. 1 7 days

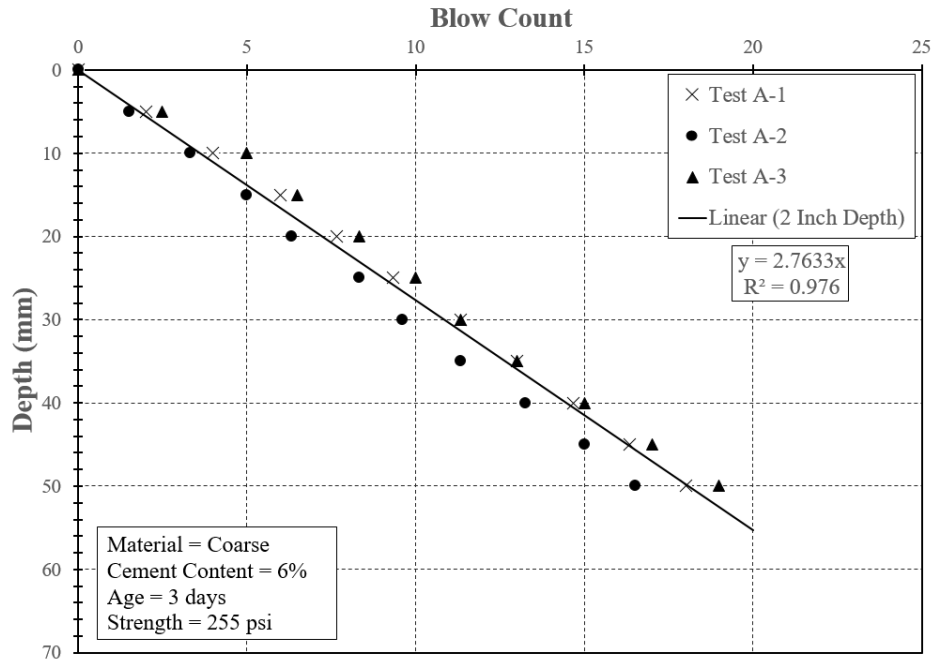


Figure E.31: Coarse 6% No. 2 3 days

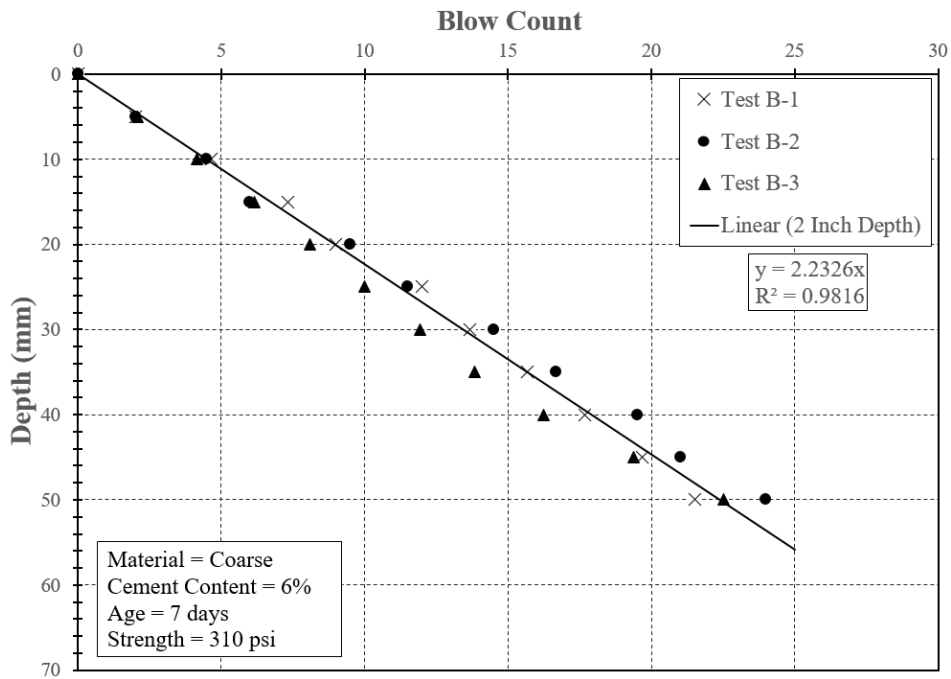


Figure E.32: Coarse 6% No. 2 7 days

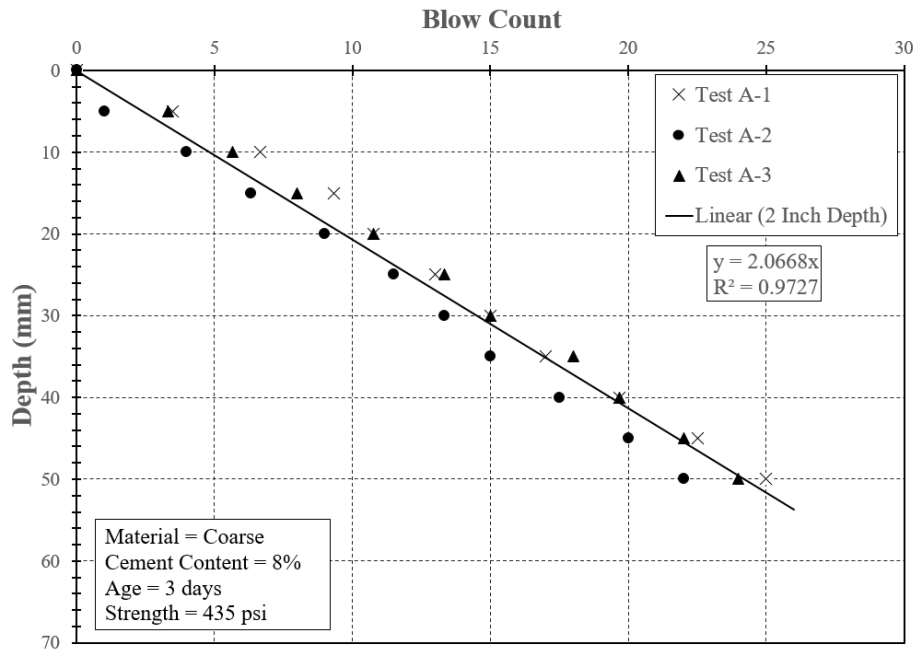


Figure E.33: Coarse 8% No. 1 3 days

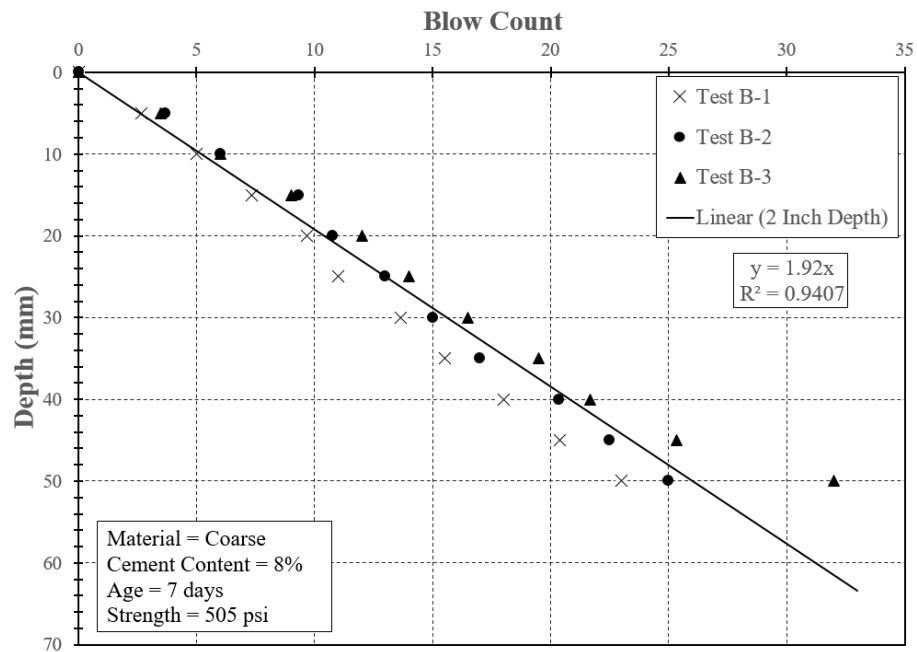


Figure E.34: Coarse 8% No. 1 7 days

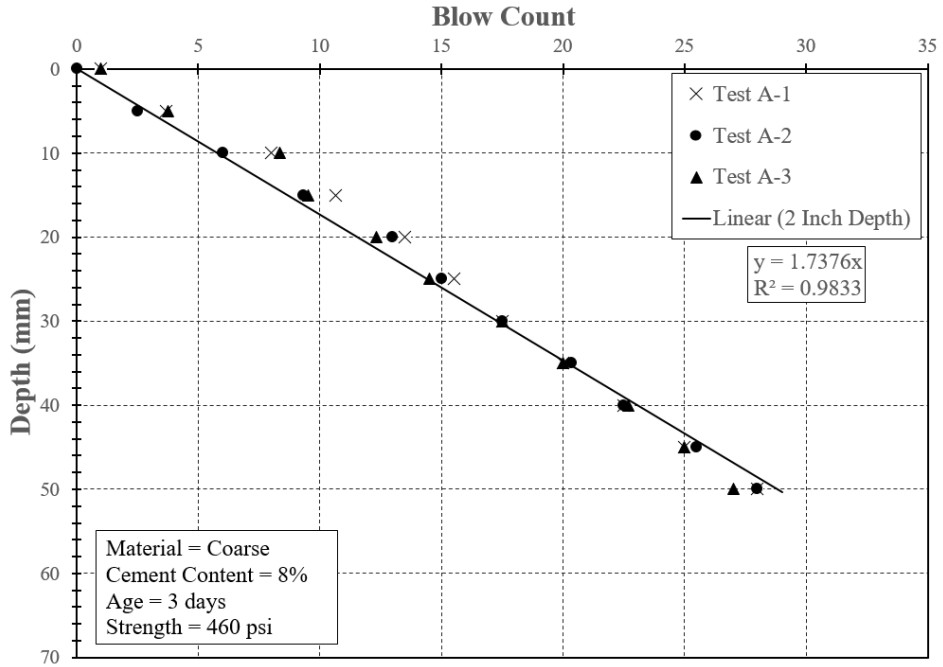


Figure E.35: Coarse 8% No. 2 3 days

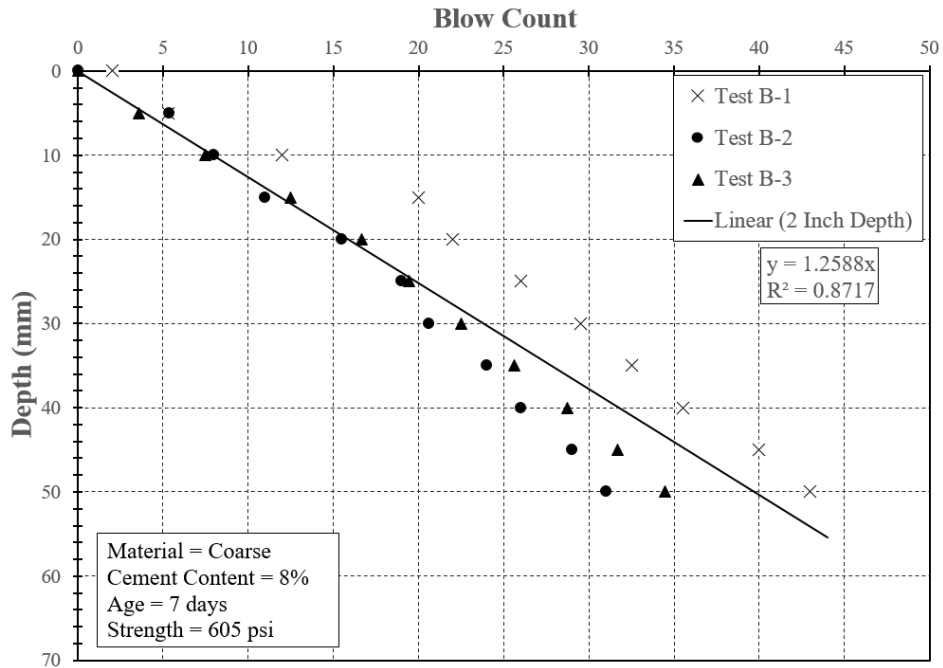


Figure E.36: Coarse 8% No. 2 7 days

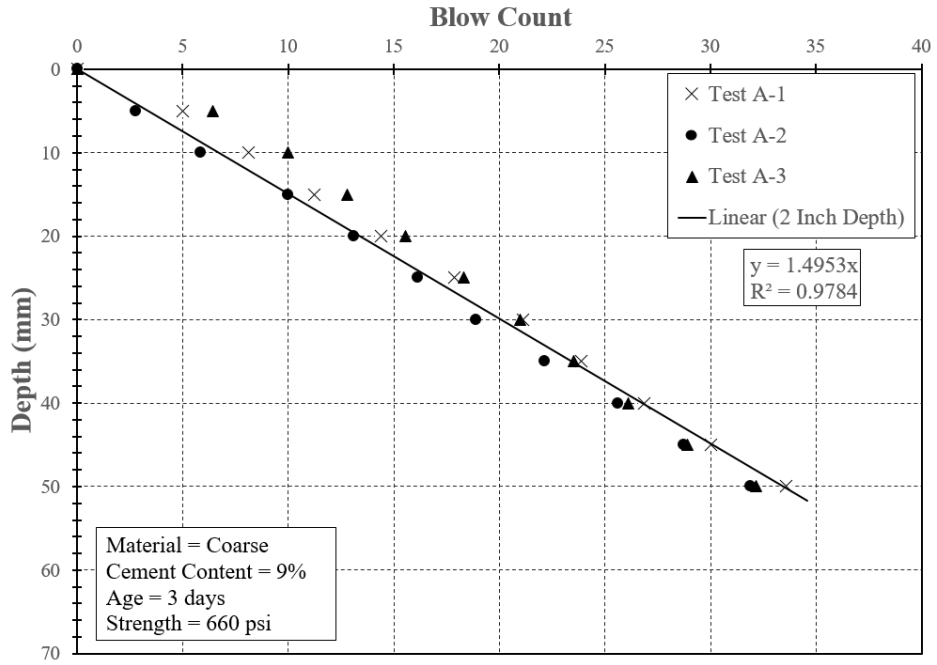


Figure E.37: Coarse 9% 3 days

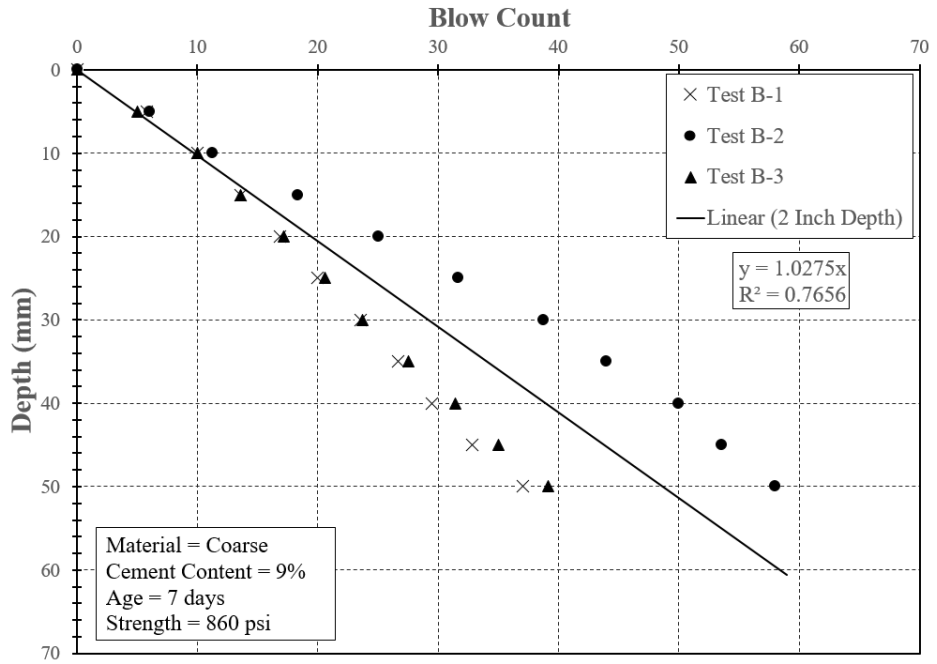


Figure E.38: Coarse 9% 7 days

Appendix F

75 Millimeter Penetration Depth Data

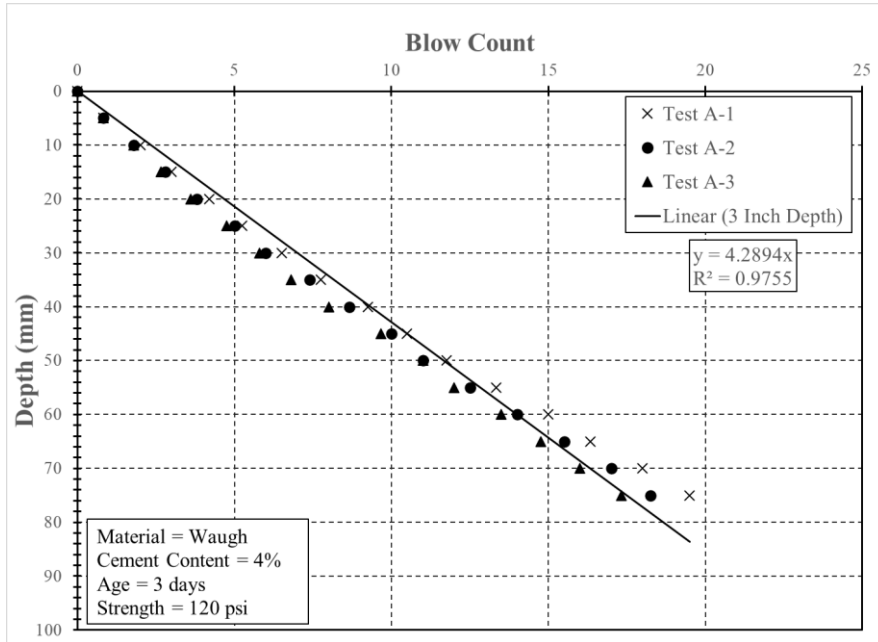


Figure F.1: Waugh 4% No. 1 3 days

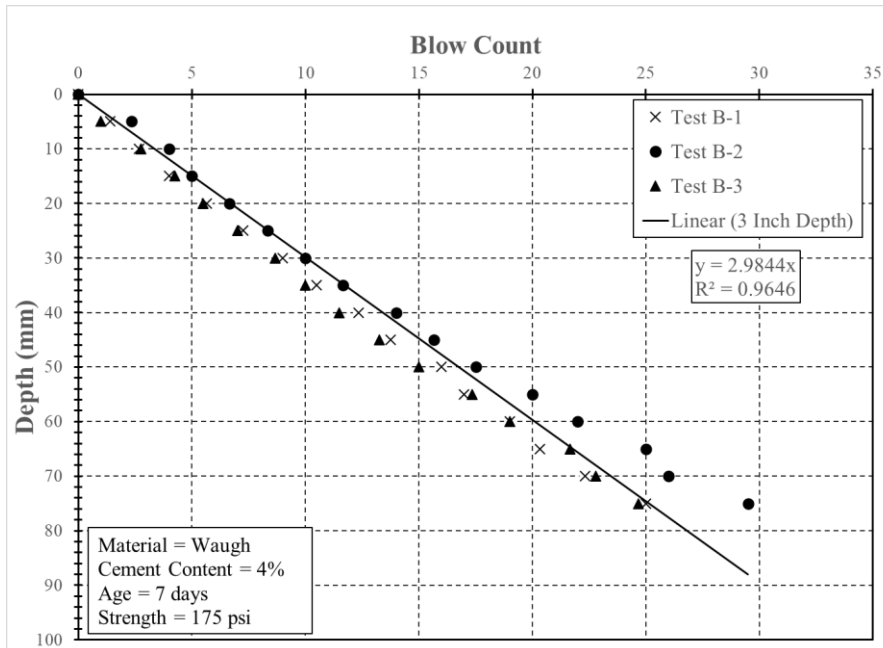


Figure F.2: Waugh 4% No. 1 7 days

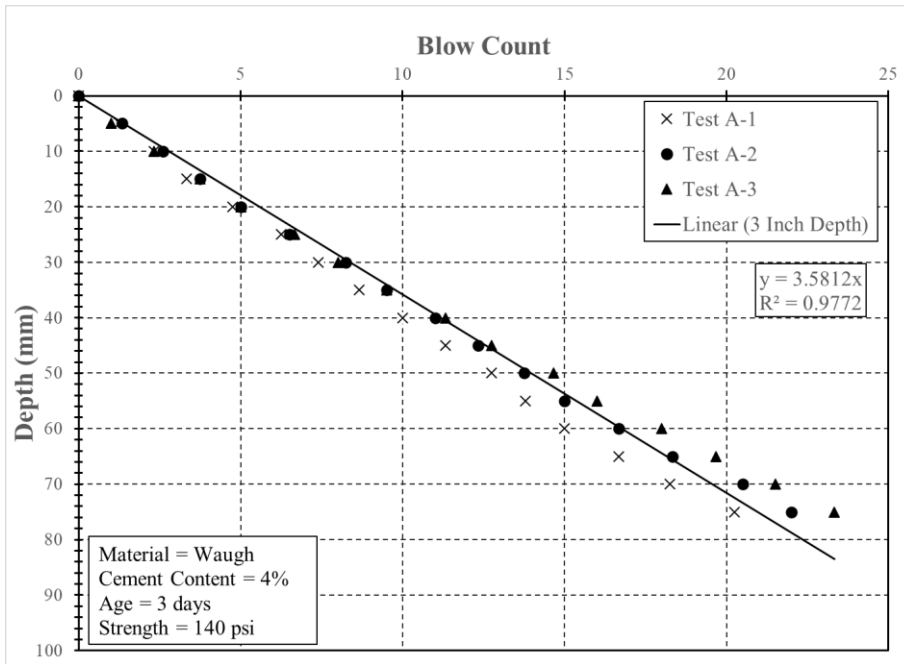


Figure F.3: Waugh 4% No. 2 3 days

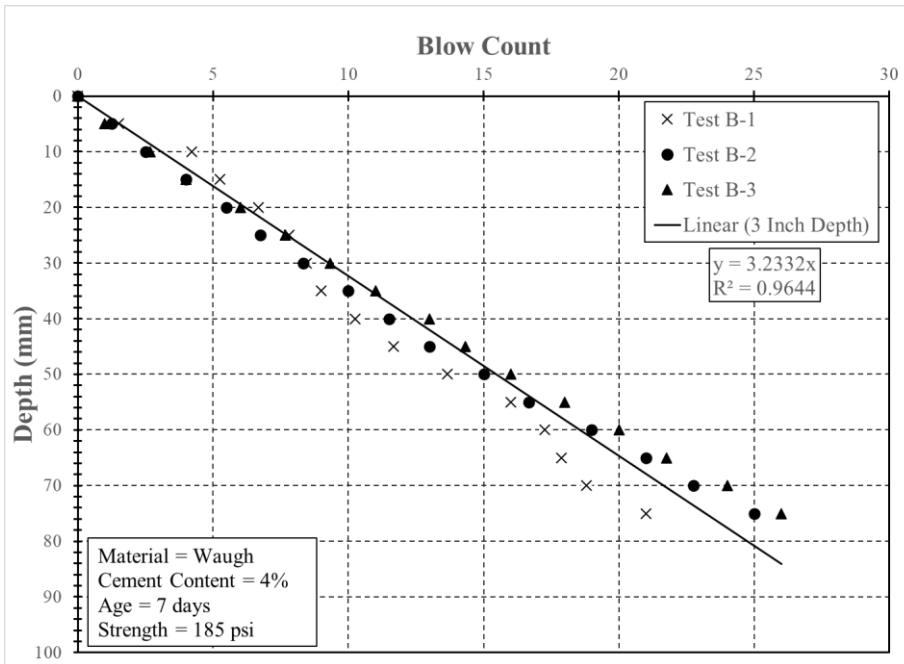


Figure F.4: Waugh 4% No. 2 7 days

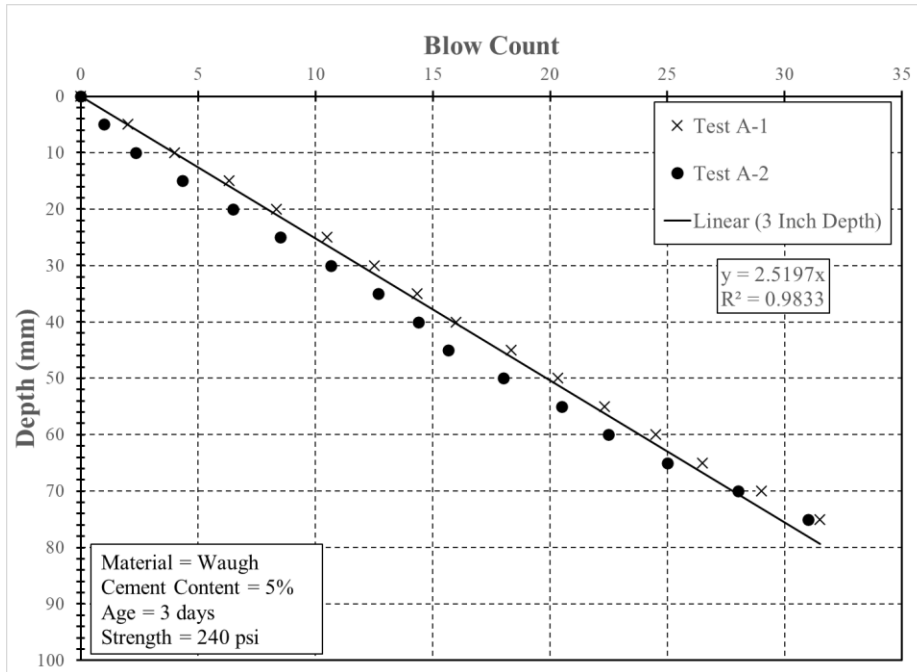


Figure F.5: Waugh 5% No. 1 3 days (Third specimen was removed due to error)

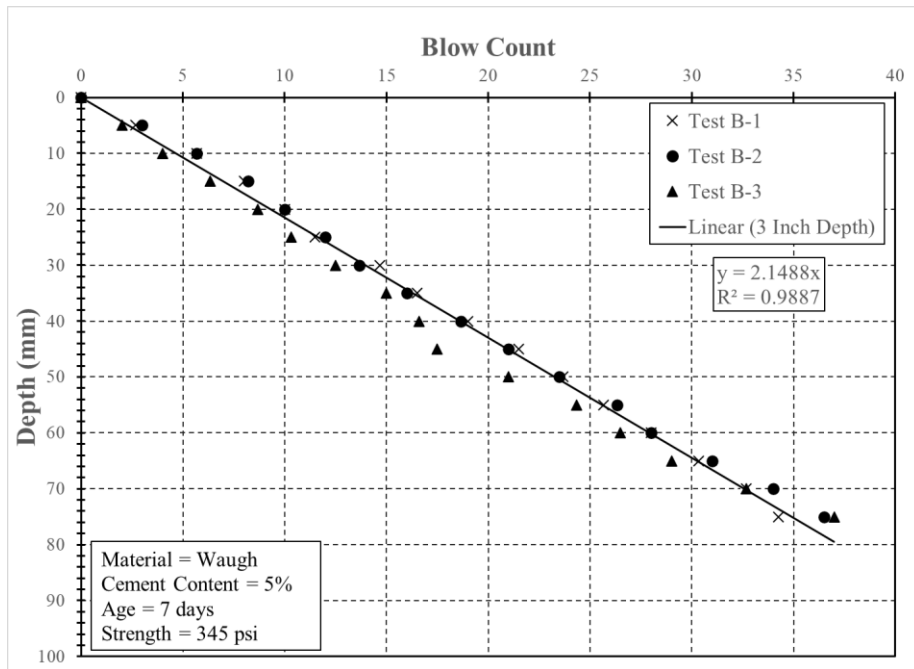


Figure F.6: Waugh 5% No. 1 7 days

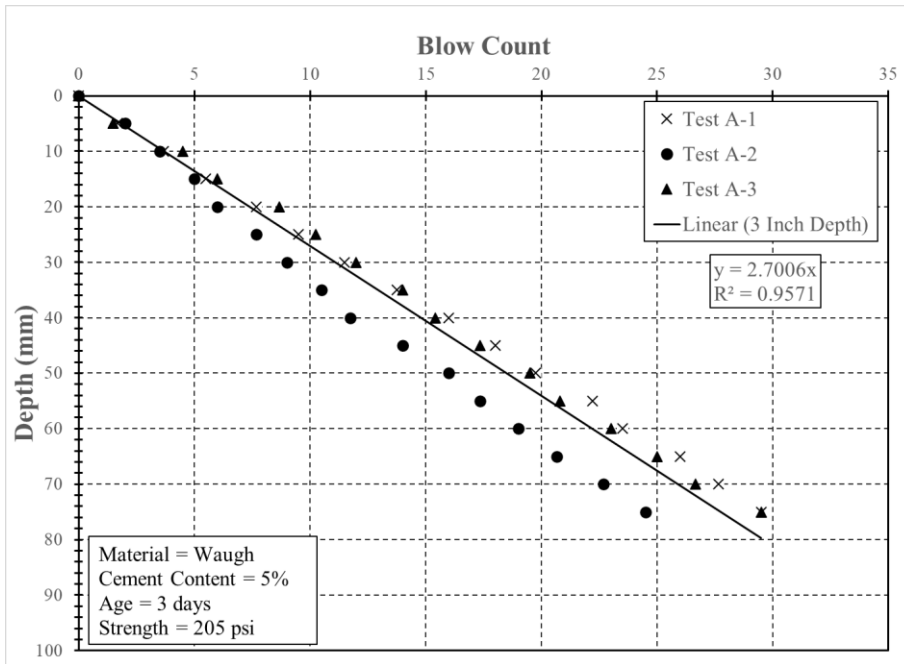


Figure F.7: Waugh 5% No. 2 3 days

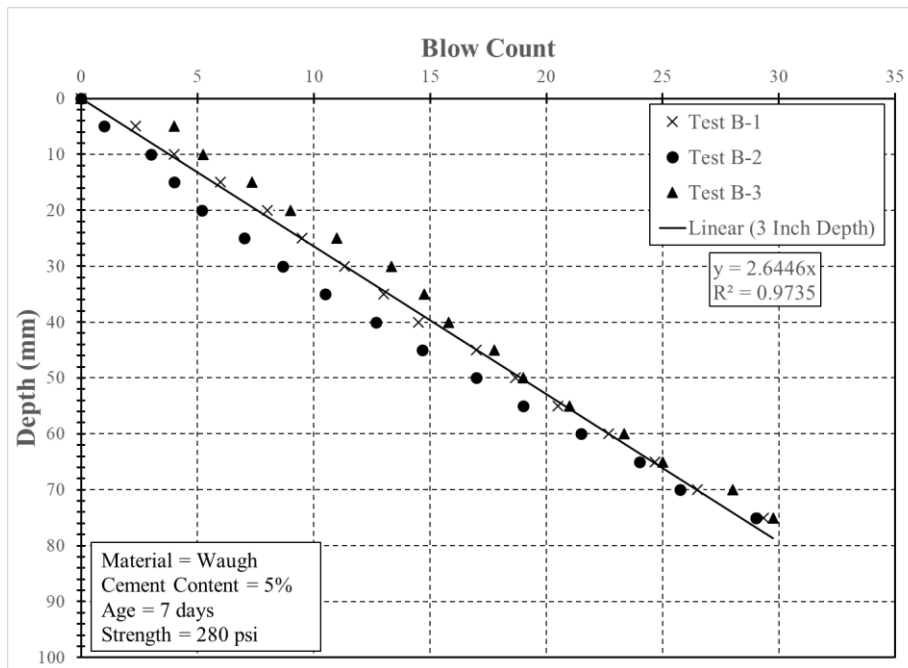


Figure F.8: Waugh 5% No. 2 7 days

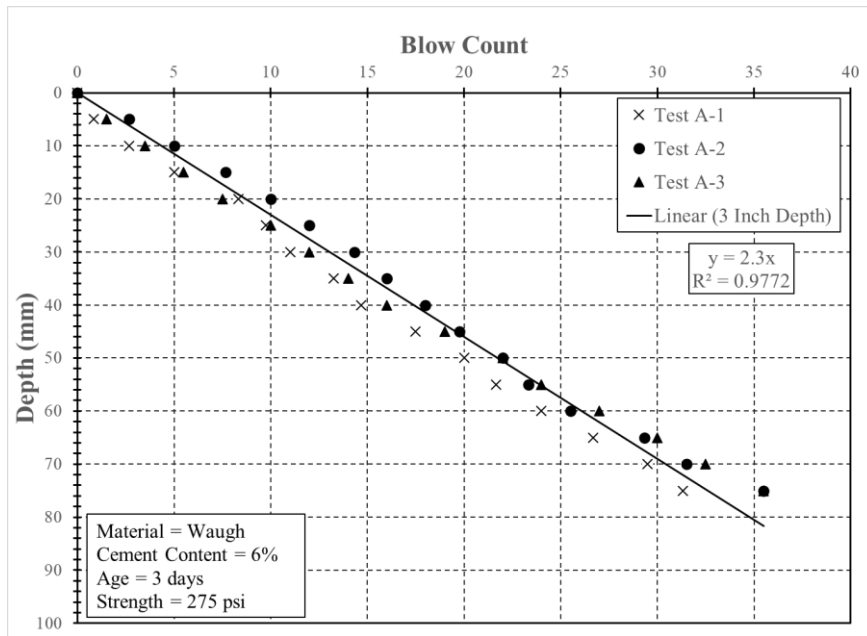


Figure F.9: Waugh 6% 3 day

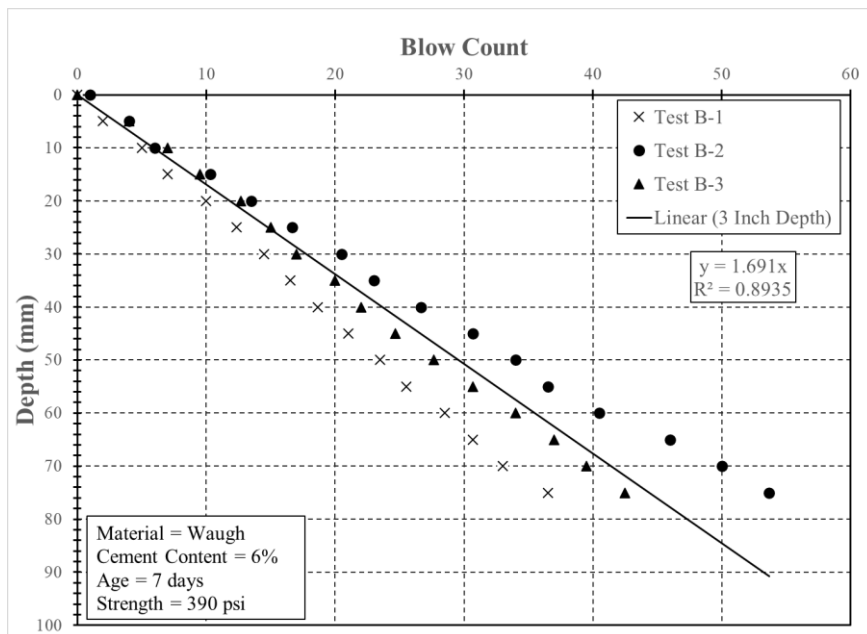


Figure F.10: Waugh 6% 7 day

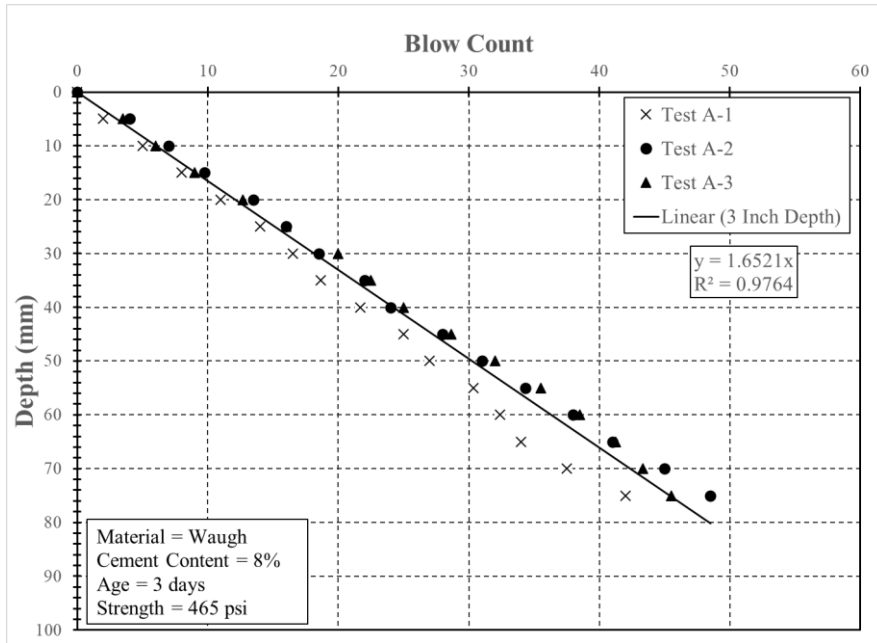


Figure F.11: Waugh 8% No. 1 3 days

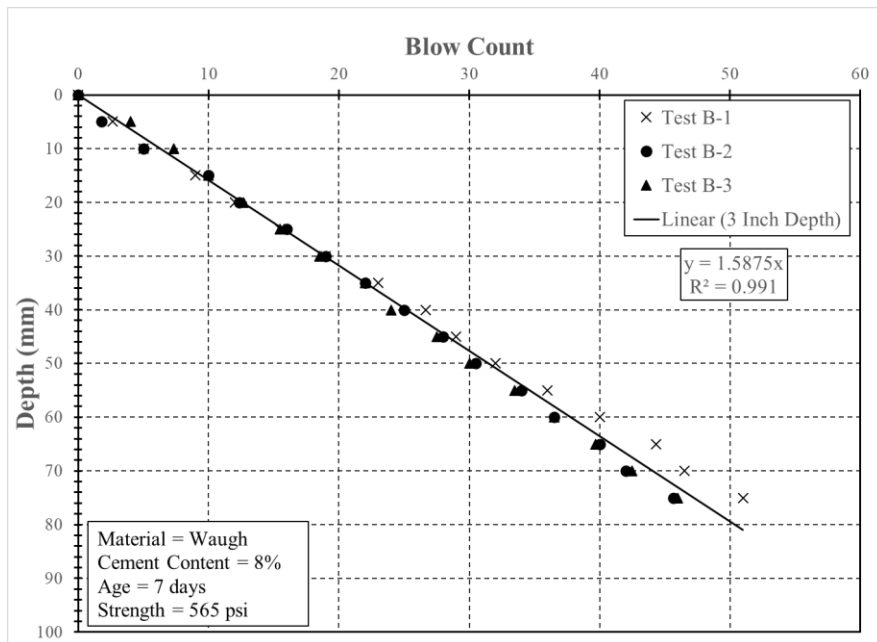


Figure F.12: Waugh 8% No. 1 7 days

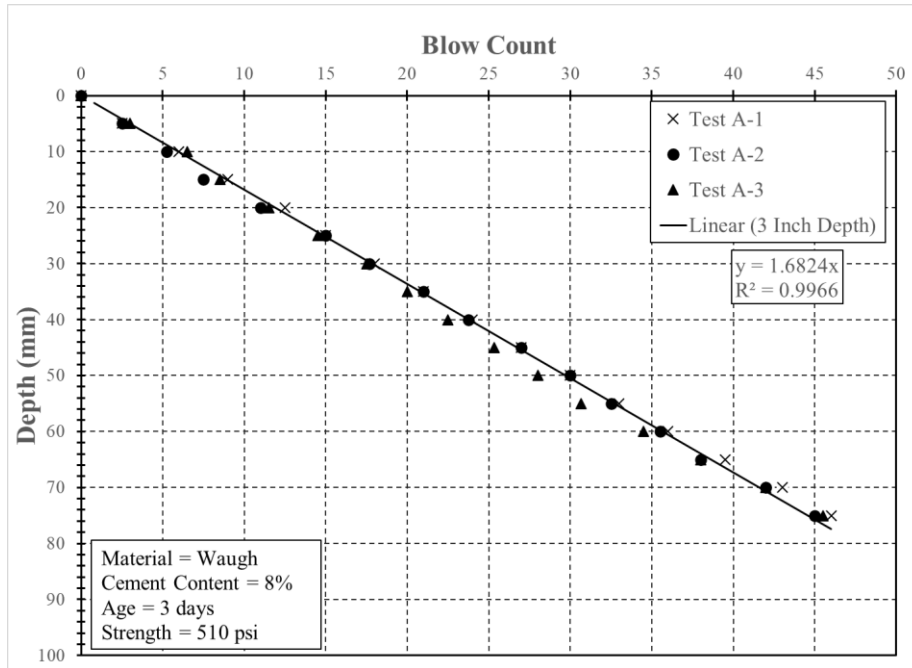


Figure F.13: Waugh 8% No. 2 3 days

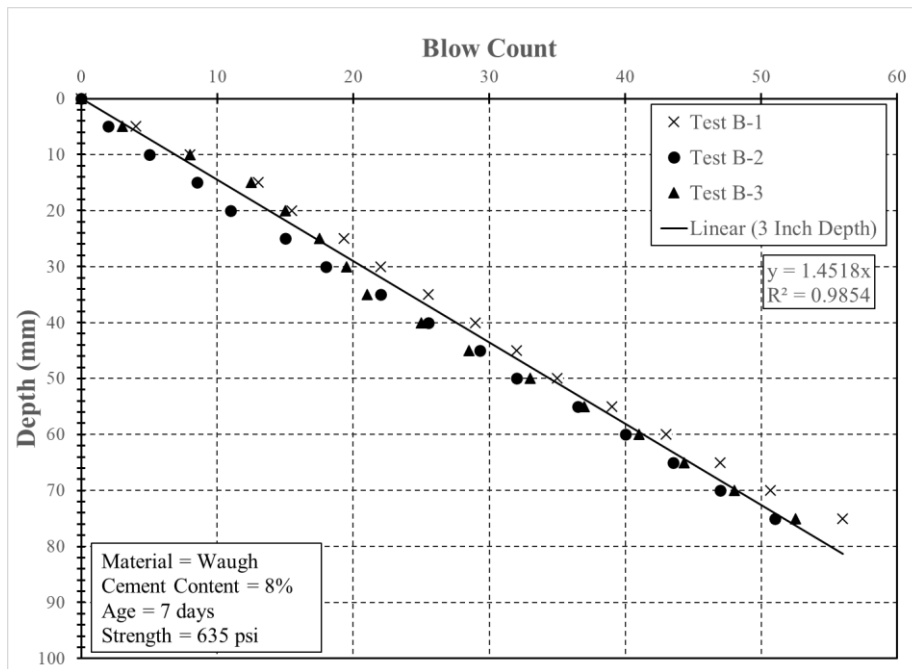


Figure F.14: Waugh 8% No. 2 7 days

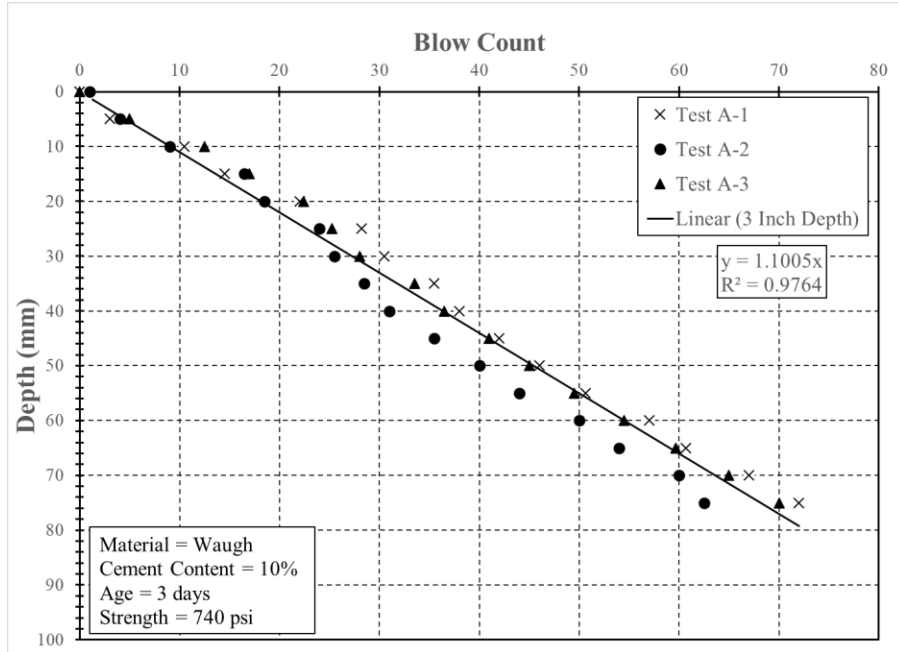


Figure F.15: Waugh 10% 3 days

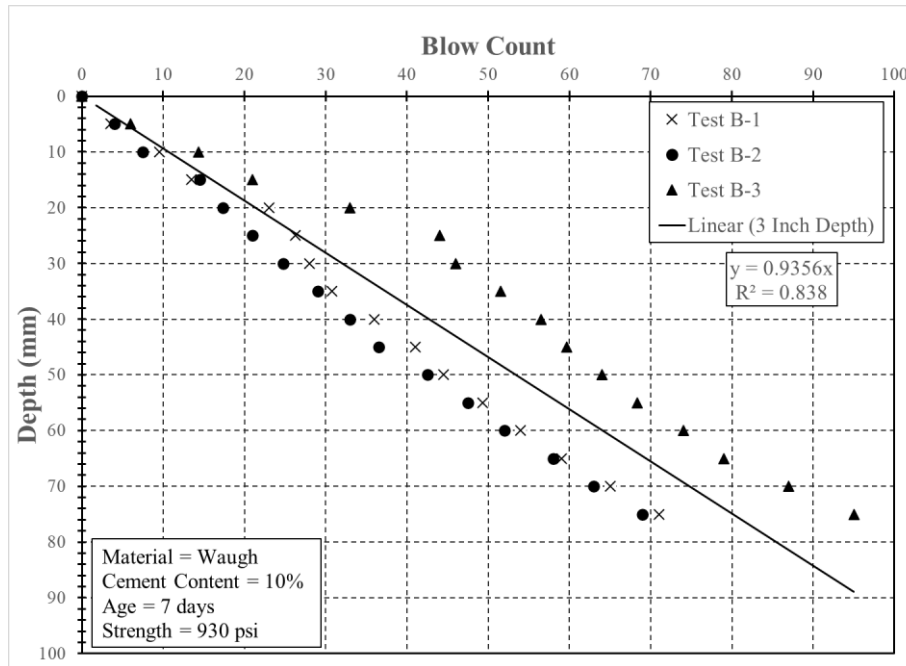


Figure F.16: Waugh 10% 7 days

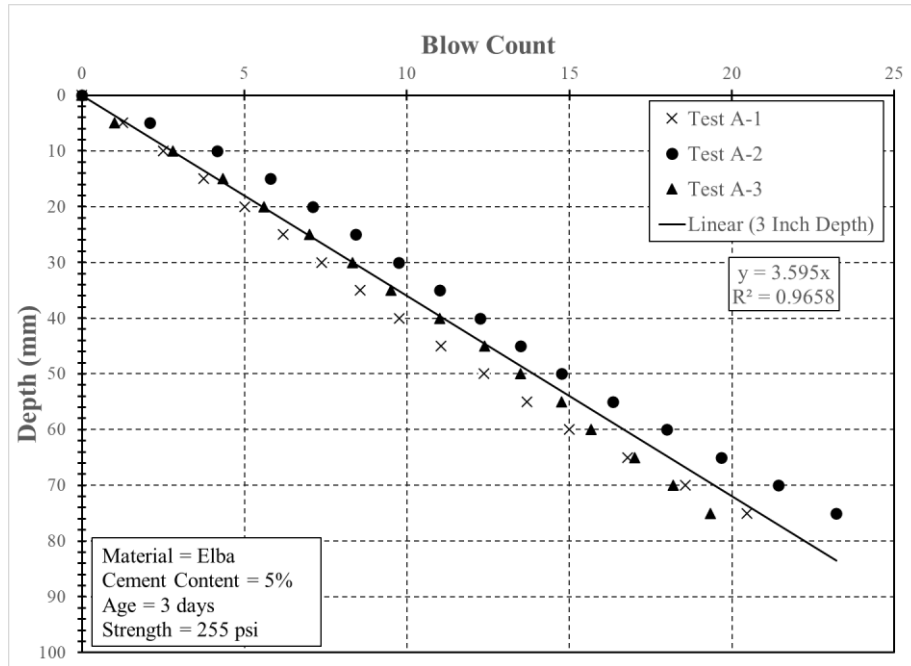


Figure F.17: Elba 5% 3 days

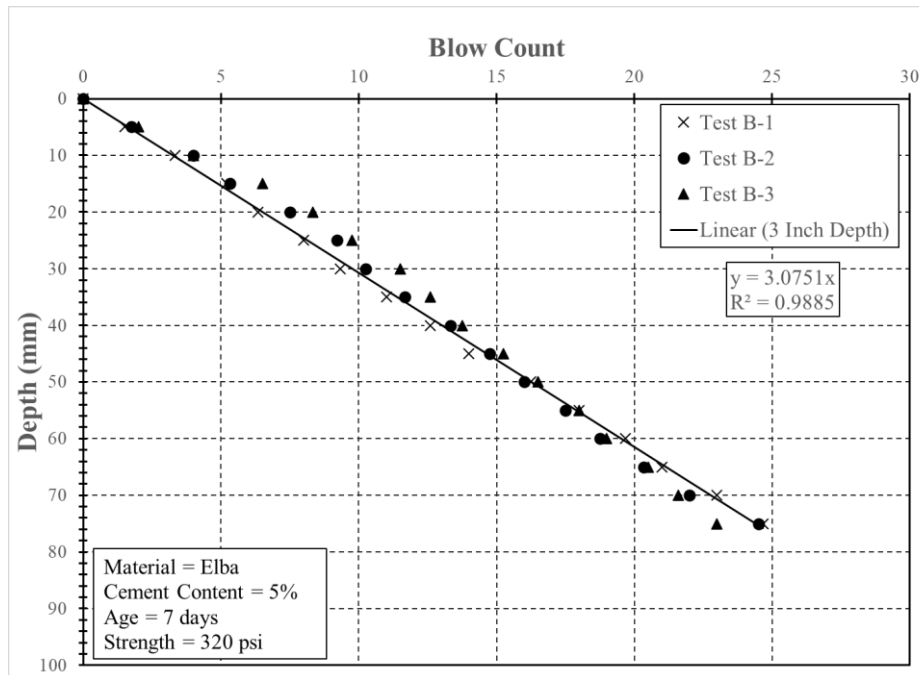


Figure F.18: Elba 5% 7 days

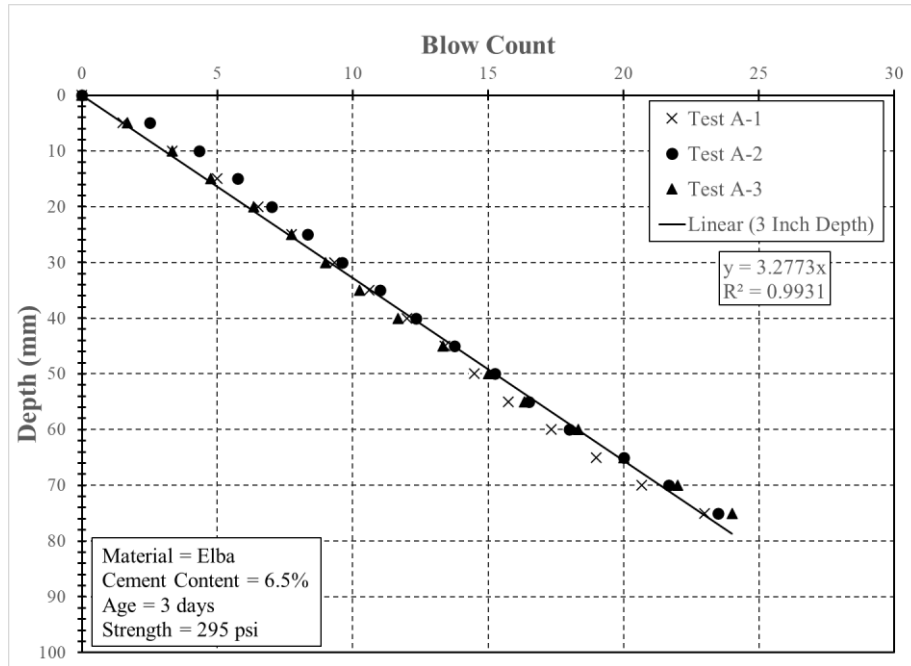


Figure F.19: Elba 6.5% No. 1 3 days

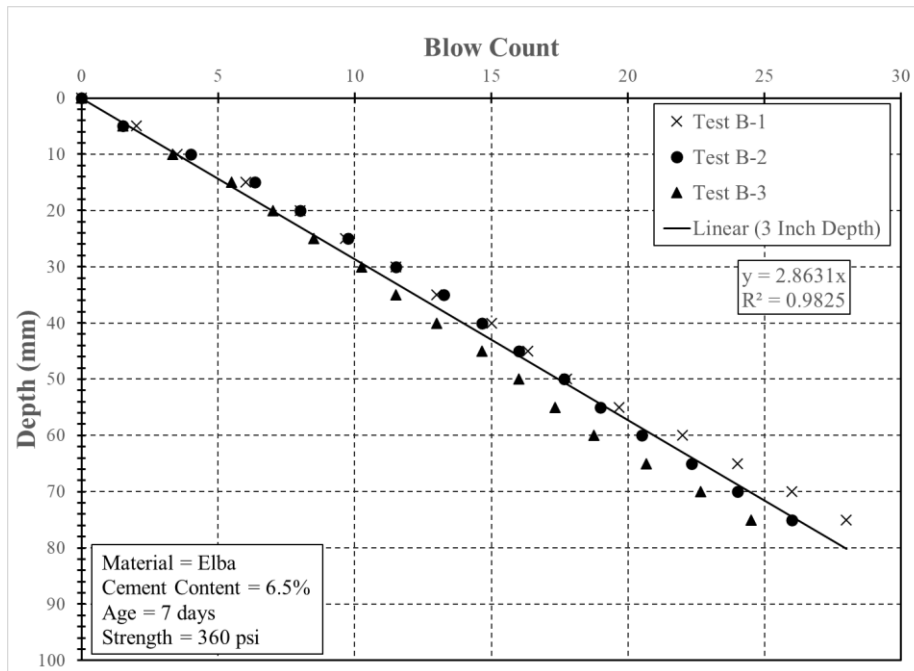


Figure F.20: Elba 6.5% No. 1 7 days

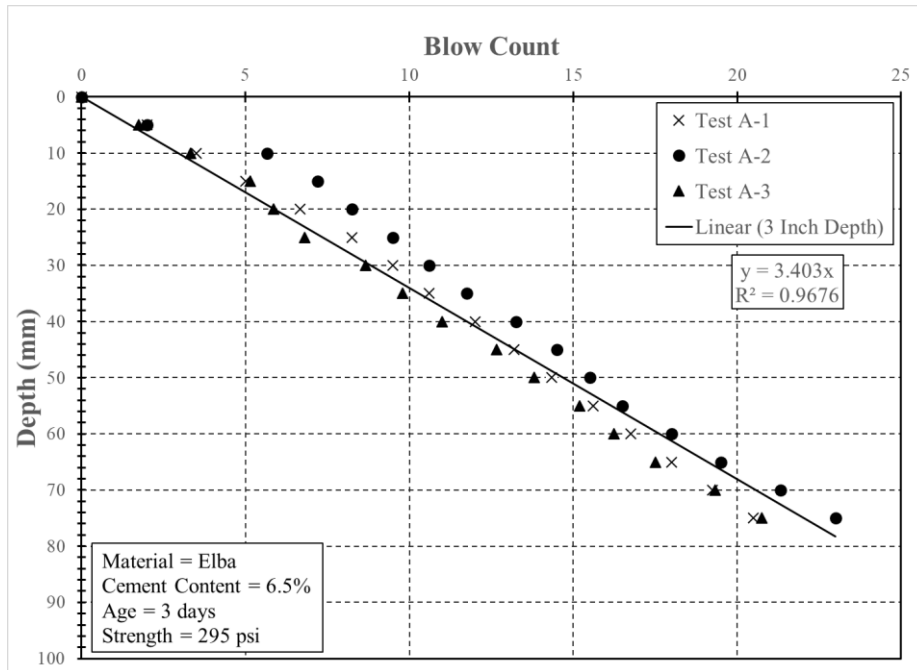


Figure F.21: Elba 6.5% No. 2 3 days

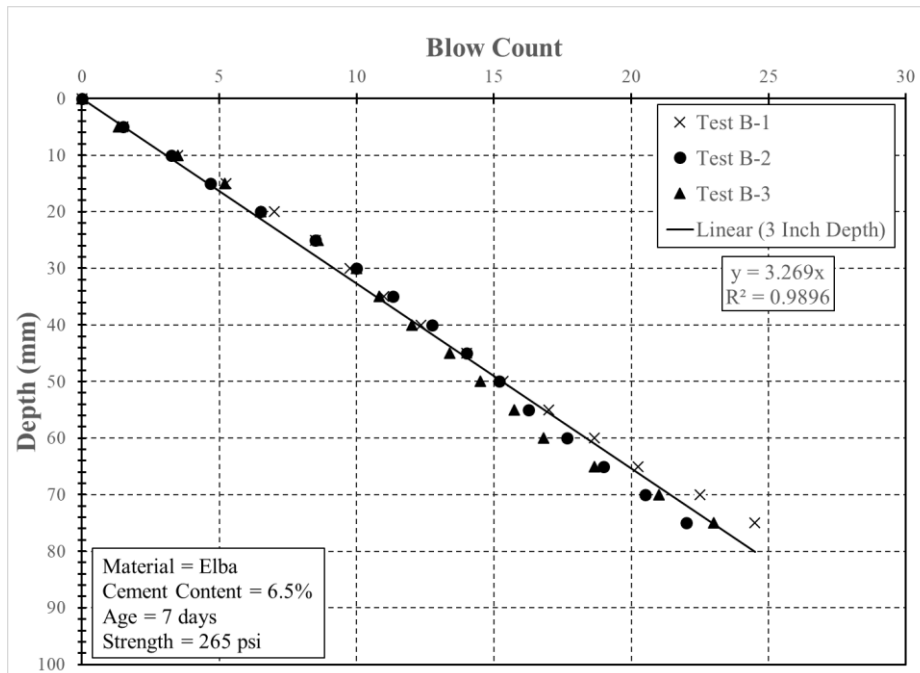


Figure F.22: Elba 6.5% No. 2 7 days

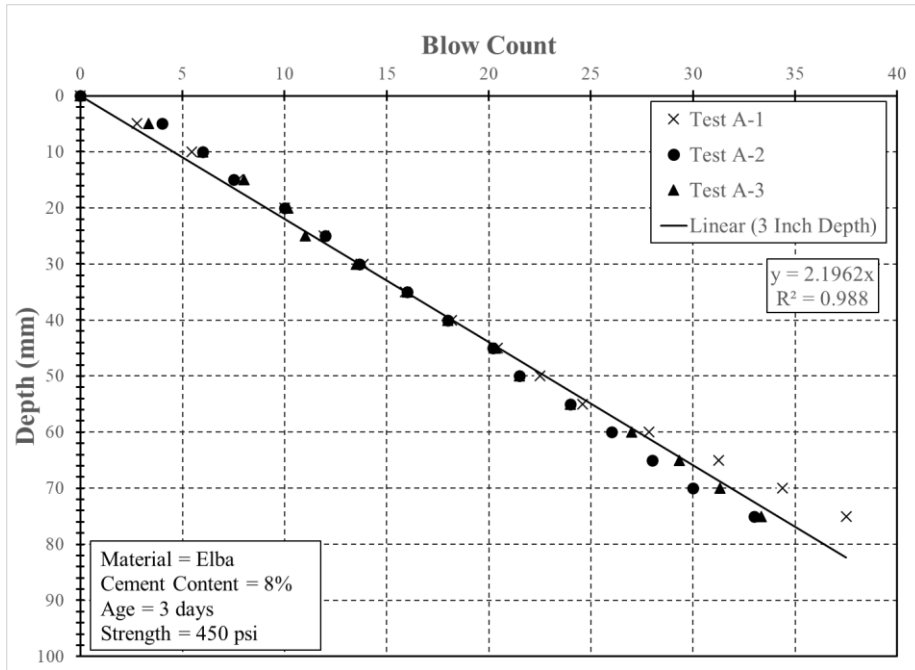


Figure F.23: Elba 8% 3 days

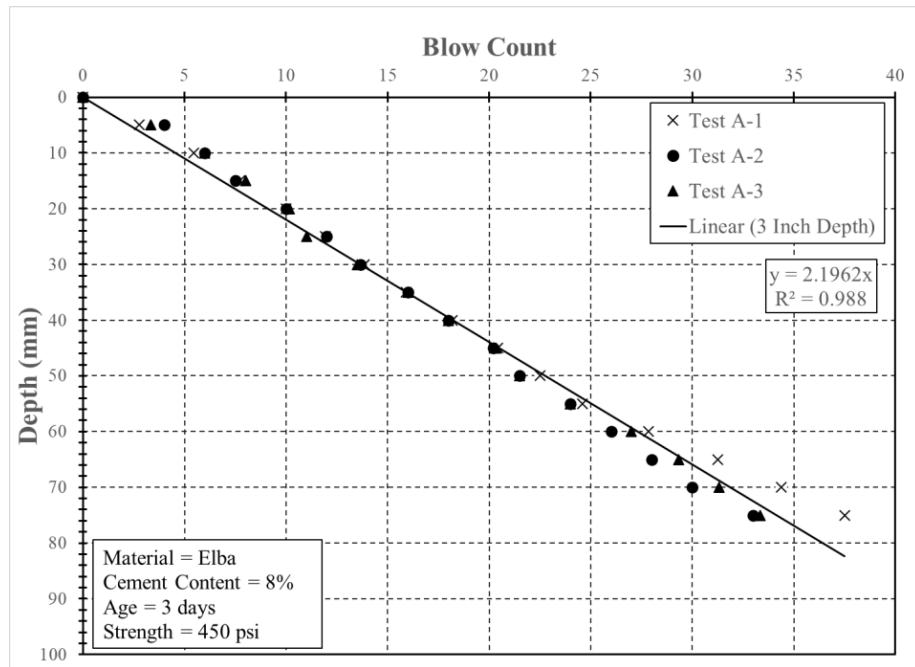


Figure F.24: Elba 8% 7 days

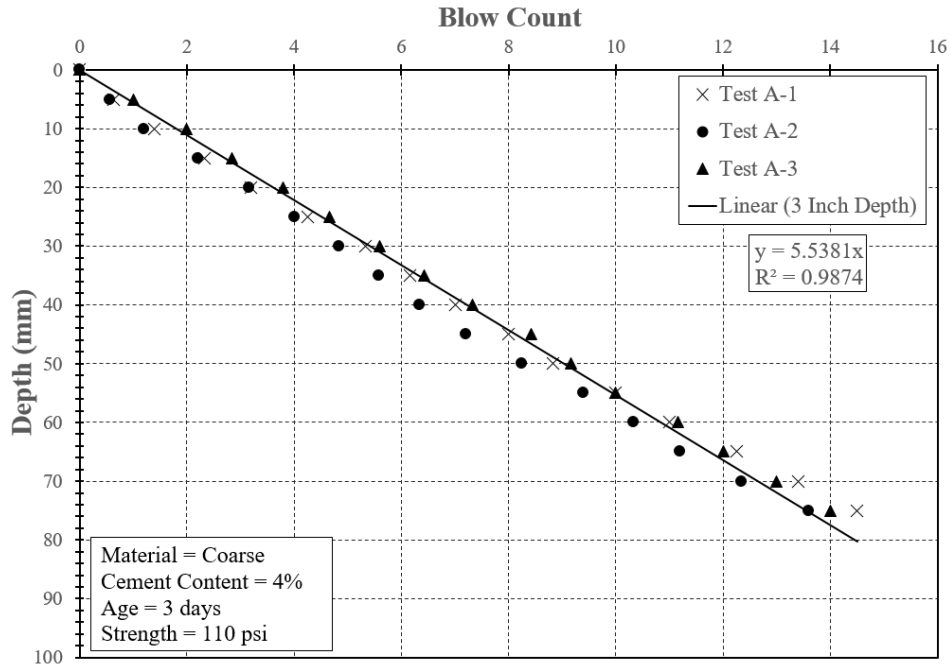


Figure F.25: Coarse 4% No. 1 3 days

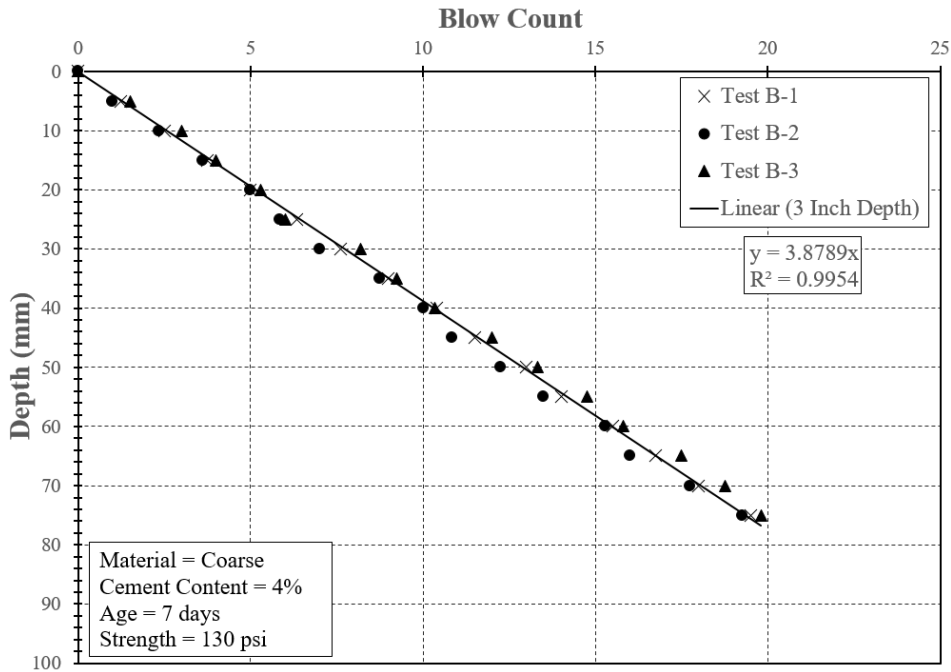


Figure F.26: Coarse 4% No. 1 7 days

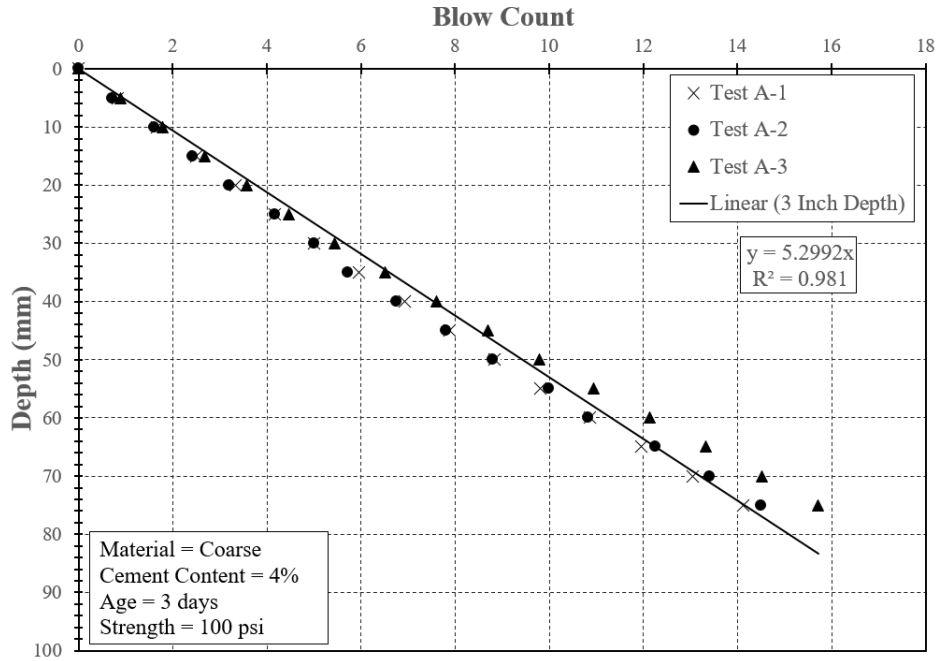


Figure F.27: Coarse 4% No. 2 3 days

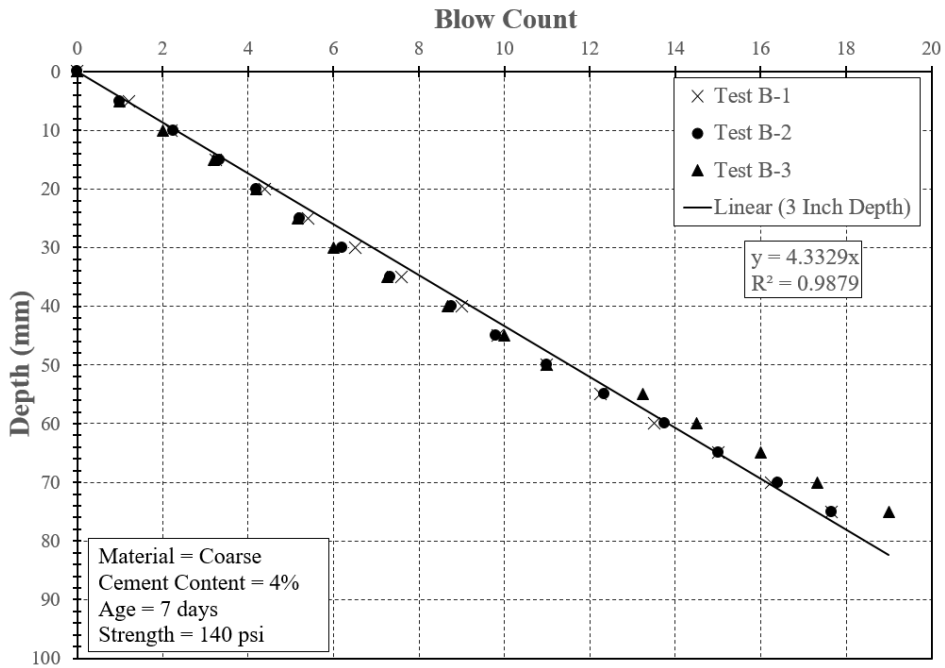


Figure F.28: Coarse 4% No. 2 7 days

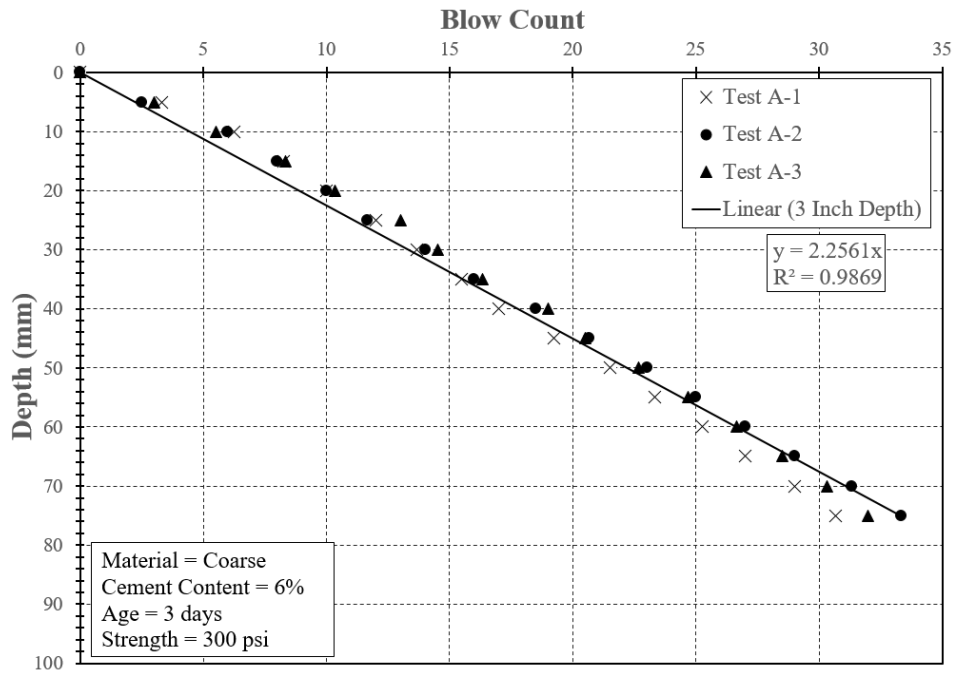


Figure F.29: Coarse 6% No. 1 3 days

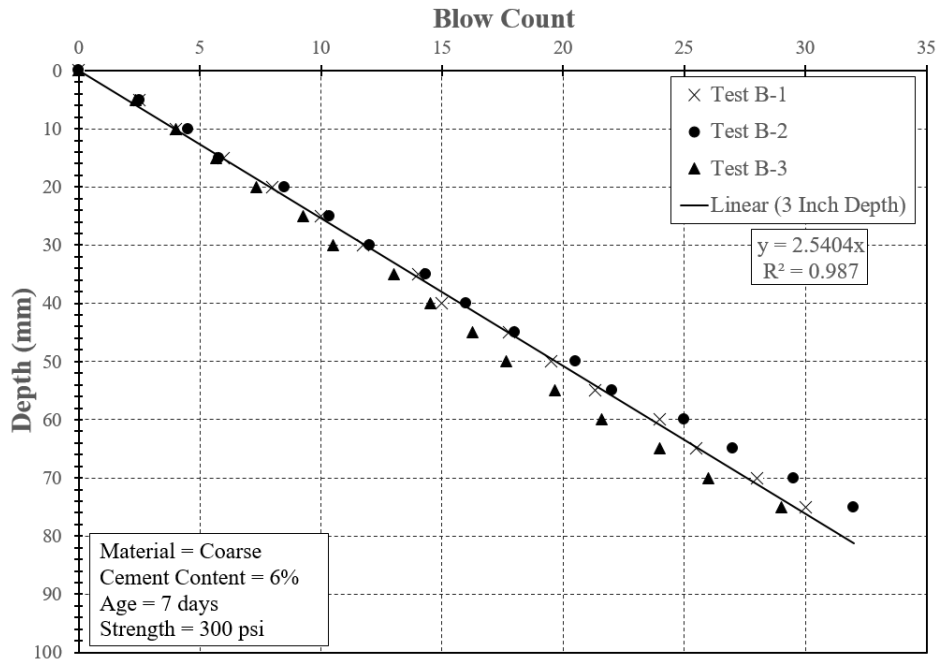


Figure F.30: Coarse 6% No. 1 7 days

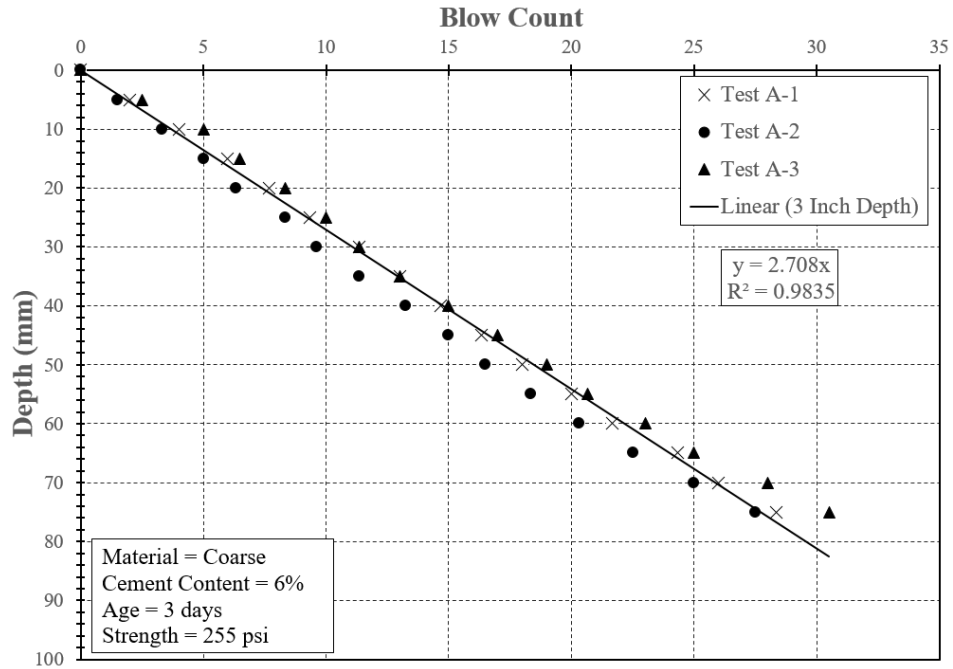


Figure F.31: Coarse 6% No. 2 3 days

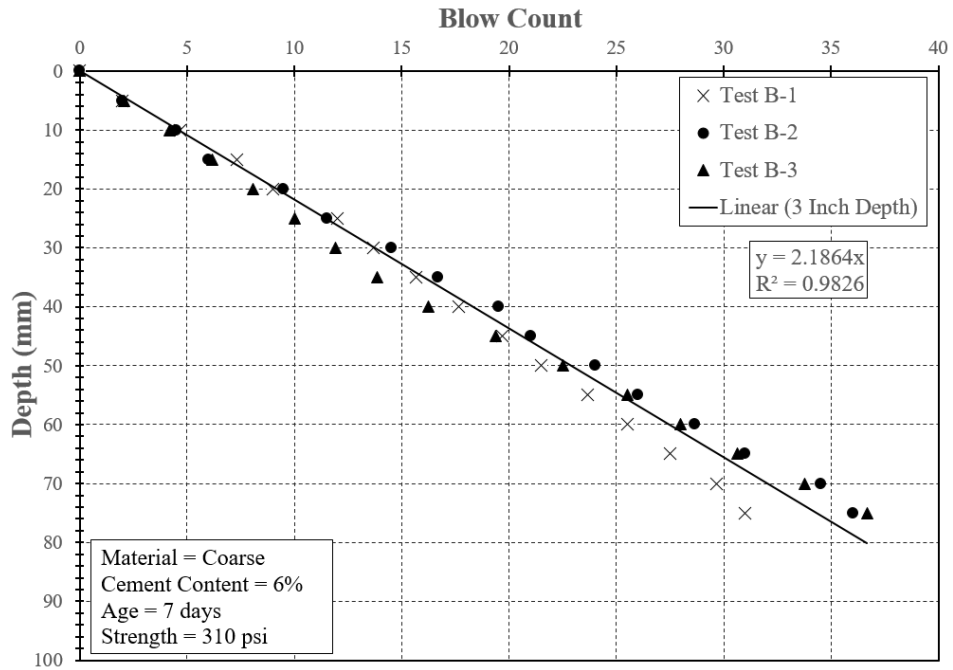


Figure F.32: Coarse 6% No. 2 7 days

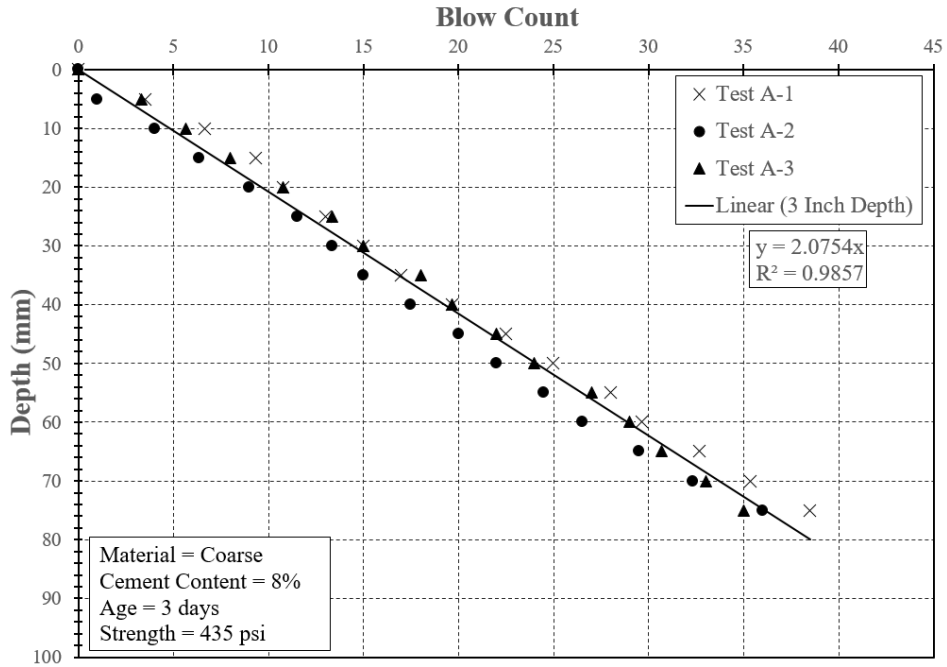


Figure F.33: Coarse 8% No. 1 3 days

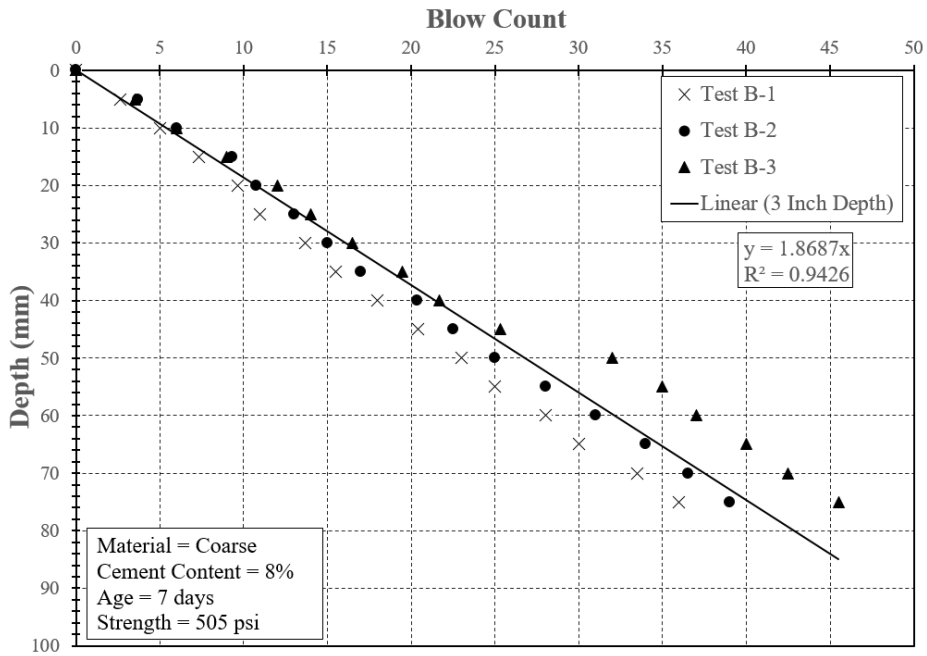


Figure F.34: Coarse 8% No. 1 7 days

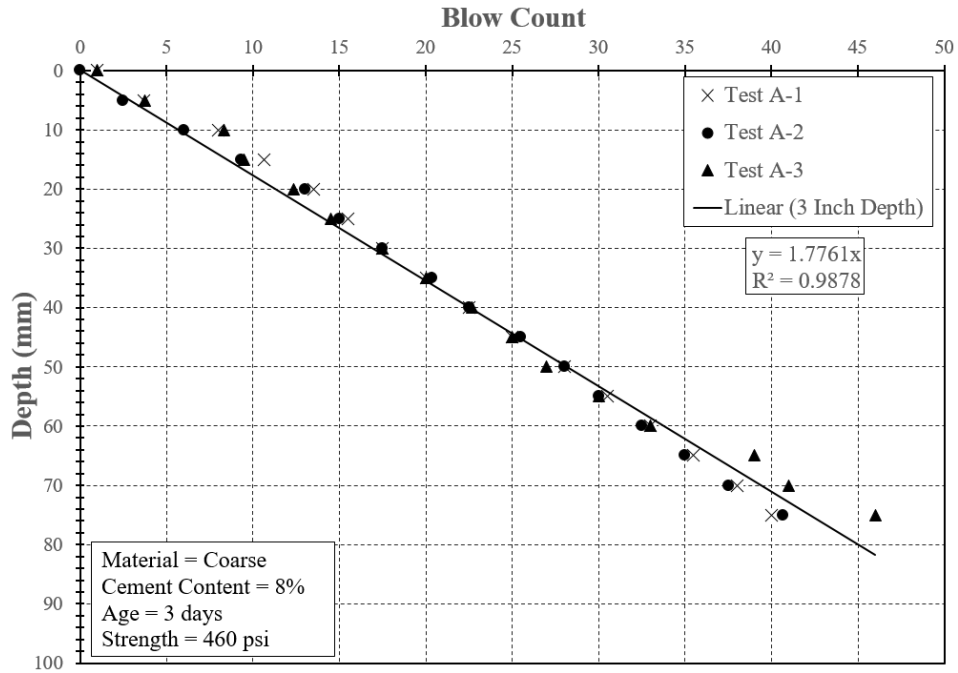


Figure F.35: Coarse 8% No. 2 3 days

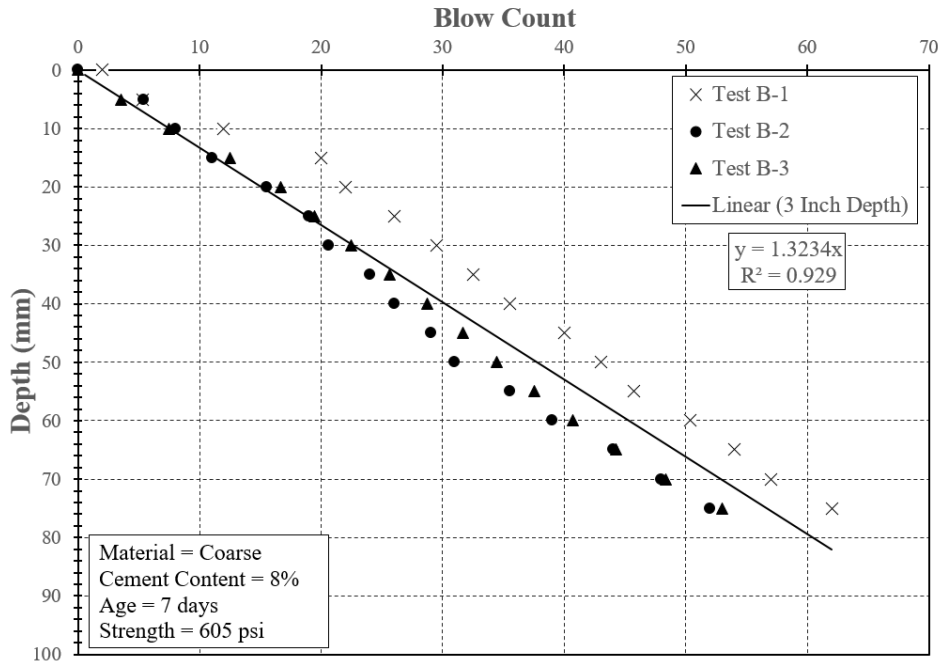


Figure F.36: Coarse 8% No. 2 7 days

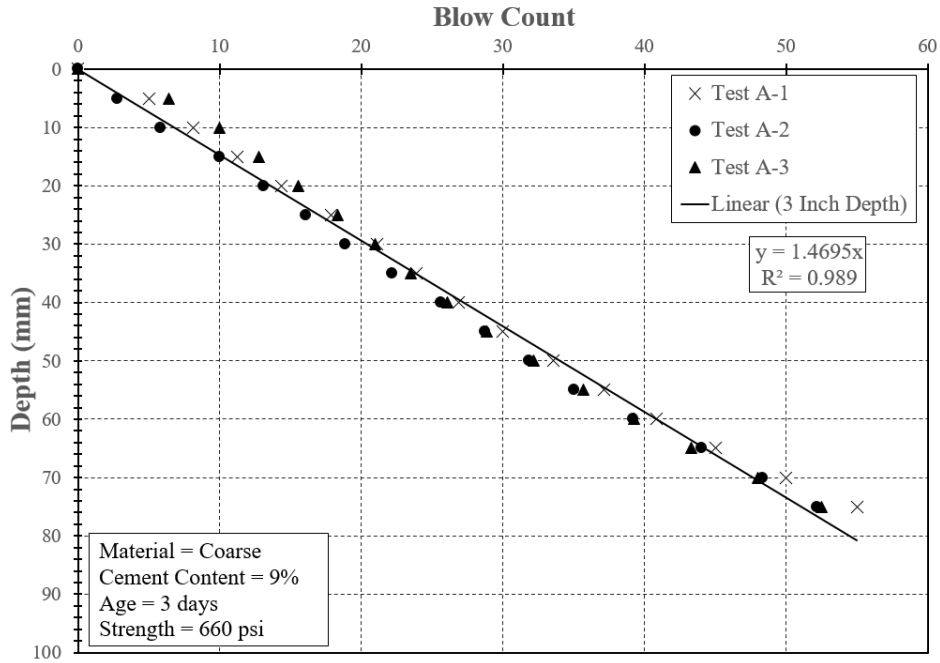


Figure F.37: Coarse 9% 3 days

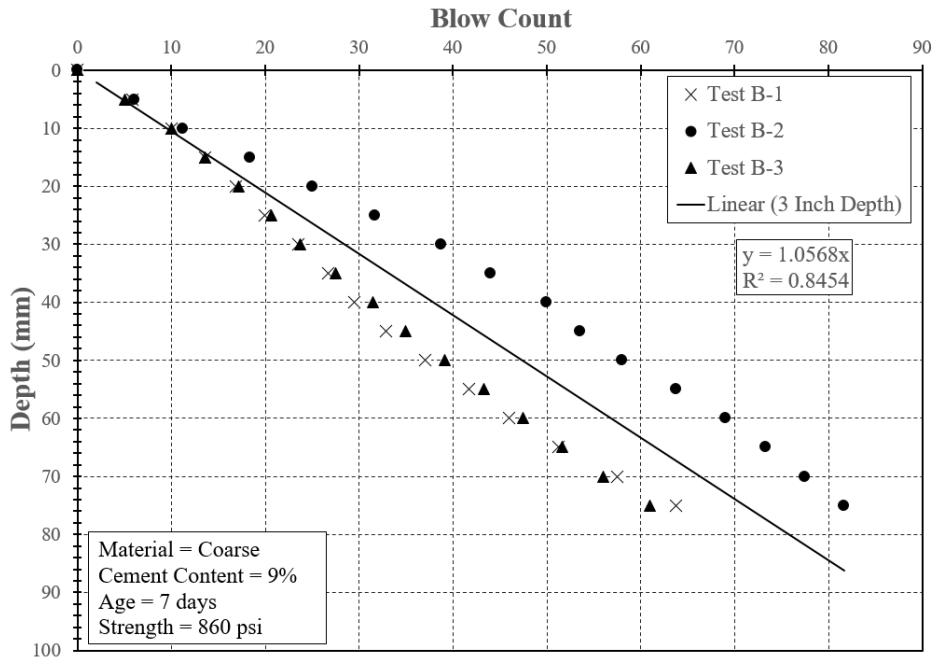


Figure F.38: Coarse 9% 7 days

Appendix G

100 Millimeter Penetration Depth Data

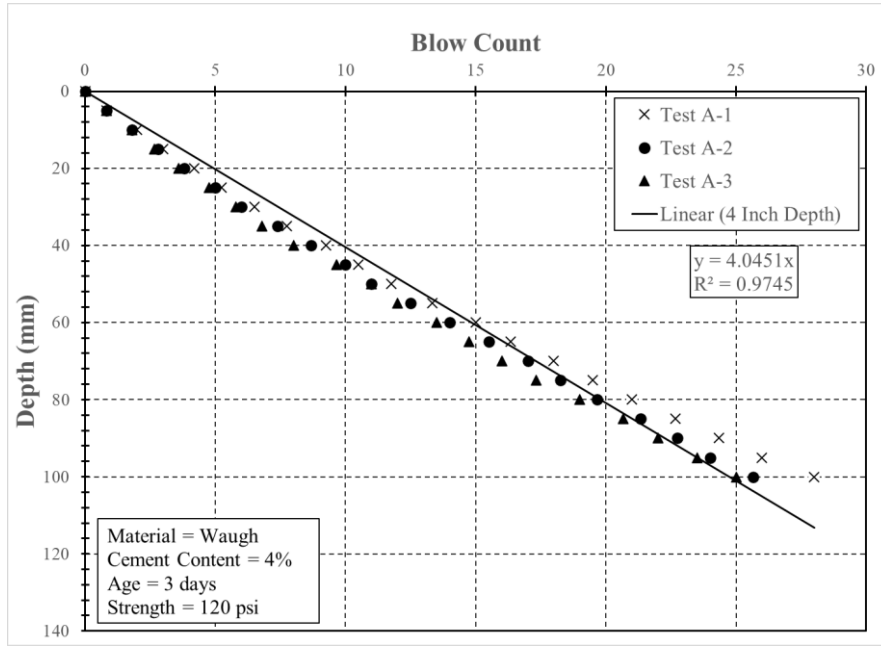


Figure G.1: Waugh 4% No. 1 3 days

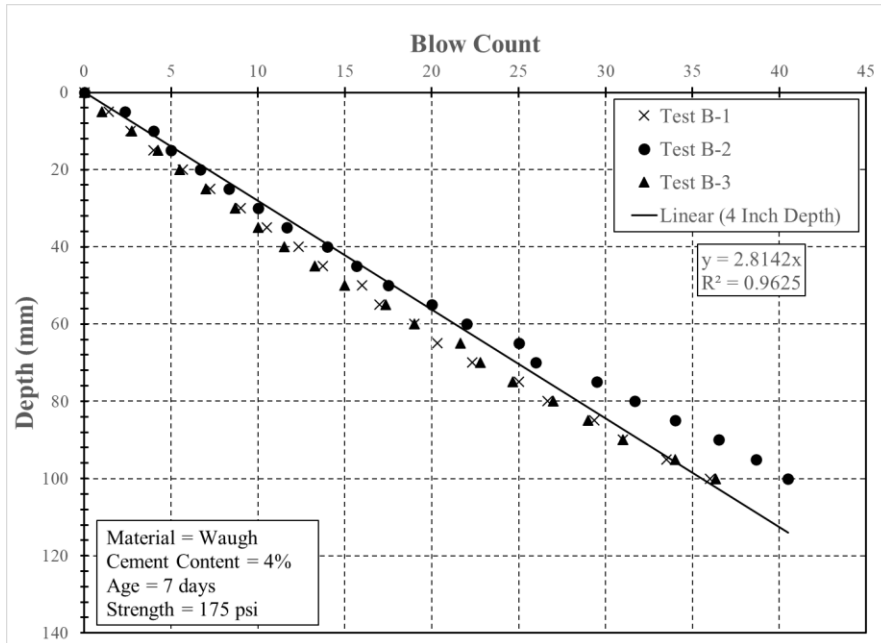


Figure G.2: Waugh 4% No. 1 7 days

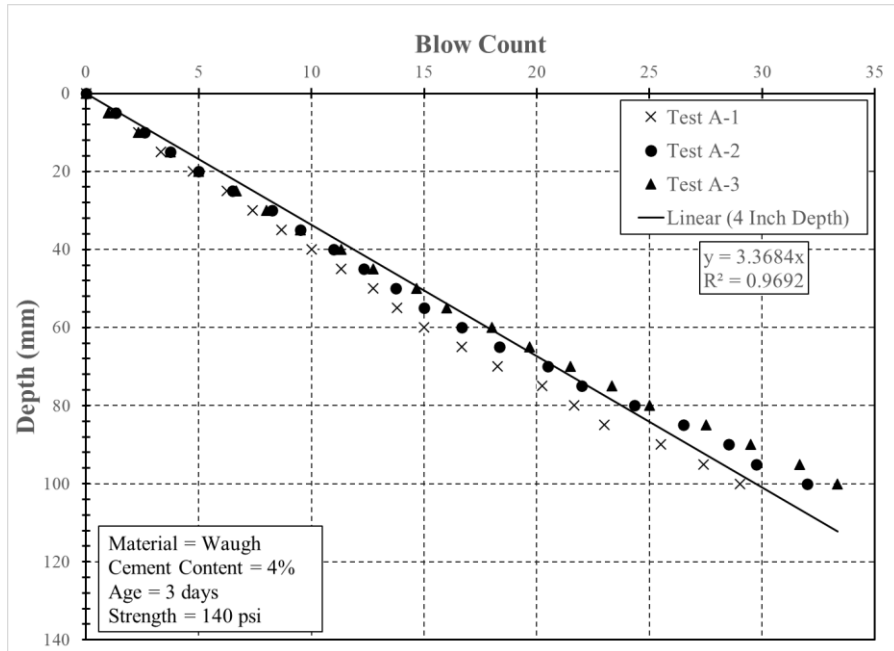


Figure G.3: Waugh 4% No. 2 3 days

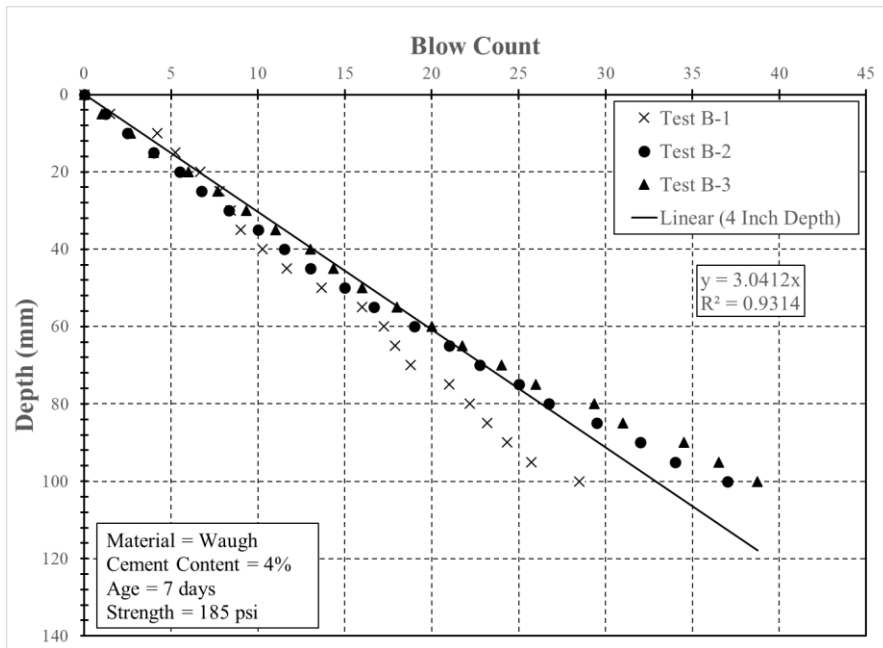


Figure G.4: Waugh 4% No. 2 7 days

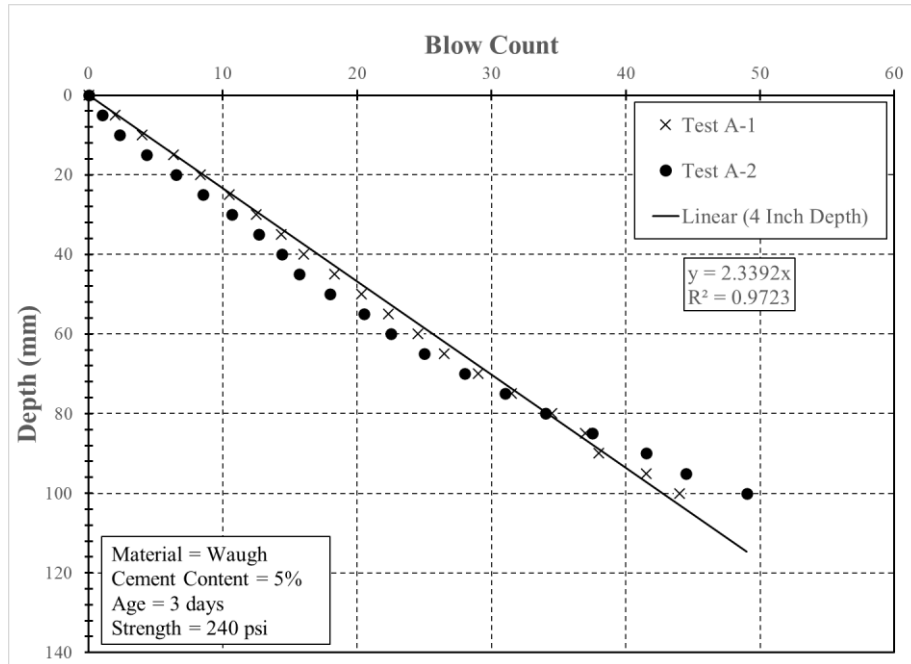


Figure G.5: Waugh 5% No. 1 3 days (Third specimen was removed due to error)

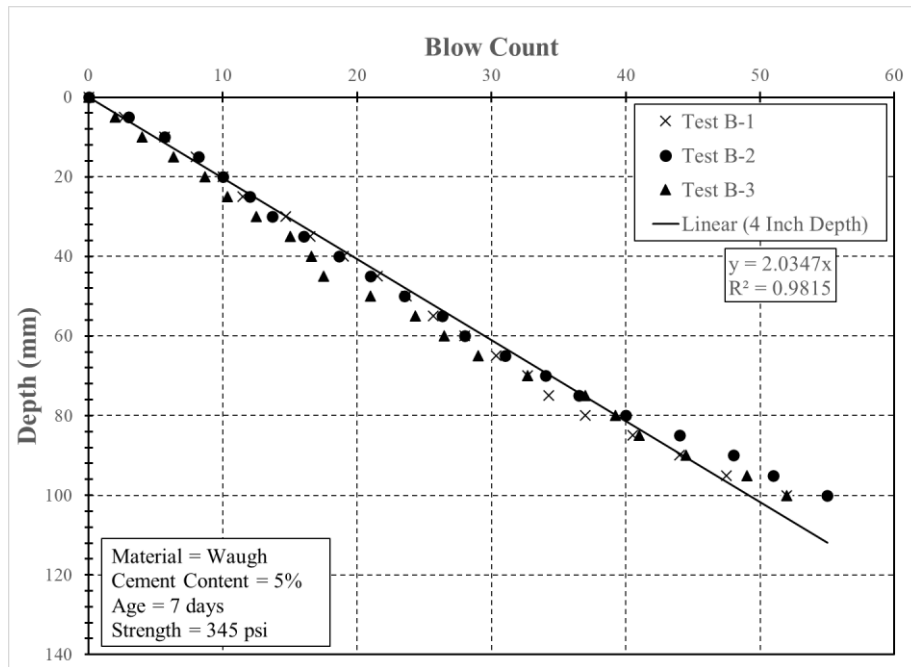


Figure G.6: Waugh 5% No. 1 7 days

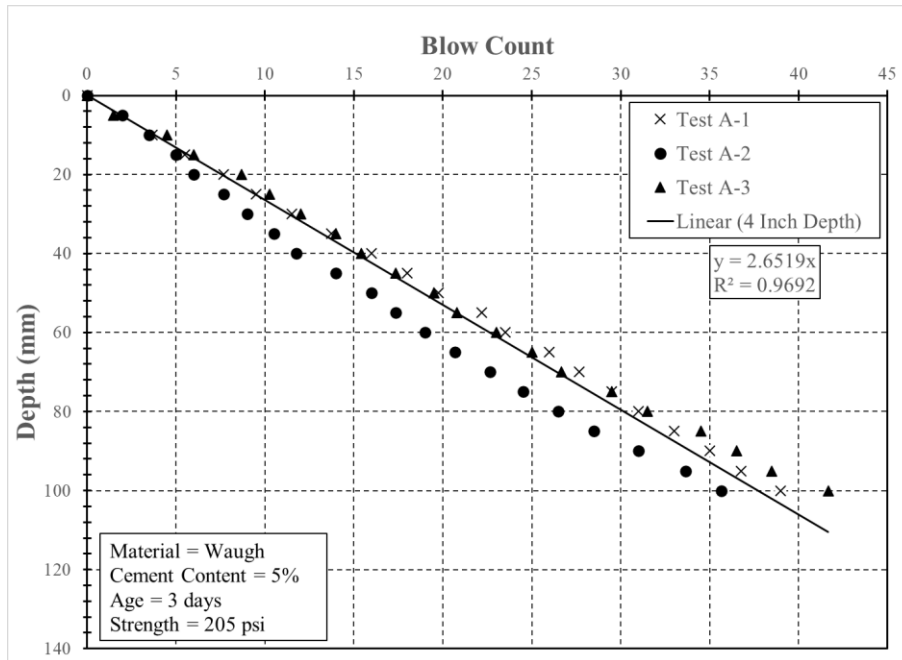


Figure G.7: Waugh 5% No. 2 3 days

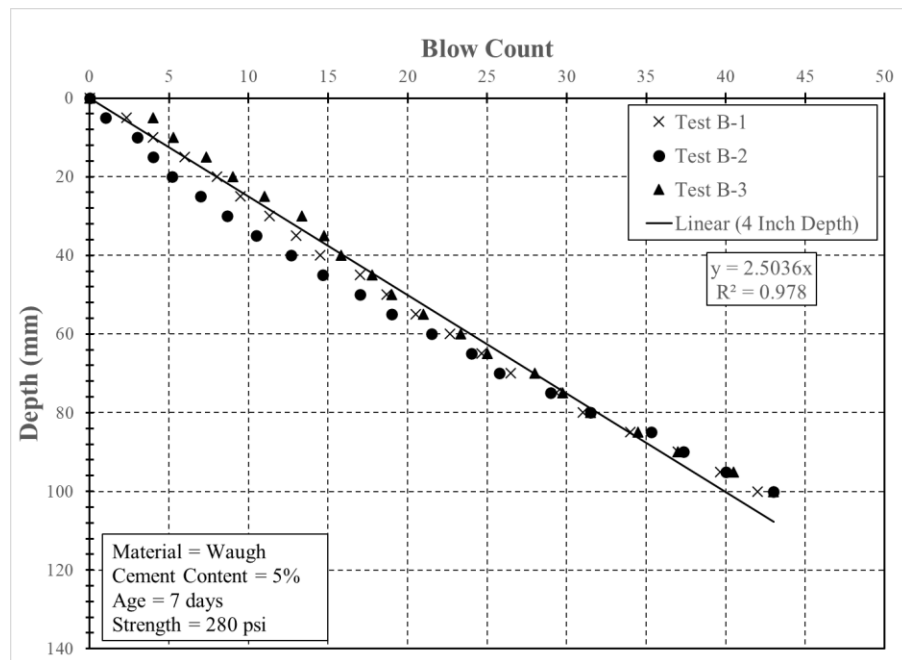


Figure G.8: Waugh 5% No. 2 7 days

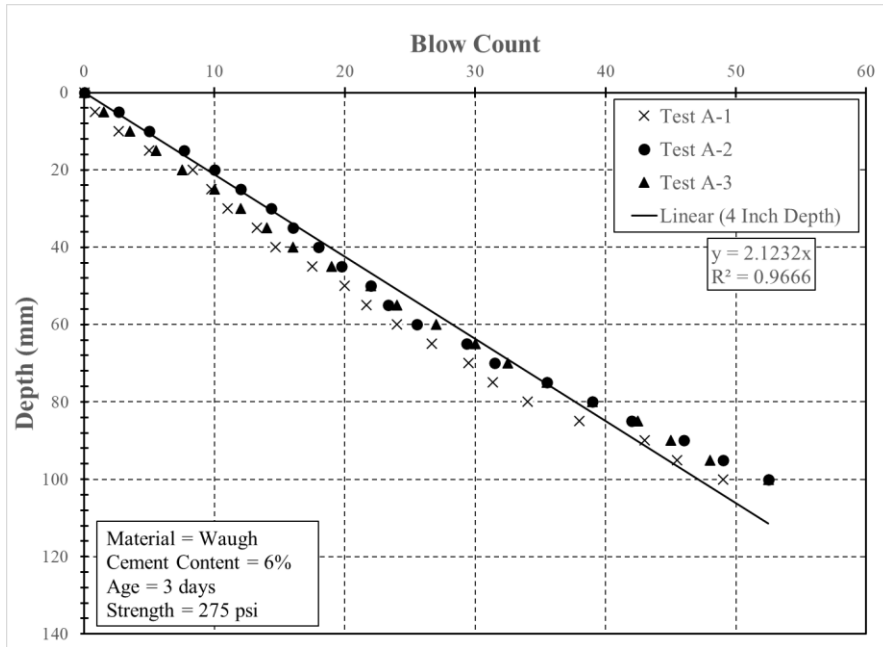


Figure G.9: Waugh 6% 3 day

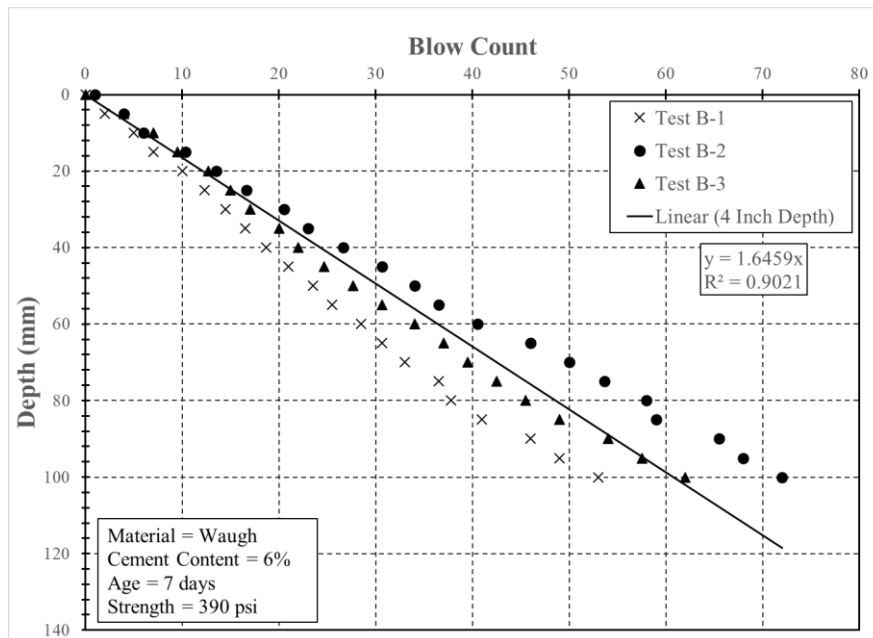


Figure G.10: Waugh 6% 7 day

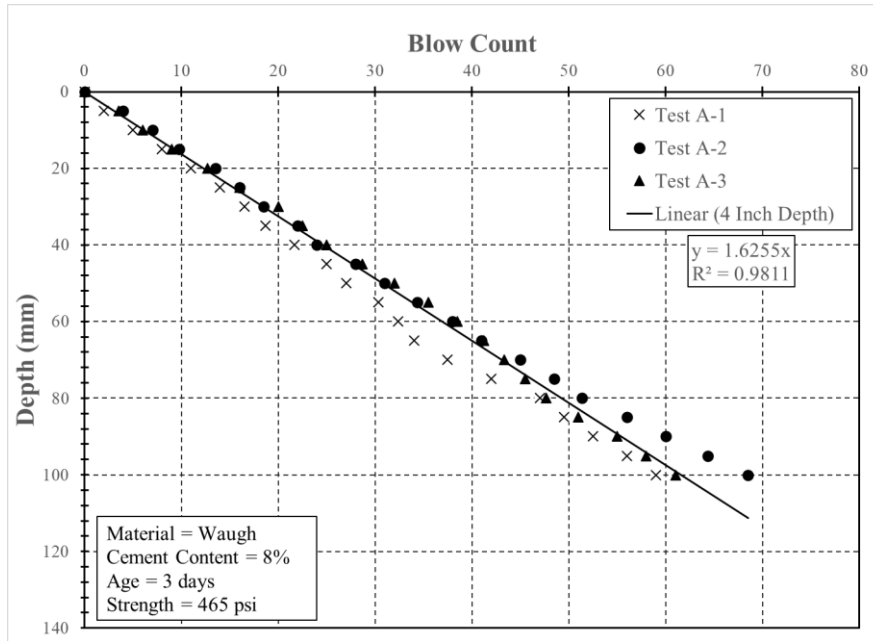


Figure G.11: Waugh 8% No. 1 3 days

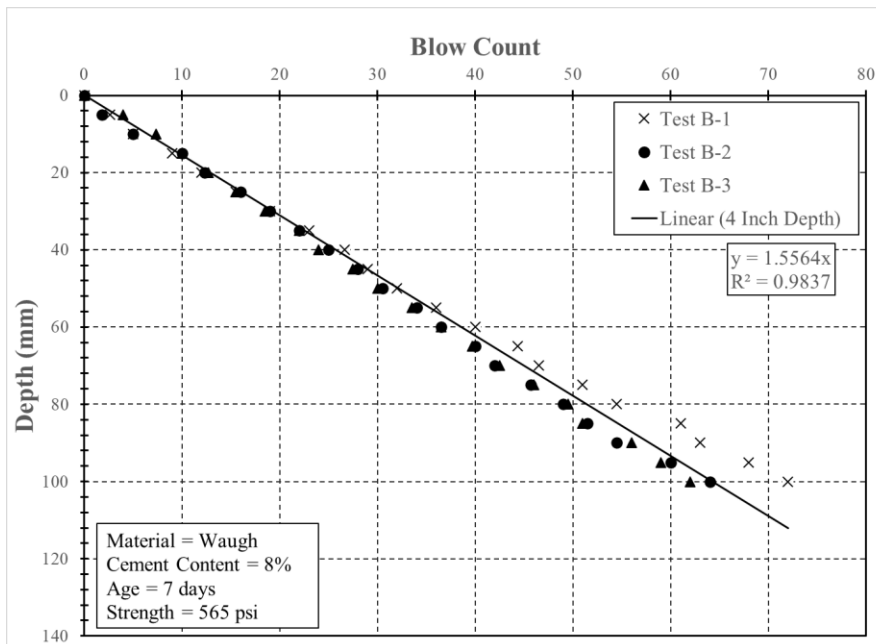


Figure G.12: Waugh 8% No. 1 7 days

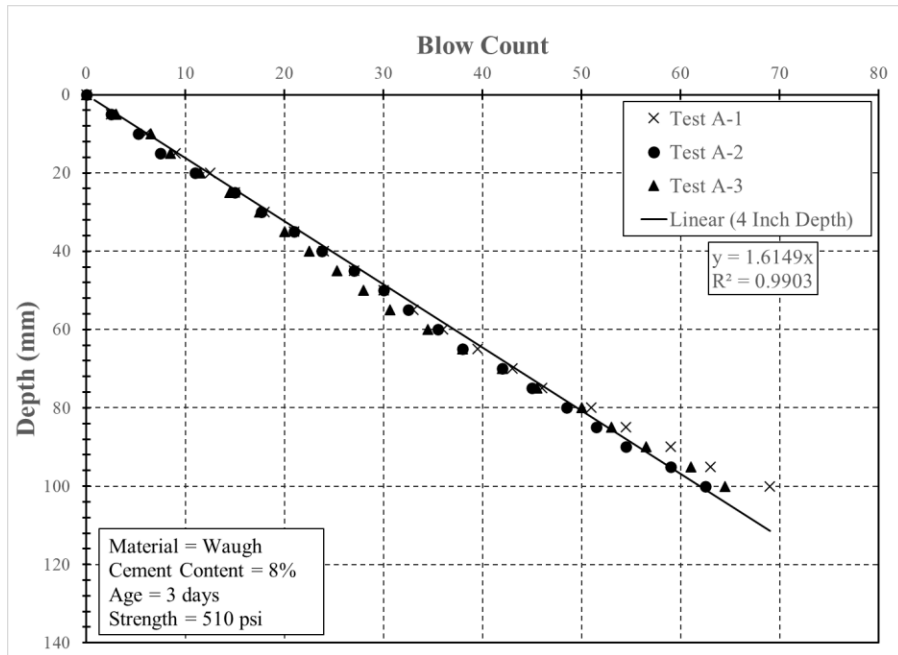


Figure G.13: Waugh 8% No. 2 3 days

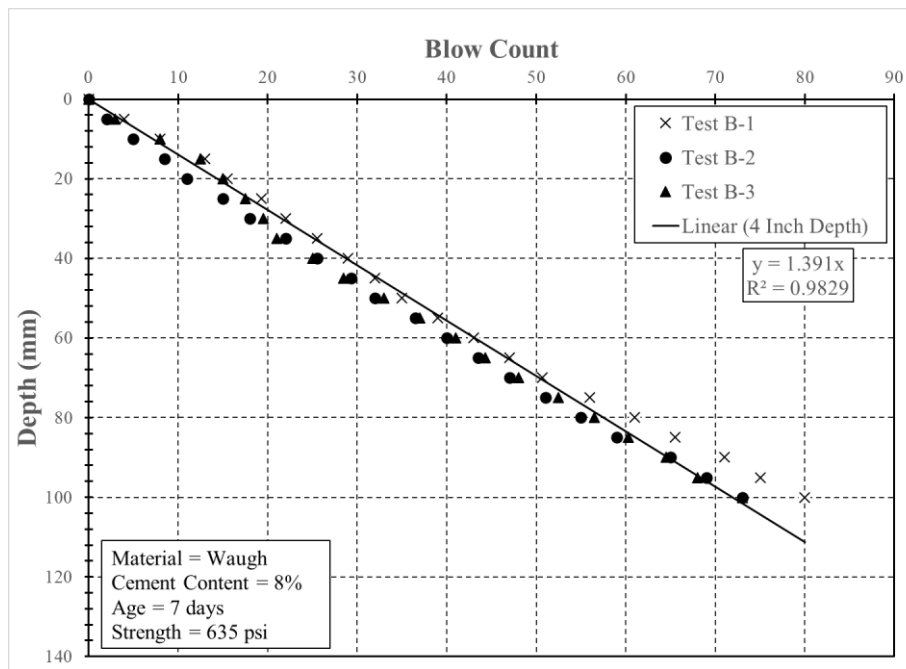


Figure G.14: Waugh 8% No. 2 7 days

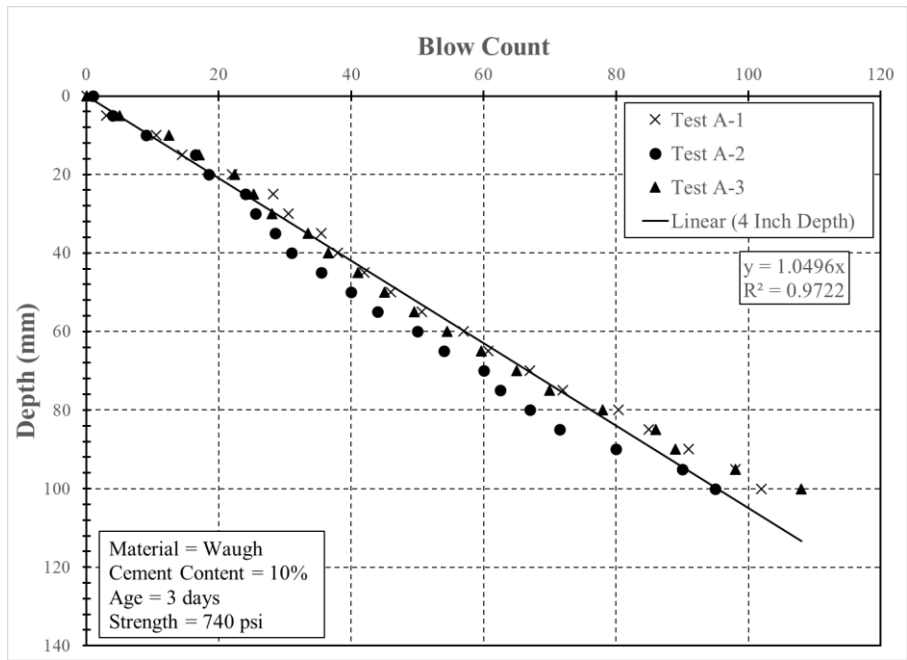


Figure G.15: Waugh 10% 3 days

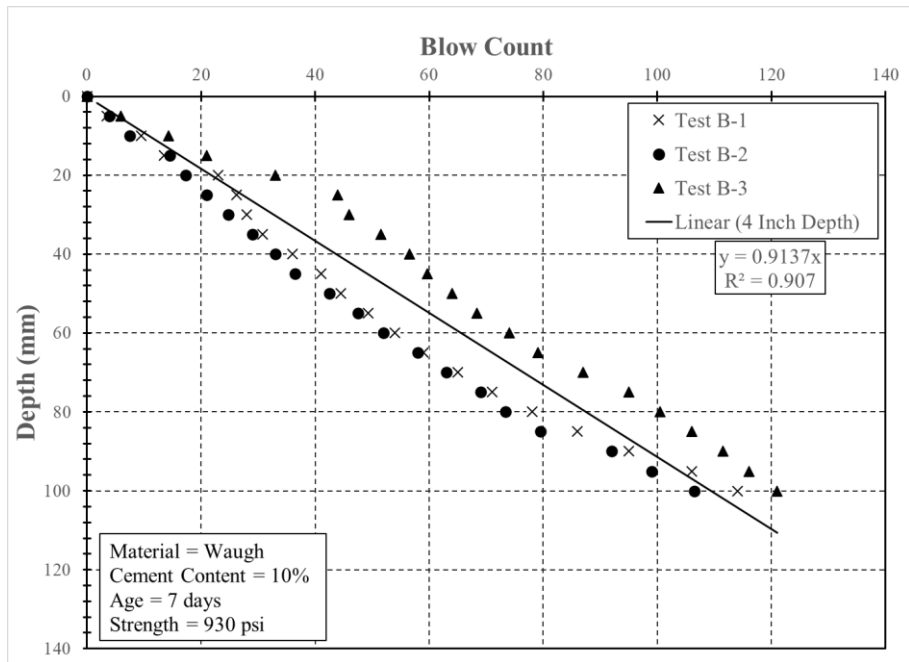


Figure G.16: Waugh 10% 7 days

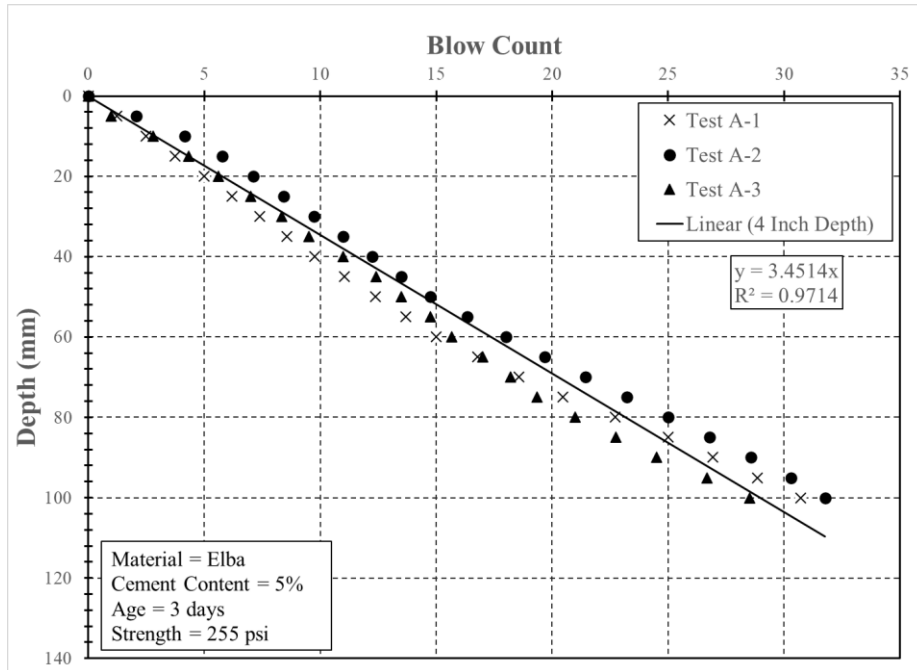


Figure G.17: Elba 5% 3 days

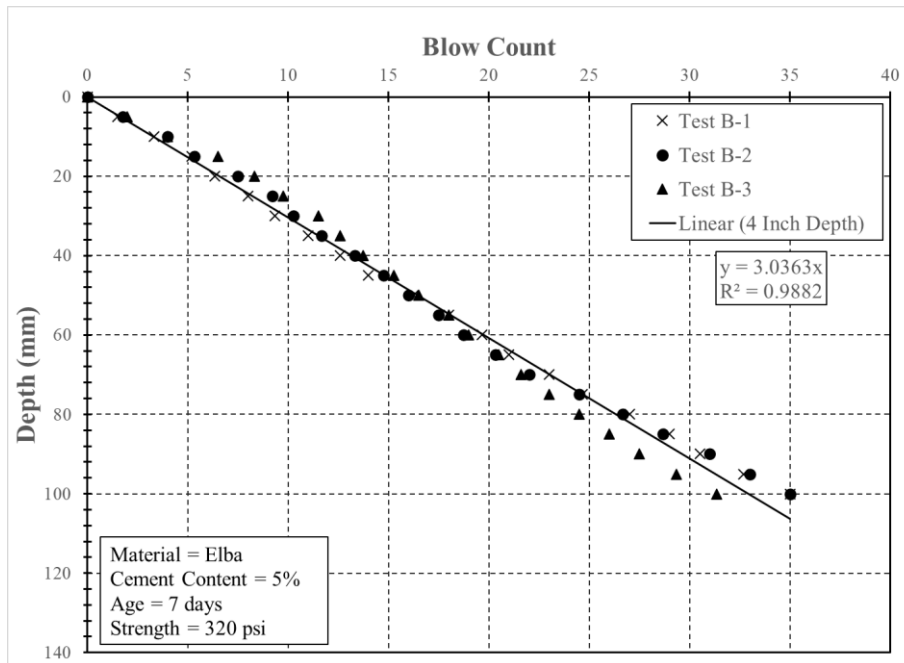


Figure G.18: Elba 5% 7 days

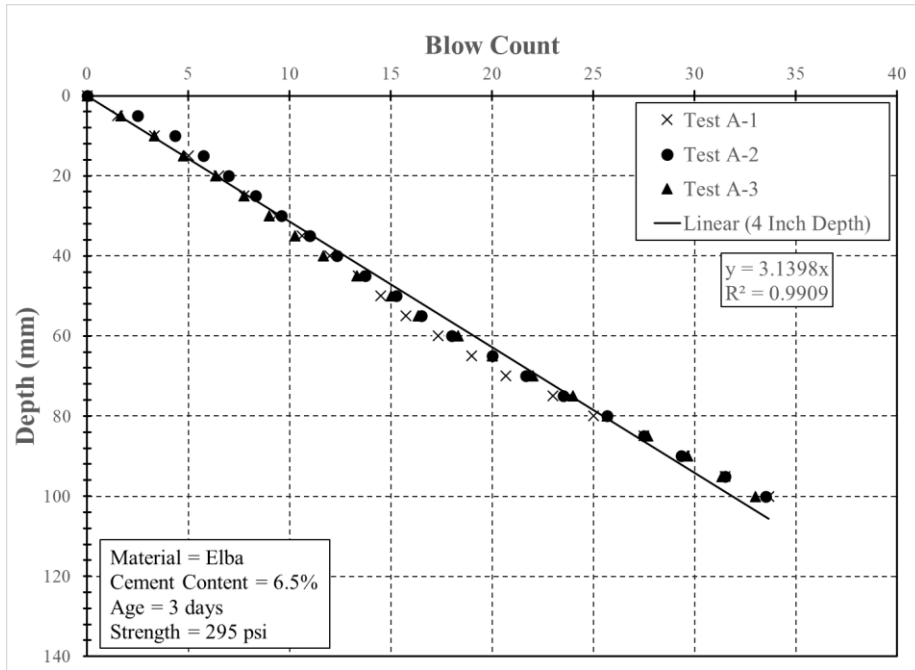


Figure G.19: Elba 6.5% No. 1 3 days

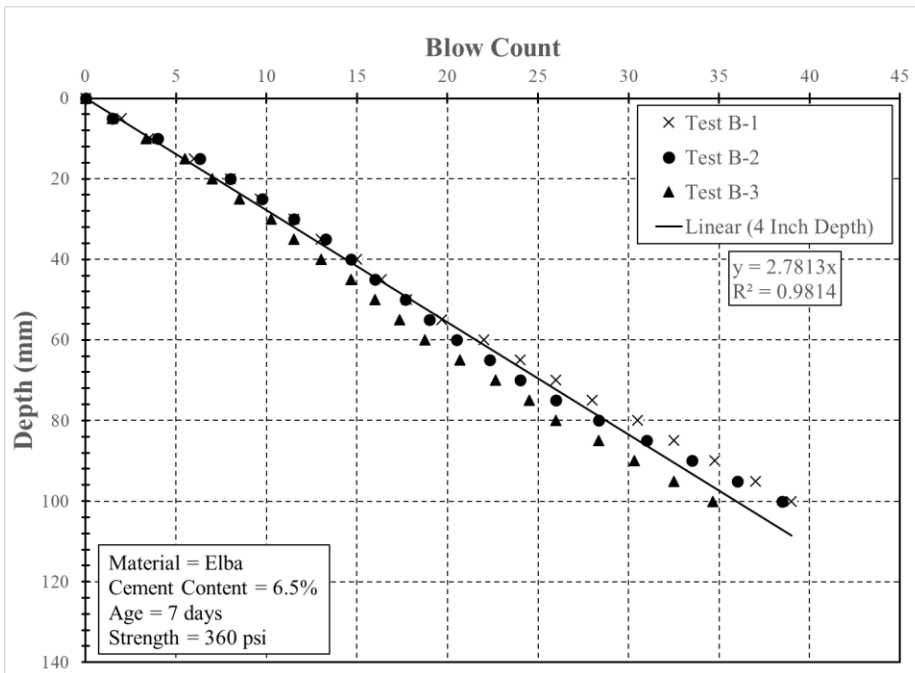


Figure G.20: Elba 6.5% No. 1 7 days

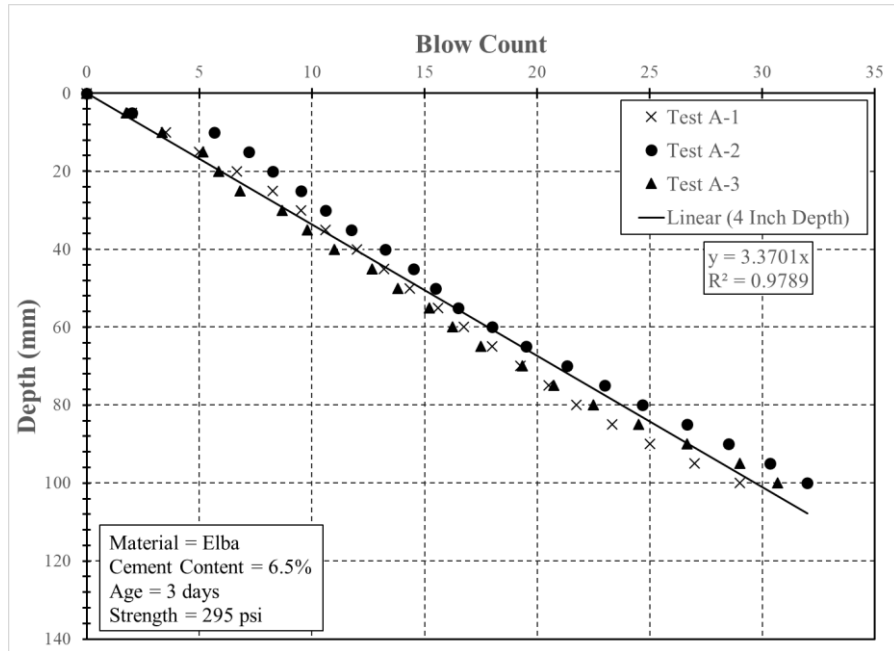


Figure G.21: Elba 6.5% No. 2 3 days

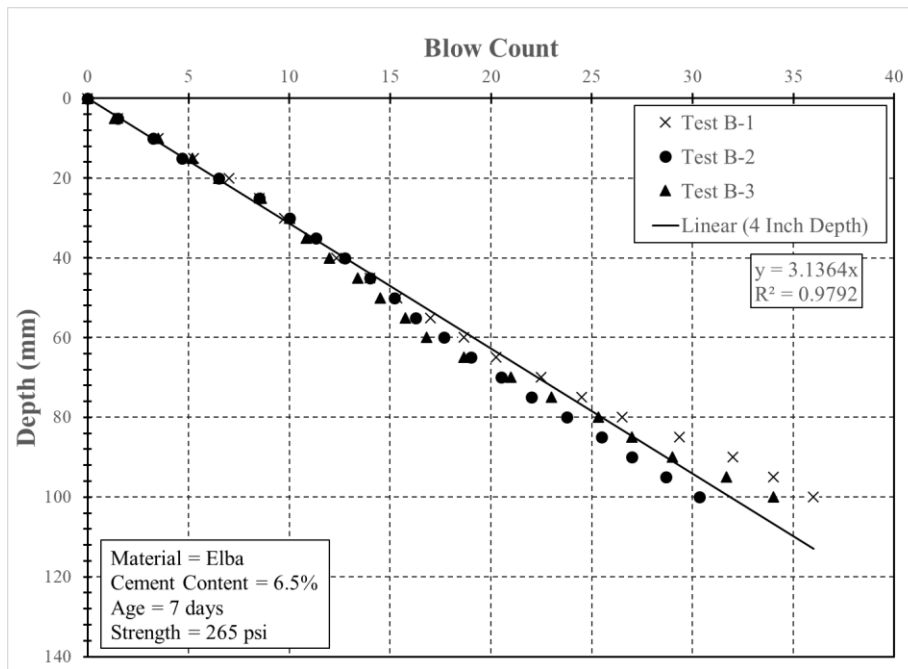


Figure G.22: Elba 6.5% No. 2 7 days

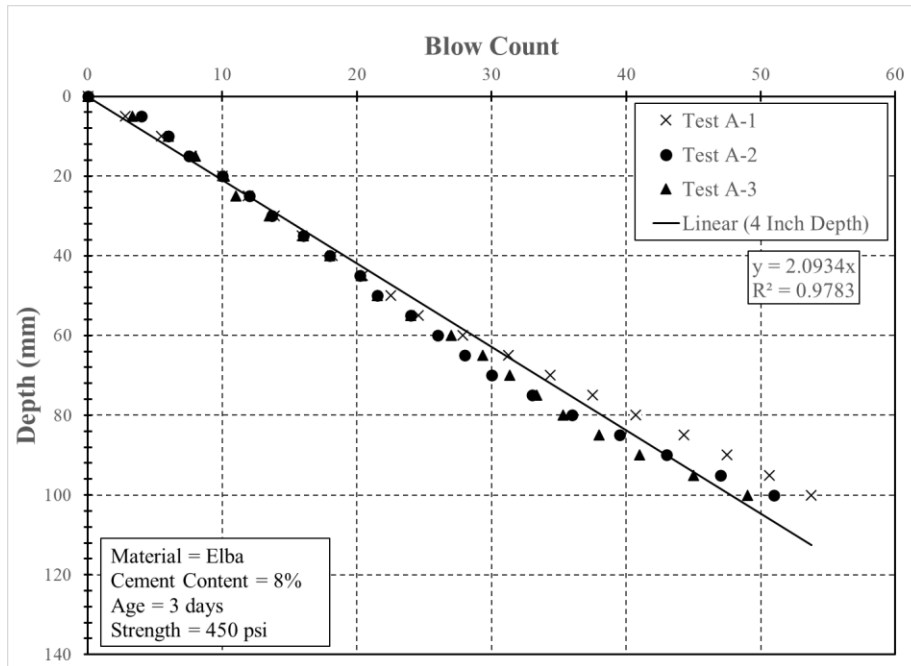


Figure G.23: Elba 8% 3 days

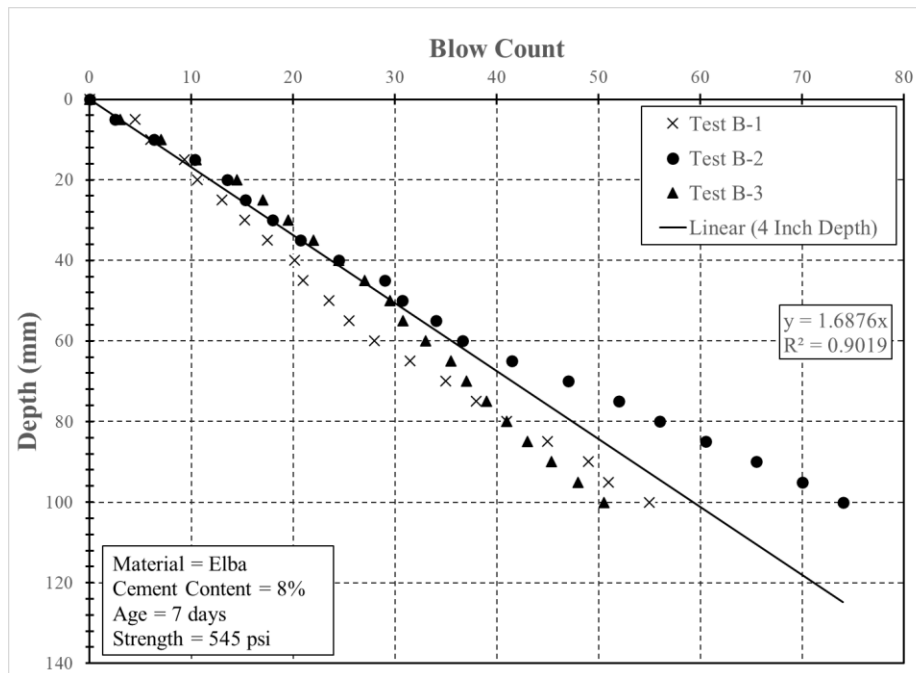


Figure G.24: Elba 8% 7 days

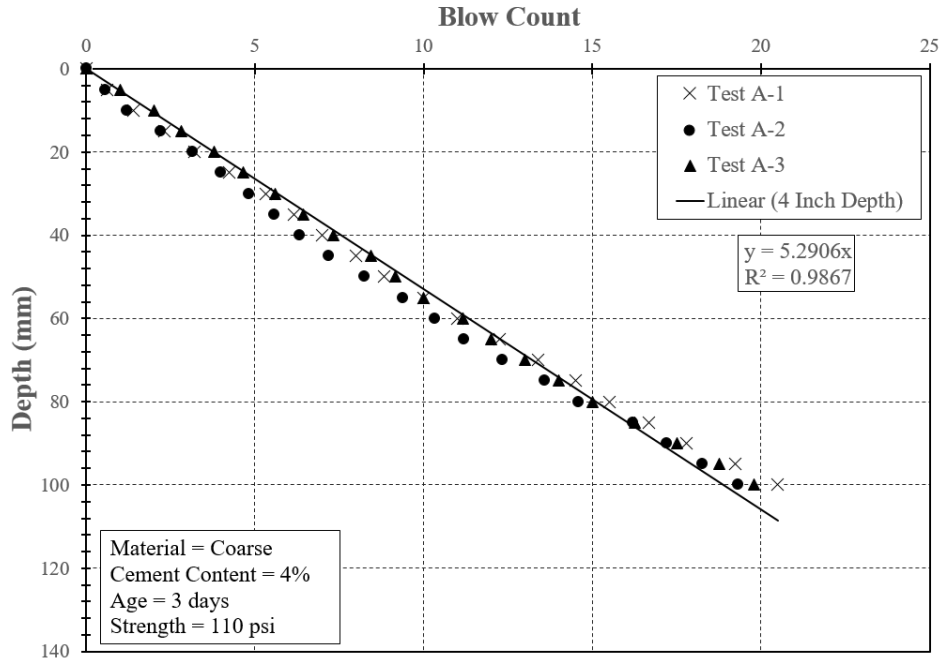


Figure G.25: Coarse 4% No. 1 3 days

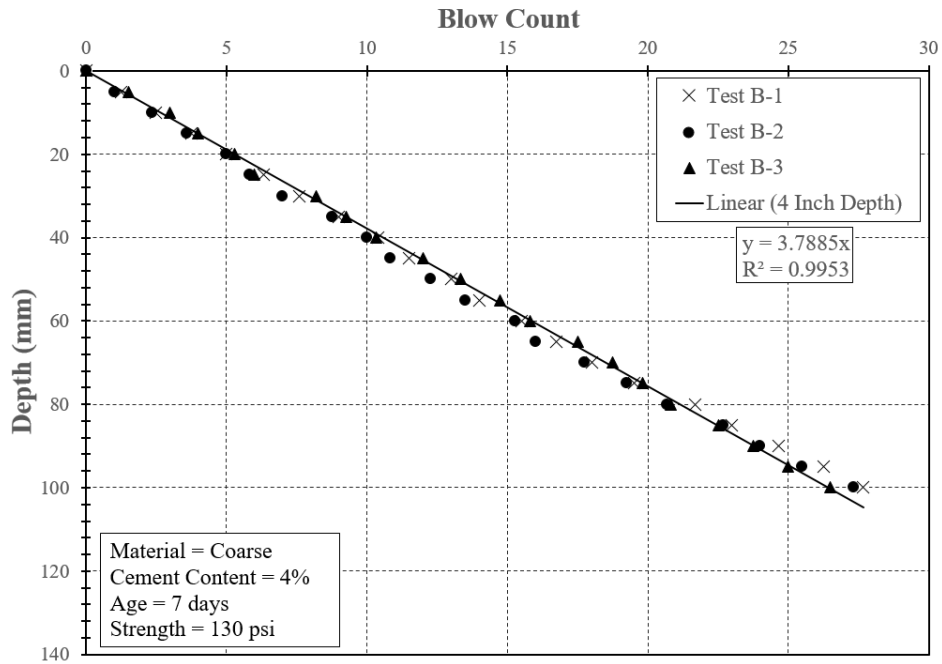


Figure G.26: Coarse 4% No. 1 7 days

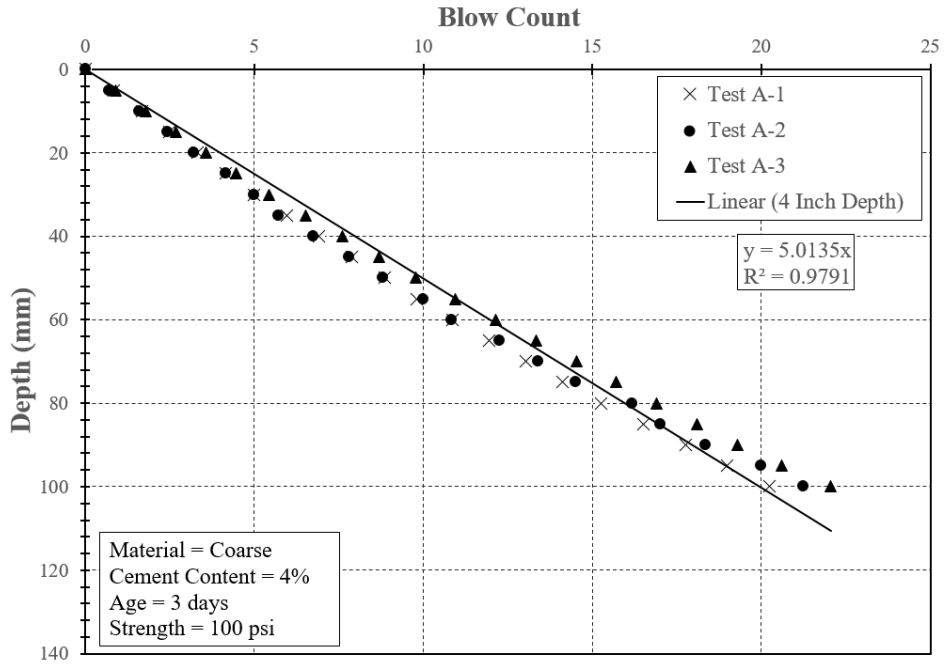


Figure G.27: Coarse 4% No. 2 3 days

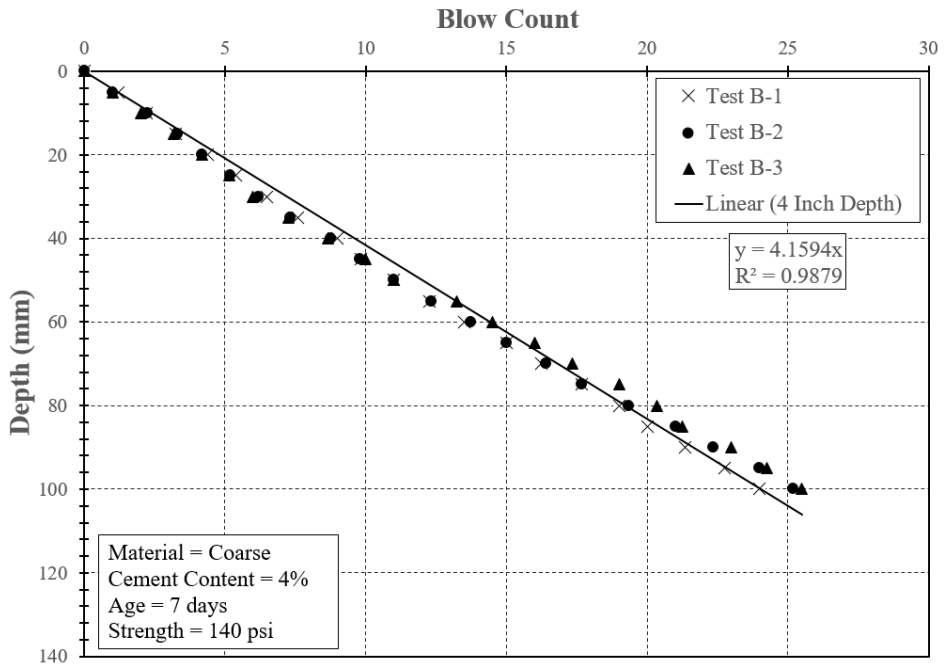


Figure G.28: Coarse 4% No. 2 7 days

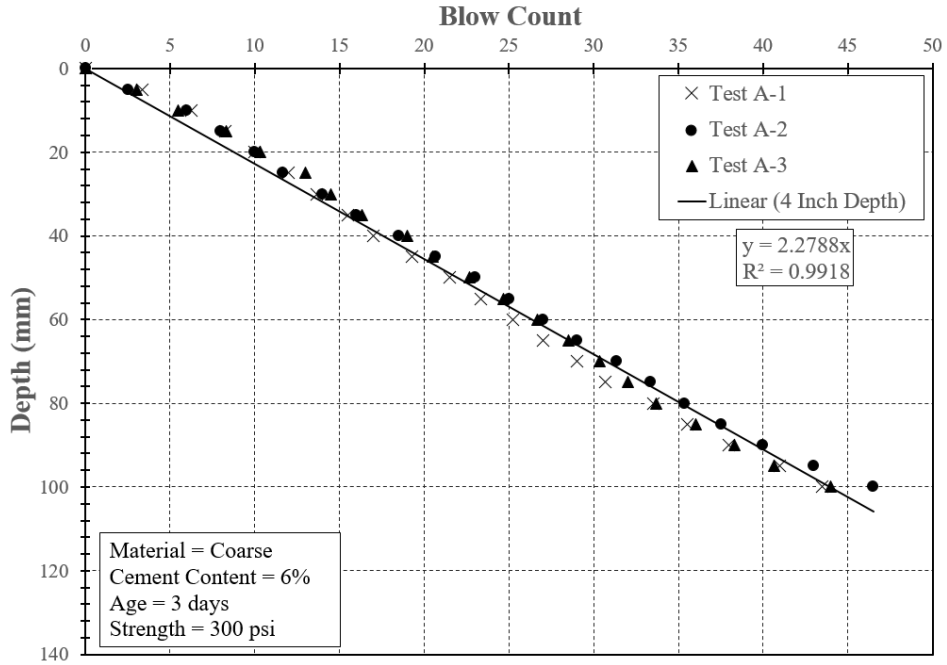


Figure G.29: Coarse 6% No. 1 3 days

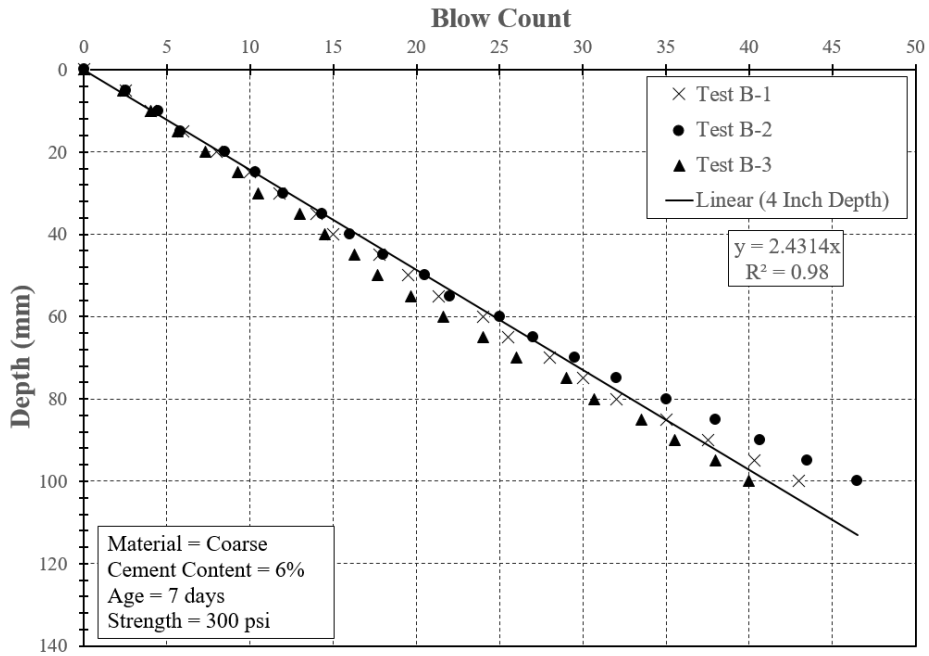


Figure G.30: Coarse 6% No. 1 7 days

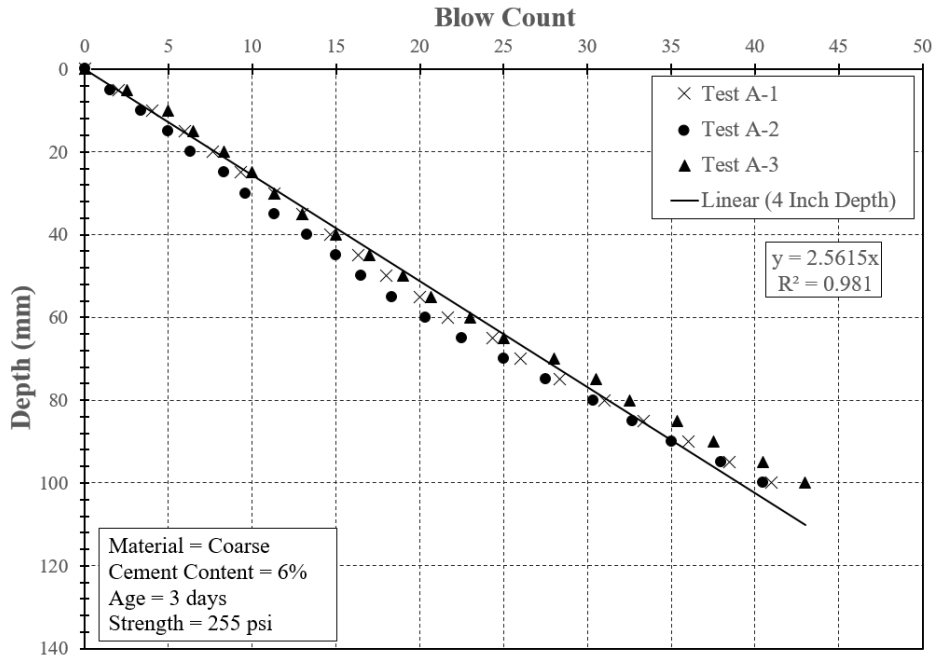


Figure G.31: Coarse 6% No. 2 3 days

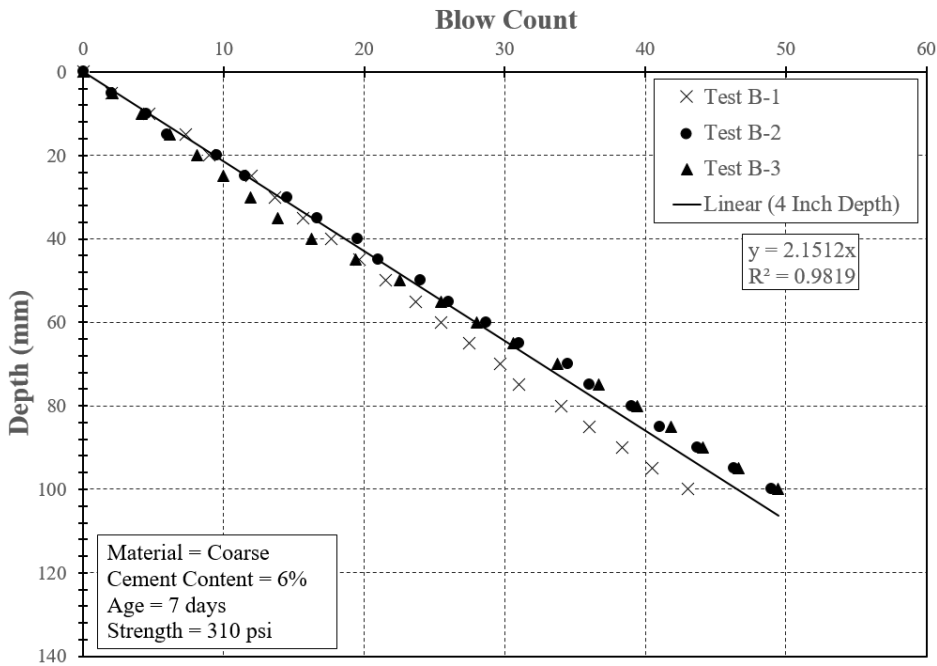


Figure G.32: Coarse 6% No. 2 7 days

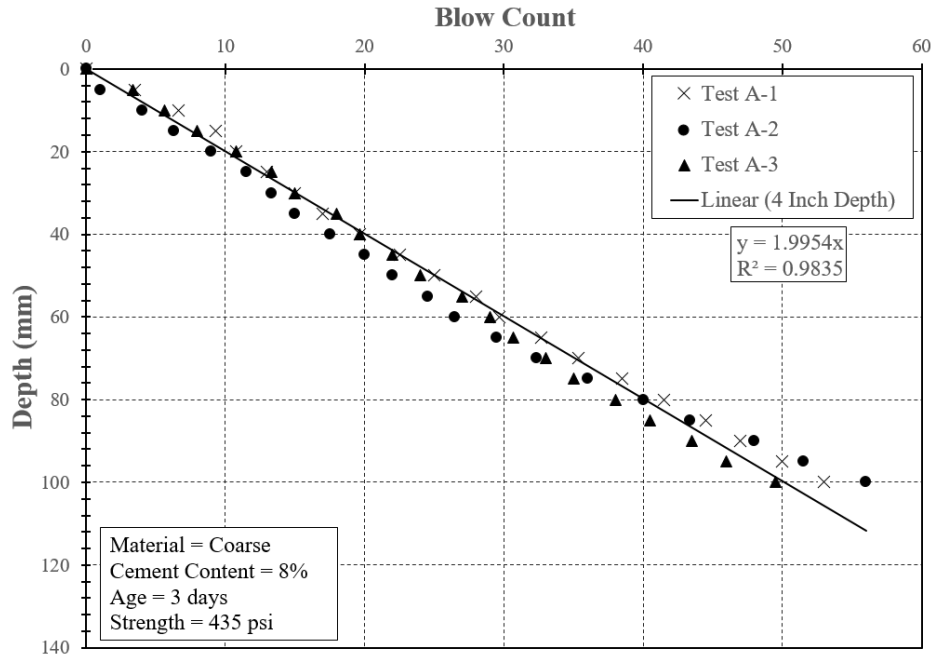


Figure G.33: Coarse 8% No. 1 3 days

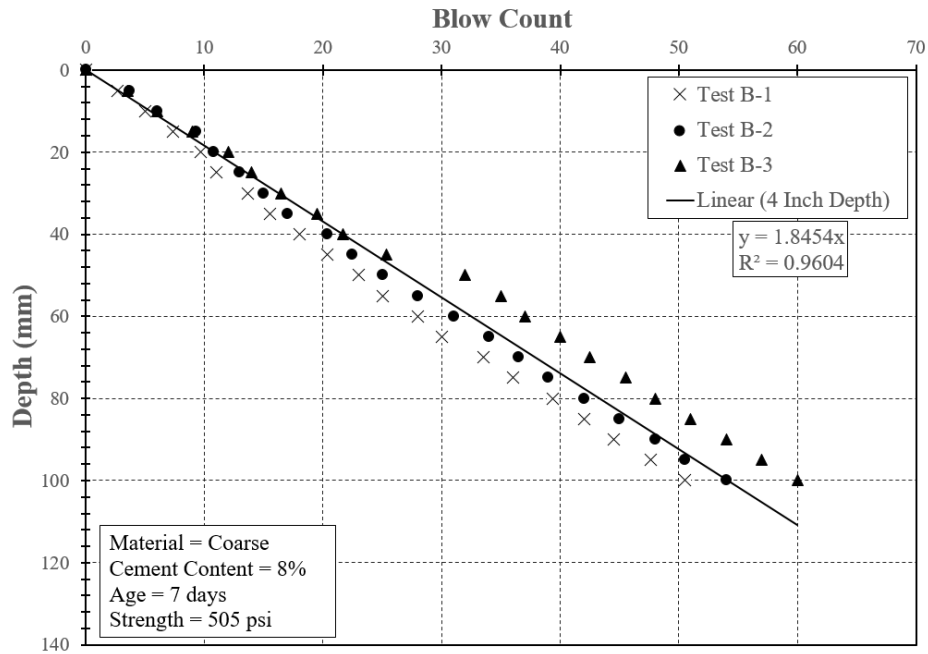


Figure G.34: Coarse 8% No. 1 7 days

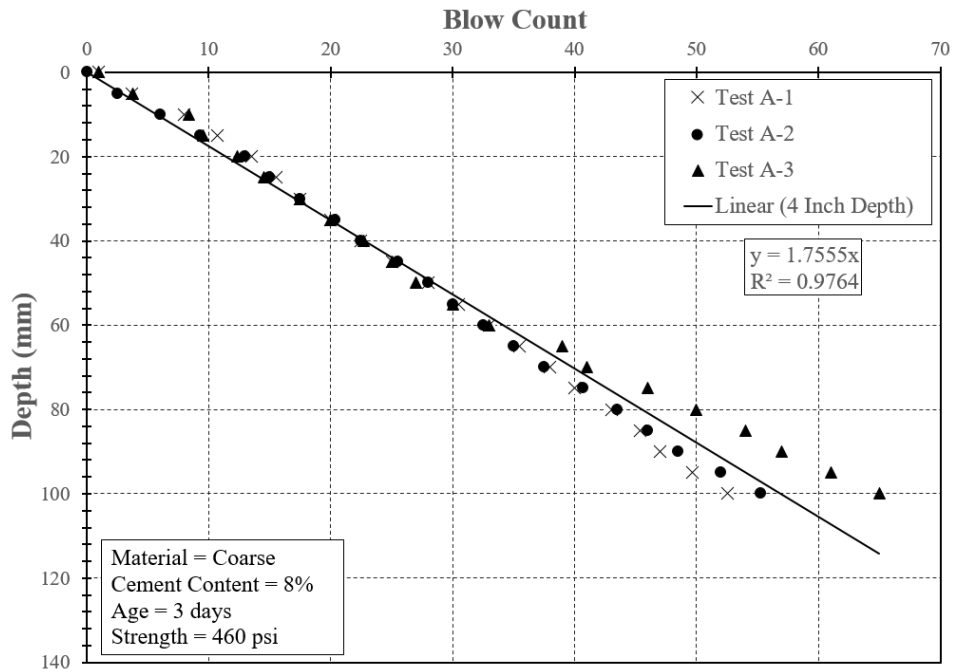


Figure G.35: Coarse 8% No. 2 3 days

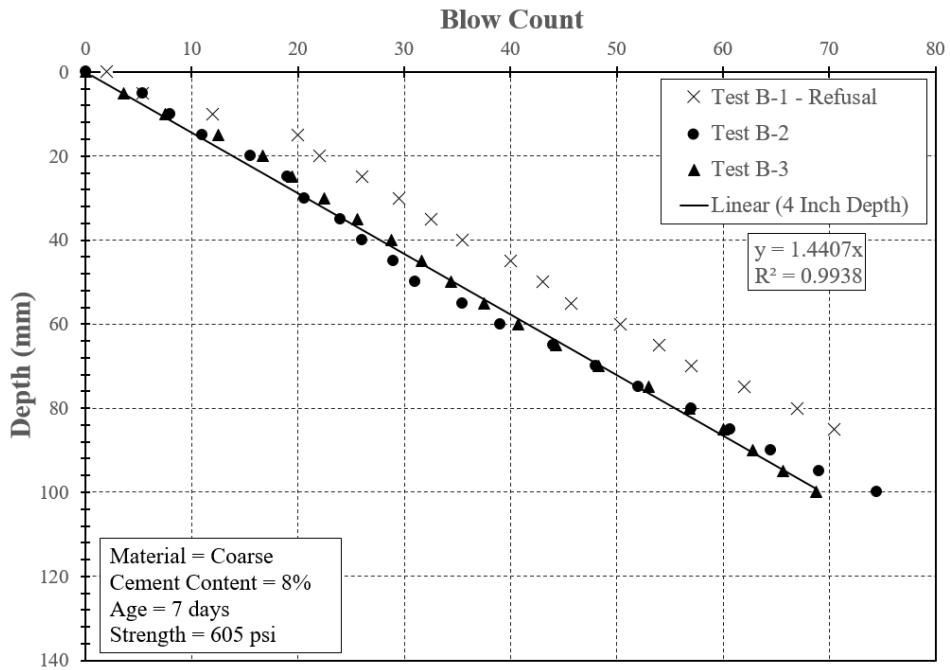


Figure G.36: Coarse 8% No. 2 7 days

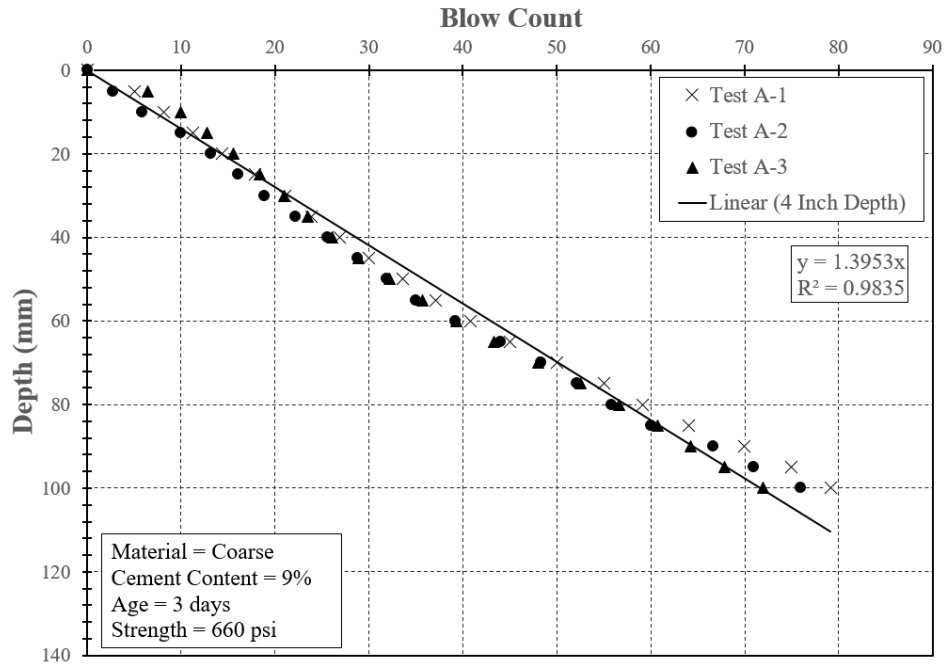


Figure G.37: Coarse 9% 3 days

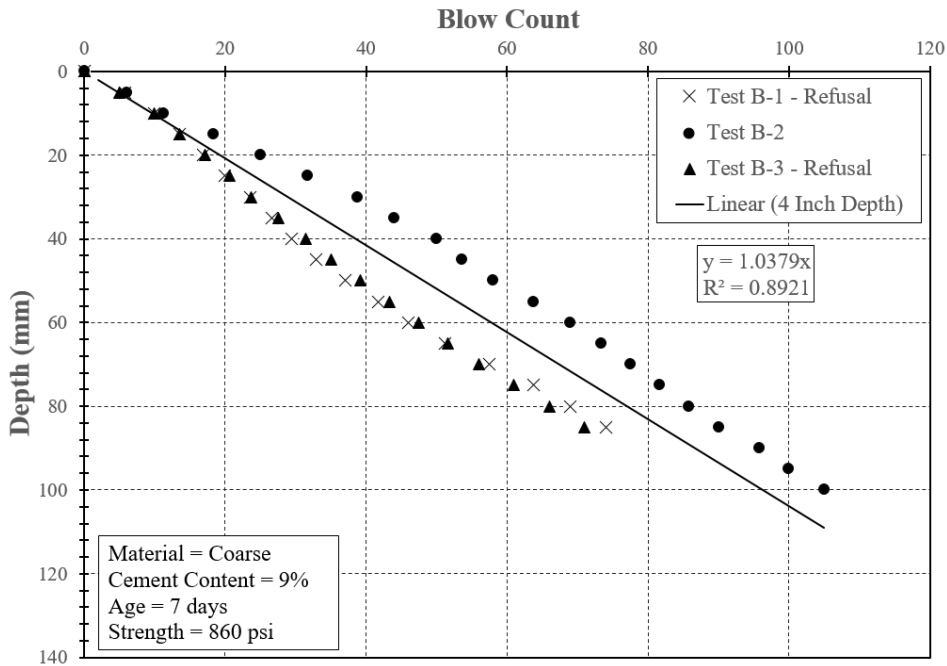


Figure G.38: Coarse 9% 7 days

Appendix H

Full Depth Penetration Data

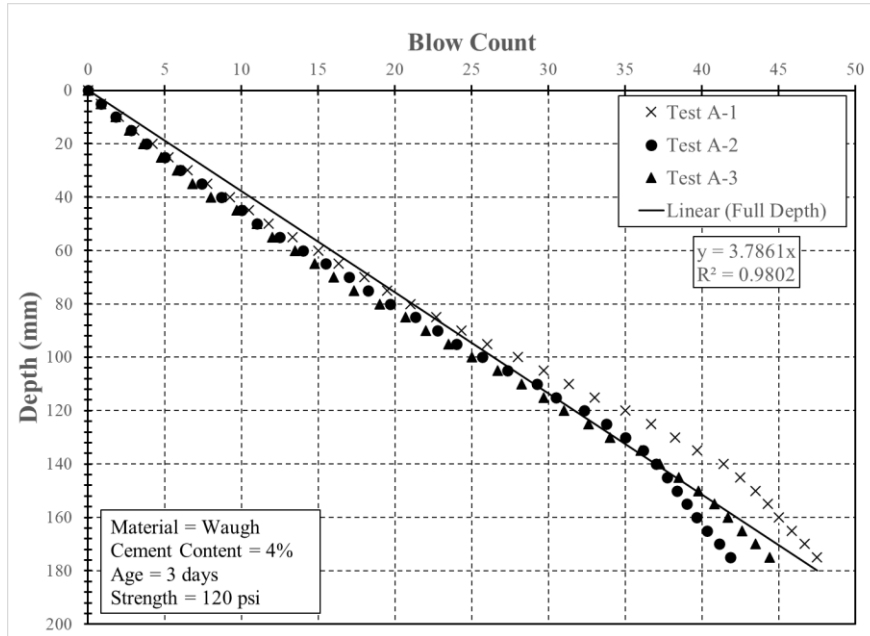


Figure H.1: Waugh 4% No. 1 3 days

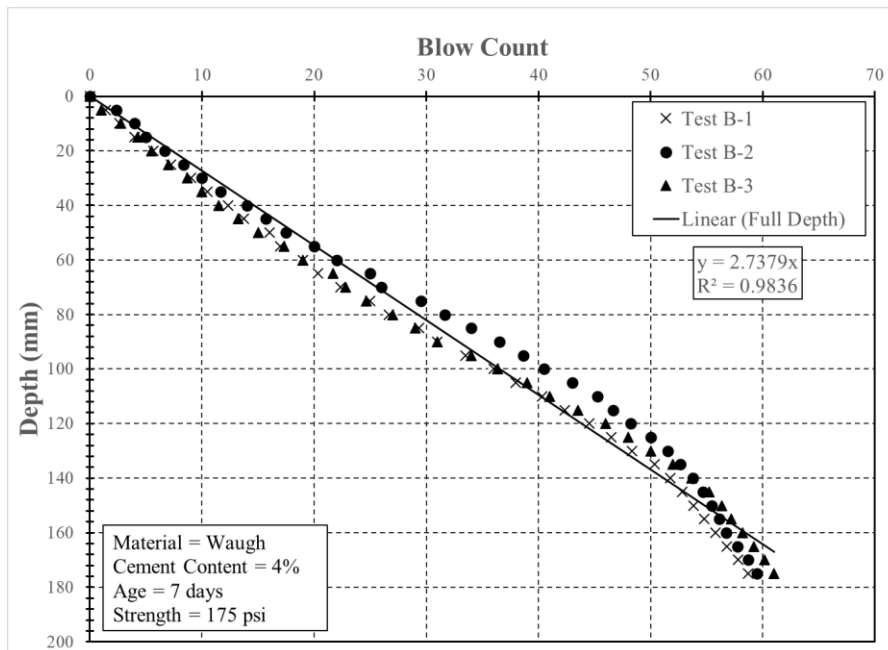


Figure H.2: Waugh 4% No. 1 7 days

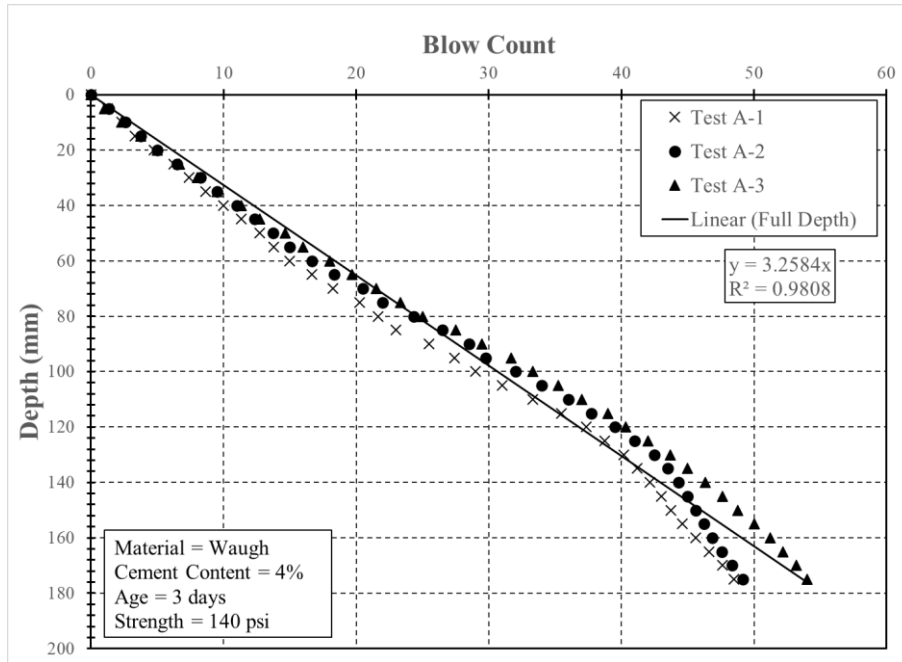


Figure H.3: Waugh 4% No. 2 3 days

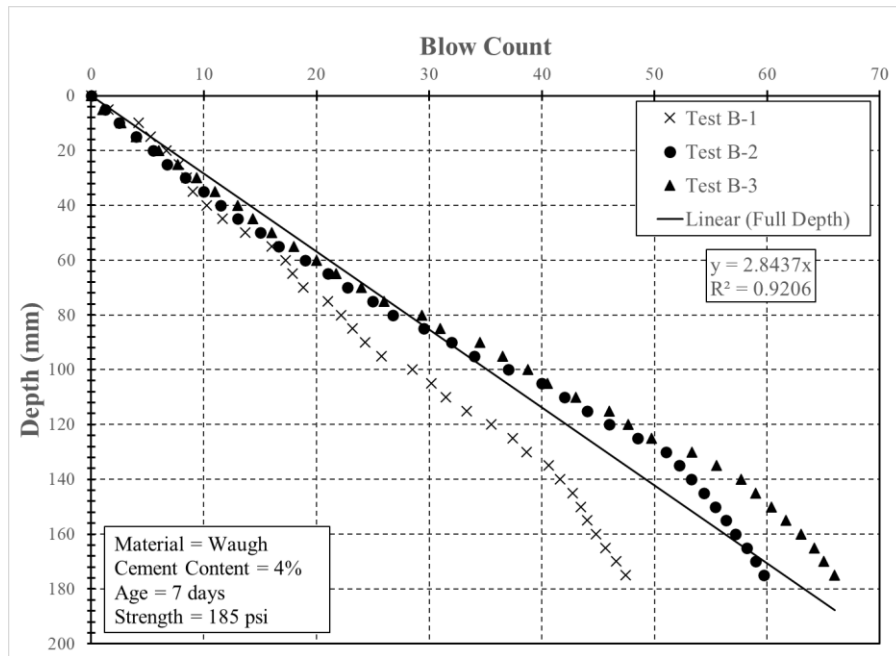


Figure H.4: Waugh 4% No. 2 7 days

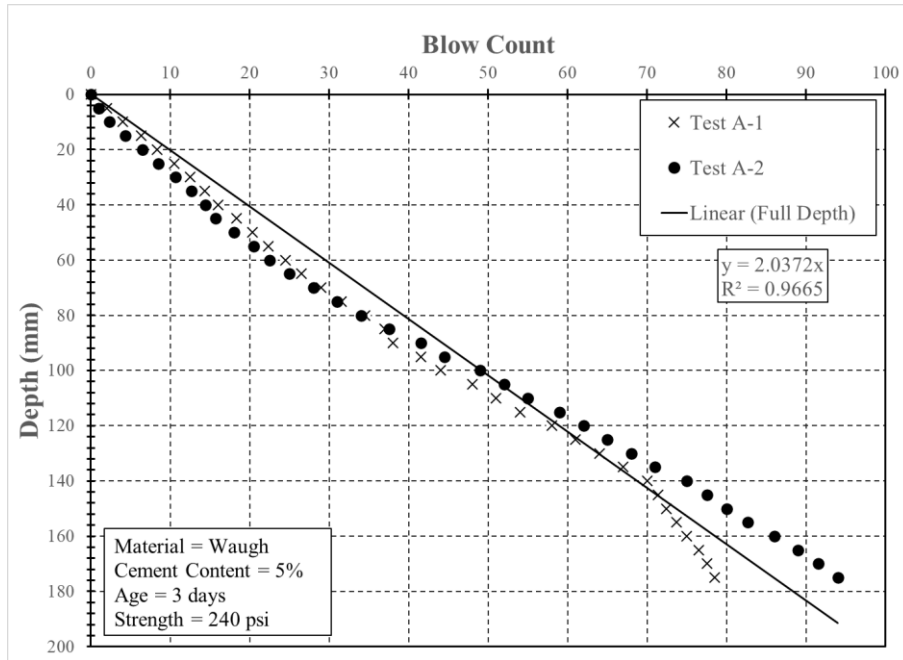


Figure H.5: Waugh 5% No. 1 3 days (Third specimen was removed due to error)

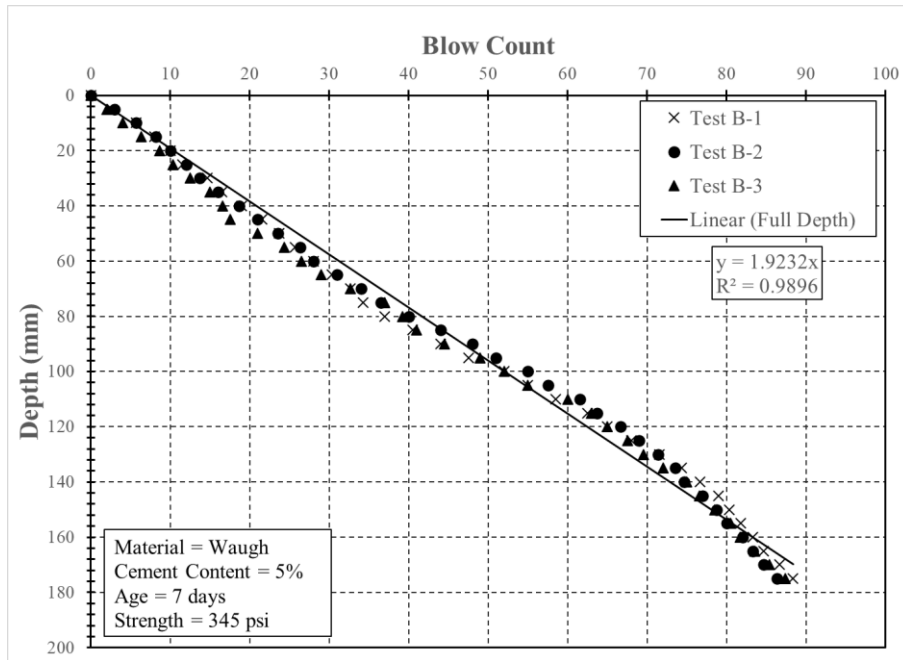


Figure H.6: Waugh 5% No. 1 7 days

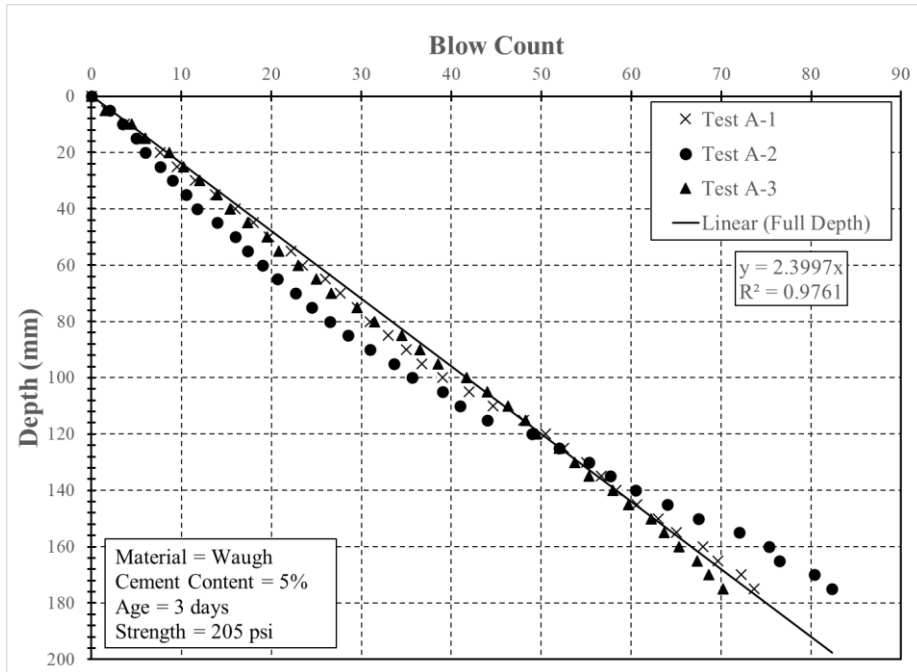


Figure H.7: Waugh 5% No. 2 3 days

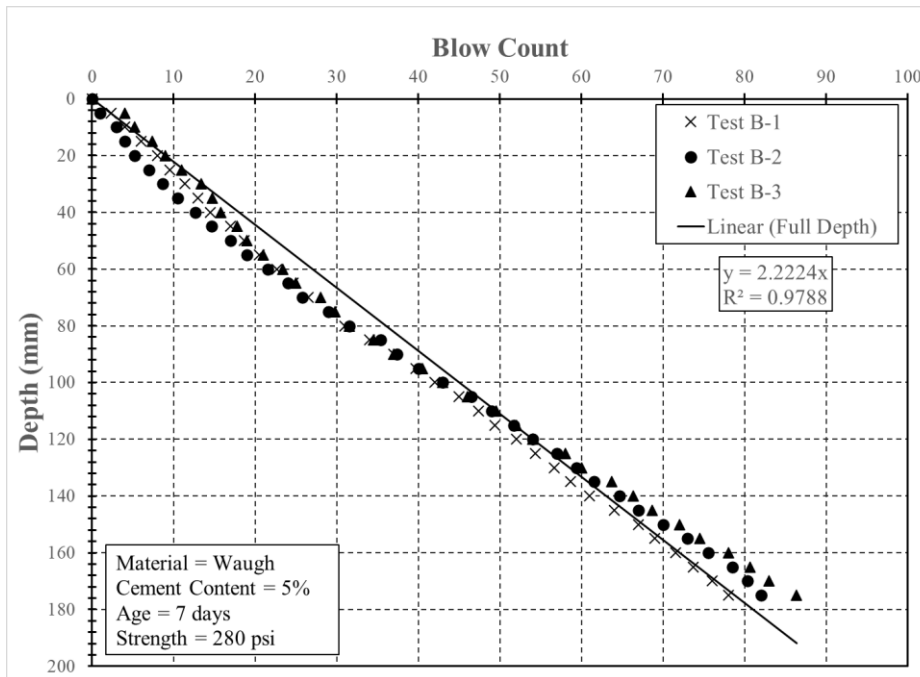


Figure H.8: Waugh 5% No. 2 7 days

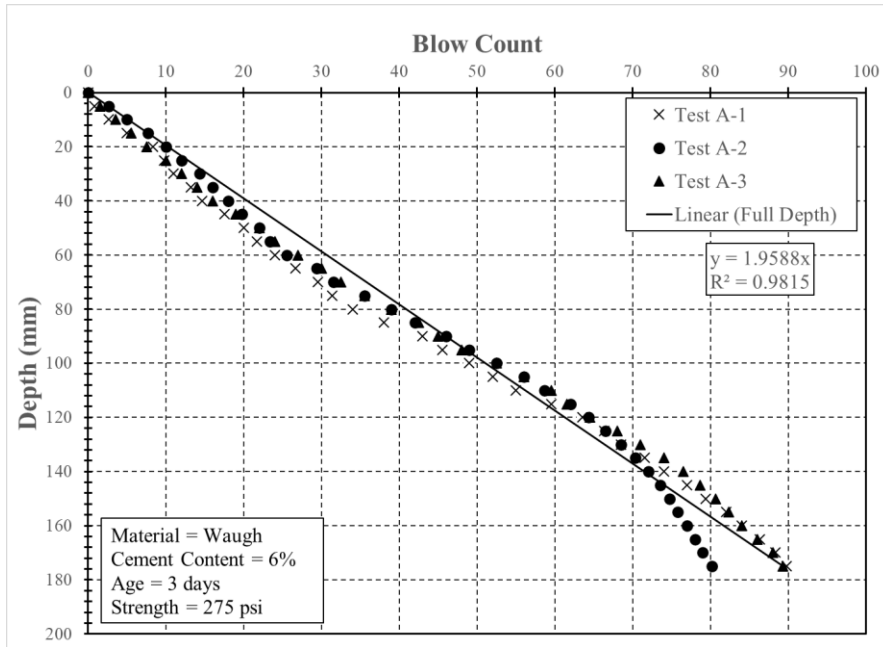


Figure H.9: Waugh 6% 3 day

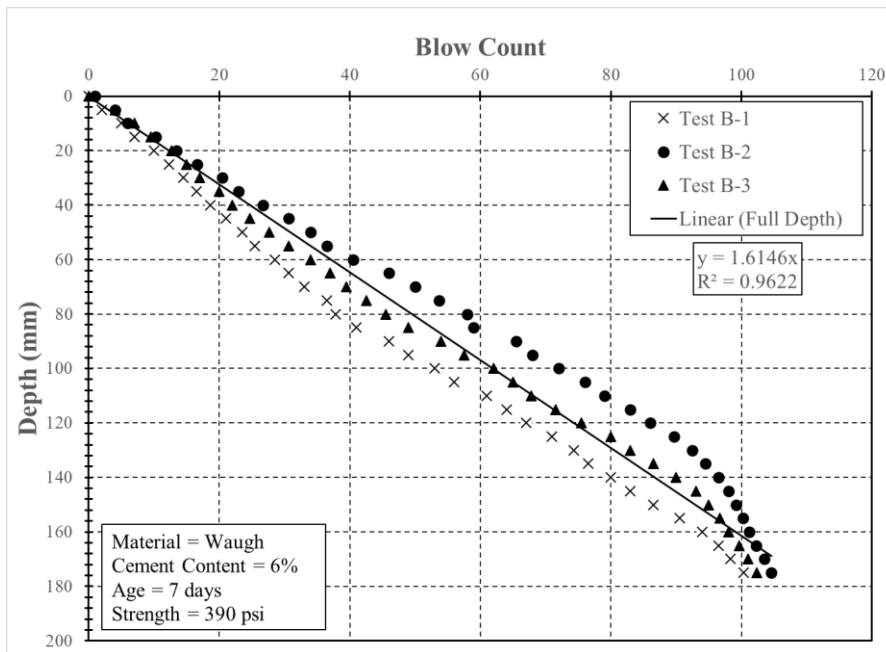


Figure H.10: Waugh 6% 7 day

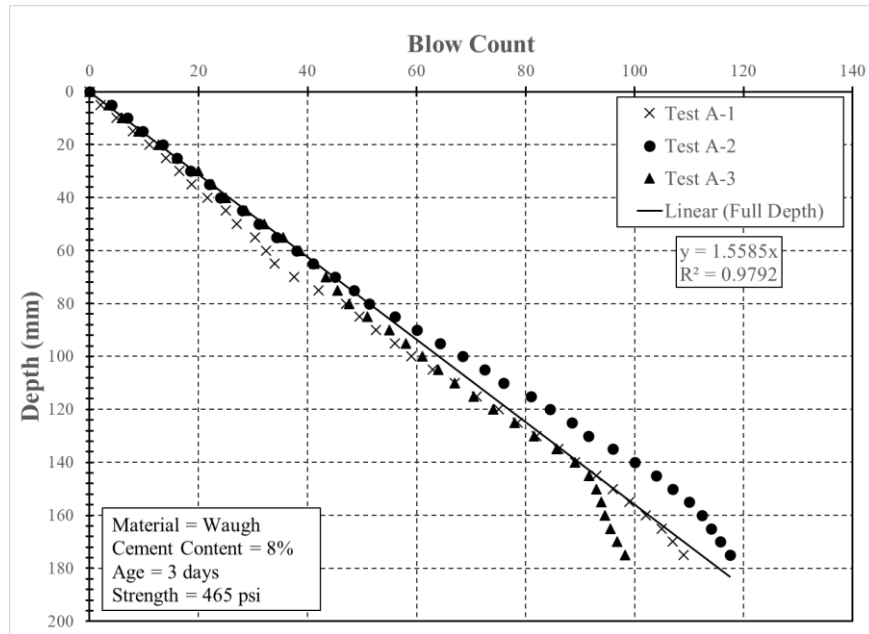


Figure H.11: Waugh 8% No. 1 3 days

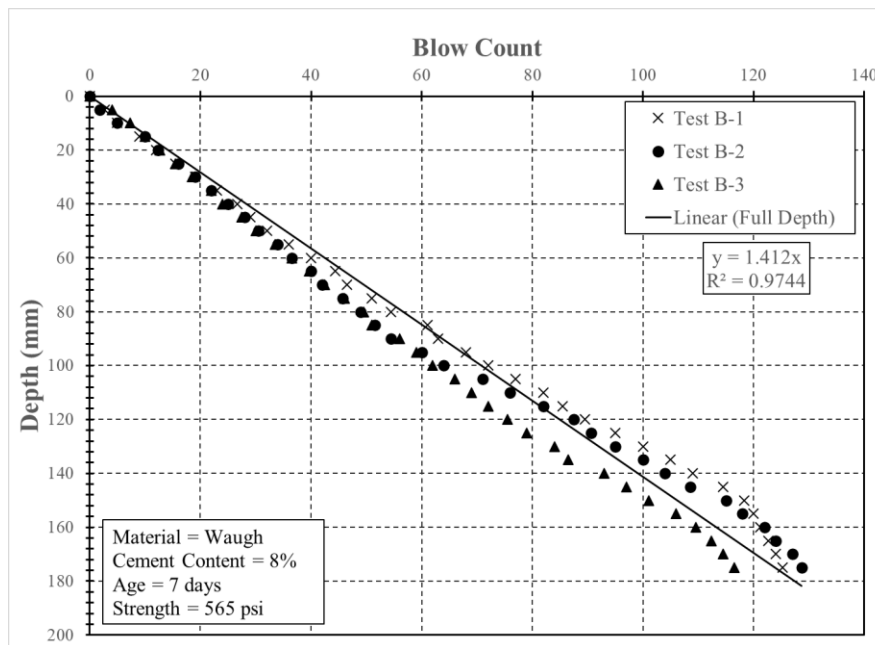


Figure H.12: Waugh 8% No. 1 7 days

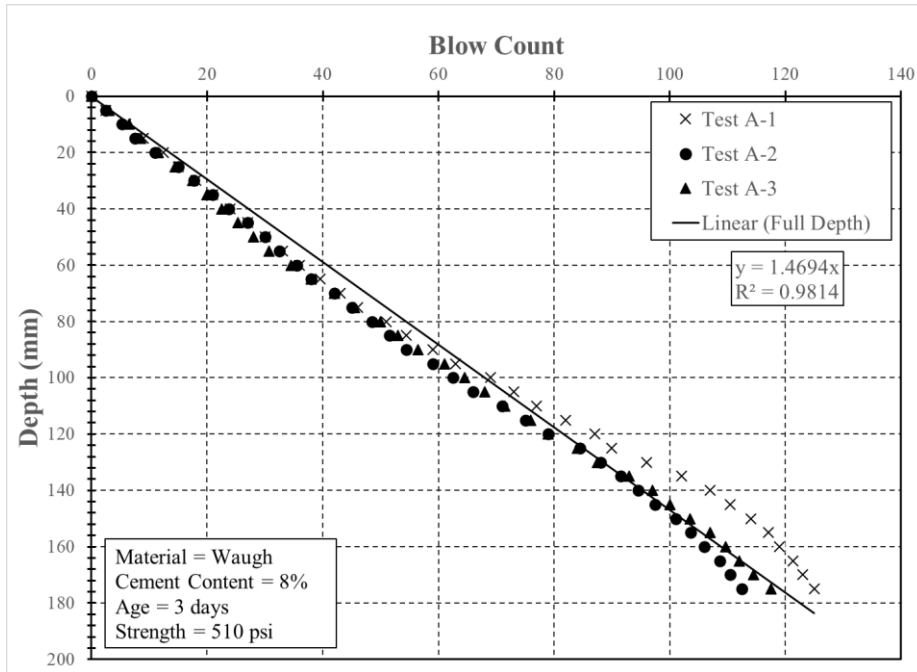


Figure H.13: Waugh 8% No. 2 3 days

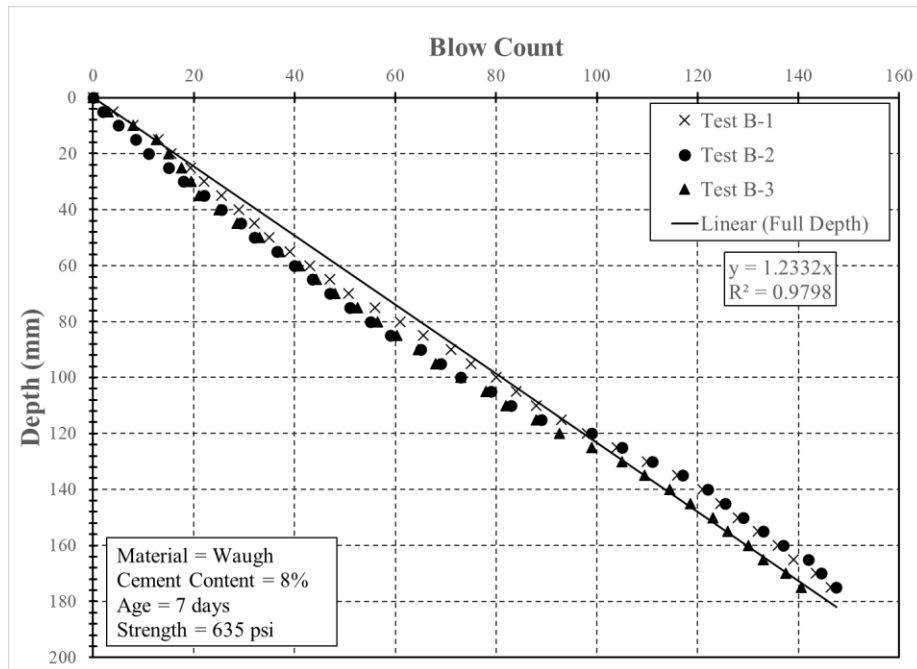


Figure H.14: Waugh 8% No. 2 7 days

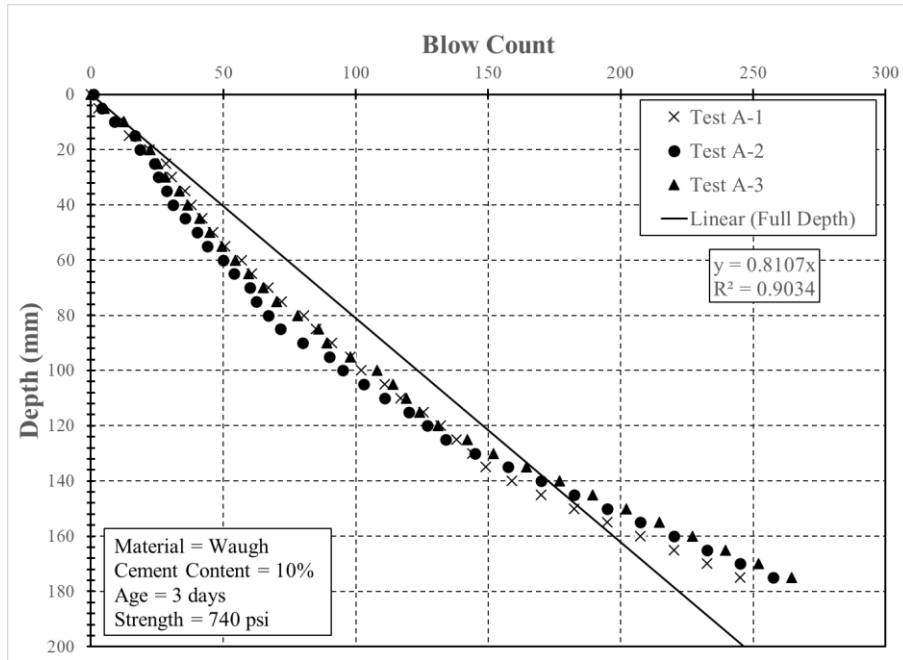


Figure H.15: Waugh 10% 3 days

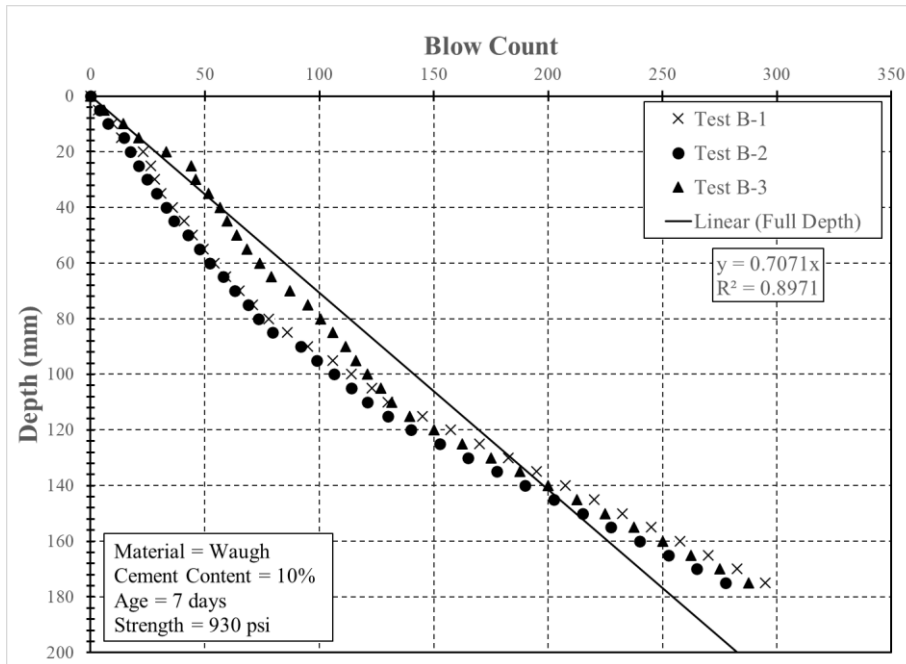


Figure H.16: Waugh 10% 7 days

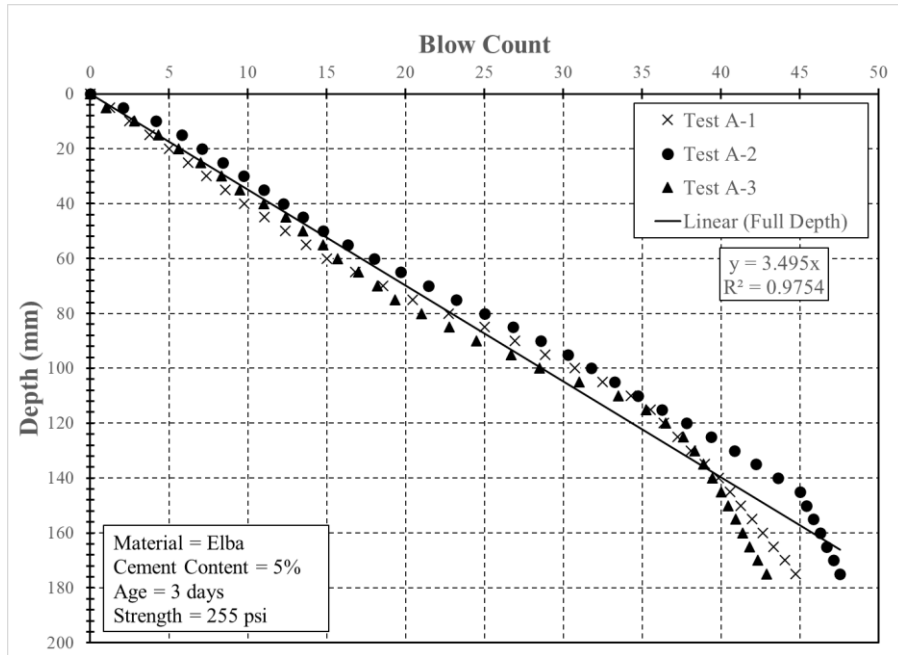


Figure H.17: Elba 5% 3 days

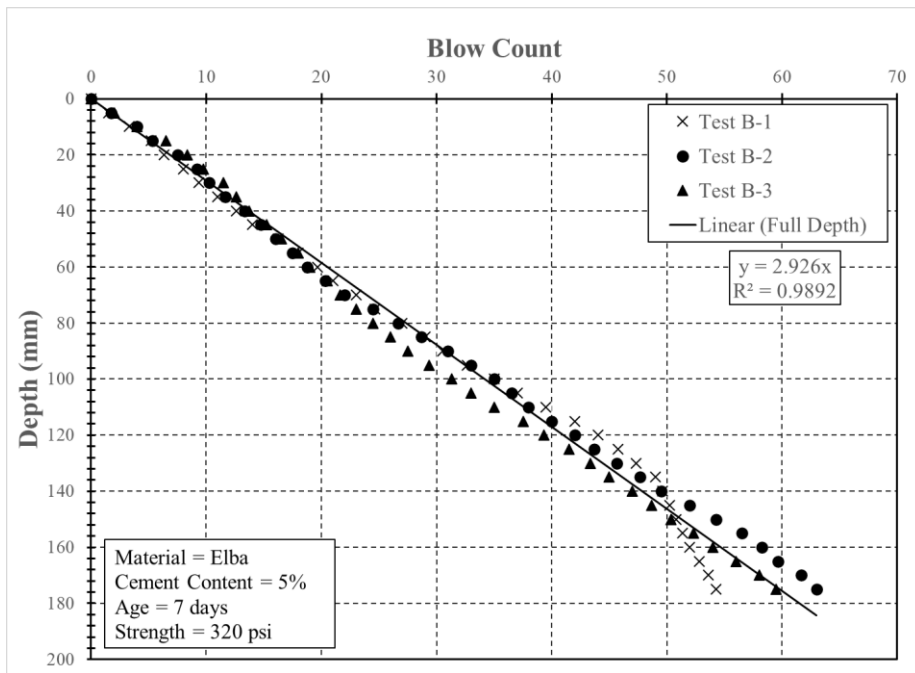


Figure H.18: Elba 5% 7 days

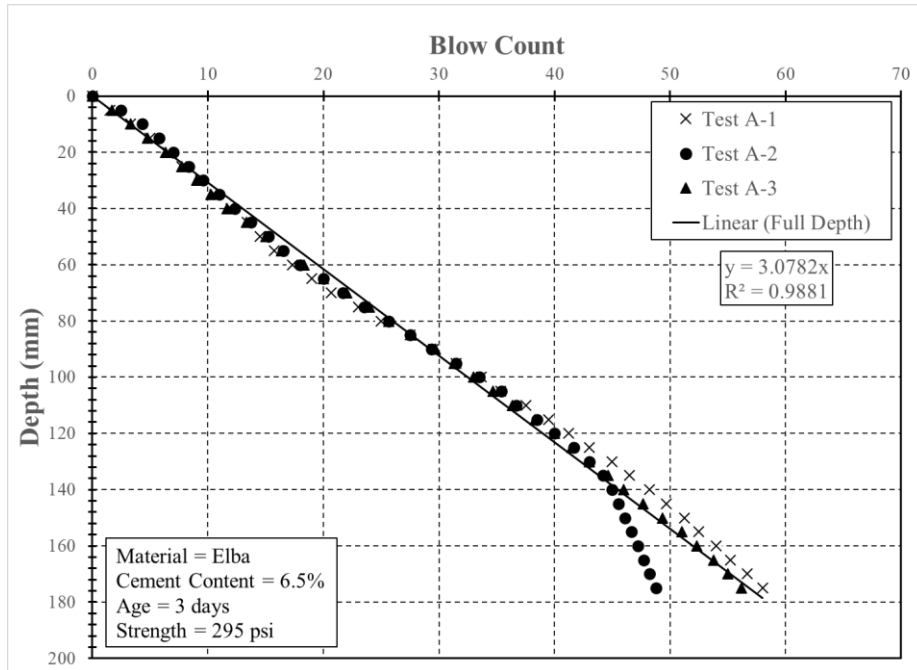


Figure H.19: Elba 6.5% No. 1 3 days

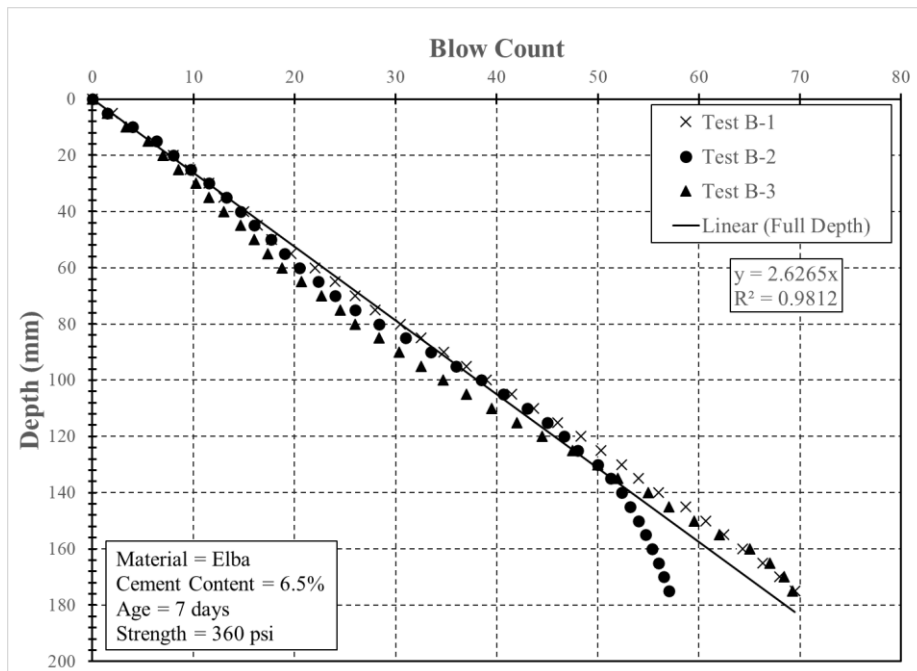


Figure H.20: Elba 6.5% No. 1 7 days

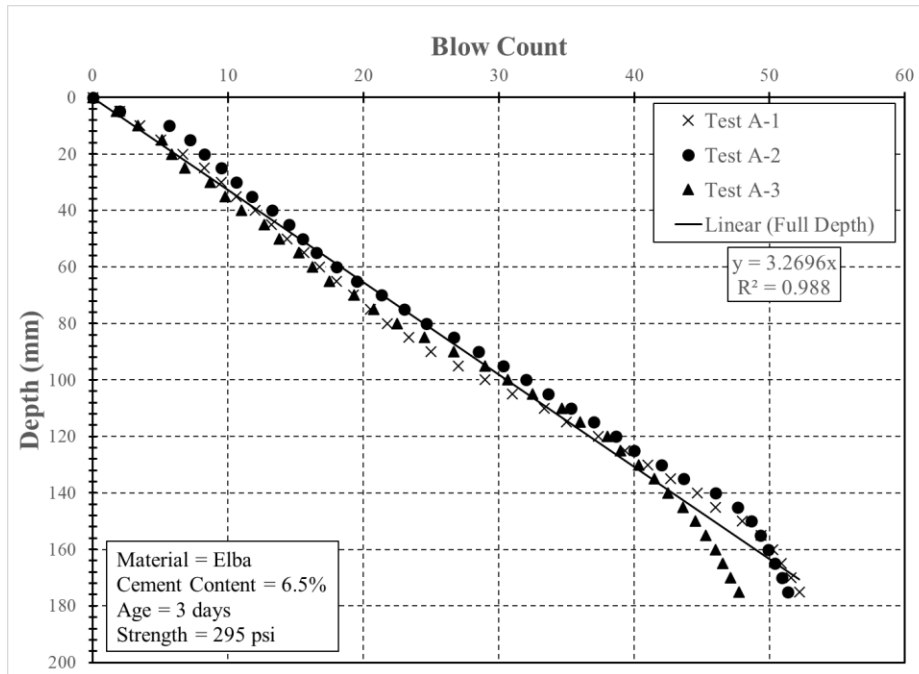


Figure H.21: Elba 6.5% No. 2 3 days

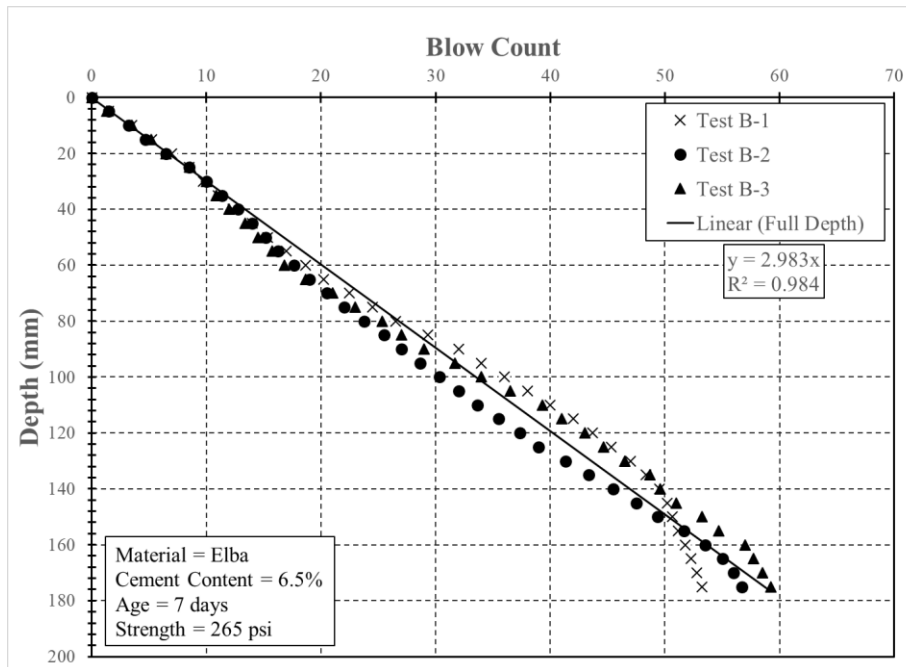


Figure H.22: Elba 6.5% No. 2 7 days

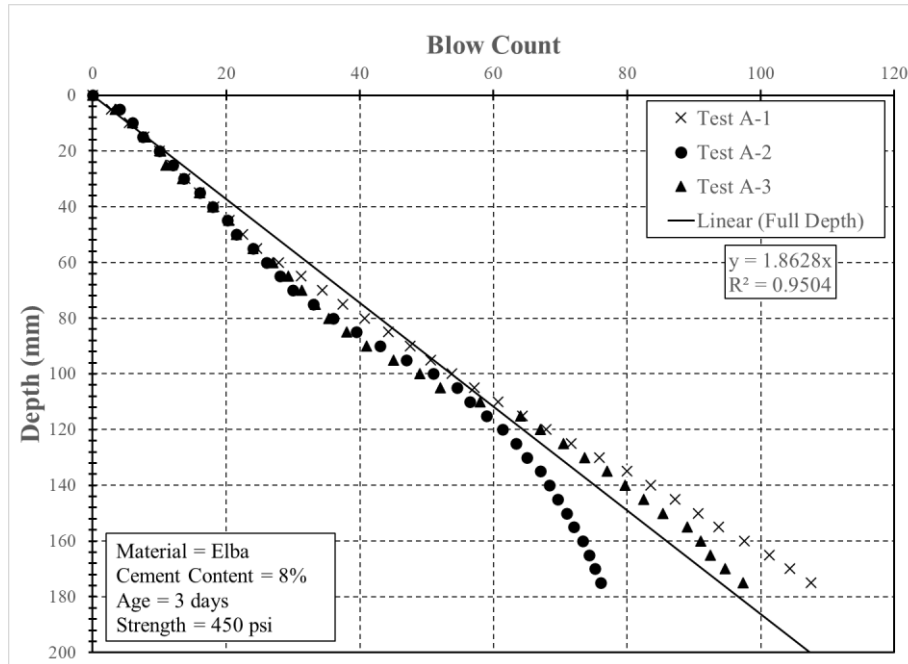


Figure H.23: Elba 8% 3 days

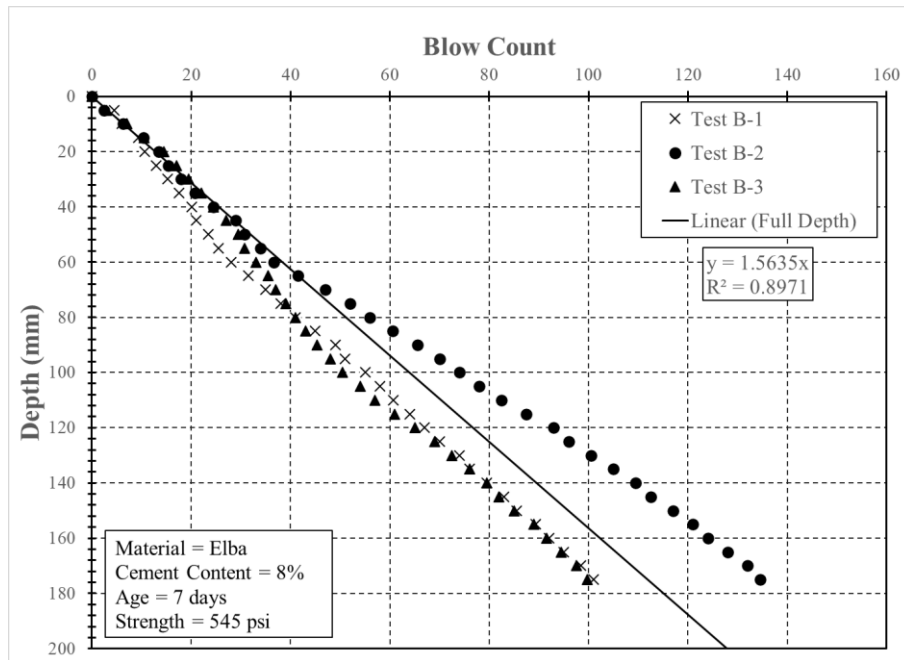


Figure H.24: Elba 8% 7 days

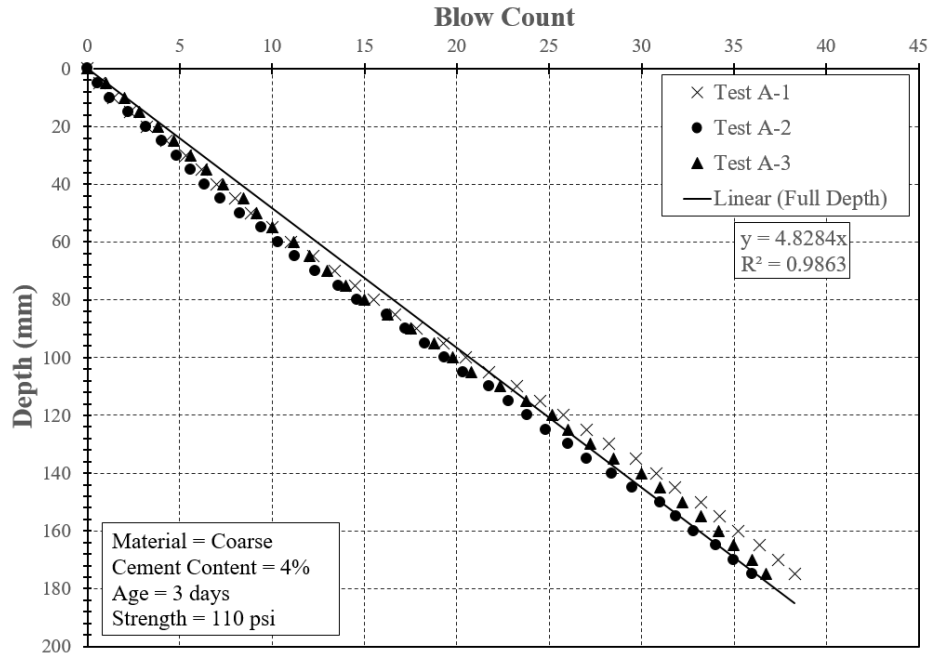


Figure H.25: Coarse 4% No. 1 3 days

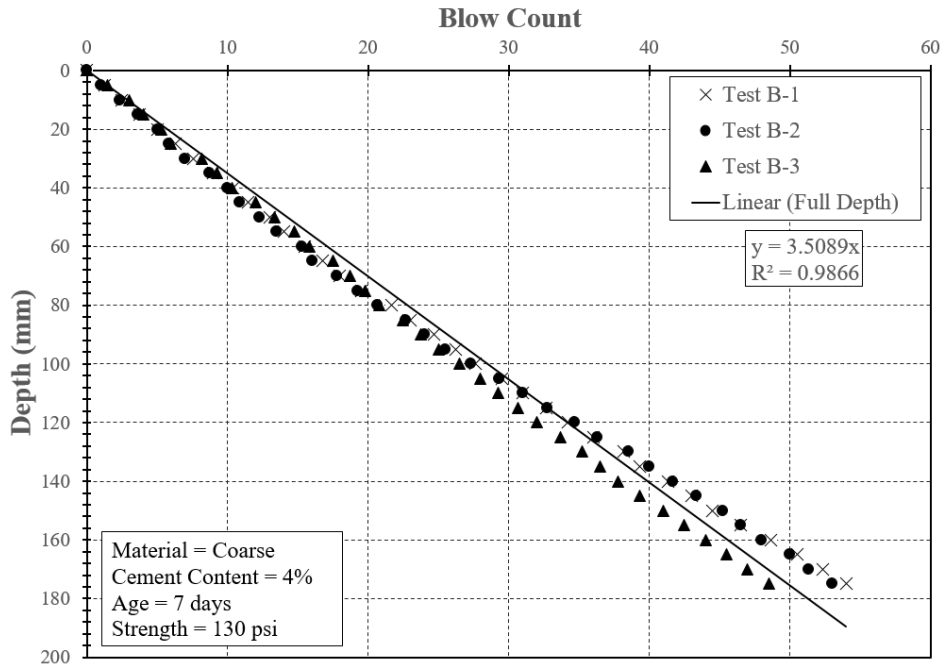


Figure H.26: Coarse 4% No. 1 7 days

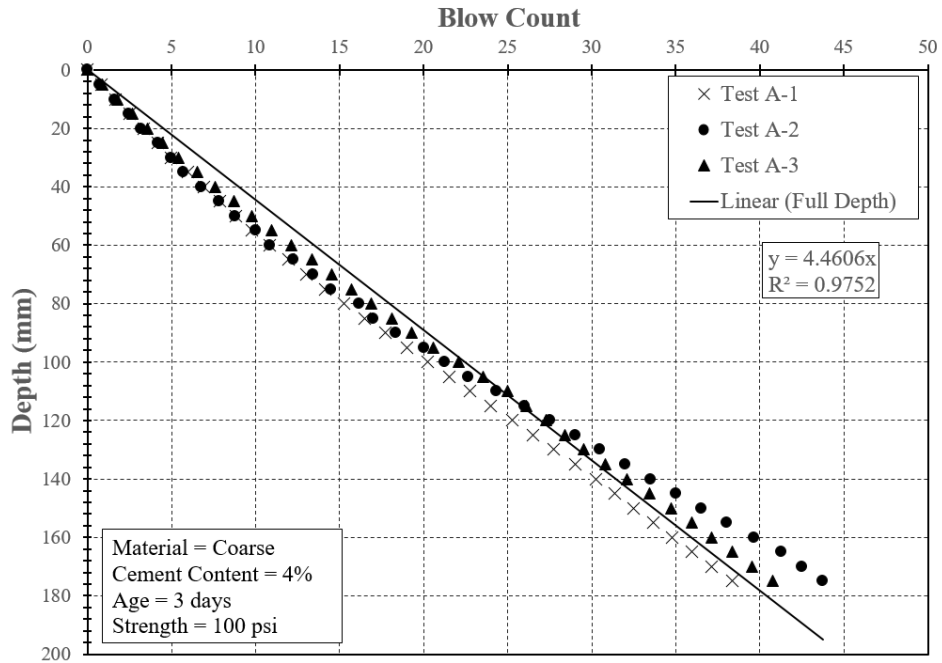


Figure H.27: Coarse 4% No. 2 3 days

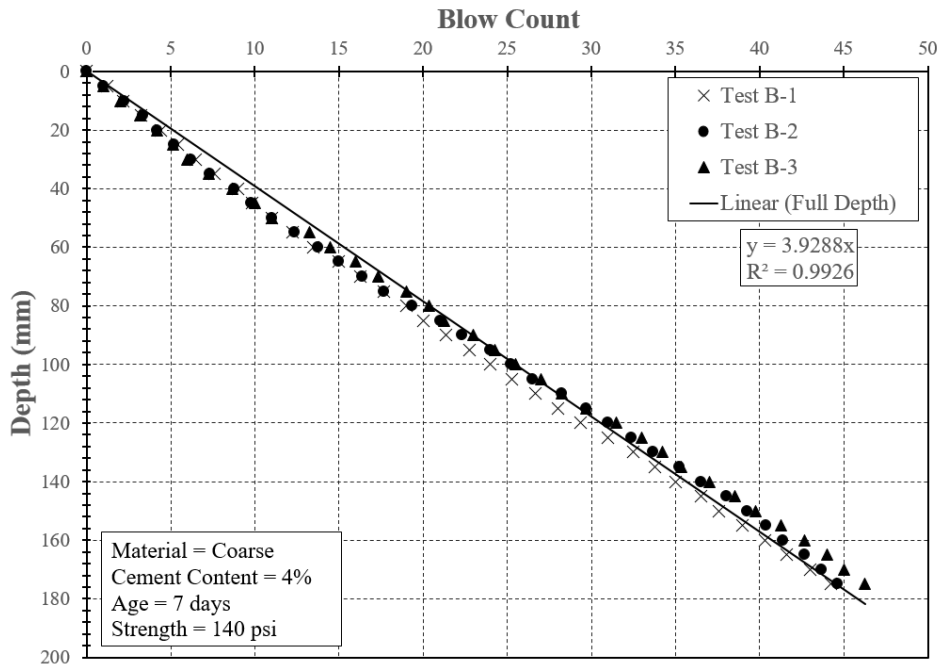


Figure H.28: Coarse 4% No. 2 7 days

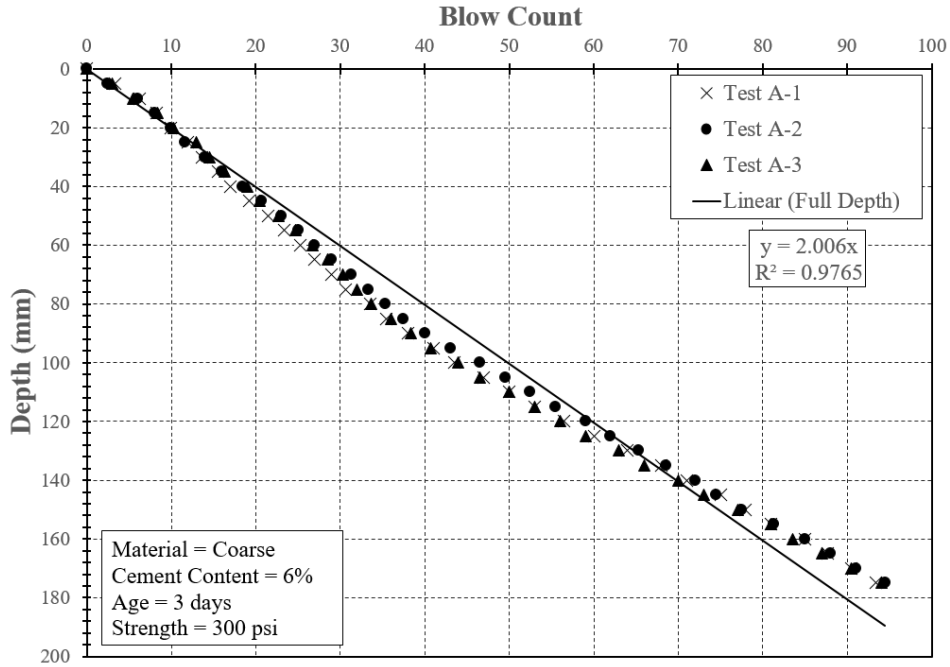


Figure H.29: Coarse 6% No. 1 3 days

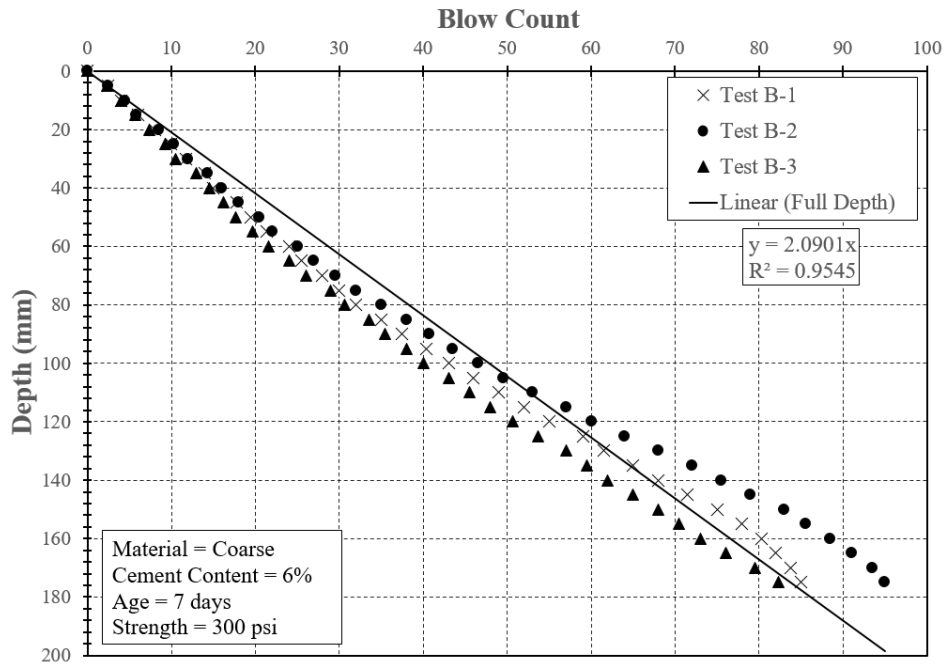


Figure H.30: Coarse 6% No. 1 7 days

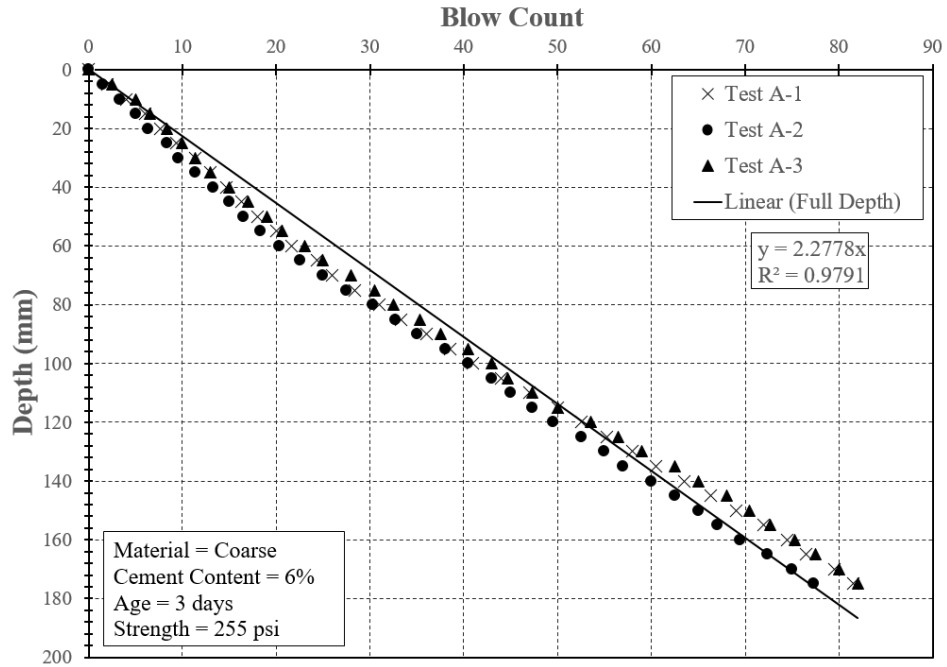


Figure H.31: Coarse 6% No. 2 3 days

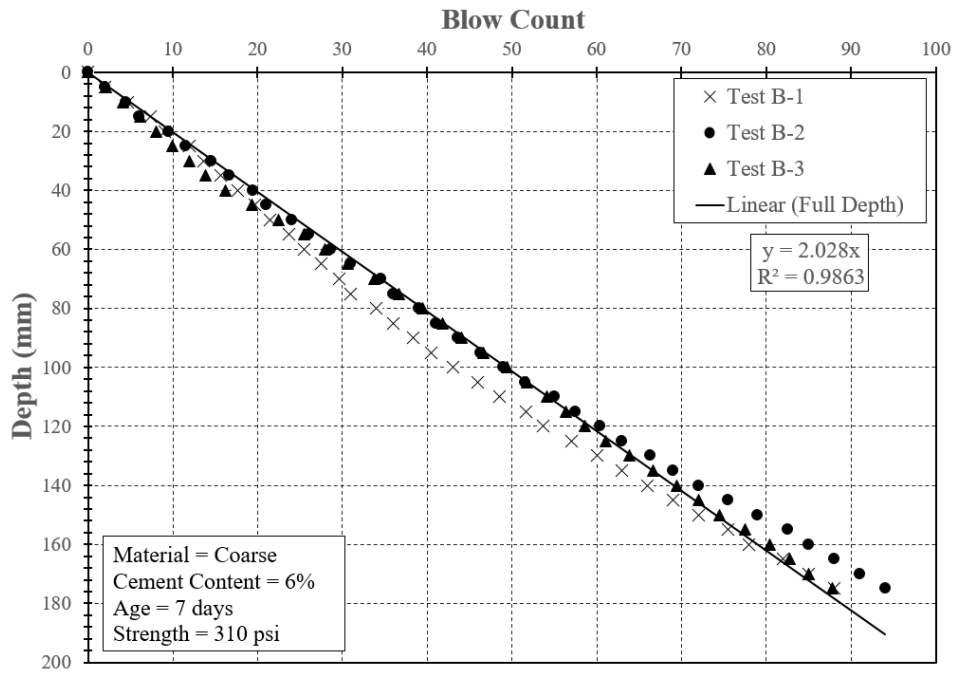


Figure H.32: Coarse 6% No. 2 7 days

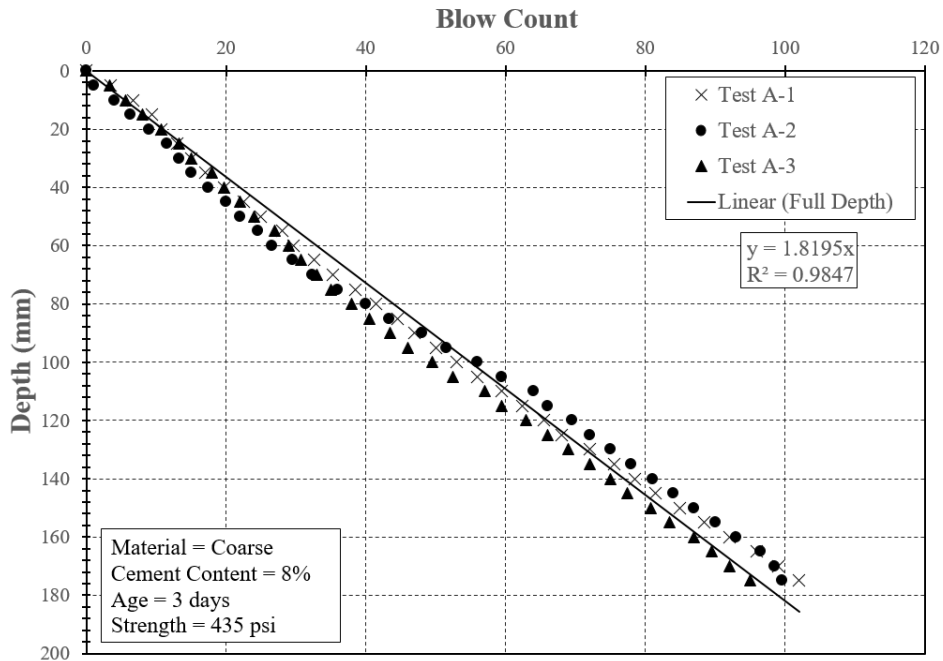


Figure H.33: Coarse 8% No. 1 3 days

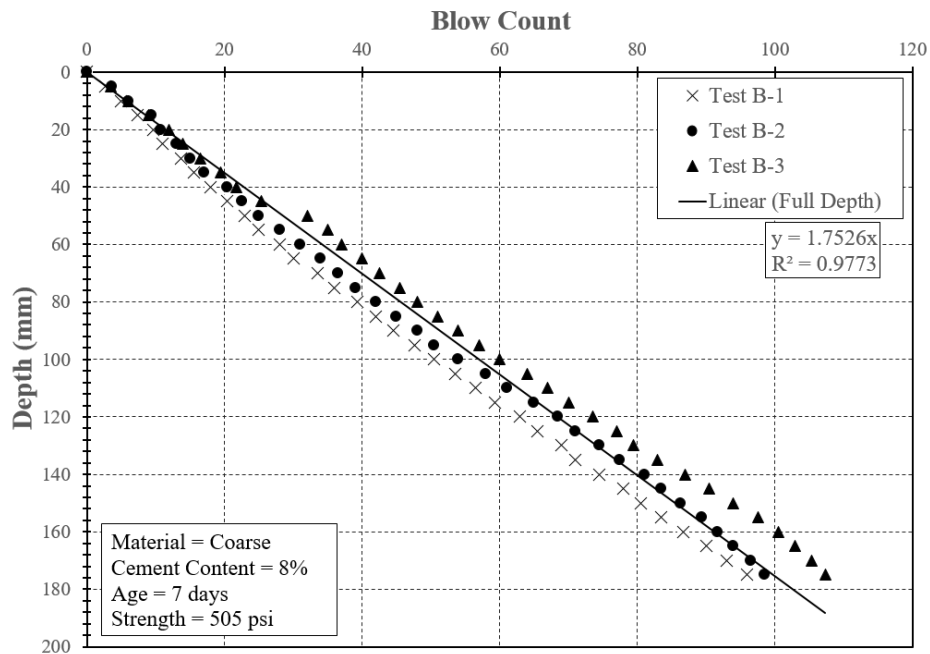


Figure H.34: Coarse 8% No. 1 7 days

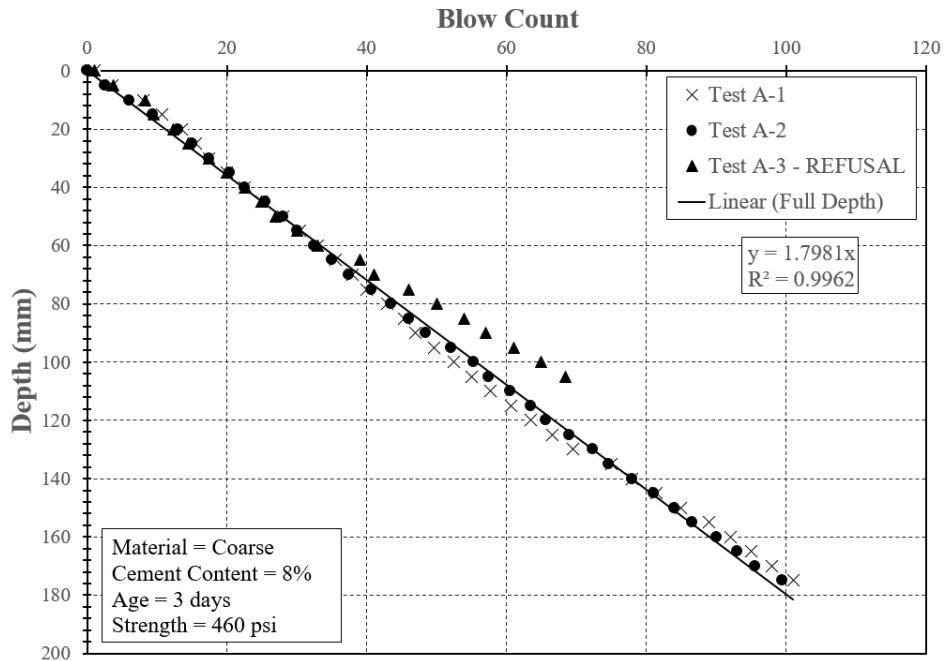


Figure H.35: Coarse 8% No. 2 3 days

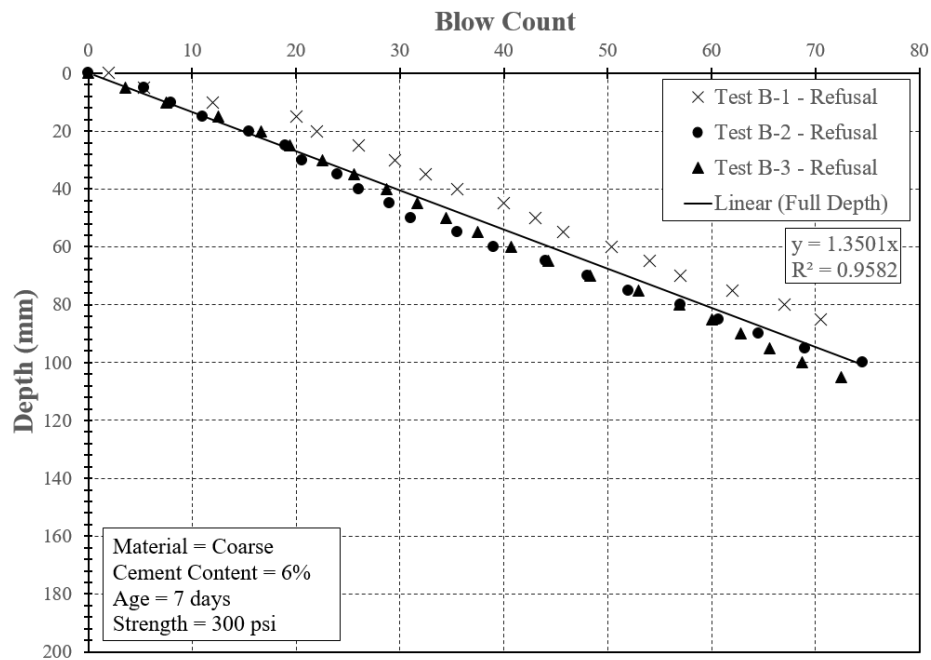


Figure H.36: Coarse 8% No. 2 7 days

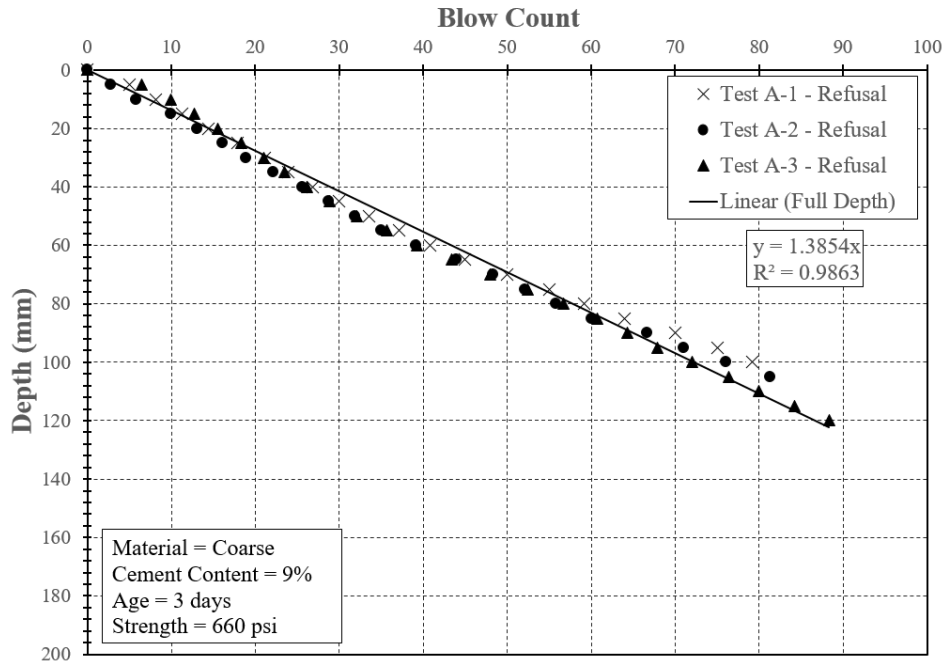


Figure H.37: Coarse 9% 3 days

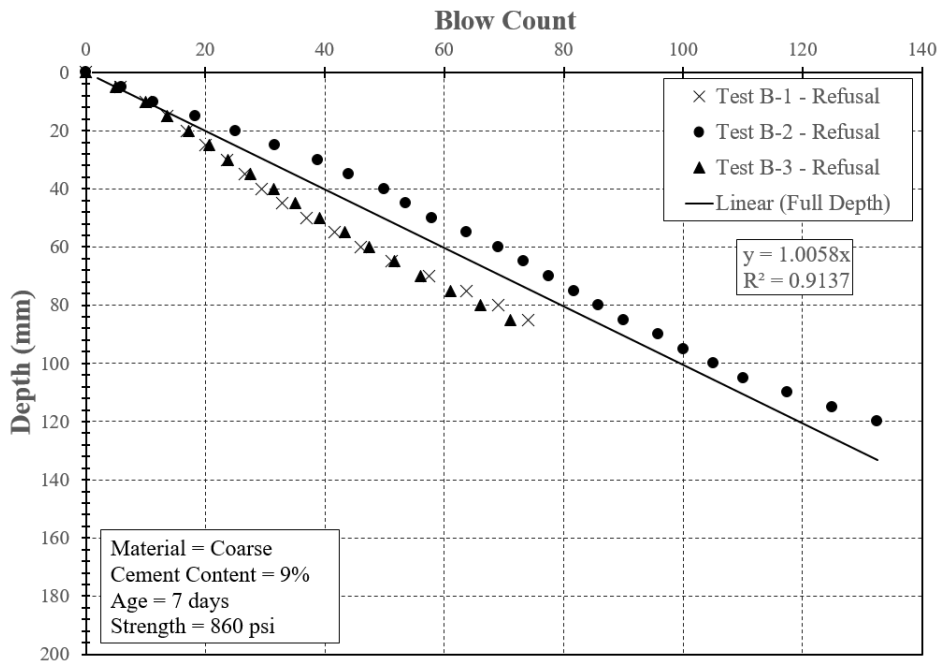


Figure H.38: Coarse 9% 7 days

Appendix I

Summary of All Field Strengths Obtained from Different Test Methods

Table I.1: Tests conducted on locations 1 through 8

Test Method	Subsection							
	1	2	2	3	4	4	5	5
	Location							
	1	2	3	4	5	6	7	8
Compressive Strength (psi)								
Plastic-Mold	-	-	-	-	-	-	-	-
DCP	499	-	-	241	443	460	163	458
Core	334	435	461	337	683	324	216	280

Table I.2: Tests conducted on locations 9 through 16

Test Method	Subsection							
	6	7	7	7	8	8	8	8
	Location							
	9	10	11	12	13	14	15	16
Compressive Strength (psi)								
Plastic-Mold	-	245	215	-	-	190	-	240
DCP	628	169	37	20	248	-	164	-
Core	326	-	-	76	251	-	321	-

Table I.3: Tests conducted on locations 17 through 24

Test Method	Subsection							
	9	9	9	9	10	10	11	11
	Location							
	17	18	19	20	21	22	23	24
Compressive Strength (psi)								
Plastic-Mold	140	-	-	214	545	-	205	-
DCP	218	502	316	350	361	451	399	225
Core	-	320	266	-	-	345	-	278

Table I.4: Tests conducted on locations 25 through 32

Test Method	Subsection							
	11	12	12	12	12	13	13	13
	Location							
	25	26	27	28	29	30	31	32
Compressive Strength (psi)								
Plastic-Mold	195	-	275	-	315	275	-	345
DCP	250	-	-	492	-	223	307	229
Core	-	316	-	306	-	-	253	-

Table I.5: Tests conducted on locations 33 through 40

Test Method	Subsection							
	14	14	14	14	15	15	15	15
	Location							
	33	34	35	36	37	38	39	40
Compressive Strength (psi)								
Plastic-Mold	-	150	-	220	135	-	-	180
DCP	341	390	75	309	435	282	132	101
Core	107	-	219	-	-	223	259	-

Table I.6: Tests conducted on locations 41 through 48

Test Method	Subsection							
	16	16	16	17	17	17	17	18
	Location							
	41	42	43	44	45	46	47	48
Compressive Strength (psi)								
Plastic-Mold	-	180	215	230	-	185	-	285
DCP	303	284	169	380	197	342	143	292
Core	532	-	-	-	215	-	266	-

Table I.7: Tests conducted on locations 49 through 57

Test Method	Subsection								
	18	18	19	19	19	19	20	20	20
	Location								
	49	50	51	52	53	54	55	56	57
Compressive Strength (psi)									
Plastic-Mold	245	-	185	-	175	-	-	185	145
DCP	156	287	-	-	-	-	-	-	-
Core	-	337	-	199	-	305	124	-	-

Appendix J

25 Millimeter Penetration Field Data

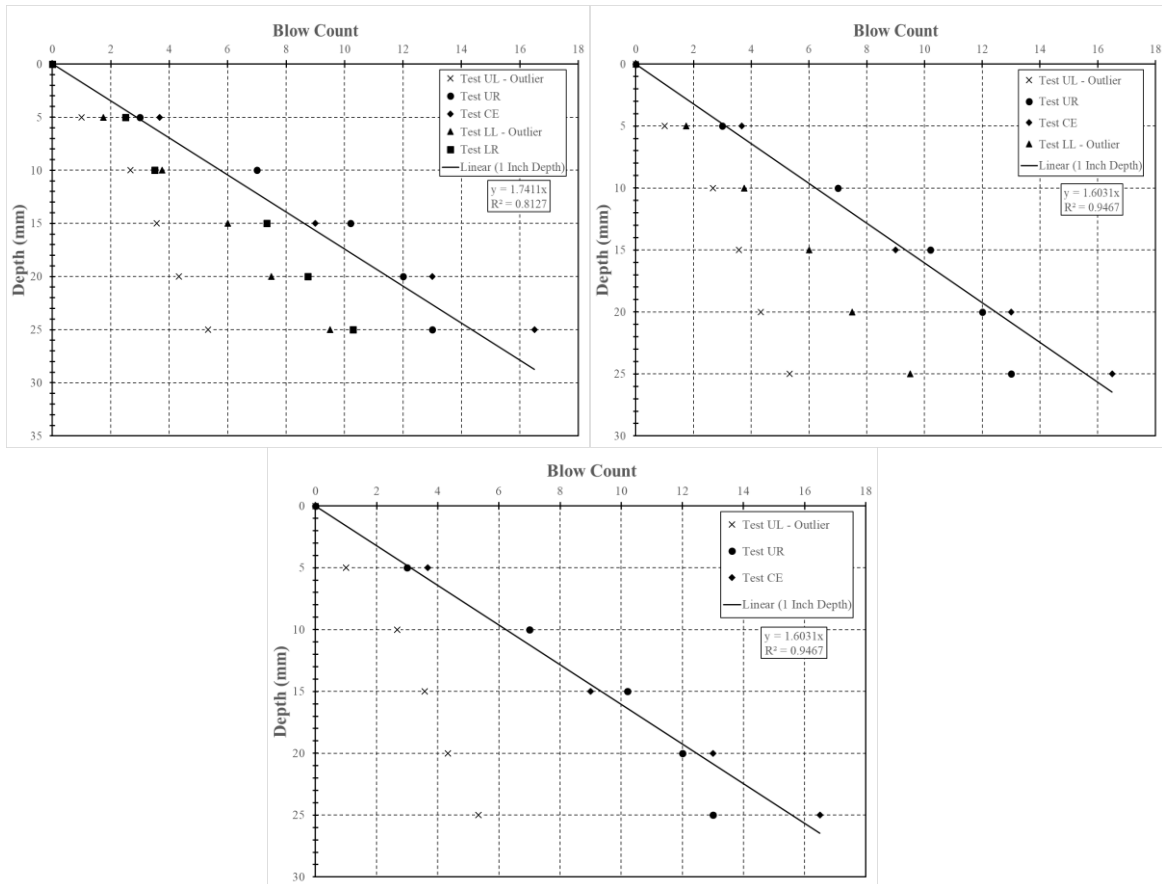


Figure J.1: Test performed on July 9, 2019, Location 1 (top left = 5 tests, top right = 4 tests, bottom = 3 tests)

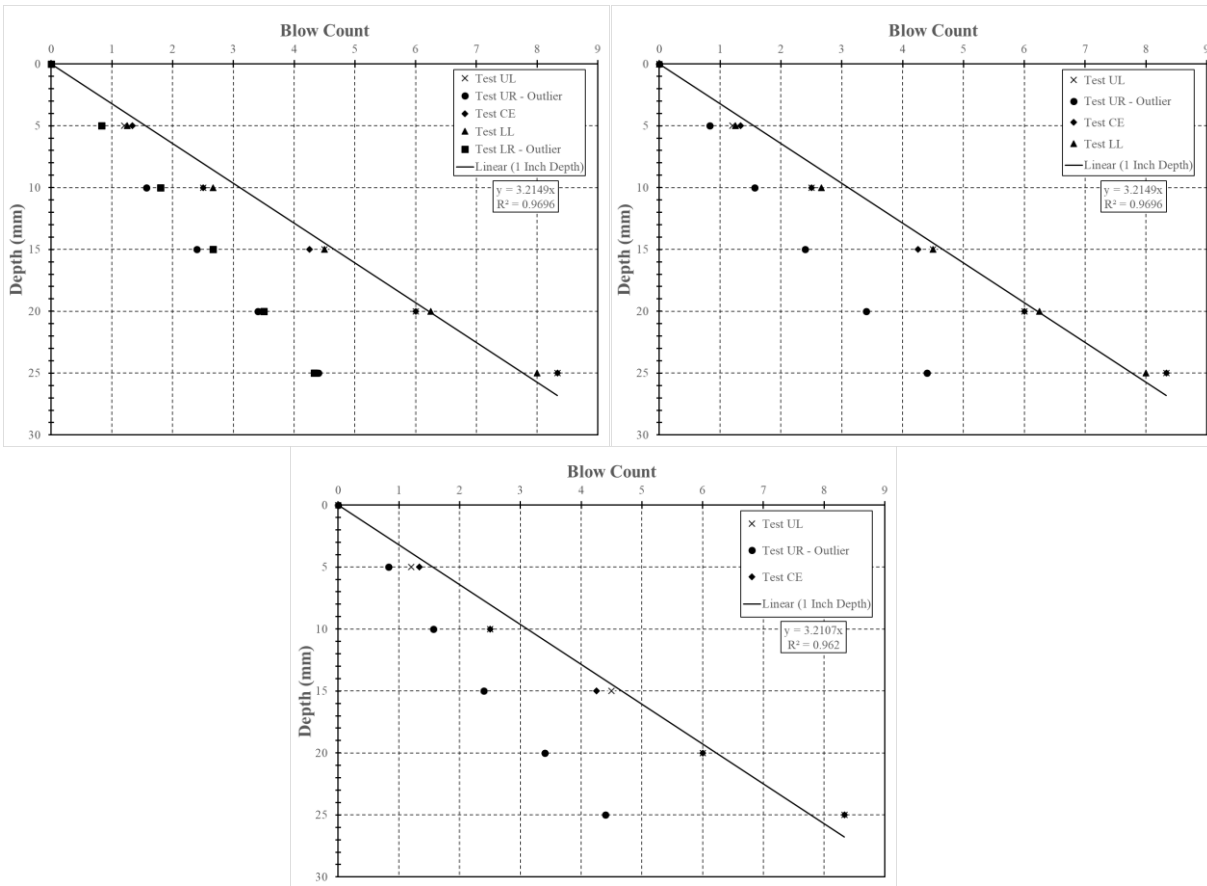


Figure J.2: Test performed on July 10, 2019, Location 4 (top left = 5 tests, top right = 4 tests, bottom = 3 tests)

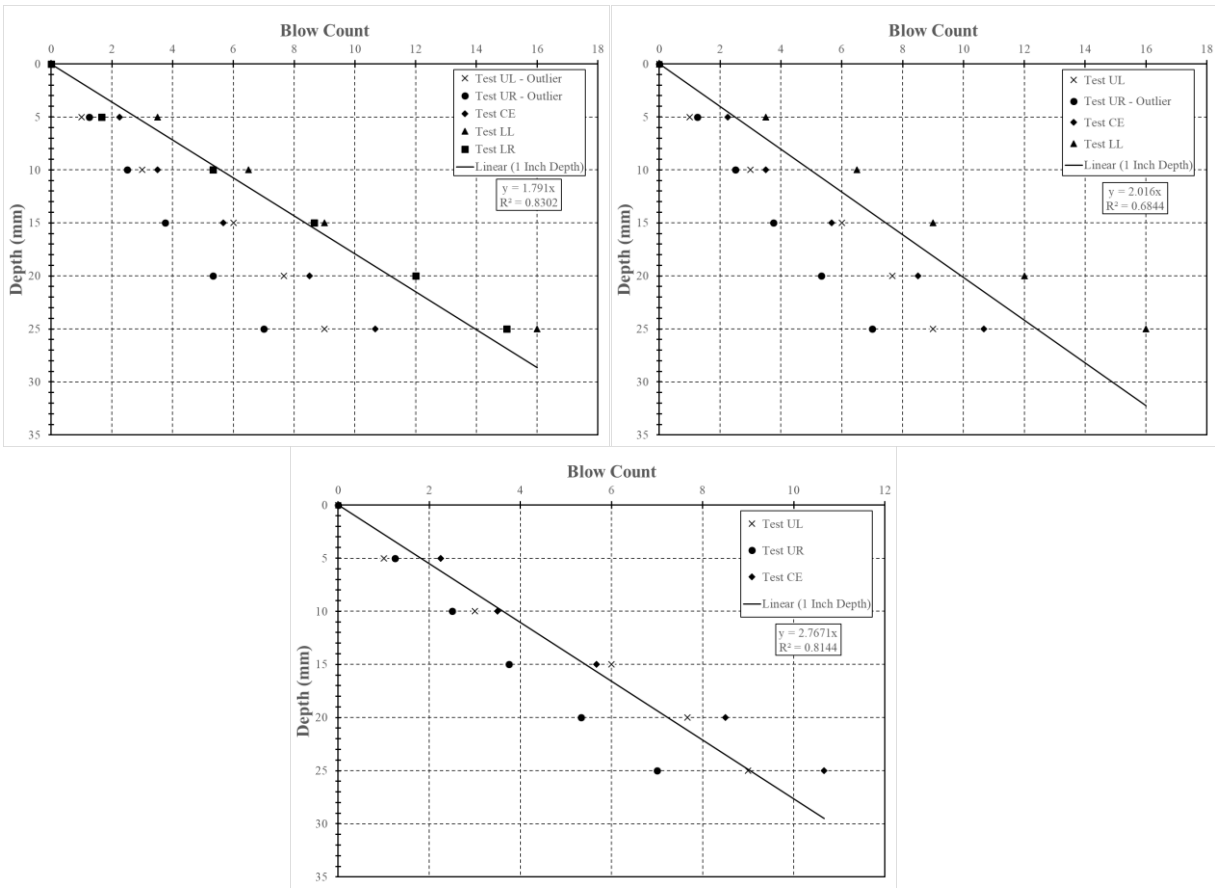


Figure J.3: Test performed on July 10, 2019, Location 5 (top left = 5 tests, top right = 4 tests, bottom = 3 tests)

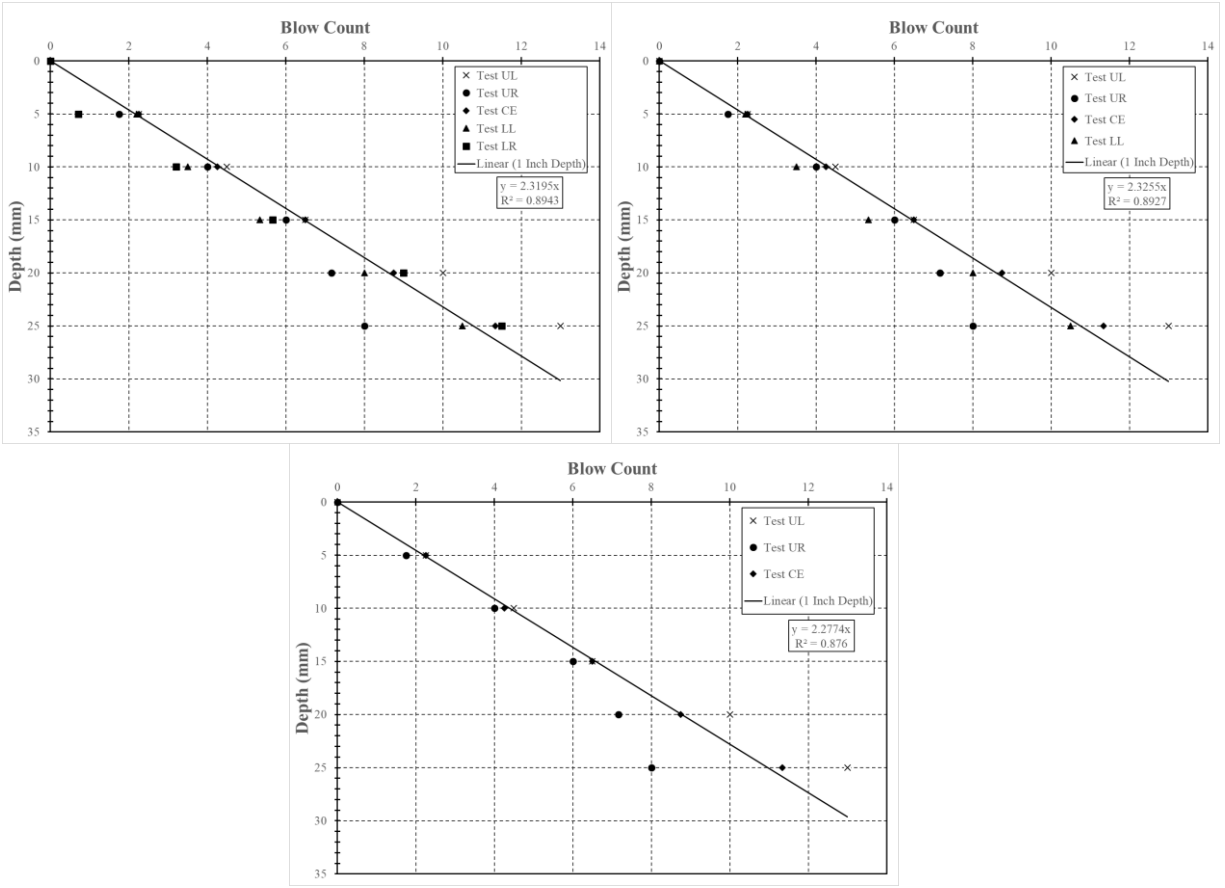


Figure J.4: Test performed on July 10, 2019, Location 6 (top left = 5 tests, top right = 4 tests, bottom = 3 tests)

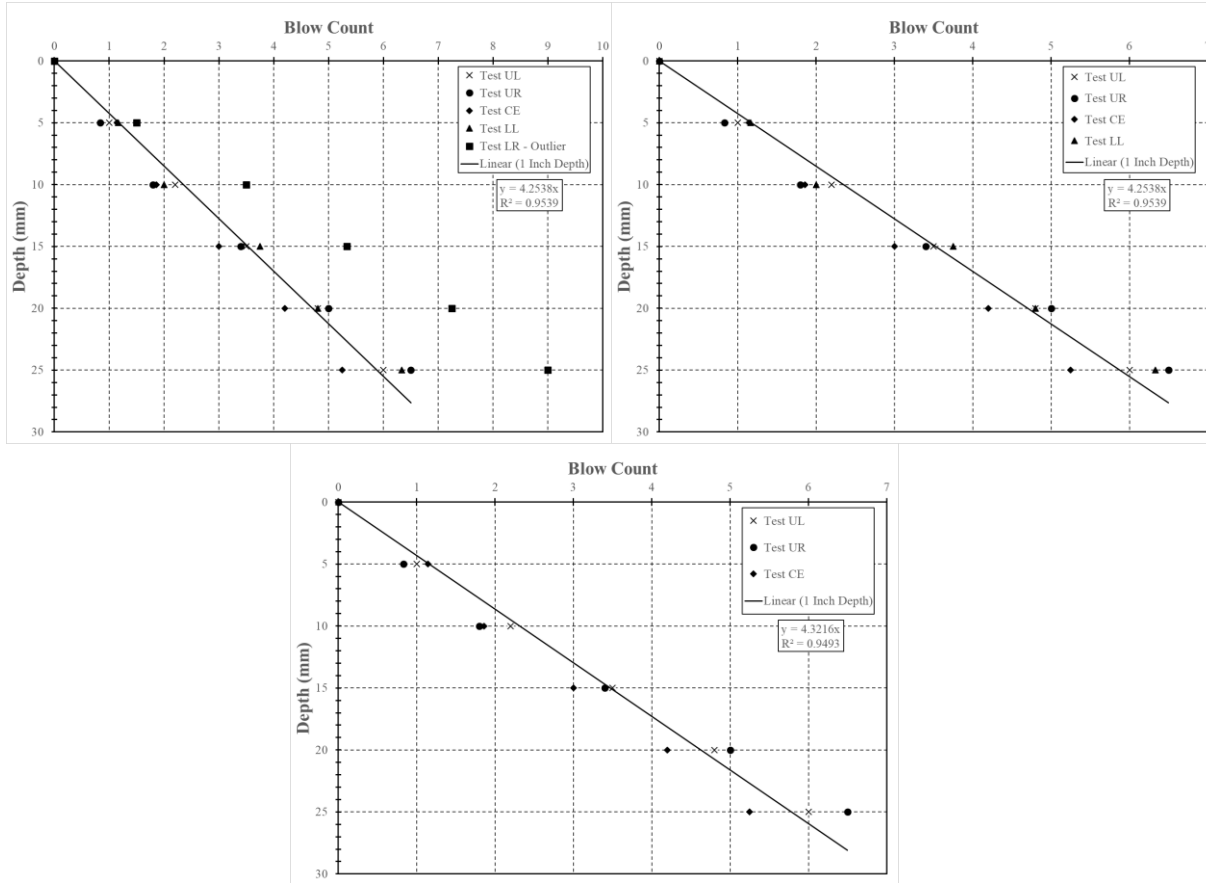


Figure J.5: Test performed on July 16, 2019, Location 7 (top left = 5 tests, top right = 4 tests, bottom = 3 tests)

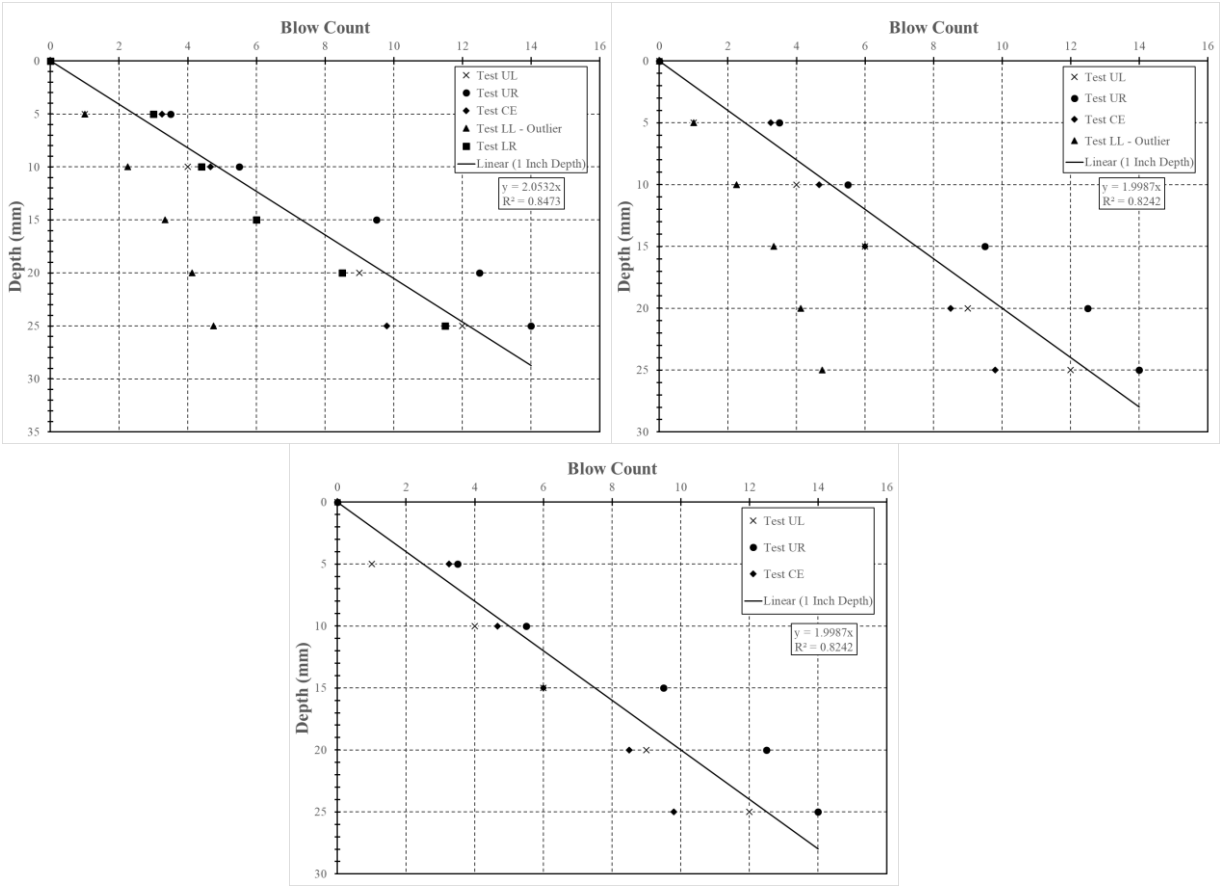


Figure J.6: Test performed on July 16, 2019, Location 8 (top left = 5 tests, top right = 4 tests, bottom = 3 tests)

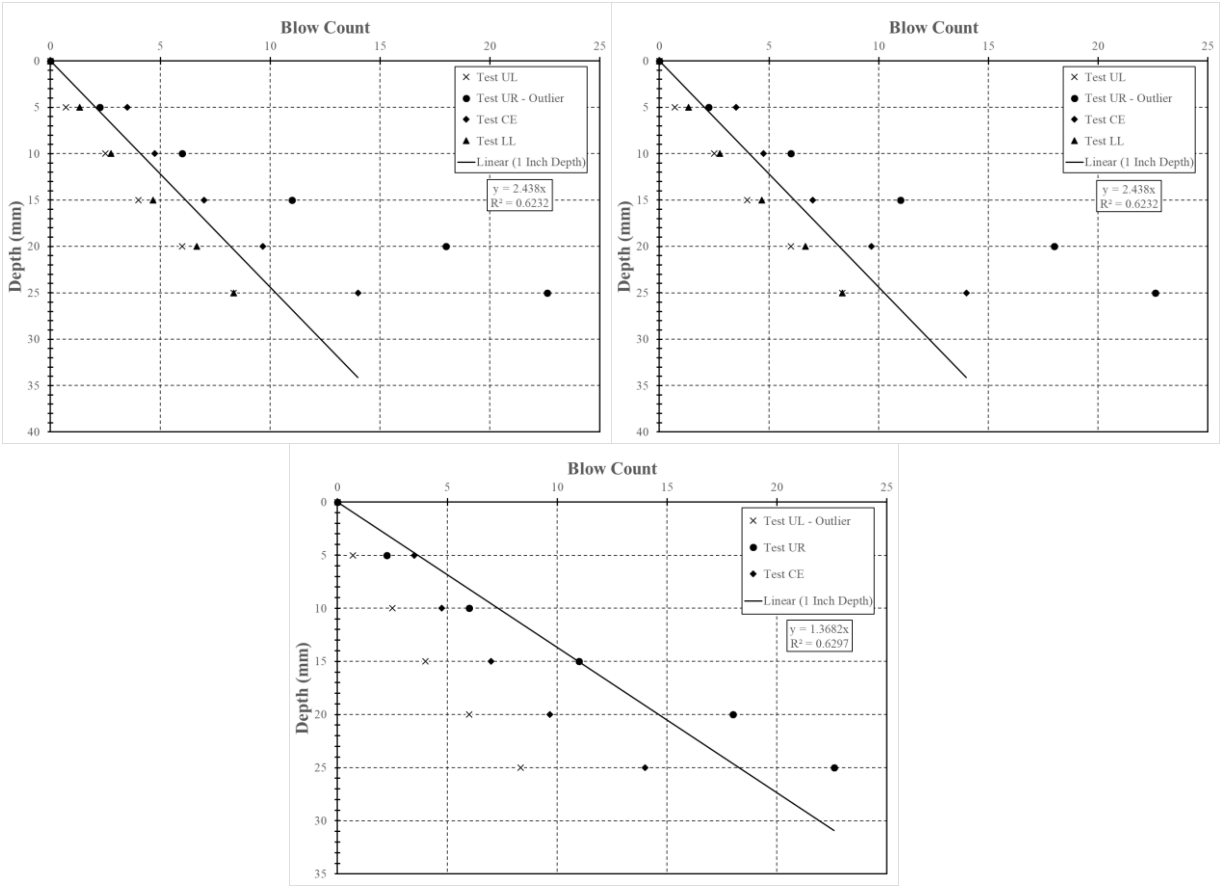


Figure J.7: Test performed on July 16, 2019, Location 9 (top left = 5 tests, top right = 4 tests, bottom = 3 tests)

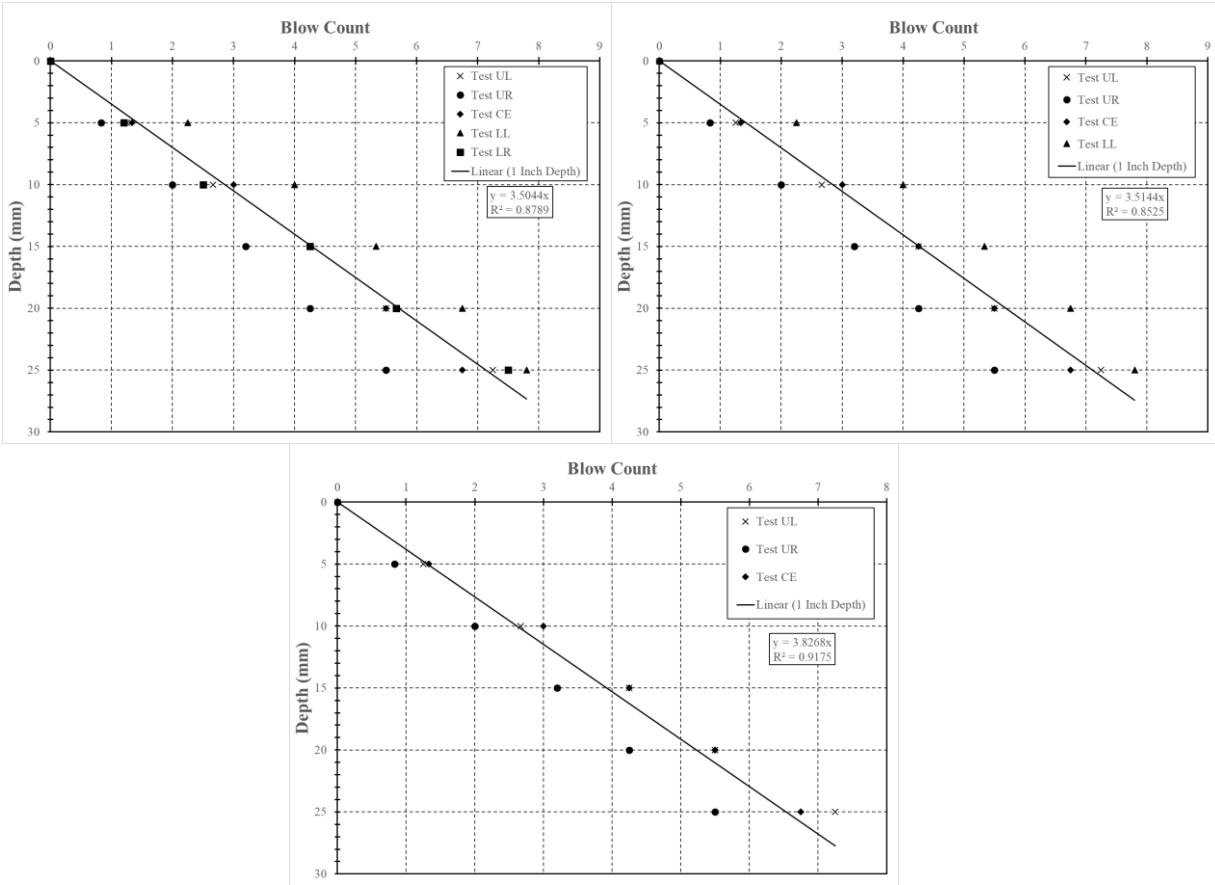


Figure J.8: Test performed on July 16, 2019, Location 10 (top left = 5 tests, top right = 4 tests, bottom = 3 tests)

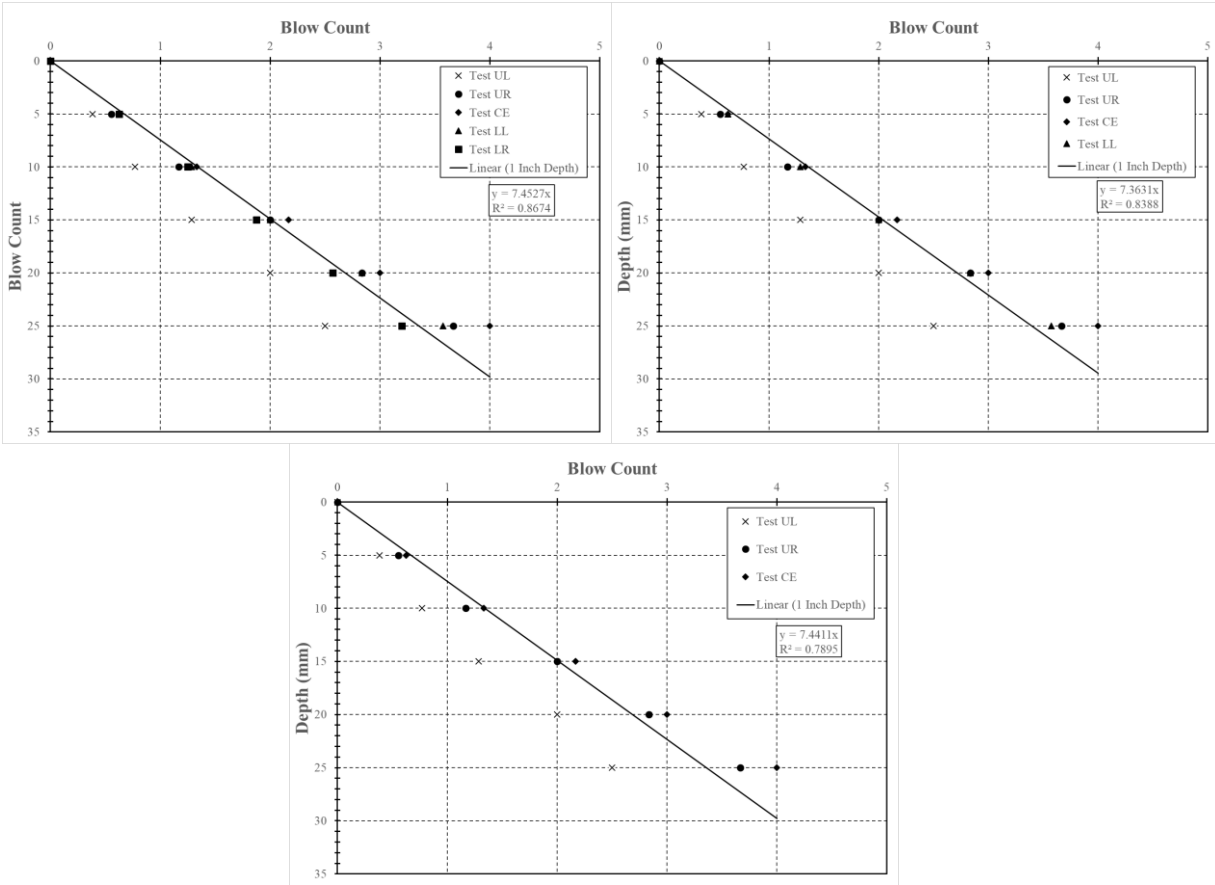


Figure J.9: Test performed on July 16, 2019, Location 11 (top left = 5 tests, top right = 4 tests, bottom = 3 tests)

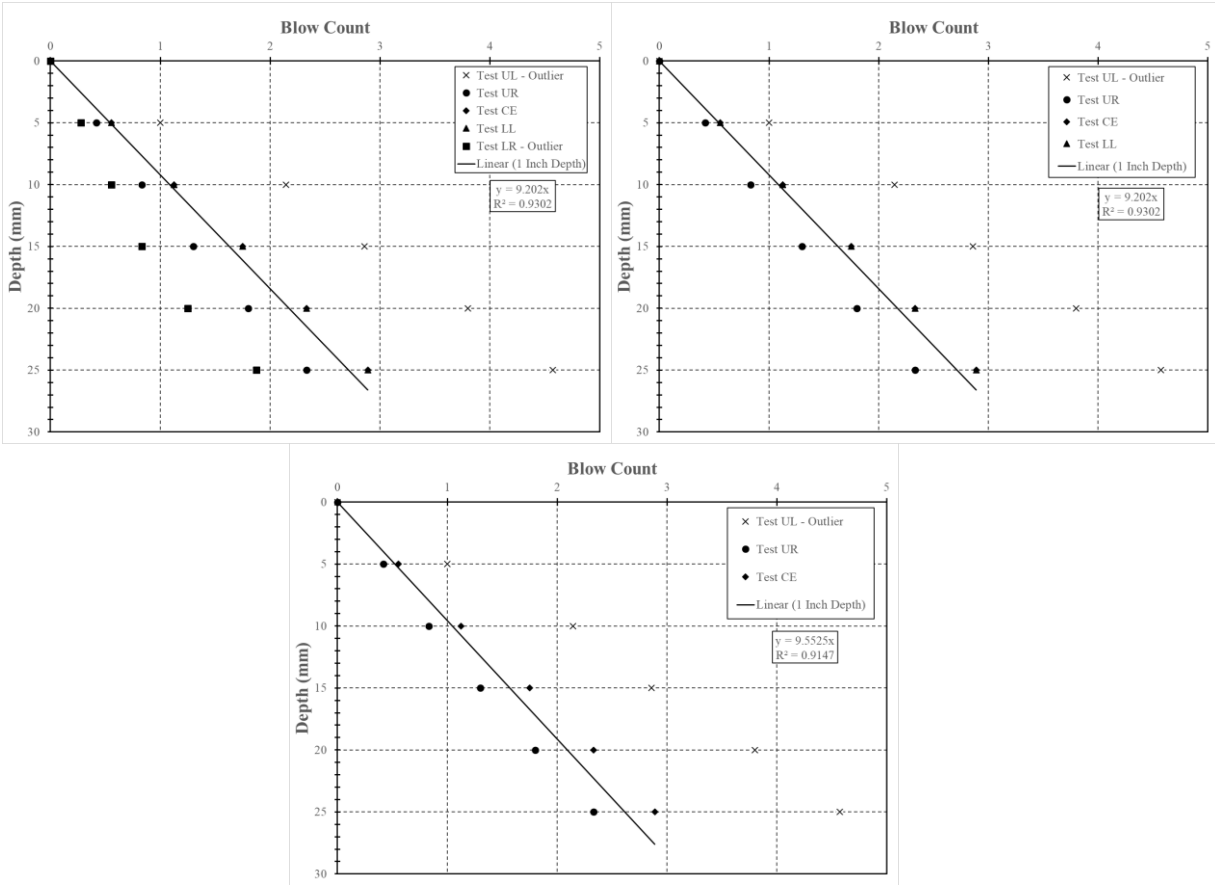


Figure J.10: Test performed on July 16, 2019, Location 12 (top left = 5 tests, top right = 4 tests, bottom = 3 tests)

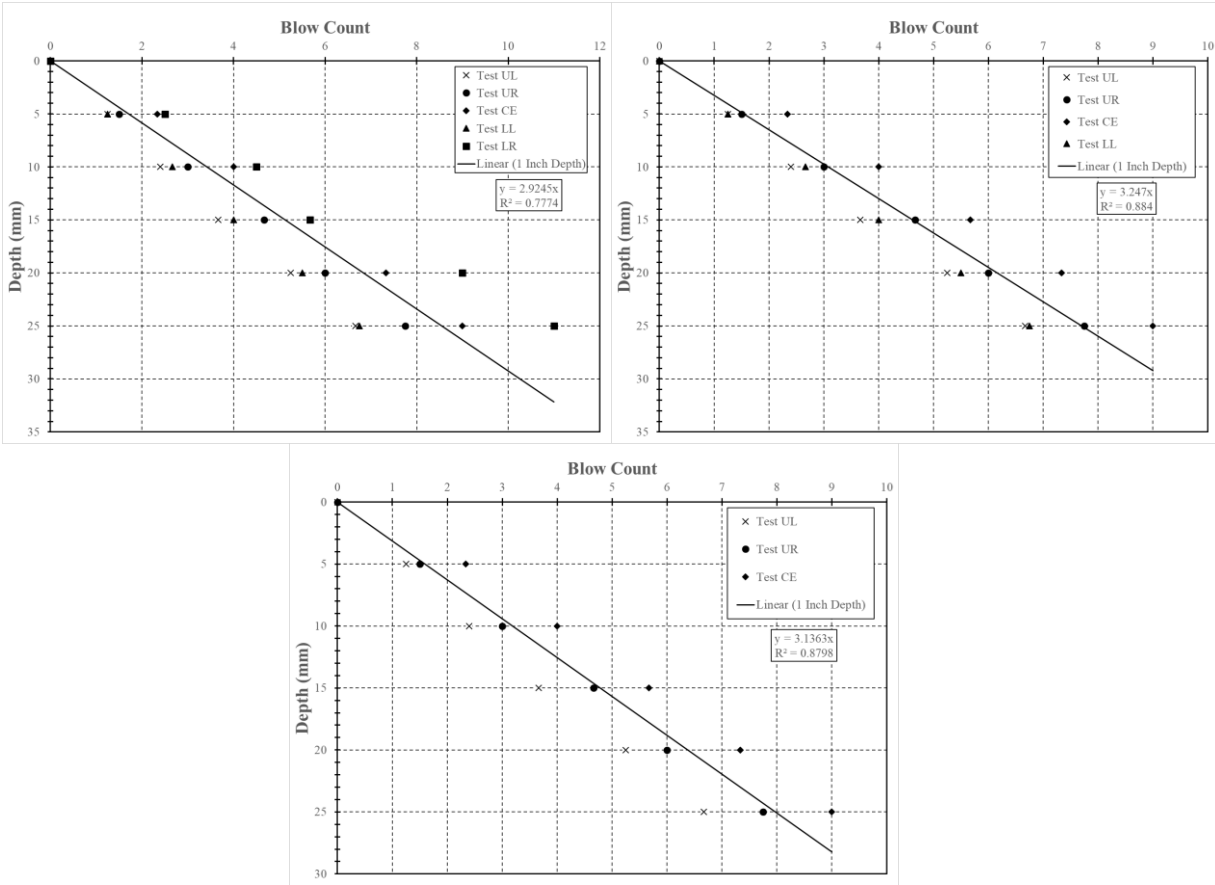


Figure J.11: Test performed on July 16, 2019, Location 13 (top left = 5 tests, top right = 4 tests, bottom = 3 tests)

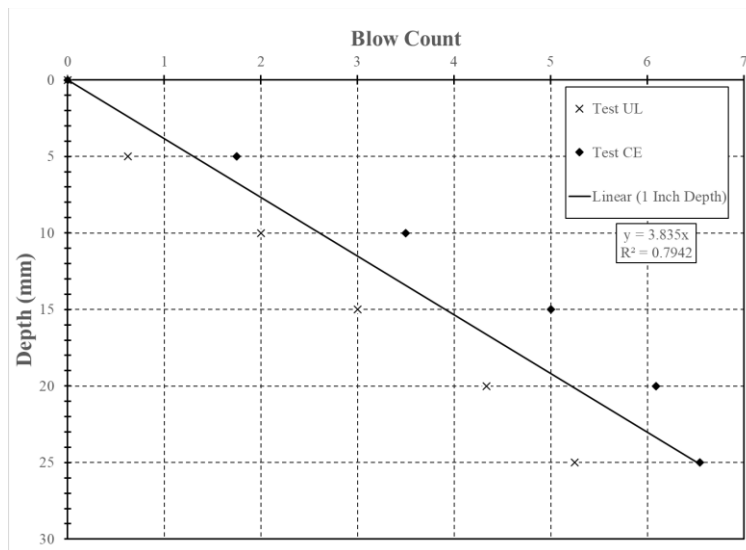


Figure J.12: Test performed on July 16, 2019, Location 15 (only 2 tests completed)

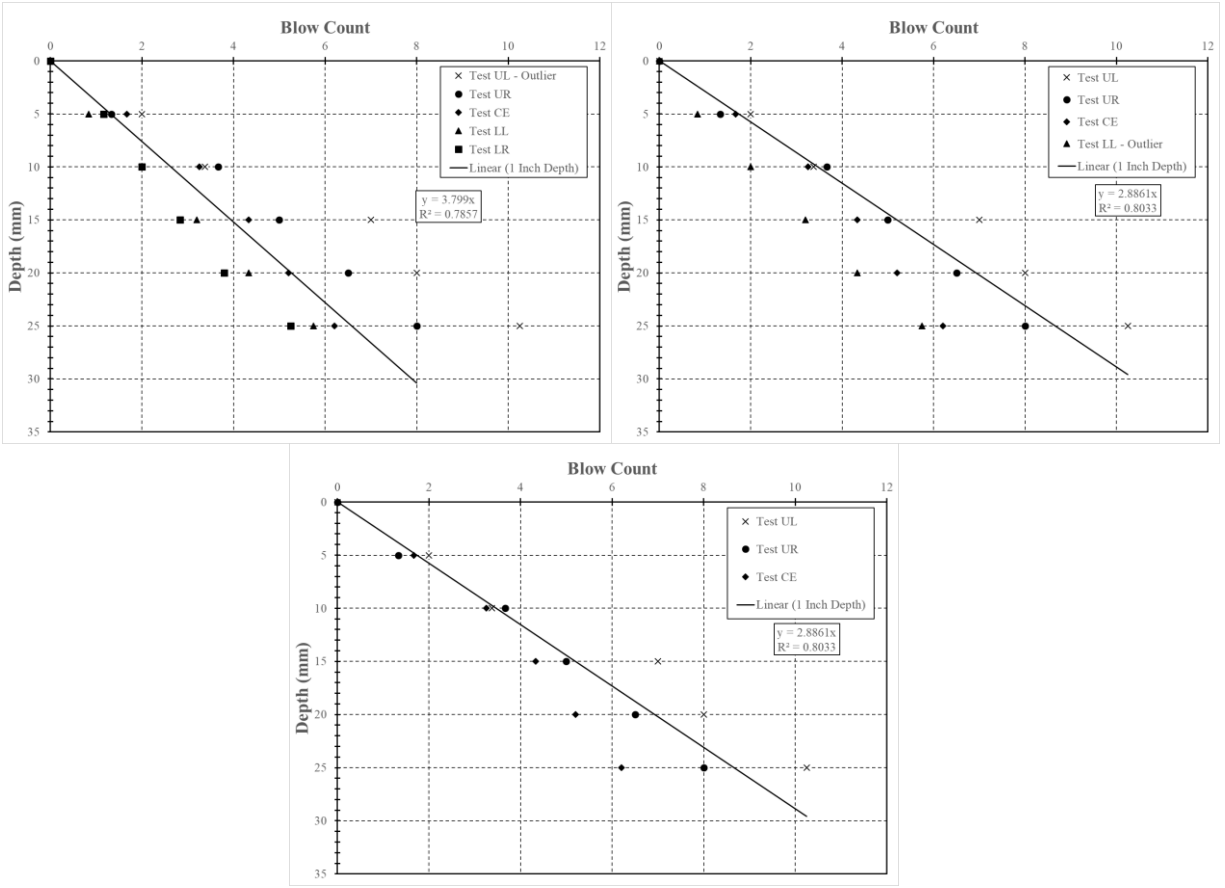


Figure J.13: Test performed on July 17, 2019, Location 17 (top left = 5 tests, top right = 4 tests, bottom = 3 tests)

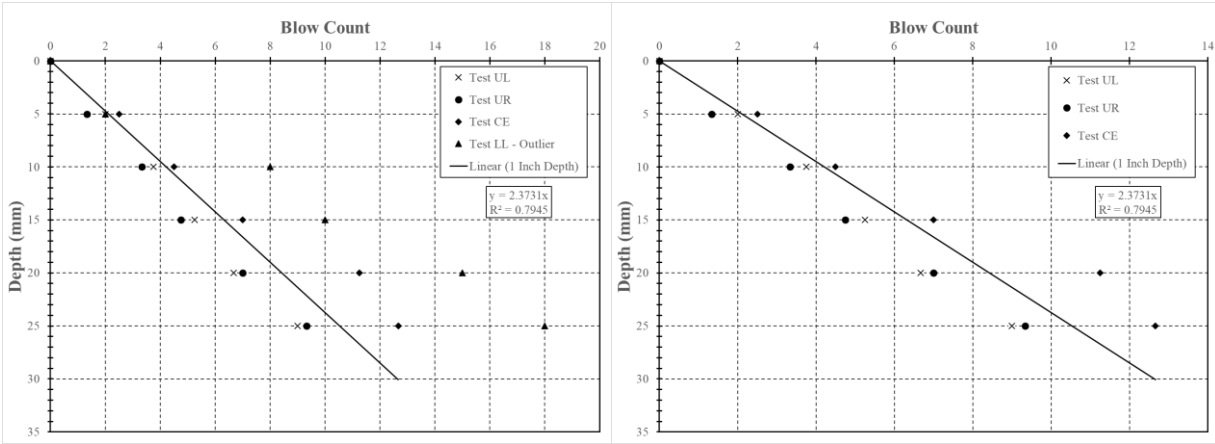


Figure J.14: Test performed on July 17, 2019, Location 18 (left = 4 tests, right = 3 tests)

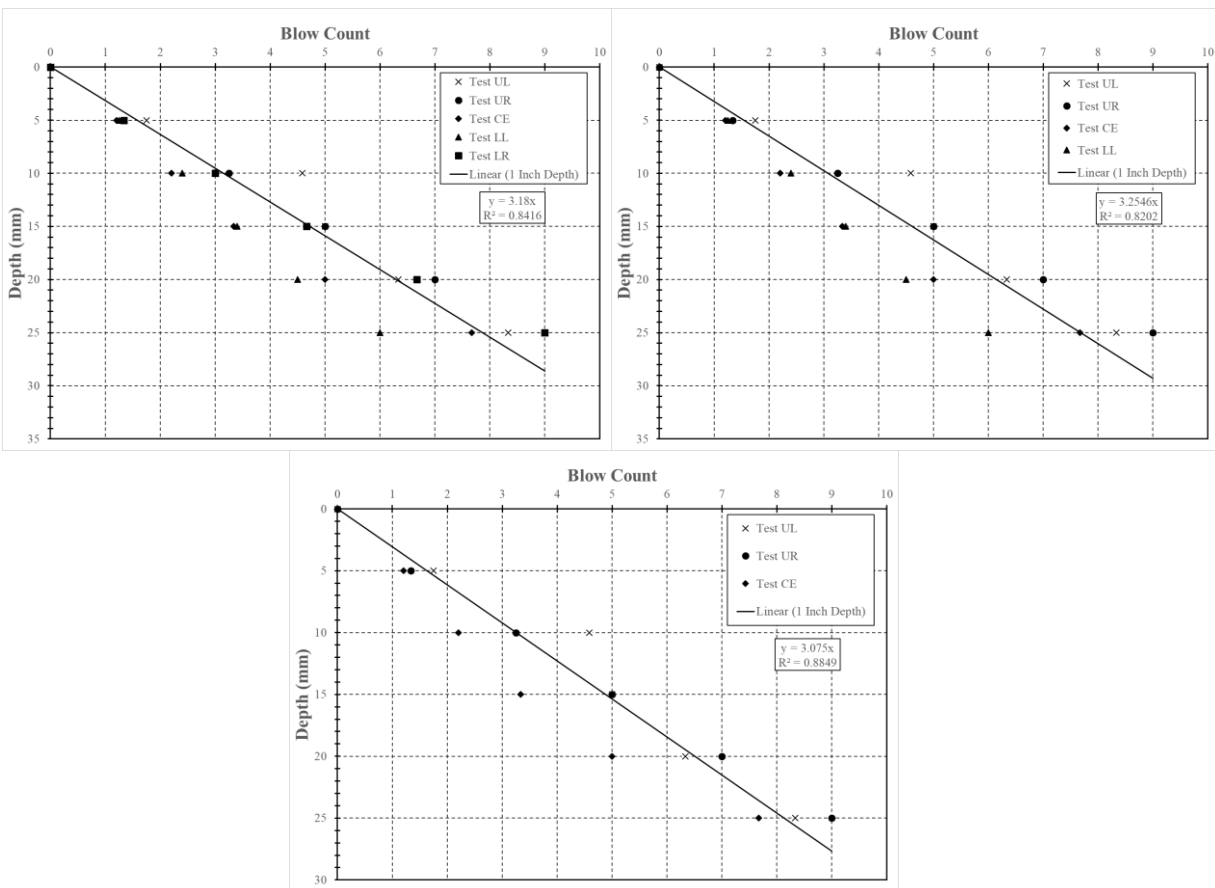


Figure J.15: Test performed on July 17, 2019, Location 19 (top left = 5 tests, top right = 4 tests, bottom = 3 tests)

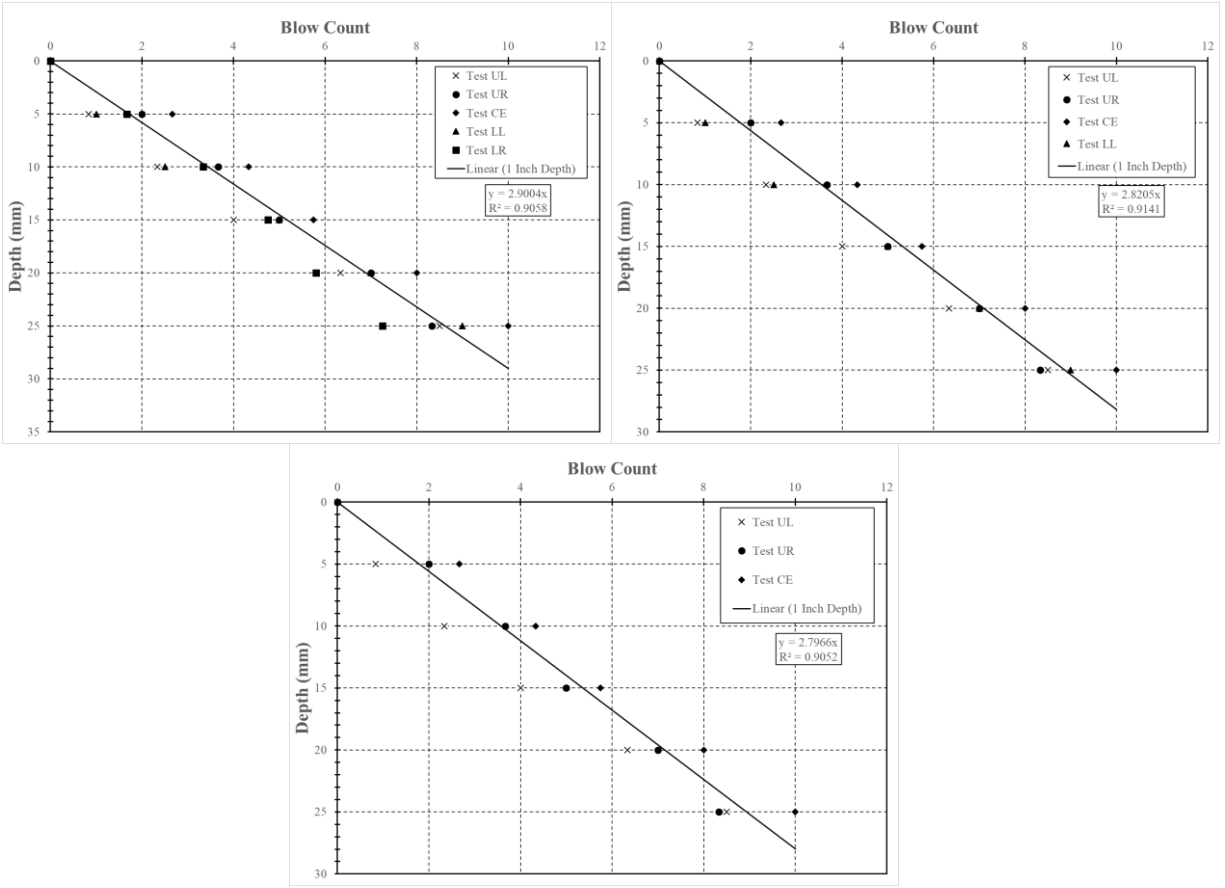


Figure J.16: Test performed on July 17, 2019, Location 20 (top left = 5 tests, top right = 4 tests, bottom = 3 tests)

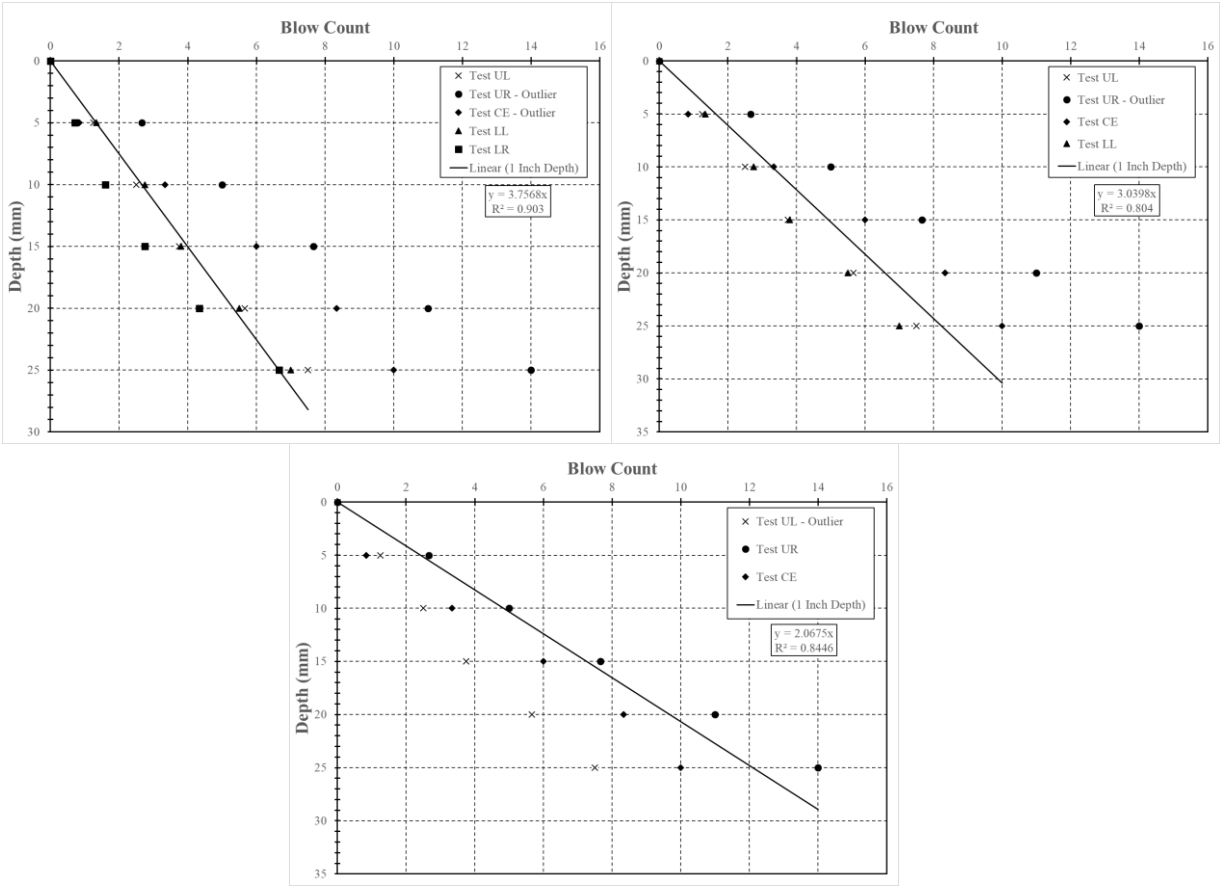


Figure J.17: Test performed on July 17, 2019, Location 21 (top left = 5 tests, top right = 4 tests, bottom = 3 tests)

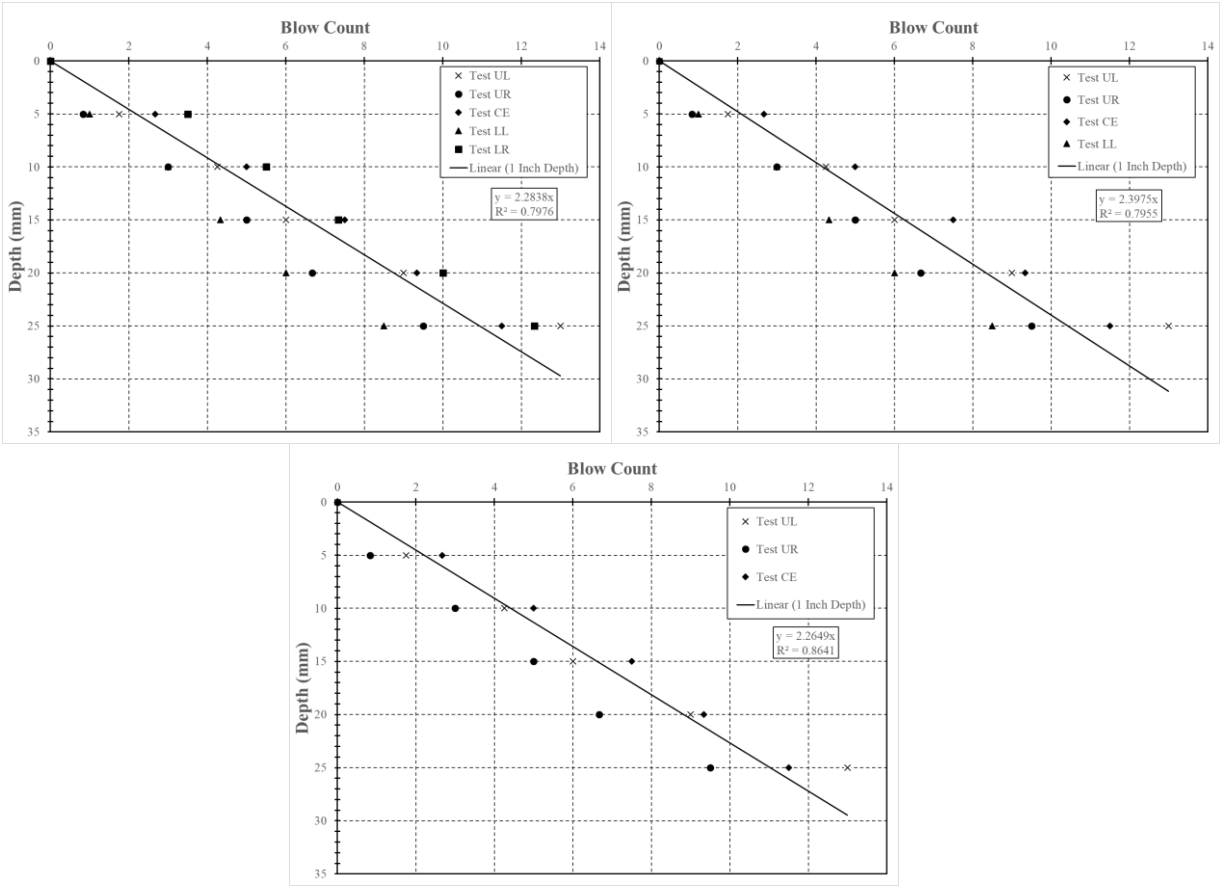


Figure J.18: Test performed on July 17, 2019, Location 22 (top left = 5 tests, top right = 4 tests, bottom = 3 tests)

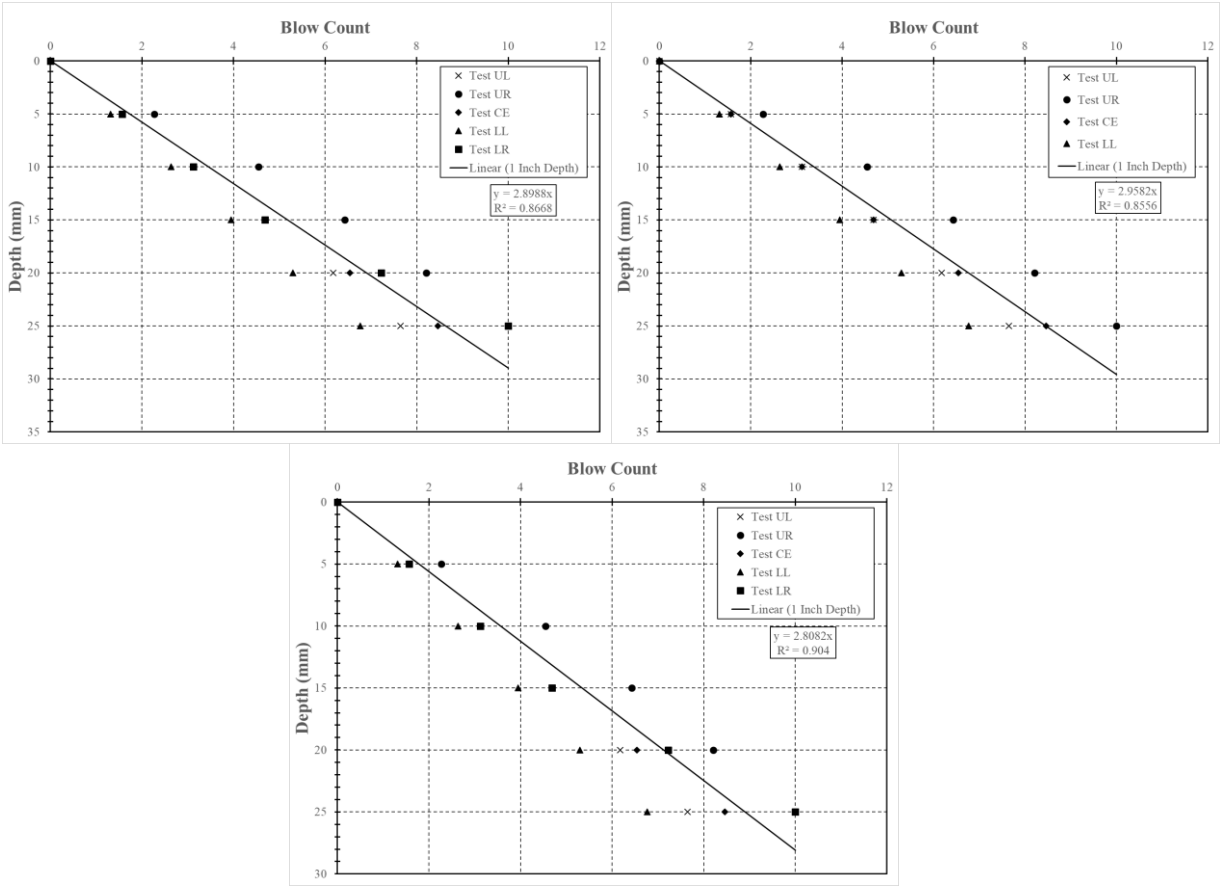


Figure J.19: Test performed on July 18, 2019, Location 23 (top left = 5 tests, top right = 4 tests, bottom = 3 tests)

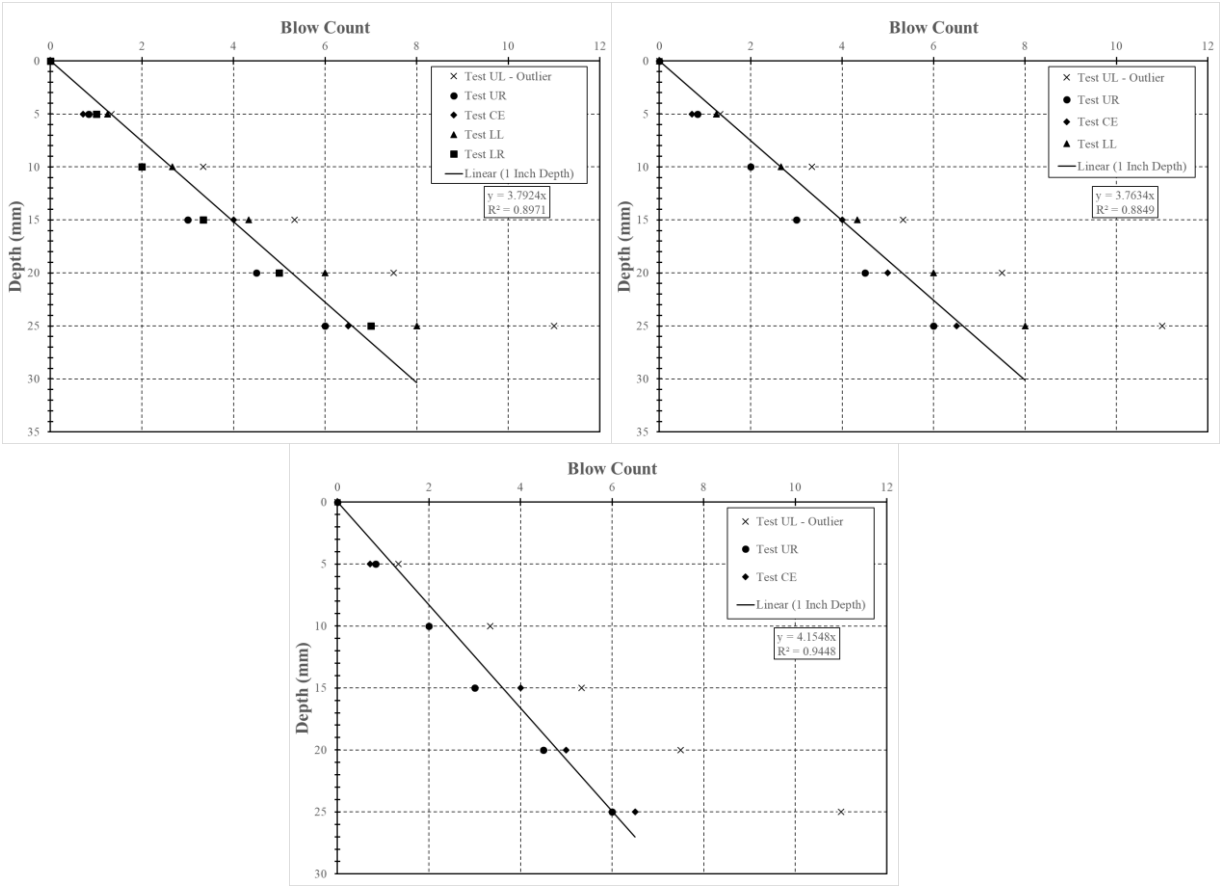


Figure J.20: Test performed on July 18, 2019, Location 24 (top left = 5 tests, top right = 4 tests, bottom = 3 tests)

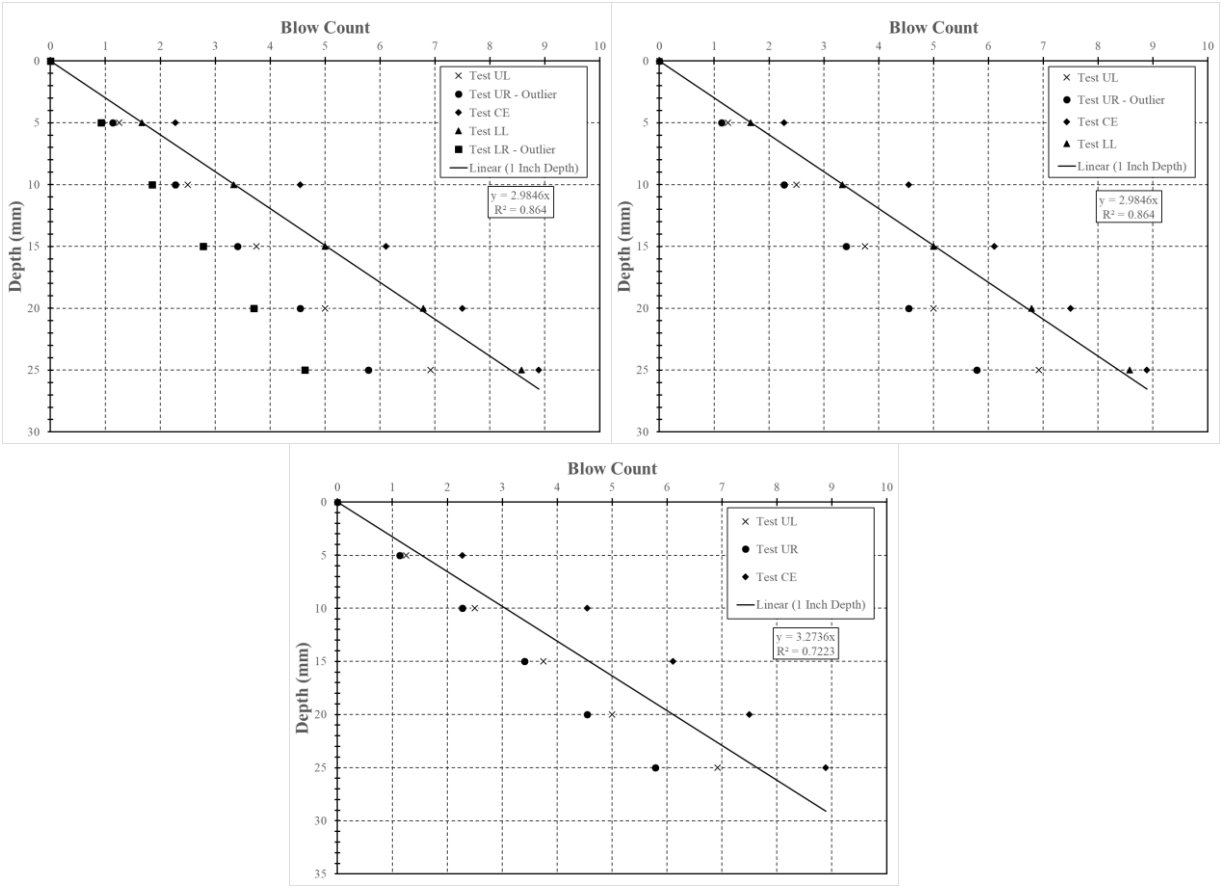


Figure J.21: Test performed on July 18, 2019, Location 25 (top left = 5 tests, top right = 4 tests, bottom = 3 tests)

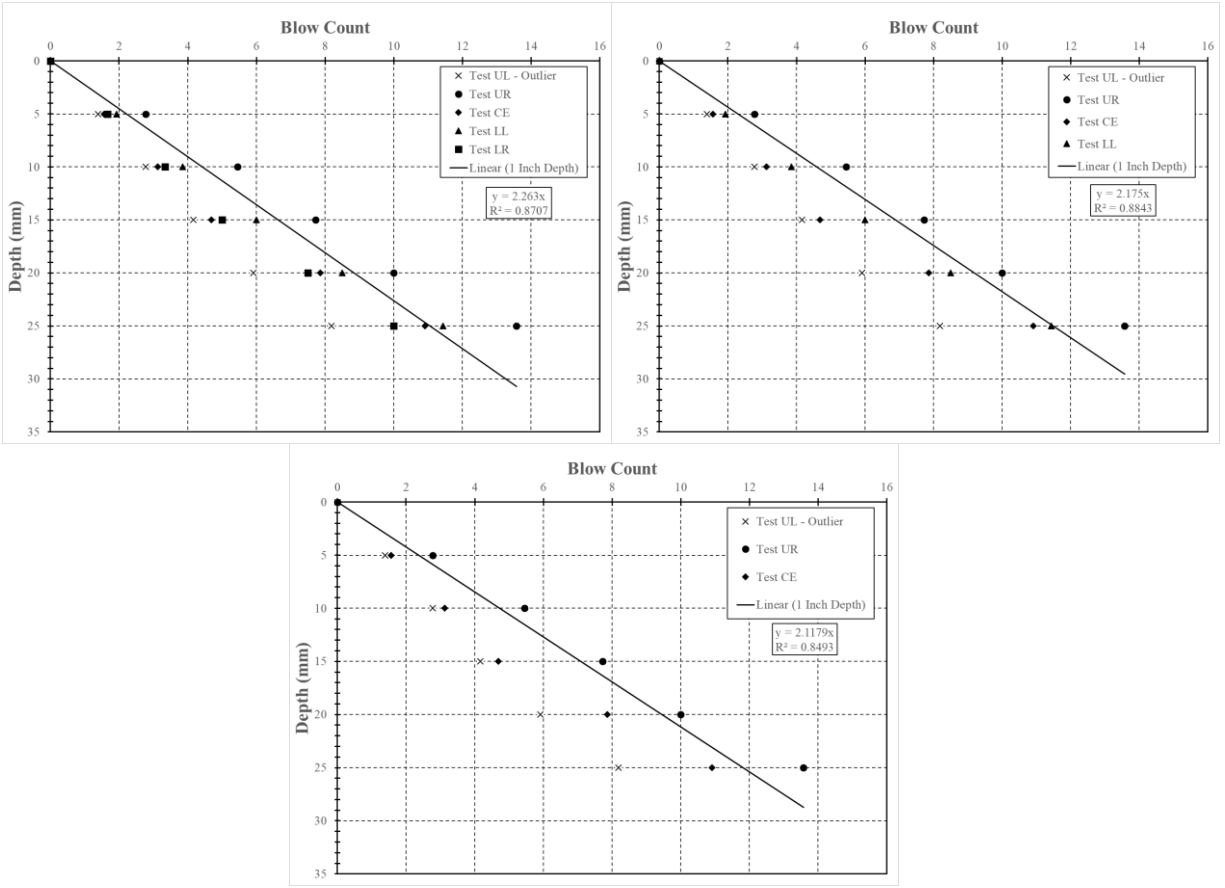


Figure J.22: Test performed on July 18, 2019, Location 28 (top left = 5 tests, top right = 4 tests, bottom = 3 tests)

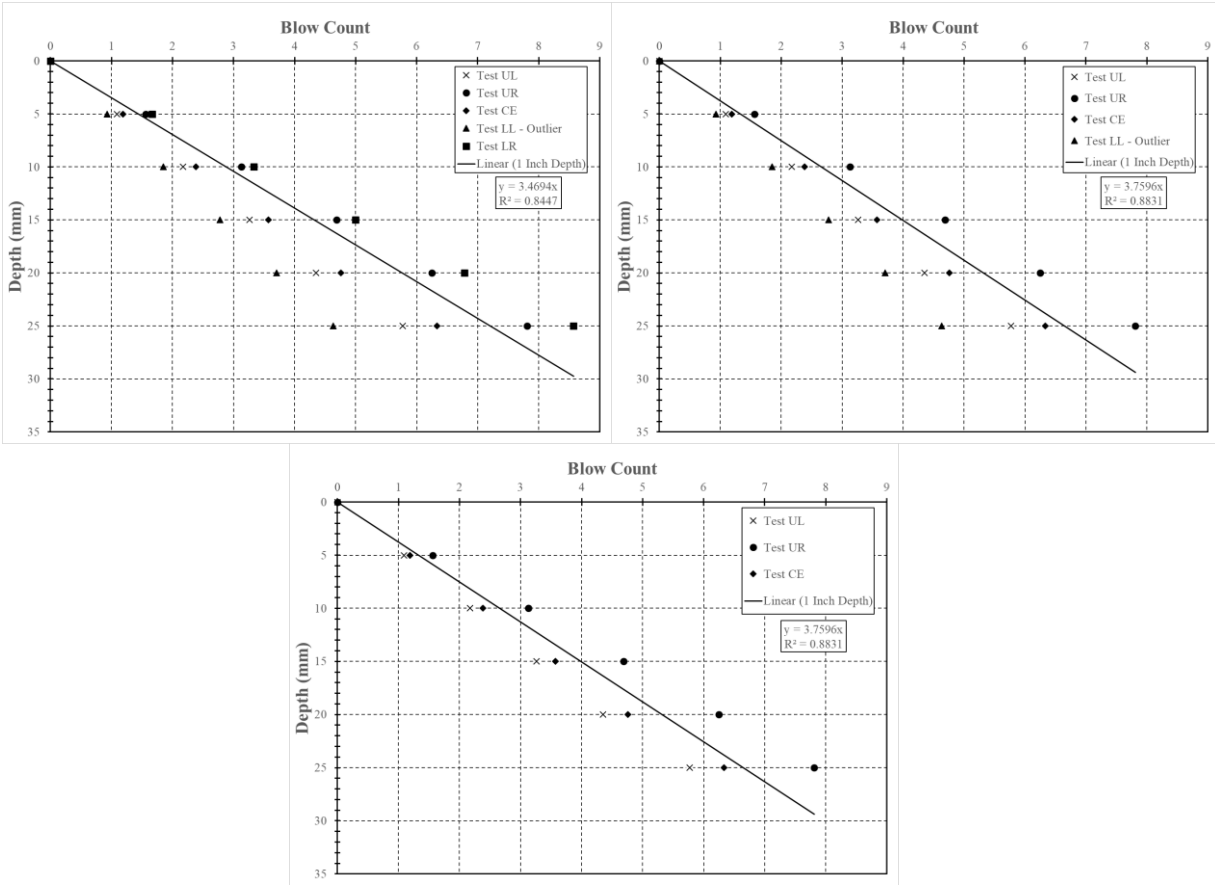


Figure J.23: Test performed on July 19, 2019, Location 30 (top left = 5 tests, top right = 4 tests, bottom = 3 tests)

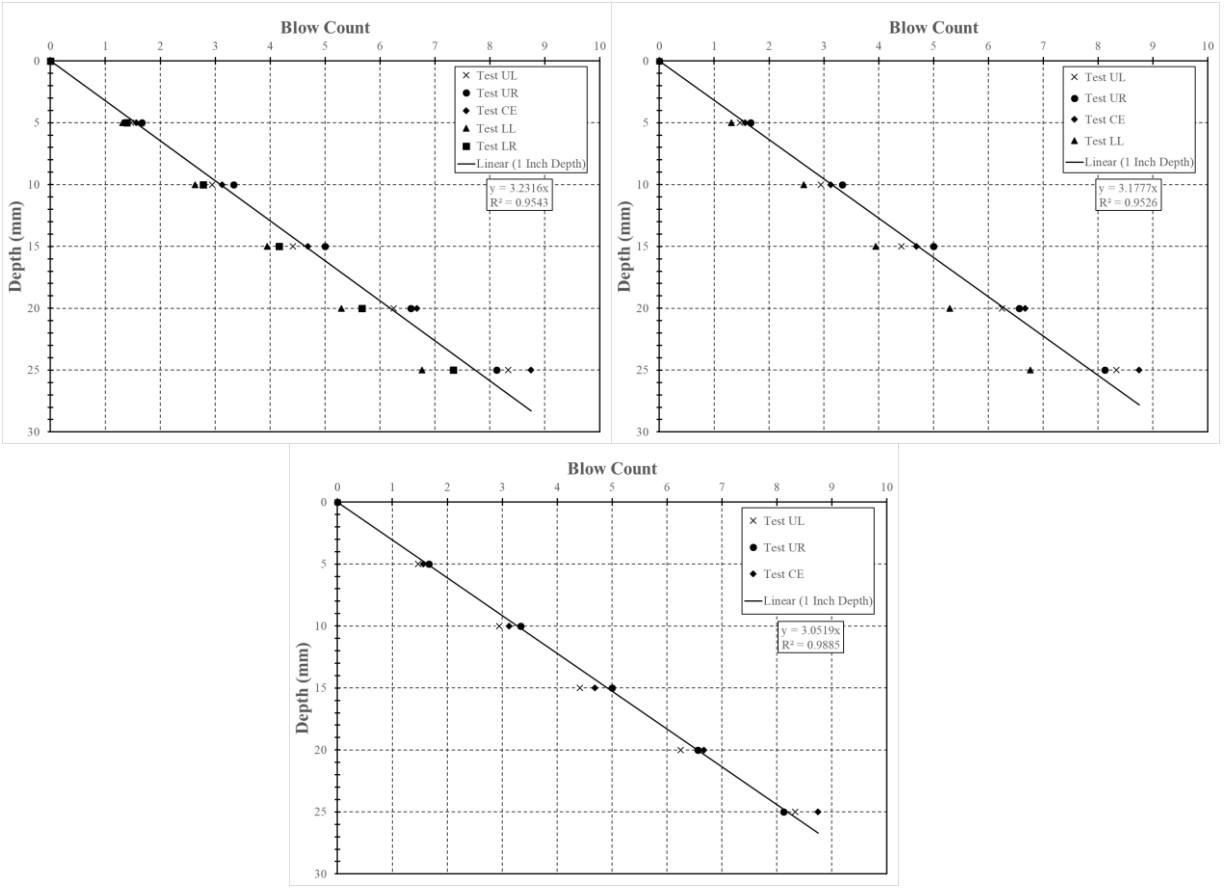


Figure J.24: Test performed on July 19, 2019, Location 31 (top left = 5 tests, top right = 4 tests, bottom = 3 tests)

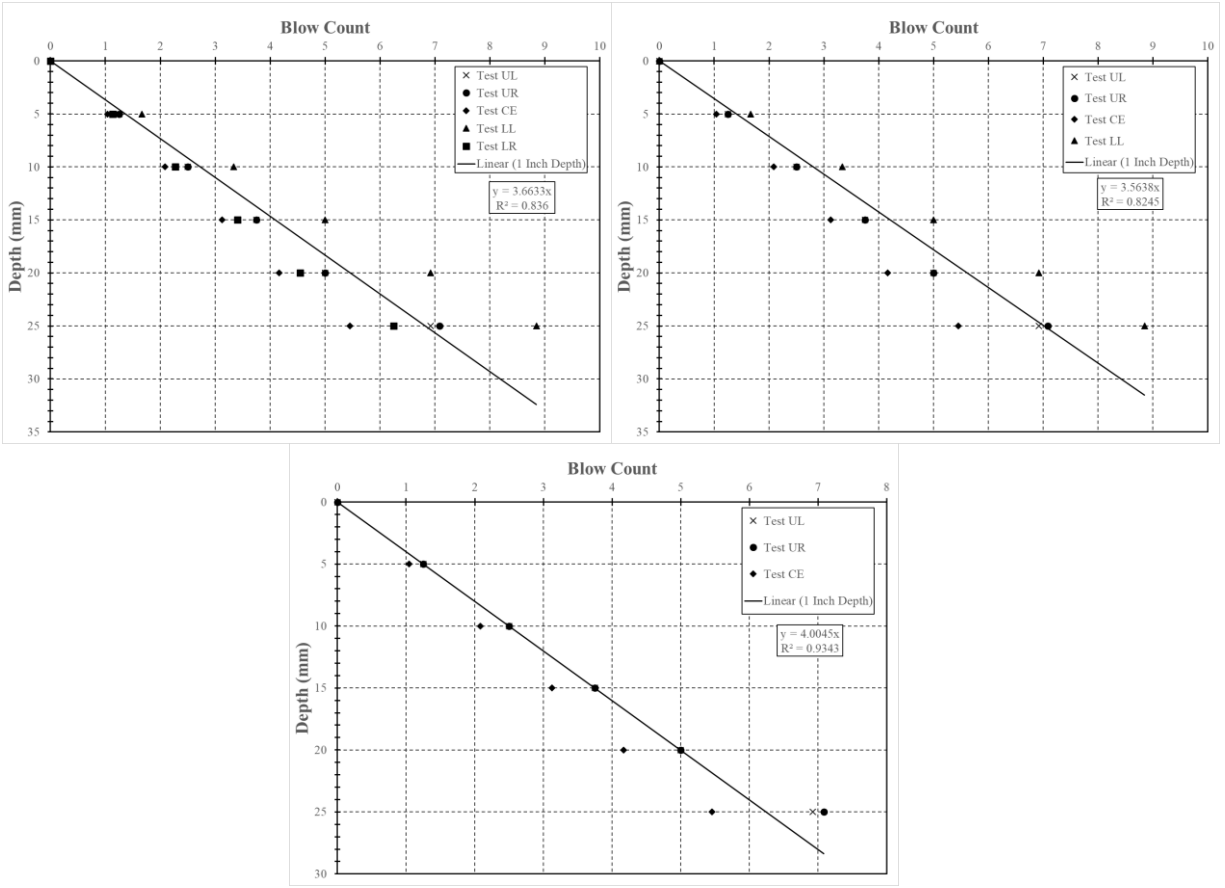


Figure J.25: Test performed on July 19, 2019, Location 32 (top left = 5 tests, top right = 4 tests, bottom = 3 tests)

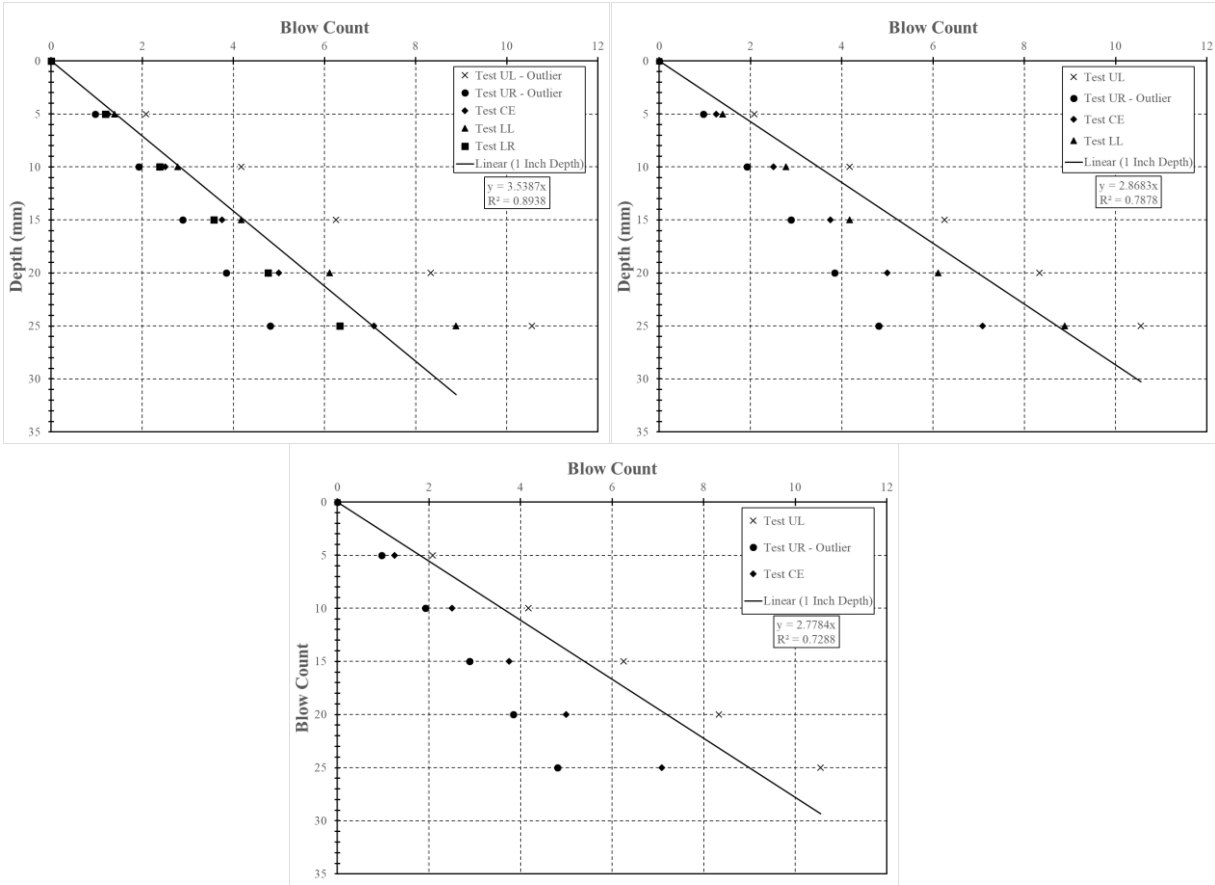


Figure J.26: Test performed on July 19, 2019, Location 33 (top left = 5 tests, top right = 4 tests, bottom = 3 tests)

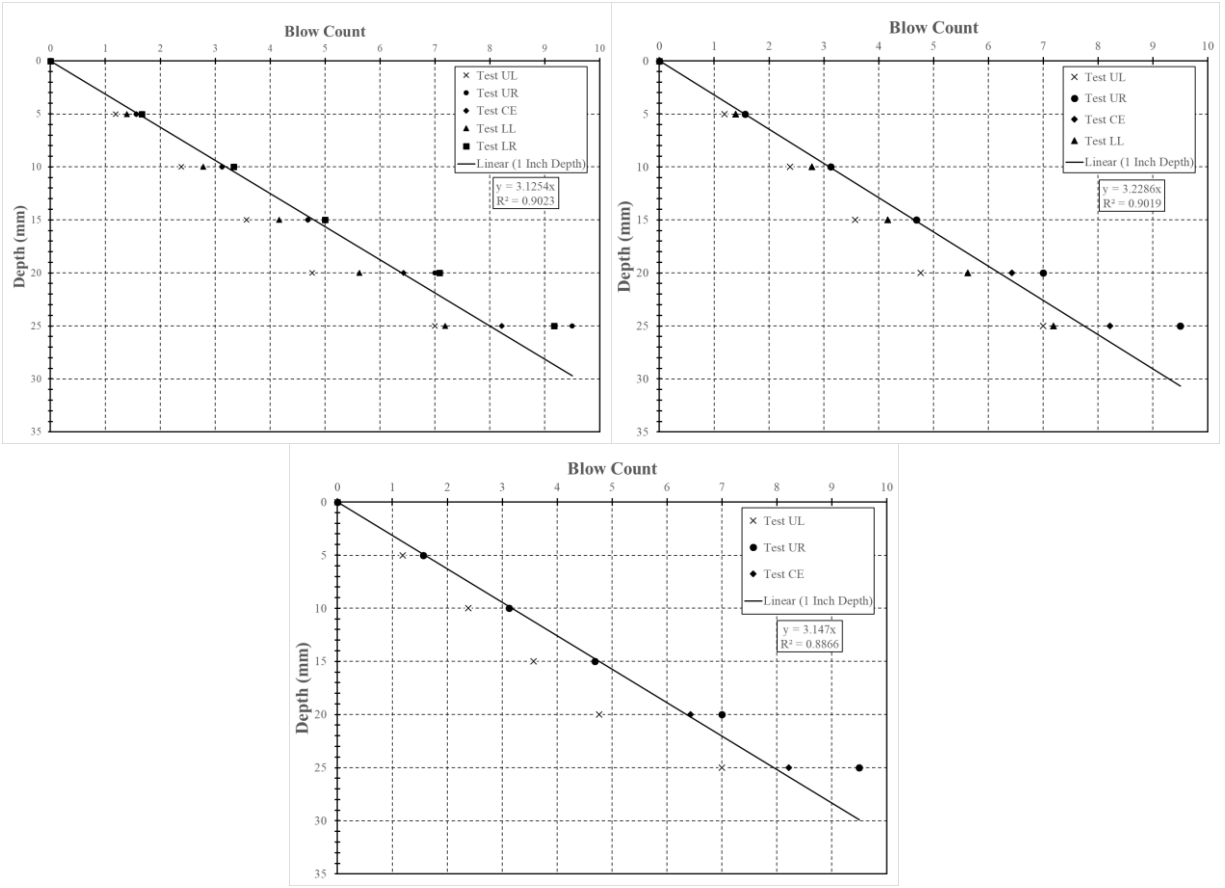


Figure J.27: Test performed on July 19, 2019, Location 34 (top left = 5 tests, top right = 4 tests, bottom = 3 tests)

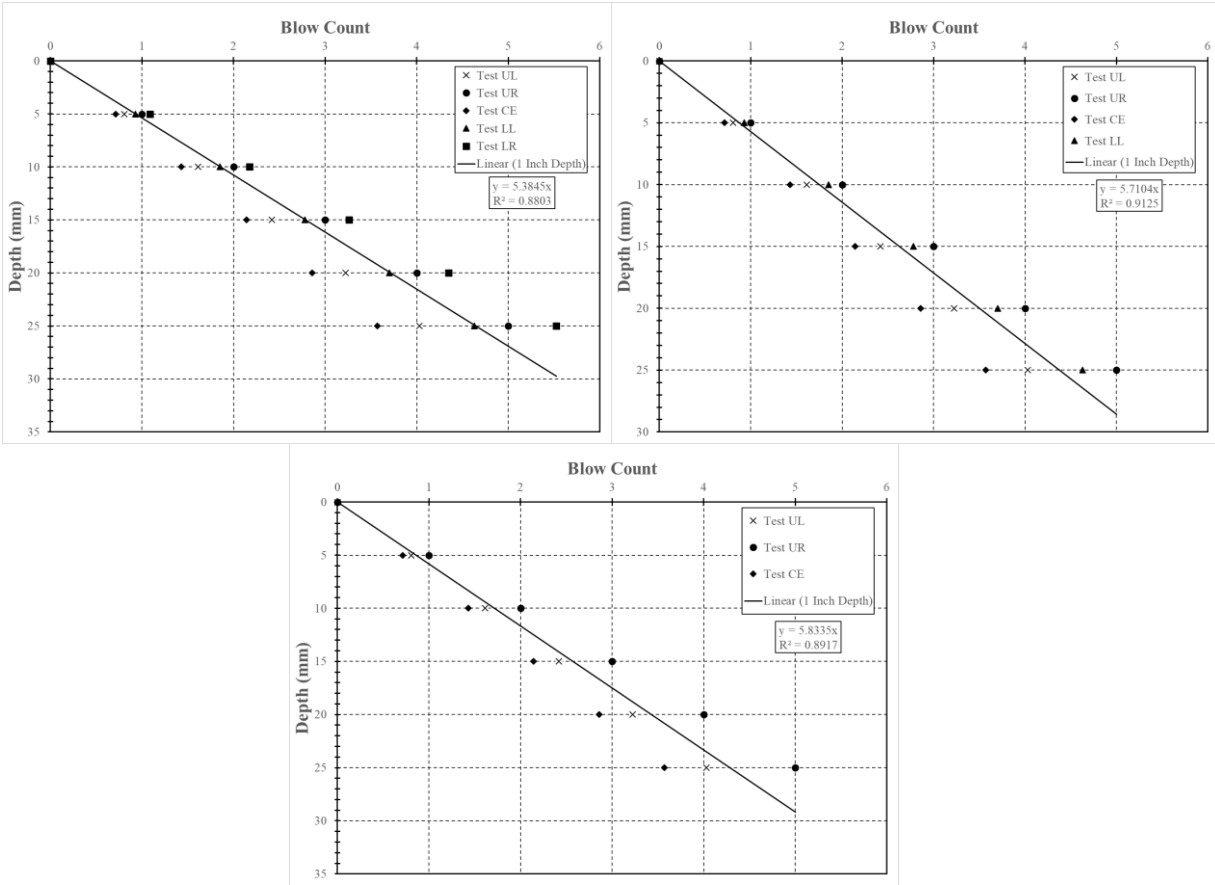


Figure J.28: Test performed on July 19, 2019, Location 35 (top left = 5 tests, top right = 4 tests, bottom = 3 tests)

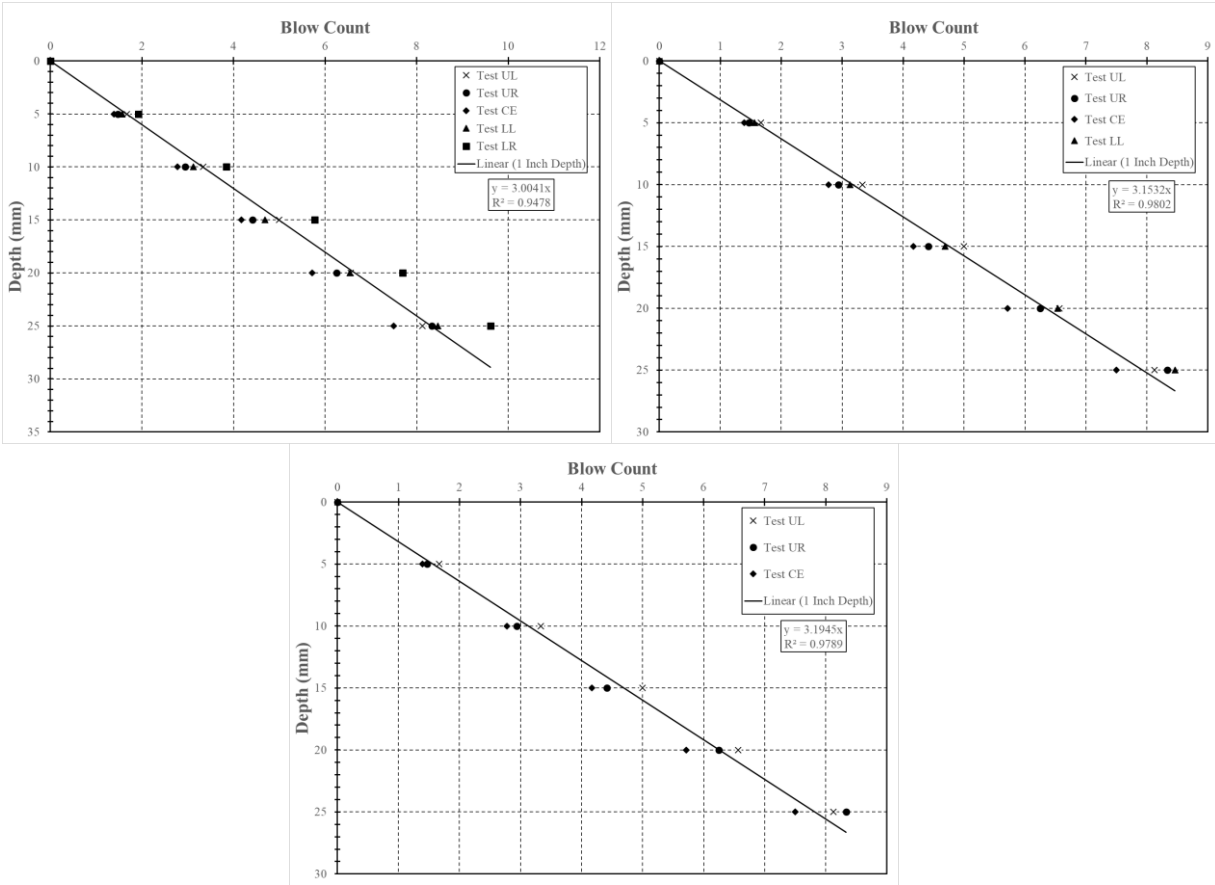


Figure J.29: Test performed on July 19, 2019, Location 36 (top left = 5 tests, top right = 4 tests, bottom = 3 tests)

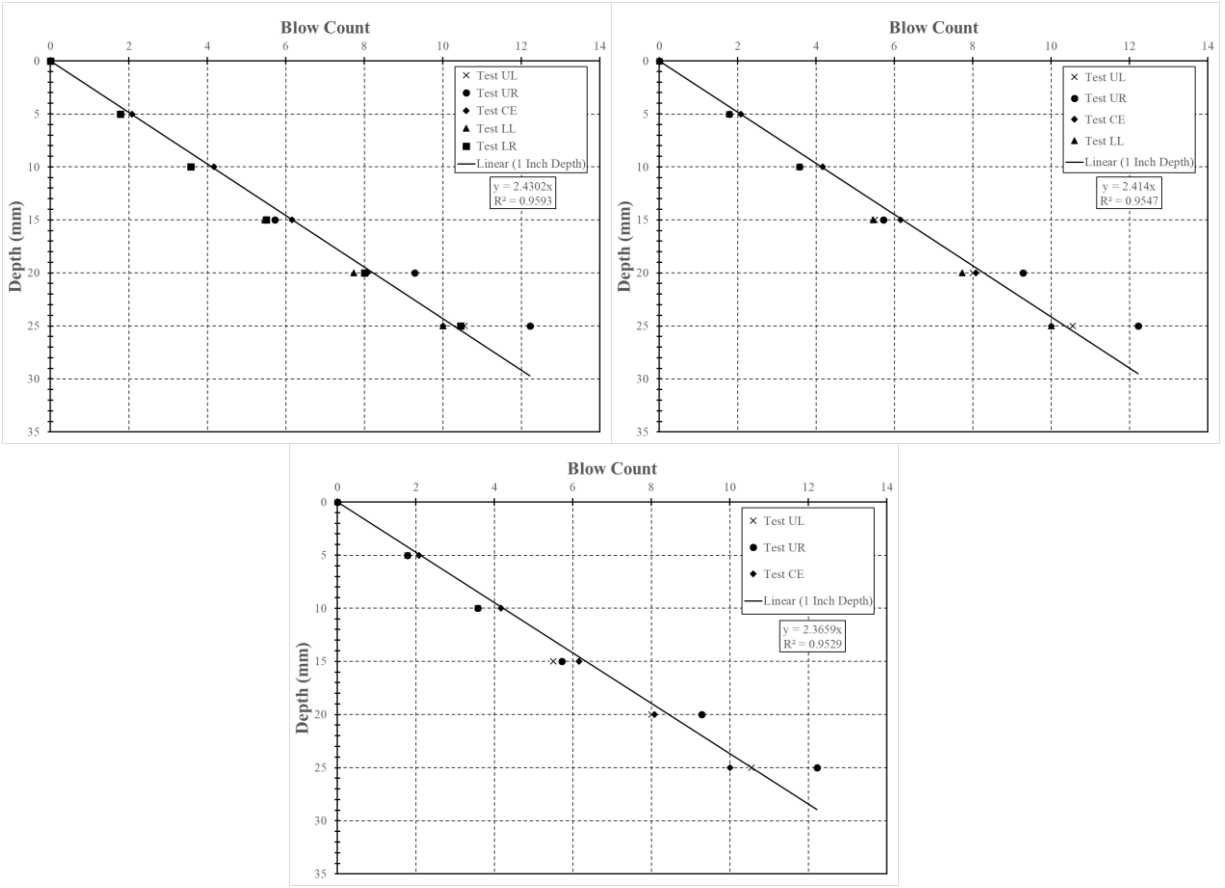


Figure J.30: Test performed on July 23, 2019, Location 37 (top left = 5 tests, top right = 4 tests, bottom = 3 tests)

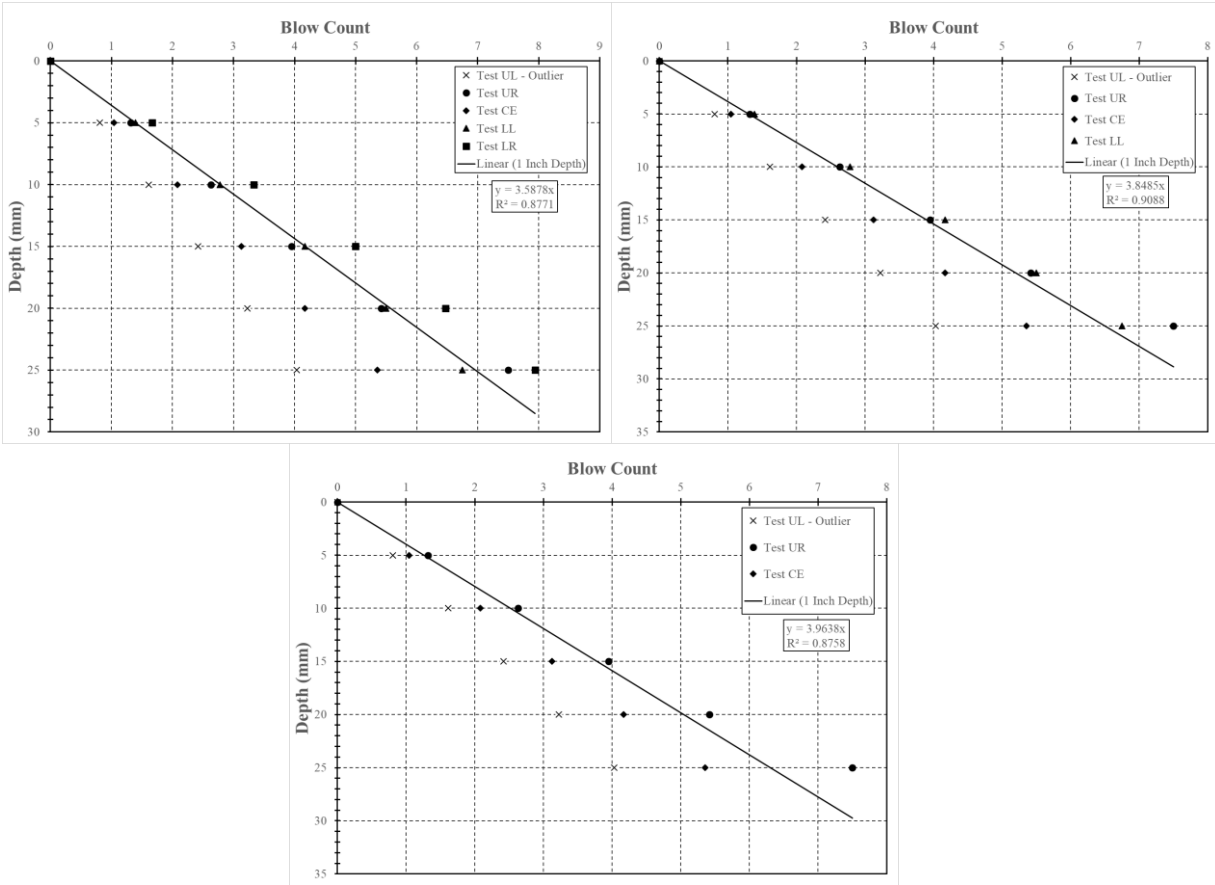


Figure J.31: Test performed on July 23, 2019, Location 38 (top left = 5 tests, top right = 4 tests, bottom = 3 tests)

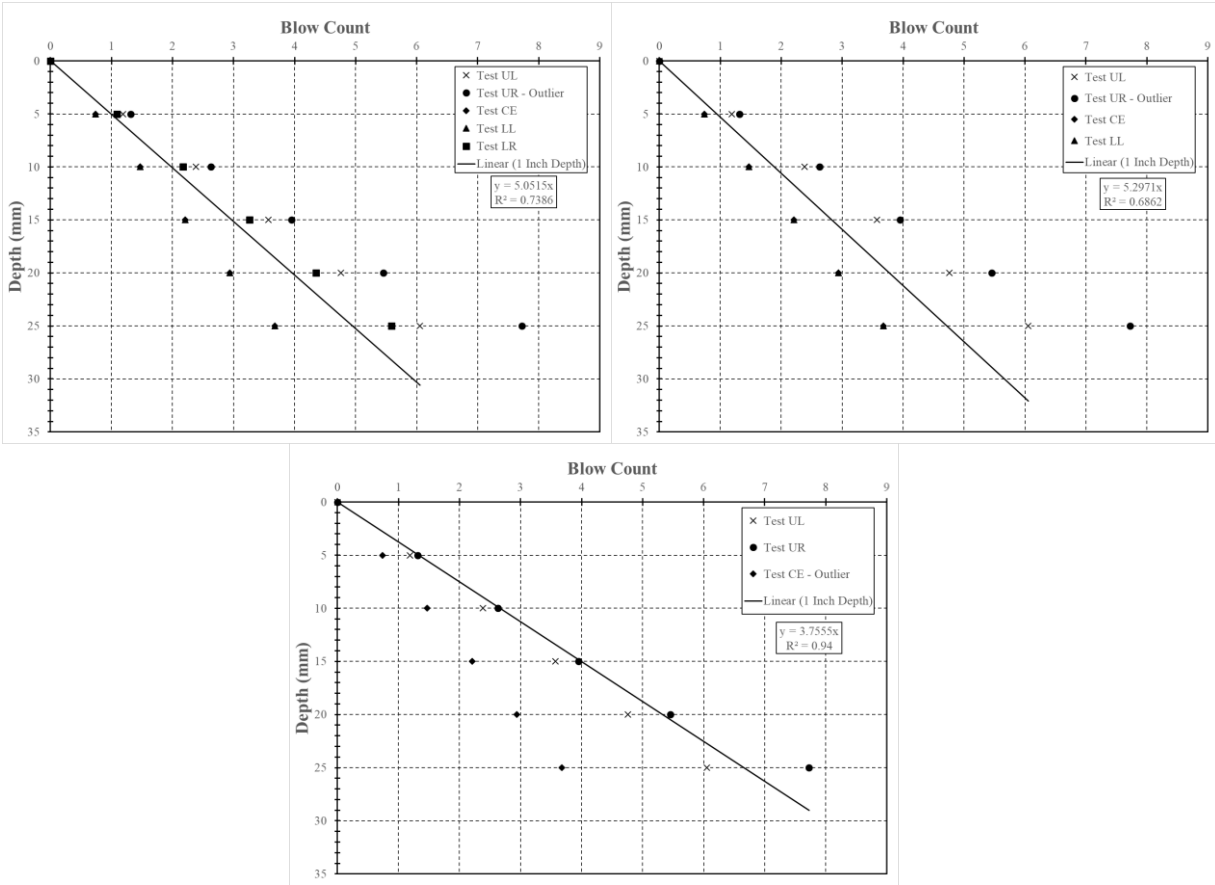


Figure J.32: Test performed on July 23, 2019, Location 39 (top left = 5 tests, top right = 4 tests, bottom = 3 tests)

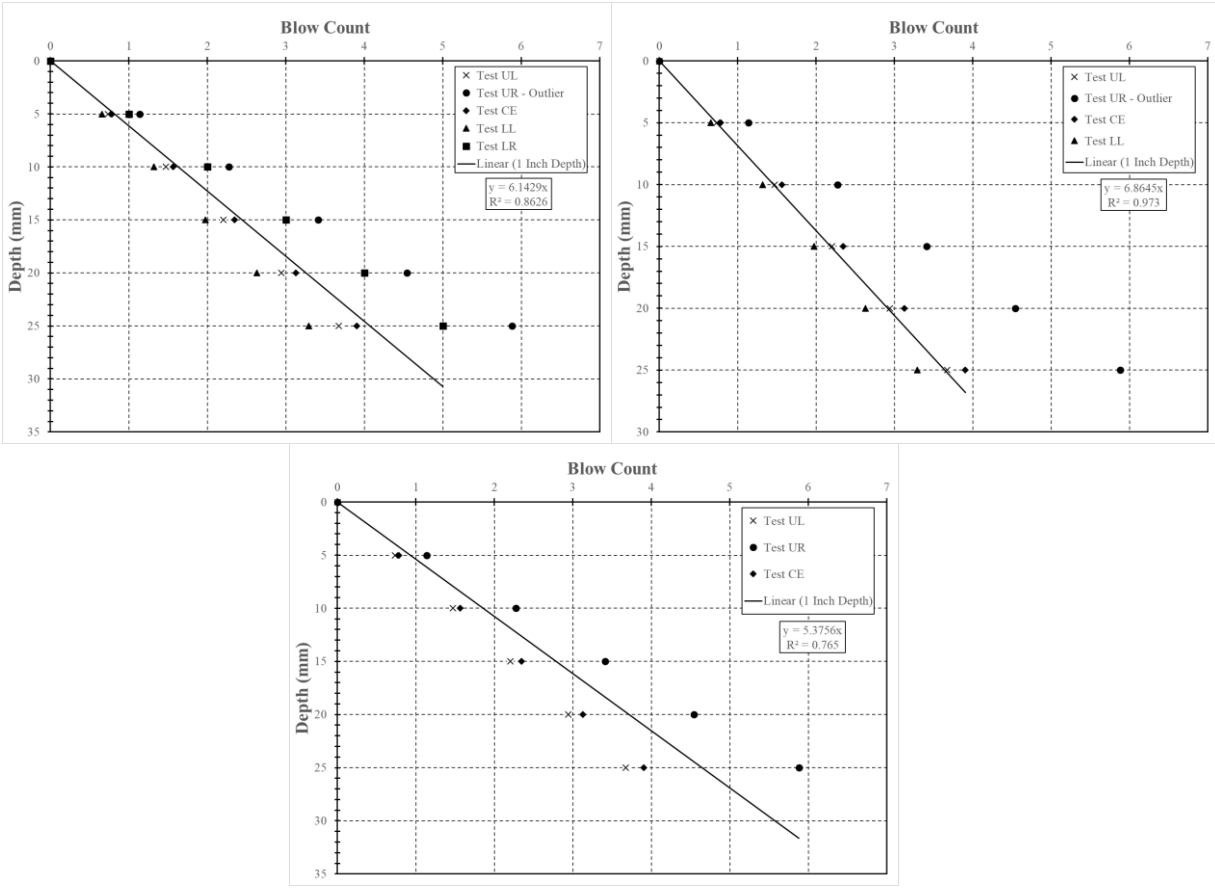


Figure J.33: Test performed on July 23, 2019, Location 40 (top left = 5 tests, top right = 4 tests, bottom = 3 tests)

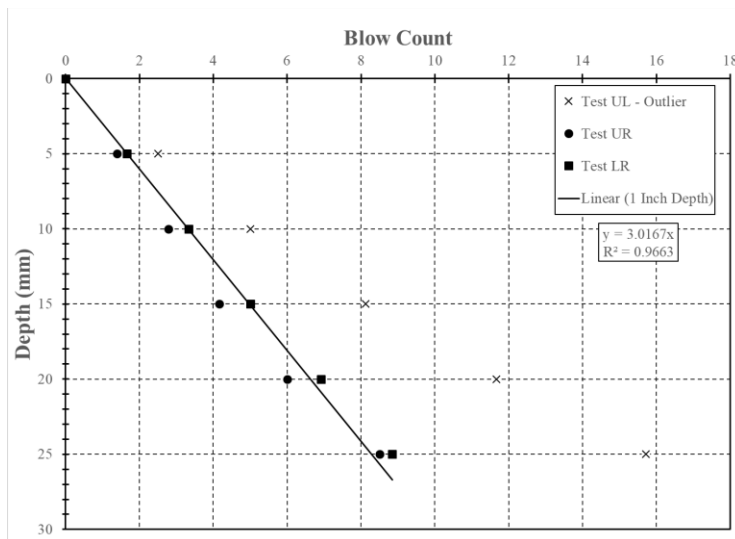


Figure J.34: Test performed on July 23, 2019, Location 41 (only 3 tests completed)

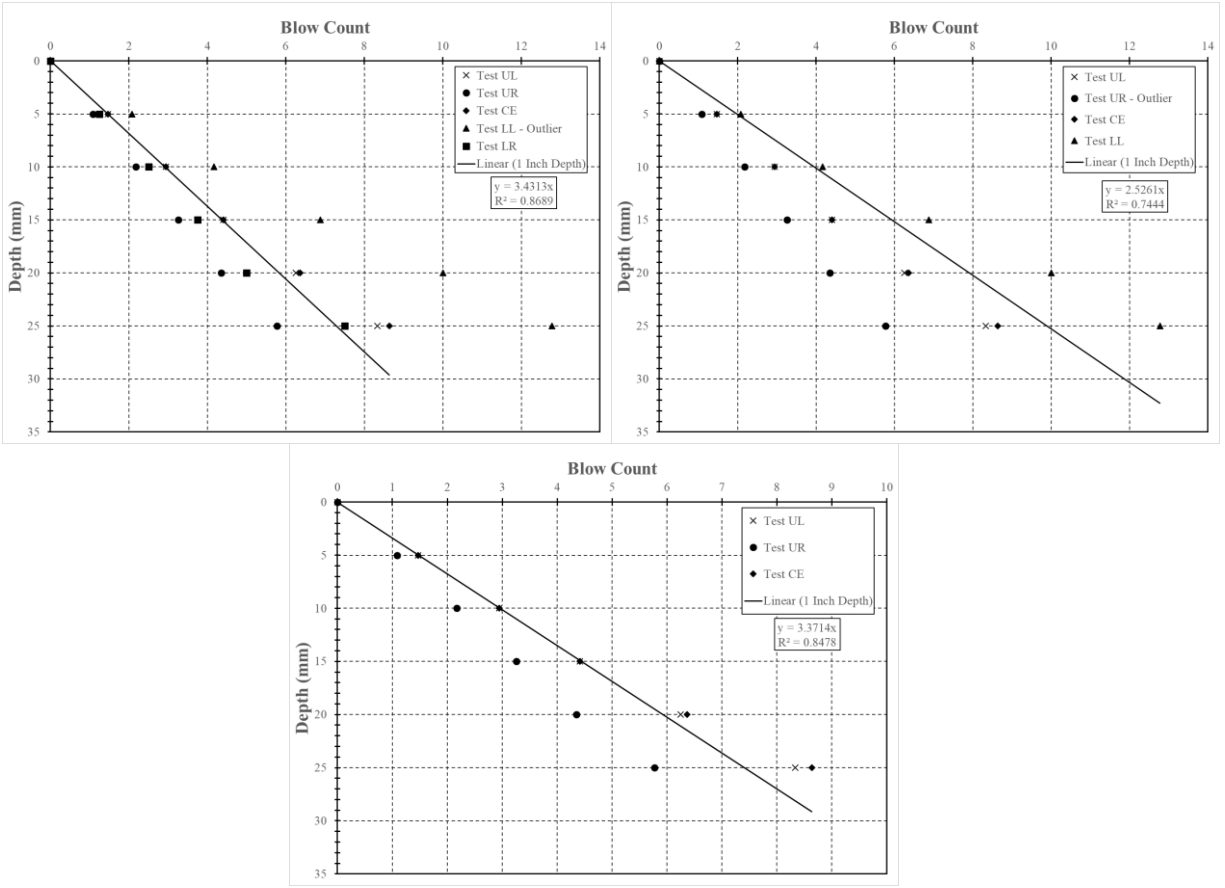


Figure J.35: Test performed on July 23, 2019, Location 42 (top left = 5 tests, top right = 4 tests, bottom = 3 tests)

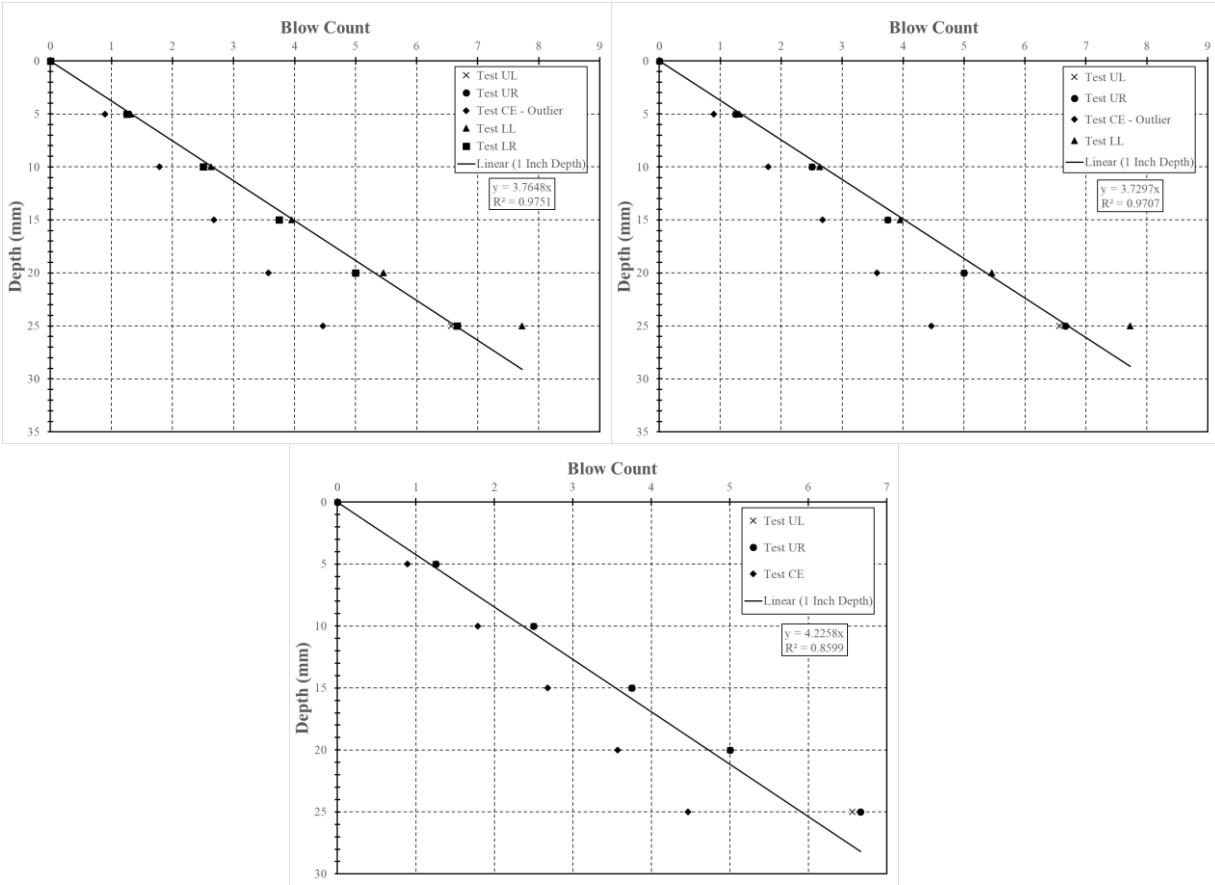


Figure J.36: Test performed on July 23, 2019, Location 43 (top left = 5 tests, top right = 4 tests, bottom = 3 tests)

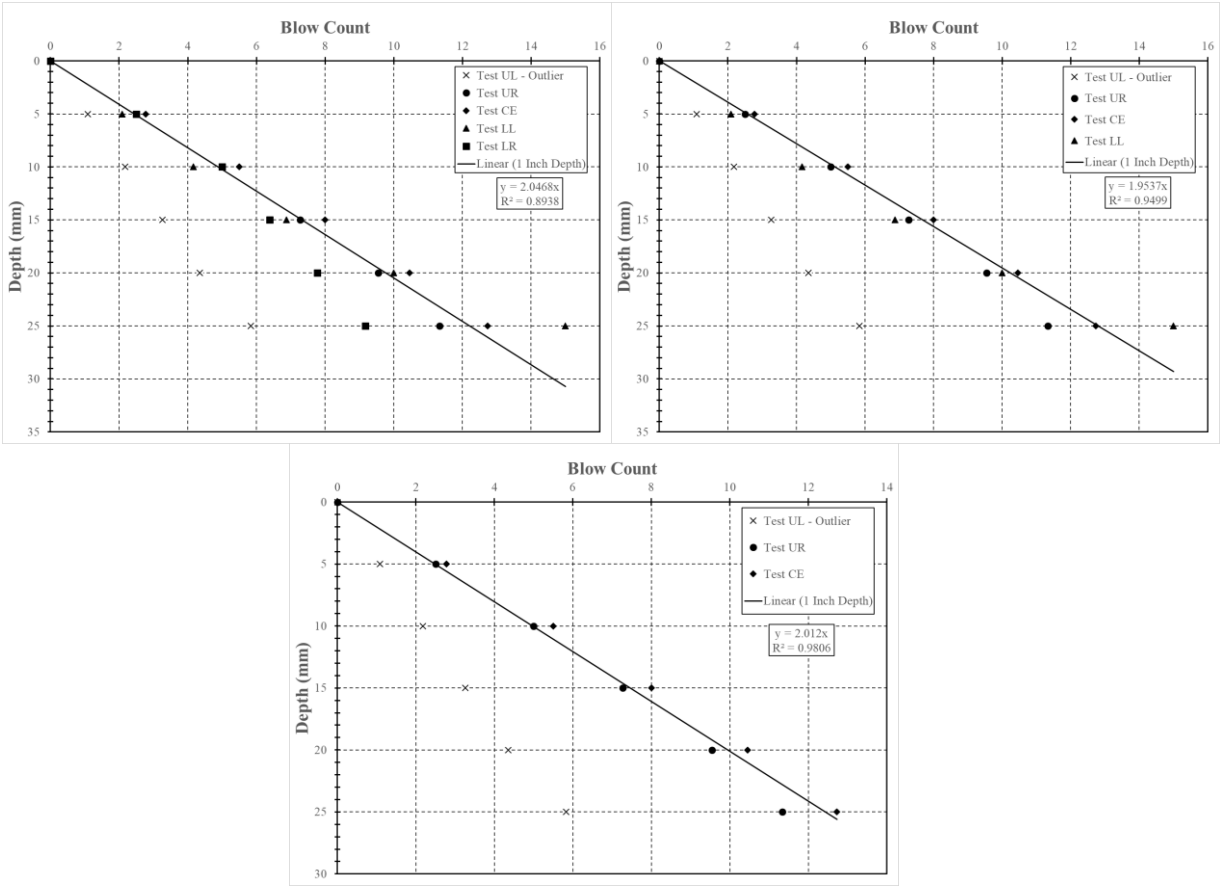


Figure J.37: Test performed on July 24, 2019, Location 44 (top left = 5 tests, top right = 4 tests, bottom = 3 tests)

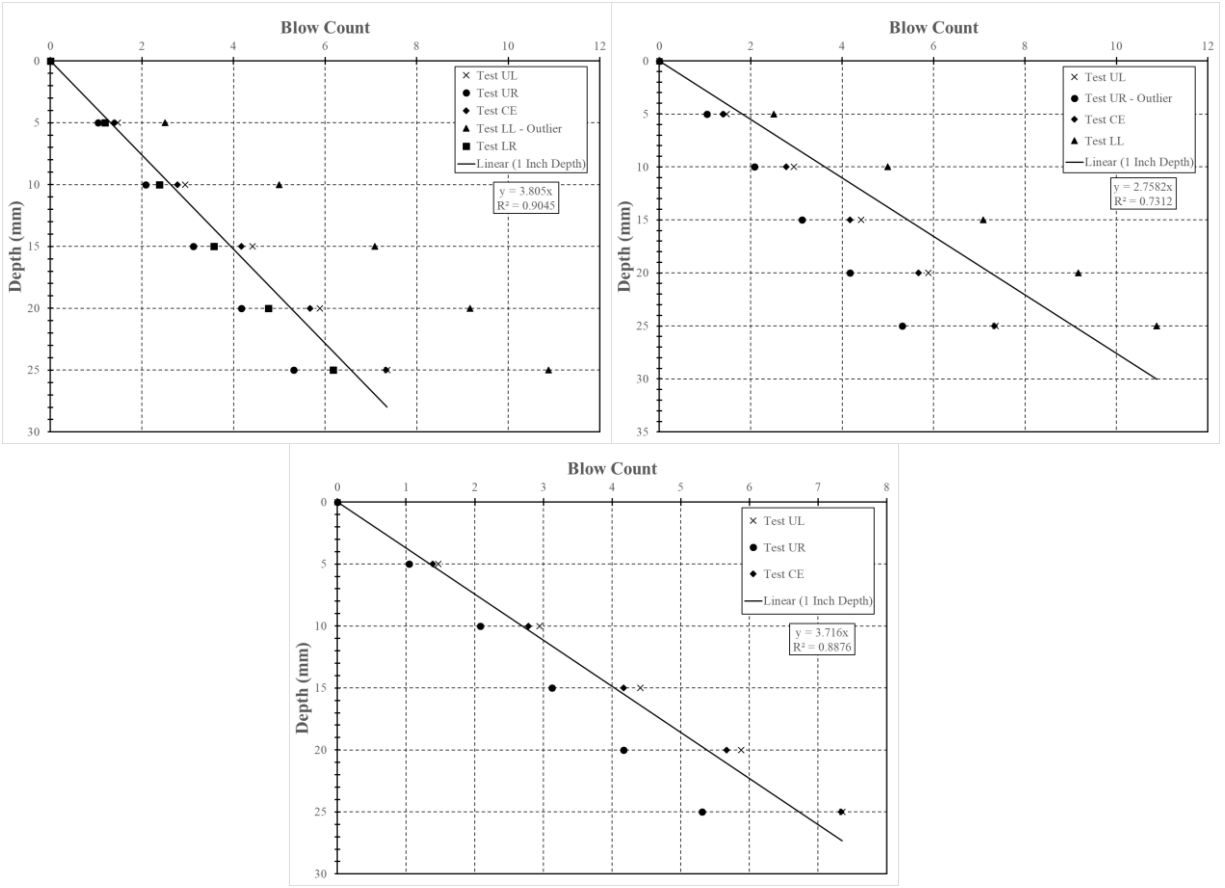


Figure J.38: Test performed on July 24, 2019, Location 45 (top left = 5 tests, top right = 4 tests, bottom = 3 tests)

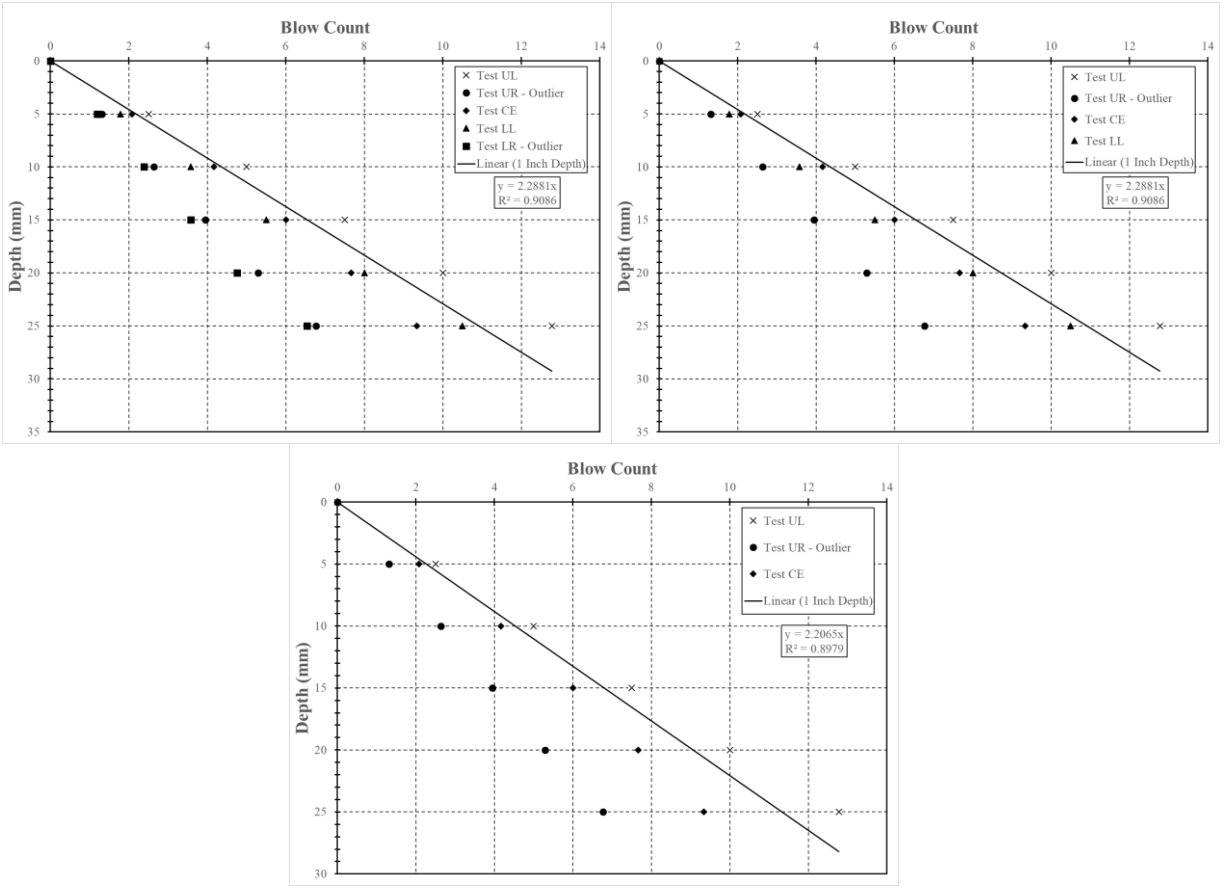


Figure J.39: Test performed on July 24, 2019, Location 46 (top left = 5 tests, top right = 4 tests, bottom = 3 tests)

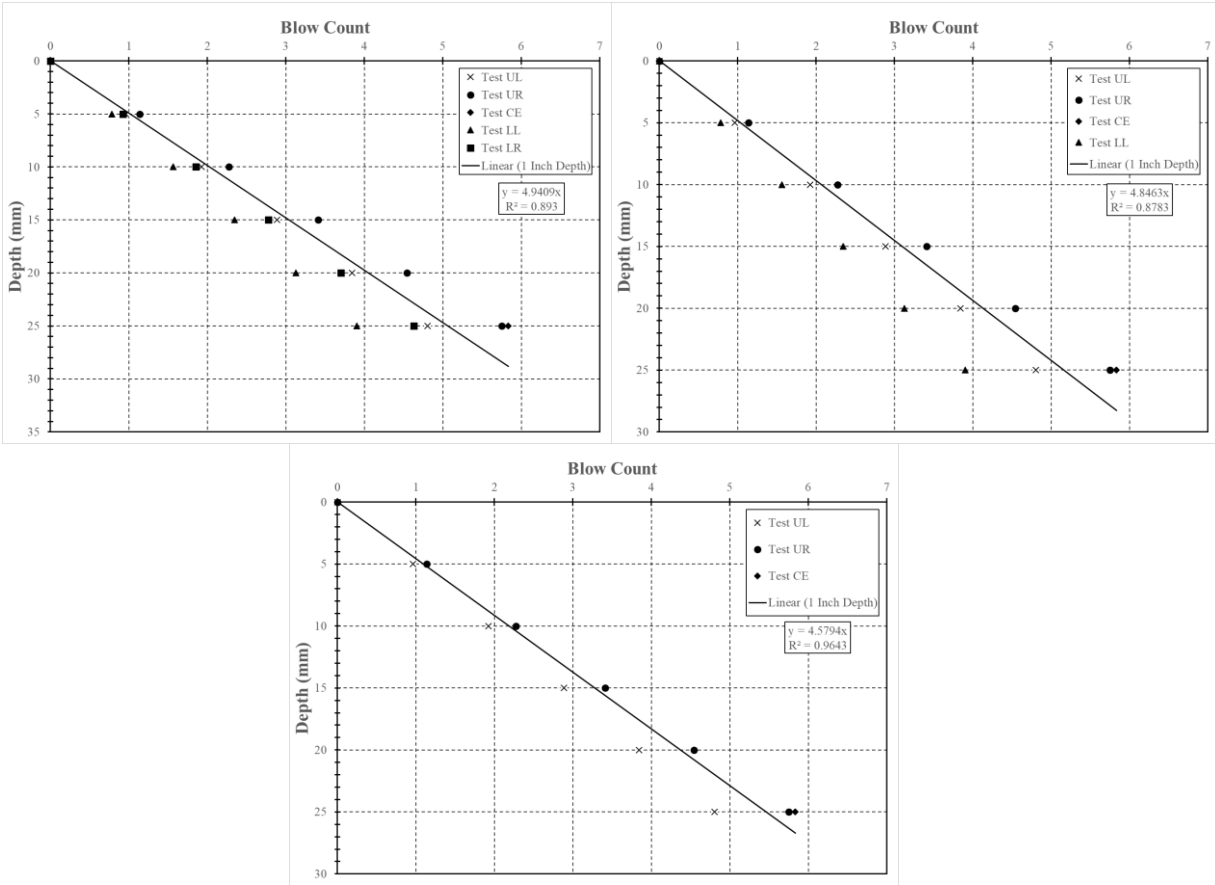


Figure J.40: Test performed on July 24, 2019, Location 47 (top left = 5 tests, top right = 4 tests, bottom = 3 tests)

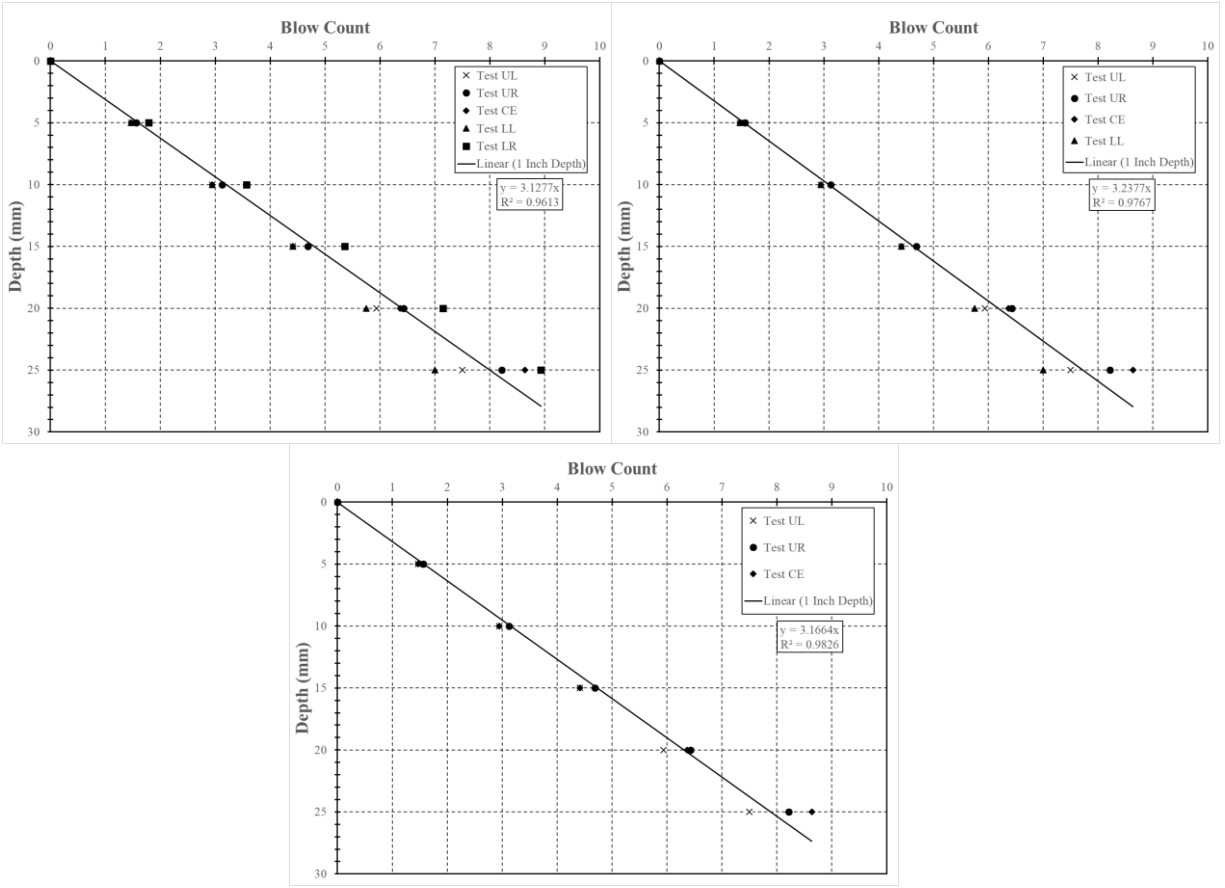


Figure J.41: Test performed on July 24, 2019, Location 48 (top left = 5 tests, top right = 4 tests, bottom = 3 tests)

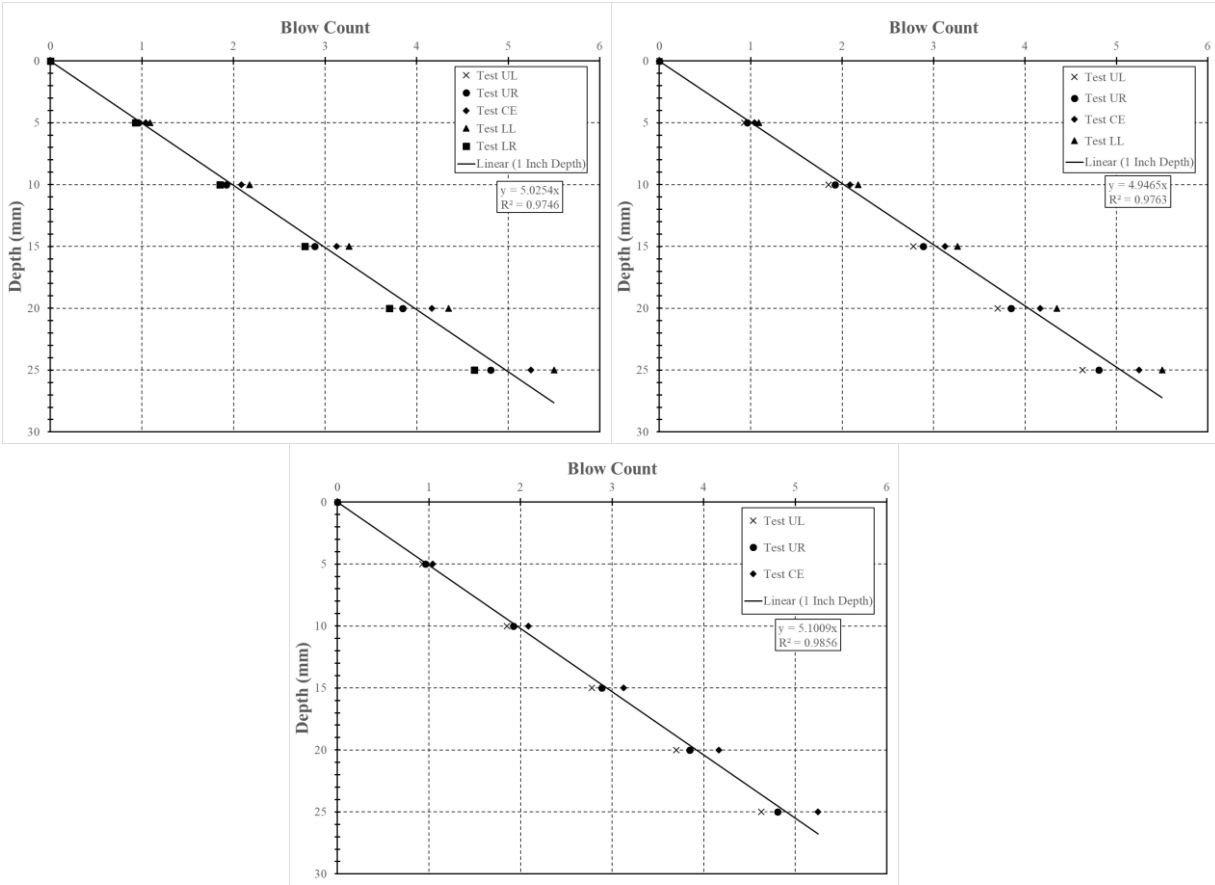


Figure J.42: Test performed on July 24, 2019, Location 49 (top left = 5 tests, top right = 4 tests, bottom = 3 tests)

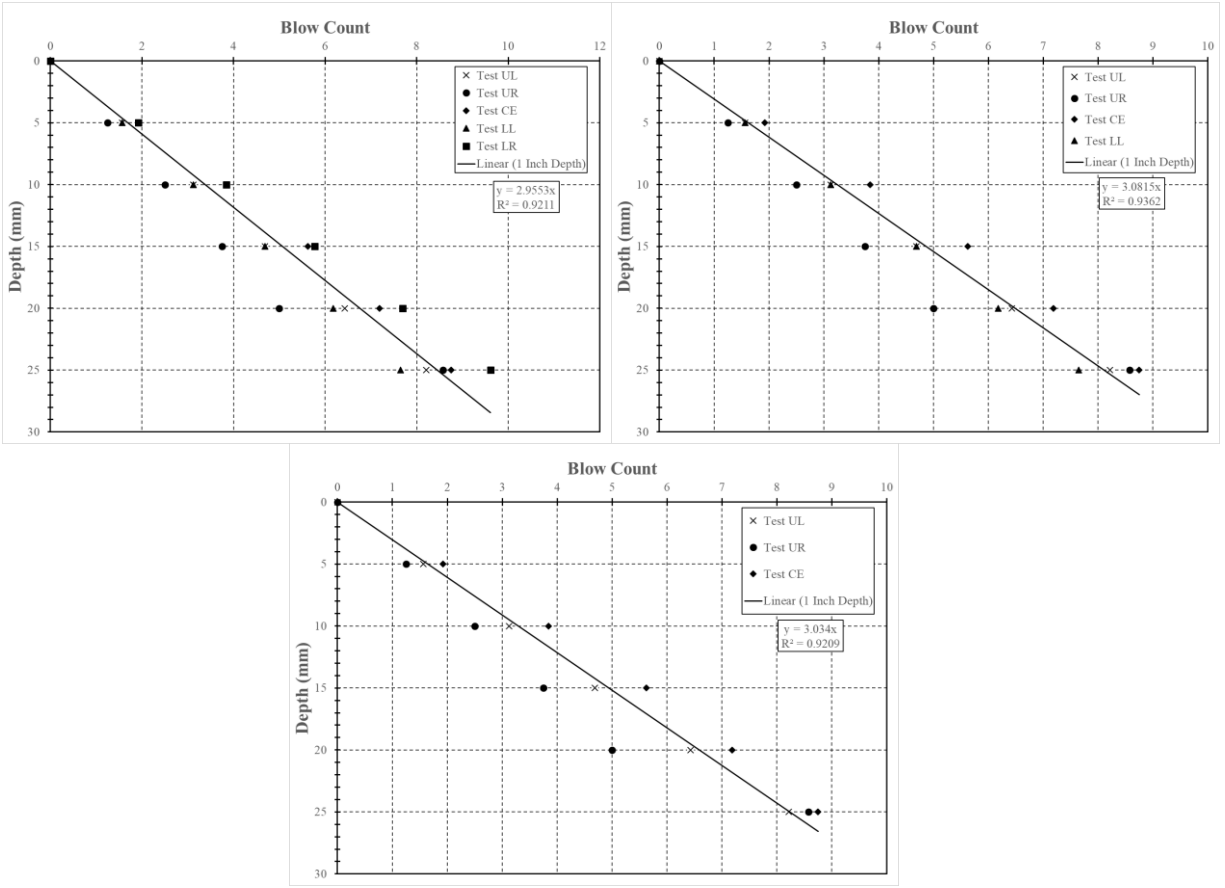


Figure J.43: Test performed on July 24, 2019, Location 50 (top left = 5 tests, top right = 4 tests, bottom = 3 tests)

Appendix K

50 Millimeter Penetration Field Data

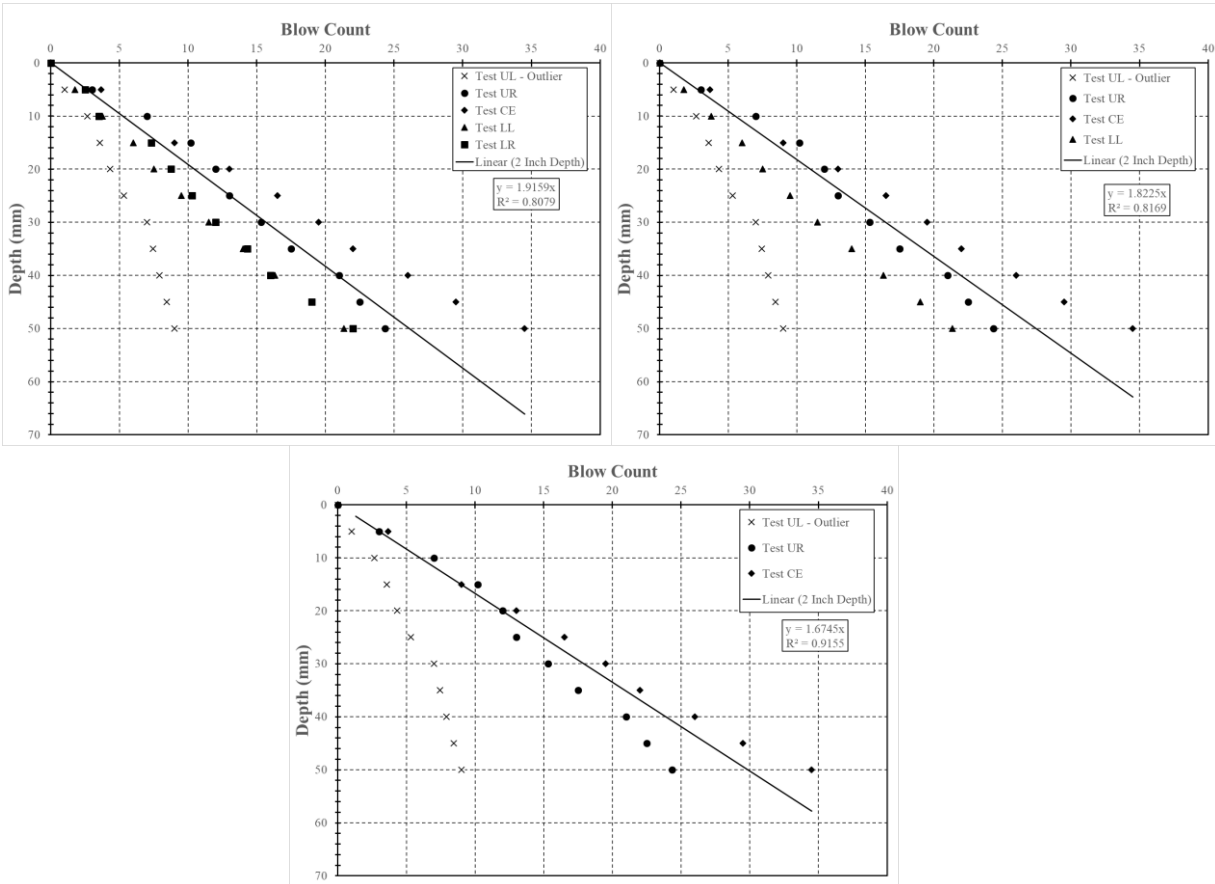


Figure K.1: Test performed on July 9, 2019, Location 1 (top left = 5 tests, top right = 4 tests, bottom = 3 tests)

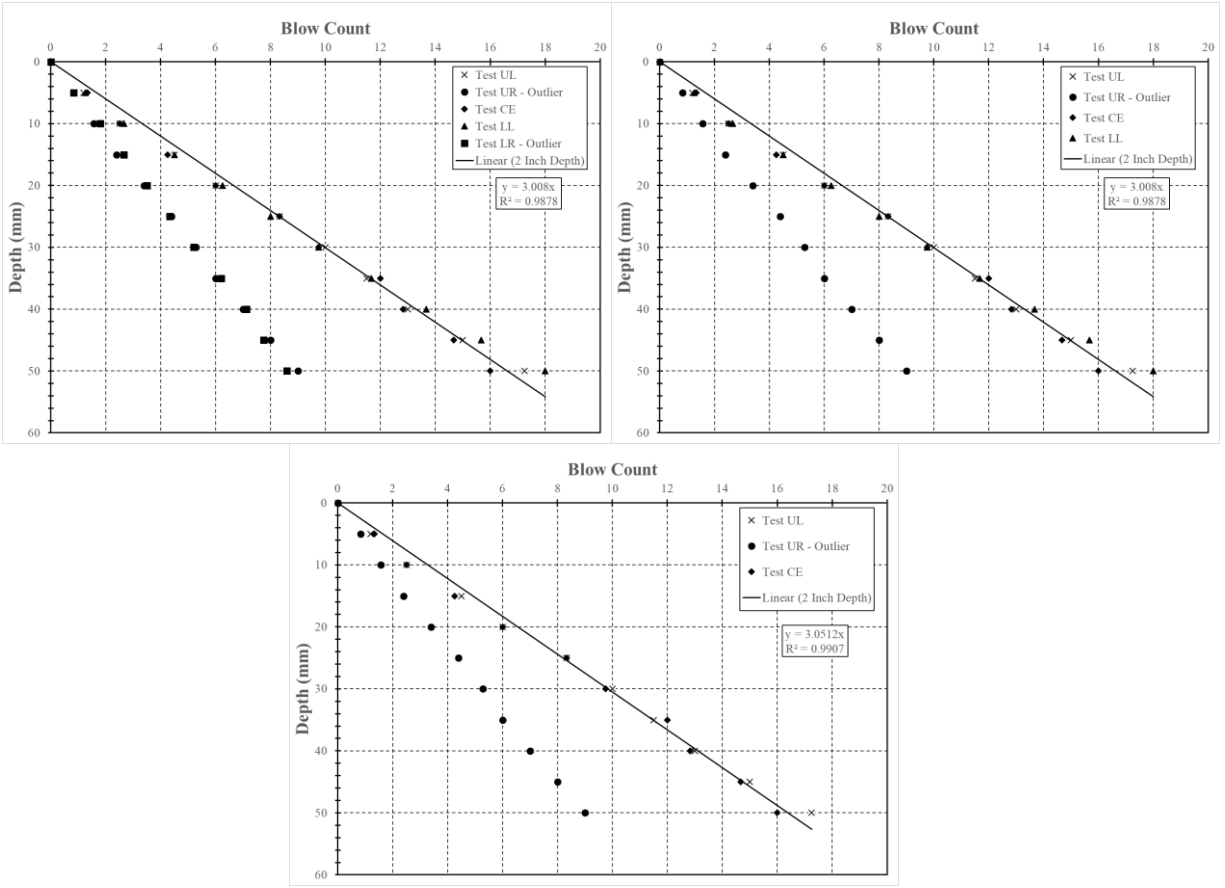


Figure K.2: Test performed on July 10, 2019, Location 4 (top left = 5 tests, top right = 4 tests, bottom = 3 tests)

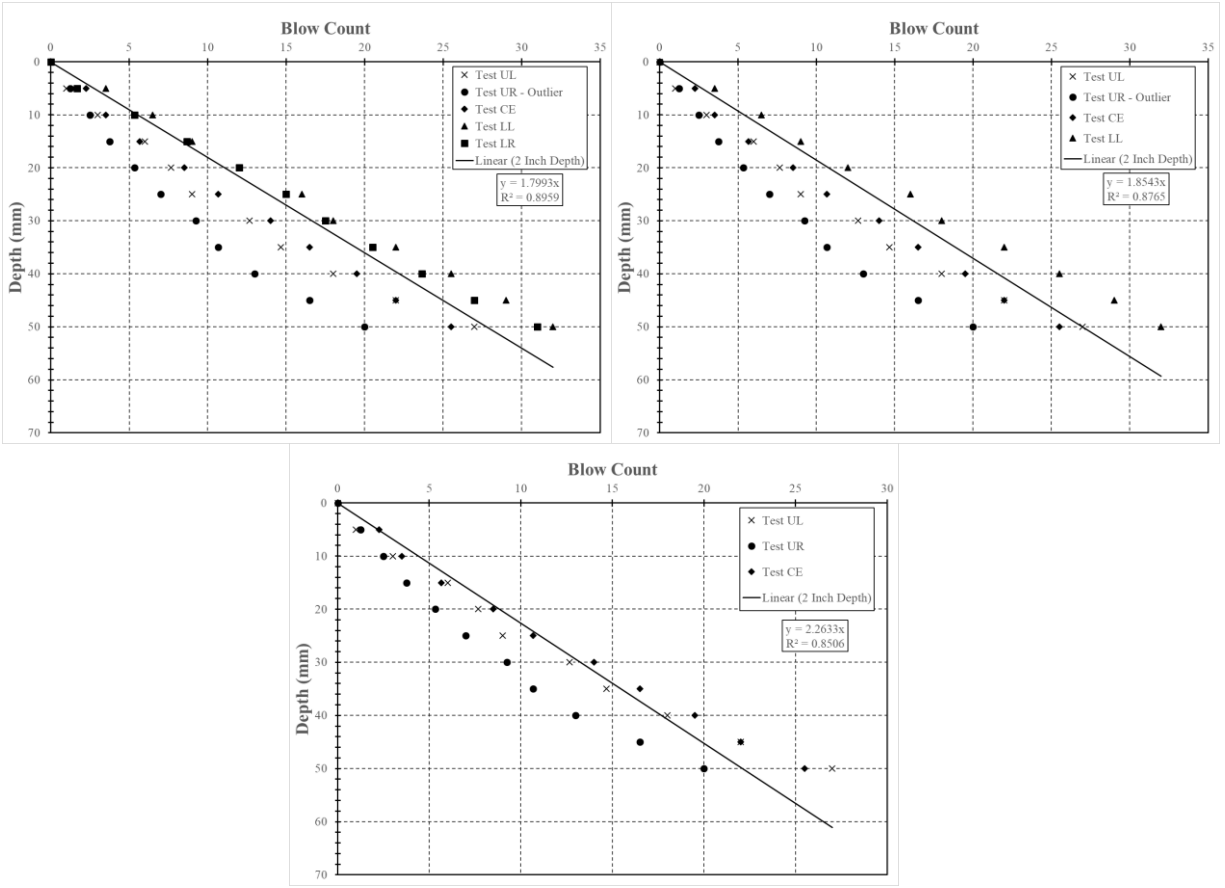


Figure K.3: Test performed on July 10, 2019, Location 5 (top left = 5 tests, top right = 4 tests, bottom = 3 tests)

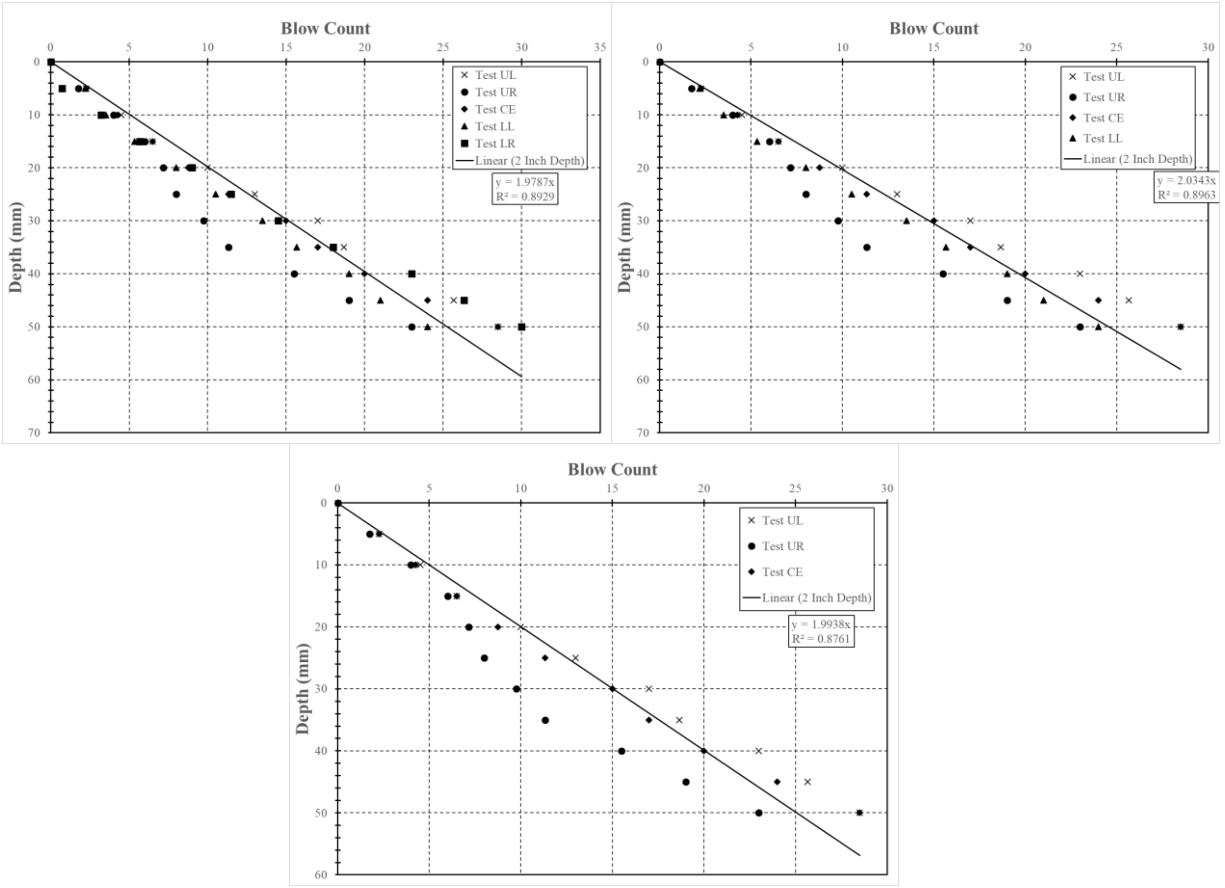


Figure K.4: Test performed on July 10, 2019, Location 6 (top left = 5 tests, top right = 4 tests, bottom = 3 tests)

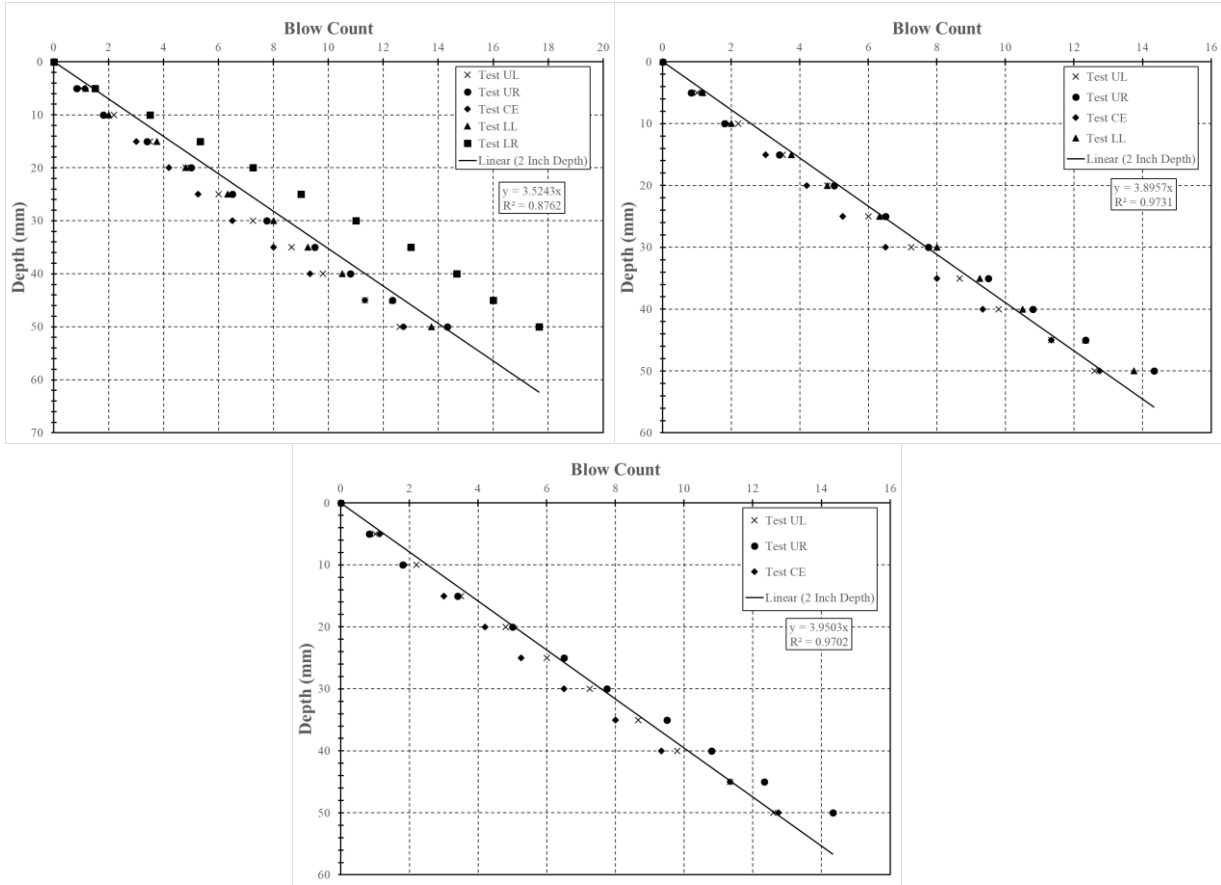


Figure K.5: Test performed on July 16, 2019, Location 7 (top left = 5 tests, top right = 4 tests, bottom = 3 tests)

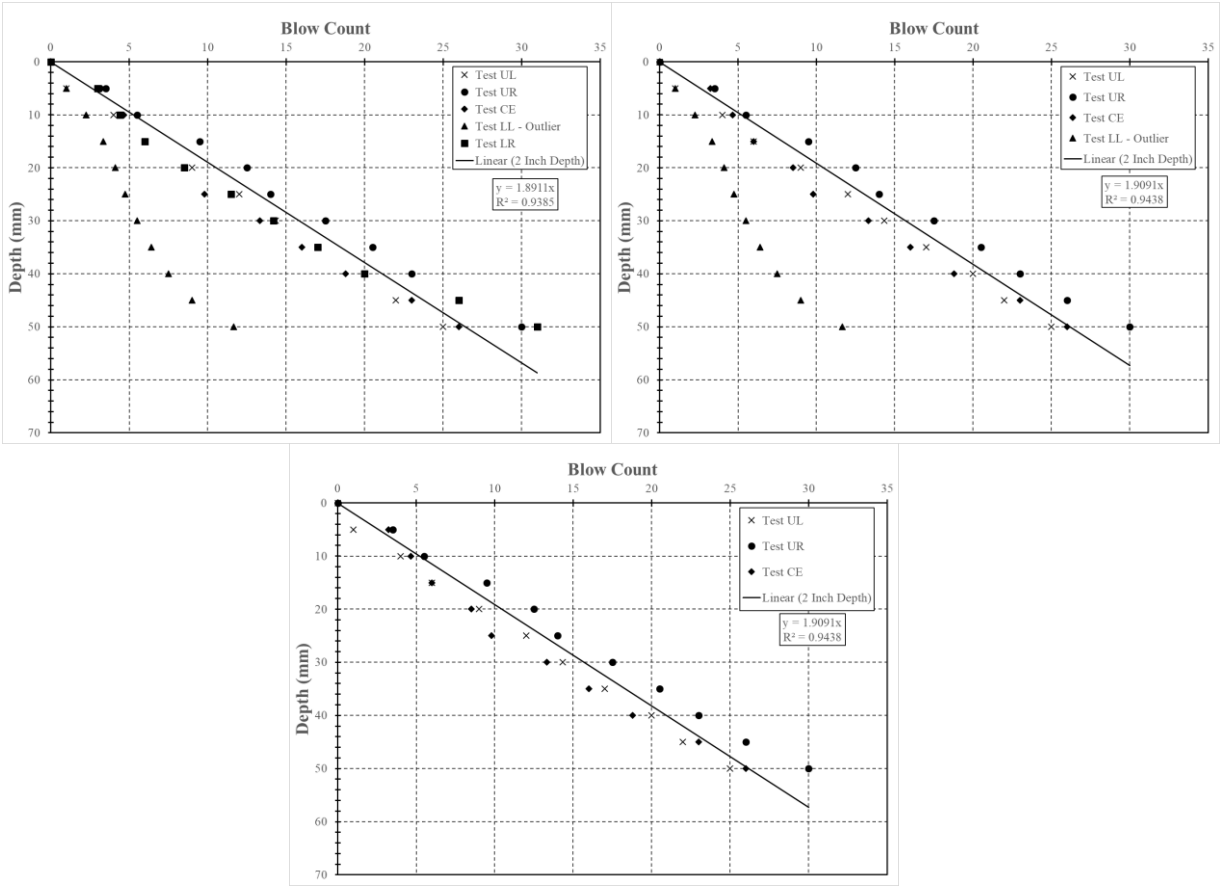


Figure K.6: Test performed on July 16, 2019, Location 8 (top left = 5 tests, top right = 4 tests, bottom = 3 tests)

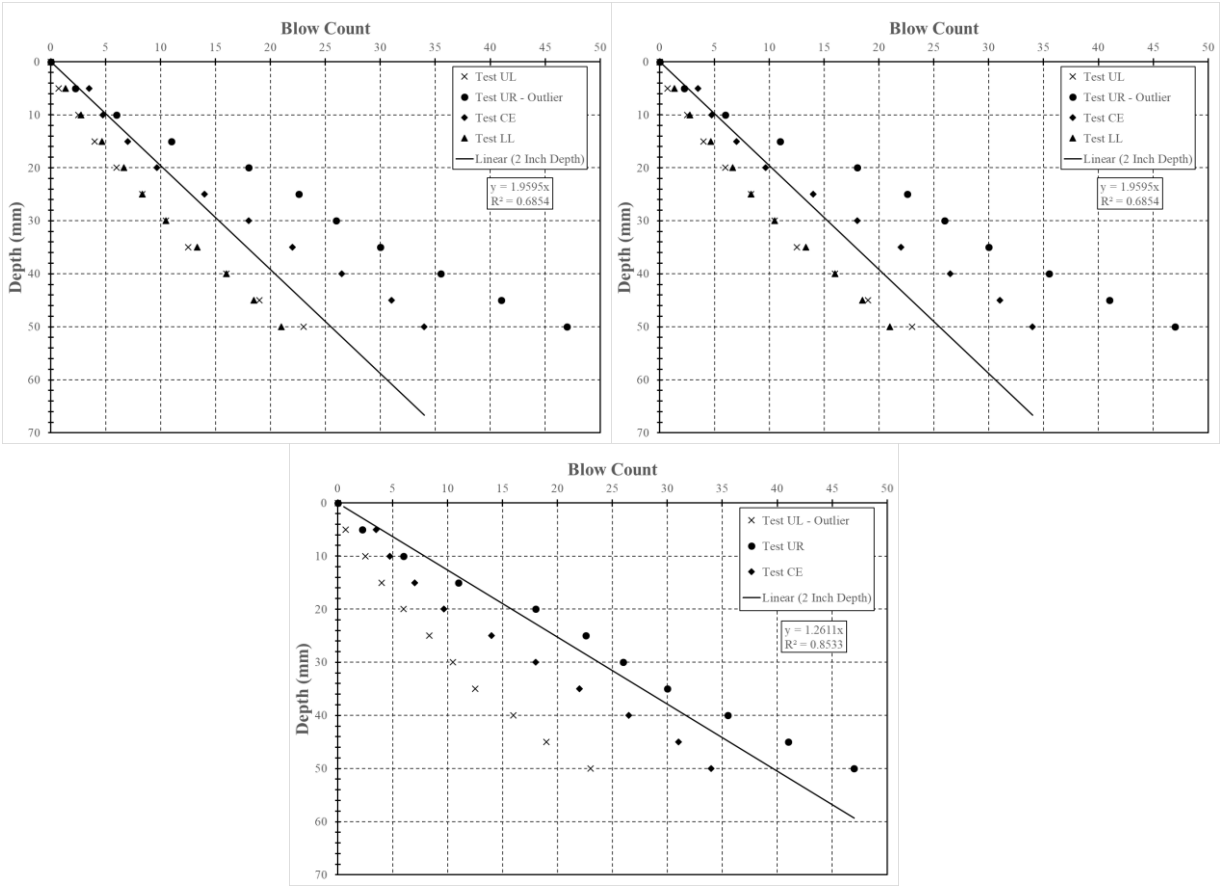


Figure K.7: Test performed on July 16, 2019, Location 9 (top left = 5 tests, top right = 4 tests, bottom = 3 tests)

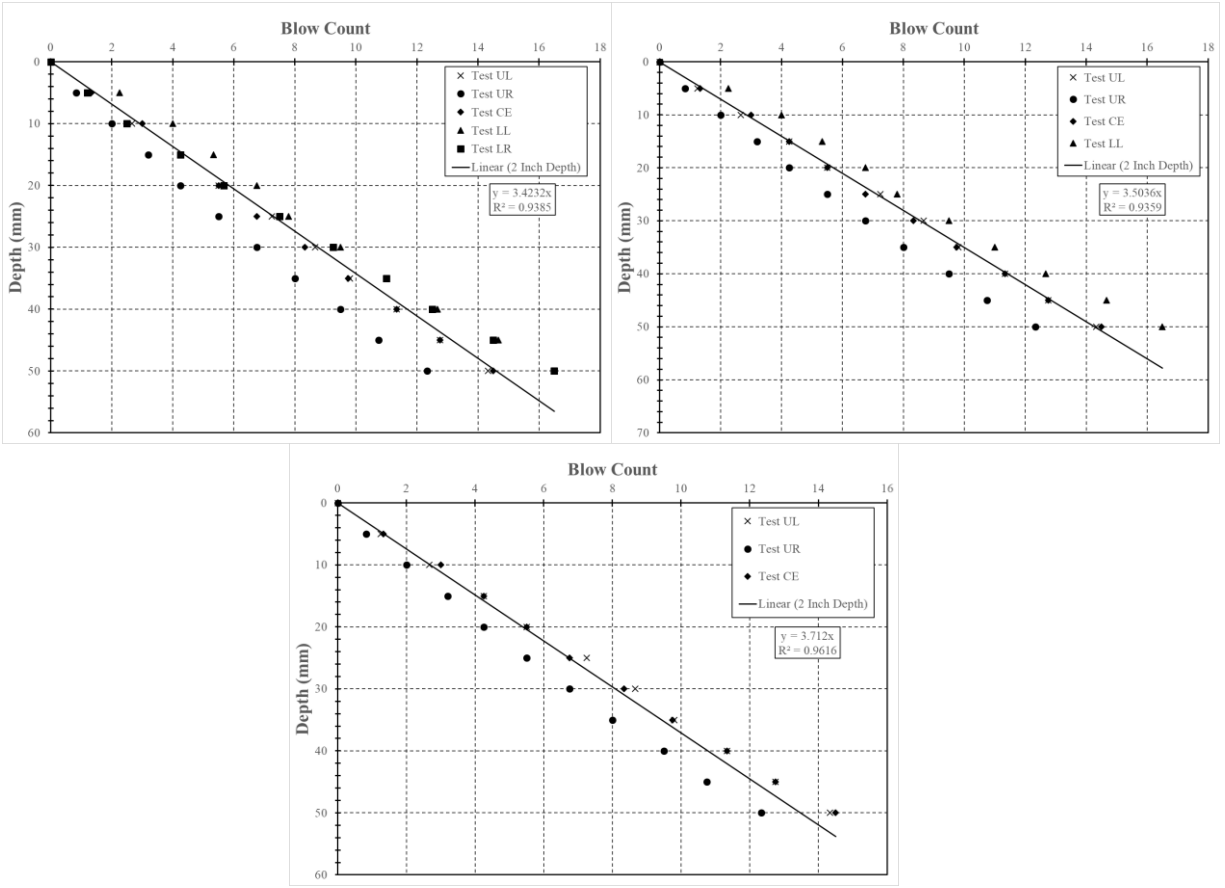


Figure K.8: Test performed on July 16, 2019, Location 10 (top left = 5 tests, top right = 4 tests, bottom = 3 tests)

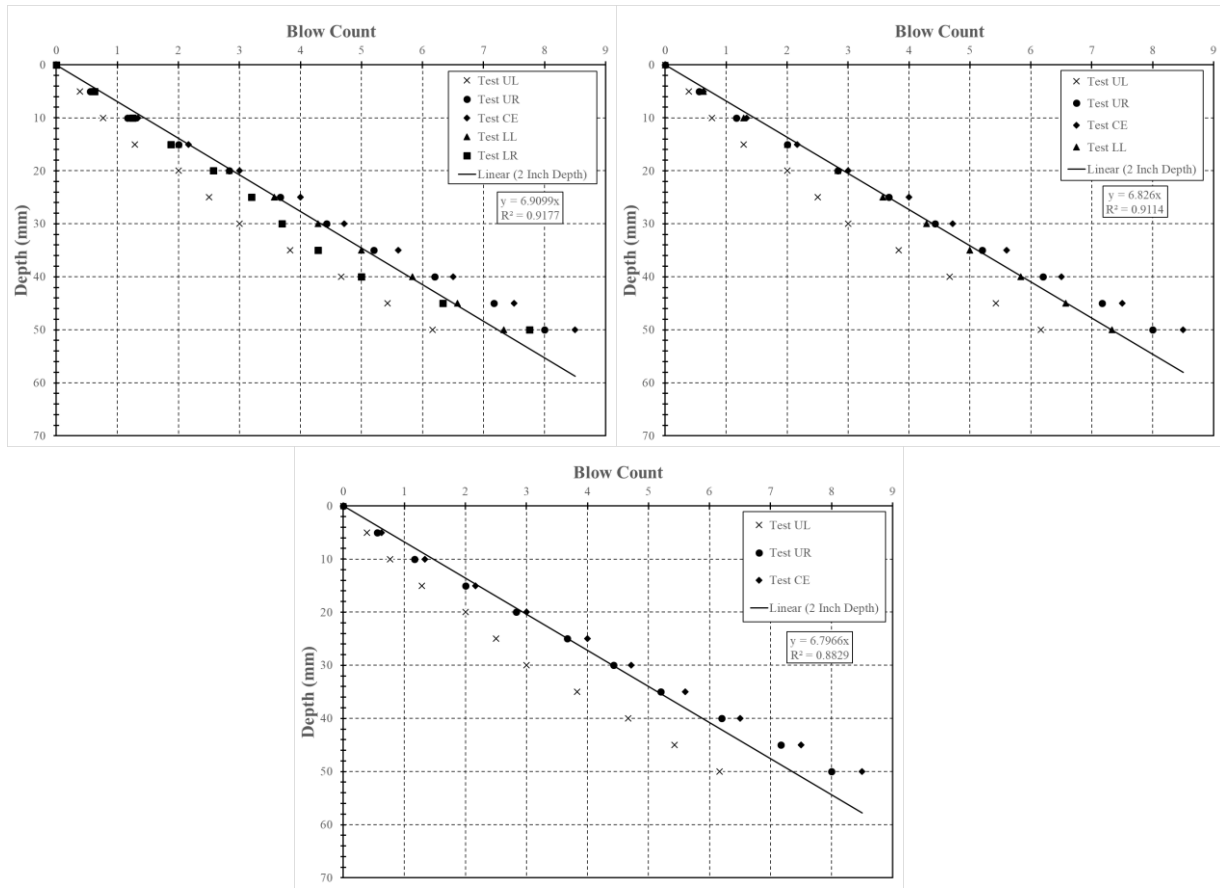


Figure K.9: Test performed on July 16, 2019, Location 11 (top left = 5 tests, top right = 4 tests, bottom = 3 tests)

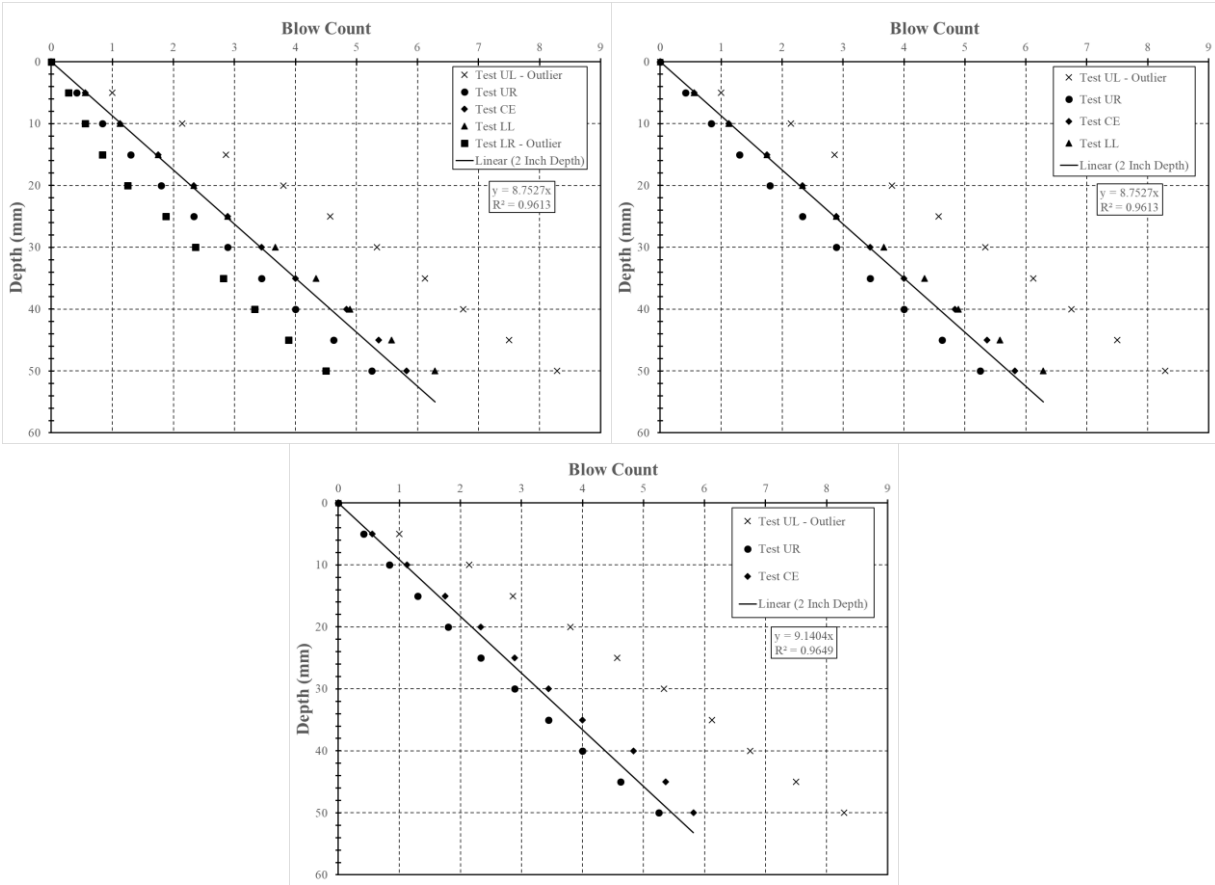


Figure K.10: Test performed on July 16, 2019, Location 12 (top left = 5 tests, top right = 4 tests, bottom = 3 tests)

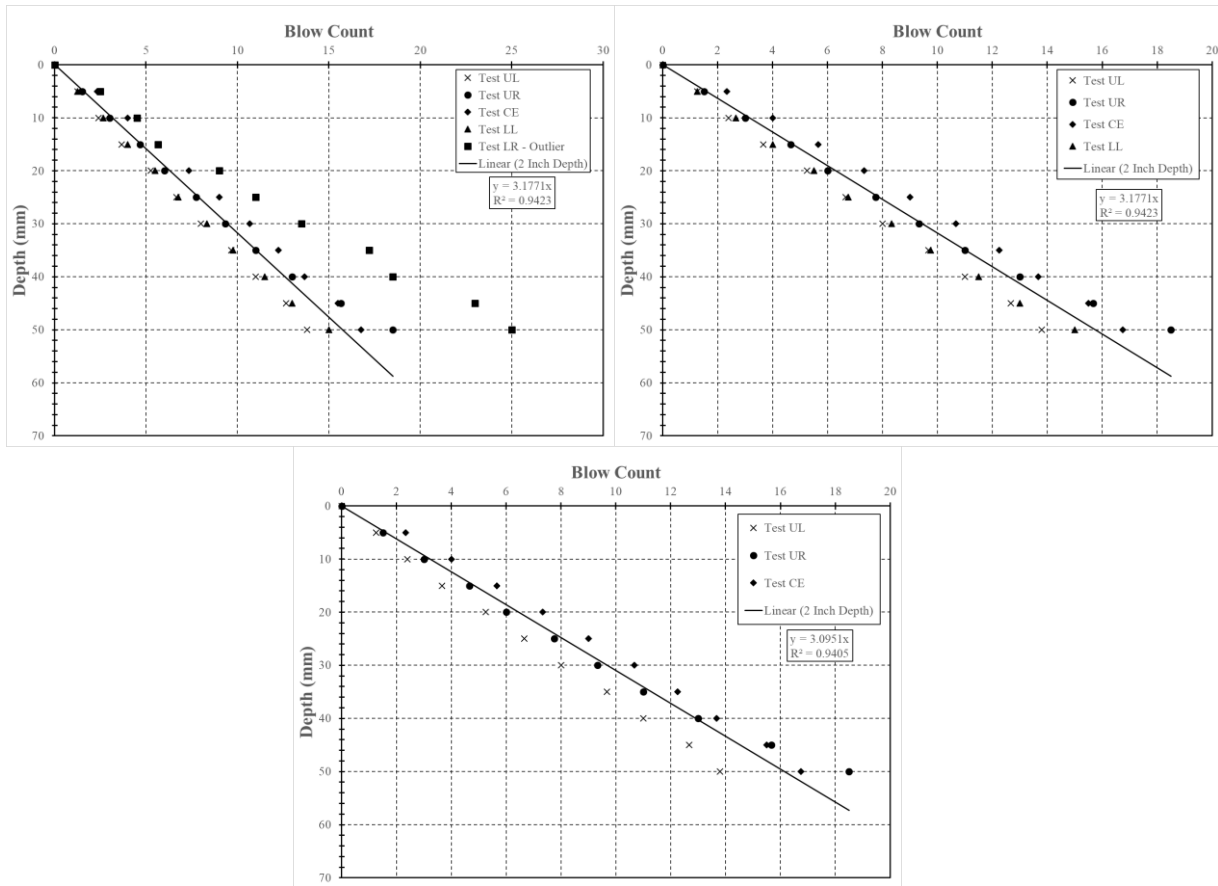


Figure K.11: Test performed on July 16, 2019, Location 13 (top left = 5 tests, top right = 4 tests, bottom = 3 tests)

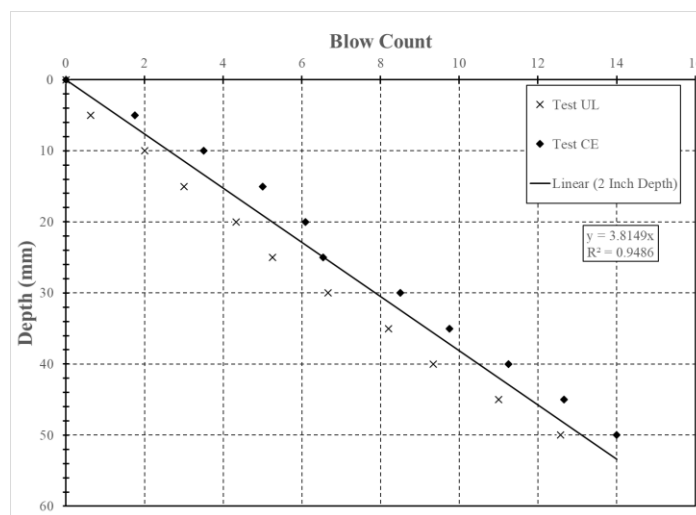


Figure K.12: Test performed on July 16, 2019, Location 15 (only 2 tests completed)

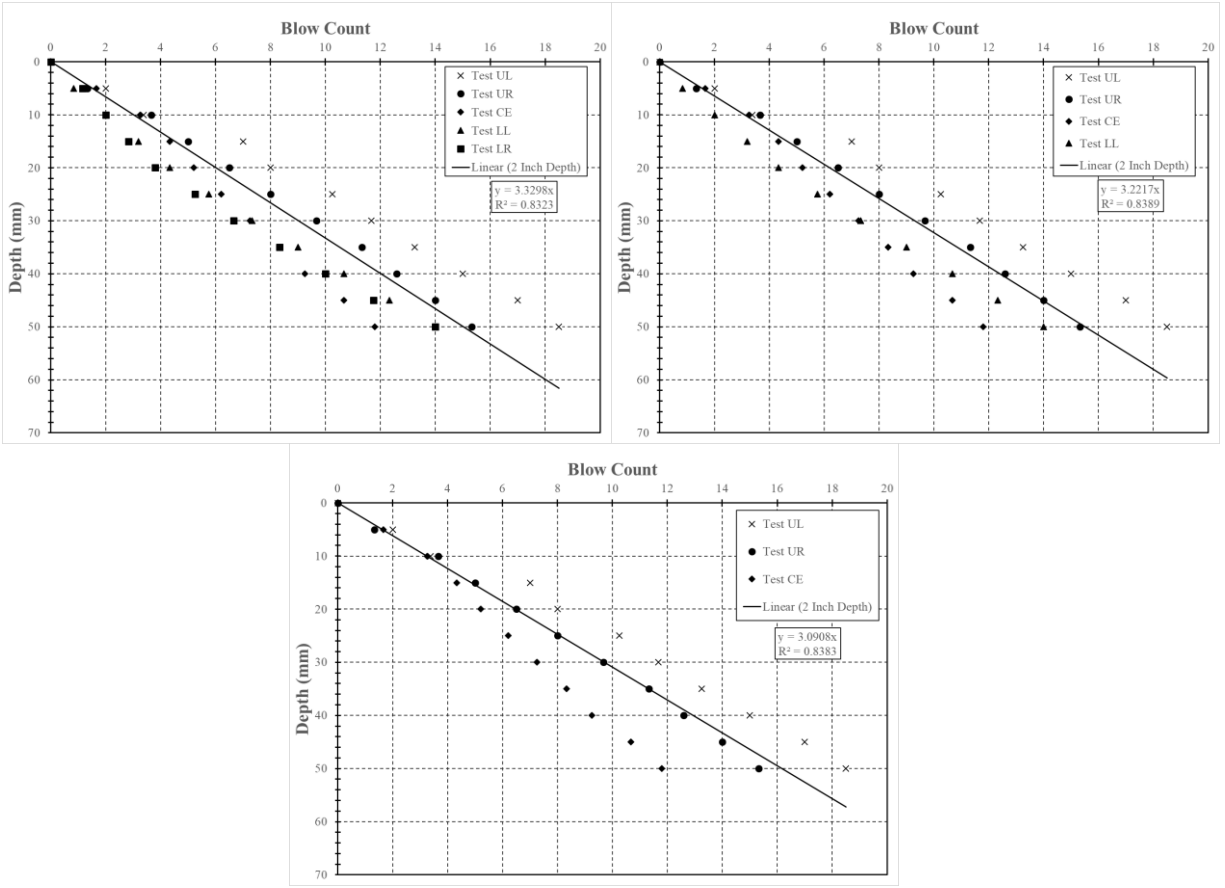


Figure K.13: Test performed on July 17, 2019, Location 17 (top left = 5 tests, top right = 4 tests, bottom = 3 tests)

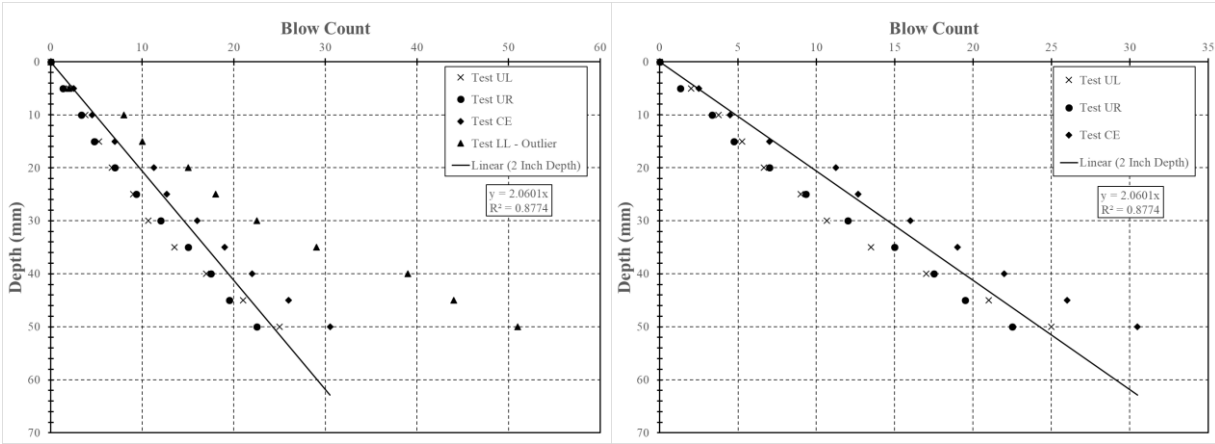


Figure K.14: Test performed on July 17, 2019, Location 18 (left = 4 tests, right = 3 tests)

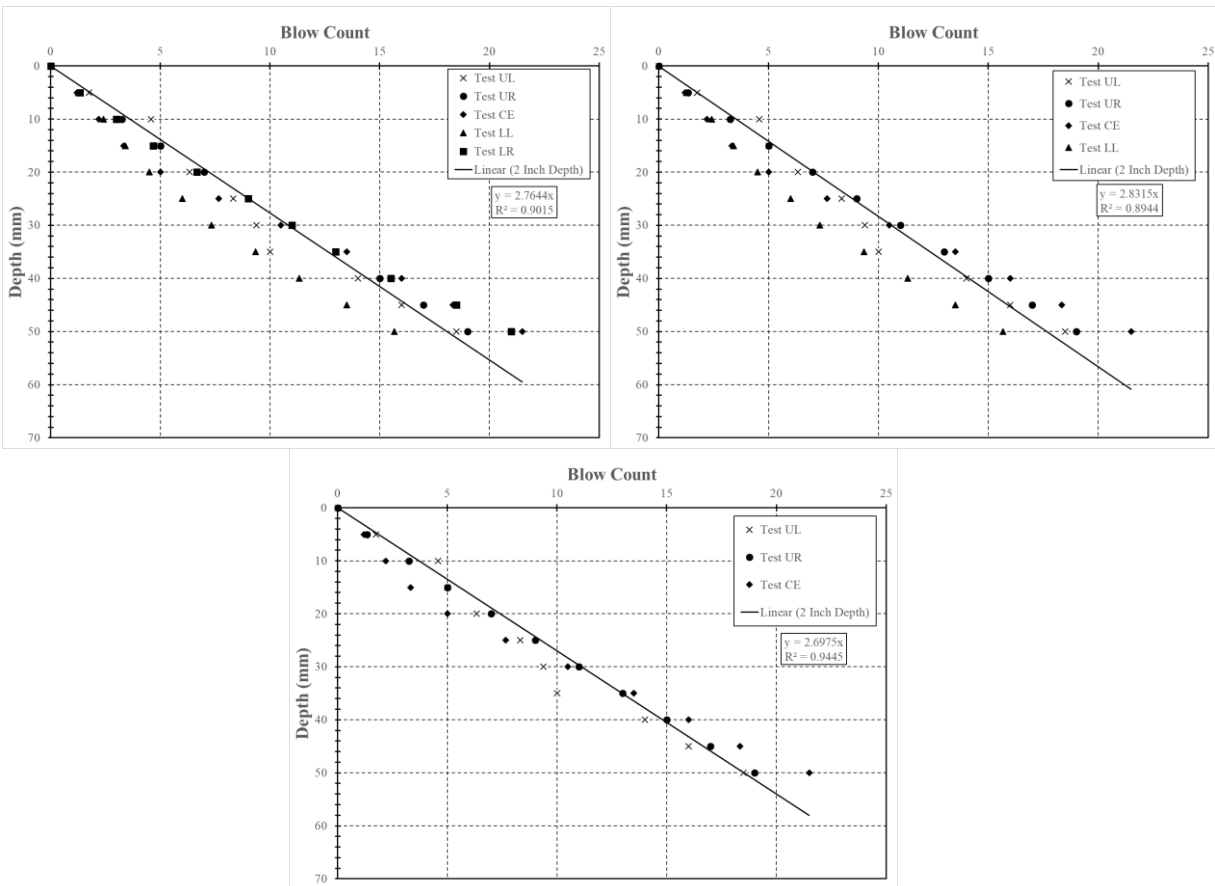


Figure K.15: Test performed on July 17, 2019, Location 19 (top left = 5 tests, top right = 4 tests, bottom = 3 tests)

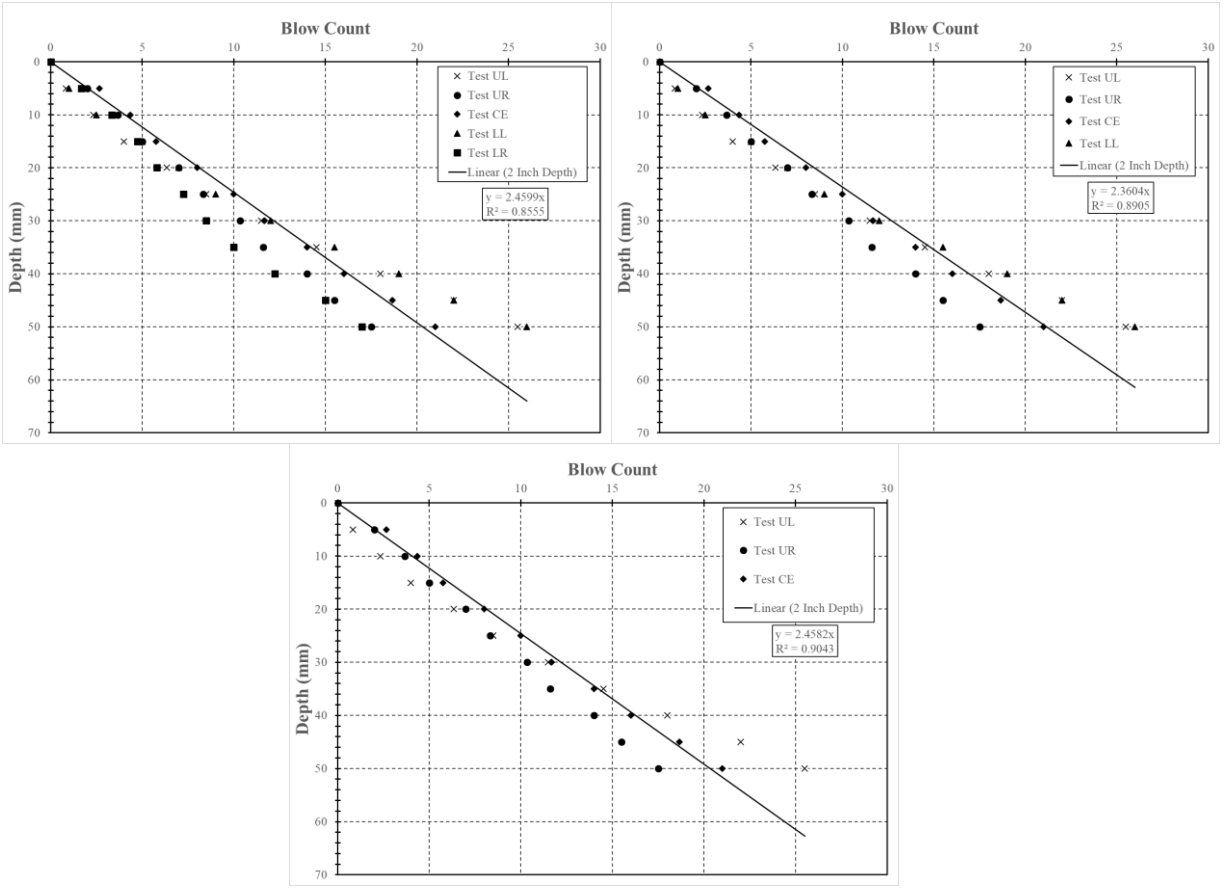


Figure K.16: Test performed on July 17, 2019, Location 20 (top left = 5 tests, top right = 4 tests, bottom = 3 tests)

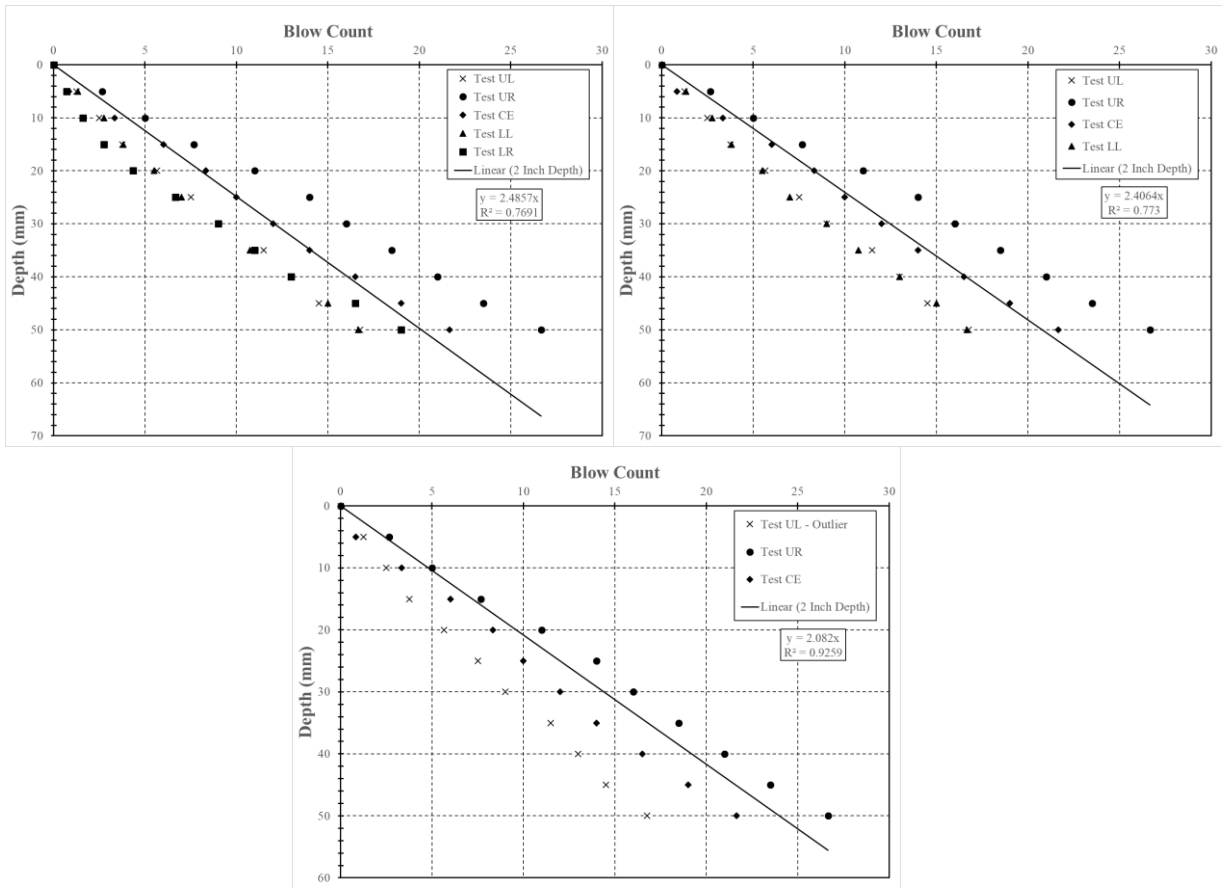


Figure K.17: Test performed on July 17, 2019, Location 21 (top left = 5 tests, top right = 4 tests, bottom = 3 tests)

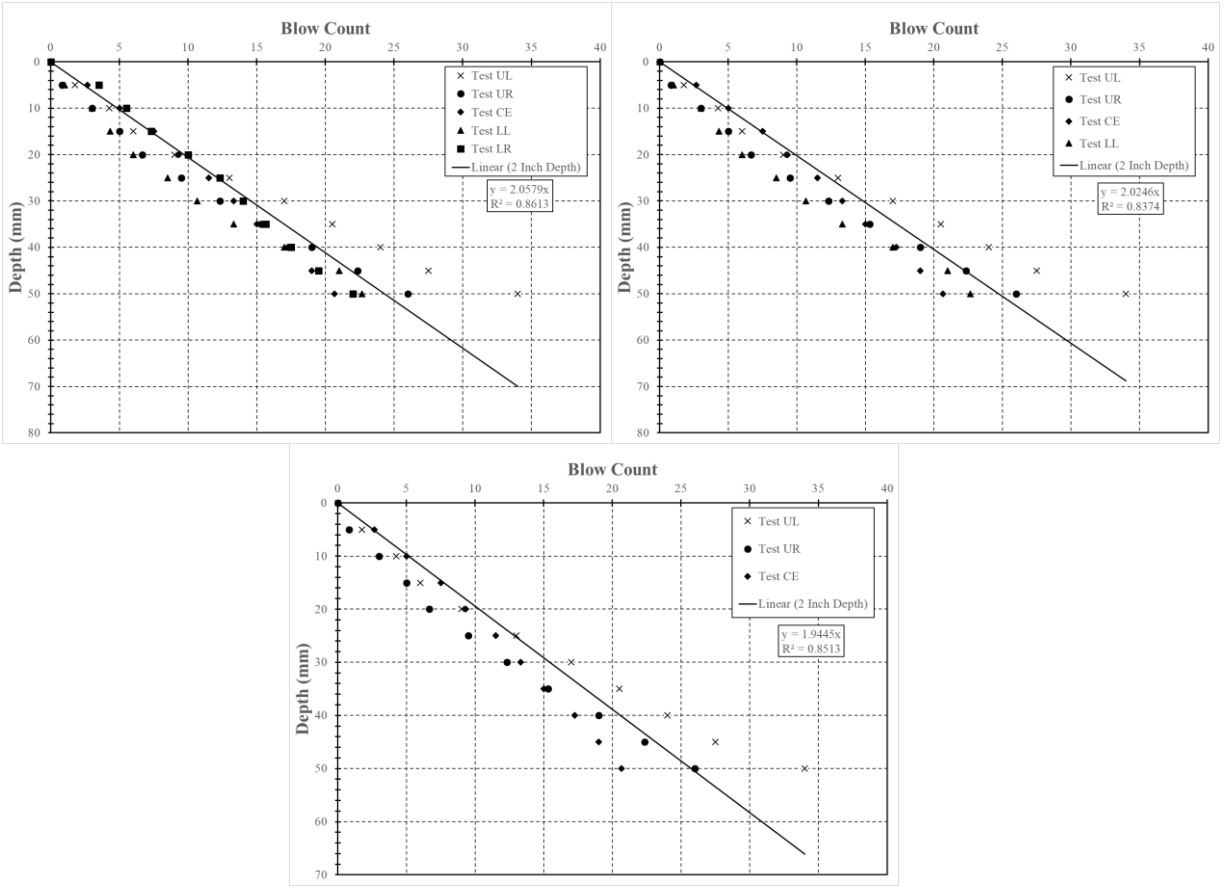


Figure K.18: Test performed on July 17, 2019, Location 22 (top left = 5 tests, top right = 4 tests, bottom = 3 tests)

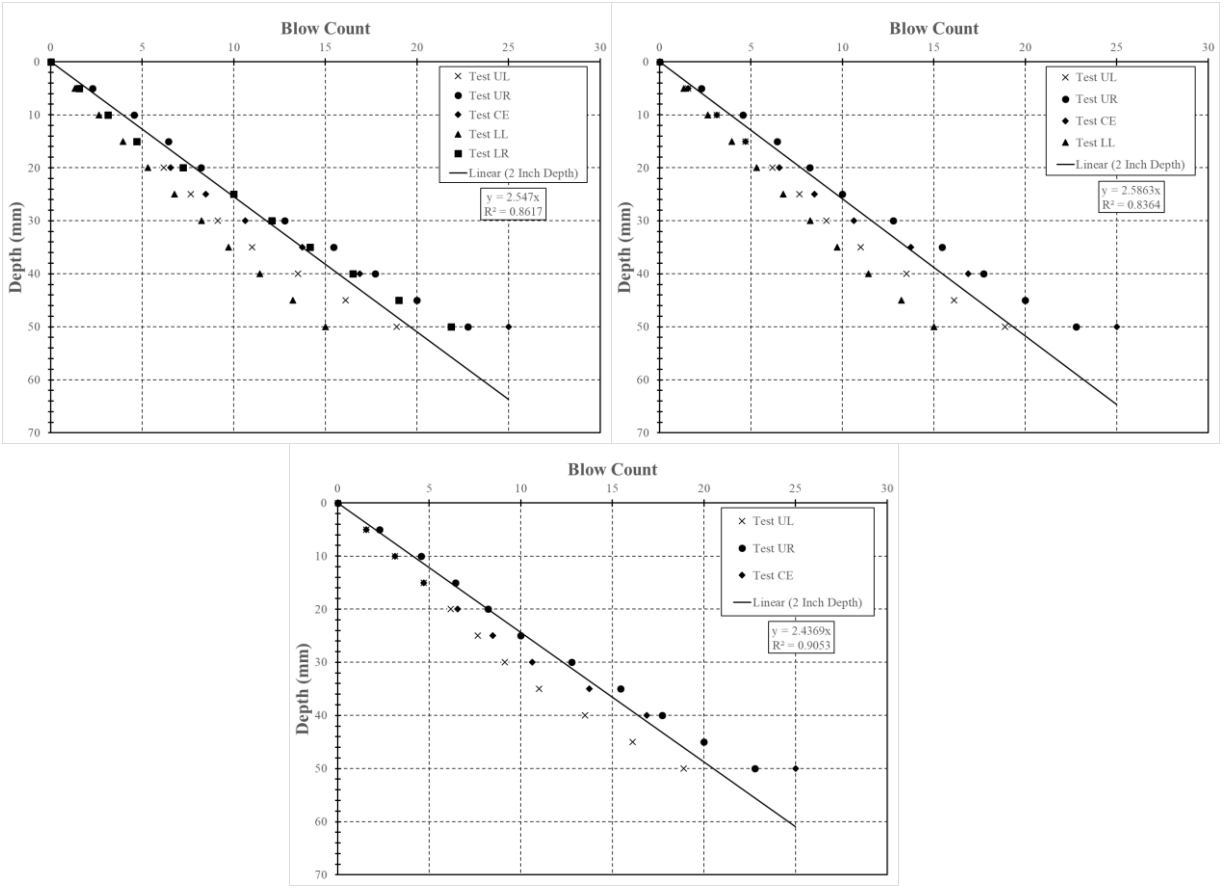


Figure K.19: Test performed on July 18, 2019, Location 23 (top left = 5 tests, top right = 4 tests, bottom = 3 tests)

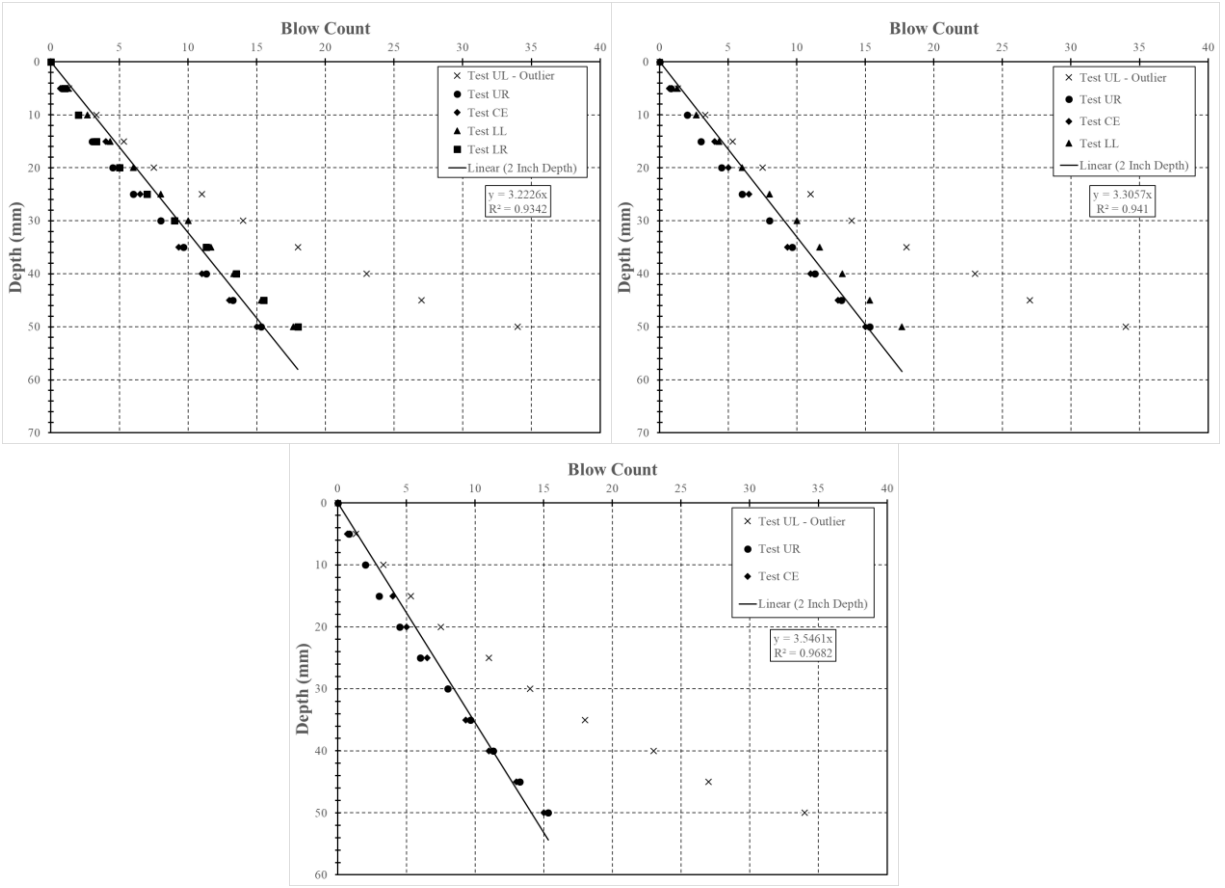


Figure K.20: Test performed on July 18, 2019, Location 24 (top left = 5 tests, top right = 4 tests, bottom = 3 tests)

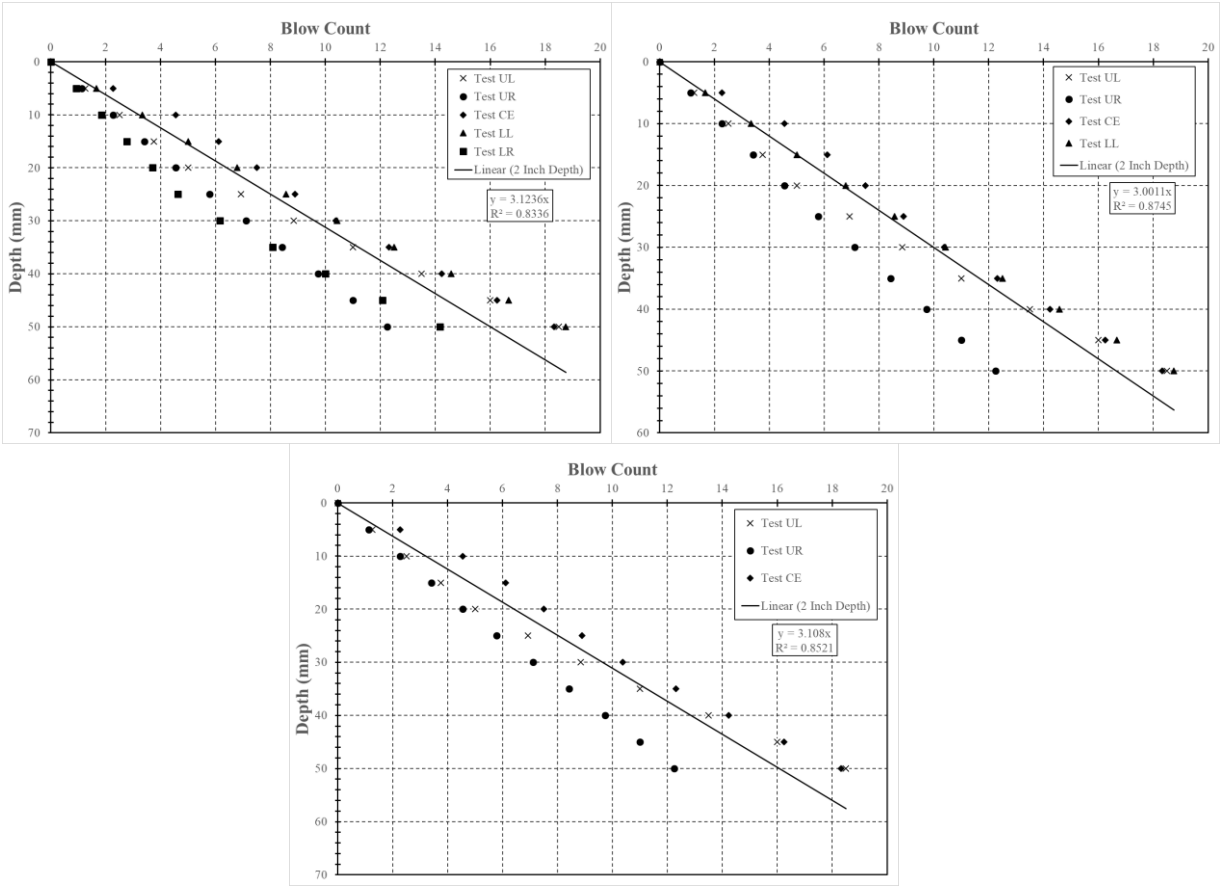


Figure K.21: Test performed on July 18, 2019, Location 25 (top left = 5 tests, top right = 4 tests, bottom = 3 tests)

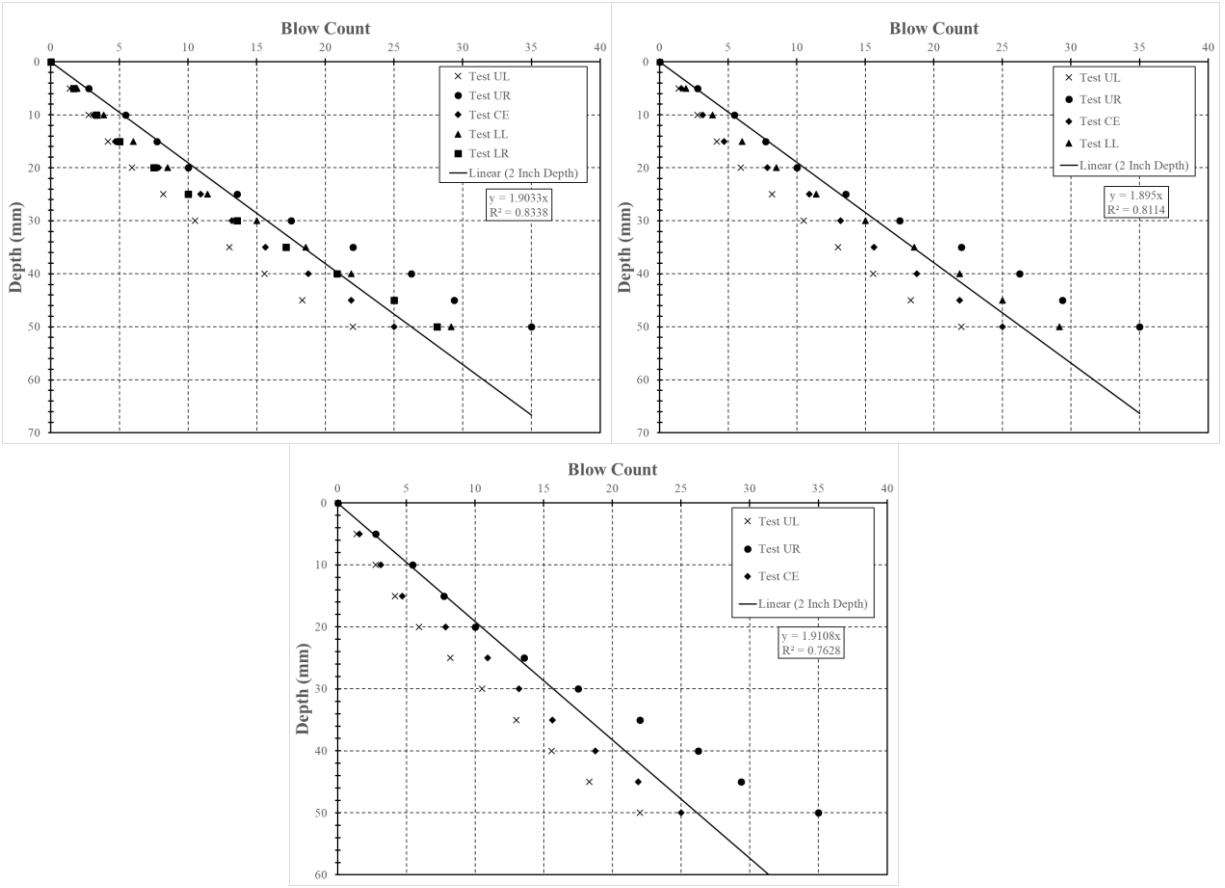


Figure K.22: Test performed on July 18, 2019, Location 28 (top left = 5 tests, top right = 4 tests, bottom = 3 tests)

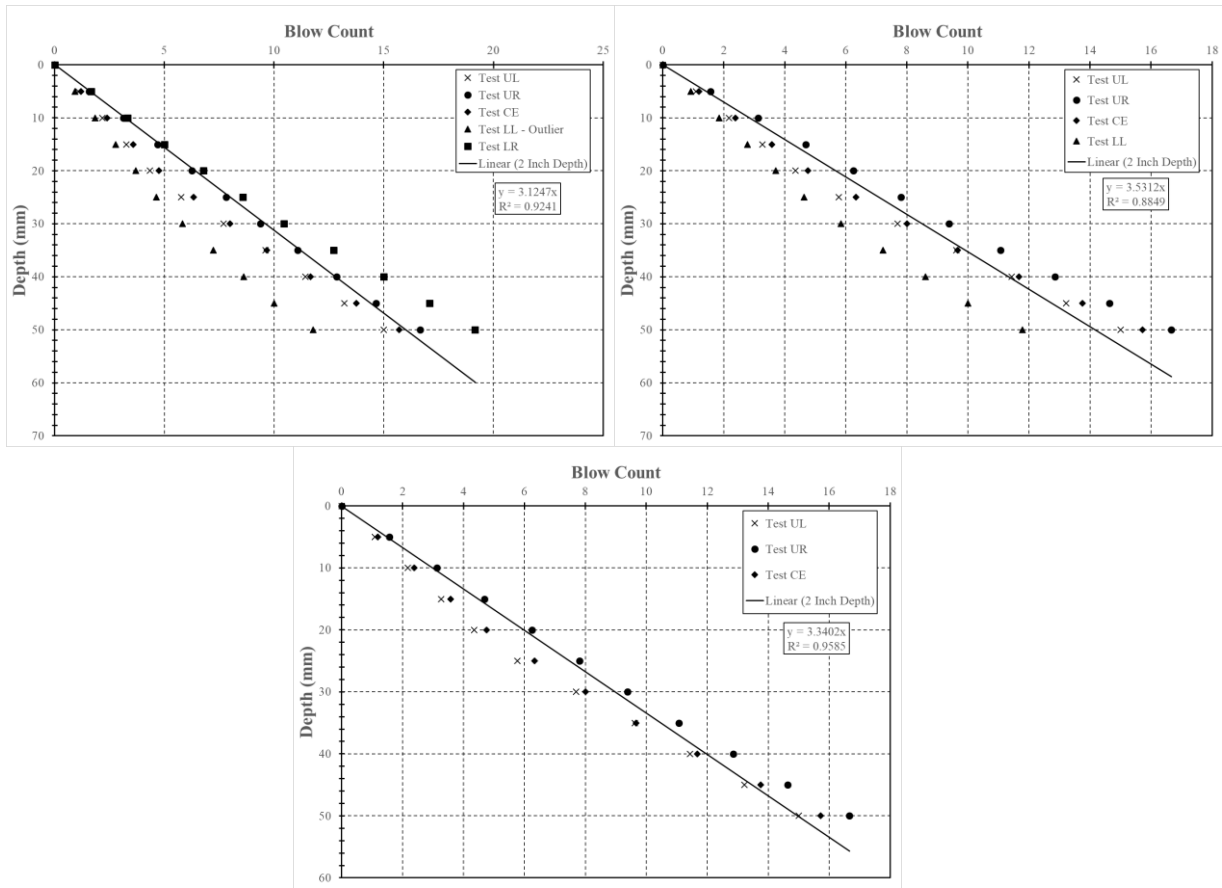


Figure K.23: Test performed on July 19, 2019, Location 30 (top left = 5 tests, top right = 4 tests, bottom = 3 tests)

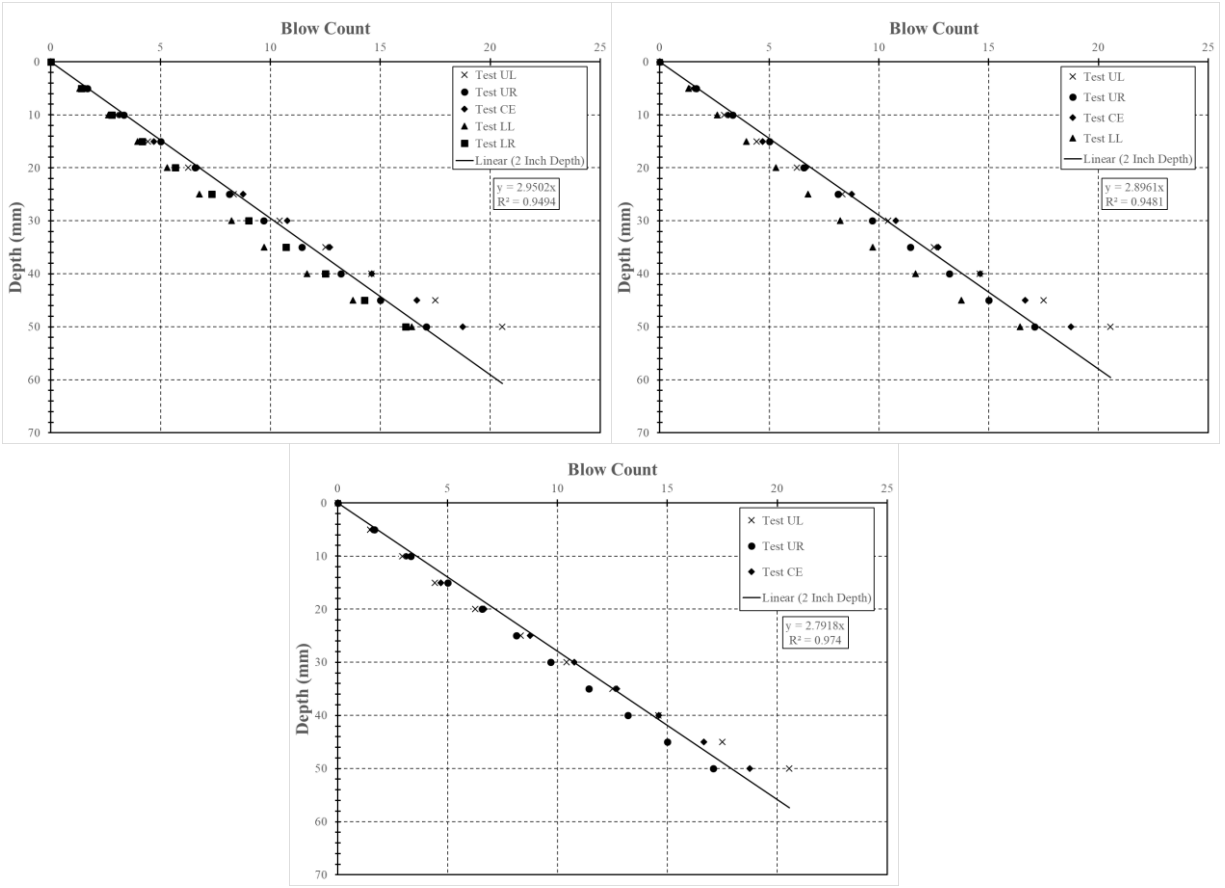


Figure K.24: Test performed on July 19, 2019, Location 31 (top left = 5 tests, top right = 4 tests, bottom = 3 tests)

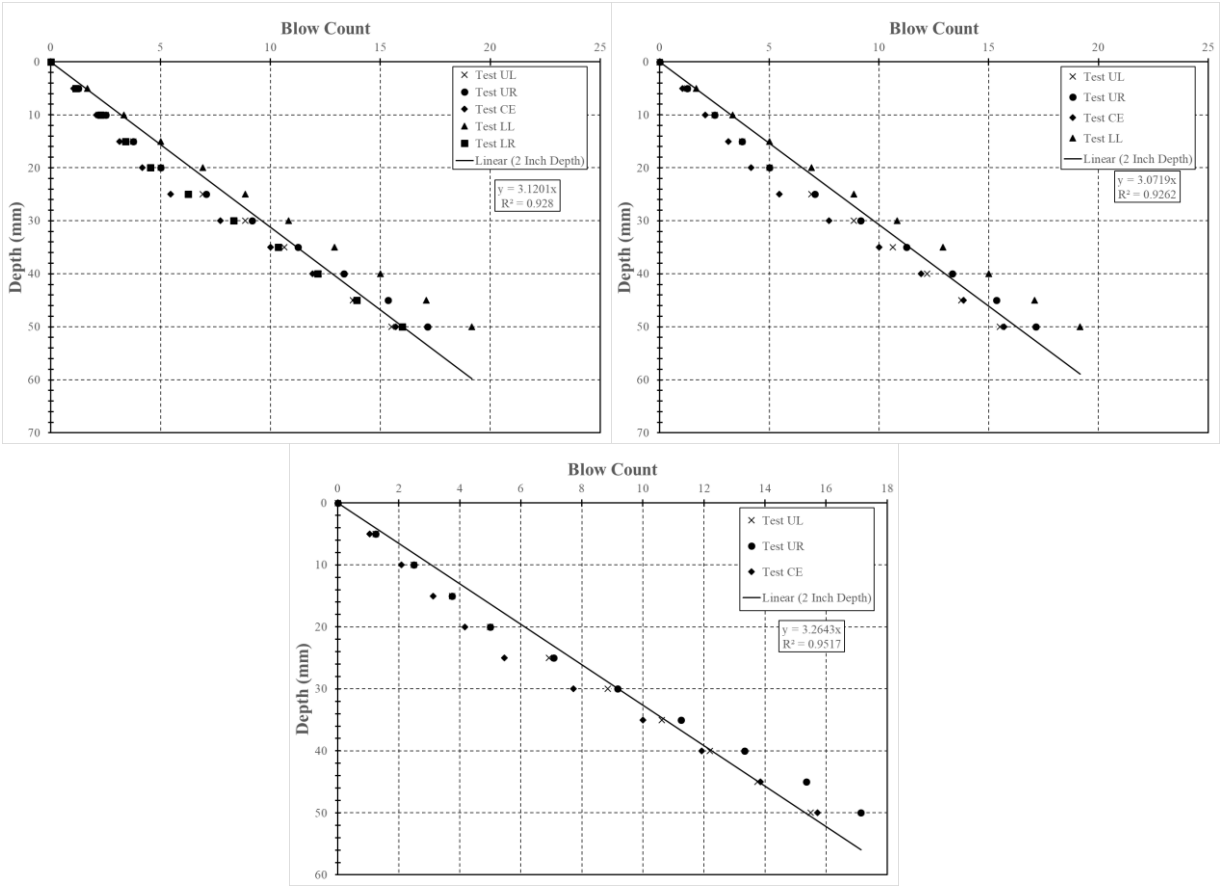


Figure K.25: Test performed on July 19, 2019, Location 32 (top left = 5 tests, top right = 4 tests, bottom = 3 tests)

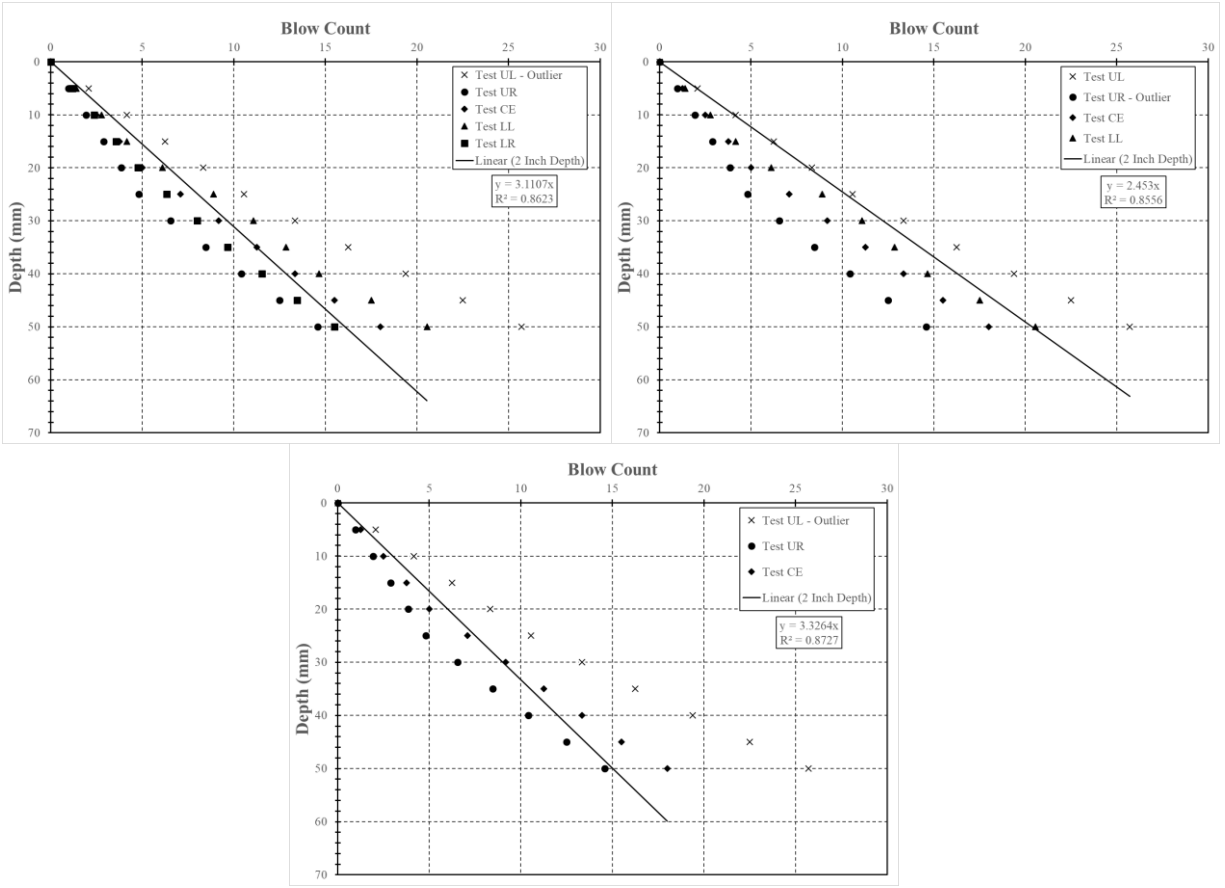


Figure K.26: Test performed on July 19, 2019, Location 33 (top left = 5 tests, top right = 4 tests, bottom = 3 tests)

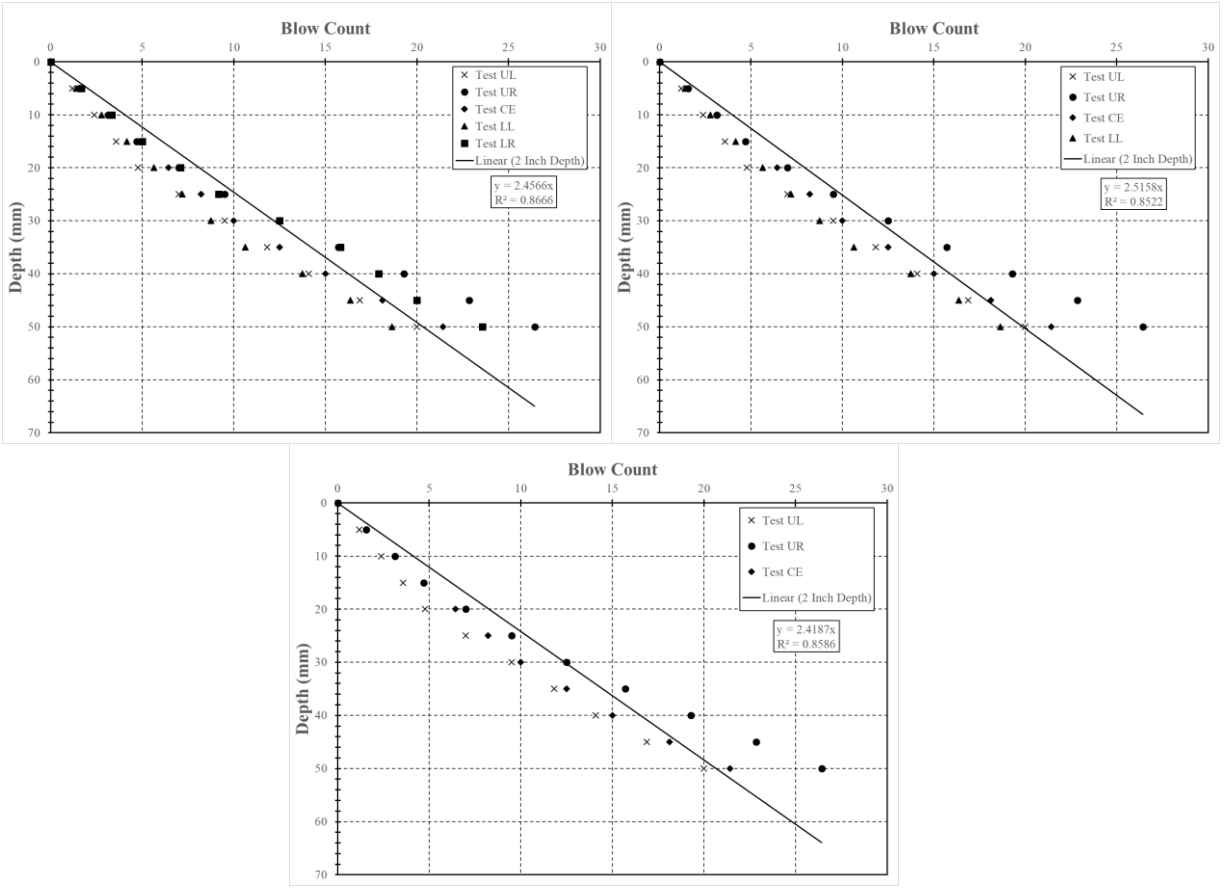


Figure K.27: Test performed on July 19, 2019, Location 34 (top left = 5 tests, top right = 4 tests, bottom = 3 tests)

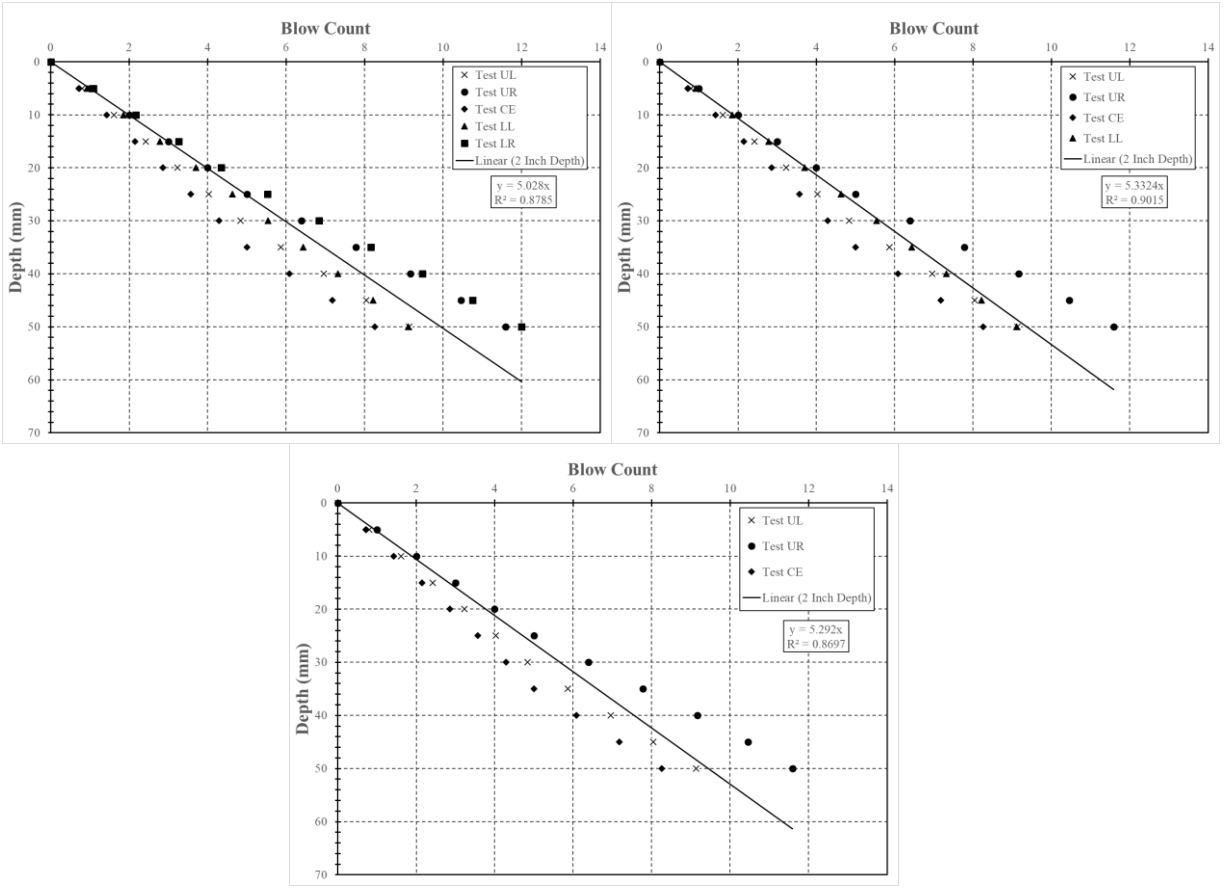


Figure K.28: Test performed on July 19, 2019, Location 35 (top left = 5 tests, top right = 4 tests, bottom = 3 tests)

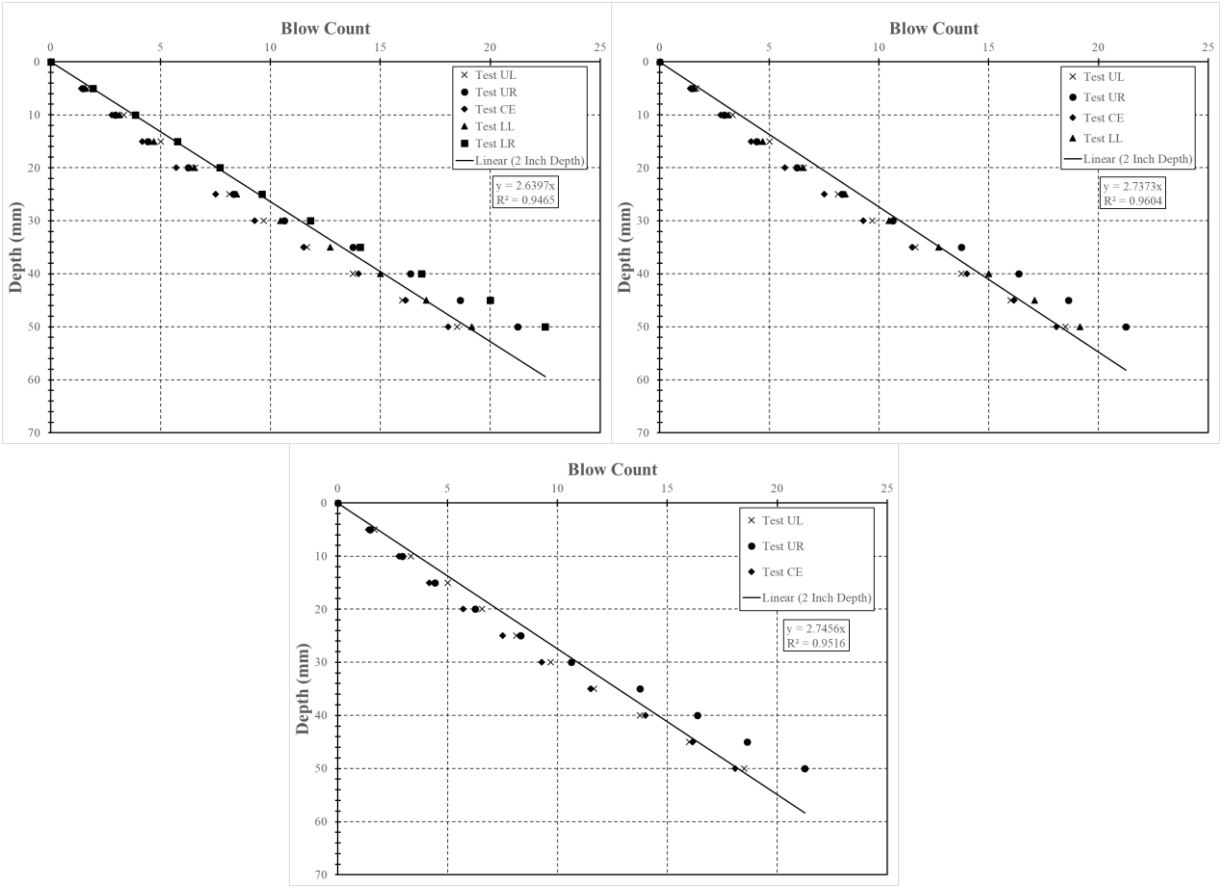


Figure K.29: Test performed on July 19, 2019, Location 36 (top left = 5 tests, top right = 4 tests, bottom = 3 tests)

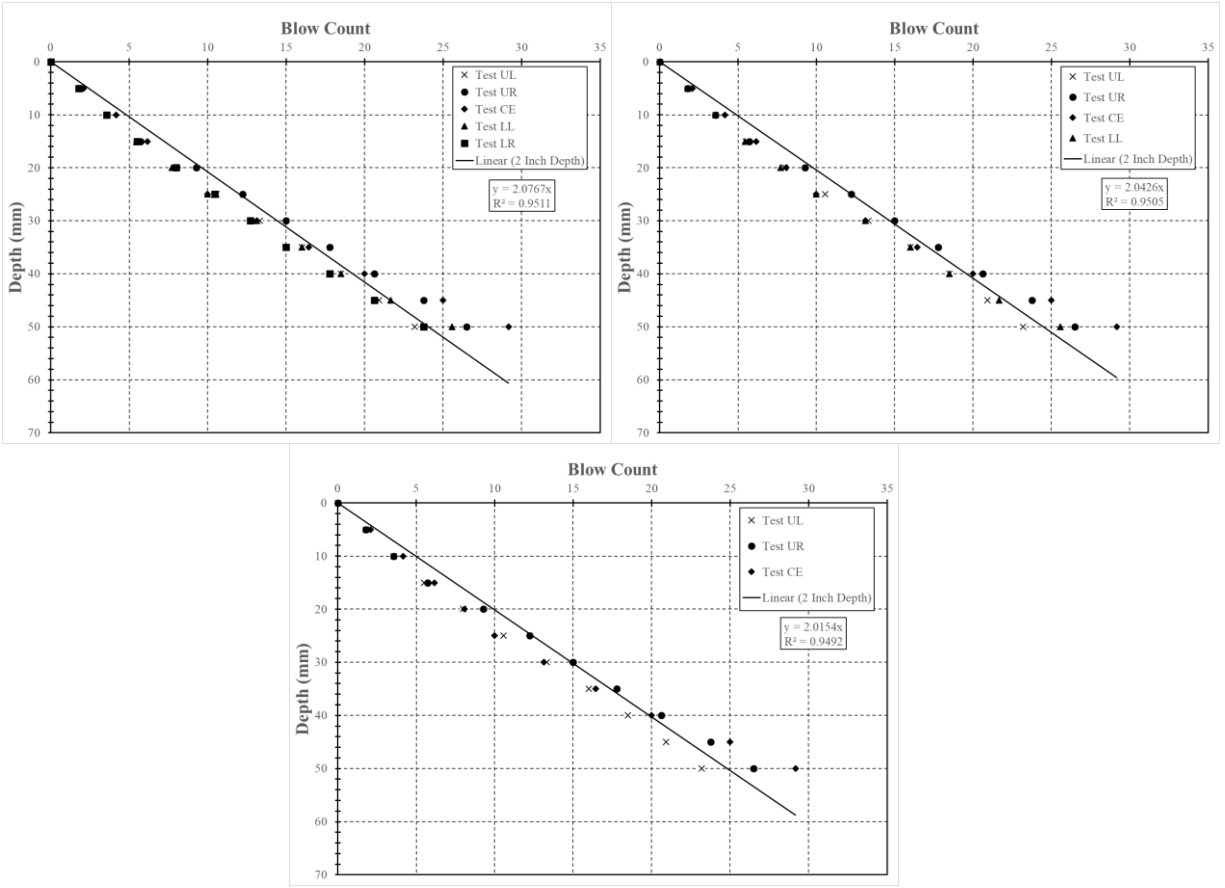


Figure K.30: Test performed on July 23, 2019, Location 37 (top left = 5 tests, top right = 4 tests, bottom = 3 tests)

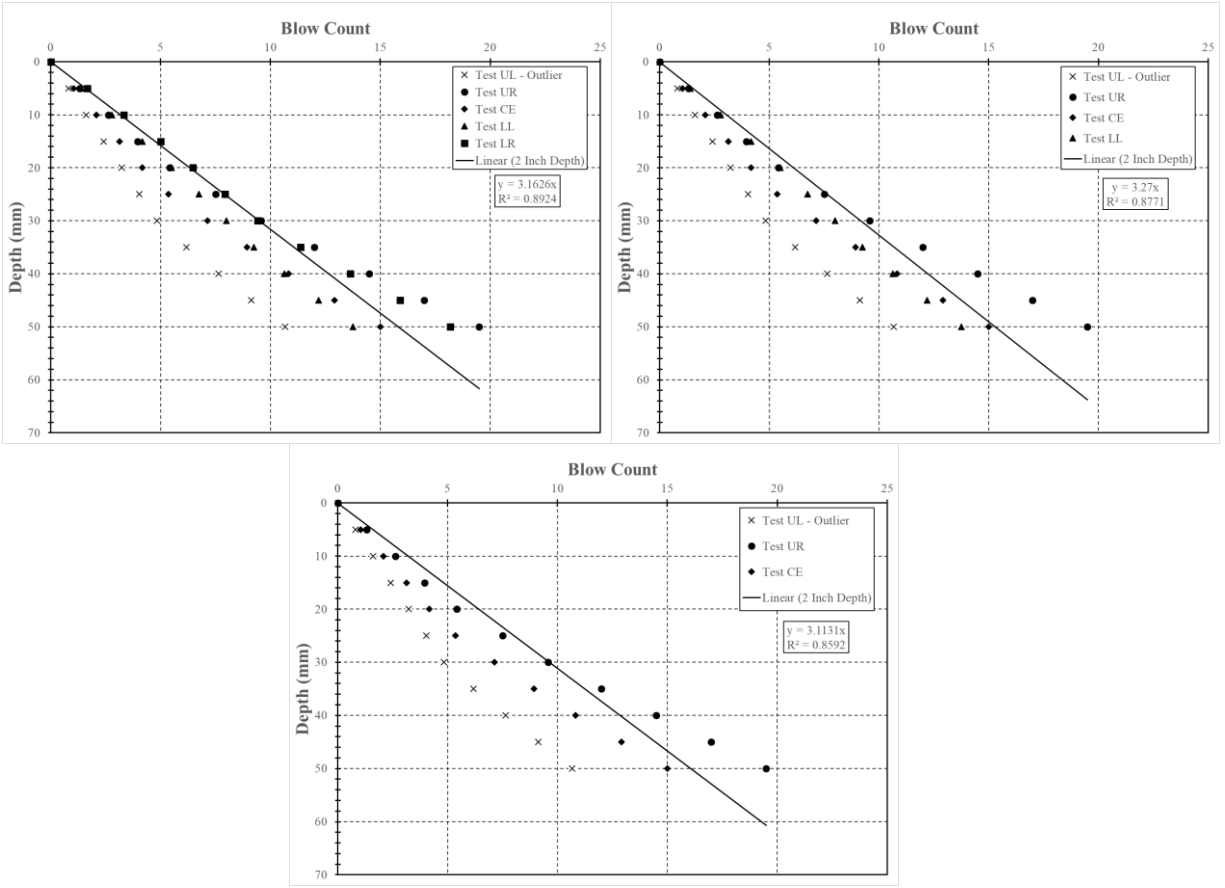


Figure K.31: Test performed on July 23, 2019, Location 38 (top left = 5 tests, top right = 4 tests, bottom = 3 tests)

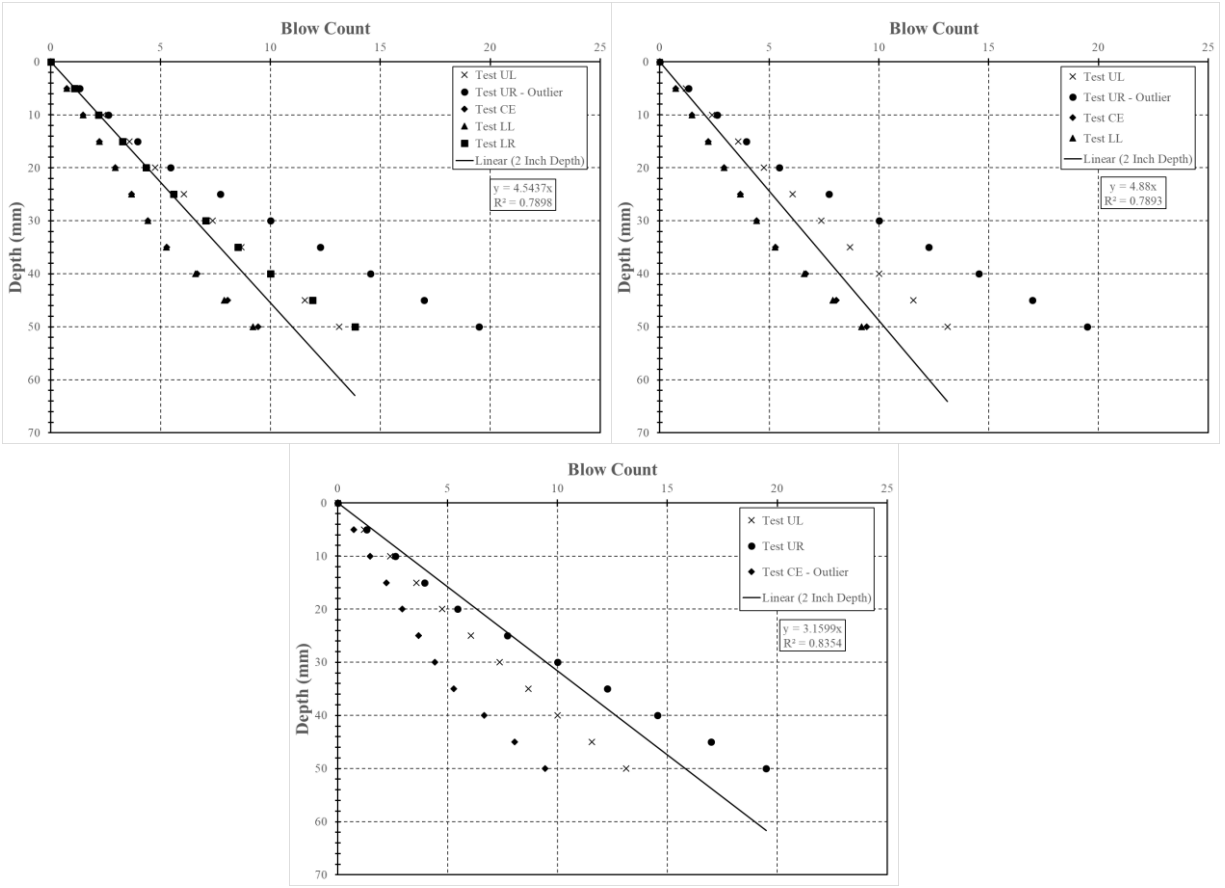


Figure K.32: Test performed on July 23, 2019, Location 39 (top left = 5 tests, top right = 4 tests, bottom = 3 tests)

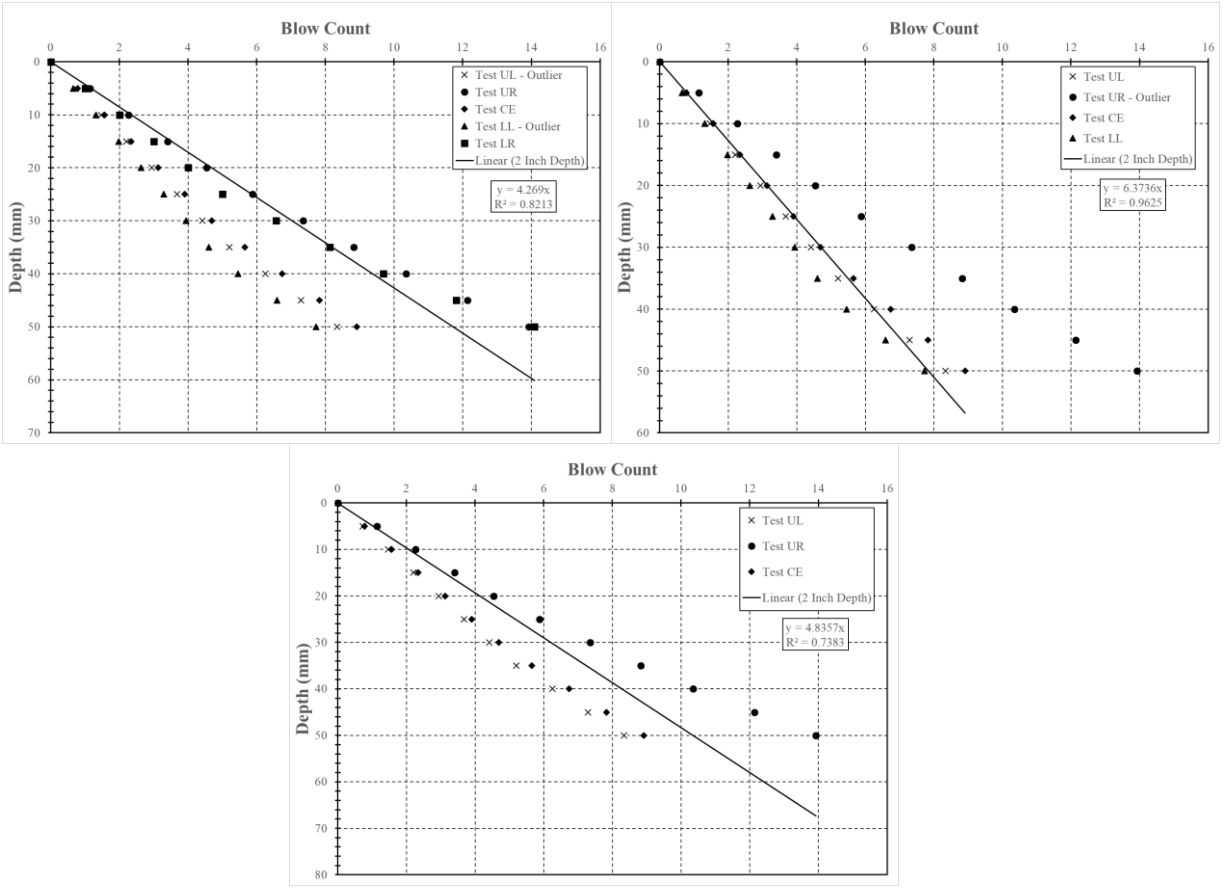


Figure K.33: Test performed on July 23, 2019, Location 40 (top left = 5 tests, top right = 4 tests, bottom = 3 tests)

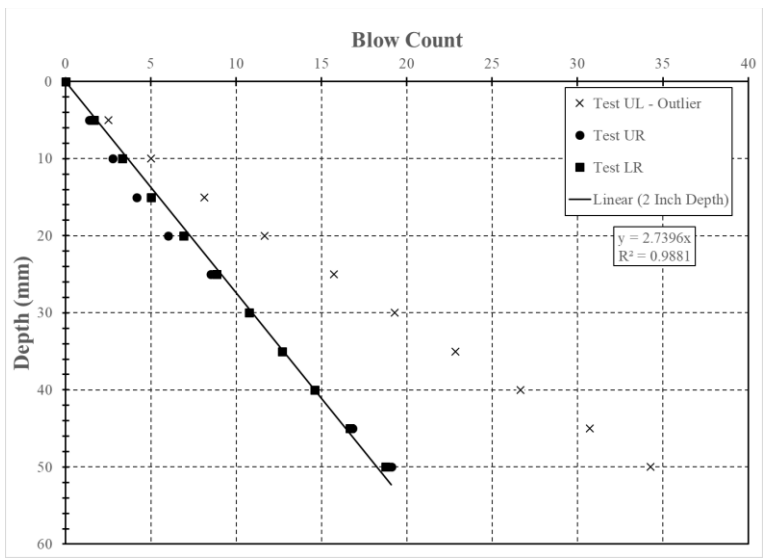


Figure K.34: Test performed on July 23, 2019, Location 41 (only 3 tests completed)

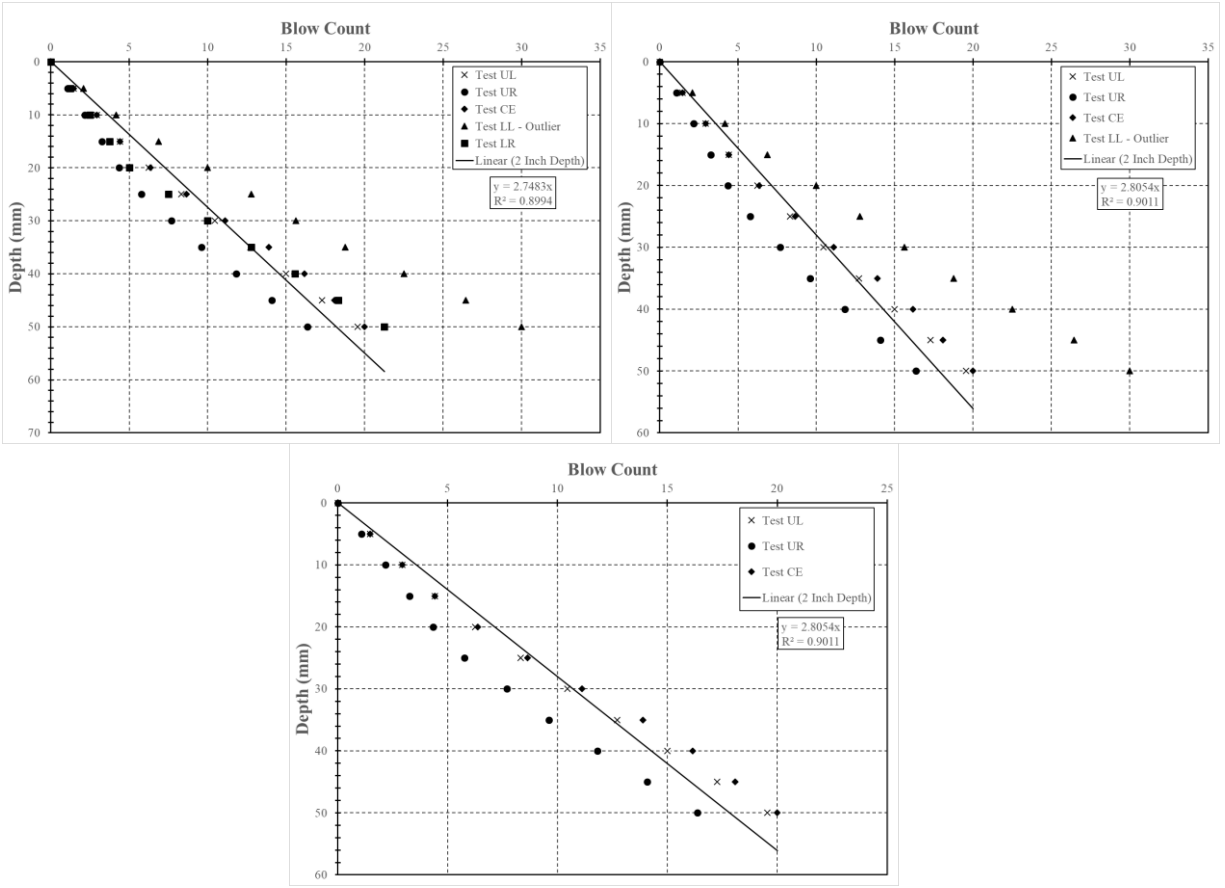


Figure K.35: Test performed on July 23, 2019, Location 42 (top left = 5 tests, top right = 4 tests, bottom = 3 tests)

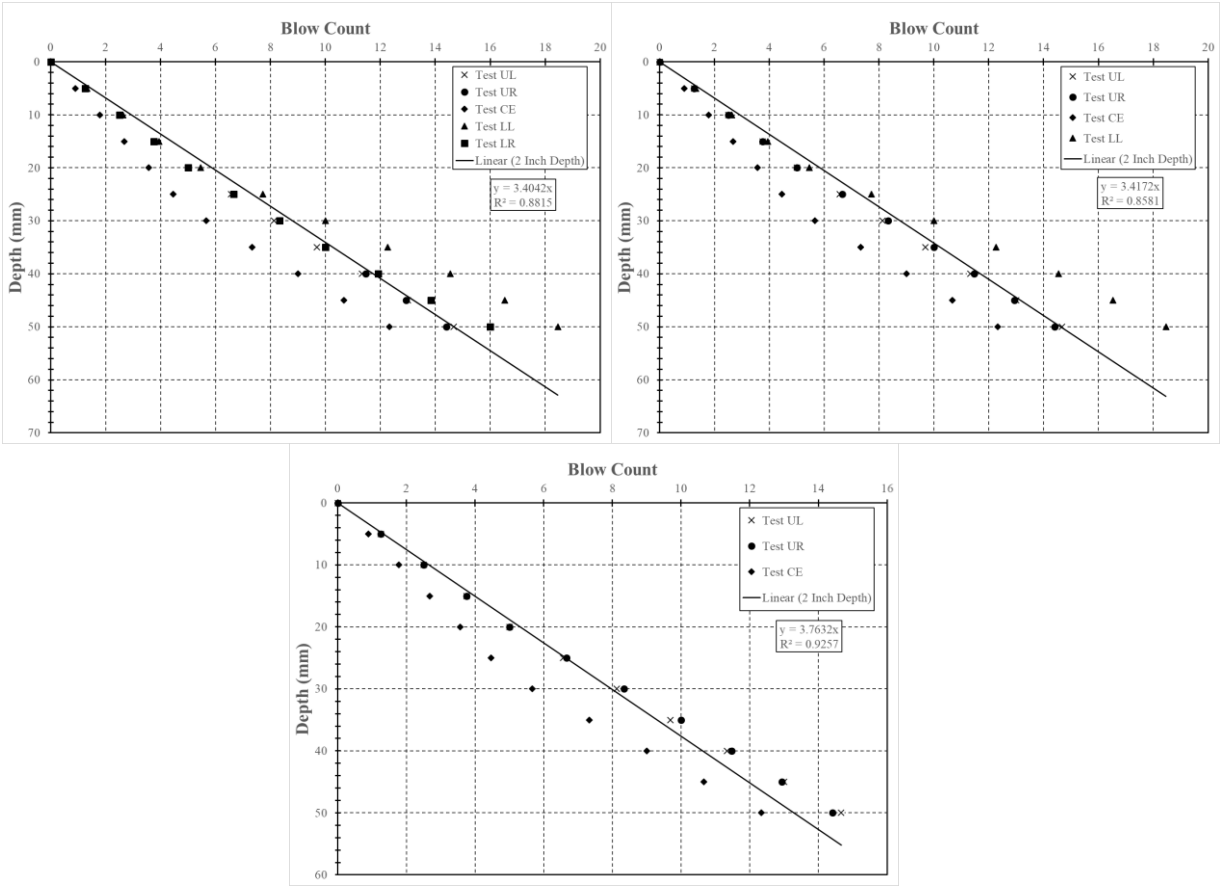


Figure K.36: Test performed on July 23, 2019, Location 43 (top left = 5 tests, top right = 4 tests, bottom = 3 tests)

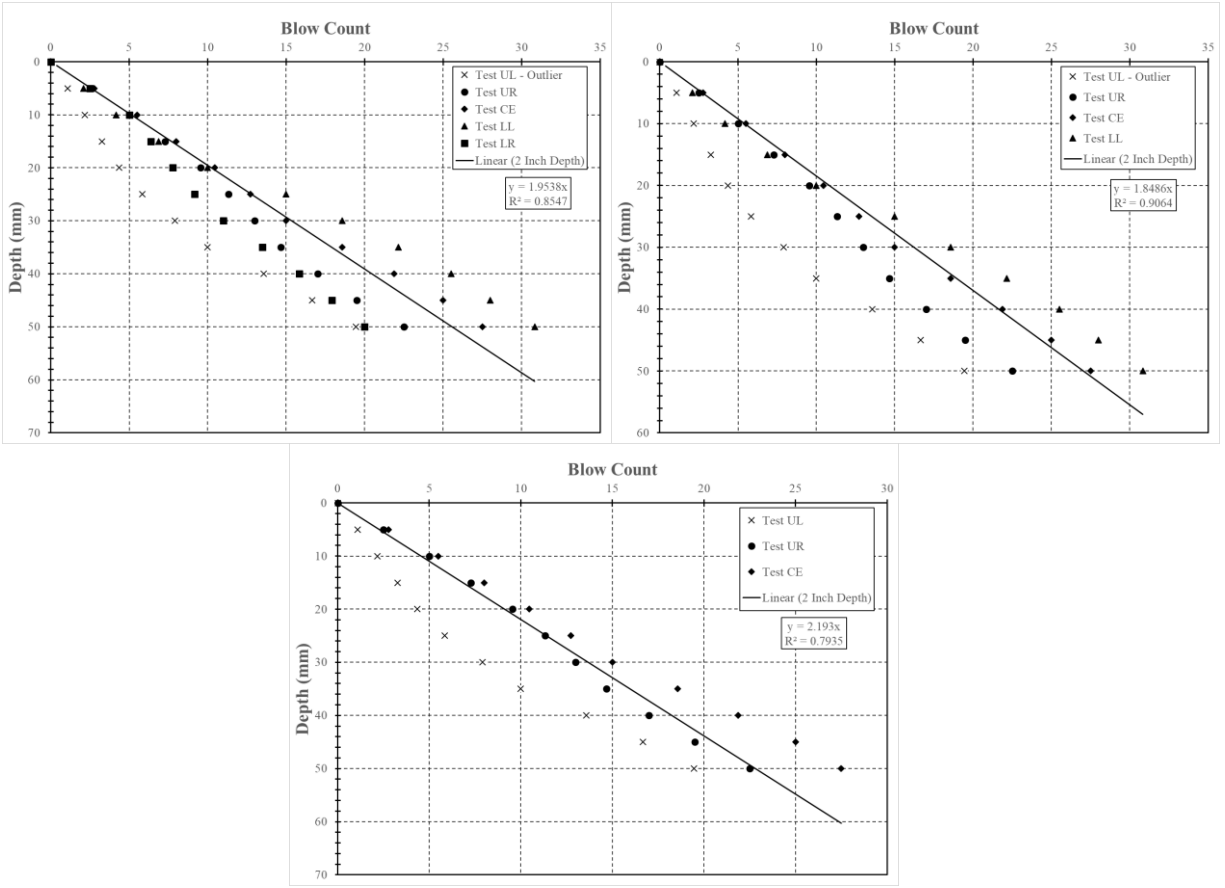


Figure K.37: Test performed on July 24, 2019, Location 44 (top left = 5 tests, top right = 4 tests, bottom = 3 tests)

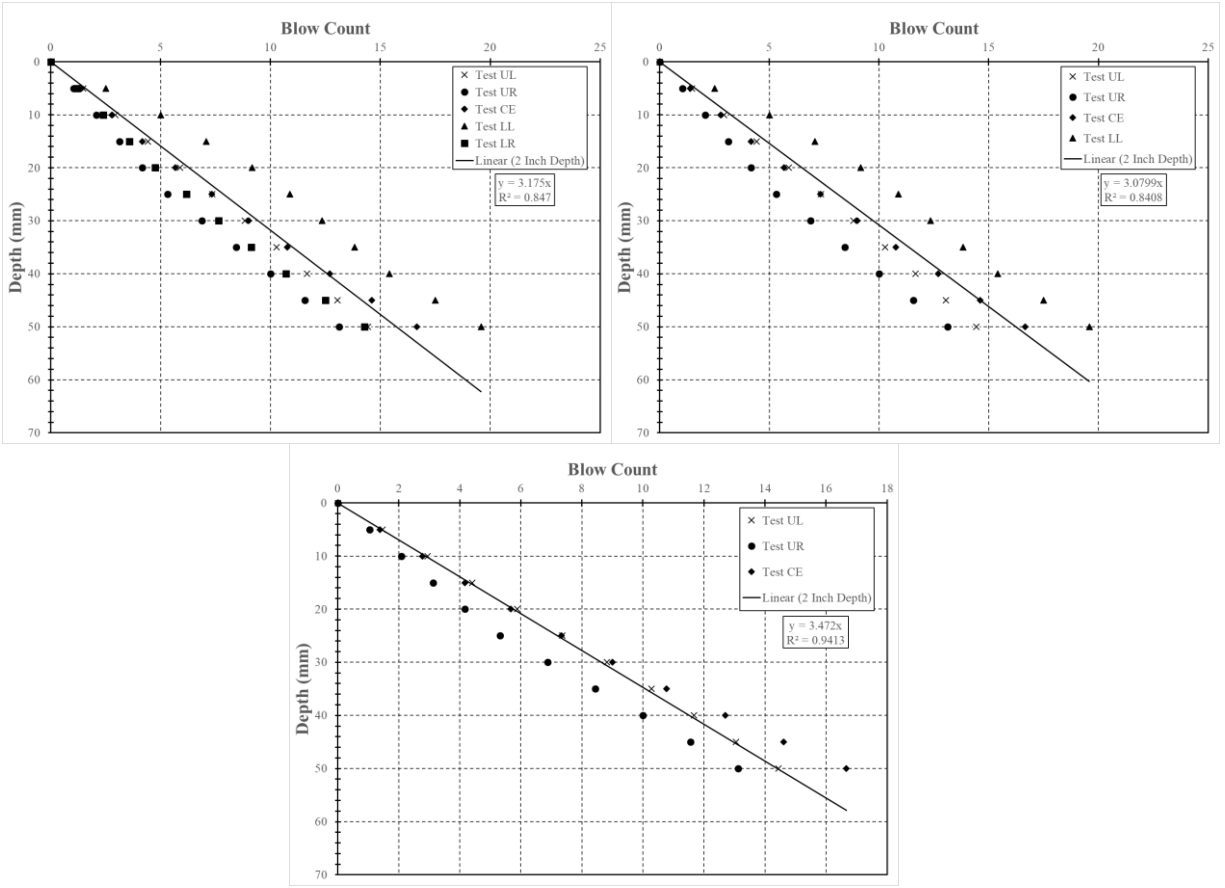


Figure K.38: Test performed on July 24, 2019, Location 45 (top left = 5 tests, top right = 4 tests, bottom = 3 tests)

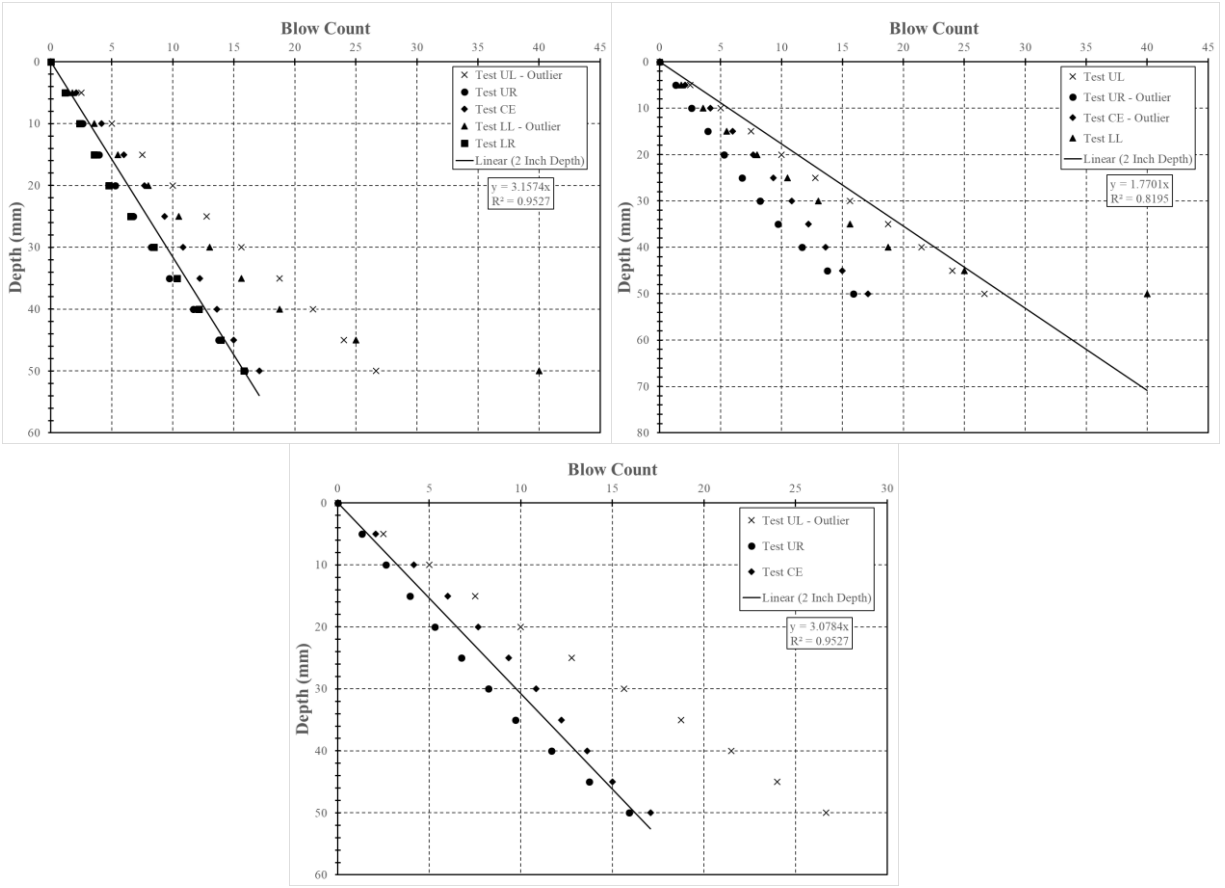


Figure K.39: Test performed on July 24, 2019, Location 46 (top left = 5 tests, top right = 4 tests, bottom = 3 tests)

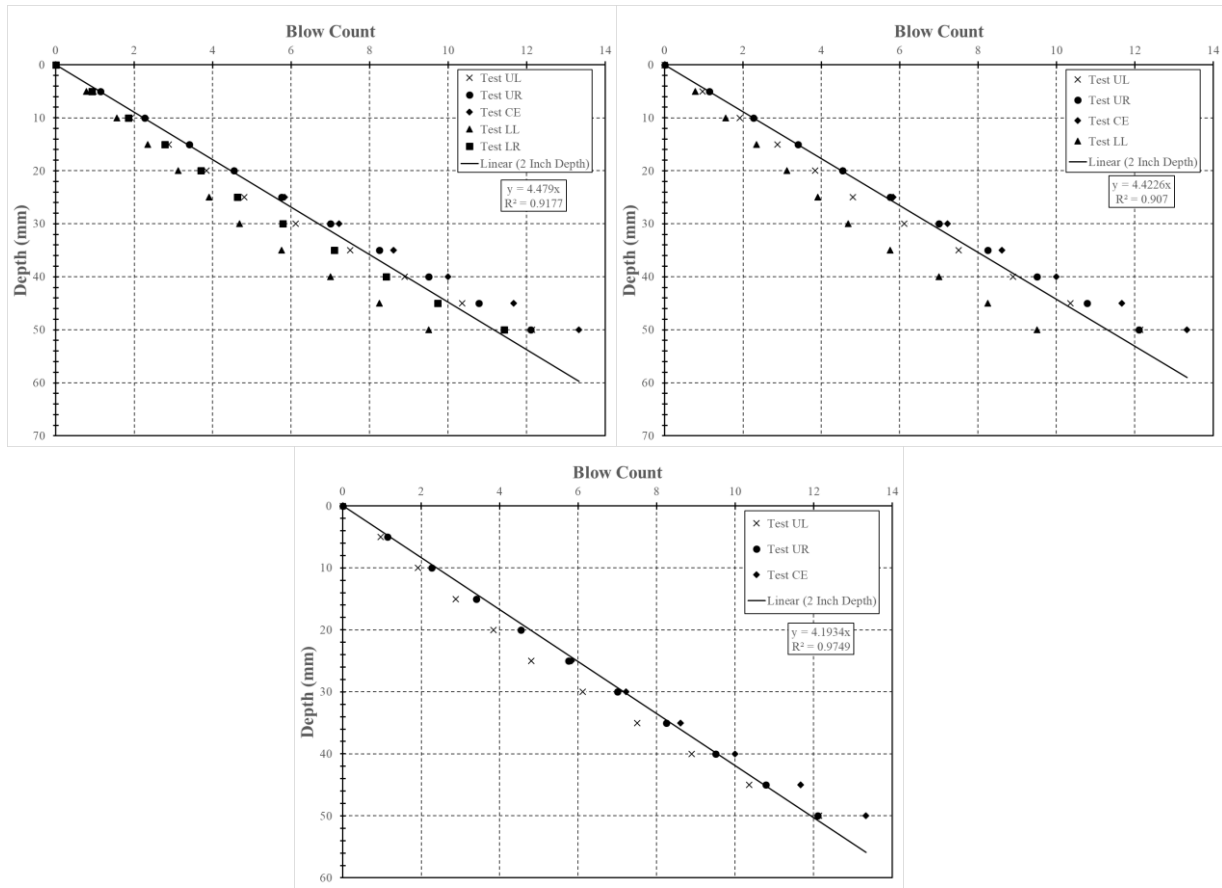


Figure K.40: Test performed on July 24, 2019, Location 47 (top left = 5 tests, top right = 4 tests, bottom = 3 tests)

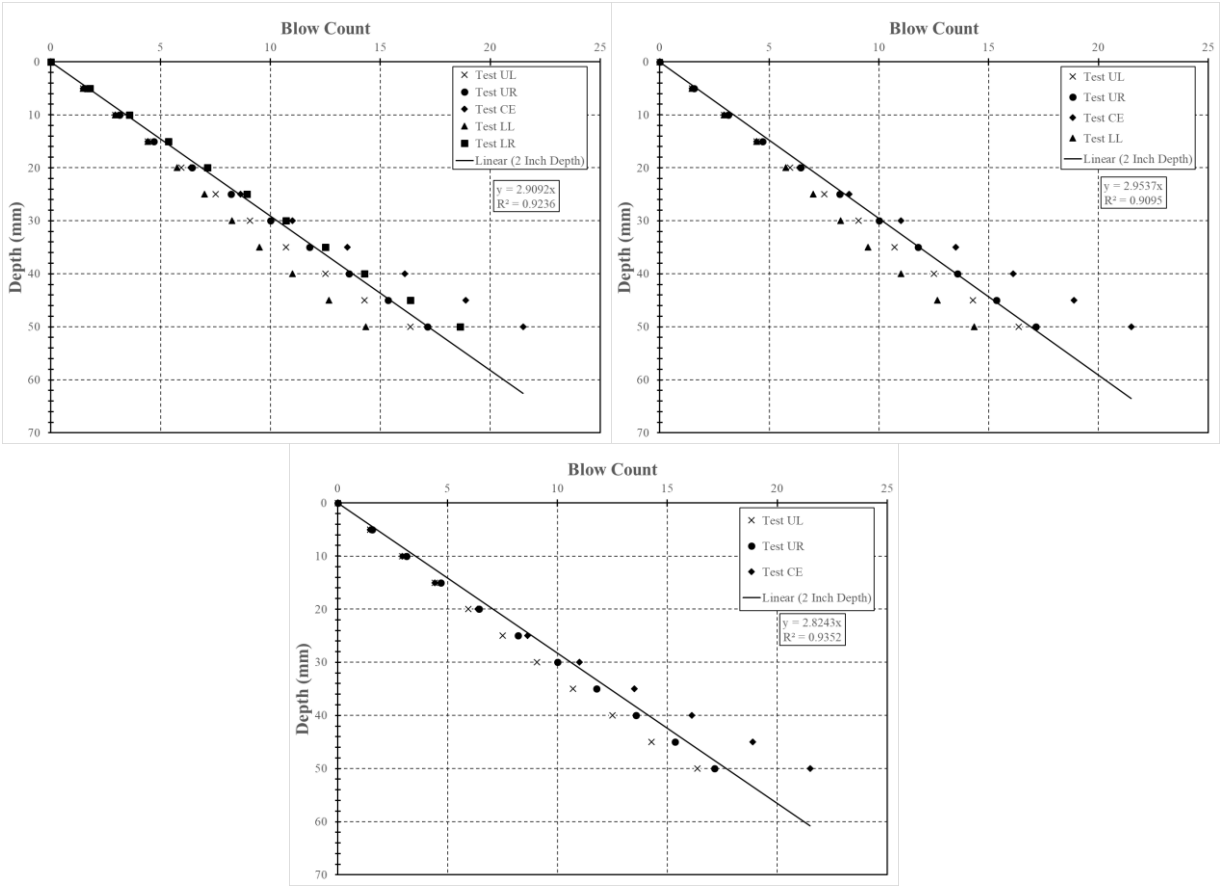


Figure K.41: Test performed on July 24, 2019, Location 48 (top left = 5 tests, top right = 4 tests, bottom = 3 tests)

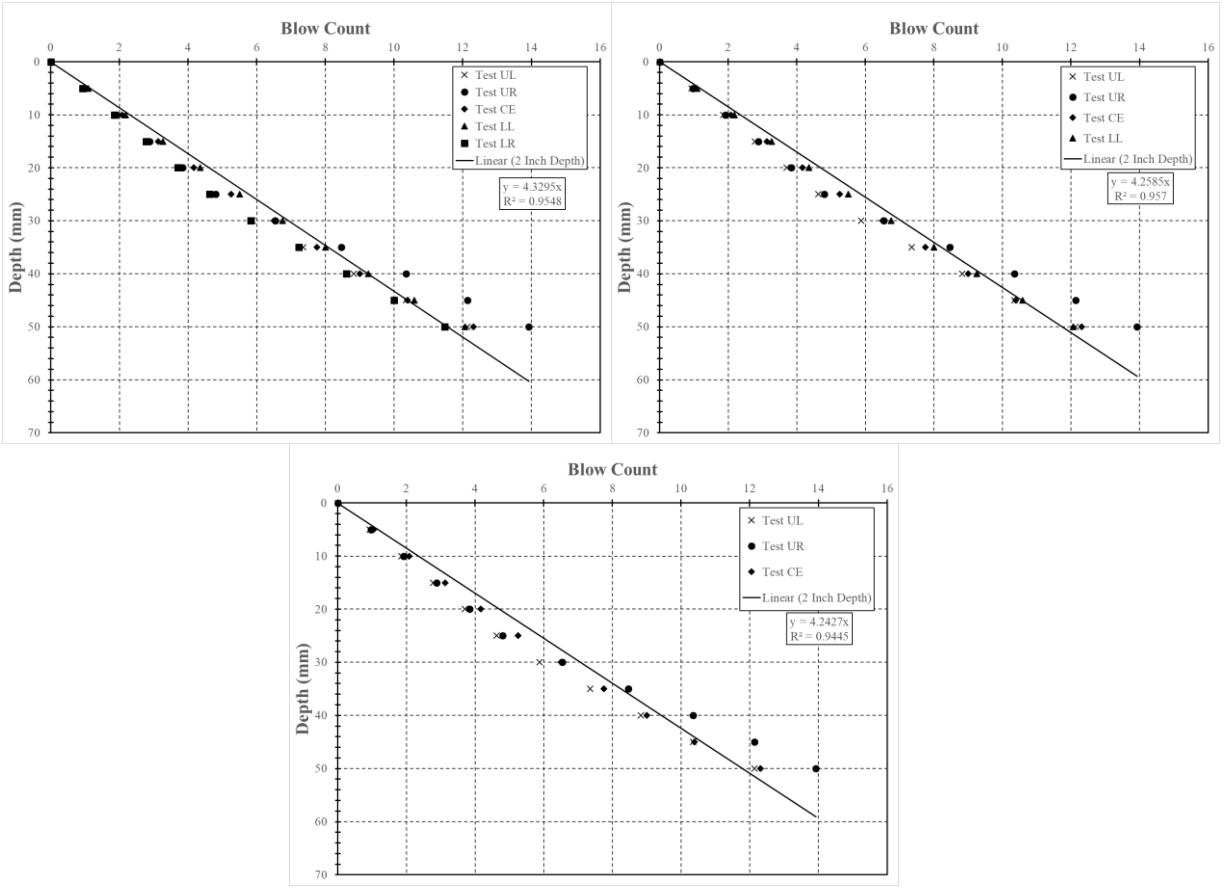


Figure K.42: Test performed on July 24, 2019, Location 49 (top left = 5 tests, top right = 4 tests, bottom = 3 tests)

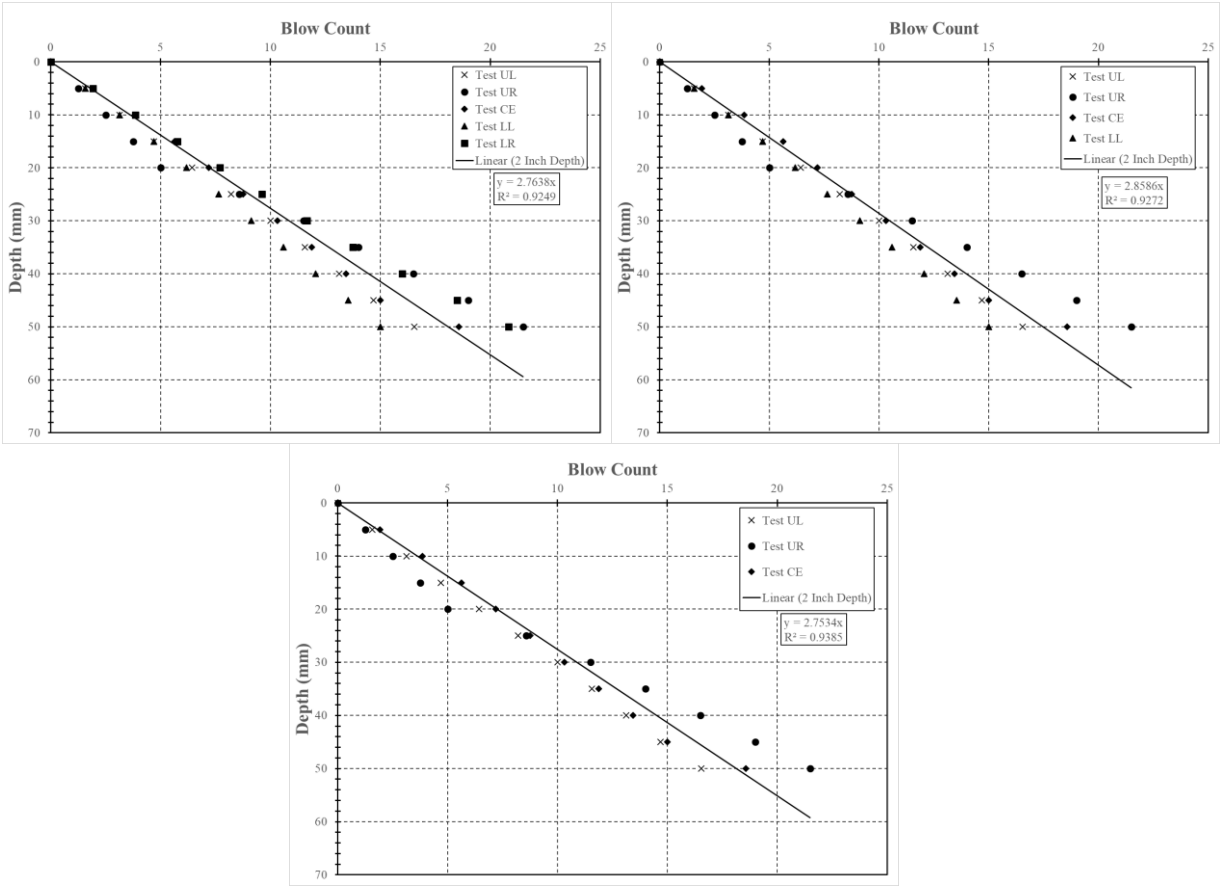


Figure K.43: Test performed on July 24, 2019, Location 50 (top left = 5 tests, top right = 4 tests, bottom = 3 tests)

Appendix L

75 Millimeter Penetration Field Data

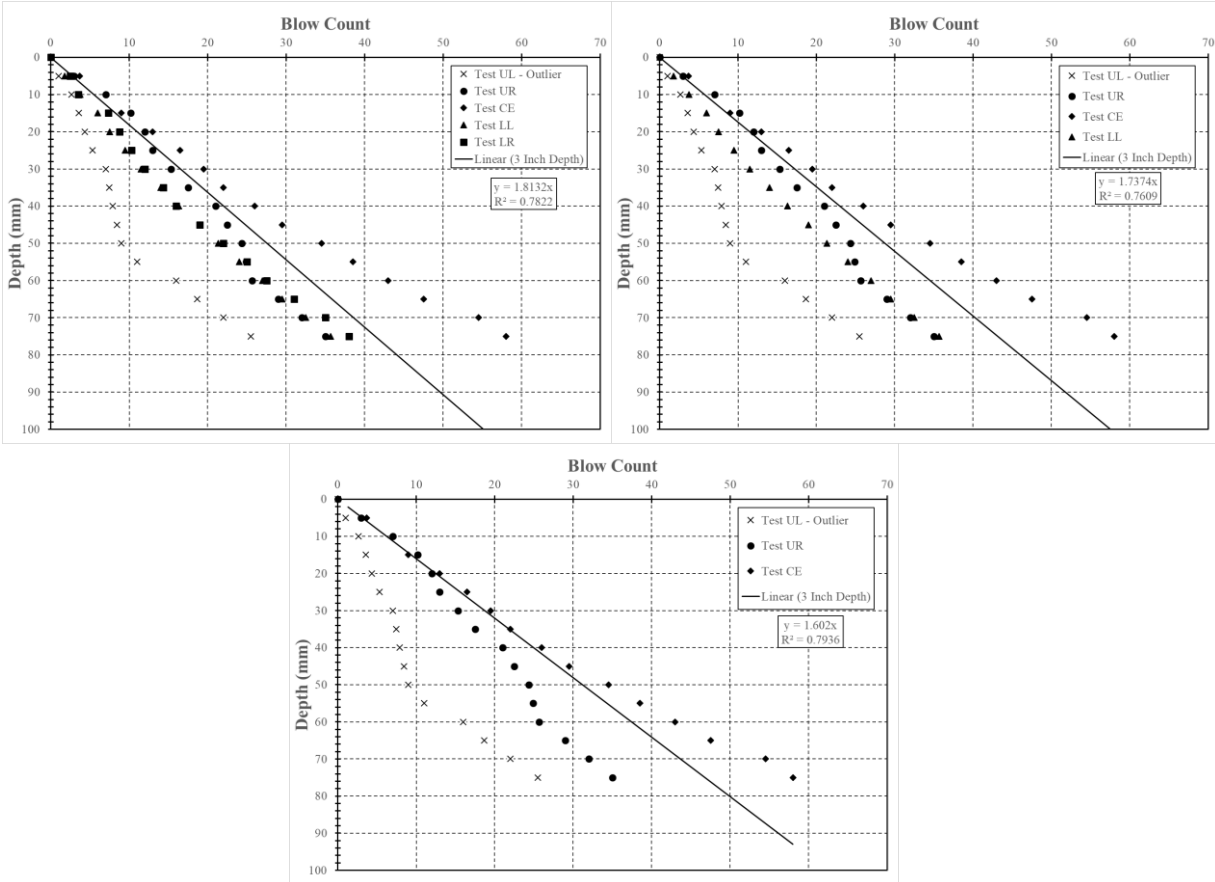


Figure L.1: Test performed on July 9, 2019, Location 1 (top left = 5 tests, top right = 4 tests, bottom = 3 tests)

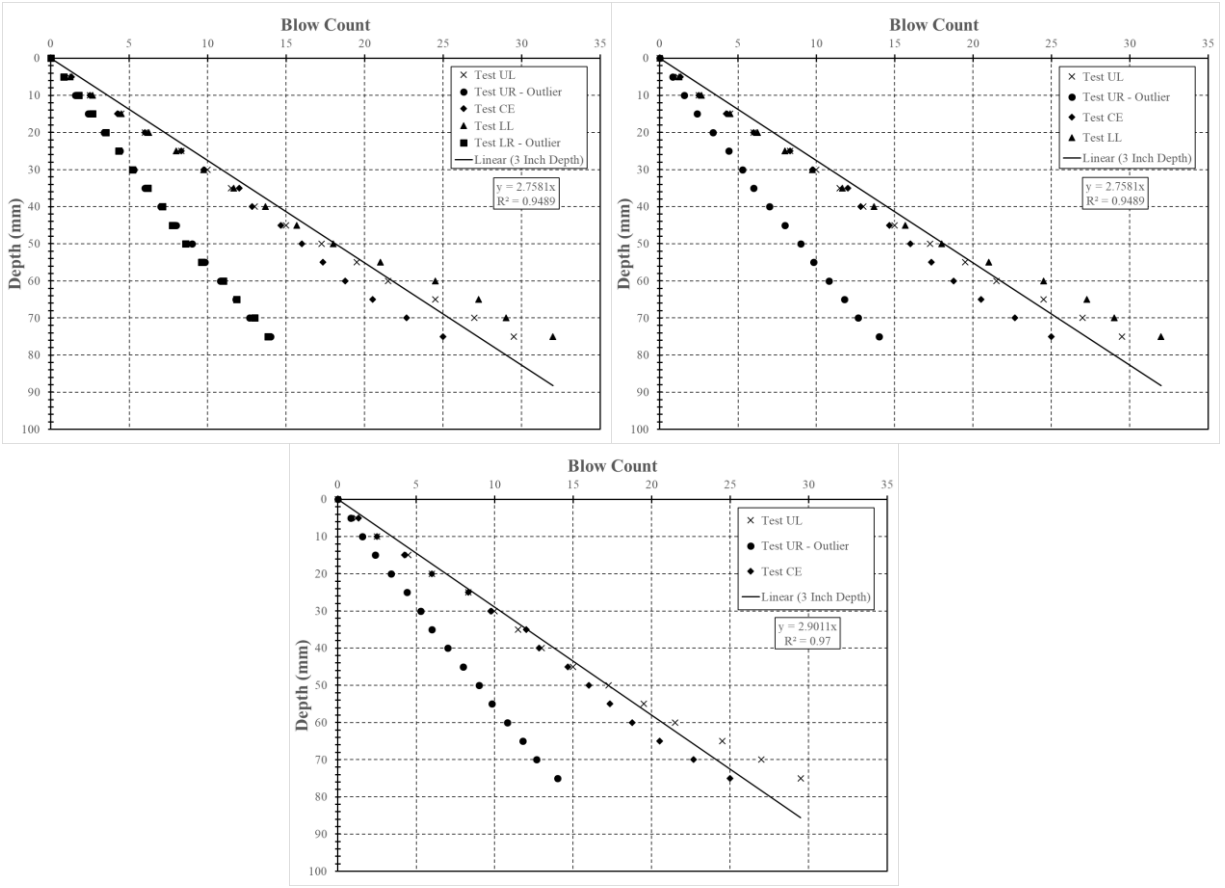


Figure L.2: Test performed on July 10, 2019, Location 4 (top left = 5 tests, top right = 4 tests, bottom = 3 tests)

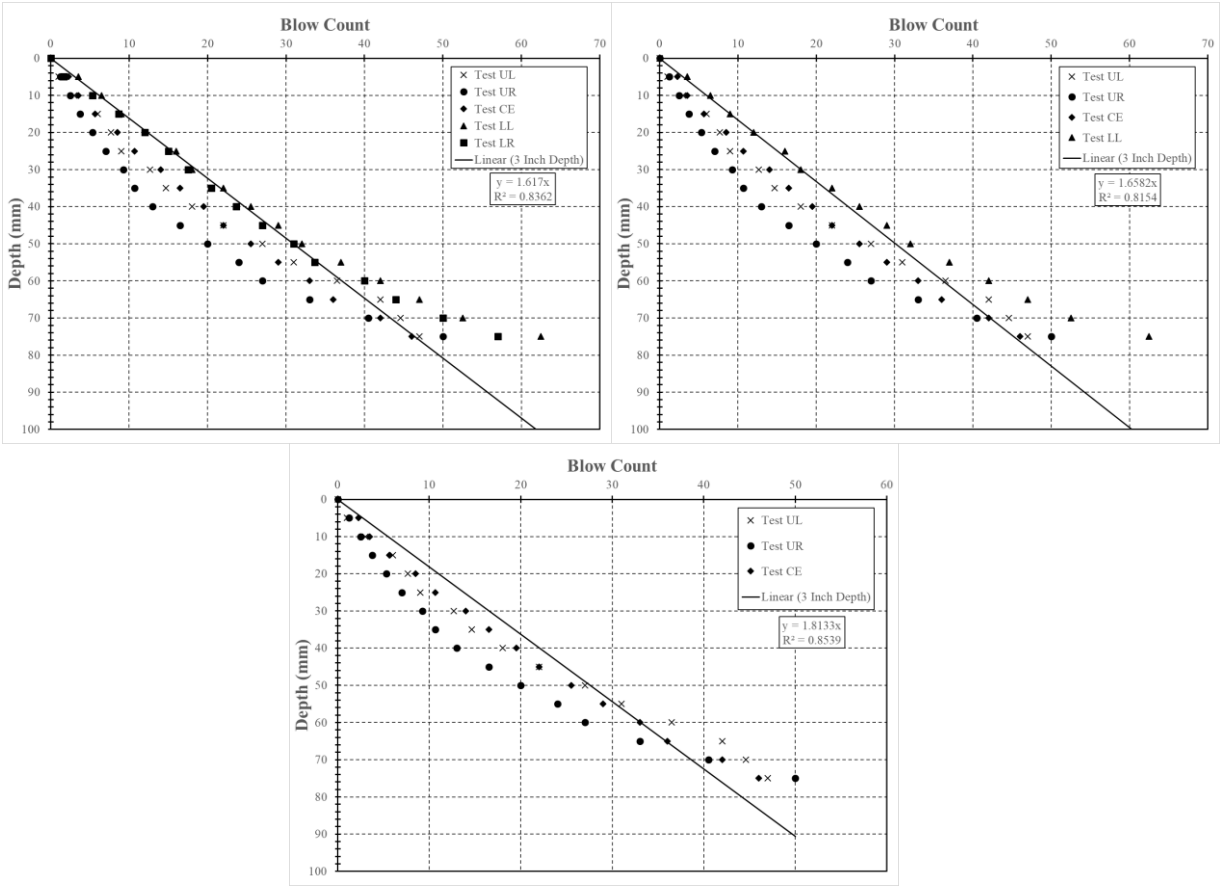


Figure L.3: Test performed on July 10, 2019, Location 5 (top left = 5 tests, top right = 4 tests, bottom = 3 tests)

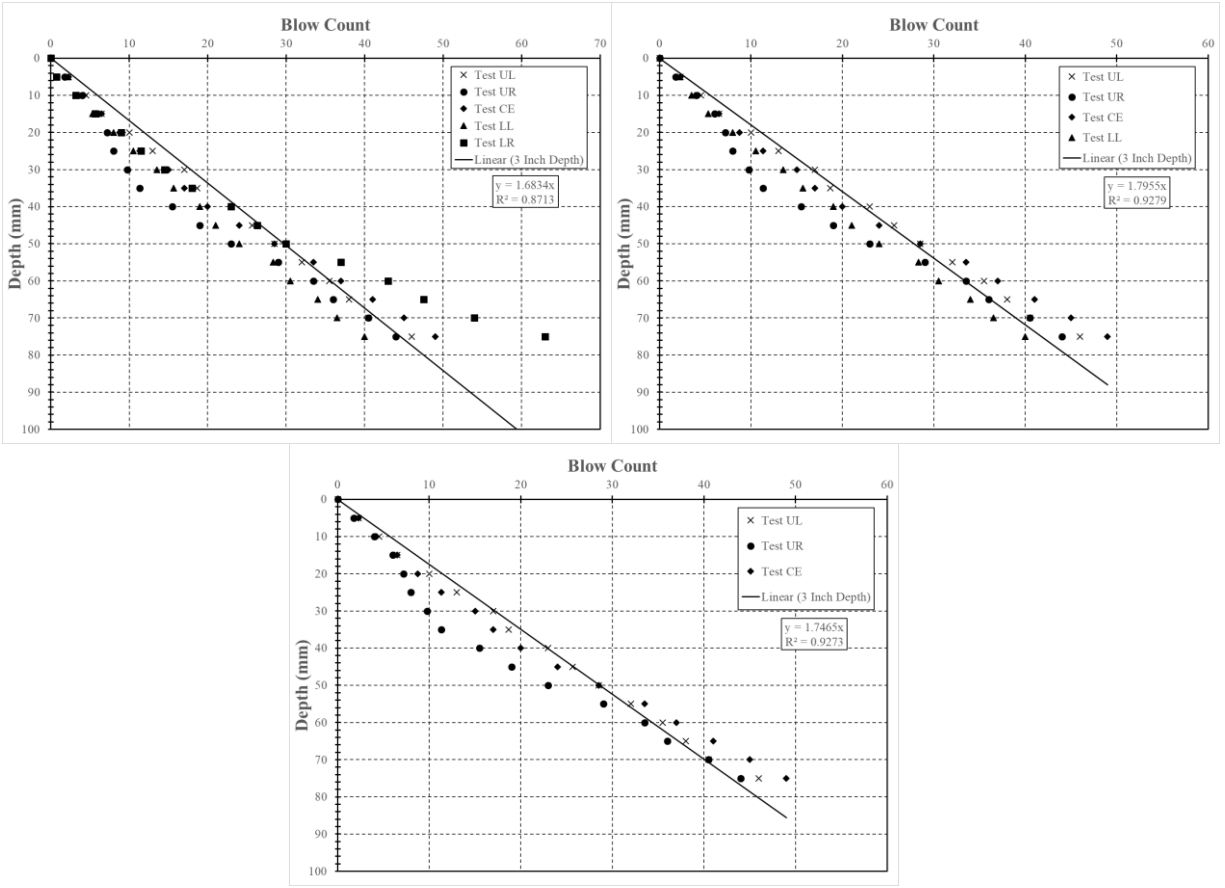


Figure L.4: Test performed on July 10, 2019, Location 6 (top left = 5 tests, top right = 4 tests, bottom = 3 tests)

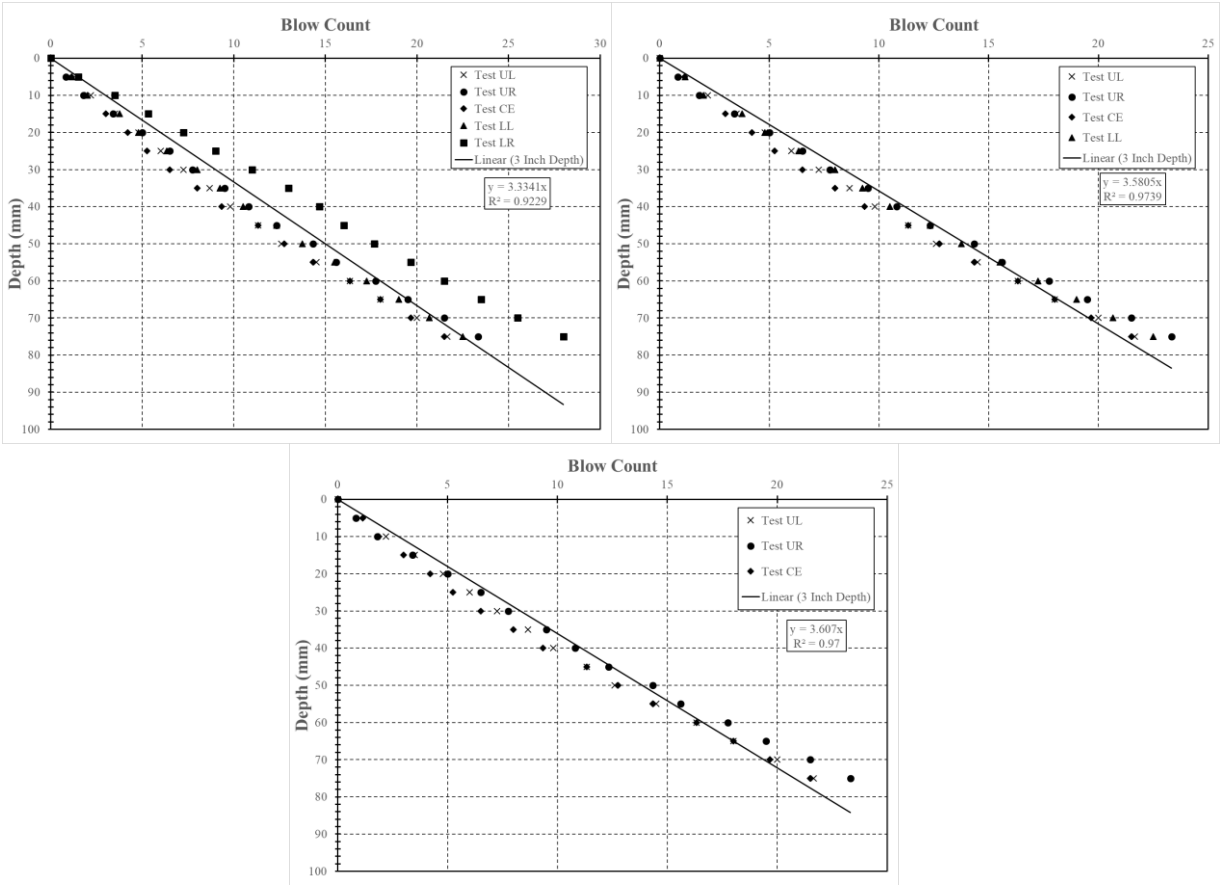


Figure L.5: Test performed on July 16, 2019, Location 7 (top left = 5 tests, top right = 4 tests, bottom = 3 tests)

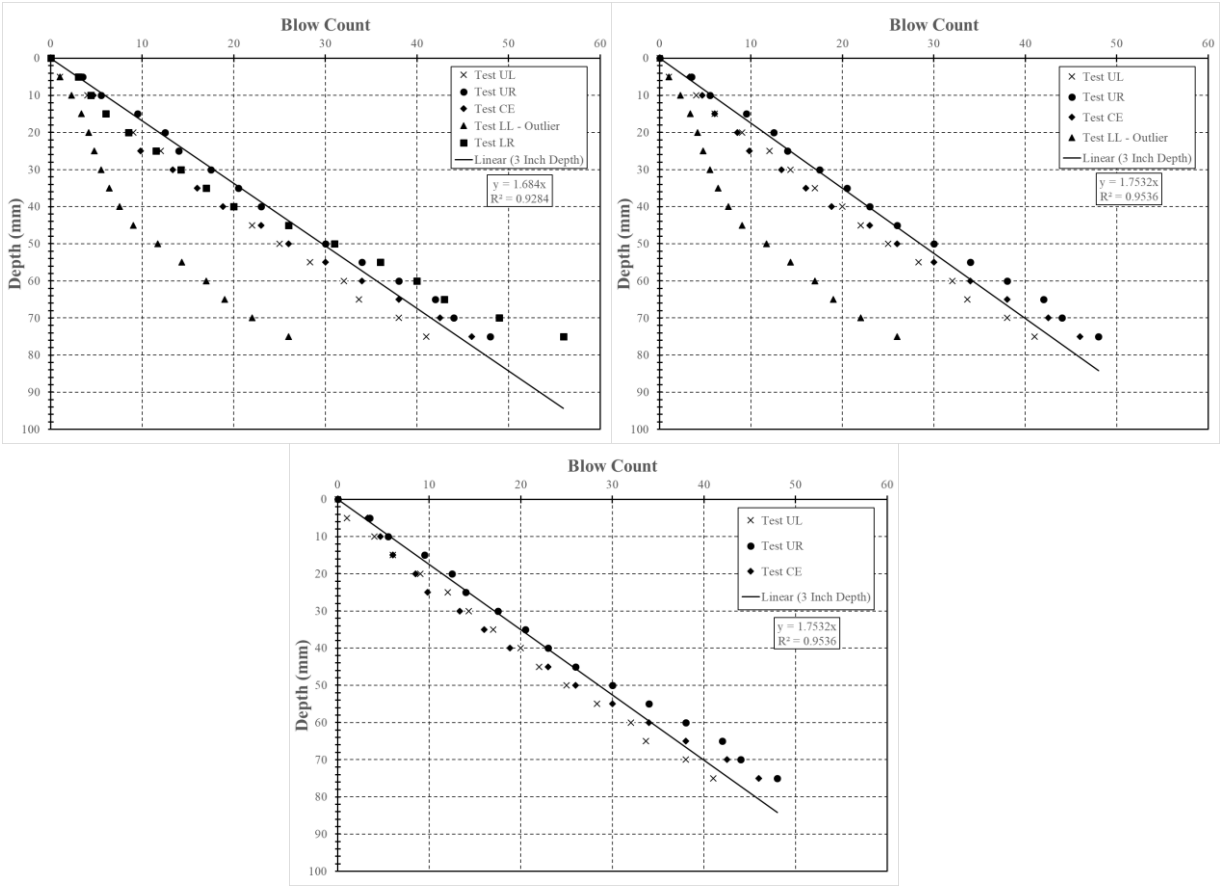


Figure L.6: Test performed on July 16, 2019, Location 8 (top left = 5 tests, top right = 4 tests, bottom = 3 tests)

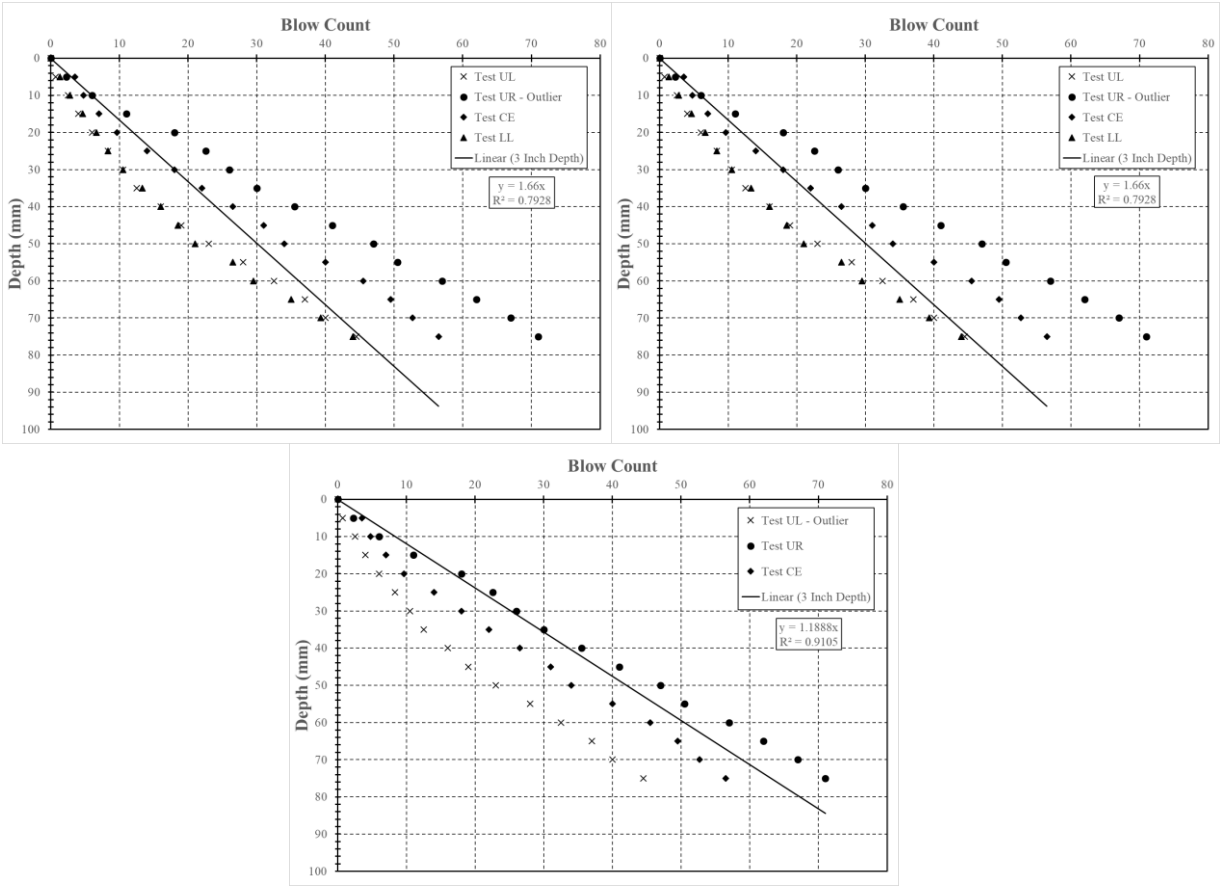


Figure L.7: Test performed on July 16, 2019, Location 9 (top left = 5 tests, top right = 4 tests, bottom = 3 tests)

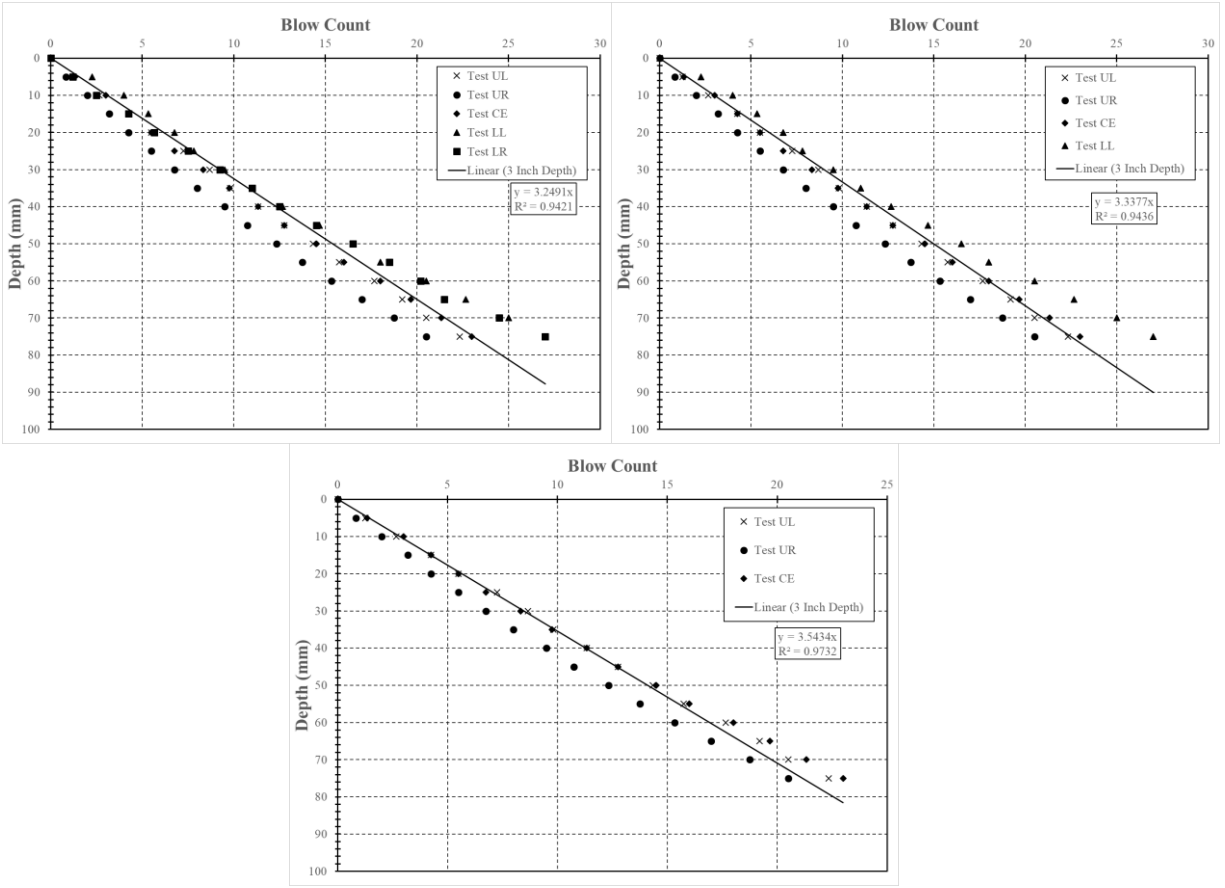


Figure L.8: Test performed on July 16, 2019, Location 10 (top left = 5 tests, top right = 4 tests, bottom = 3 tests)

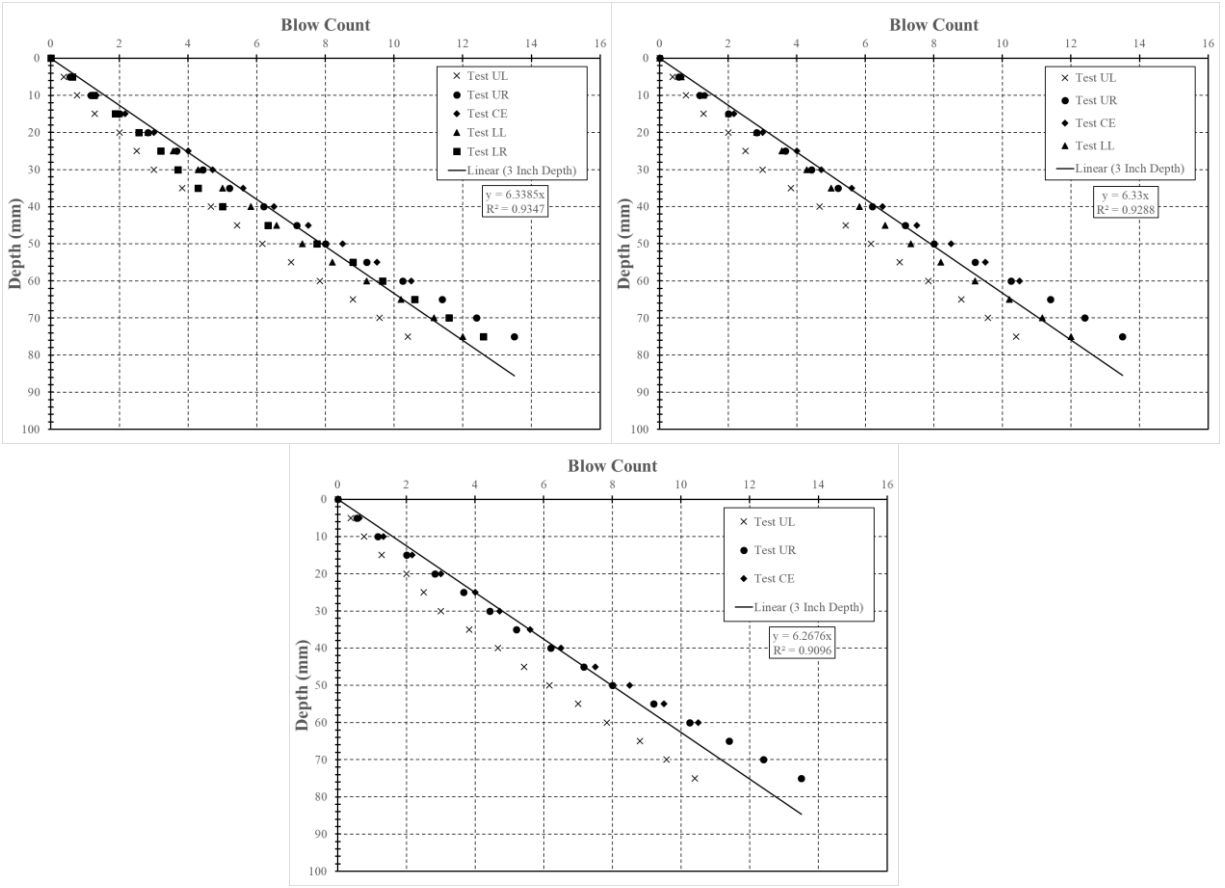


Figure L.9: Test performed on July 16, 2019, Location 11 (top left = 5 tests, top right = 4 tests, bottom = 3 tests)

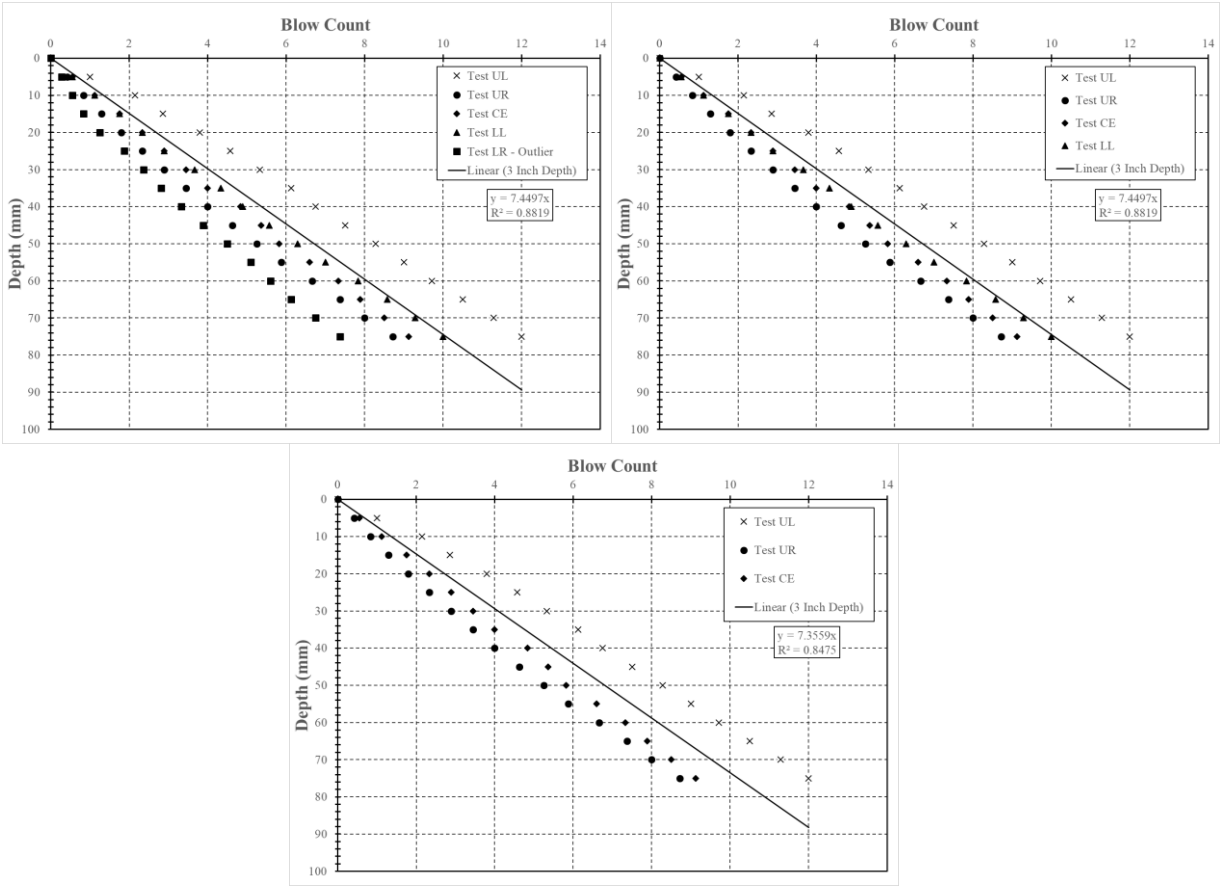


Figure L.10: Test performed on July 16, 2019, Location 12 (top left = 5 tests, top right = 4 tests, bottom = 3 tests)

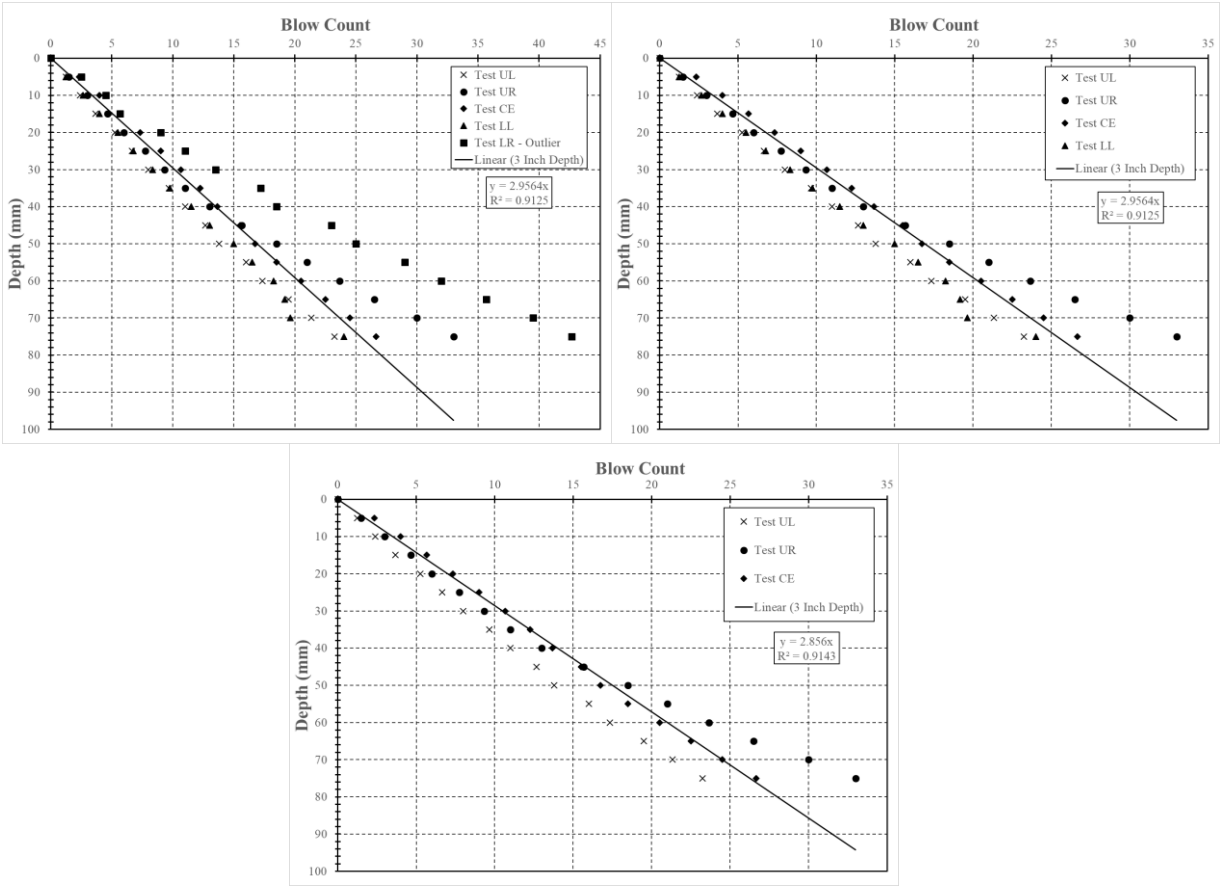


Figure L.11: Test performed on July 16, 2019, Location 13 (top left = 5 tests, top right = 4 tests, bottom = 3 tests)

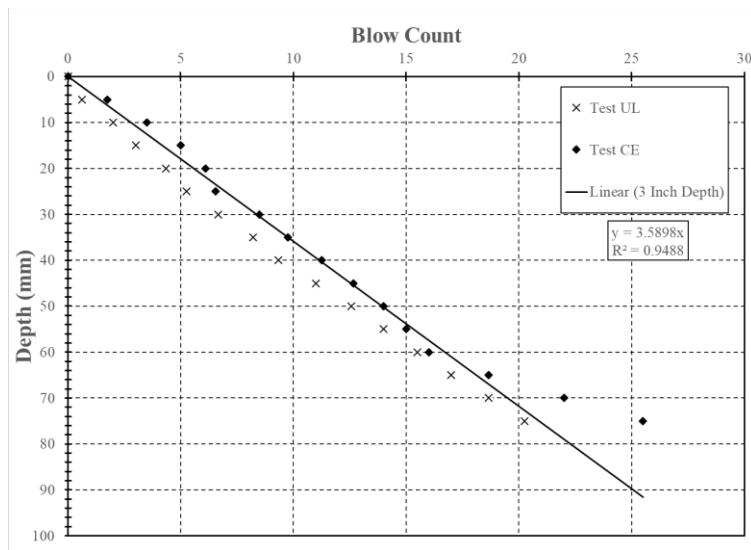


Figure L.12: Test performed on July 16, 2019, Location 15 (only 2 tests completed)

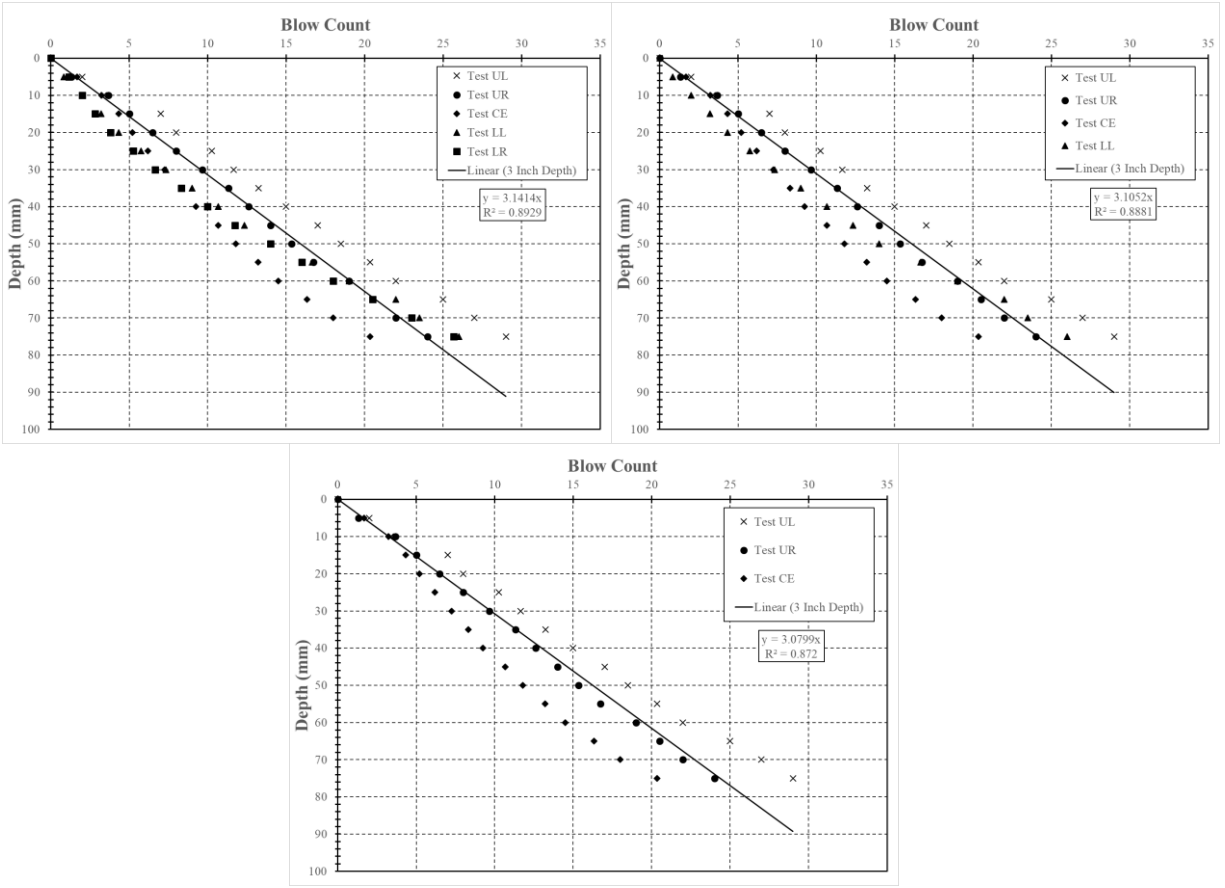


Figure L.13: Test performed on July 17, 2019, Location 17 (top left = 5 tests, top right = 4 tests, bottom = 3 tests)

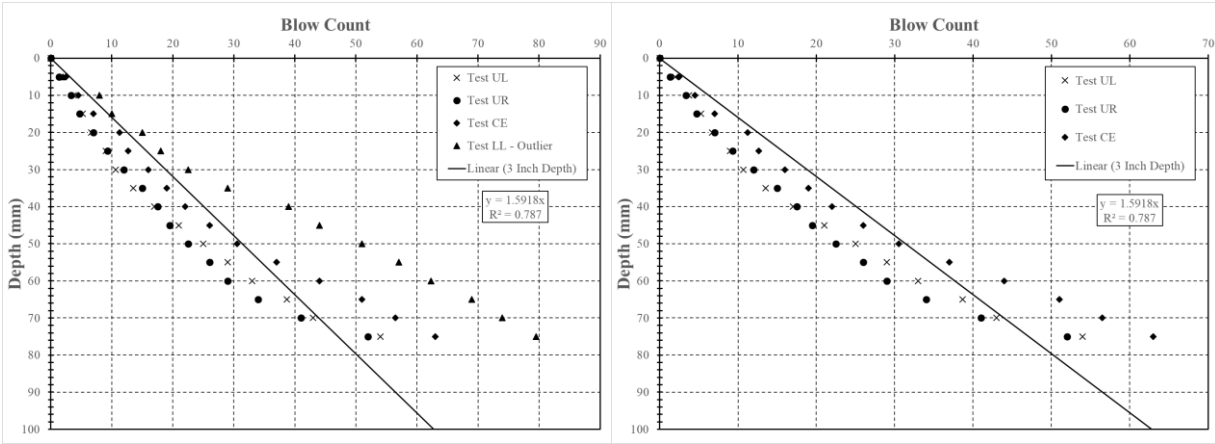


Figure L.14: Test performed on July 17, 2019, Location 18 (left = 4 tests, right = 3 tests)

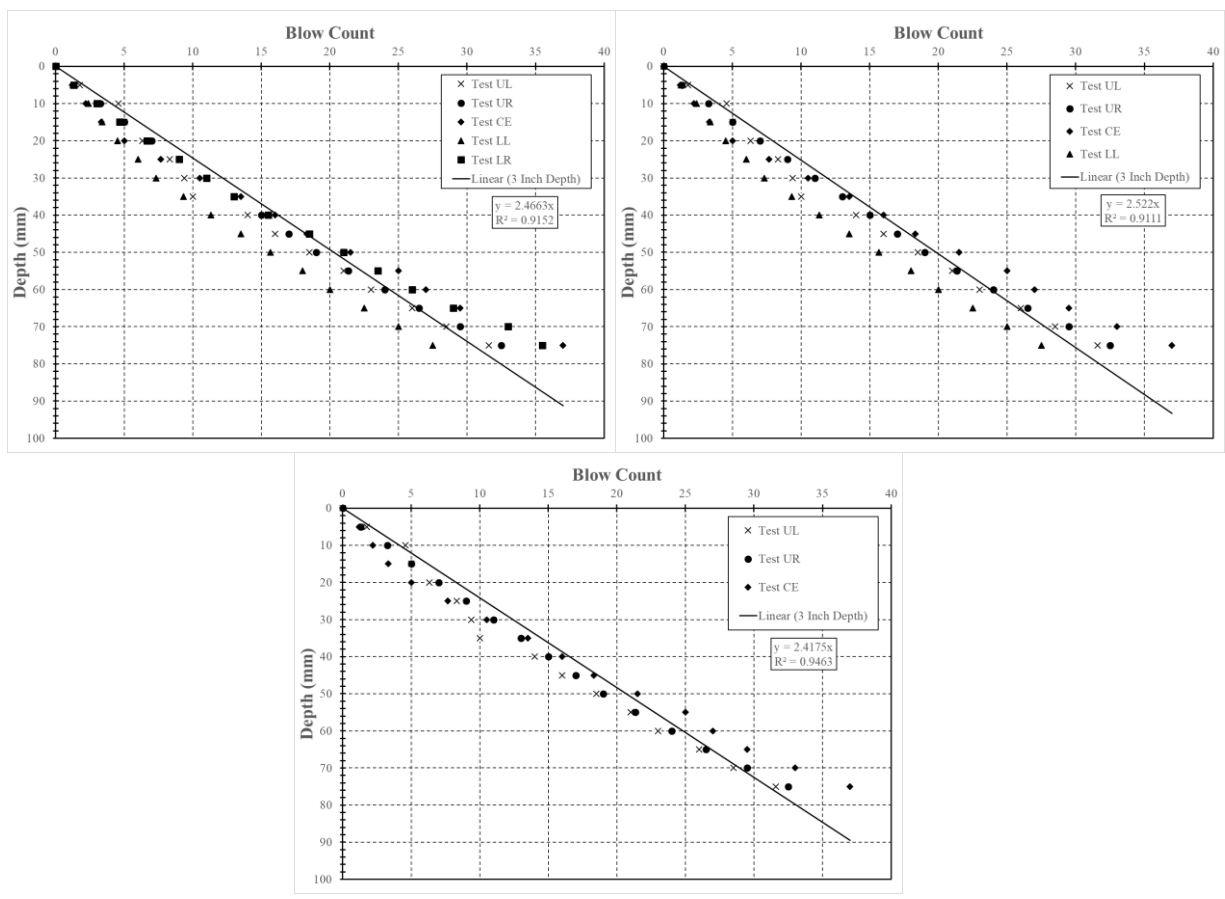


Figure L.15: Test performed on July 17, 2019, Location 19 (top left = 5 tests, top right = 4 tests, bottom = 3 tests)

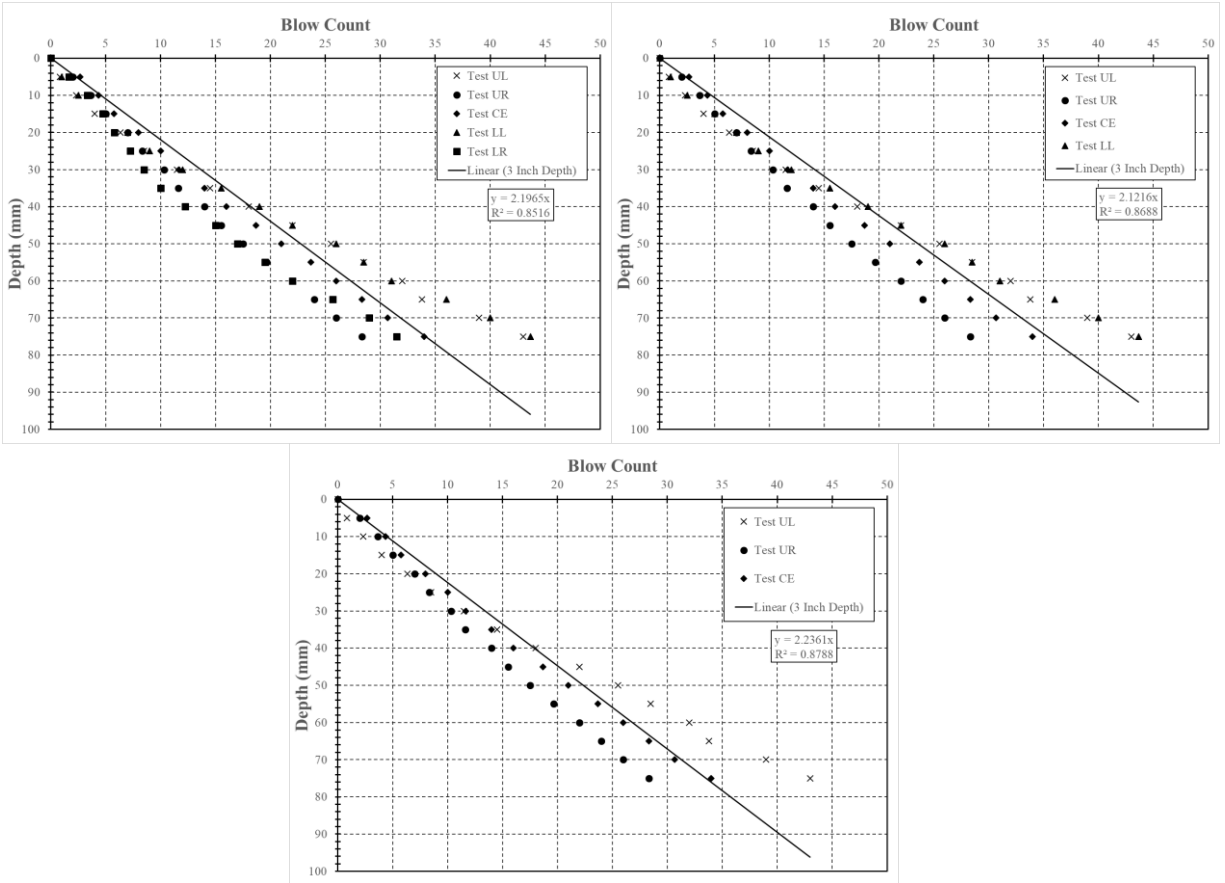


Figure L.16: Test performed on July 17, 2019, Location 20 (top left = 5 tests, top right = 4 tests, bottom = 3 tests)

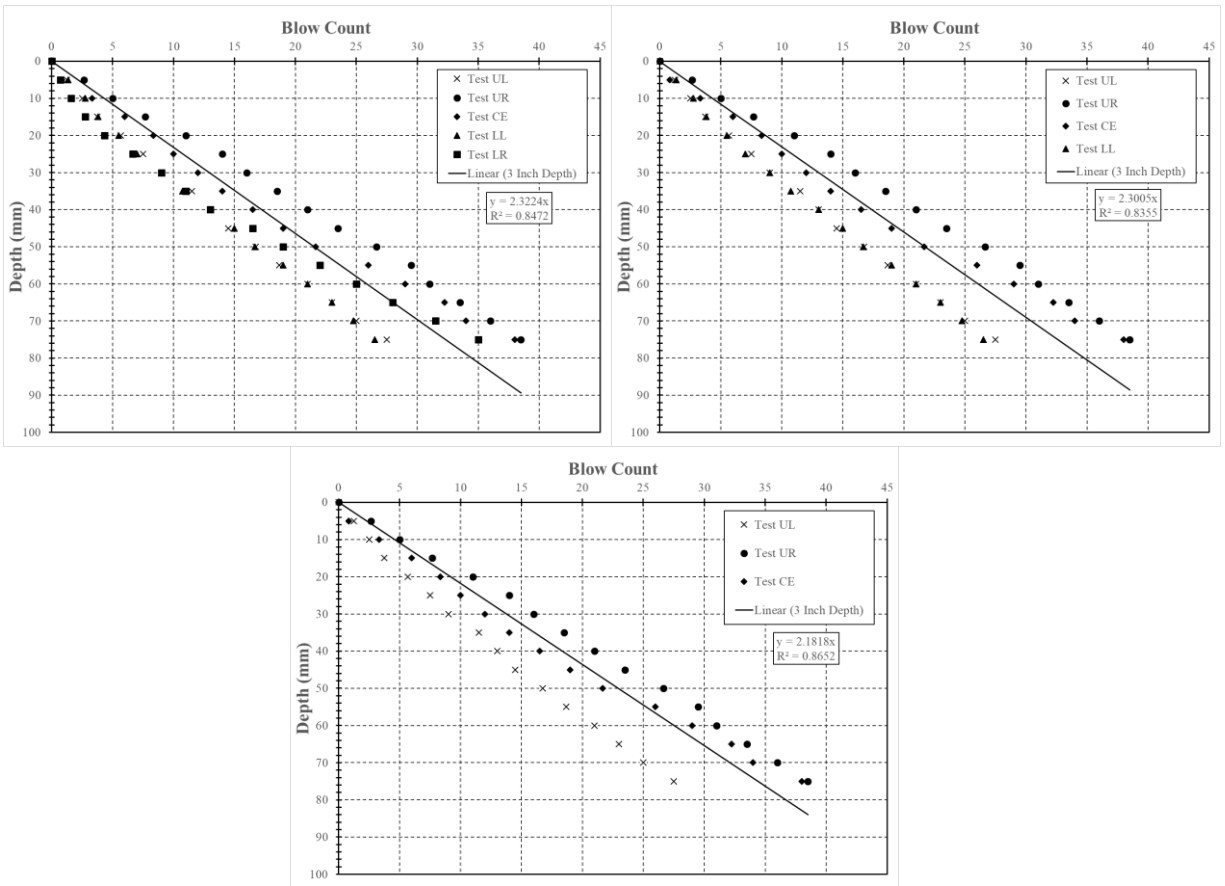


Figure L.17: Test performed on July 17, 2019, Location 21 (top left = 5 tests, top right = 4 tests, bottom = 3 tests)

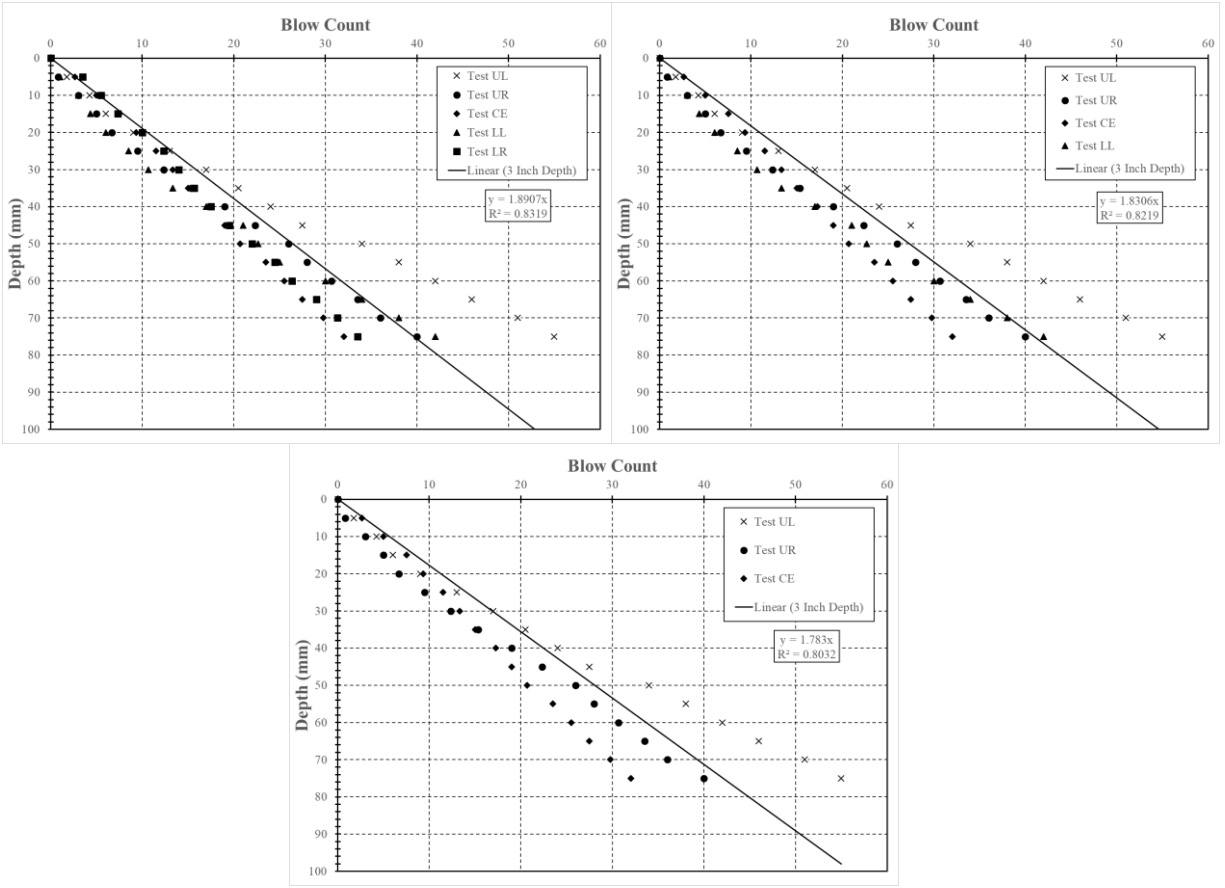


Figure L.18: Test performed on July 17, 2019, Location 22 (top left = 5 tests, top right = 4 tests, bottom = 3 tests)

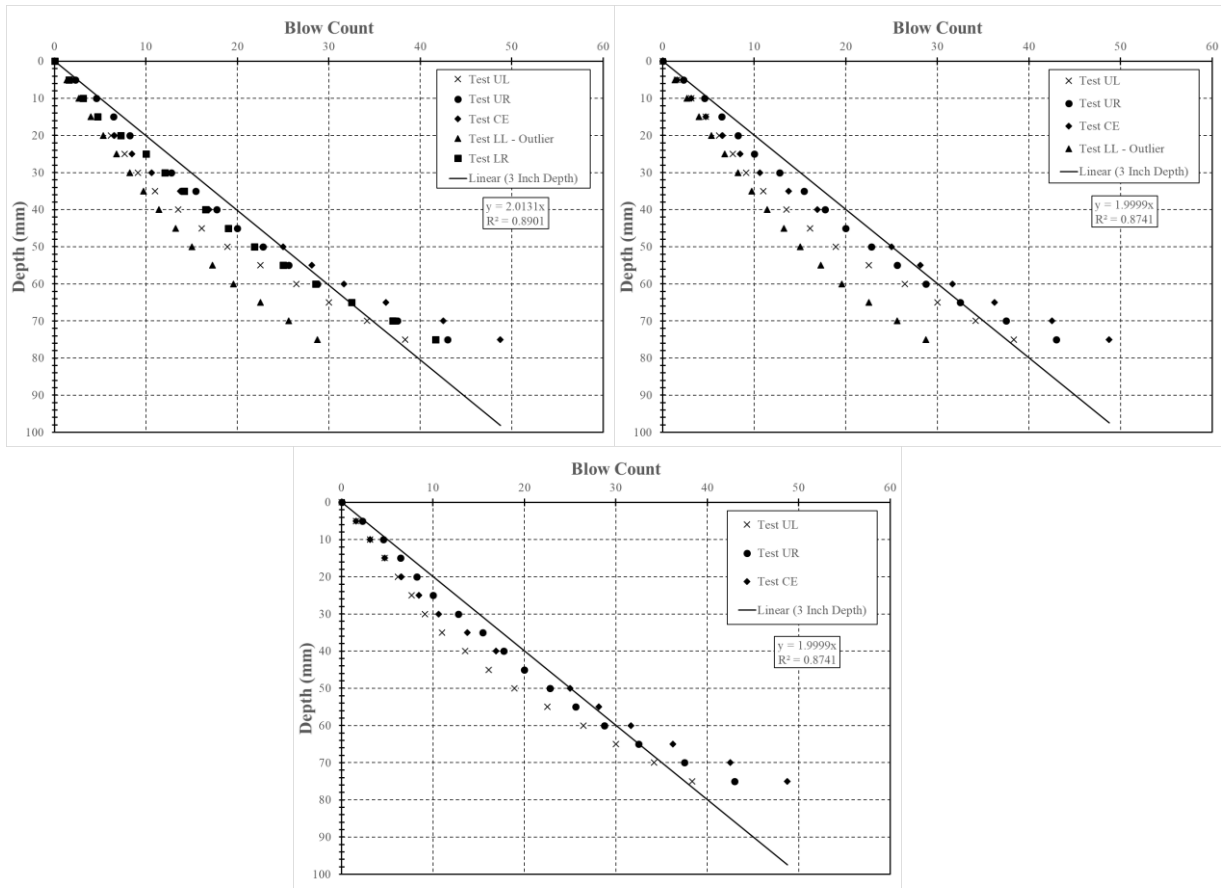


Figure L.19: Test performed on July 18, 2019, Location 23 (top left = 5 tests, top right = 4 tests, bottom = 3 tests)

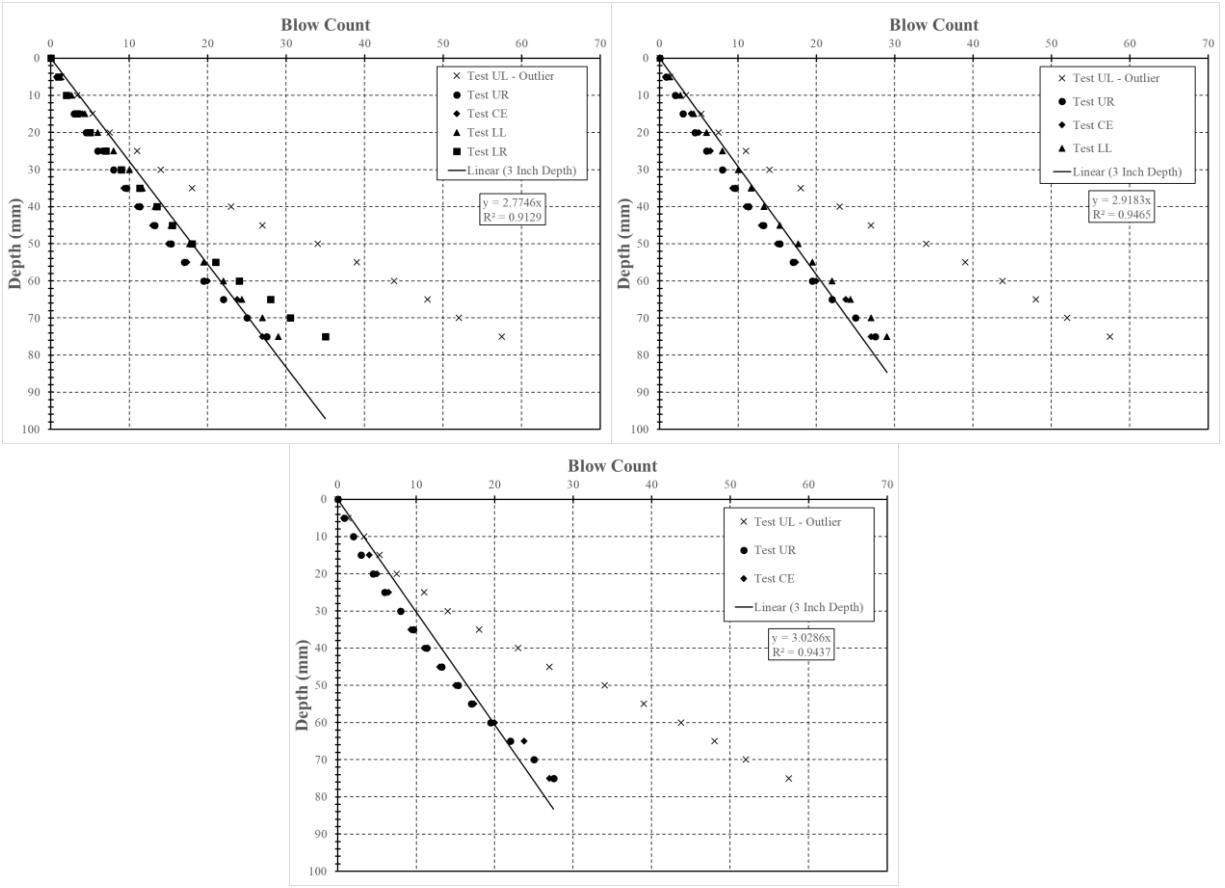


Figure L.20: Test performed on July 18, 2019, Location 24 (top left = 5 tests, top right = 4 tests, bottom = 3 tests)

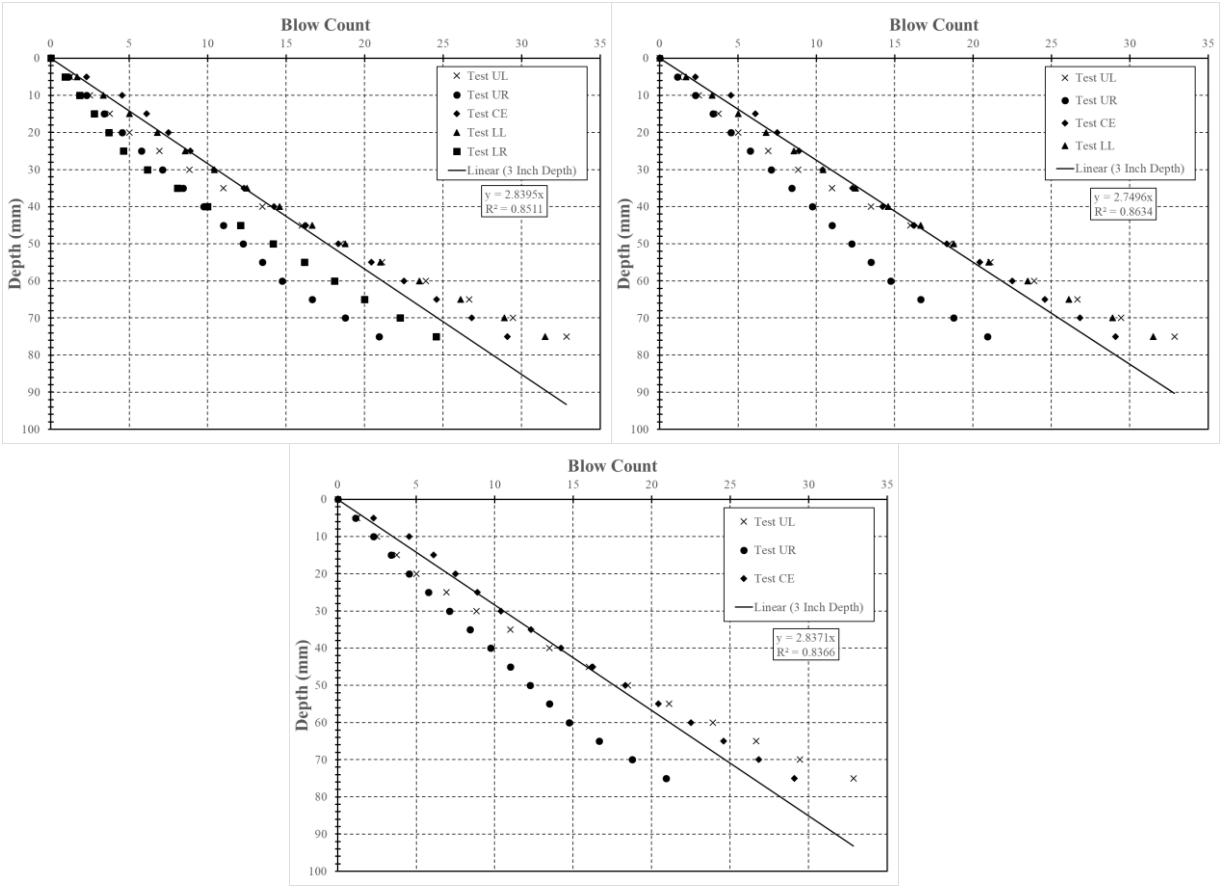


Figure L.21: Test performed on July 18, 2019, Location 25 (top left = 5 tests, top right = 4 tests, bottom = 3 tests)

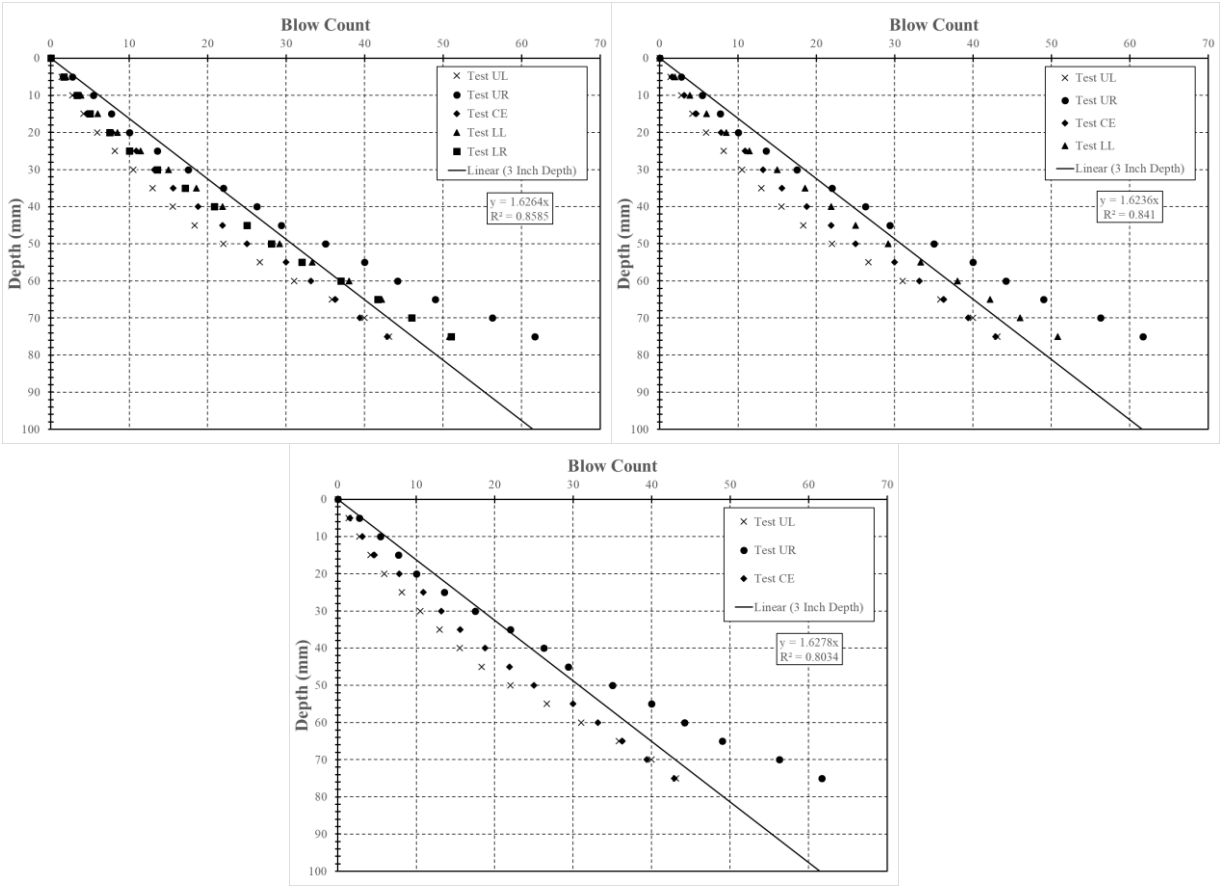


Figure L.22: Test performed on July 18, 2019, Location 28 (top left = 5 tests, top right = 4 tests, bottom = 3 tests)

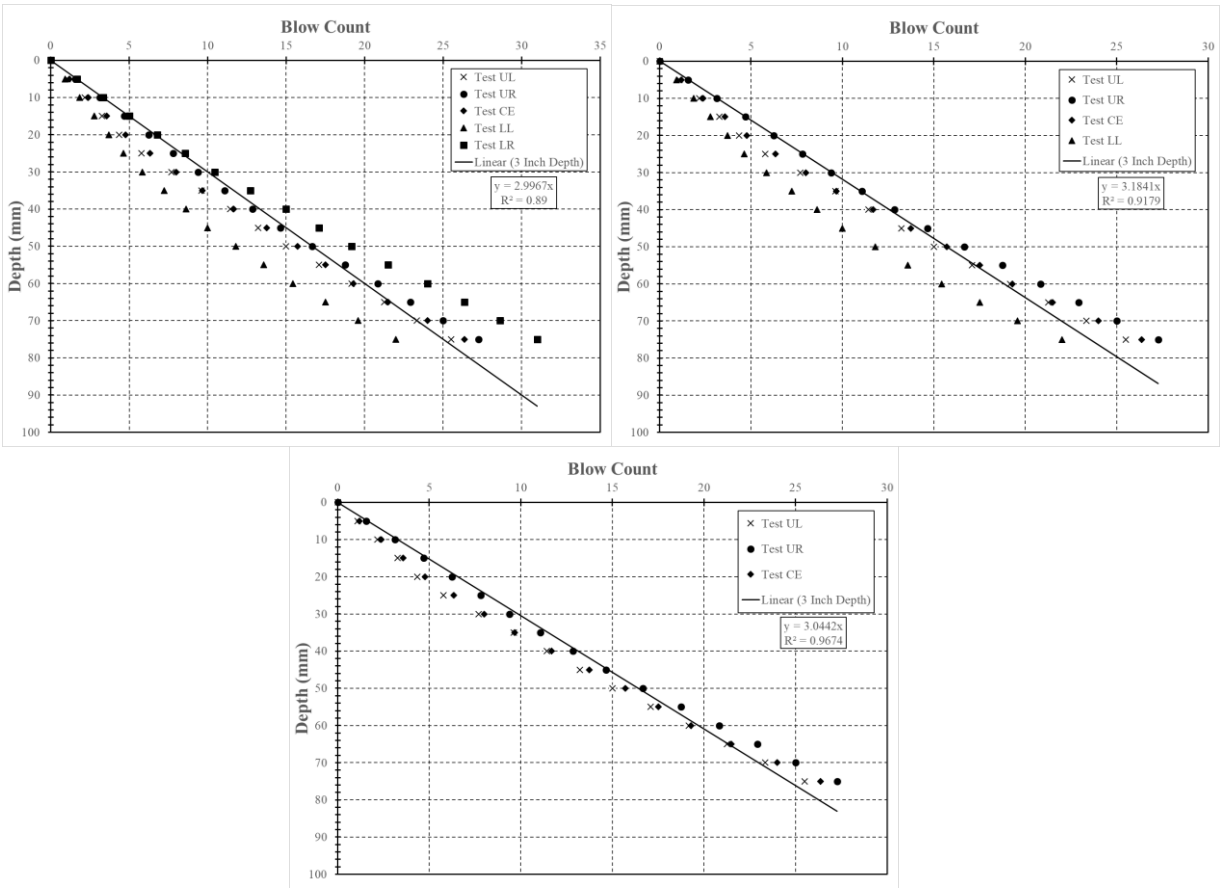


Figure L.23: Test performed on July 19, 2019, Location 30 (top left = 5 tests, top right = 4 tests, bottom = 3 tests)

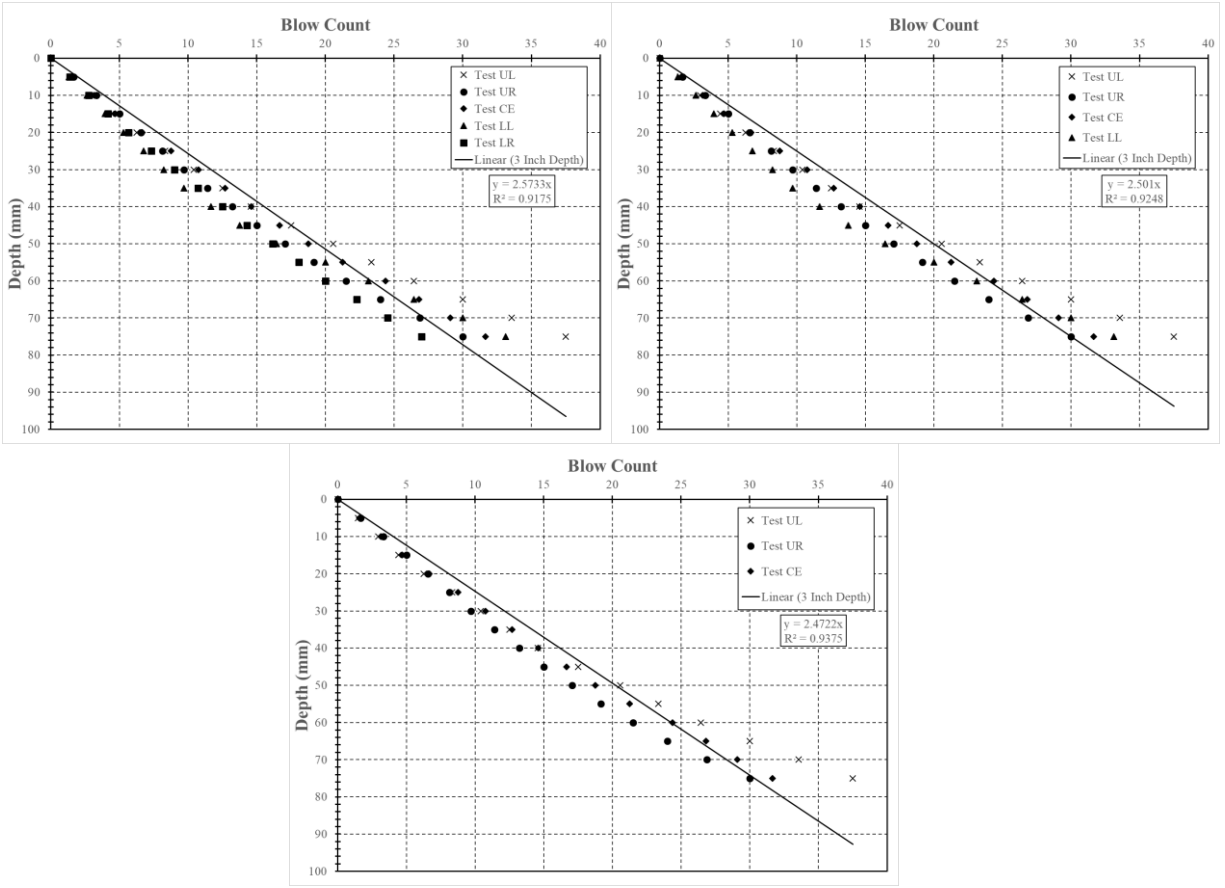


Figure L.24: Test performed on July 19, 2019, Location 31 (top left = 5 tests, top right = 4 tests, bottom = 3 tests)

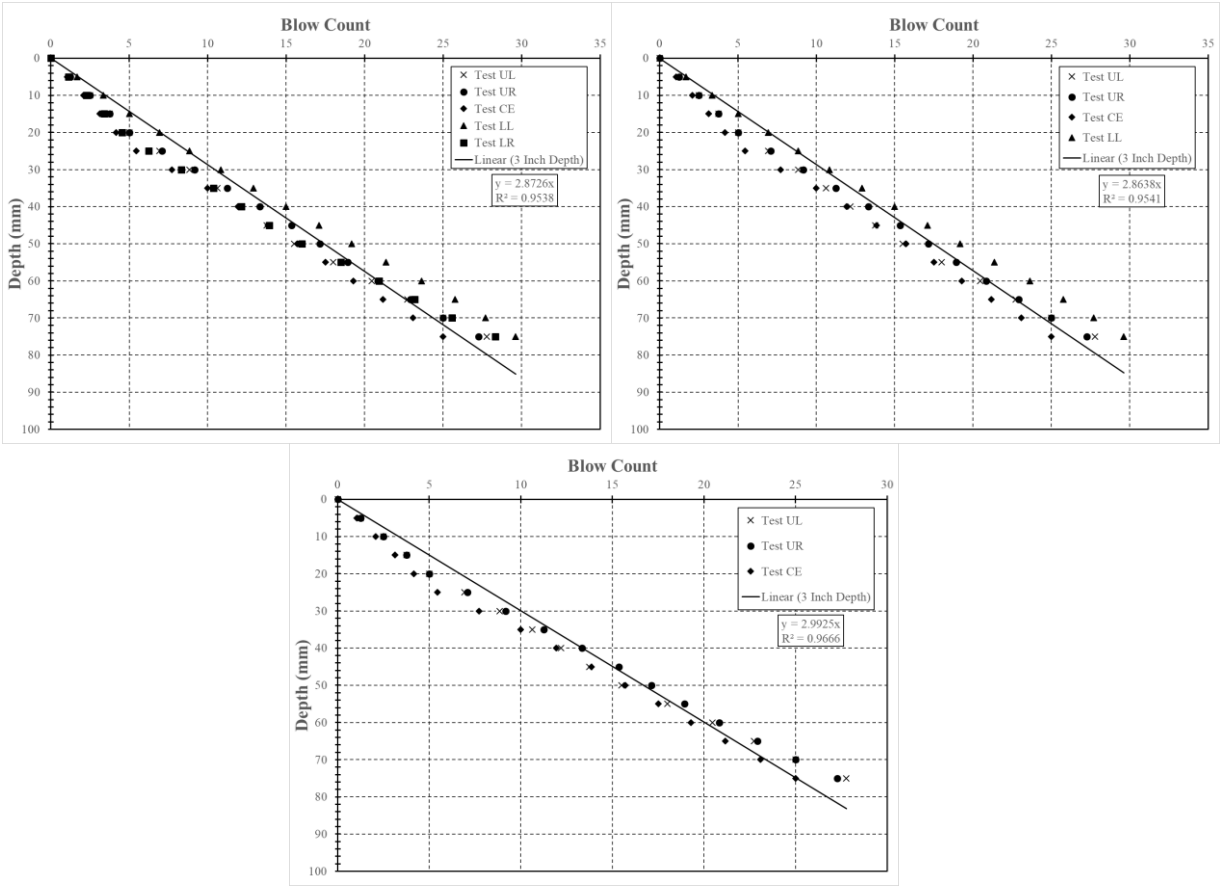


Figure L.25: Test performed on July 19, 2019, Location 32 (top left = 5 tests, top right = 4 tests, bottom = 3 tests)

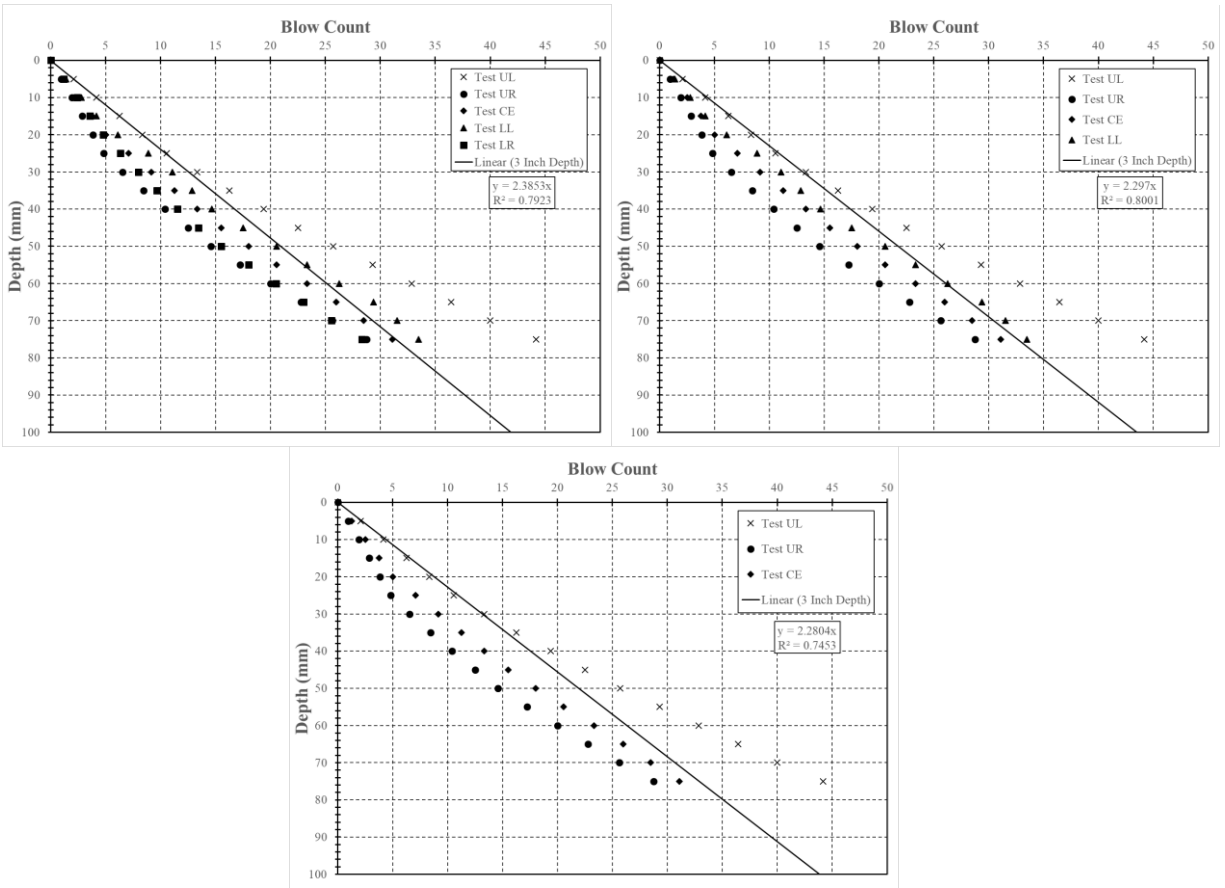


Figure L.26: Test performed on July 19, 2019, Location 33 (top left = 5 tests, top right = 4 tests, bottom = 3 tests)

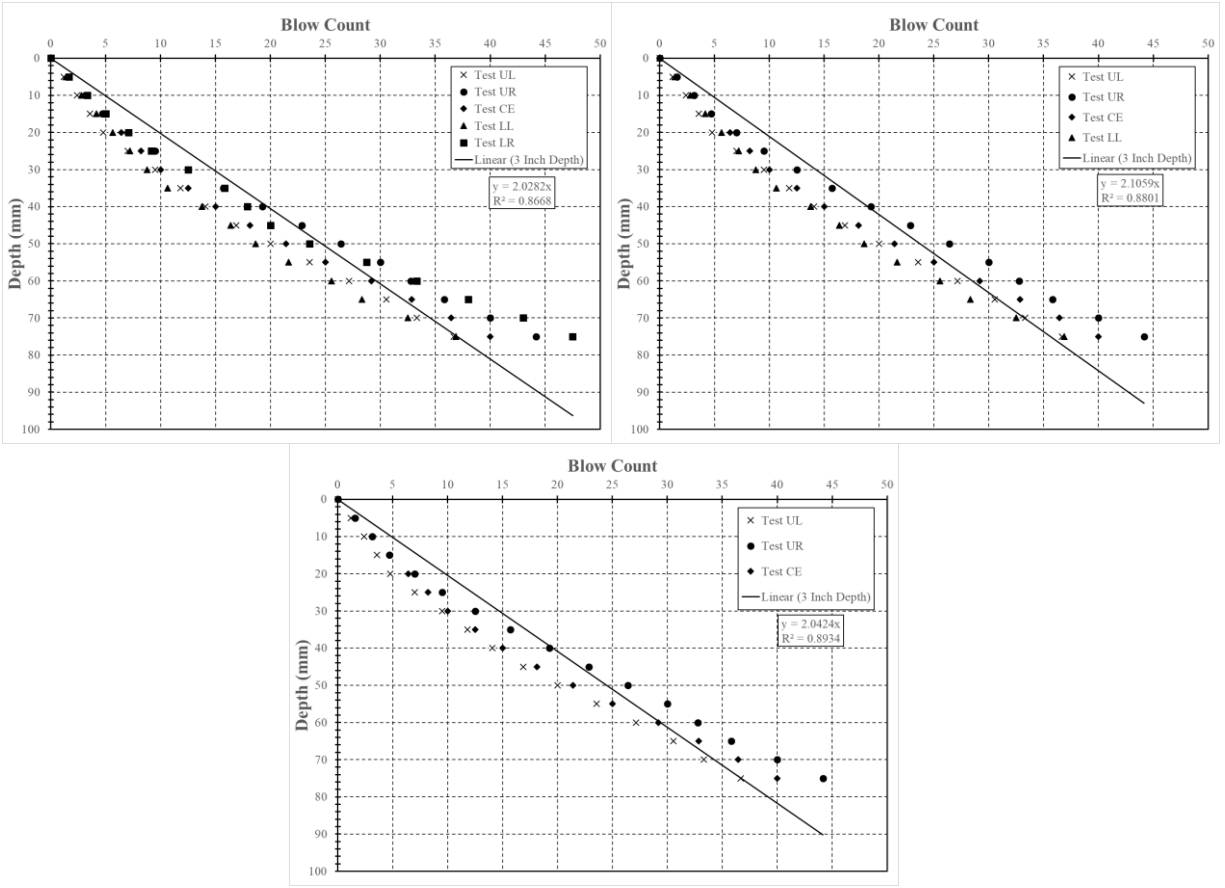


Figure L.27: Test performed on July 19, 2019, Location 34 (top left = 5 tests, top right = 4 tests, bottom = 3 tests)

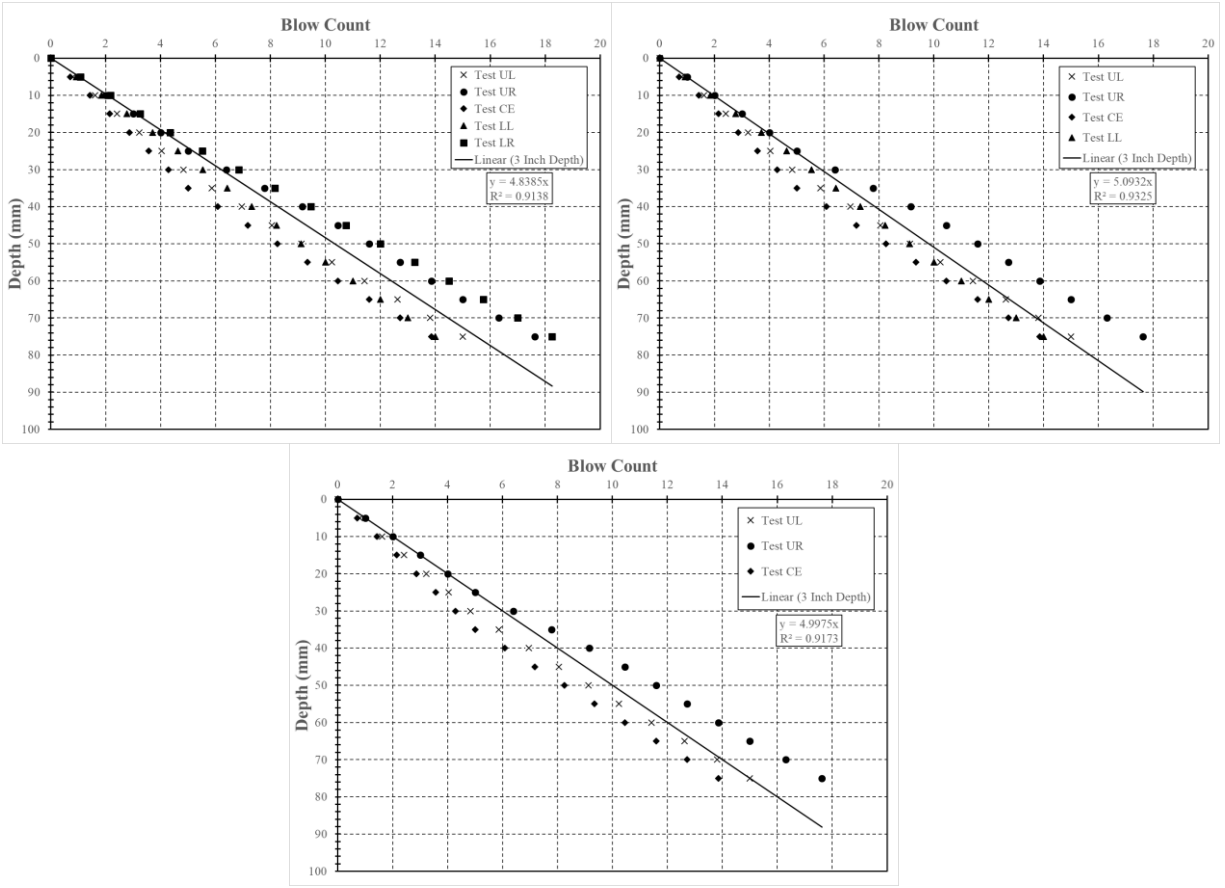


Figure L.28: Test performed on July 19, 2019, Location 35 (top left = 5 tests, top right = 4 tests, bottom = 3 tests)

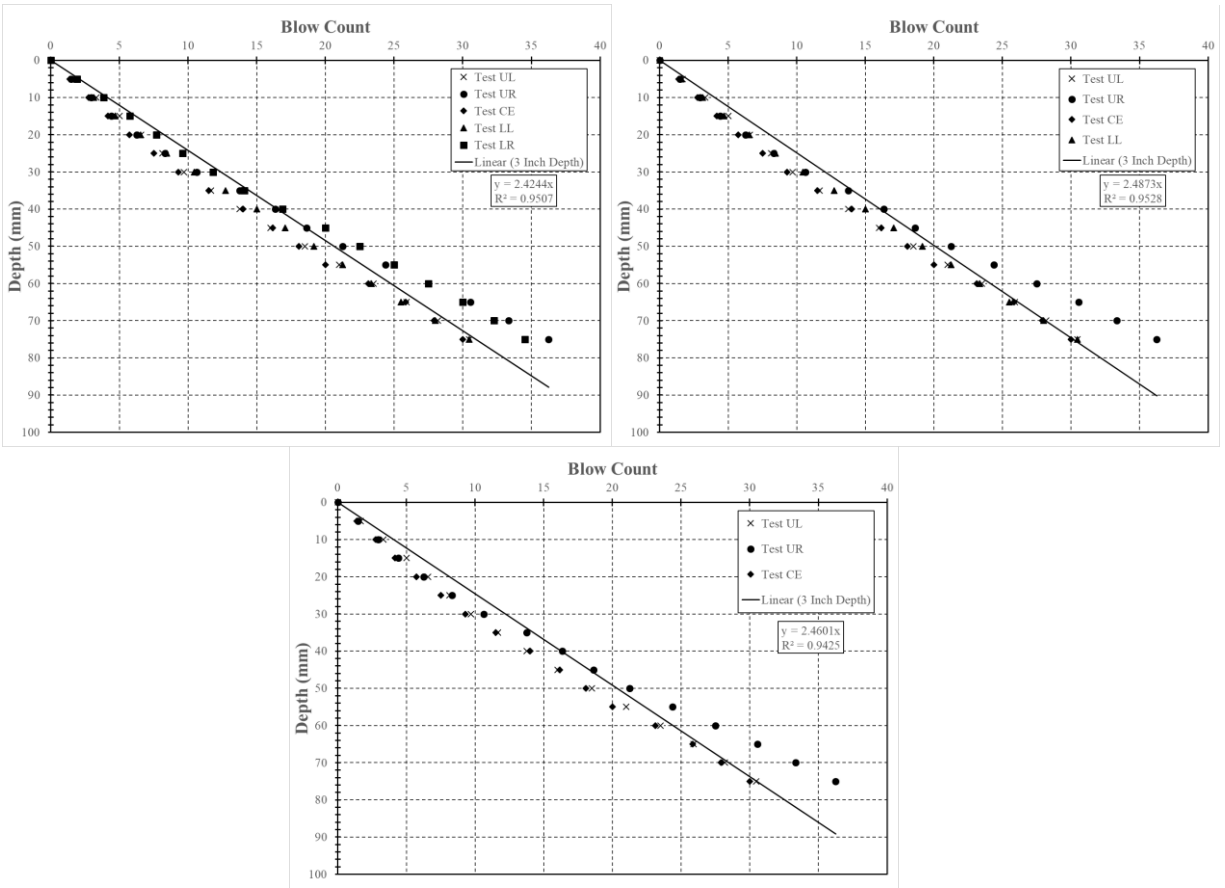


Figure L.29: Test performed on July 19, 2019, Location 36 (top left = 5 tests, top right = 4 tests, bottom = 3 tests)

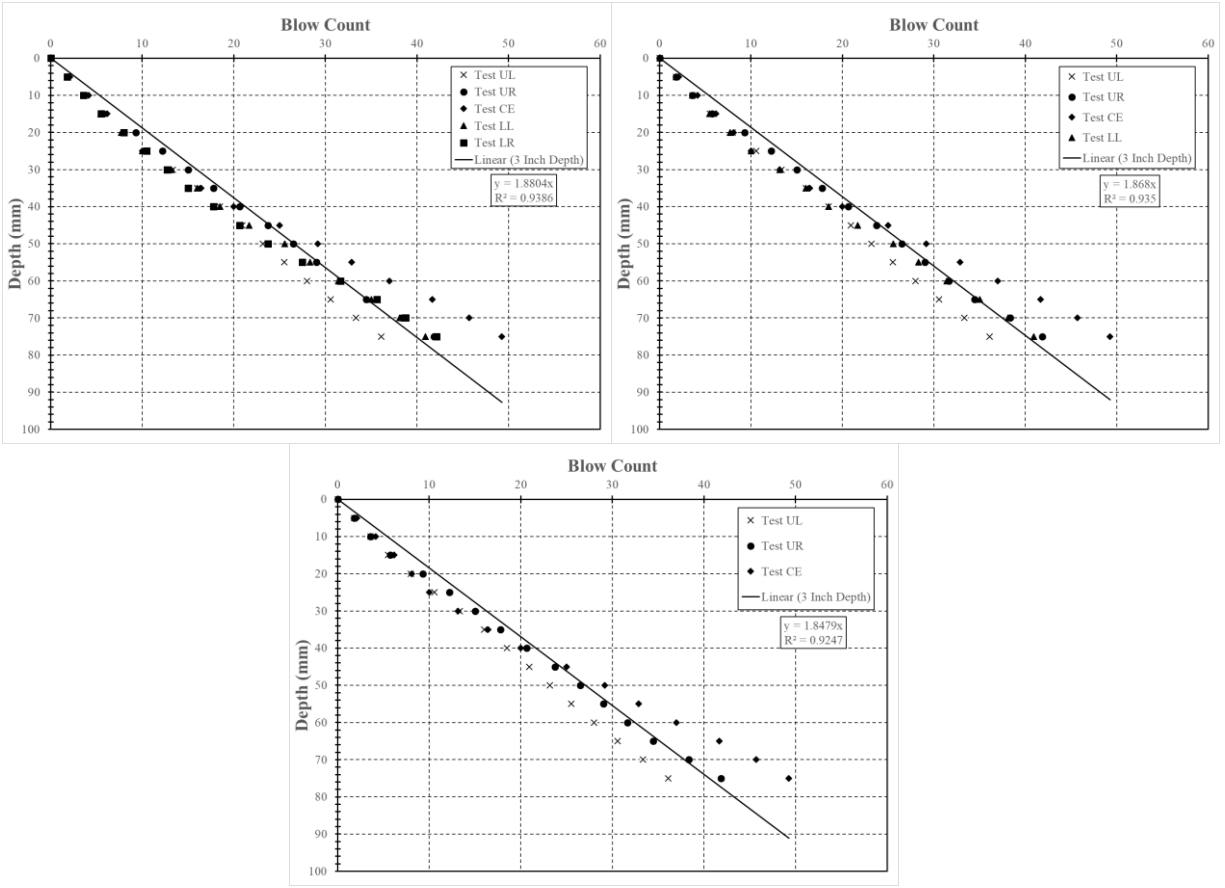


Figure L.30: Test performed on July 23, 2019, Location 37 (top left = 5 tests, top right = 4 tests, bottom = 3 tests)

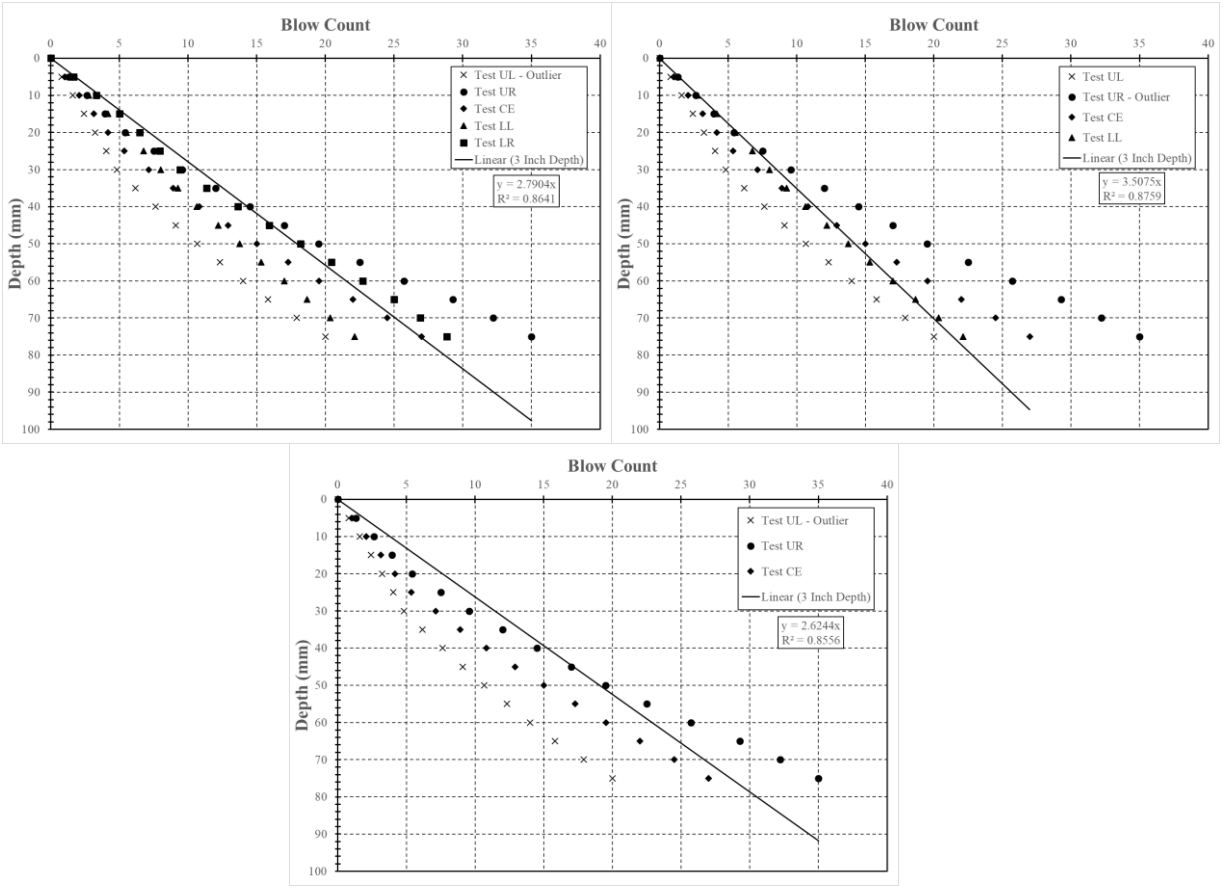


Figure L.31: Test performed on July 23, 2019, Location 38 (top left = 5 tests, top right = 4 tests, bottom = 3 tests)

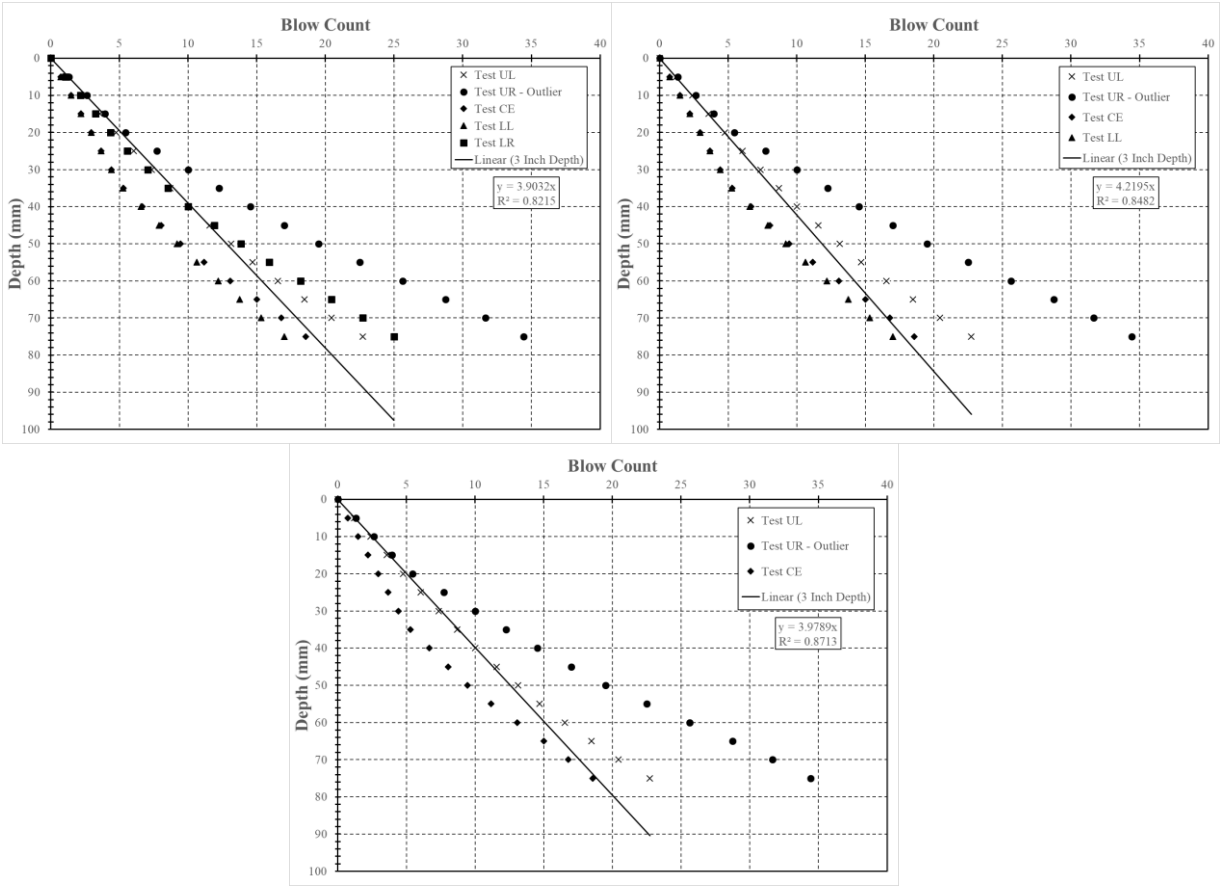


Figure L.32: Test performed on July 23, 2019, Location 39 (top left = 5 tests, top right = 4 tests, bottom = 3 tests)

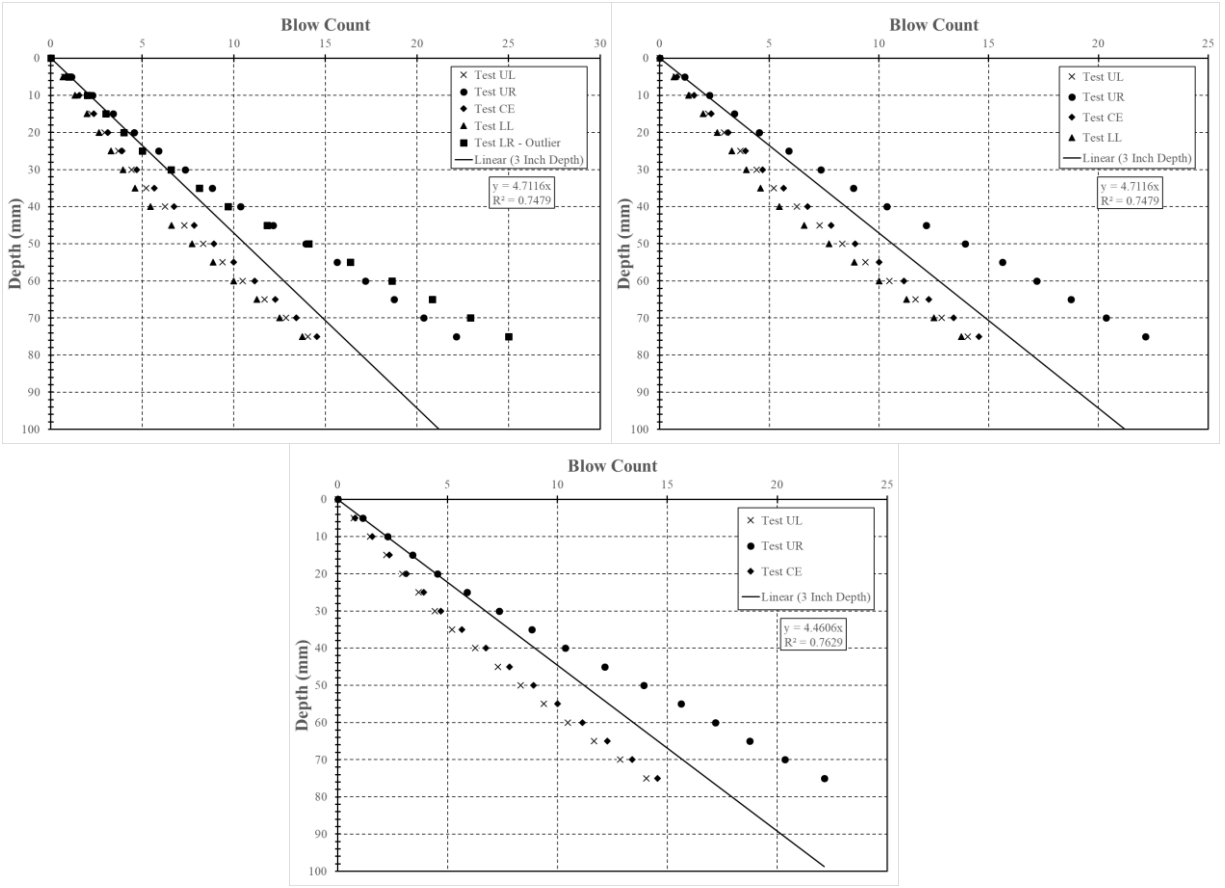


Figure L.33: Test performed on July 23, 2019, Location 40 (top left = 5 tests, top right = 4 tests, bottom = 3 tests)

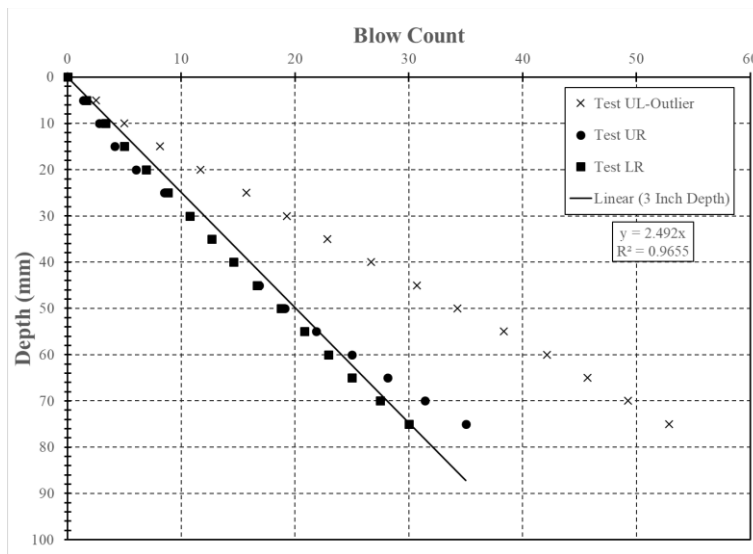


Figure L.34: Test performed on July 23, 2019, Location 41 (only 3 tests completed)

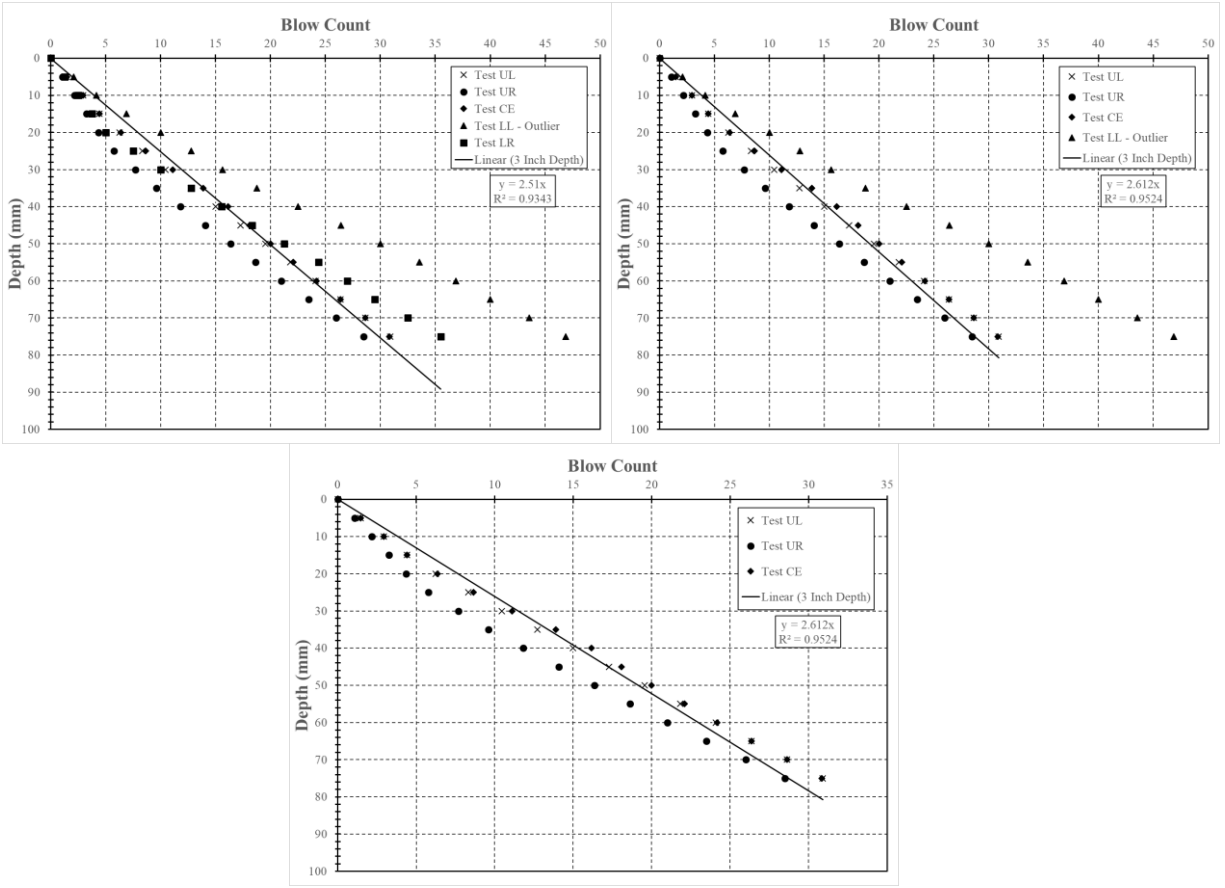


Figure L.35: Test performed on July 23, 2019, Location 42 (top left = 5 tests, top right = 4 tests, bottom = 3 tests)

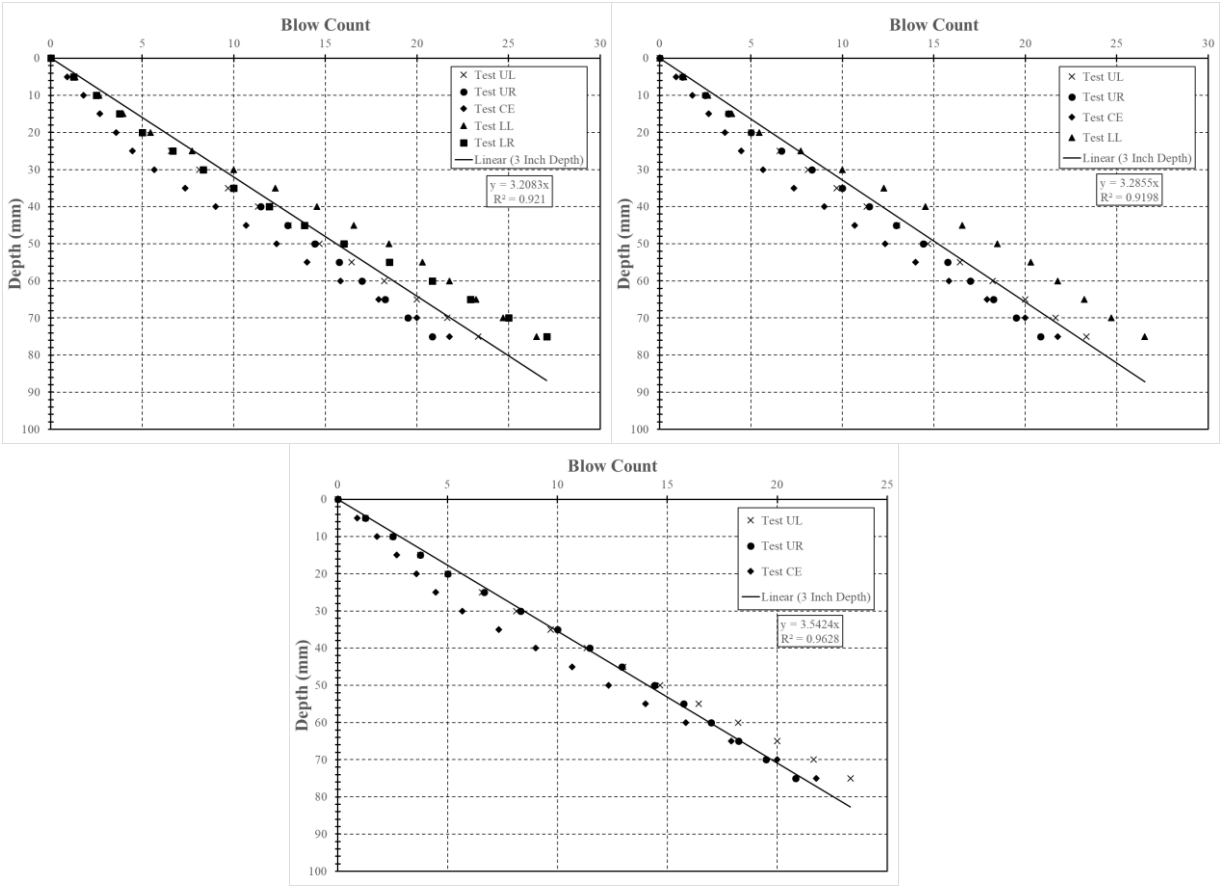


Figure L.36: Test performed on July 23, 2019, Location 43 (top left = 5 tests, top right = 4 tests, bottom = 3 tests)

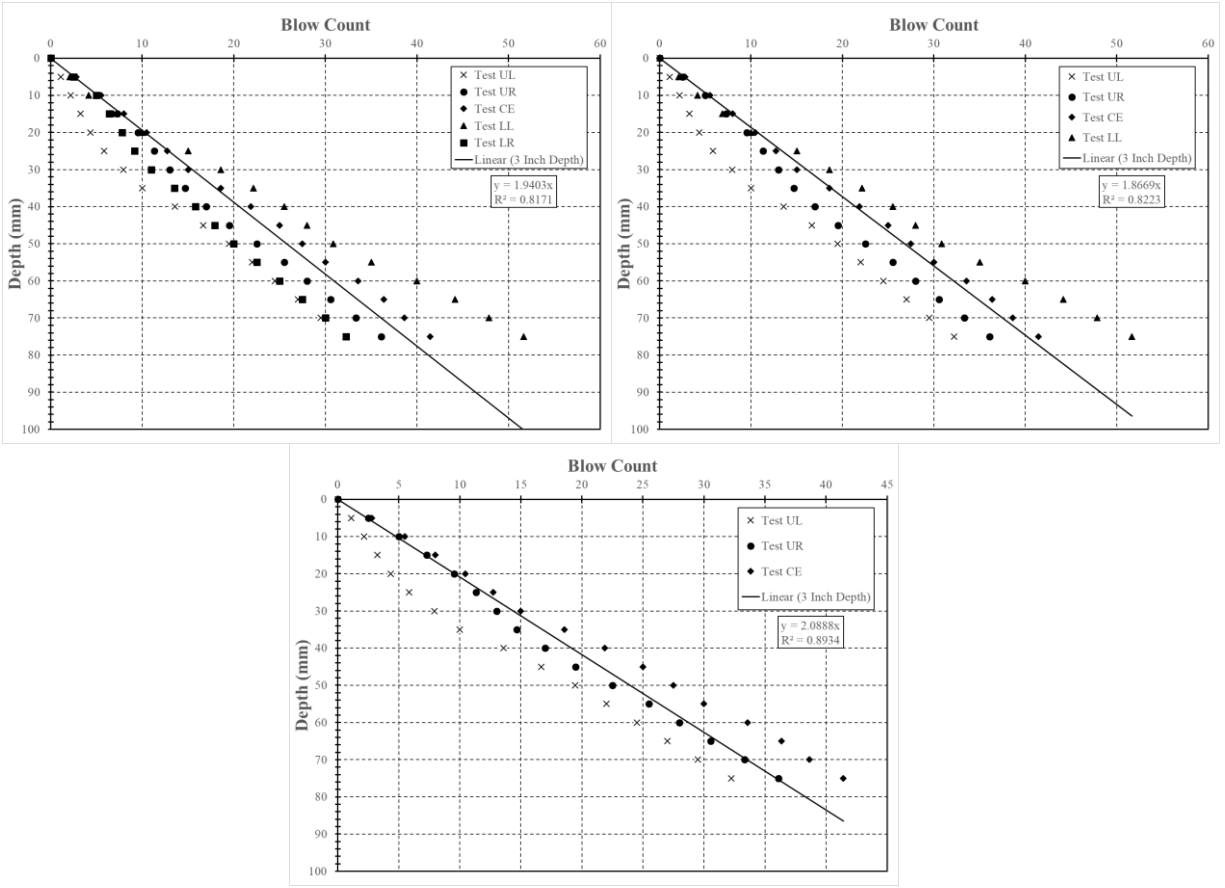


Figure L.37: Test performed on July 24, 2019, Location 44 (top left = 5 tests, top right = 4 tests, bottom = 3 tests)

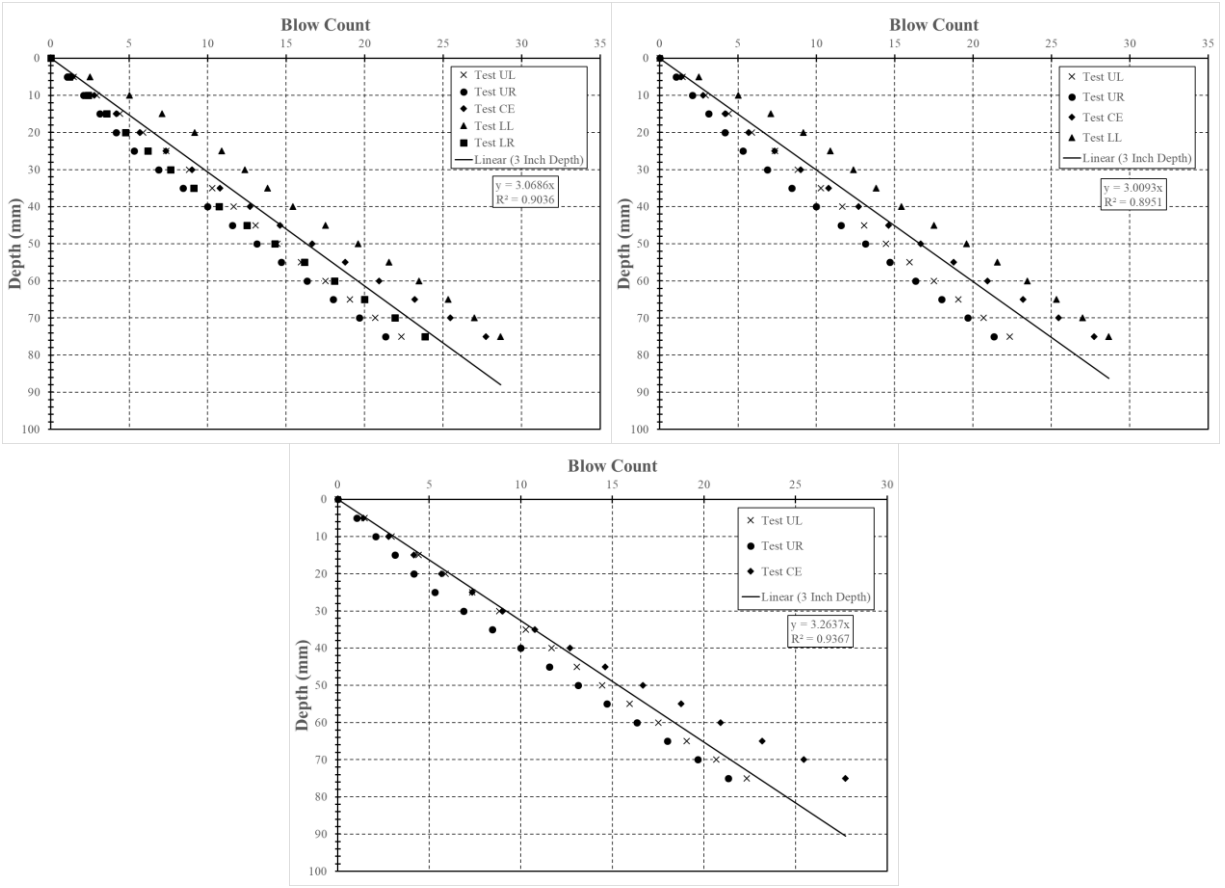


Figure L.38: Test performed on July 24, 2019, Location 45 (top left = 5 tests, top right = 4 tests, bottom = 3 tests)

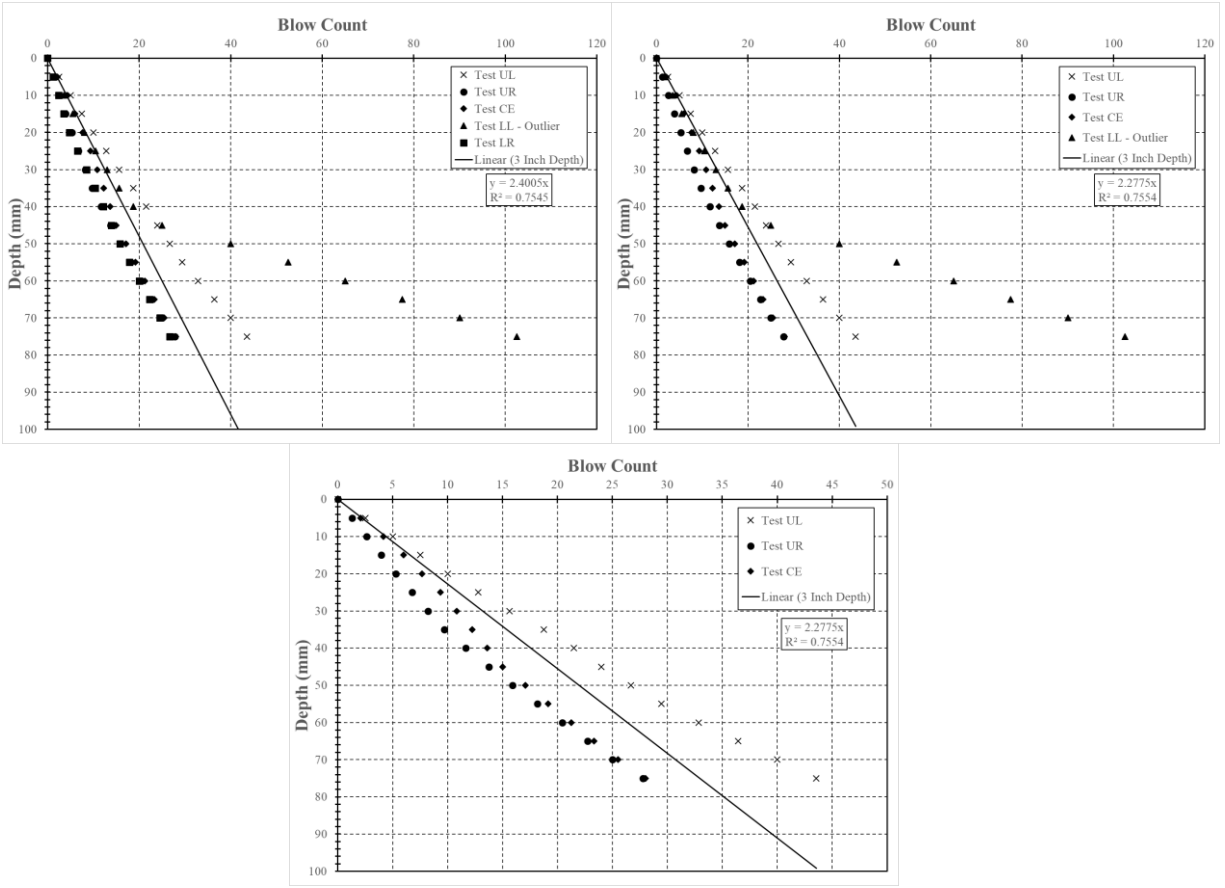


Figure L.39: Test performed on July 24, 2019, Location 46 (top left = 5 tests, top right = 4 tests, bottom = 3 tests)

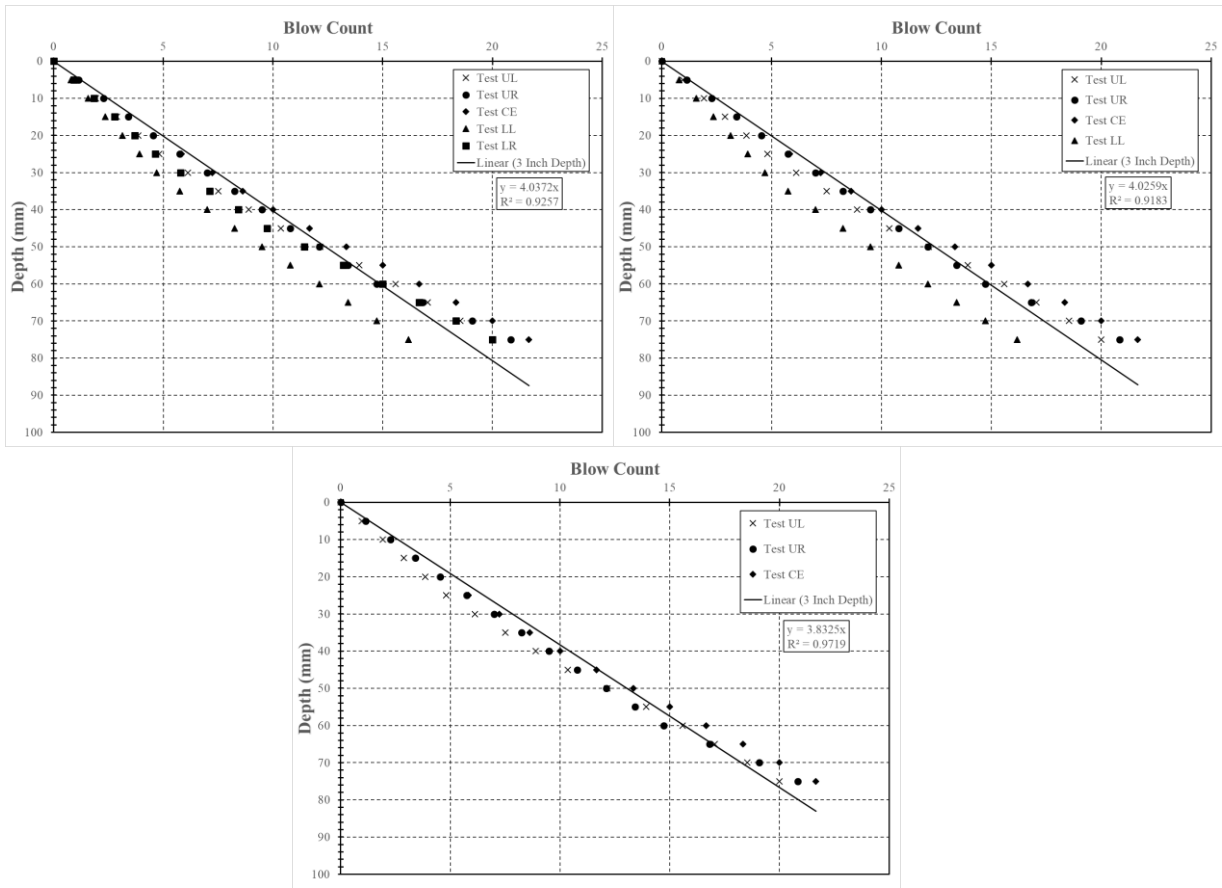


Figure L.40: Test performed on July 24, 2019, Location 47 (top left = 5 tests, top right = 4 tests, bottom = 3 tests)

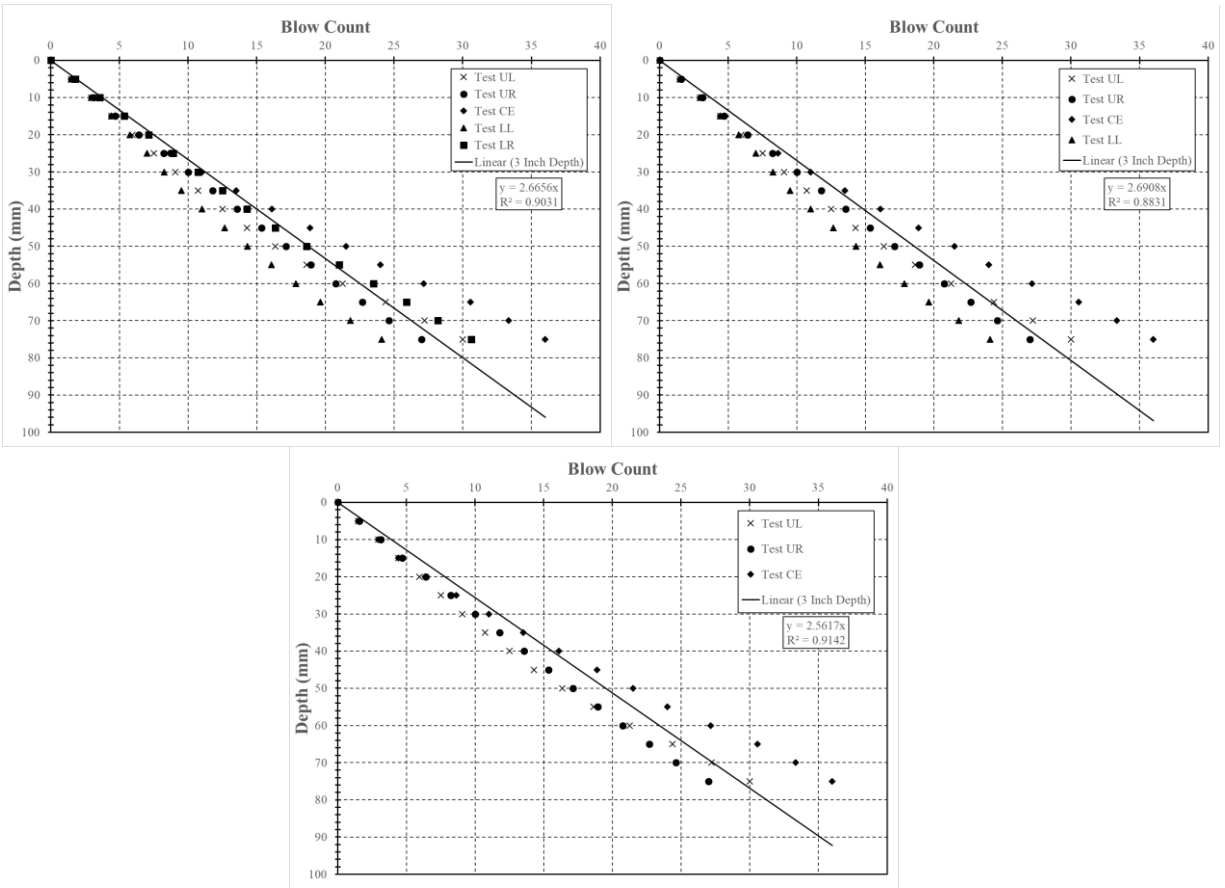


Figure L.41: Test performed on July 24, 2019, Location 48 (top left = 5 tests, top right = 4 tests, bottom = 3 tests)

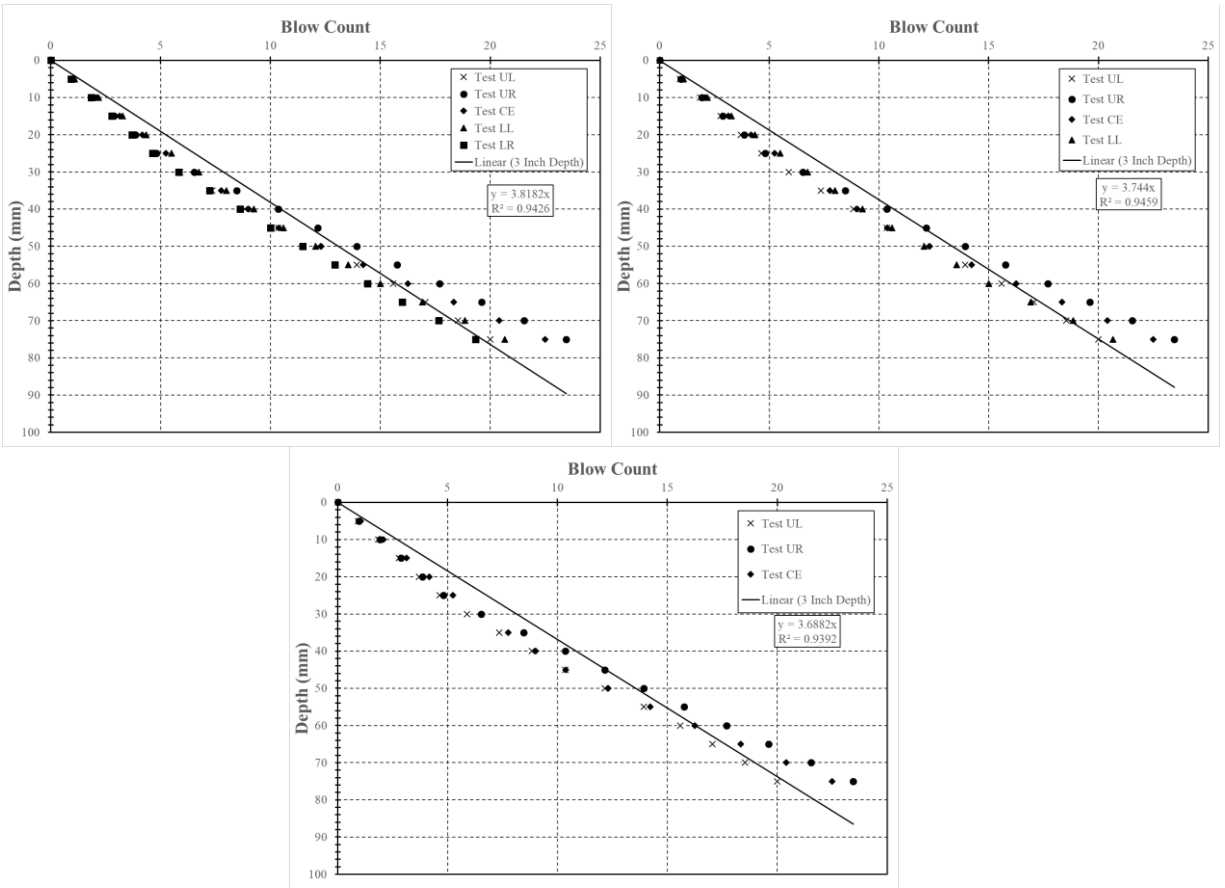


Figure L.42: Test performed on July 24, 2019, Location 49 (top left = 5 tests, top right = 4 tests, bottom = 3 tests)

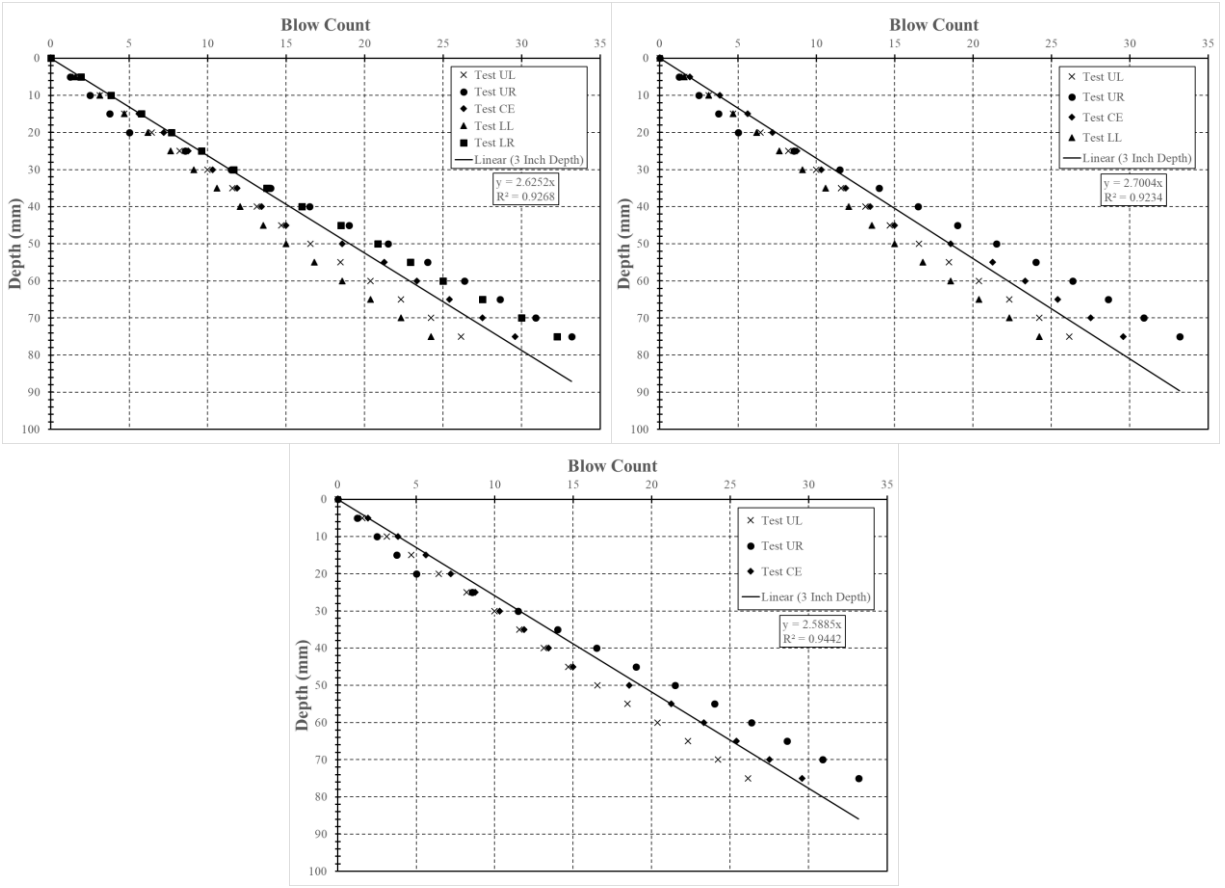


Figure L.43: Test performed on July 24, 2019, Location 50 (top left = 5 tests, top right = 4 tests, bottom = 3 tests)

Appendix M

100 Millimeter Penetration Field Data

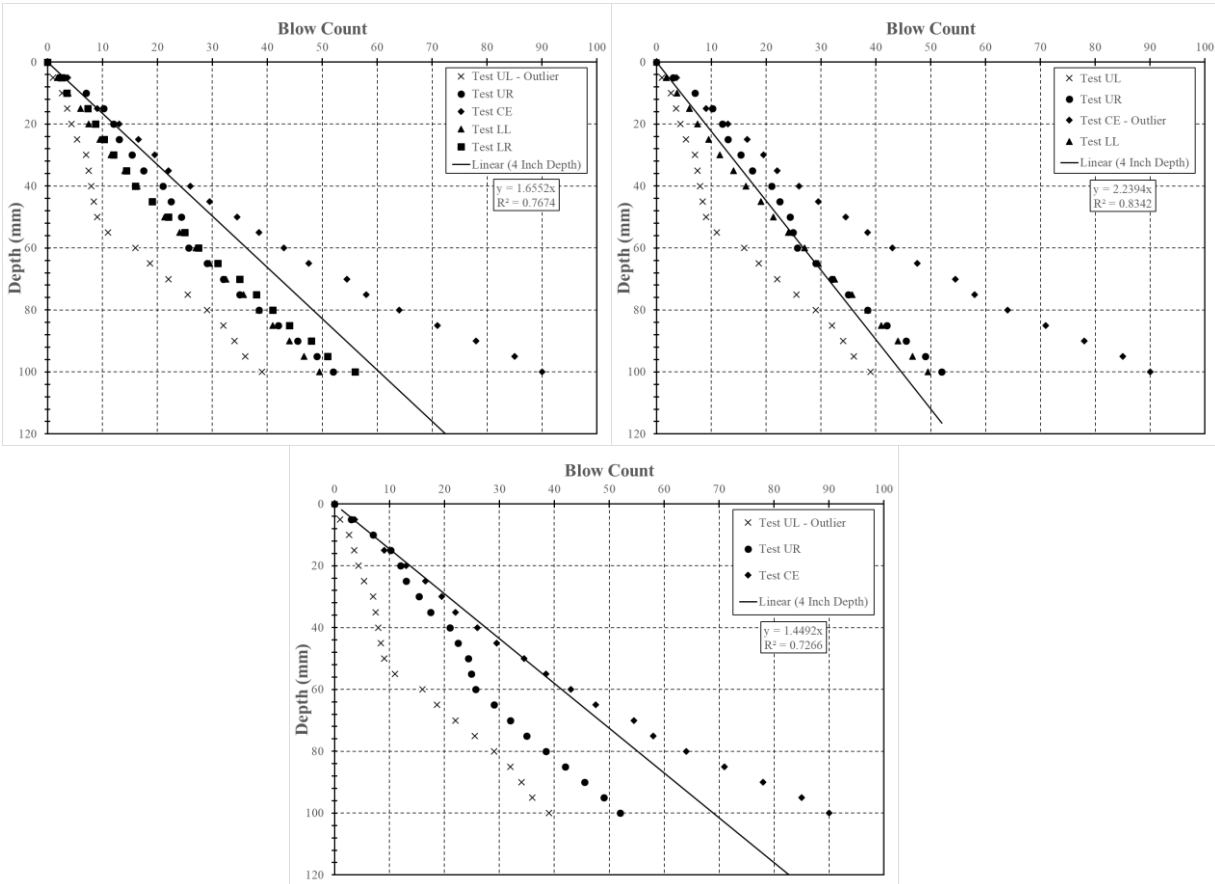


Figure M.1: Test performed on July 9, 2019, Location 1 (top left = 5 tests, top right = 4 tests, bottom = 3 tests)

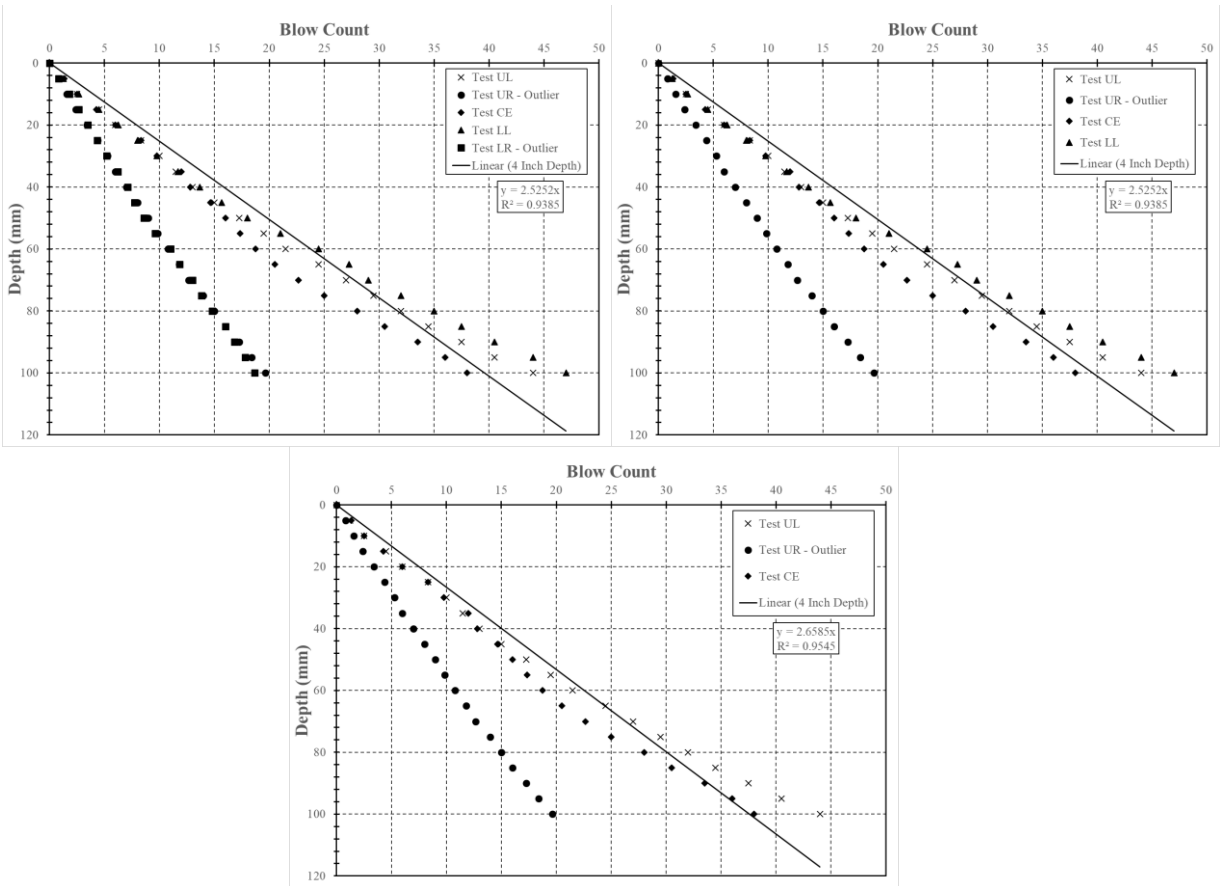


Figure M.2: Test performed on July 10, 2019, Location 4 (top left = 5 tests, top right = 4 tests, bottom = 3 tests)

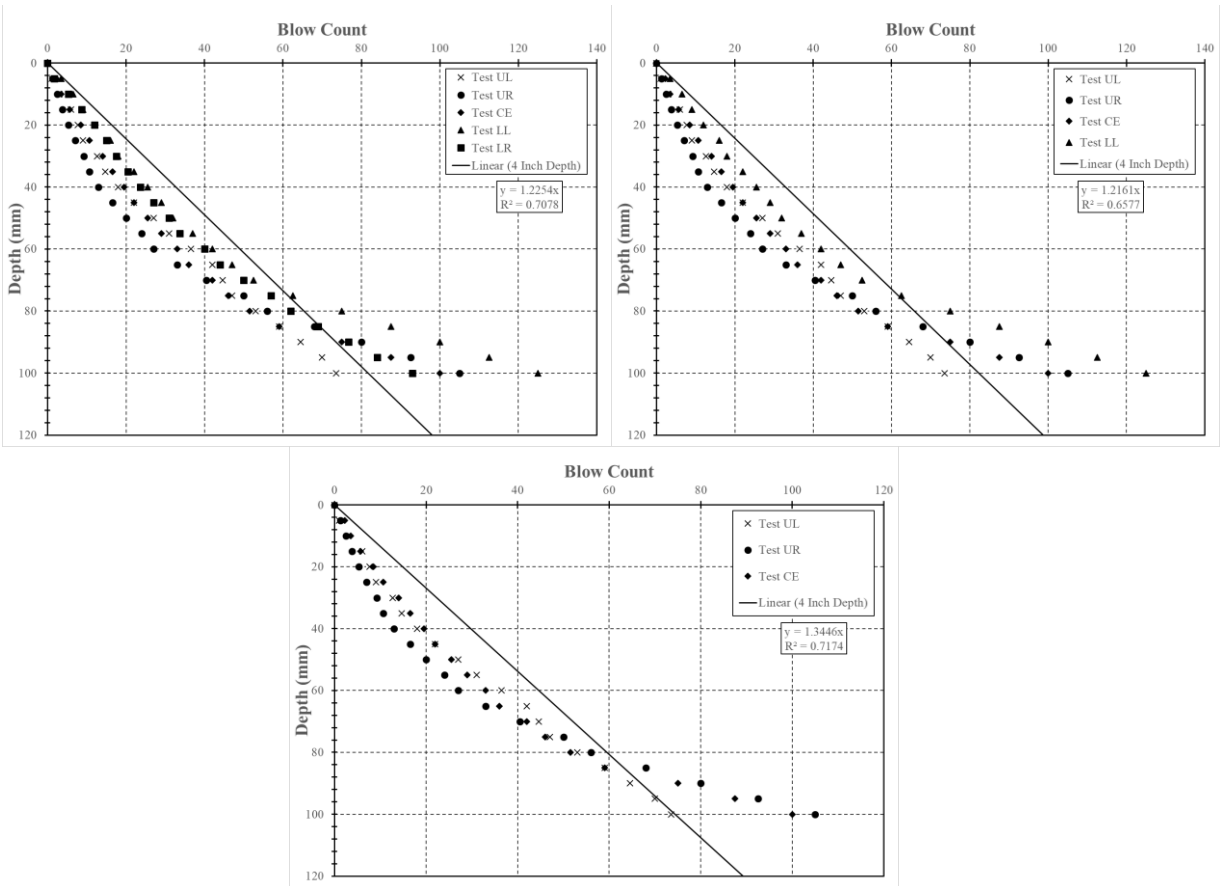


Figure M.3: Test performed on July 10, 2019, Location 5 (top left = 5 tests, top right = 4 tests, bottom = 3 tests)

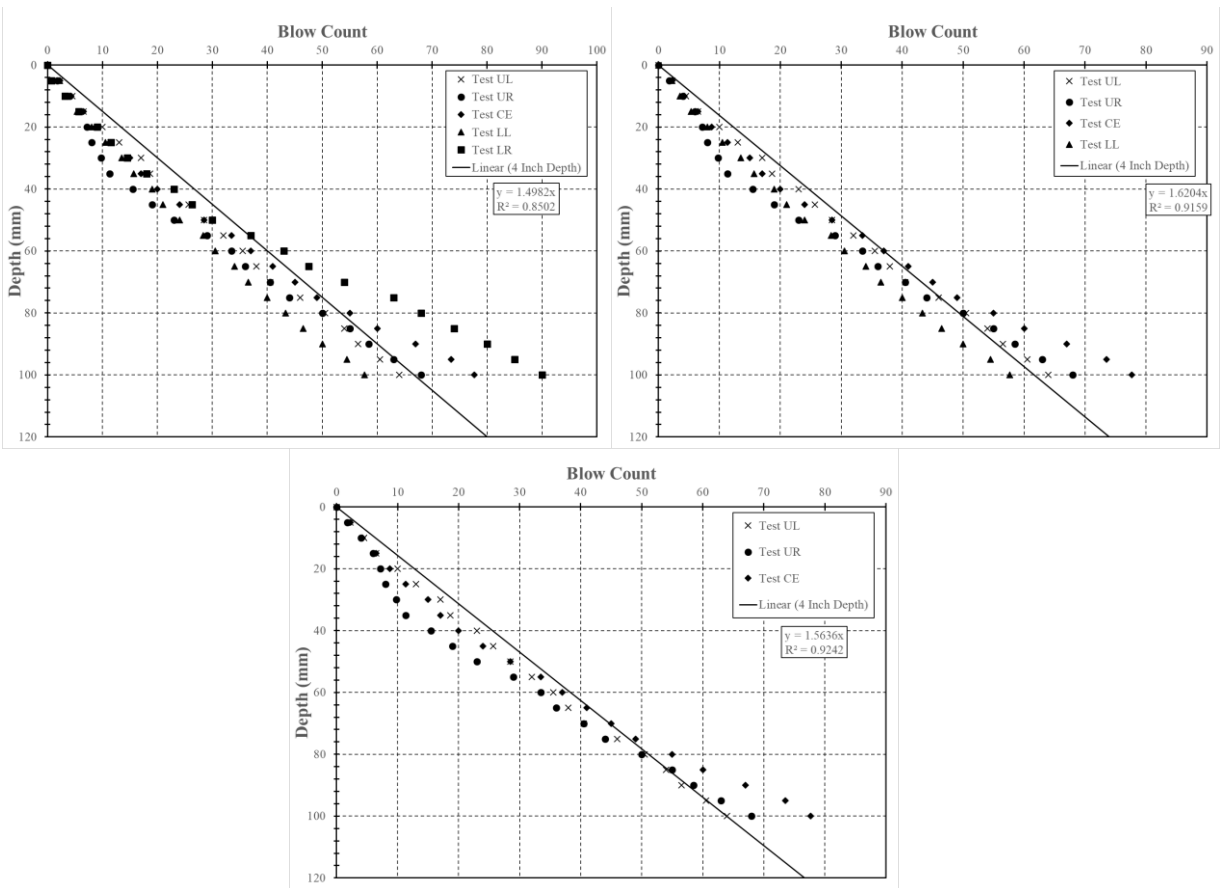


Figure M.4: Test performed on July 10, 2019, Location 6 (top left = 5 tests, top right = 4 tests, bottom = 3 tests)

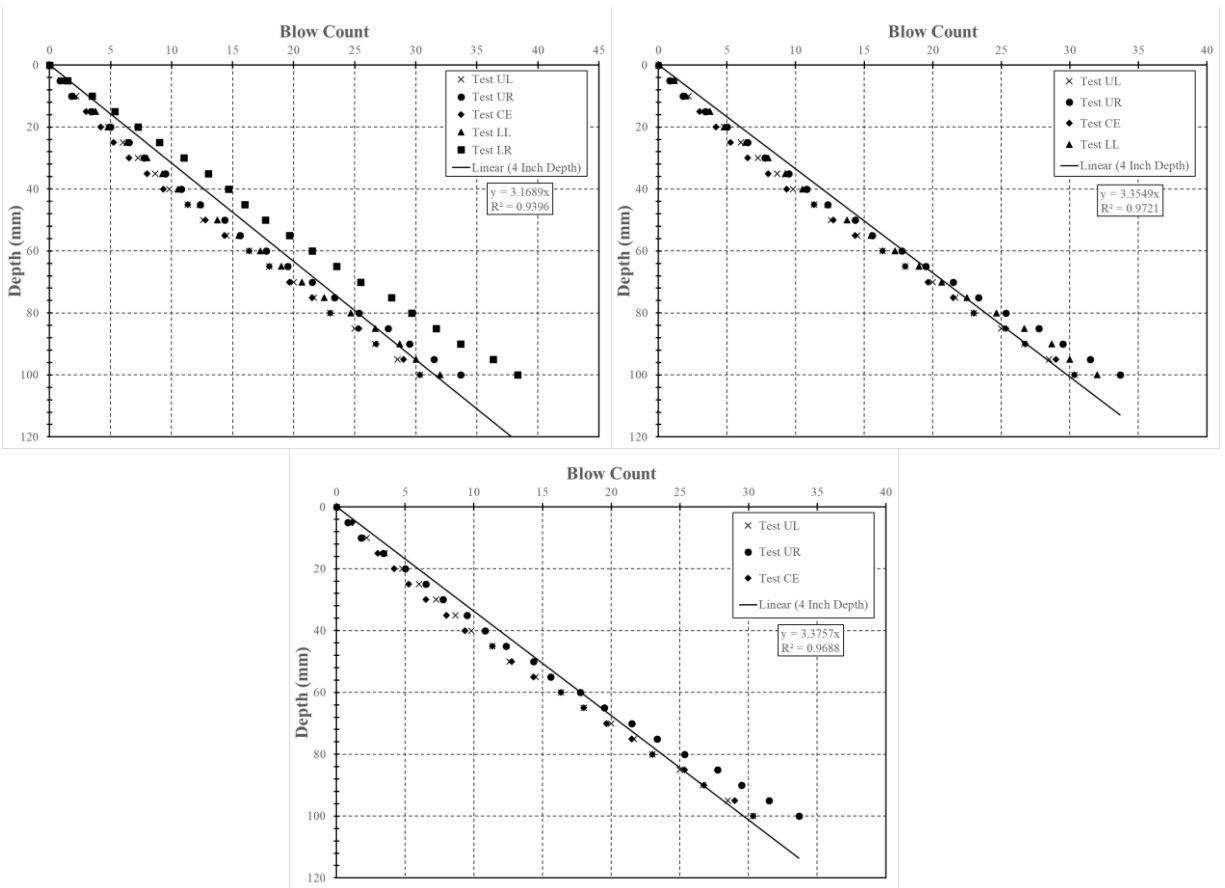


Figure M.5: Test performed on July 16, 2019, Location 7 (top left = 5 tests, top right = 4 tests, bottom = 3 tests)

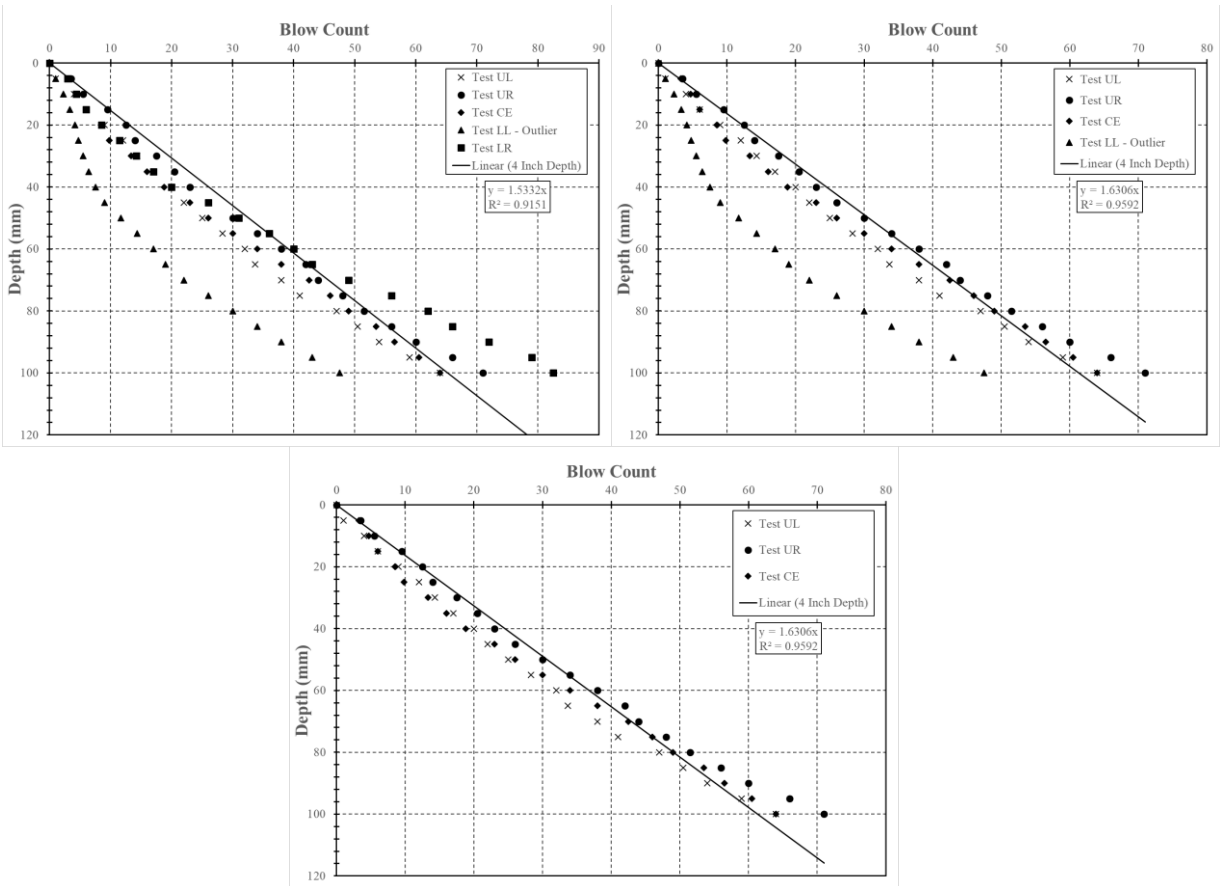


Figure M.6: Test performed on July 16, 2019, Location 8 (top left = 5 tests, top right = 4 tests, bottom = 3 tests)

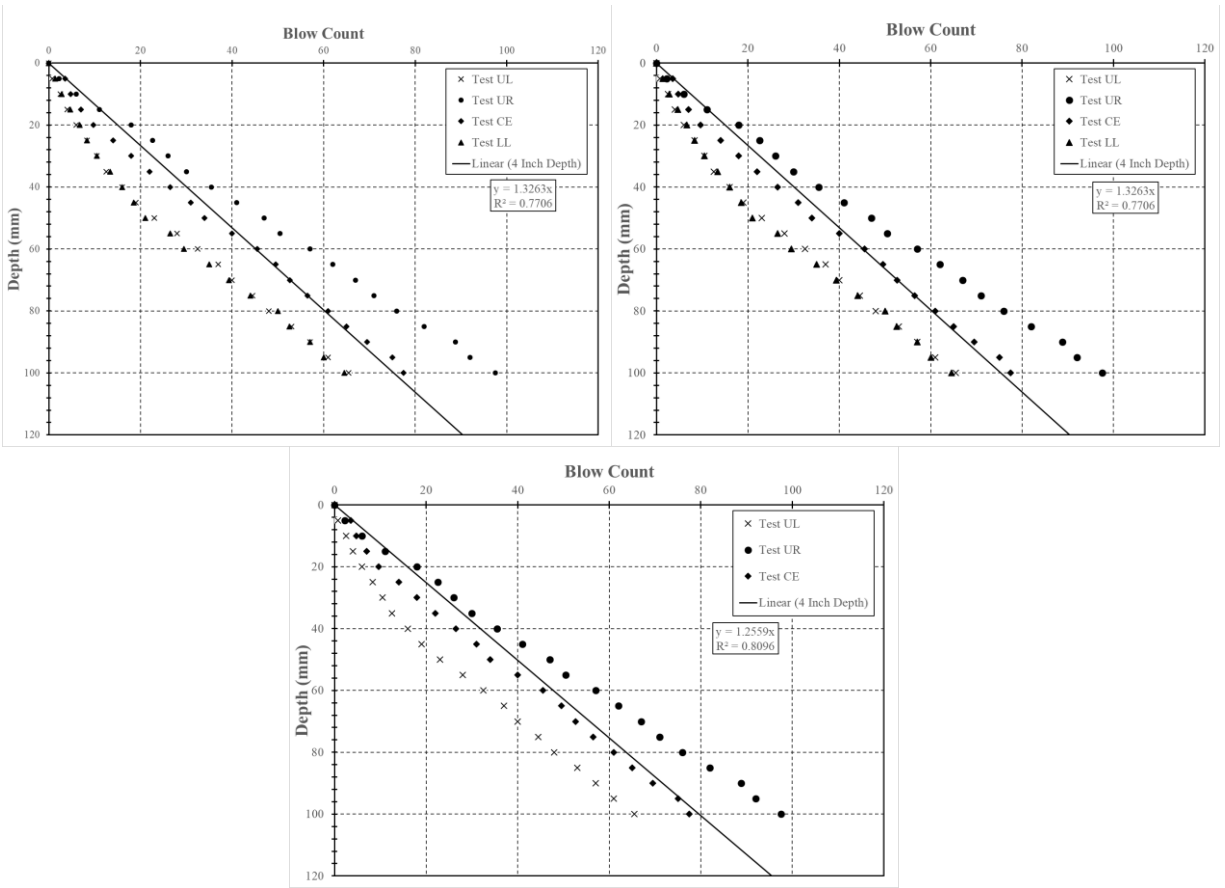


Figure M.7: Test performed on July 16, 2019, Location 9 (top left = 5 tests, top right = 4 tests, bottom = 3 tests)

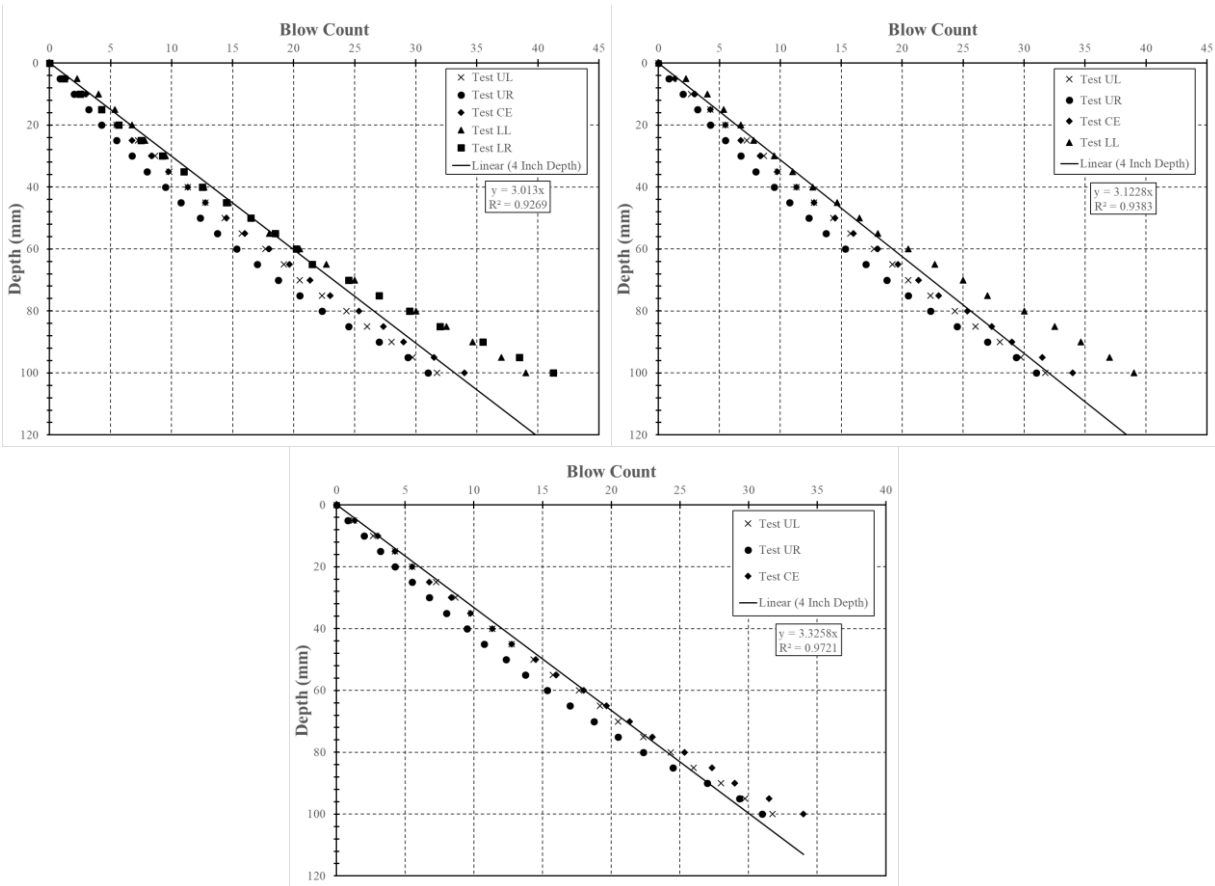


Figure M.8: Test performed on July 16, 2019, Location 10 (top left = 5 tests, top right = 4 tests, bottom = 3 tests)

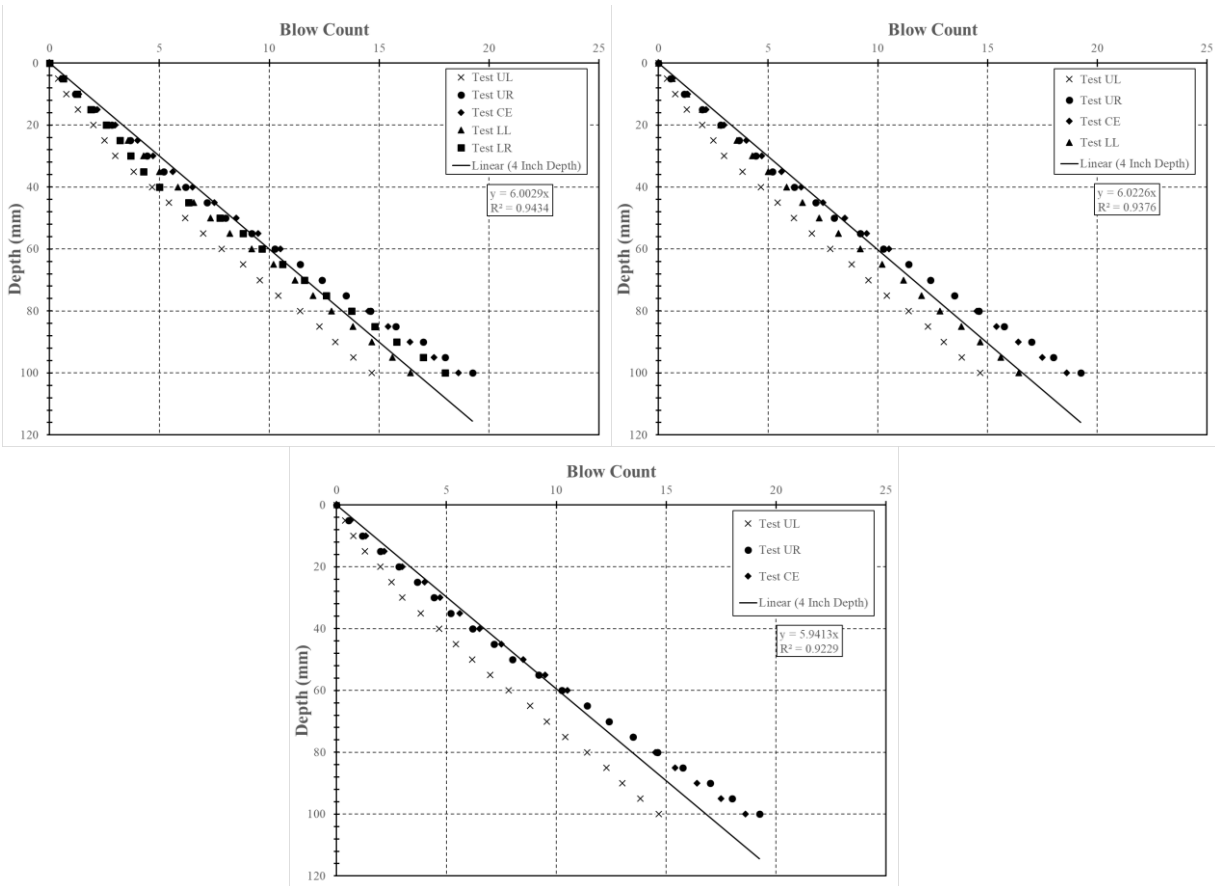


Figure M.9: Test performed on July 16, 2019, Location 11 (top left = 5 tests, top right = 4 tests, bottom = 3 tests)

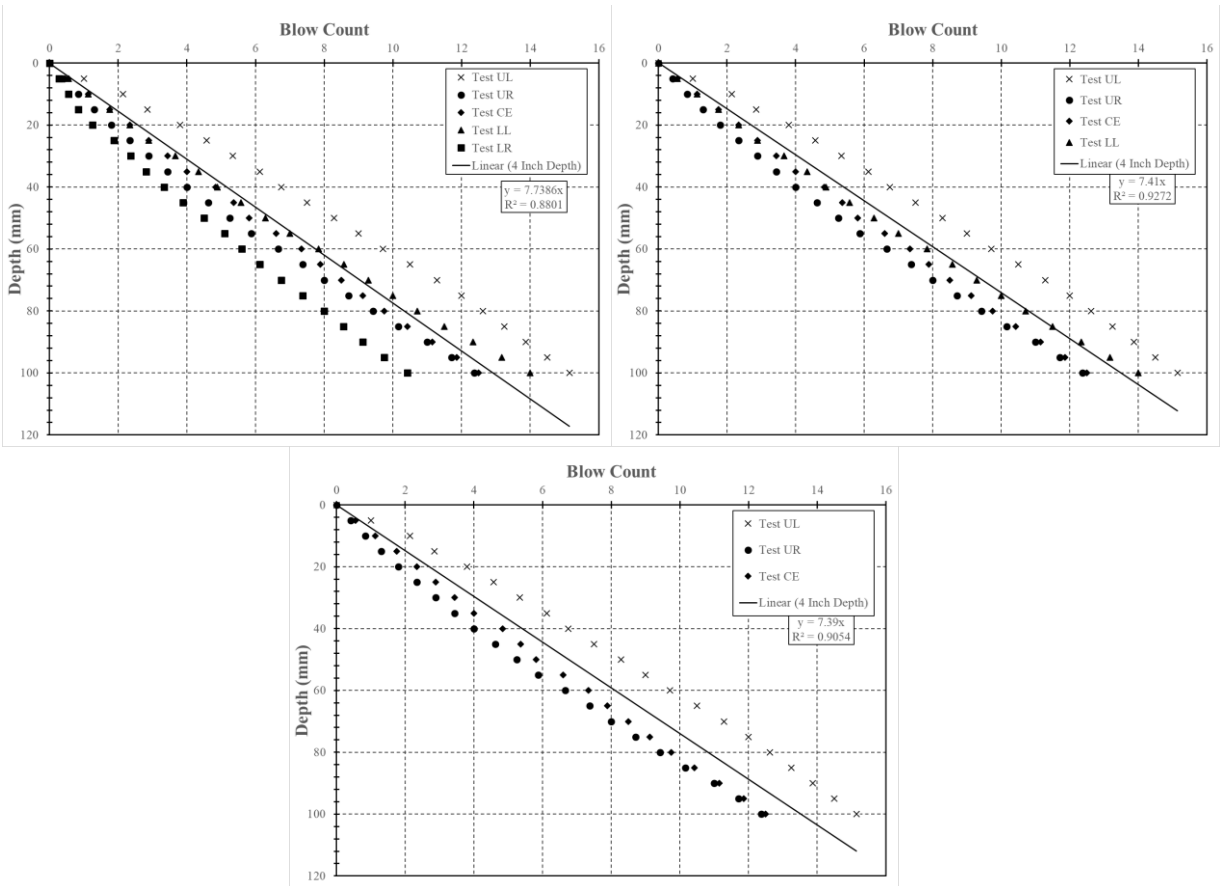


Figure M.10: Test performed on July 16, 2019, Location 12 (top left = 5 tests, top right = 4 tests, bottom = 3 tests)

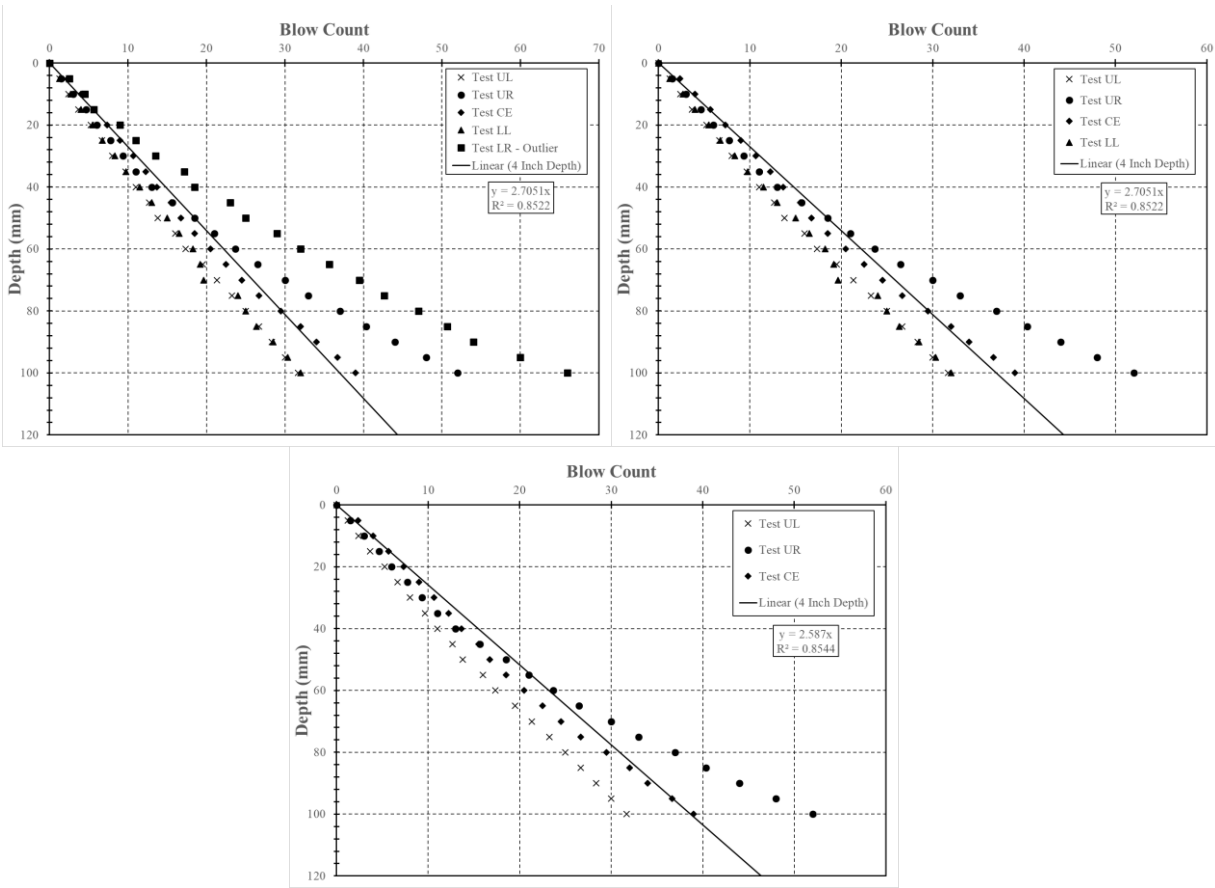


Figure M.11: Test performed on July 16, 2019, Location 13 (top left = 5 tests, top right = 4 tests, bottom = 3 tests)

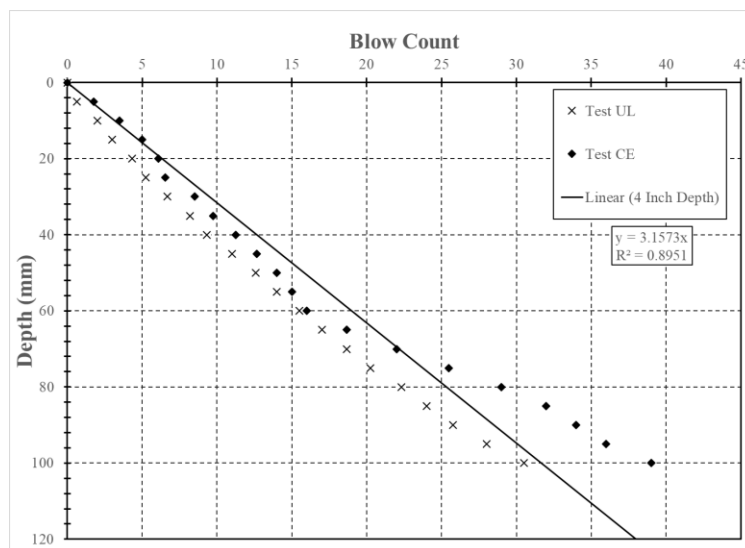


Figure M.12: Test performed on July 16, 2019, Location 15 (only 2 tests completed)

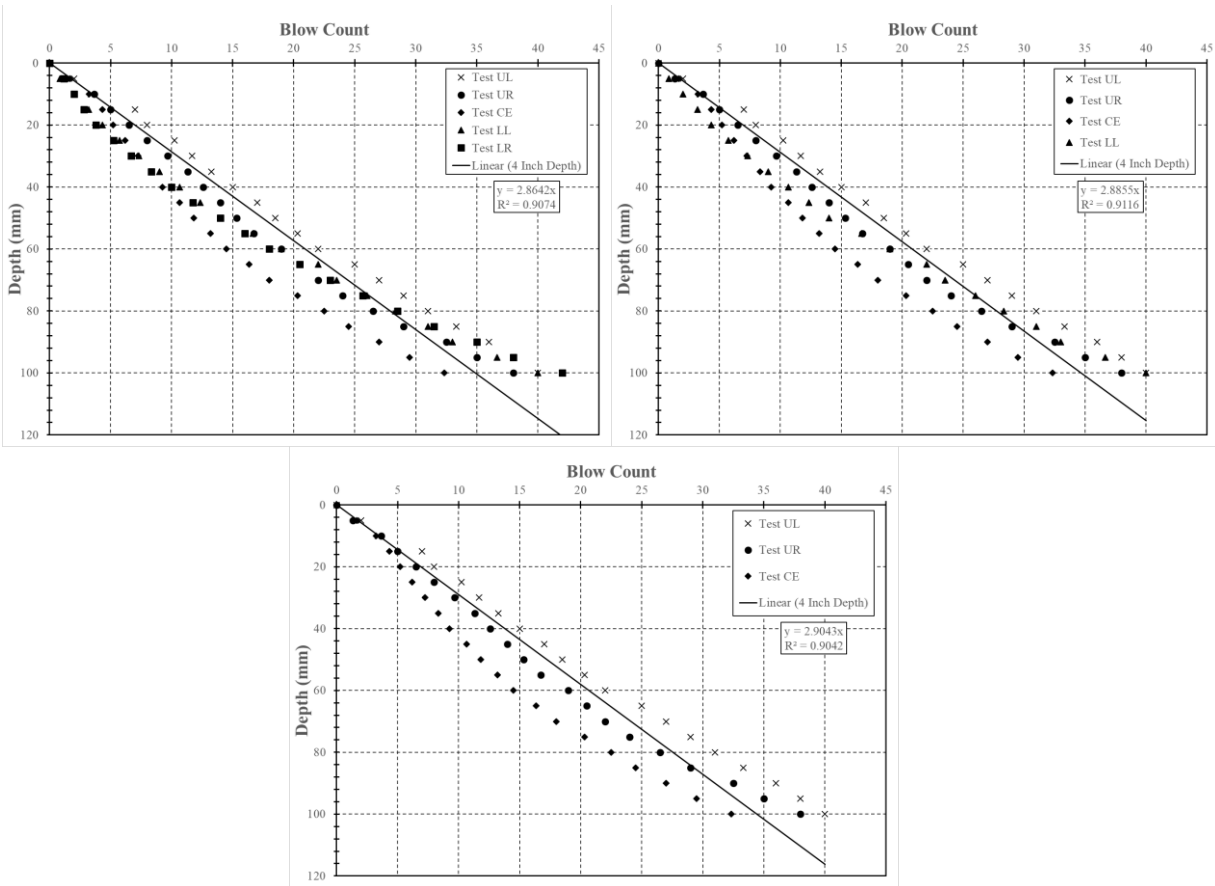


Figure M.13: Test performed on July 17, 2019, Location 17 (top left = 5 tests, top right = 4 tests, bottom = 3 tests)

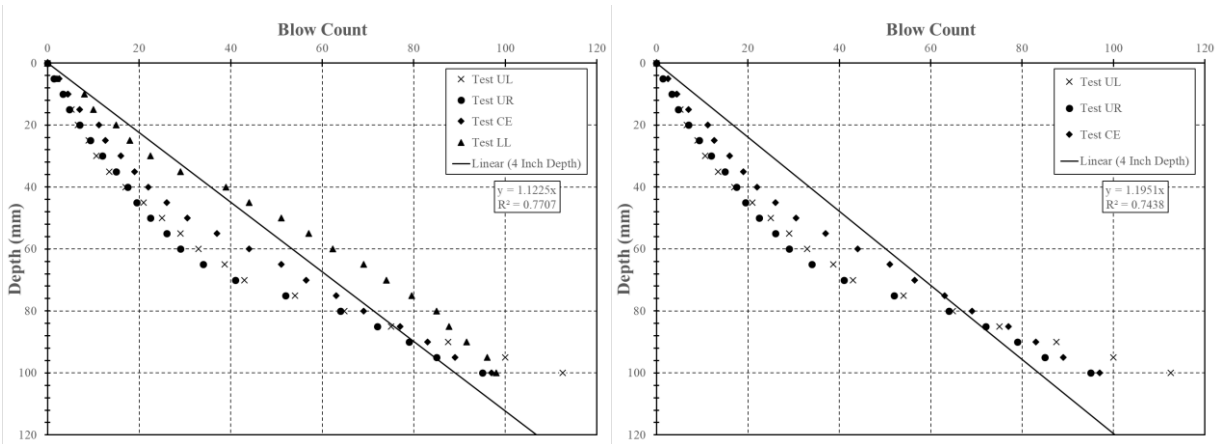


Figure M.14: Test performed on July 17, 2019, Location 18 (left = 4 tests, right = 3 tests)

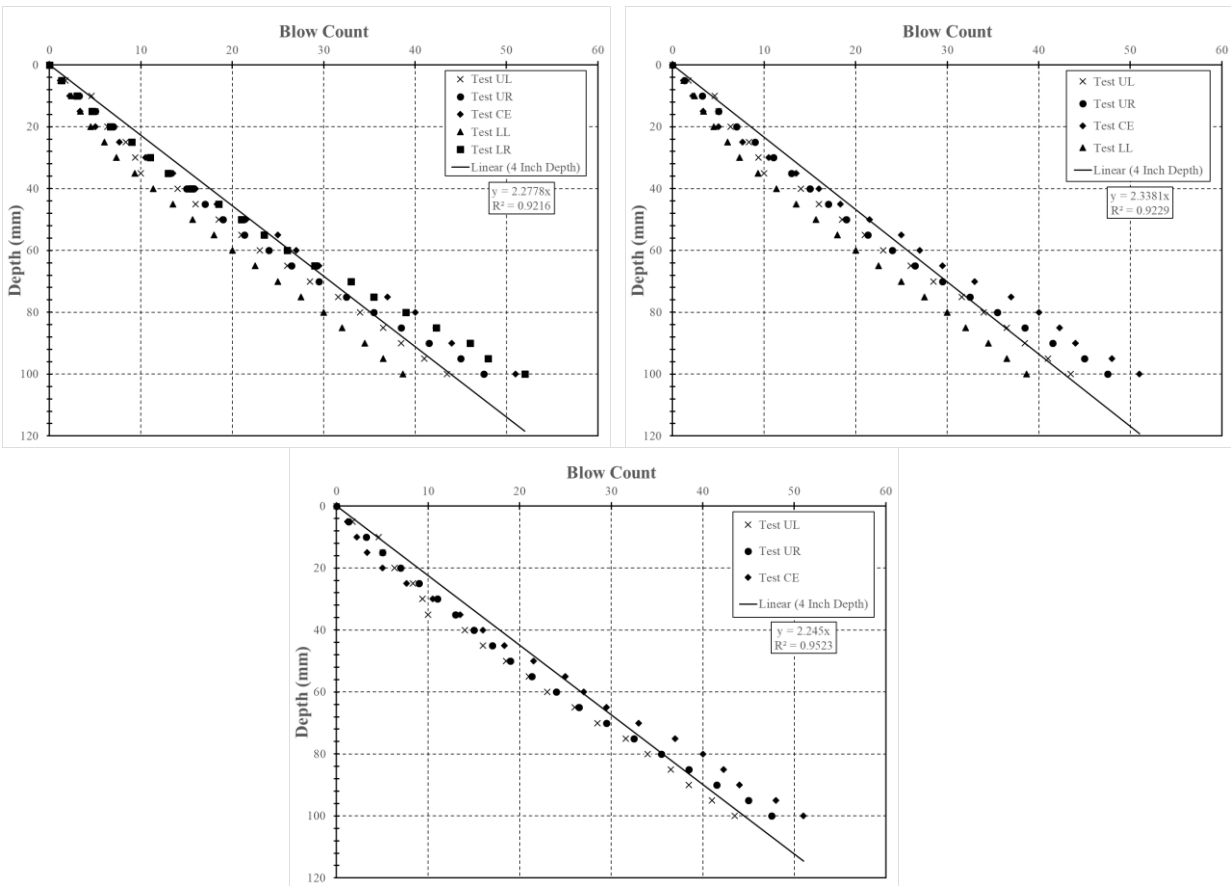


Figure M.15: Test performed on July 17, 2019, Location 19 (top left = 5 tests, top right = 4 tests, bottom = 3 tests)

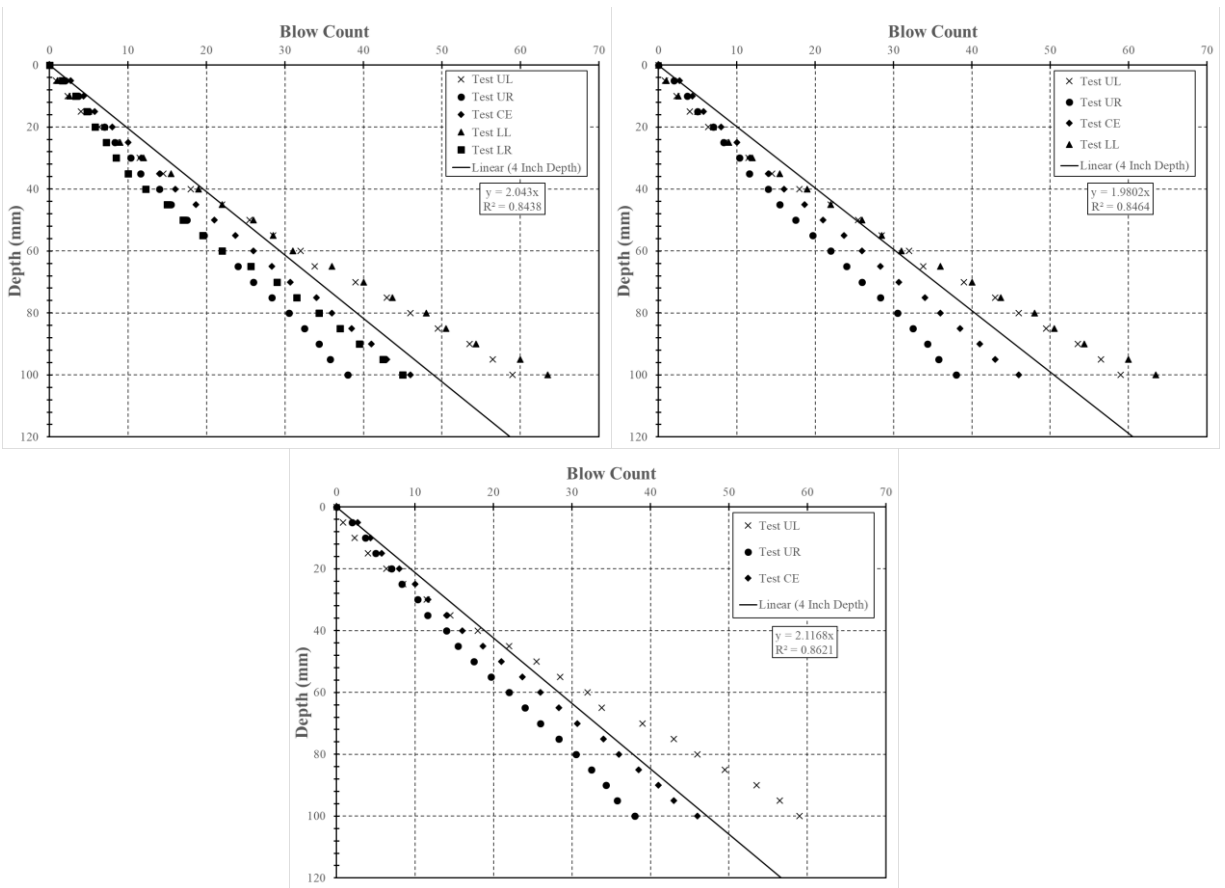


Figure M.16: Test performed on July 17, 2019, Location 20 (top left = 5 tests, top right = 4 tests, bottom = 3 tests)

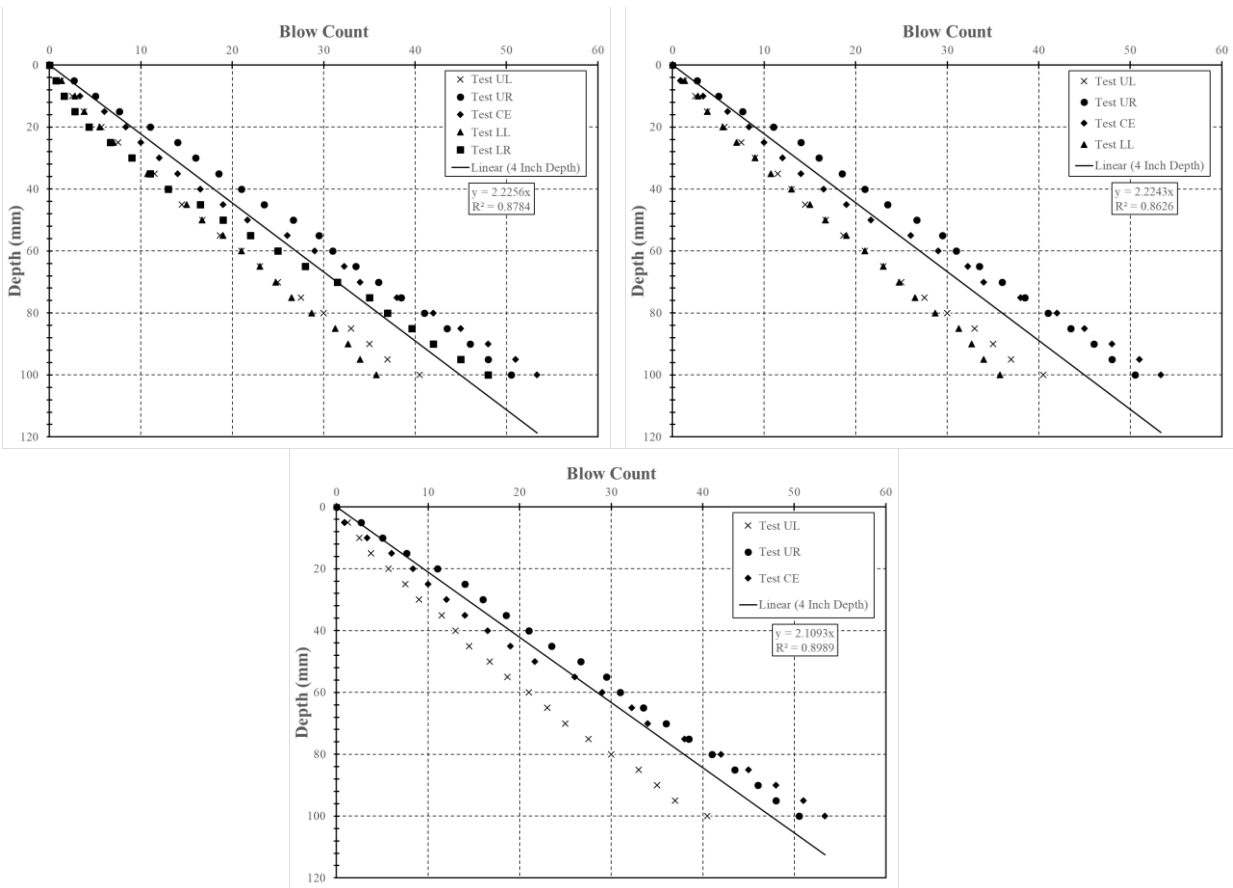


Figure M.17: Test performed on July 17, 2019, Location 21 (top left = 5 tests, top right = 4 tests, bottom = 3 tests)

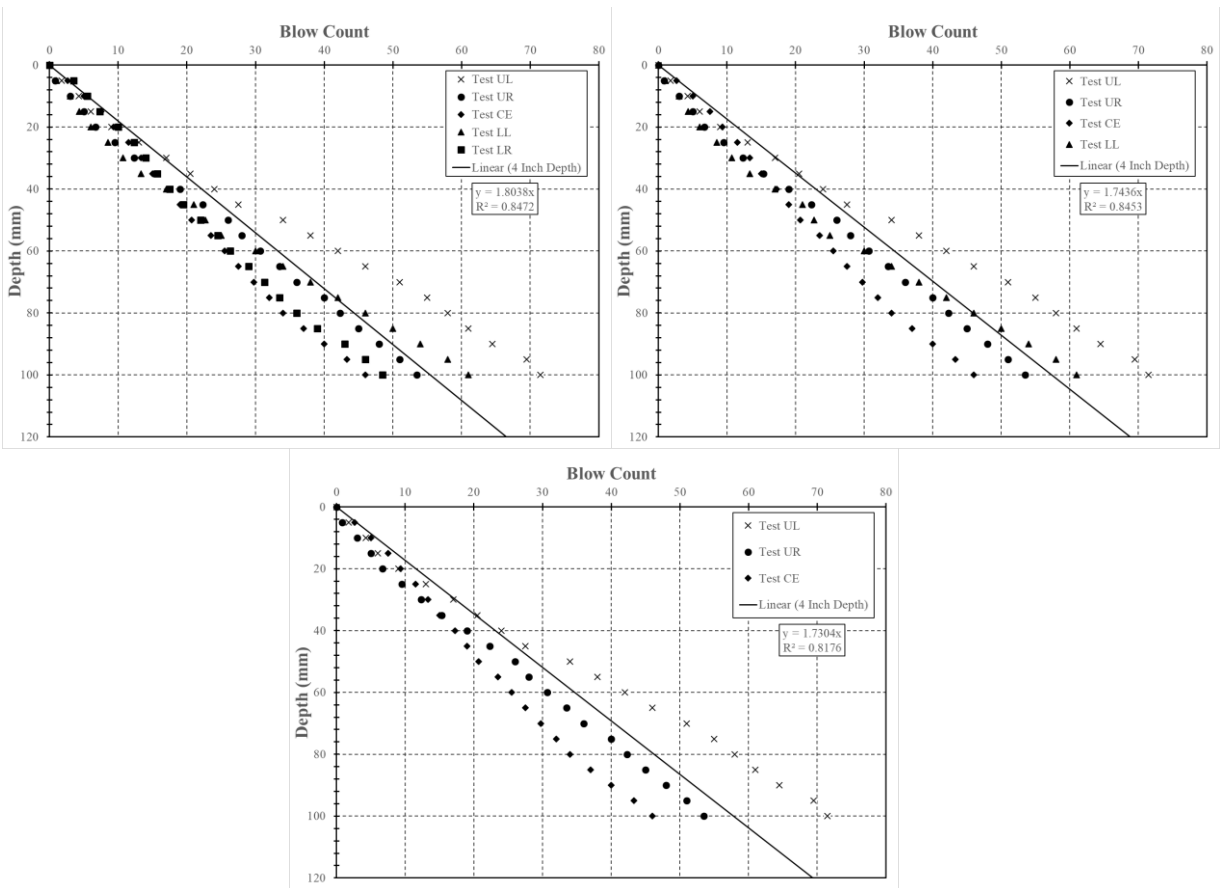


Figure M.18: Test performed on July 17, 2019, Location 22 (top left = 5 tests, top right = 4 tests, bottom = 3 tests)

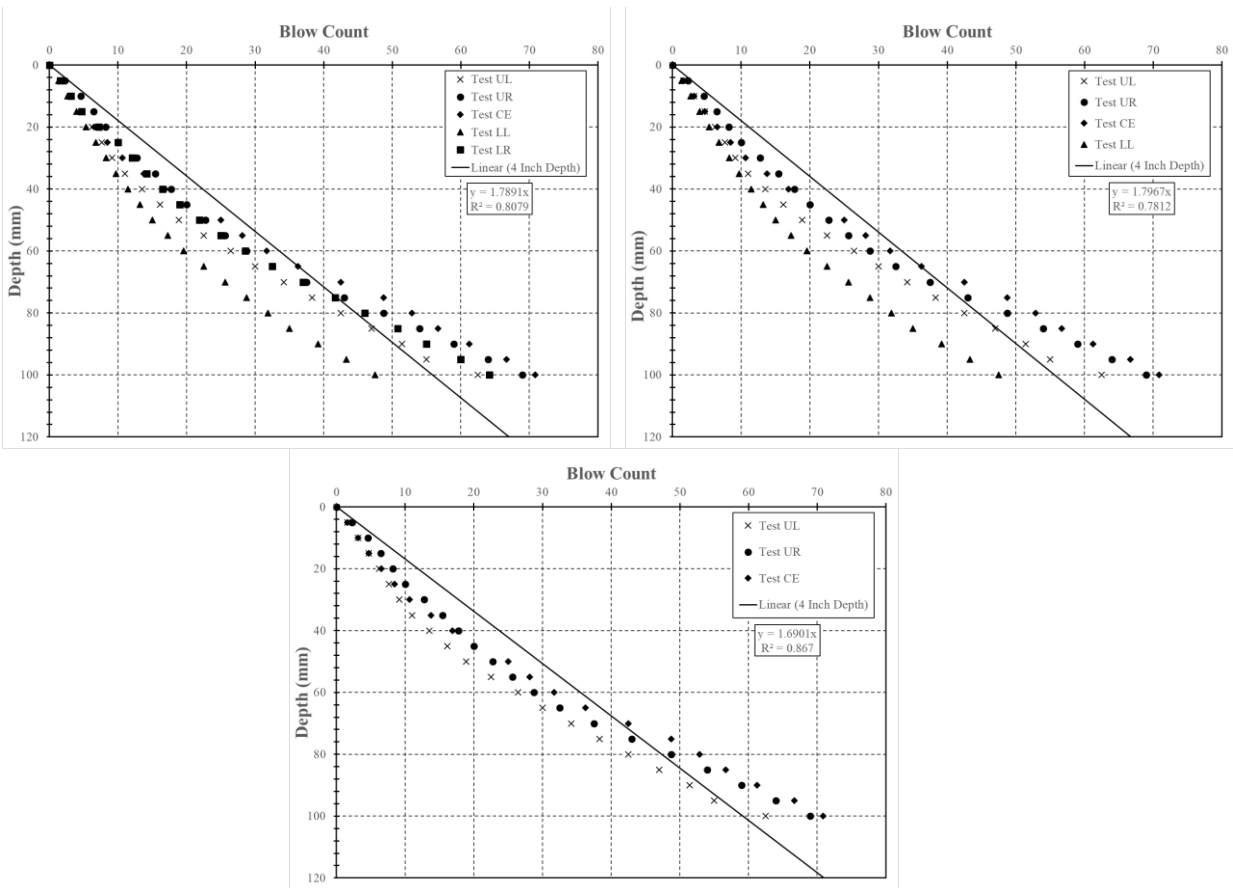


Figure M.19: Test performed on July 18, 2019, Location 23 (top left = 5 tests, top right = 4 tests, bottom = 3 tests)

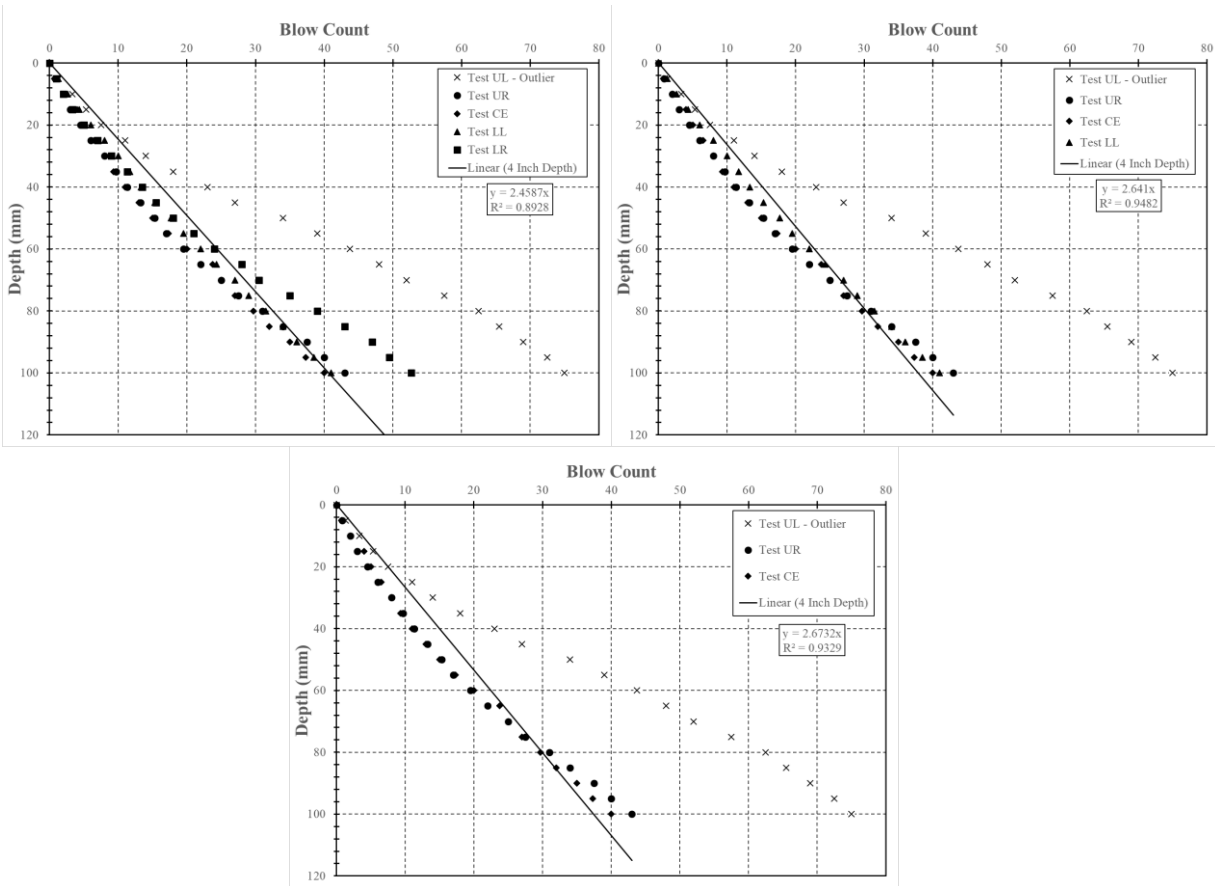


Figure M.20: Test performed on July 18, 2019, Location 24 (top left = 5 tests, top right = 4 tests, bottom = 3 tests)

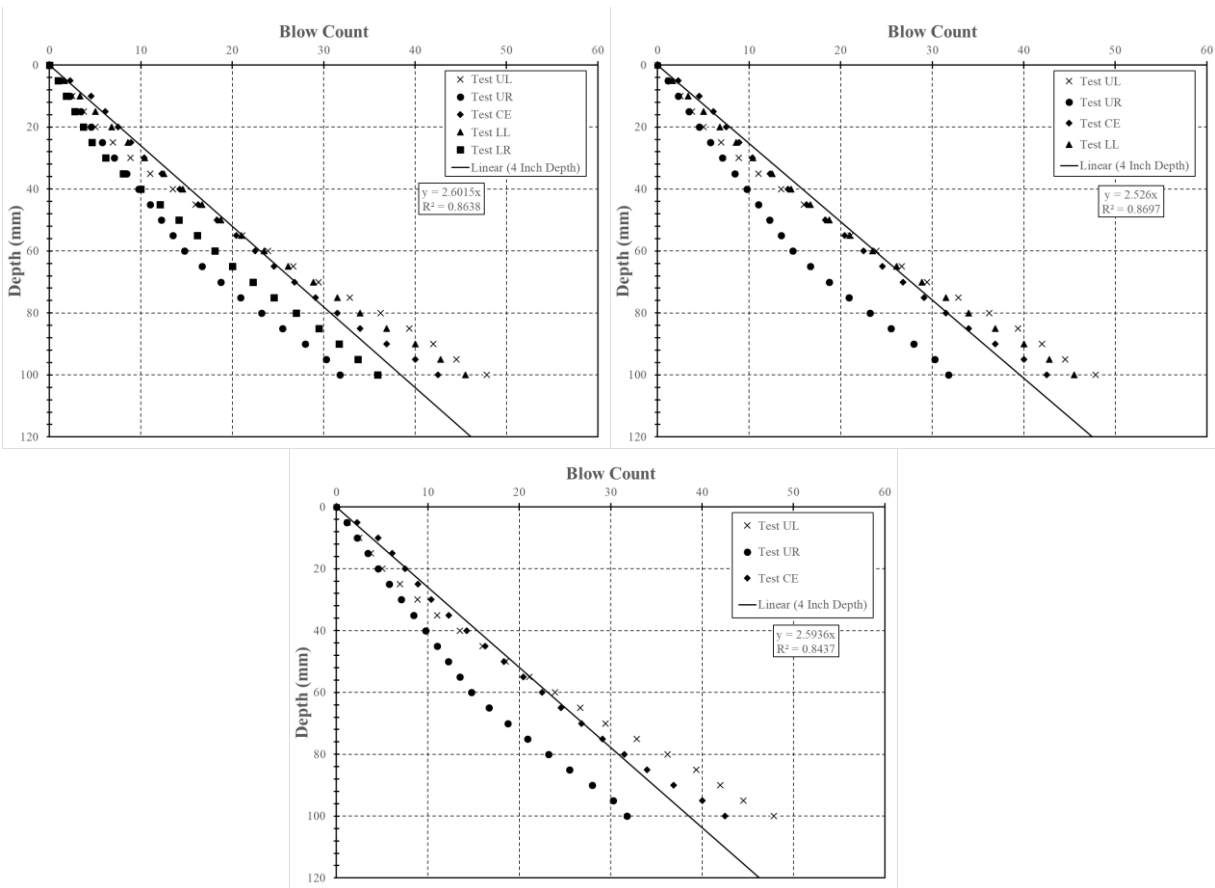


Figure M.21: Test performed on July 18, 2019, Location 25 (top left = 5 tests, top right = 4 tests, bottom = 3 tests)

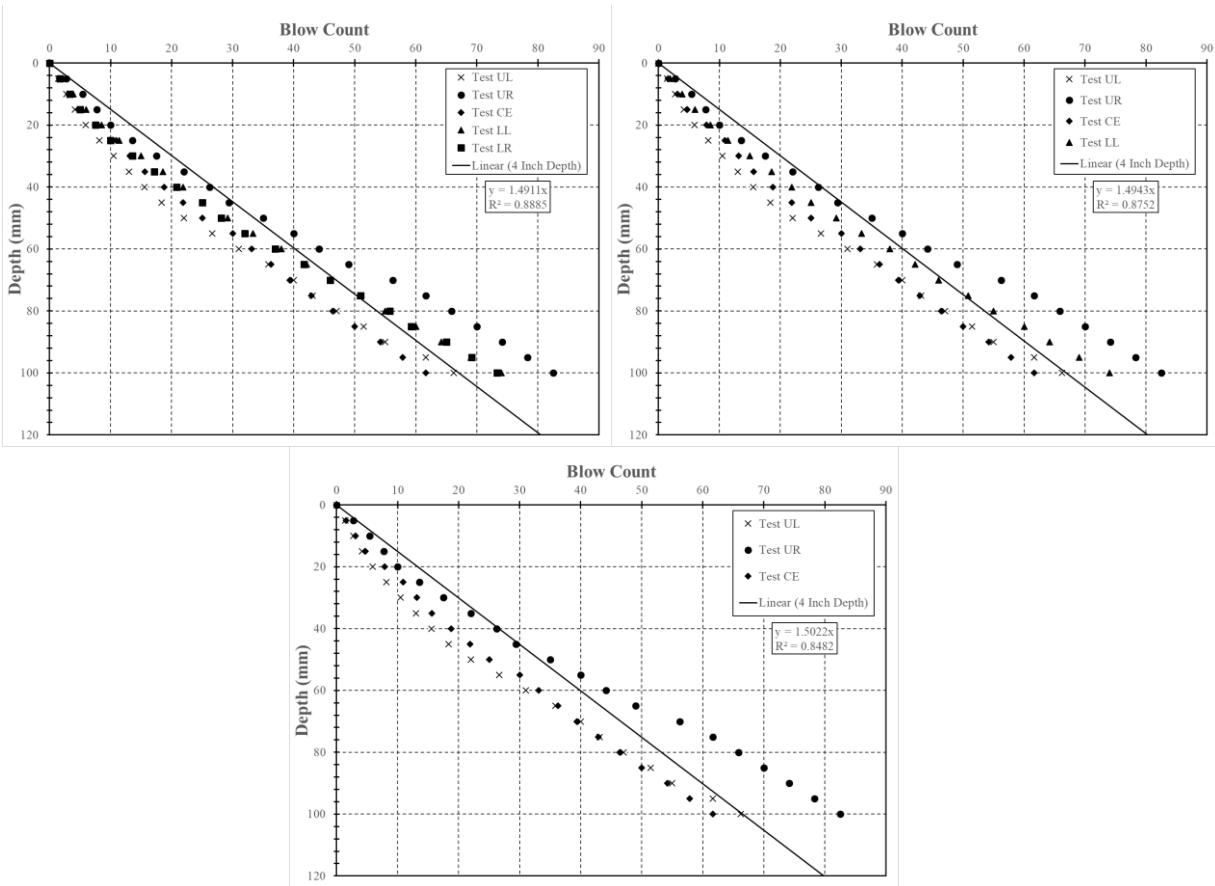


Figure M.22: Test performed on July 18, 2019, Location 28 (top left = 5 tests, top right = 4 tests, bottom = 3 tests)

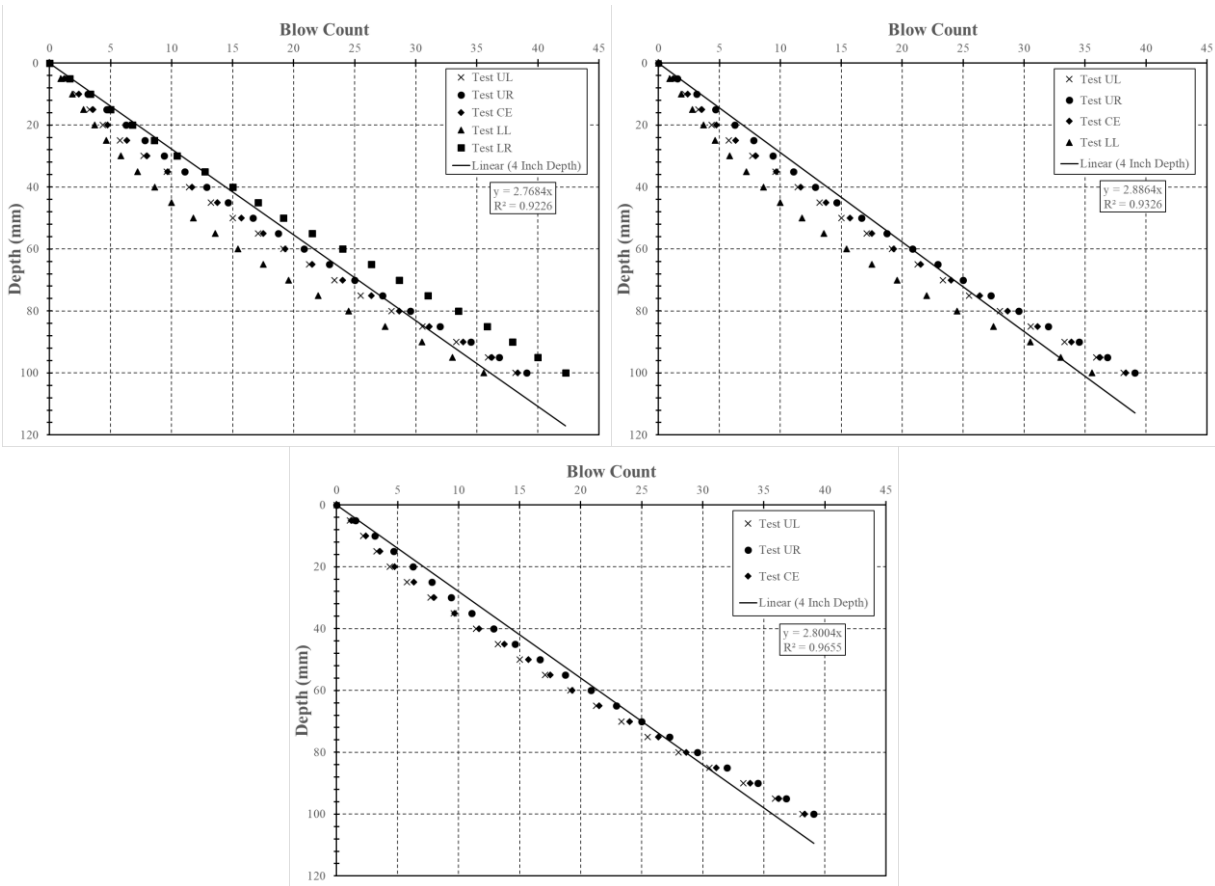


Figure M.23: Test performed on July 19, 2019, Location 30 (top left = 5 tests, top right = 4 tests, bottom = 3 tests)

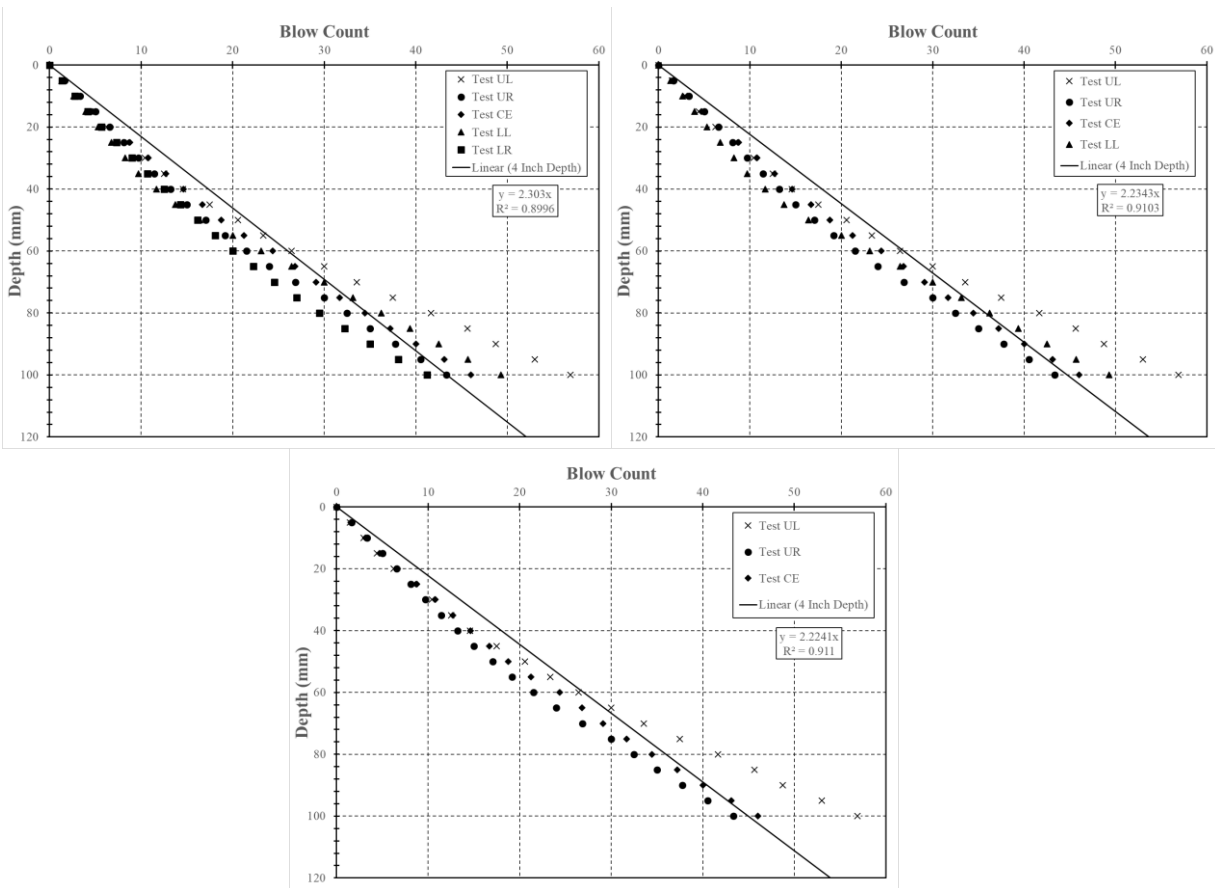


Figure M.24: Test performed on July 19, 2019, Location 31 (top left = 5 tests, top right = 4 tests, bottom = 3 tests)

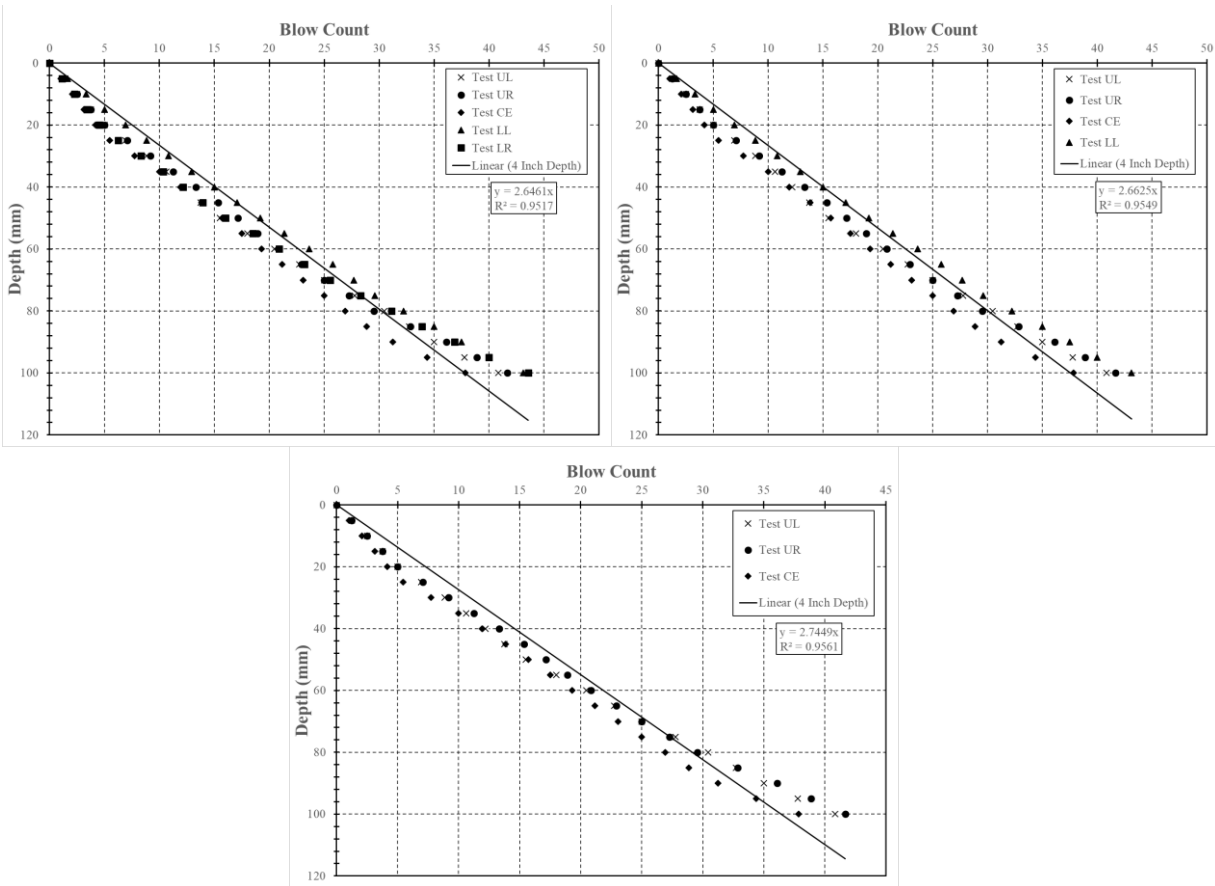


Figure M.25: Test performed on July 19, 2019, Location 32 (top left = 5 tests, top right = 4 tests, bottom = 3 tests)

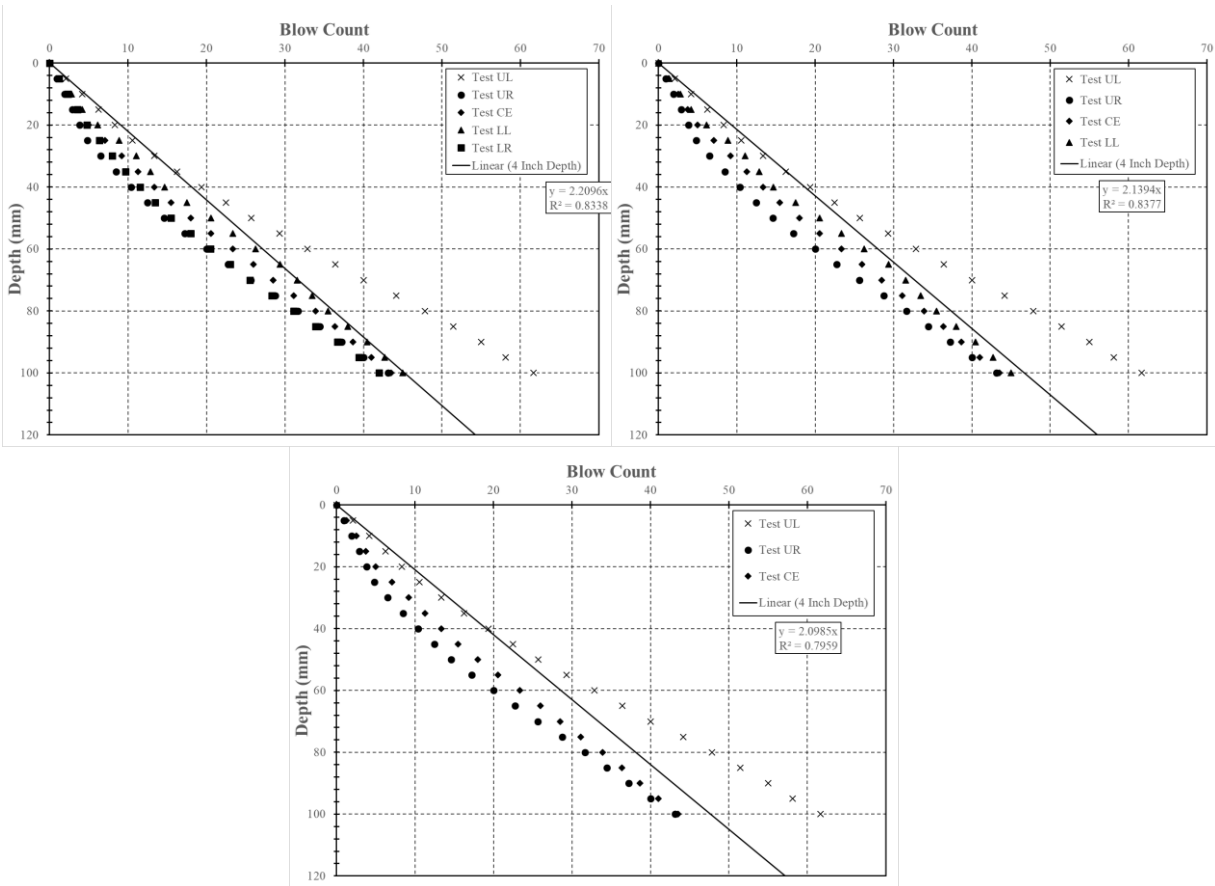


Figure M.26: Test performed on July 19, 2019, Location 33 (top left = 5 tests, top right = 4 tests, bottom = 3 tests)

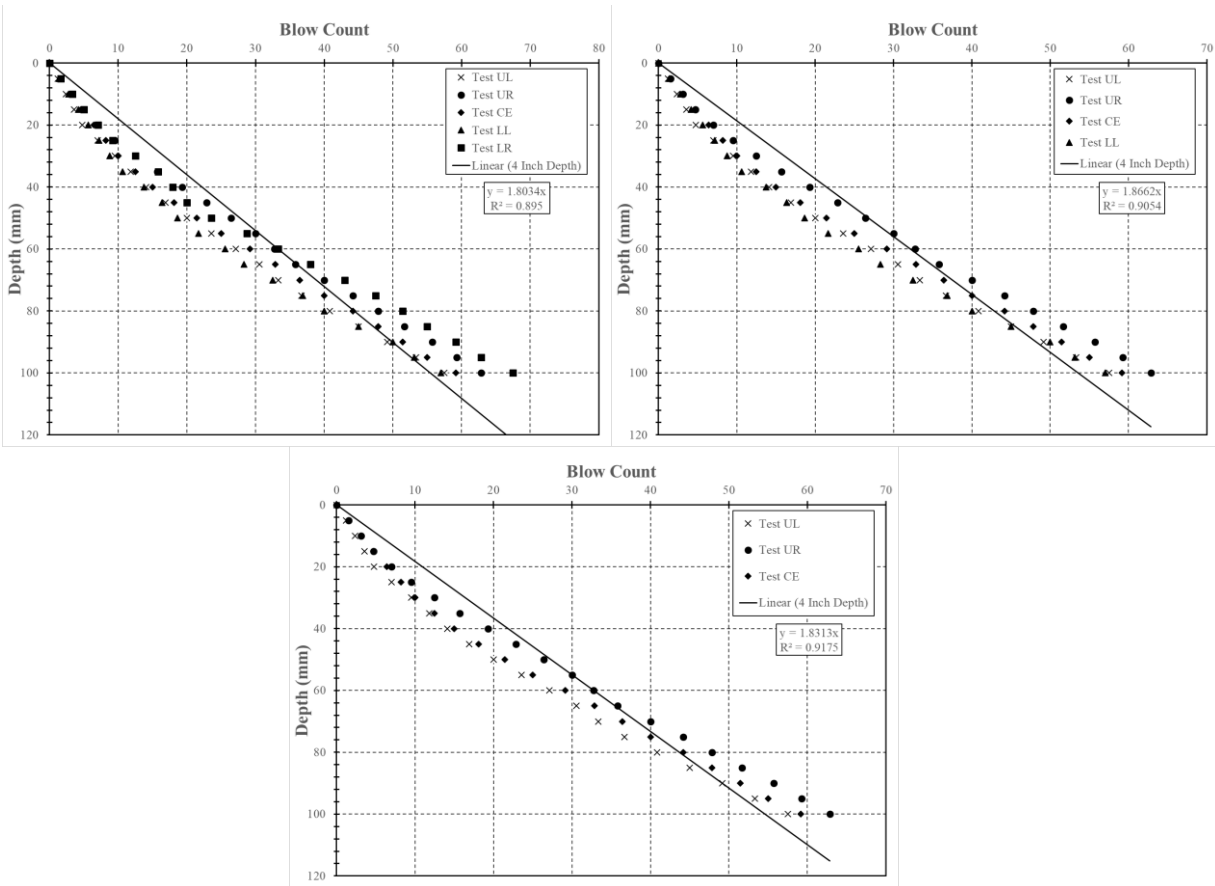


Figure M.27: Test performed on July 19, 2019, Location 34 (top left = 5 tests, top right = 4 tests, bottom = 3 tests)

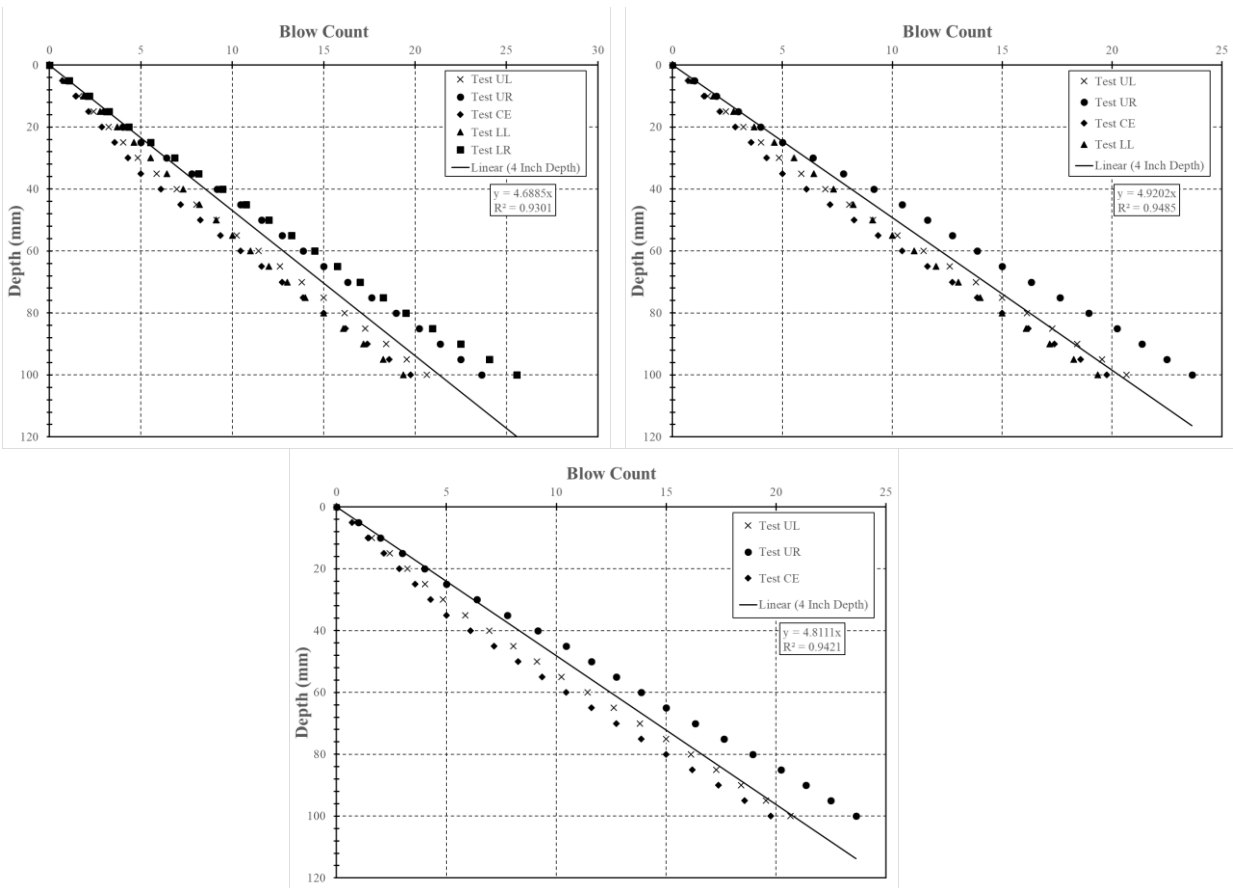


Figure M.28: Test performed on July 19, 2019, Location 35 (top left = 5 tests, top right = 4 tests, bottom = 3 tests)

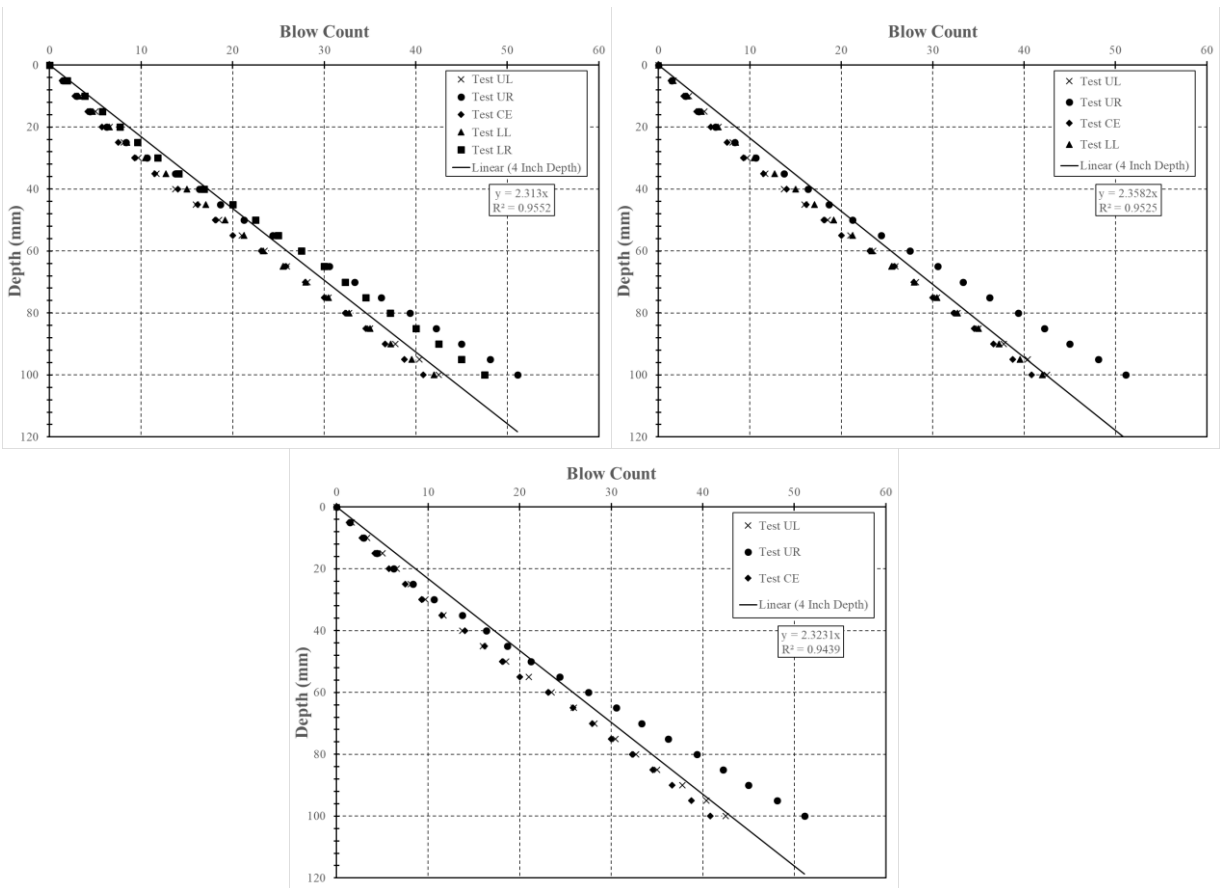


Figure M.29: Test performed on July 19, 2019, Location 36 (top left = 5 tests, top right = 4 tests, bottom = 3 tests)

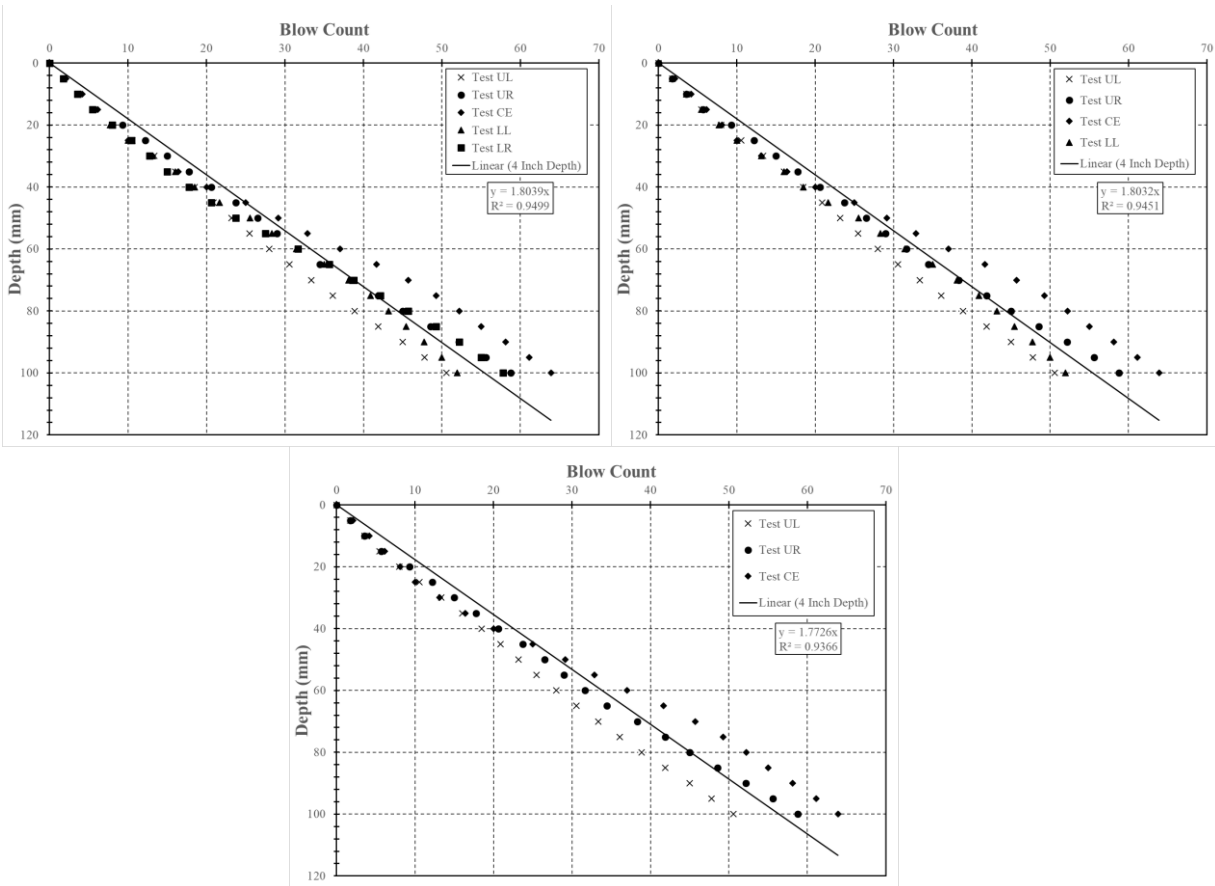


Figure M.30: Test performed on July 23, 2019, Location 37 (top left = 5 tests, top right = 4 tests, bottom = 3 tests)

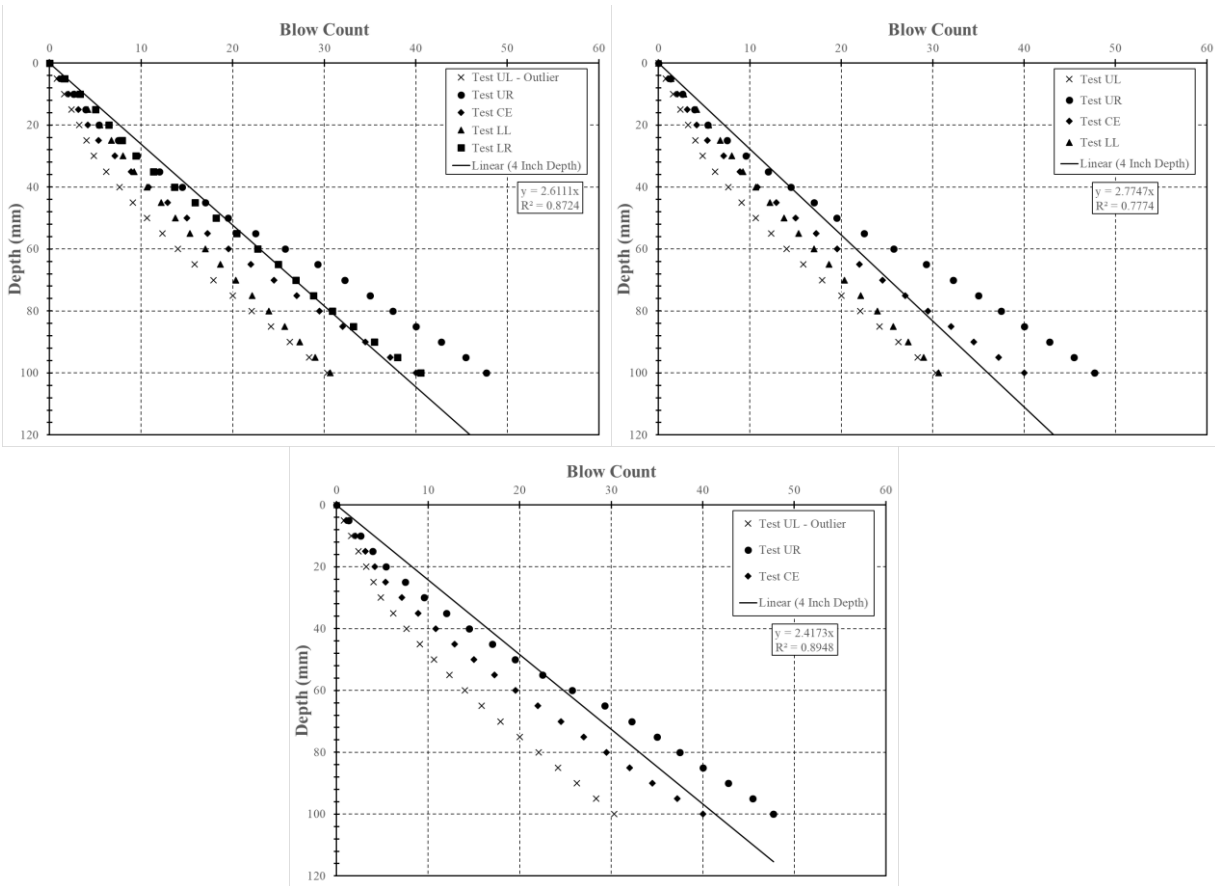


Figure M.31: Test performed on July 23, 2019, Location 38 (top left = 5 tests, top right = 4 tests, bottom = 3 tests)

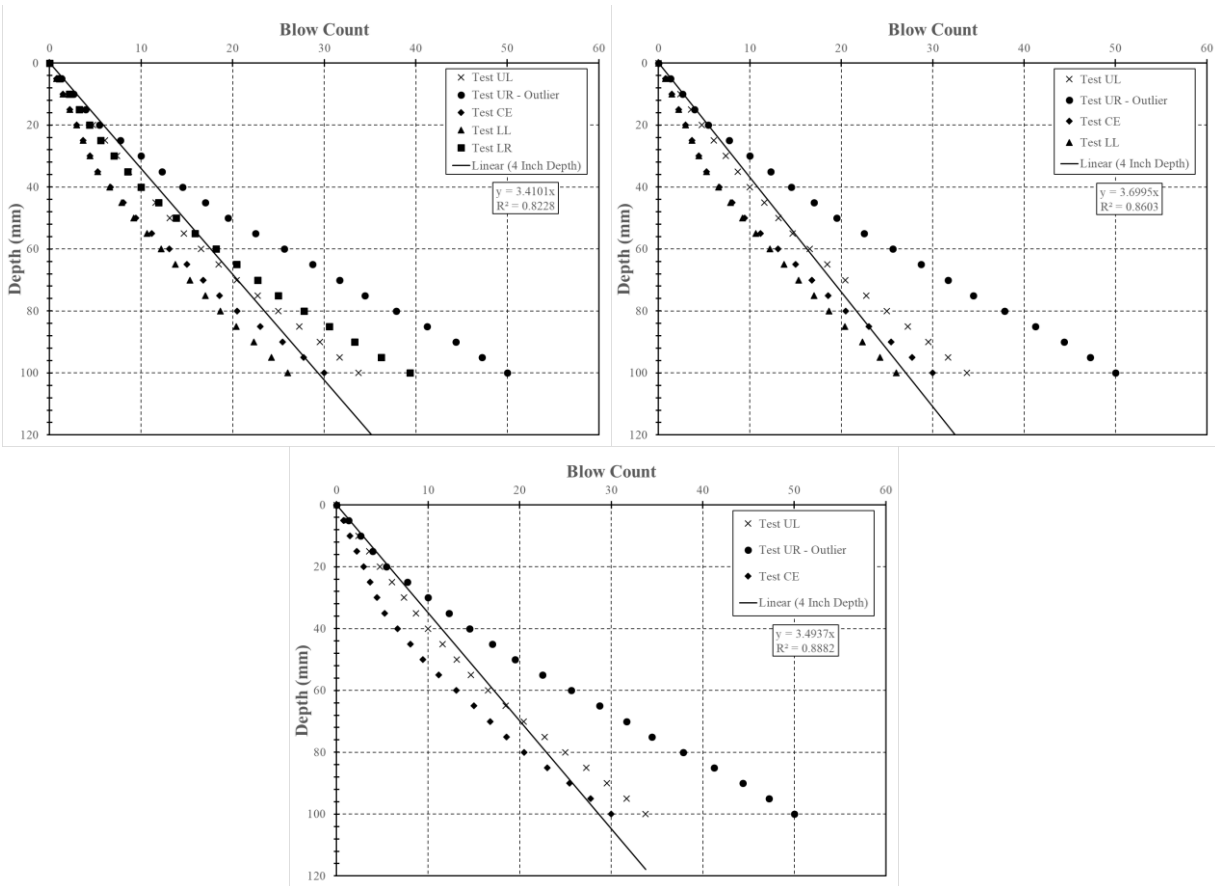


Figure M.32: Test performed on July 23, 2019, Location 39 (top left = 5 tests, top right = 4 tests, bottom = 3 tests)

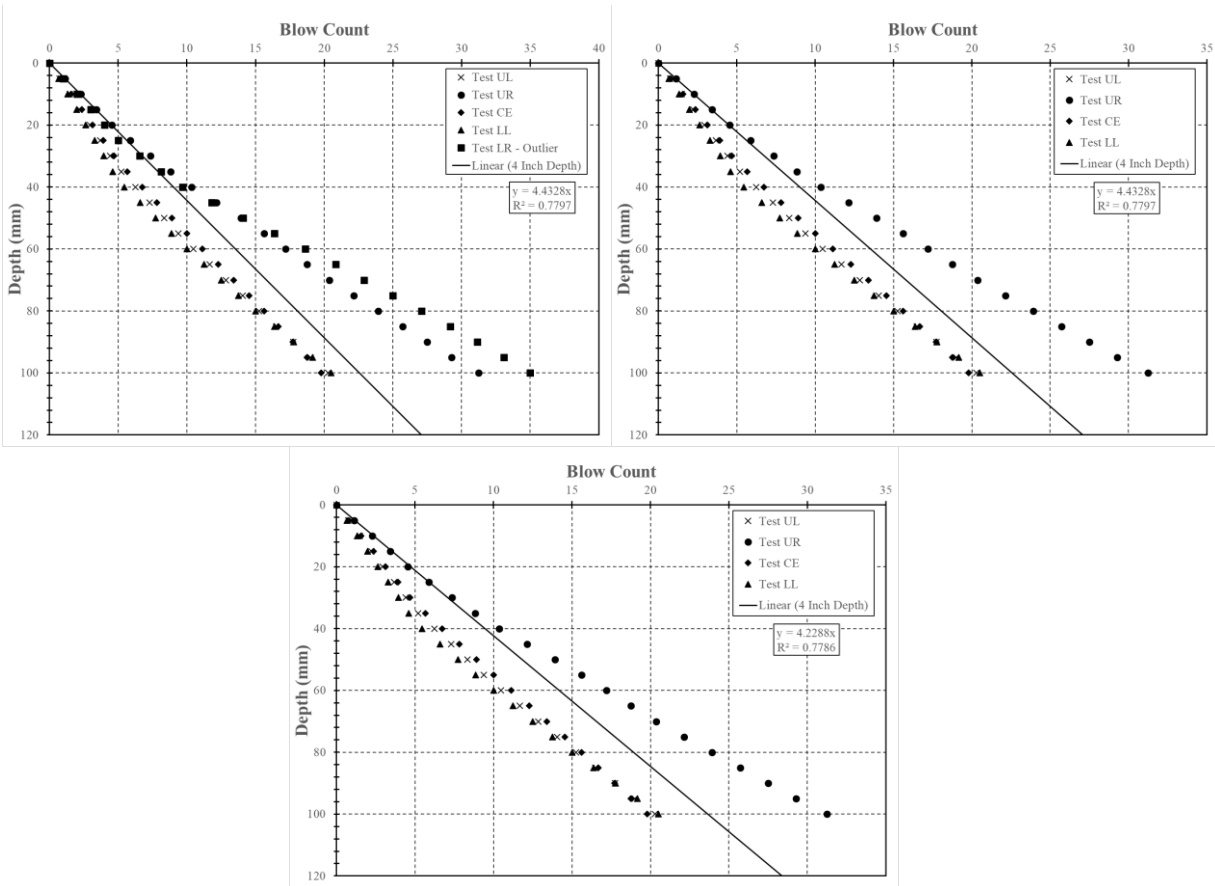


Figure M.33: Test performed on July 23, 2019, Location 40 (top left = 5 tests, top right = 4 tests, bottom = 3 tests)

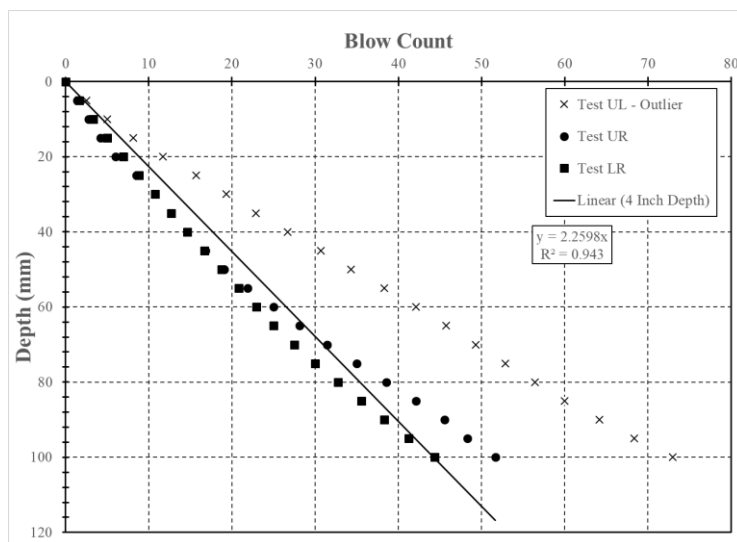


Figure M.34: Test performed on July 23, 2019, Location 41 (only 3 tests completed)

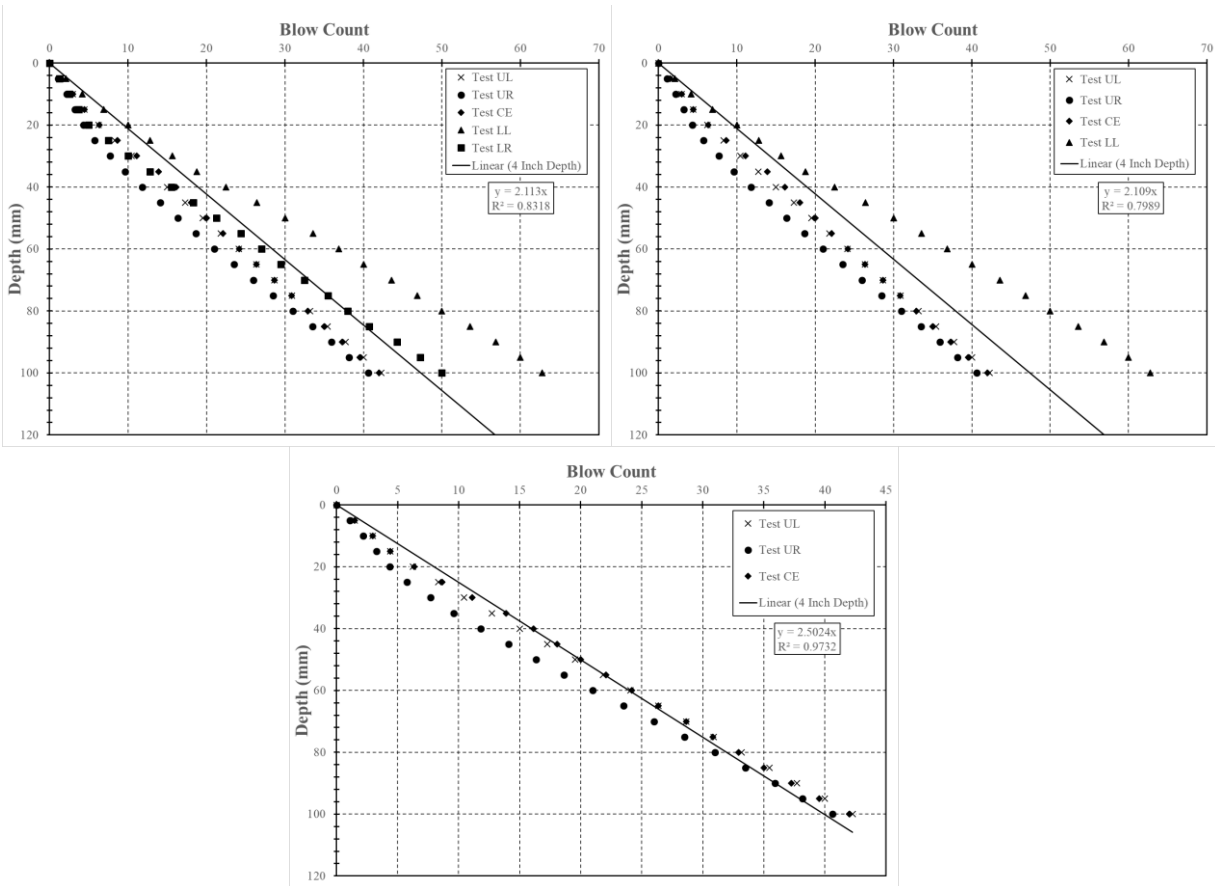


Figure M.35: Test performed on July 23, 2019, Location 42 (top left = 5 tests, top right = 4 tests, bottom = 3 tests)

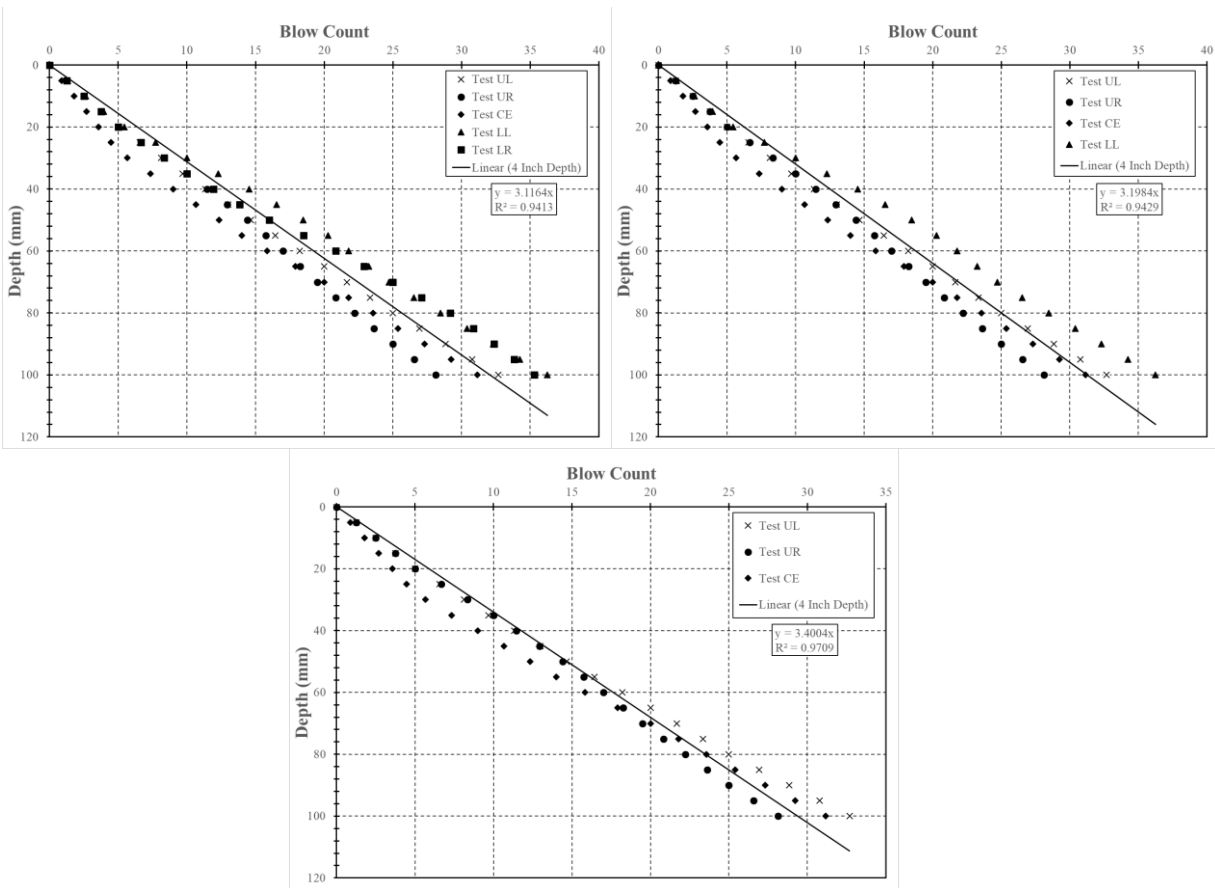


Figure M.36: Test performed on July 23, 2019, Location 43 (top left = 5 tests, top right = 4 tests, bottom = 3 tests)

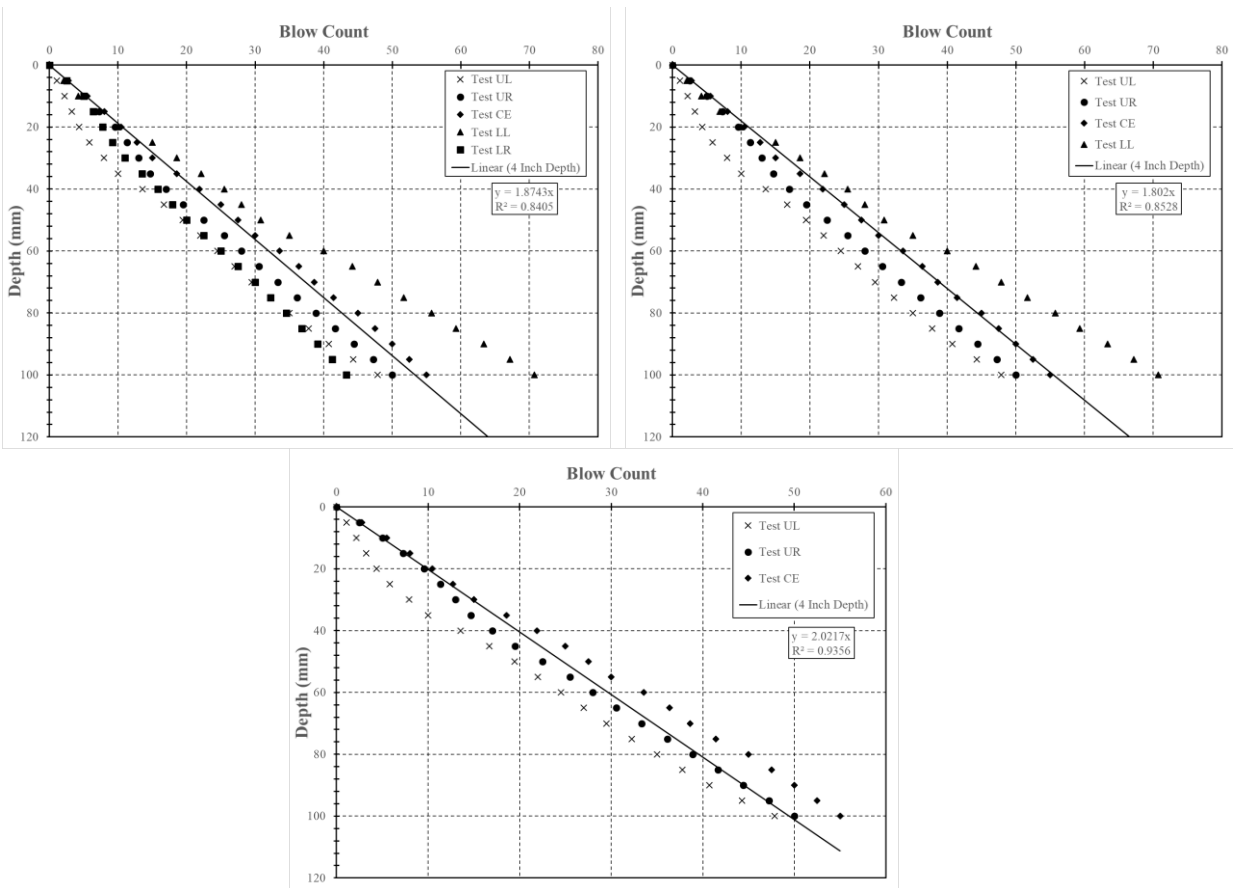


Figure M.37: Test performed on July 24, 2019, Location 44 (top left = 5 tests, top right = 4 tests, bottom = 3 tests)

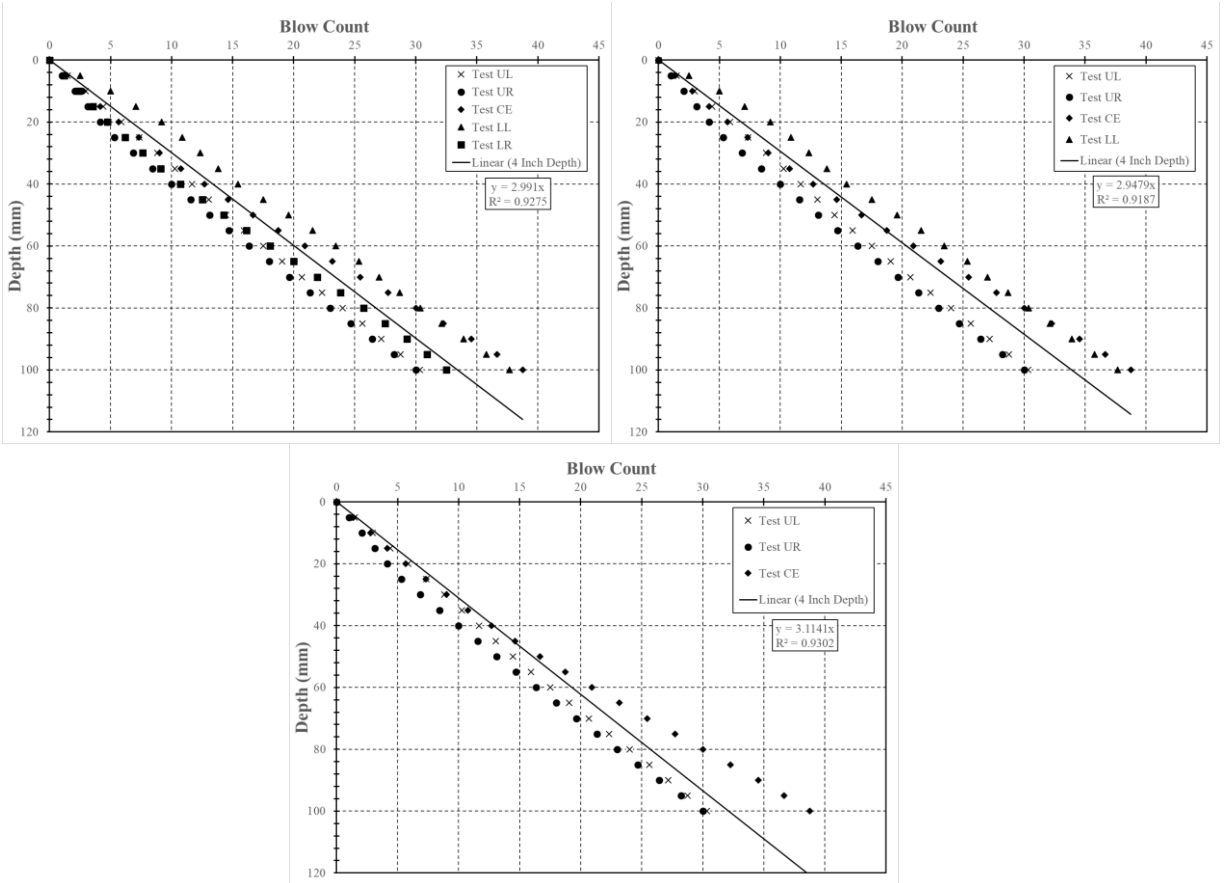


Figure M.38: Test performed on July 24, 2019, Location 45 (top left = 5 tests, top right = 4 tests, bottom = 3 tests)

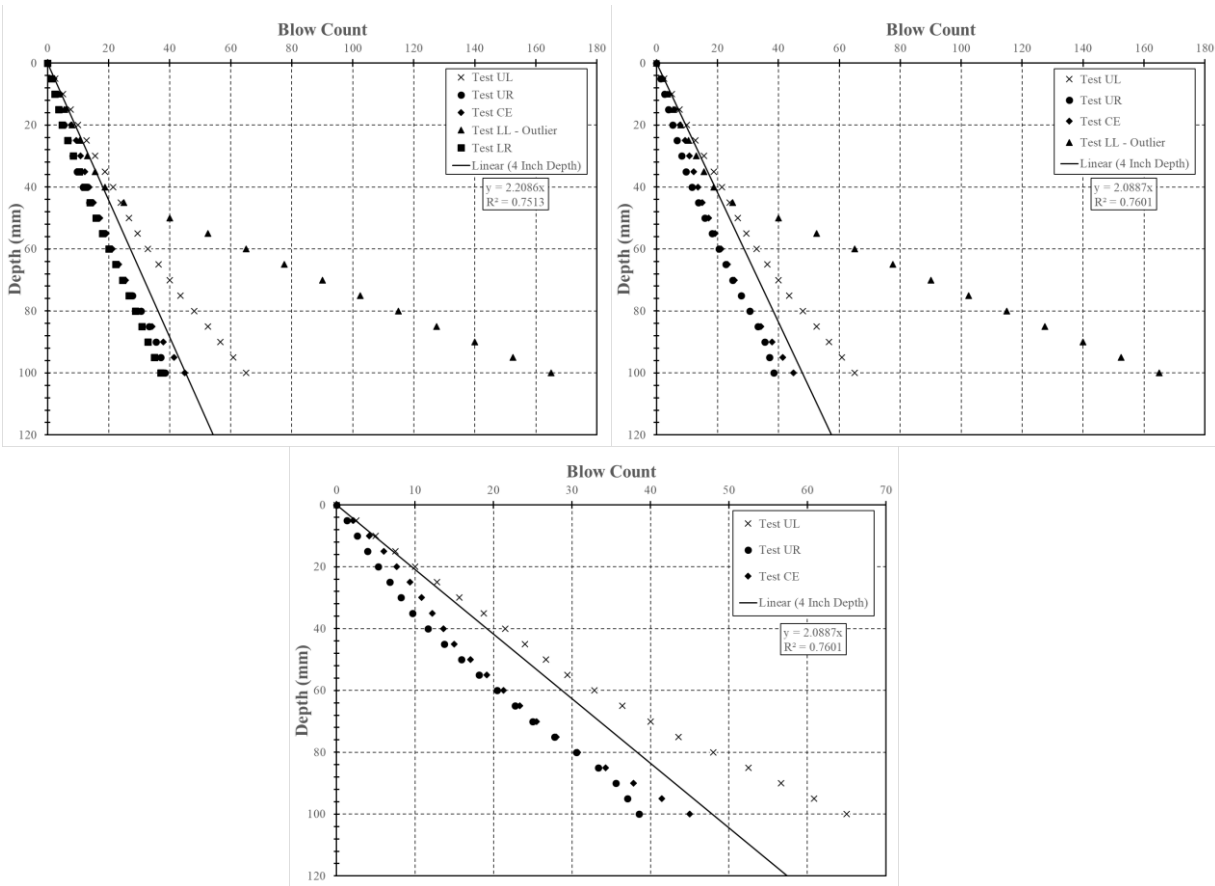


Figure M.39: Test performed on July 24, 2019, Location 46 (top left = 5 tests, top right = 4 tests, bottom = 3 tests)

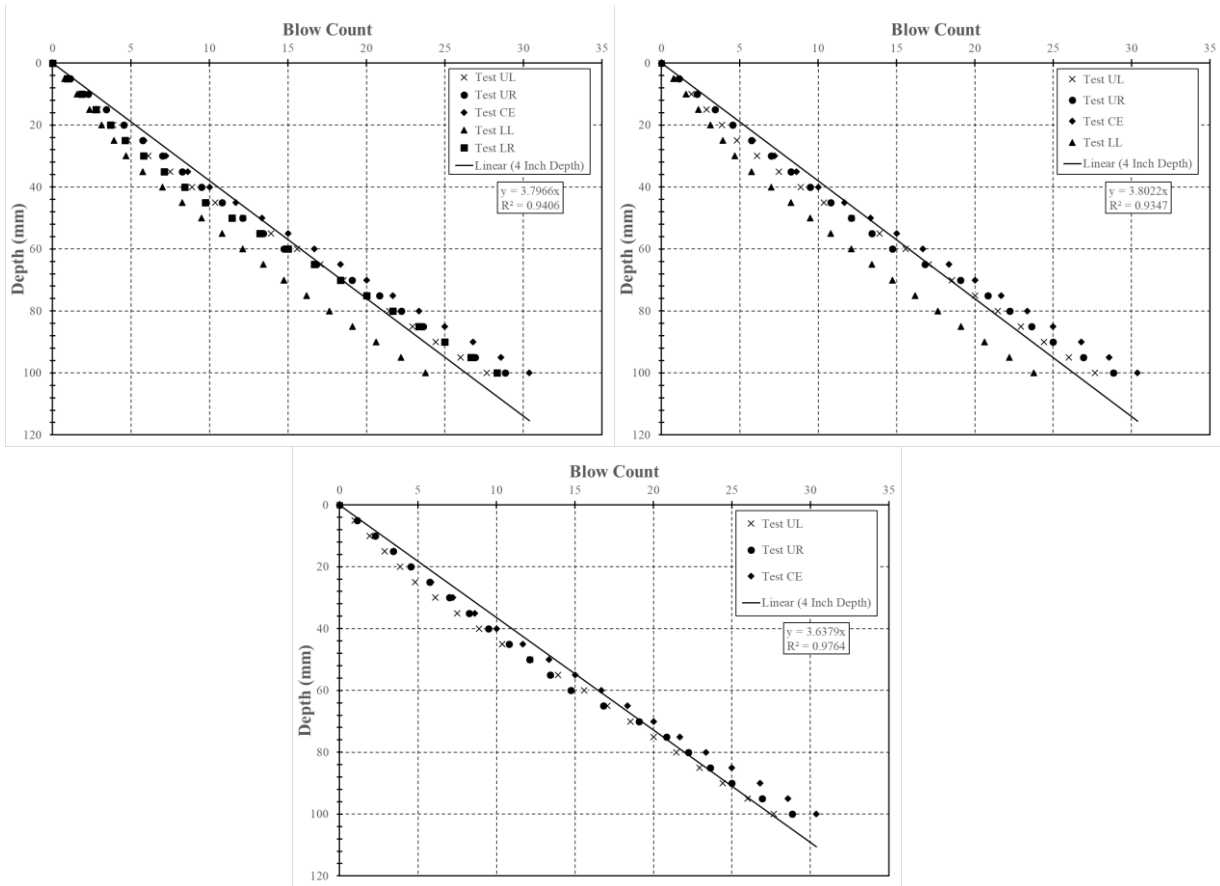


Figure M.40: Test performed on July 24, 2019, Location 47 (top left = 5 tests, top right = 4 tests, bottom = 3 tests)

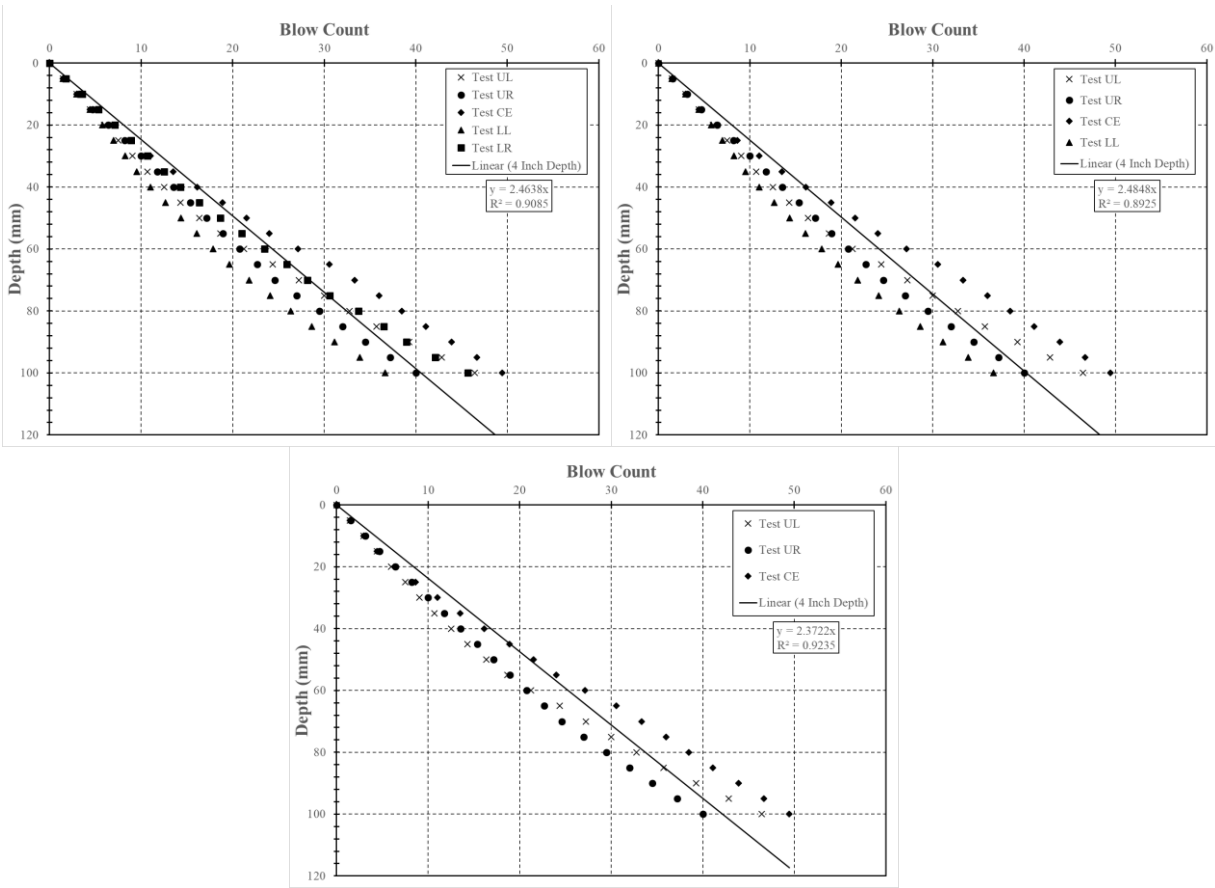


Figure M.41: Test performed on July 24, 2019, Location 48 (top left = 5 tests, top right = 4 tests, bottom = 3 tests)

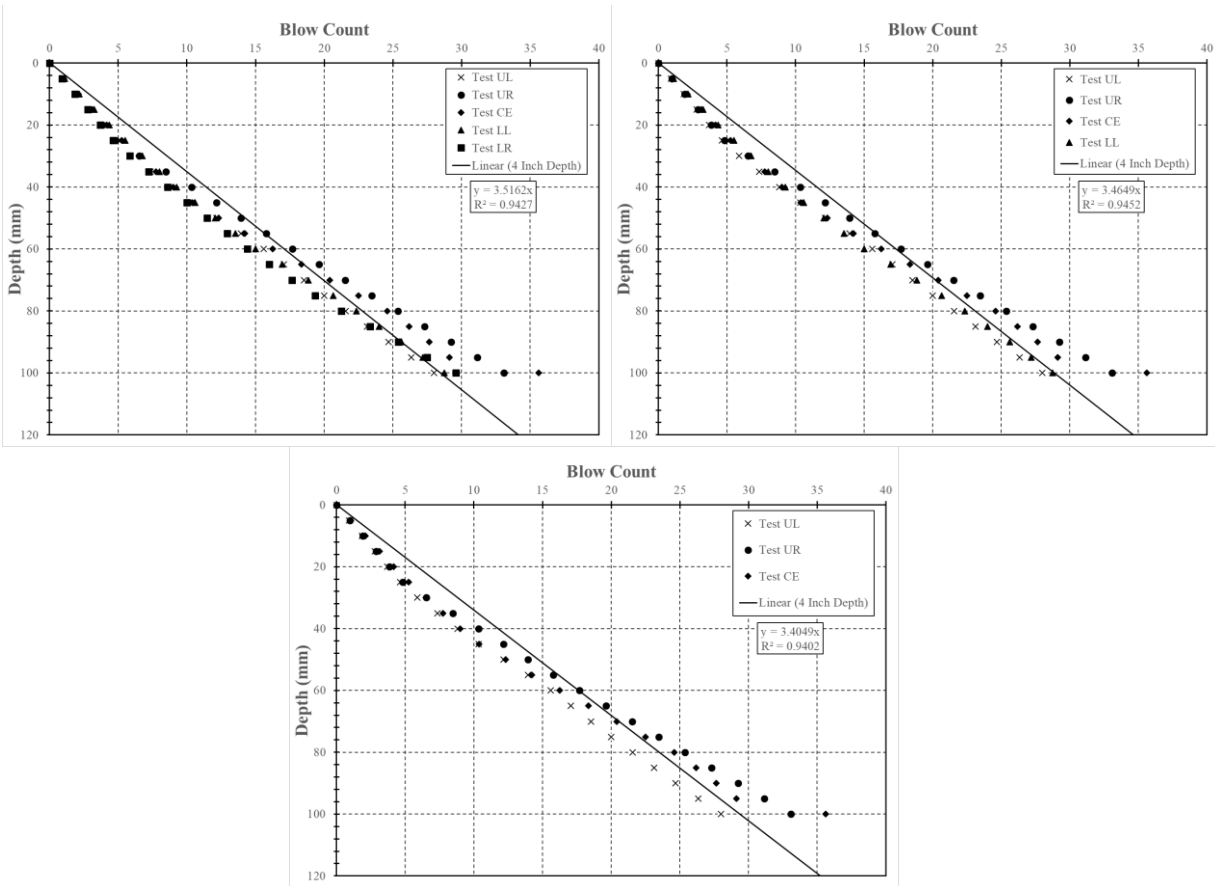


Figure M.42: Test performed on July 24, 2019, Location 49 (top left = 5 tests, top right = 4 tests, bottom = 3 tests)

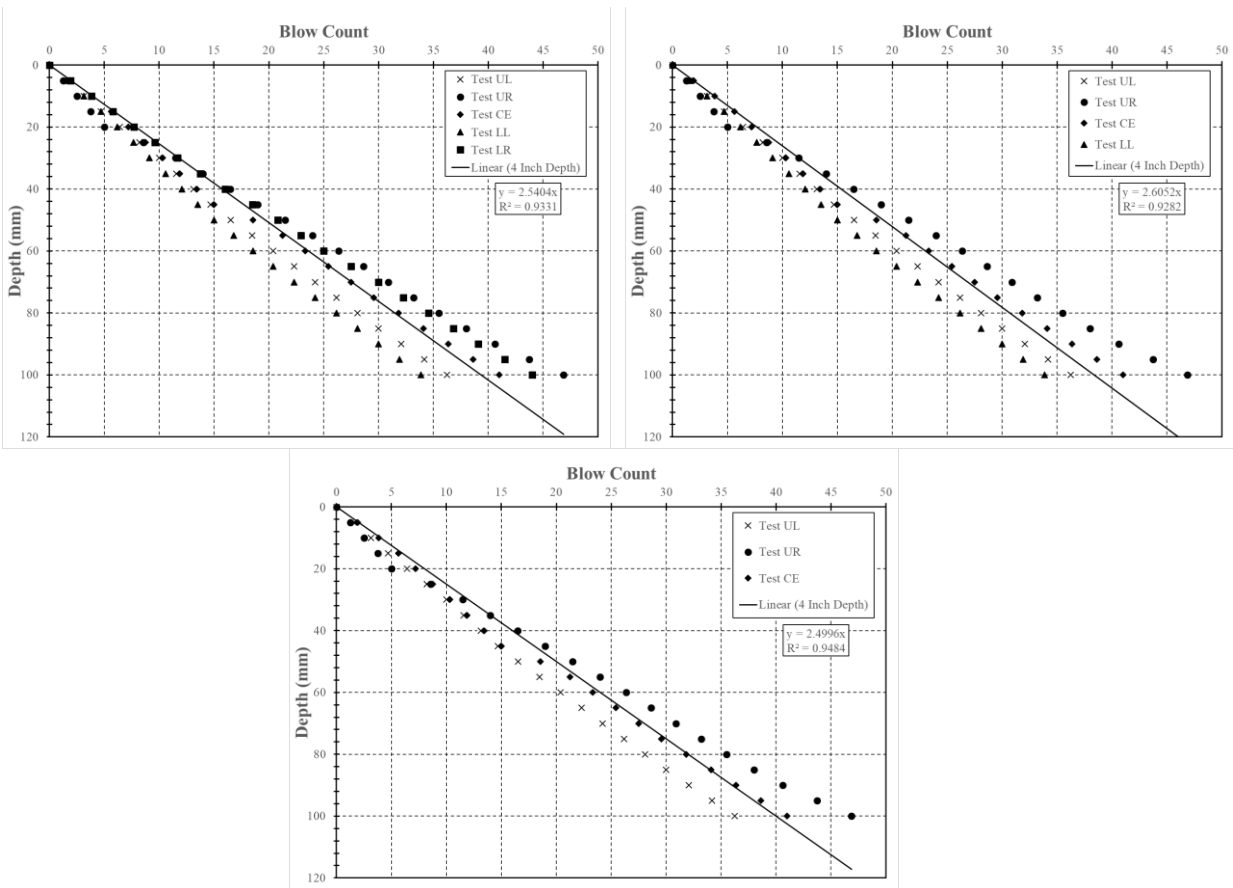


Figure M.43: Test performed on July 24, 2019, Location 50 (top left = 5 tests, top right = 4 tests, bottom = 3 tests)

Appendix N

Full Depth Penetration Field Data

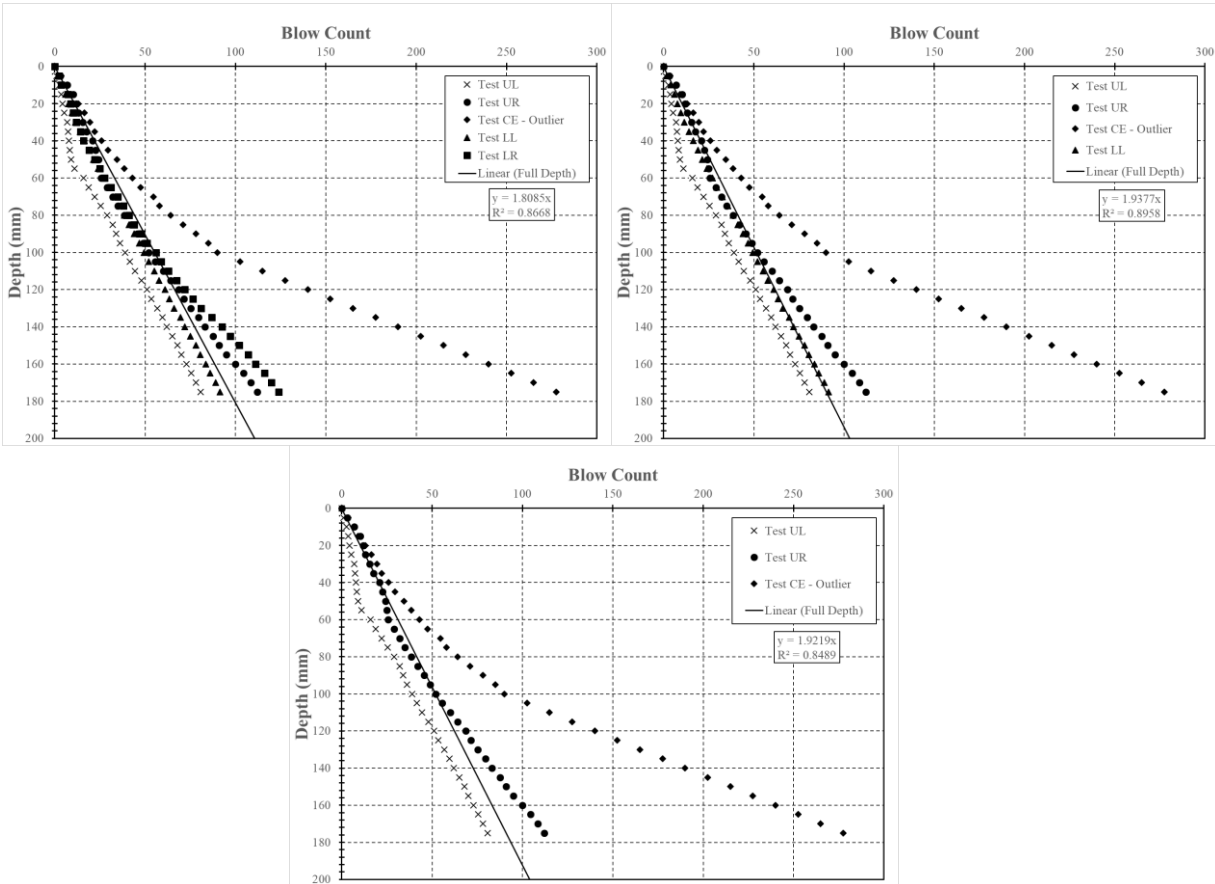


Figure N.1: Test performed on July 9, 2019, Location 1 (top left = 5 tests, top right = 4 tests, bottom = 3 tests)

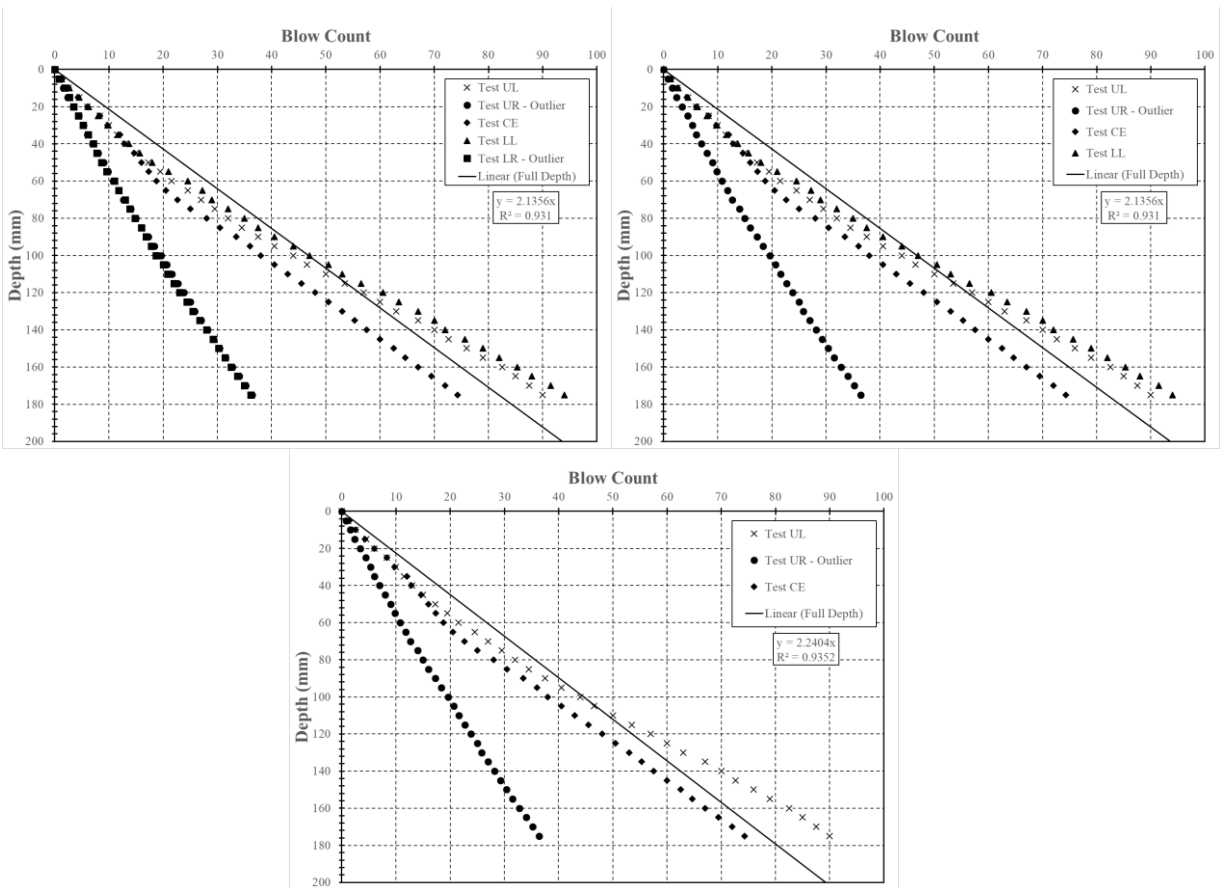


Figure N.2: Test performed on July 10, 2019, Location 4 (top left = 5 tests, top right = 4 tests, bottom = 3 tests)

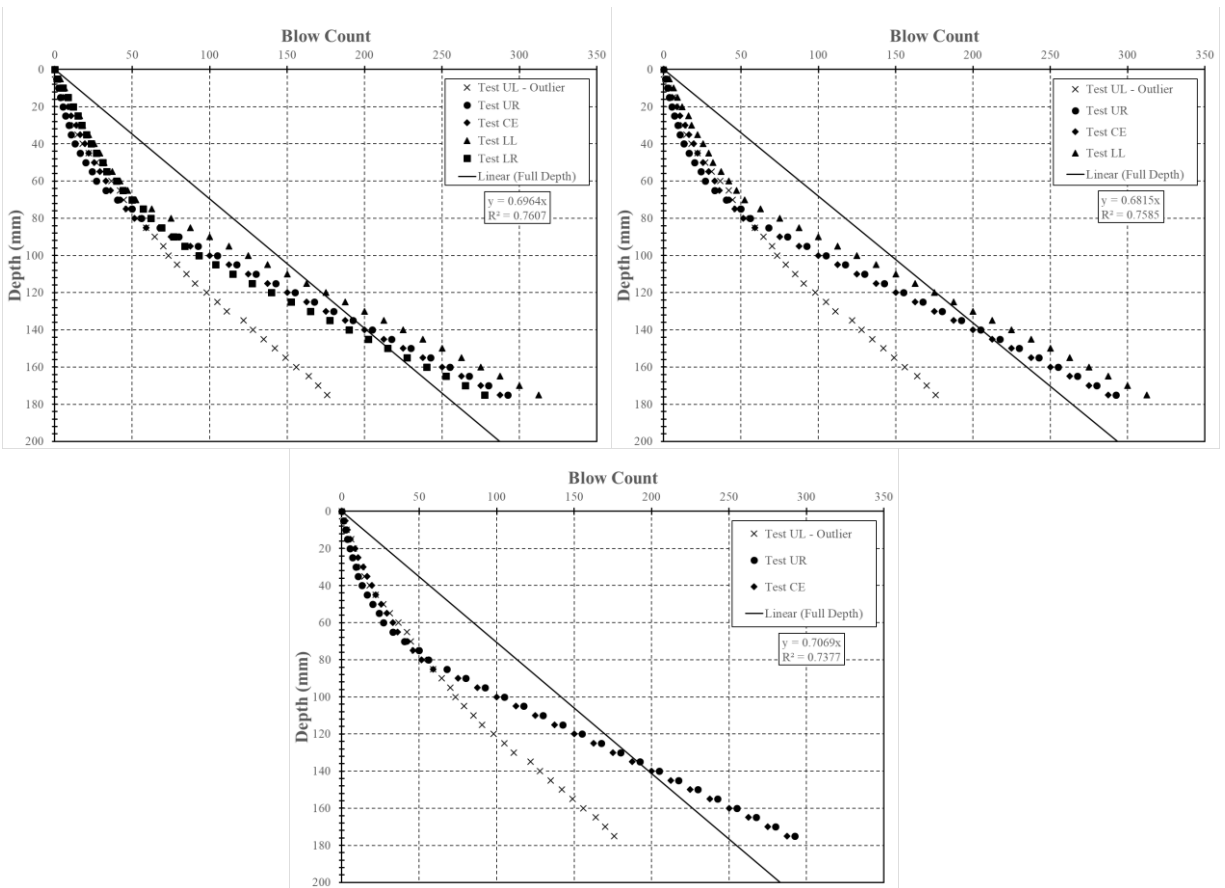


Figure N.3: Test performed on July 10, 2019, Location 5 (top left = 5 tests, top right = 4 tests, bottom = 3 tests)

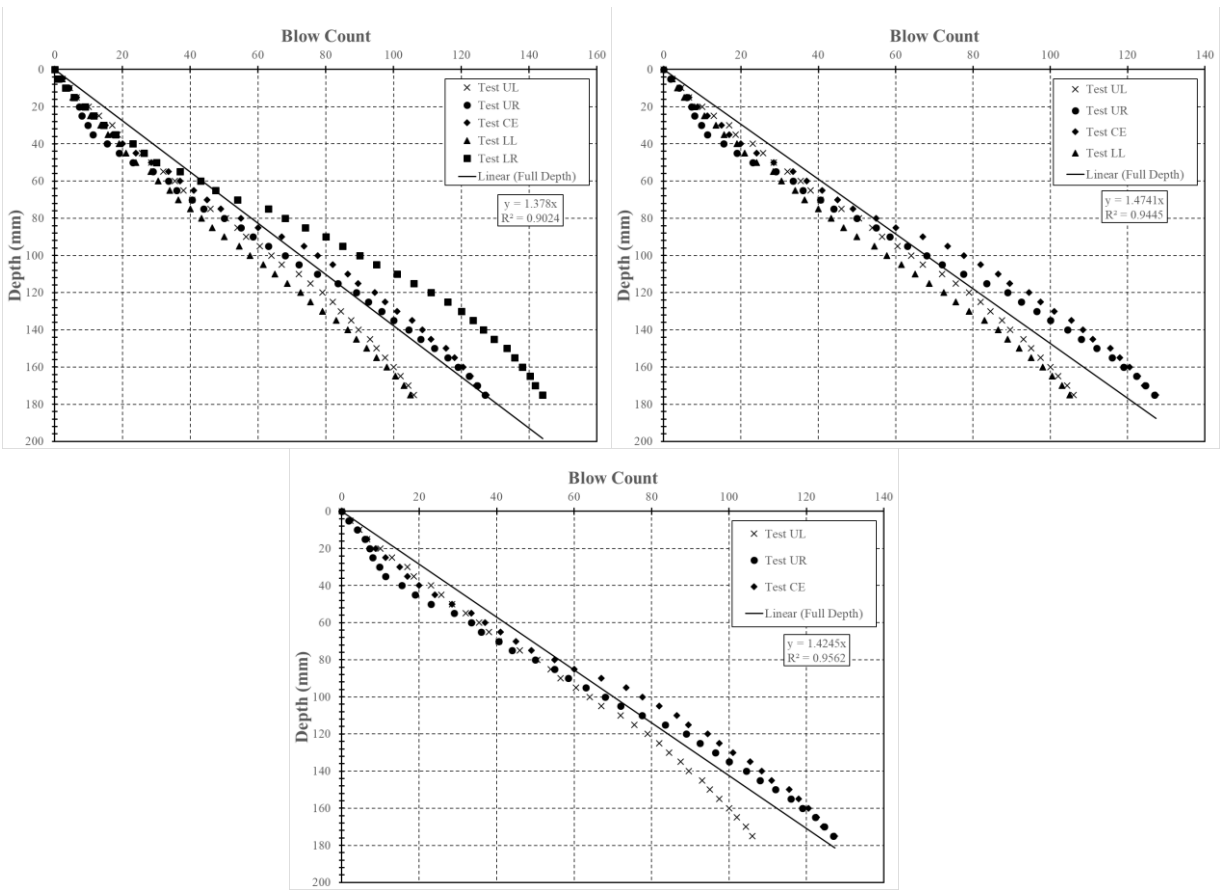


Figure N.4: Test performed on July 10, 2019, Location 6 (top left = 5 tests, top right = 4 tests, bottom = 3 tests)

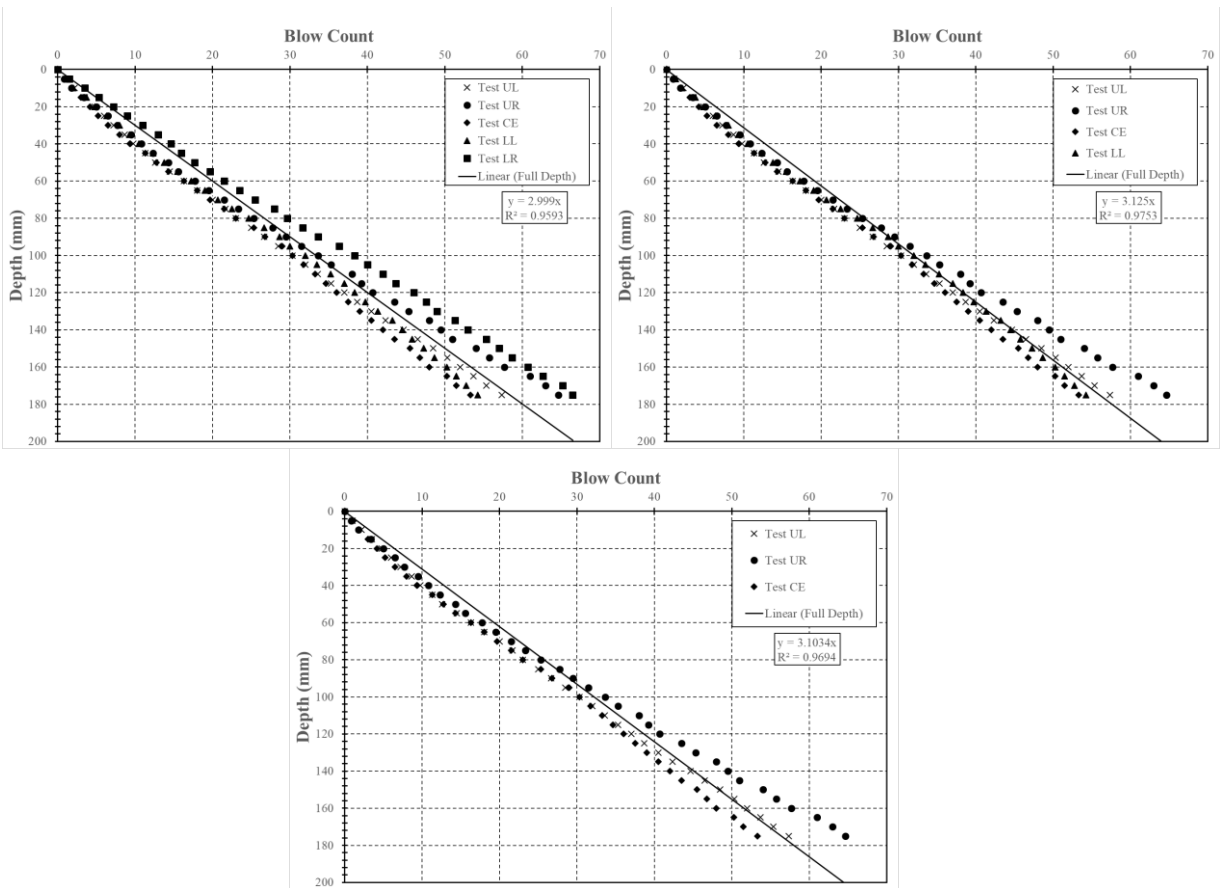


Figure N.5: Test performed on July 16, 2019, Location 7 (top left = 5 tests, top right = 4 tests, bottom = 3 tests)

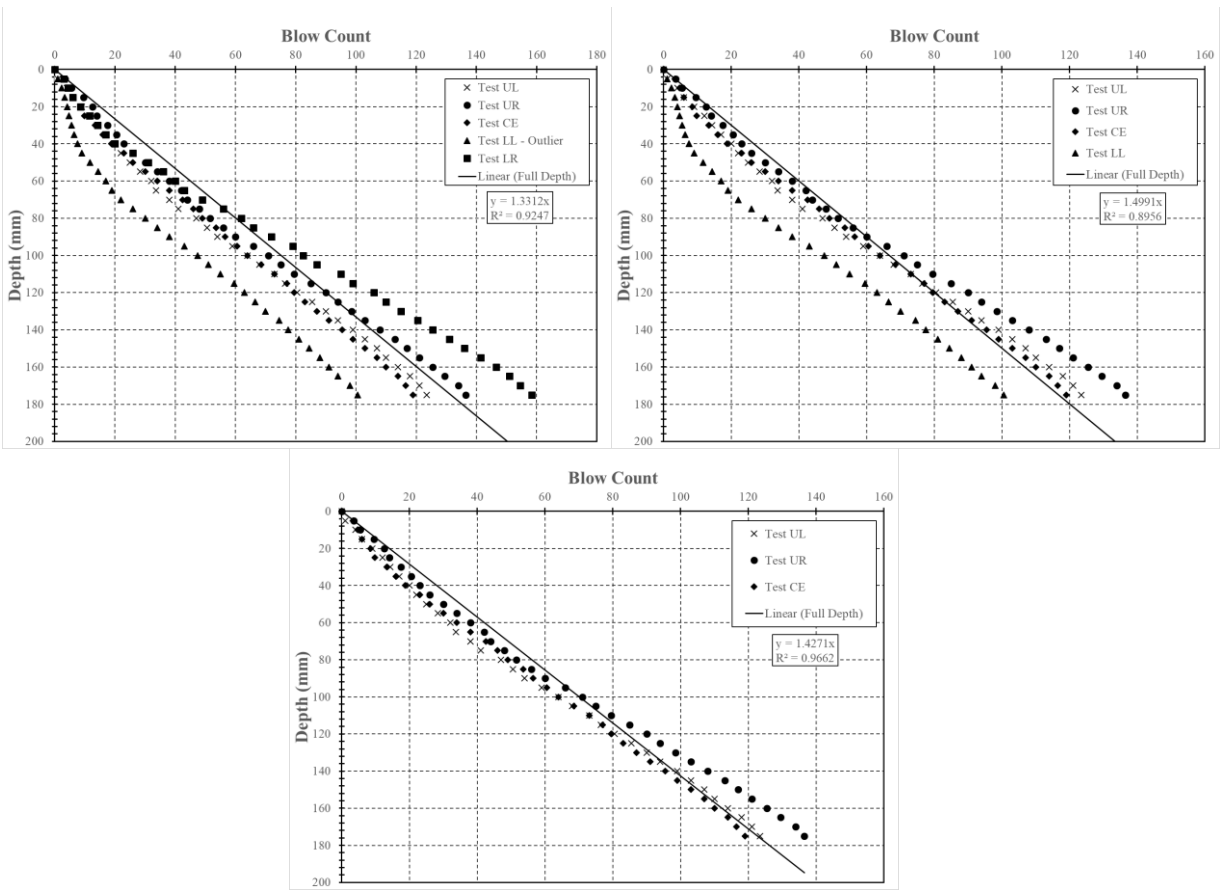


Figure N.6: Test performed on July 16, 2019, Location 8 (top left = 5 tests, top right = 4 tests, bottom = 3 tests)

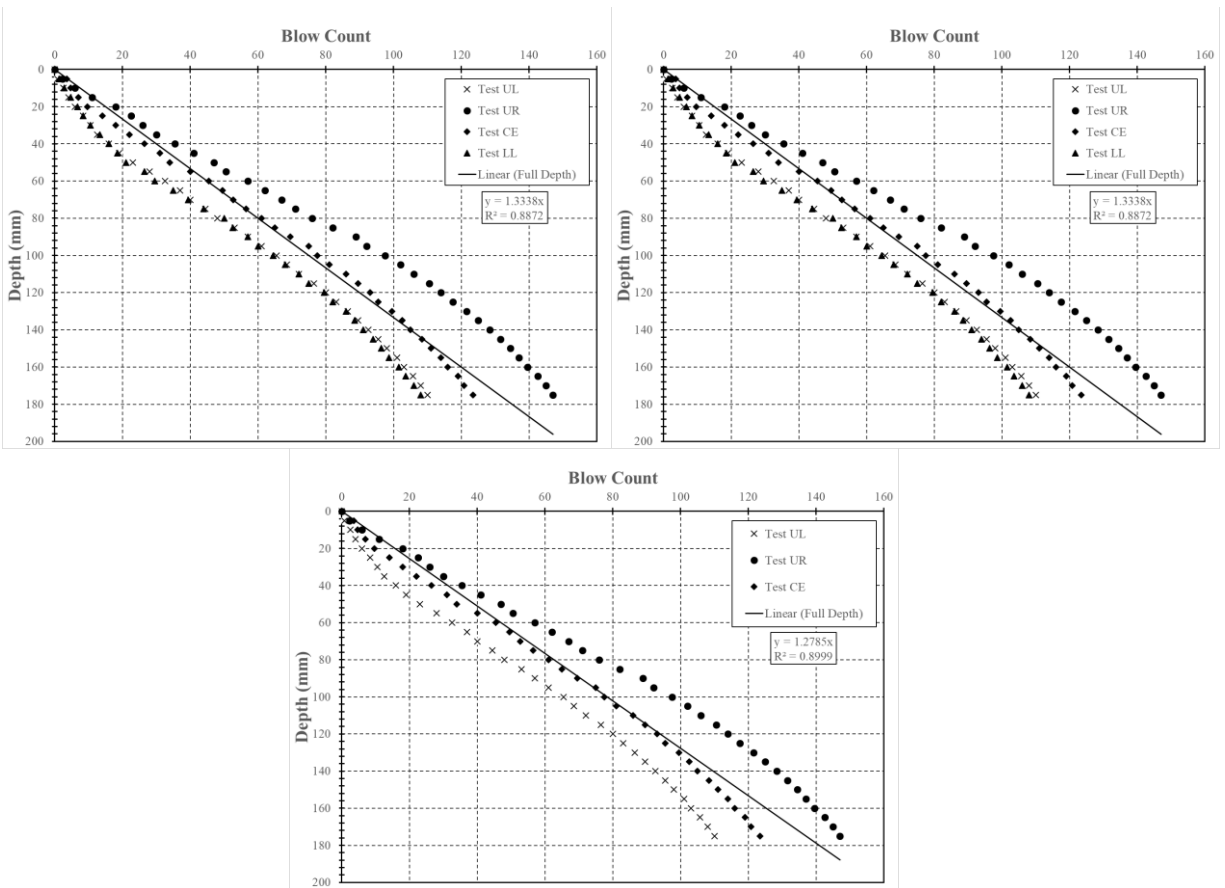


Figure N.7: Test performed on July 16, 2019, Location 9 (top left = 5 tests, top right = 4 tests, bottom = 3 tests)

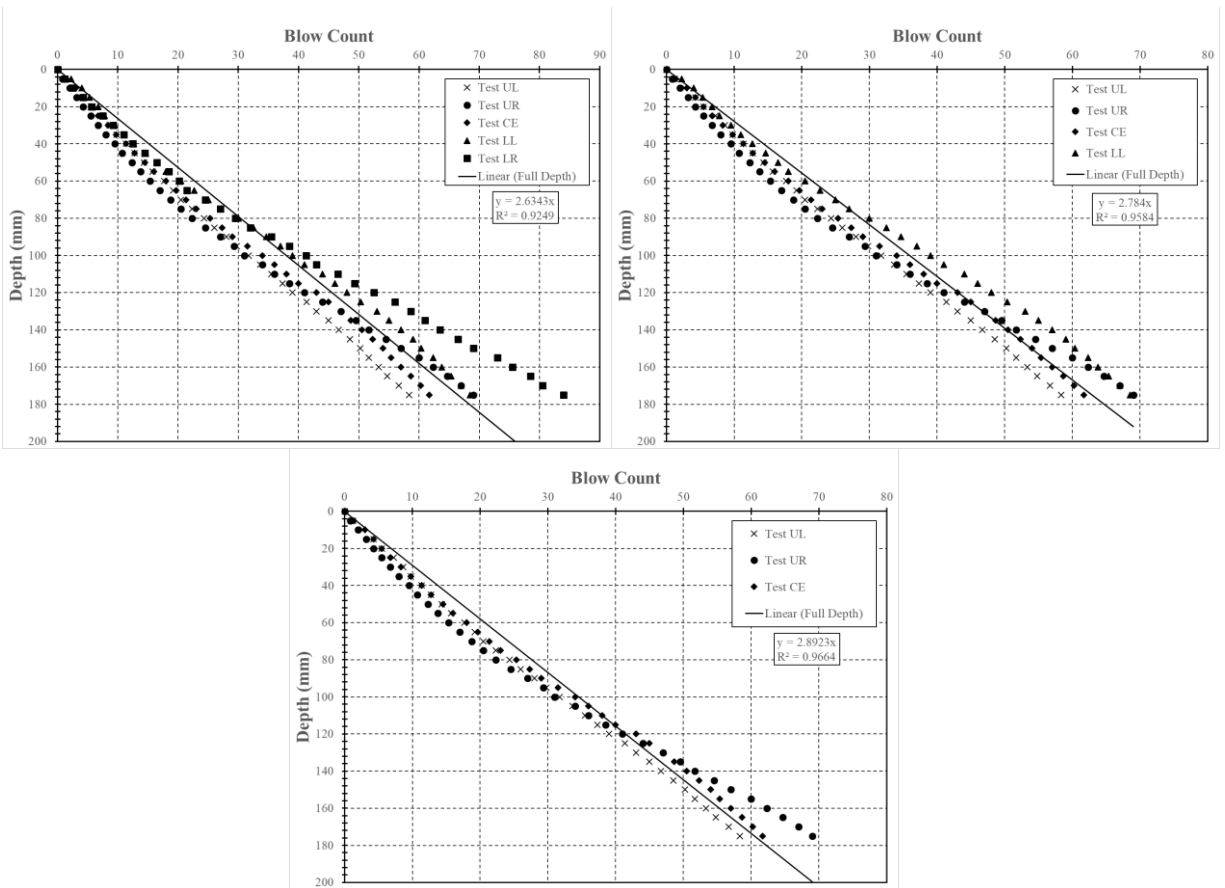


Figure N.8: Test performed on July 16, 2019, Location 10 (top left = 5 tests, top right = 4 tests, bottom = 3 tests)

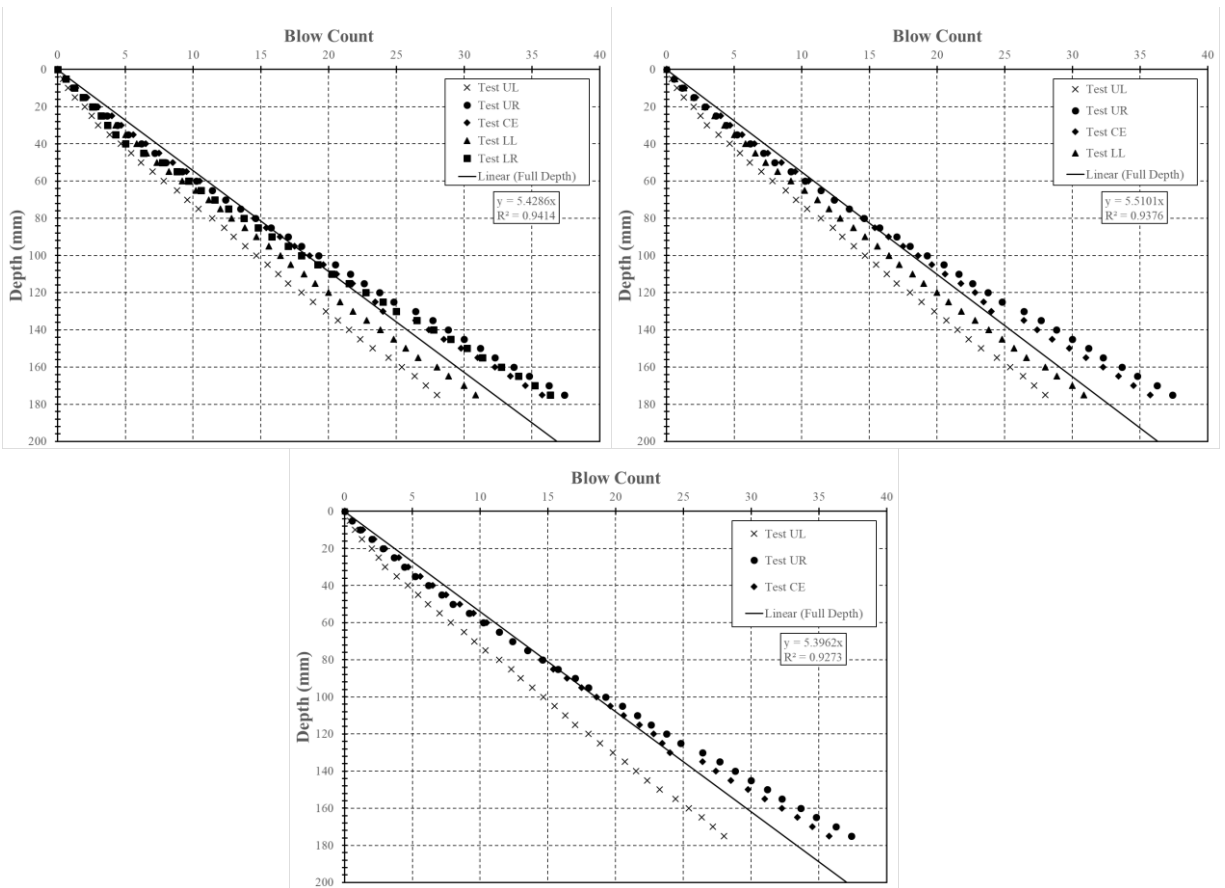


Figure N.9: Test performed on July 16, 2019, Location 11 (top left = 5 tests, top right = 4 tests, bottom = 3 tests)

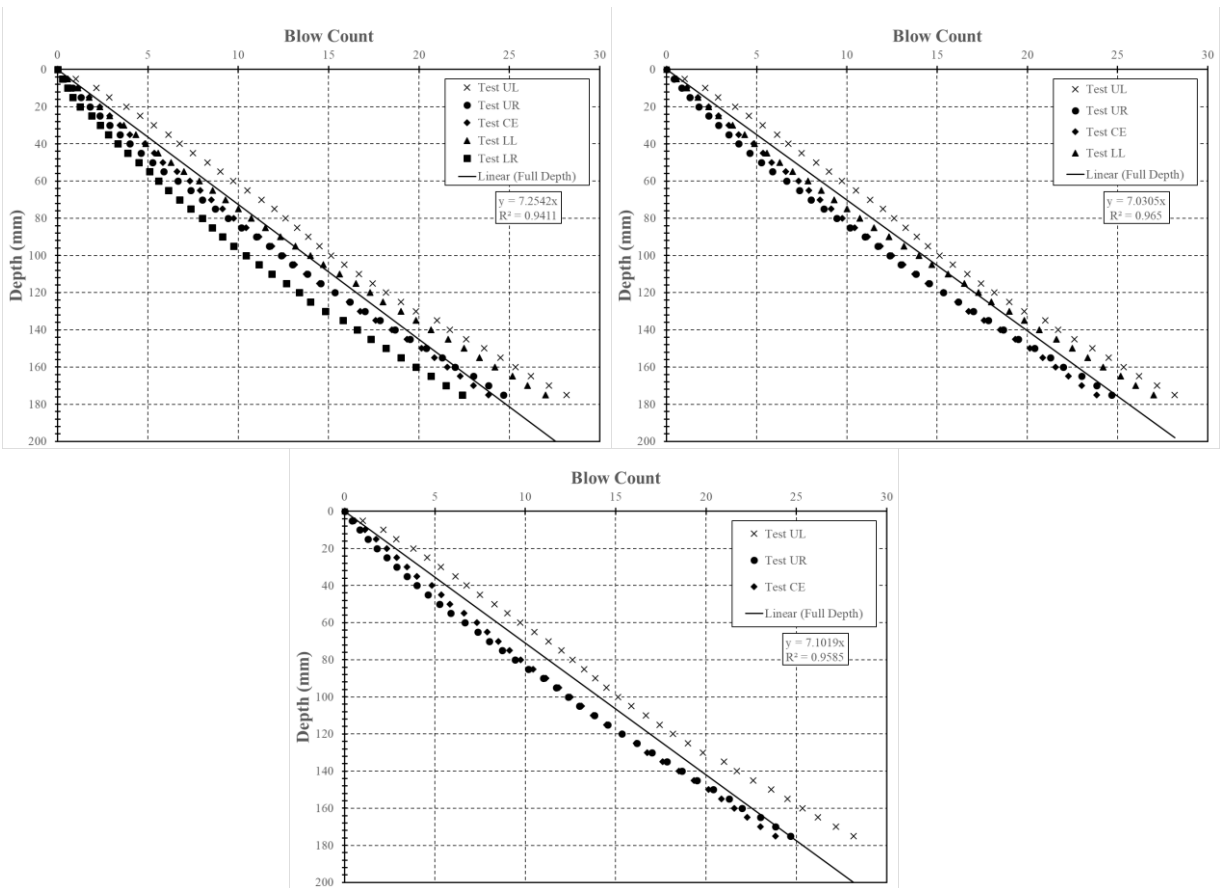


Figure N.10: Test performed on July 16, 2019, Location 12 (top left = 5 tests, top right = 4 tests, bottom = 3 tests)

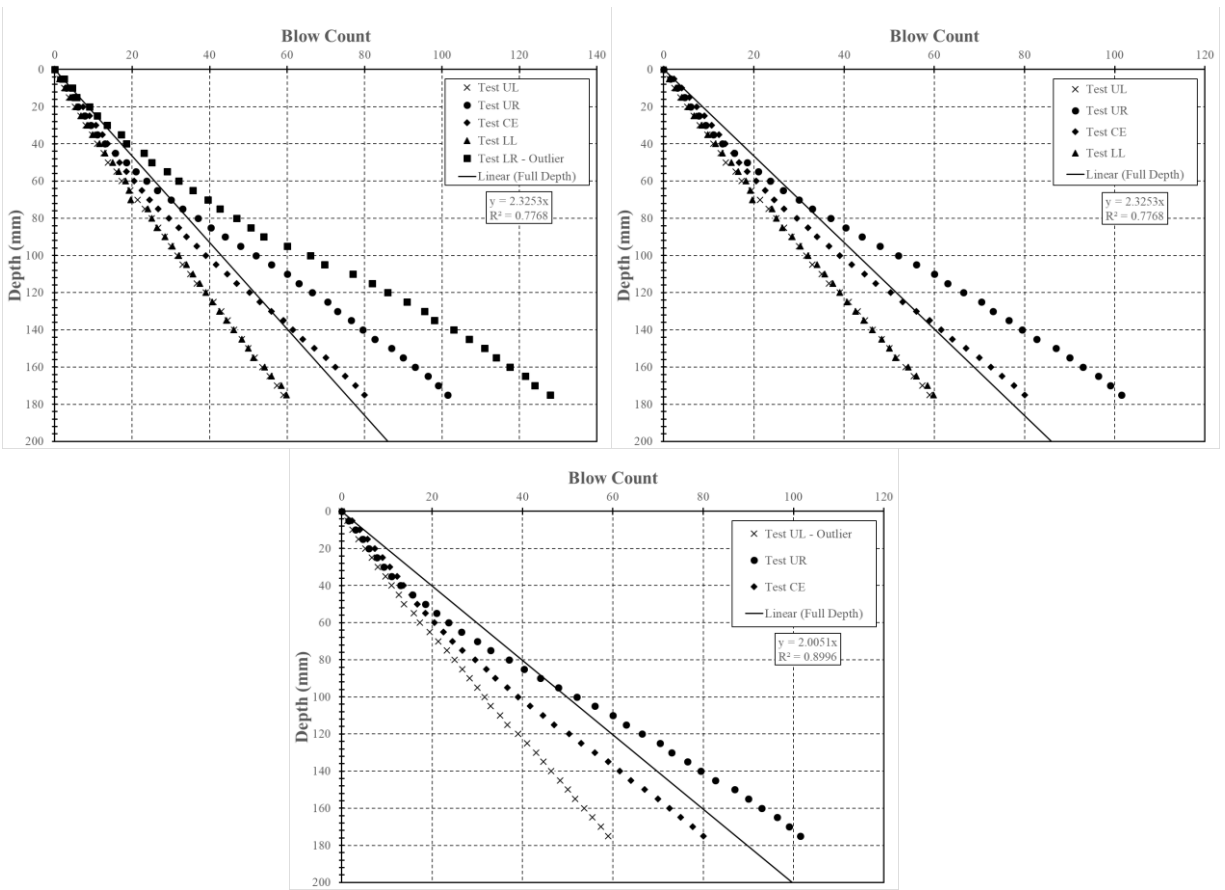


Figure N.11: Test performed on July 16, 2019, Location 13 (top left = 5 tests, top right = 4 tests, bottom = 3 tests)

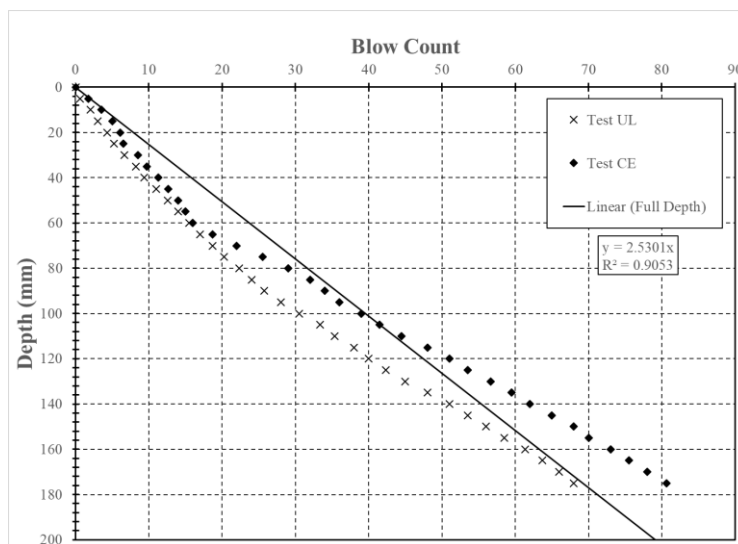


Figure N.12: Test performed on July 16, 2019, Location 15 (only 2 tests completed)

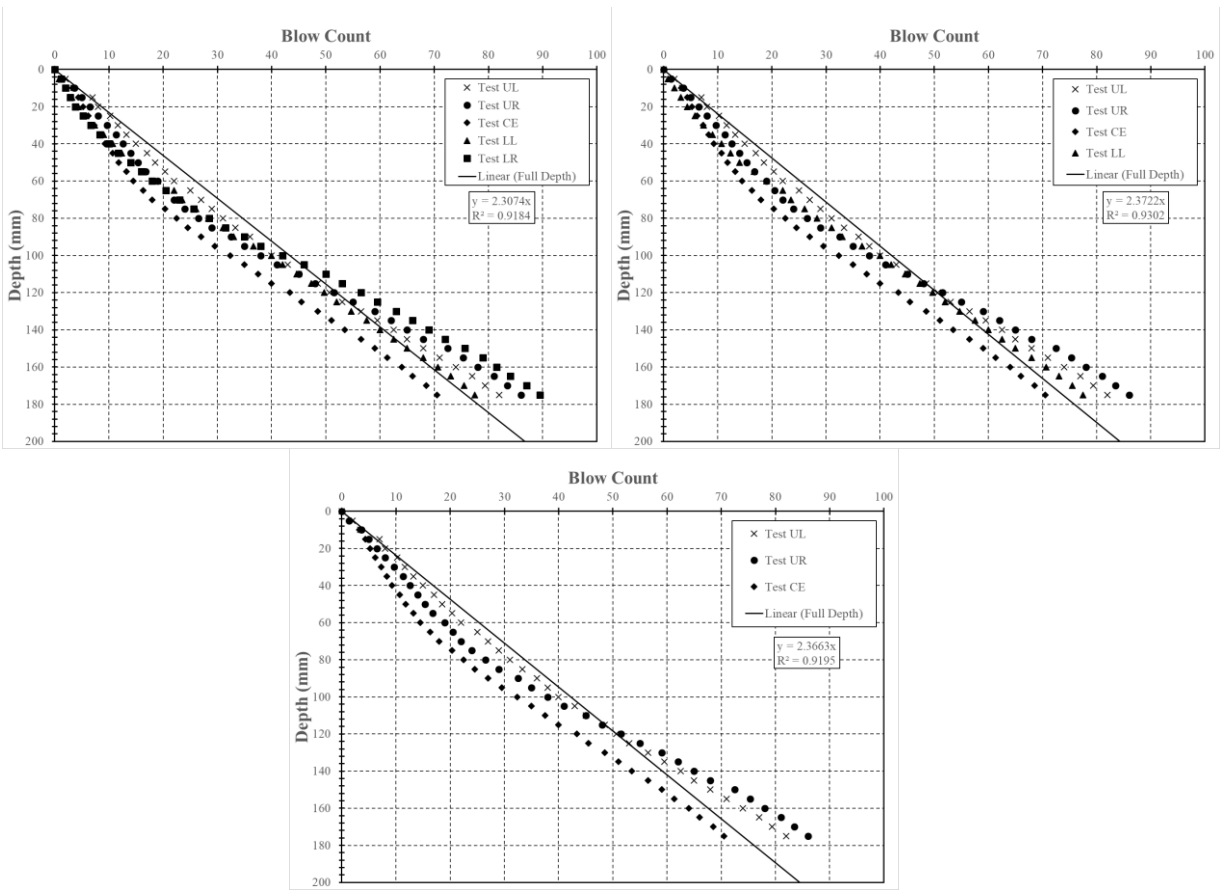


Figure N.13: Test performed on July 17, 2019, Location 17 (top left = 5 tests, top right = 4 tests, bottom = 3 tests)

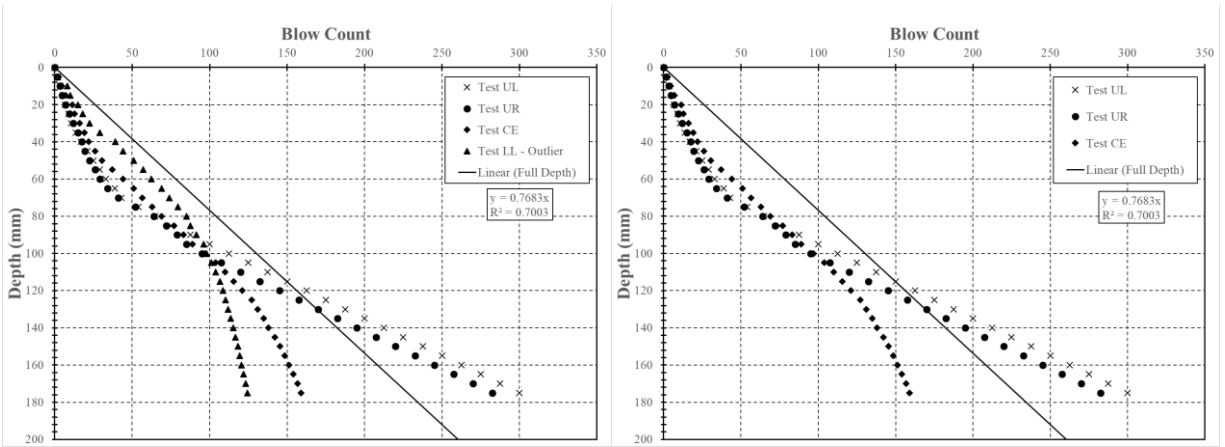


Figure N.14: Test performed on July 17, 2019, Location 18 (left = 4 tests, right = 3 tests)

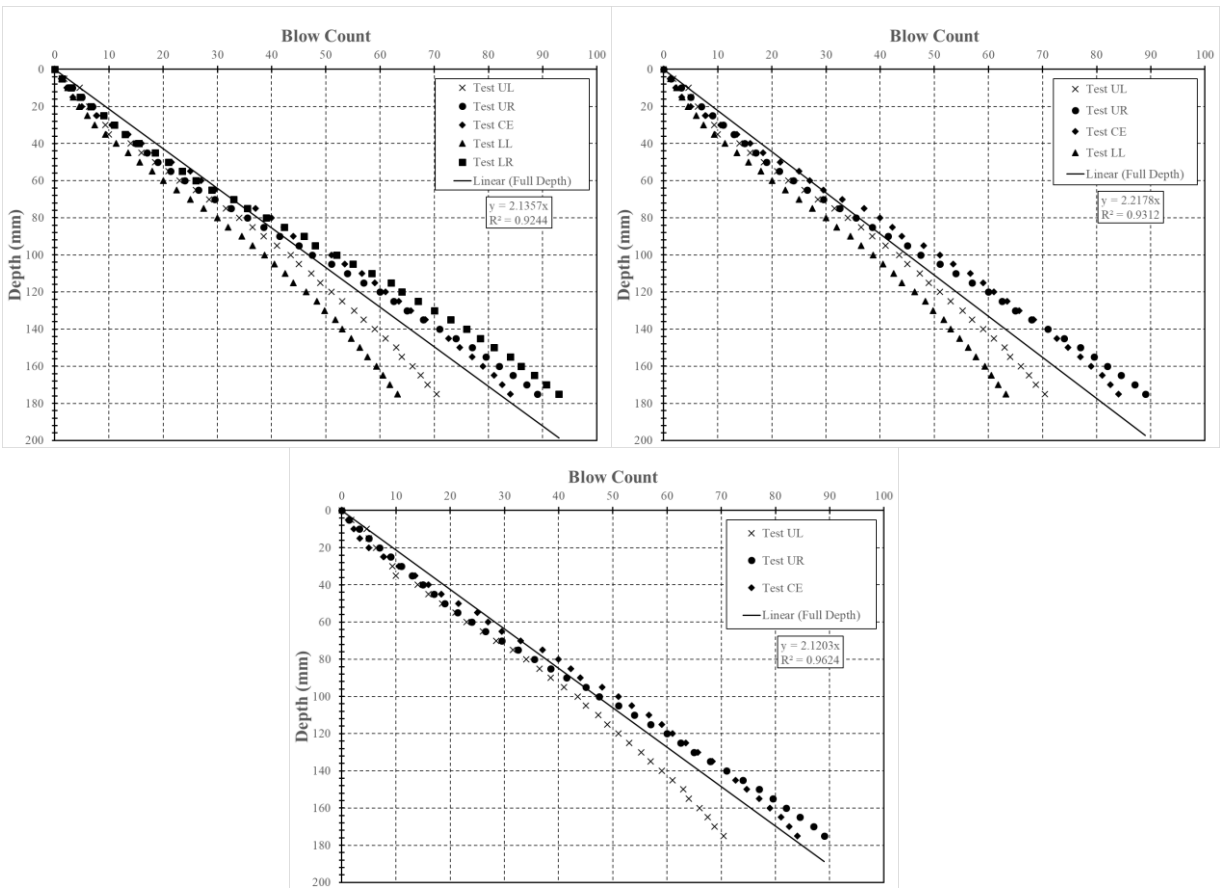


Figure N.15: Test performed on July 17, 2019, Location 19 (top left = 5 tests, top right = 4 tests, bottom = 3 tests)

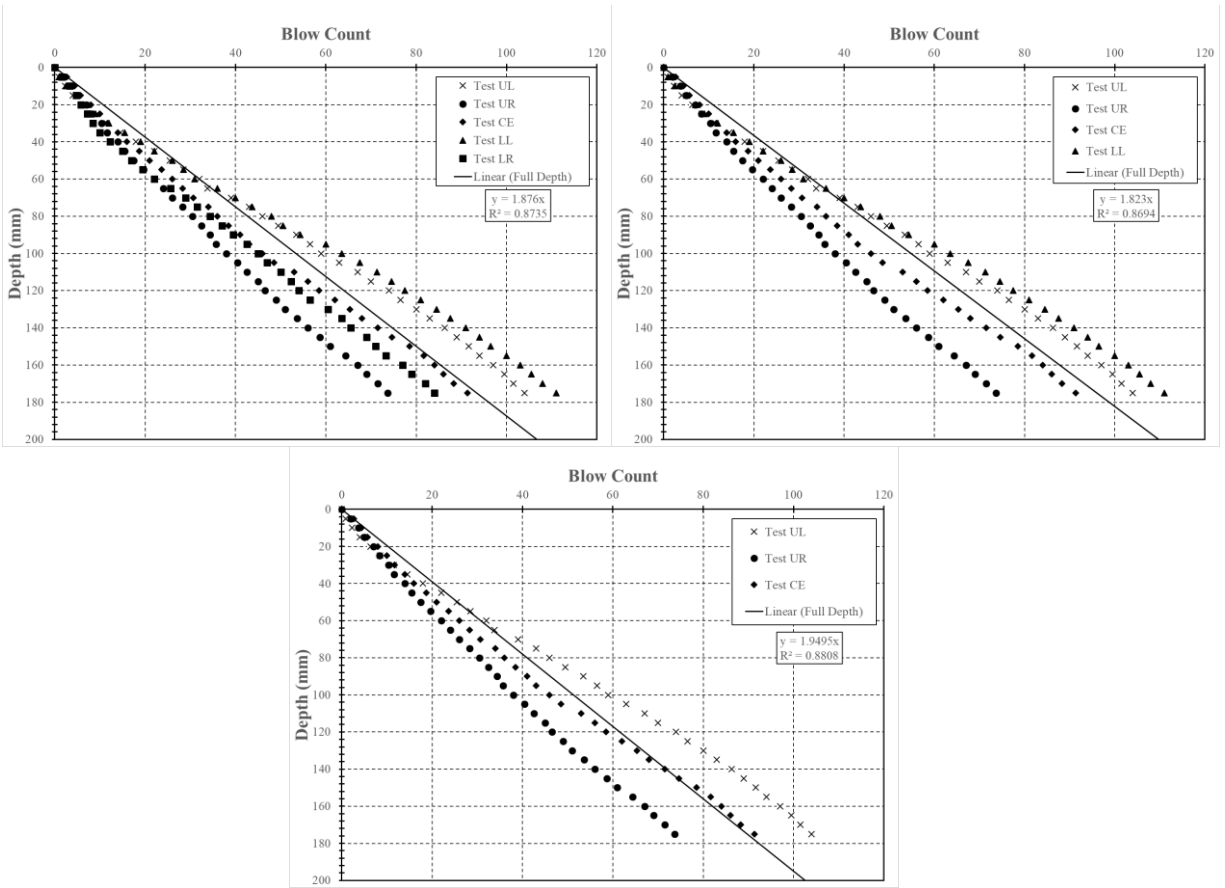


Figure N.16: Test performed on July 17, 2019, Location 20 (top left = 5 tests, top right = 4 tests, bottom = 3 tests)

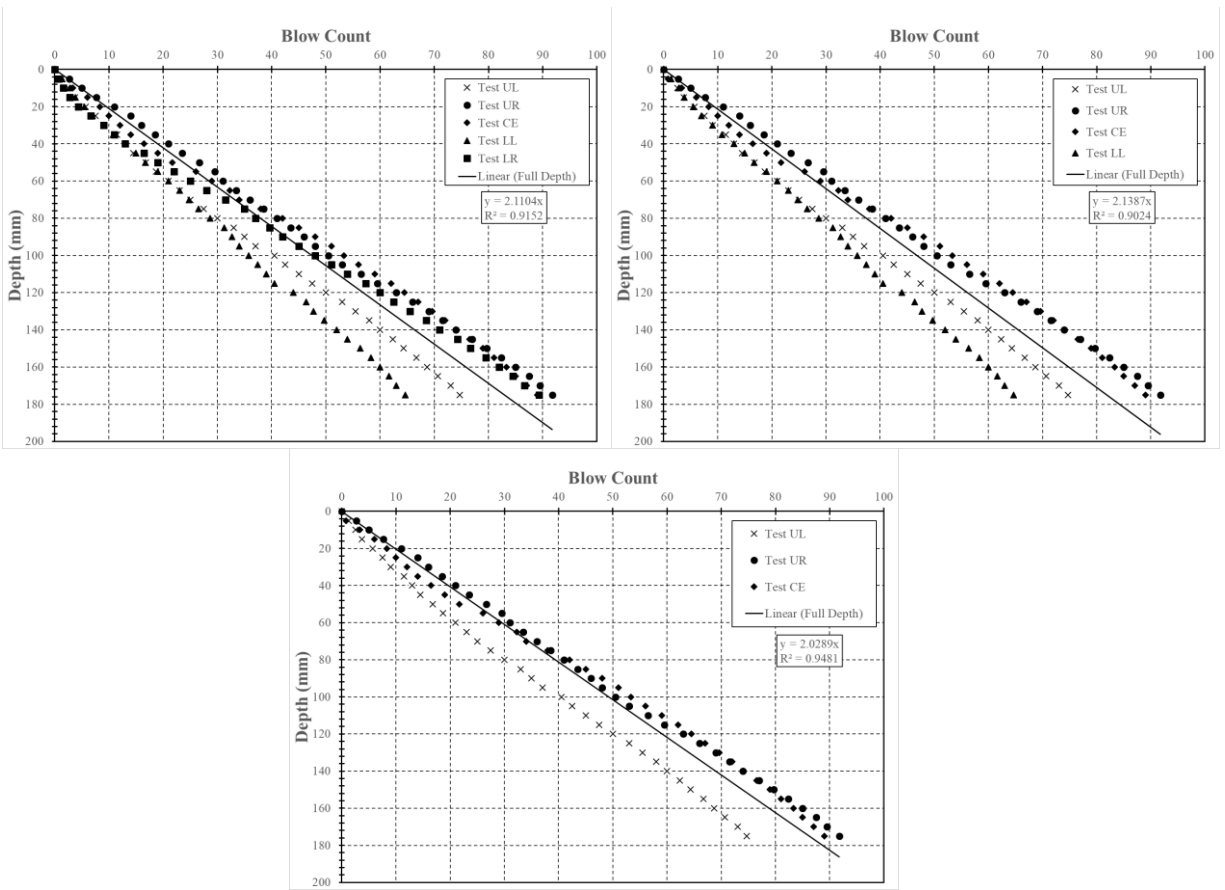


Figure N.17: Test performed on July 17, 2019, Location 21 (top left = 5 tests, top right = 4 tests, bottom = 3 tests)

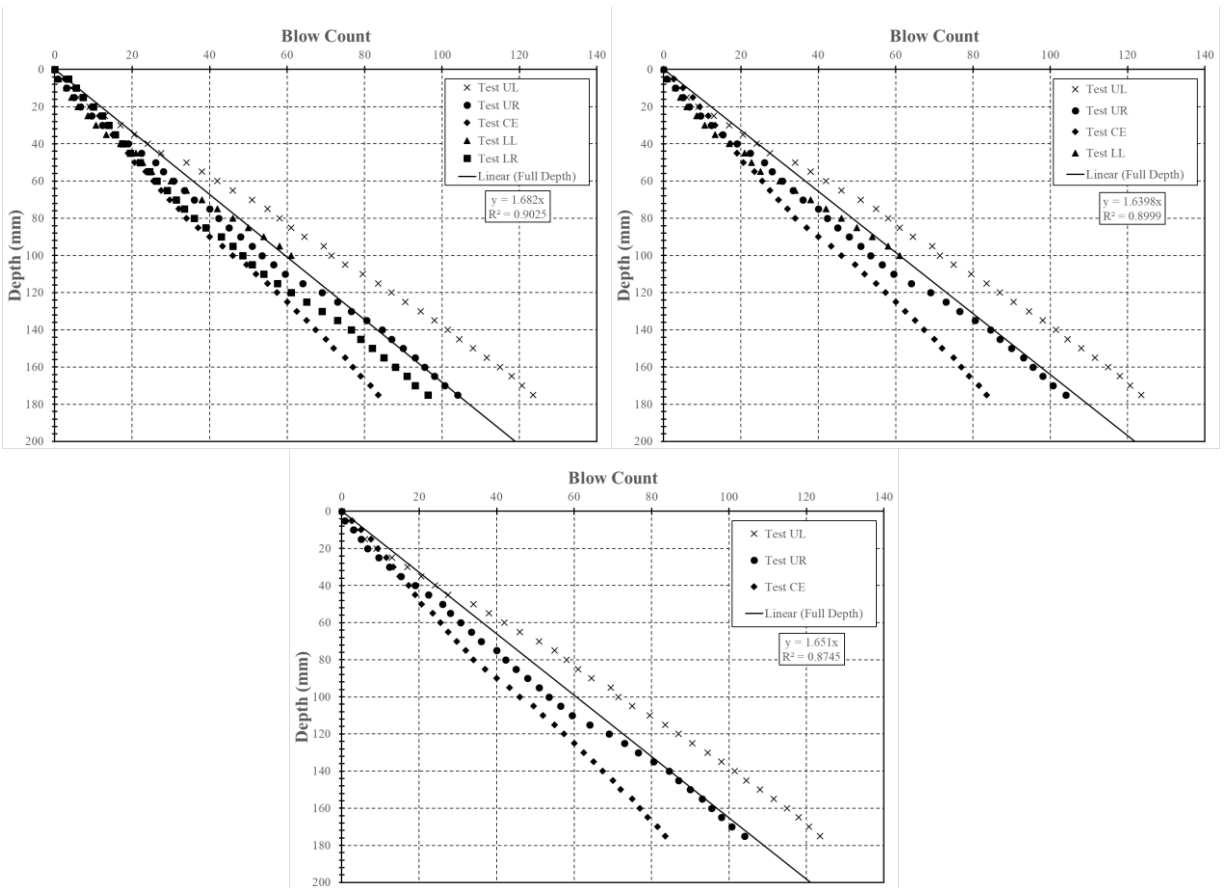


Figure N.18: Test performed on July 17, 2019, Location 22 (top left = 5 tests, top right = 4 tests, bottom = 3 tests)

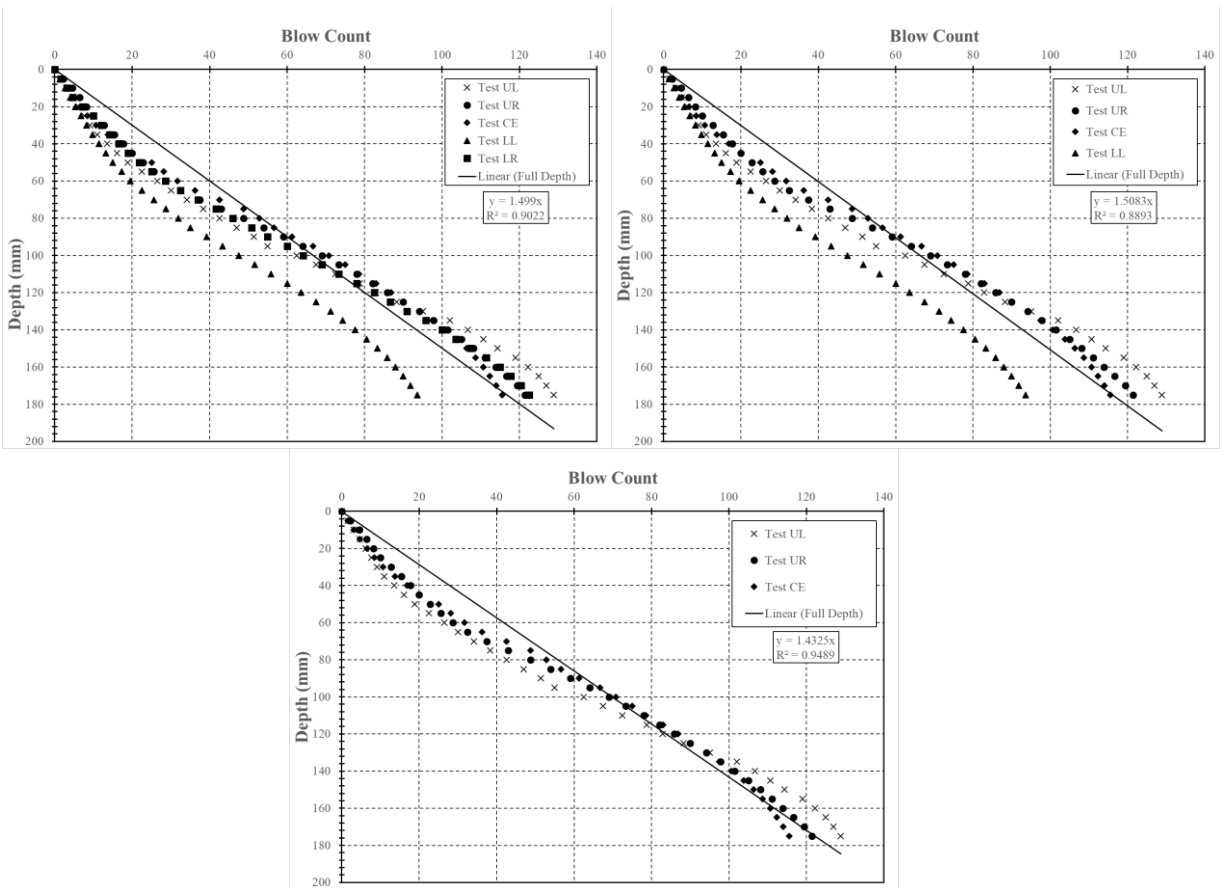


Figure N.19: Test performed on July 18, 2019, Location 23 (top left = 5 tests, top right = 4 tests, bottom = 3 tests)

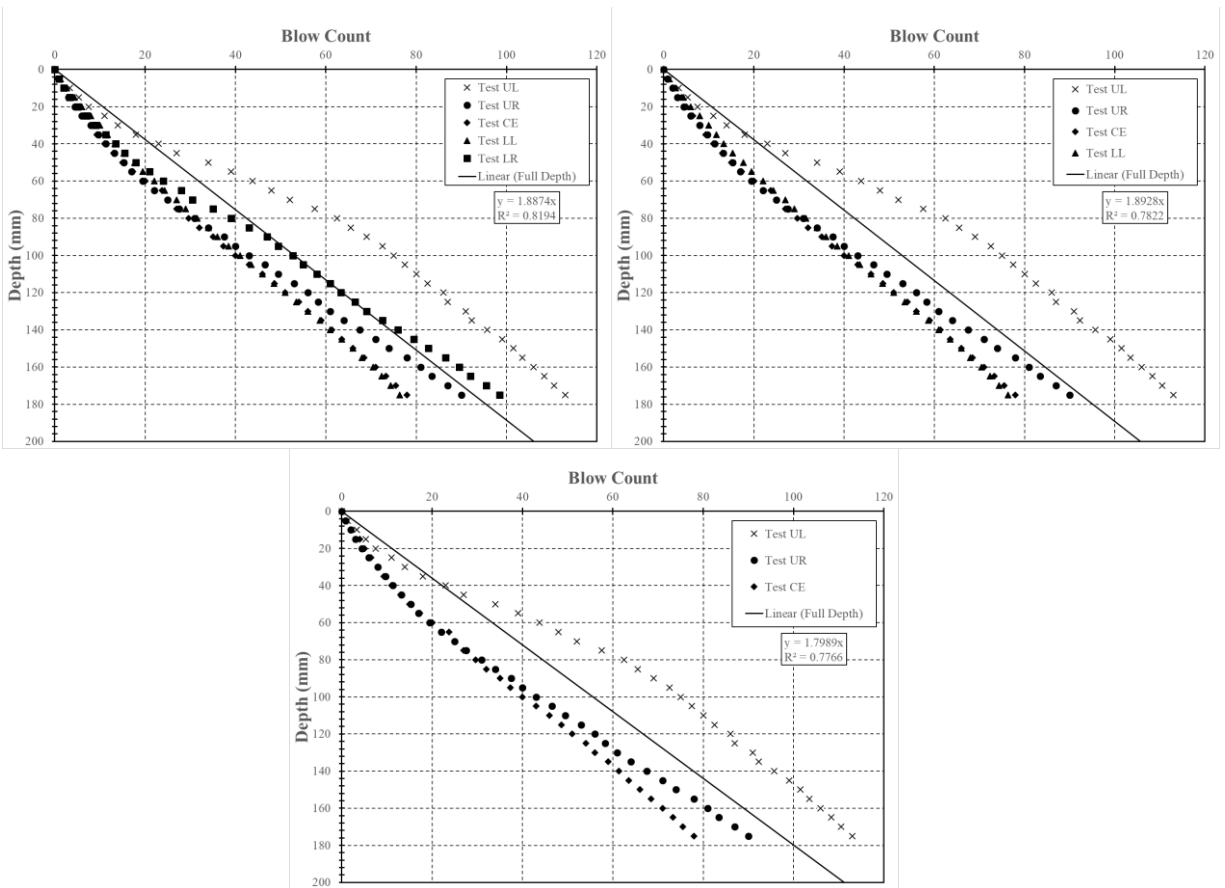


Figure N.20: Test performed on July 18, 2019, Location 24 (top left = 5 tests, top right = 4 tests, bottom = 3 tests)

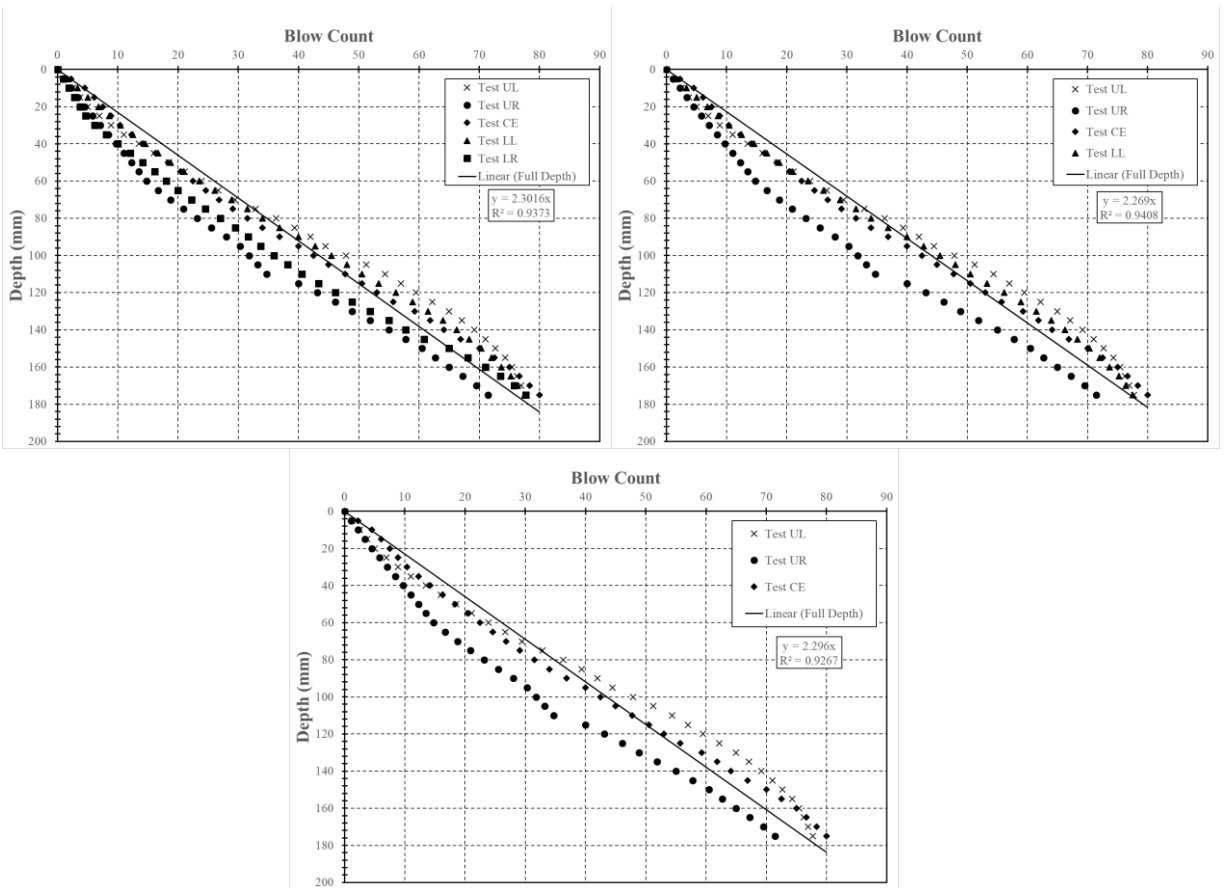


Figure N.21: Test performed on July 18, 2019, Location 25 (top left = 5 tests, top right = 4 tests, bottom = 3 tests)

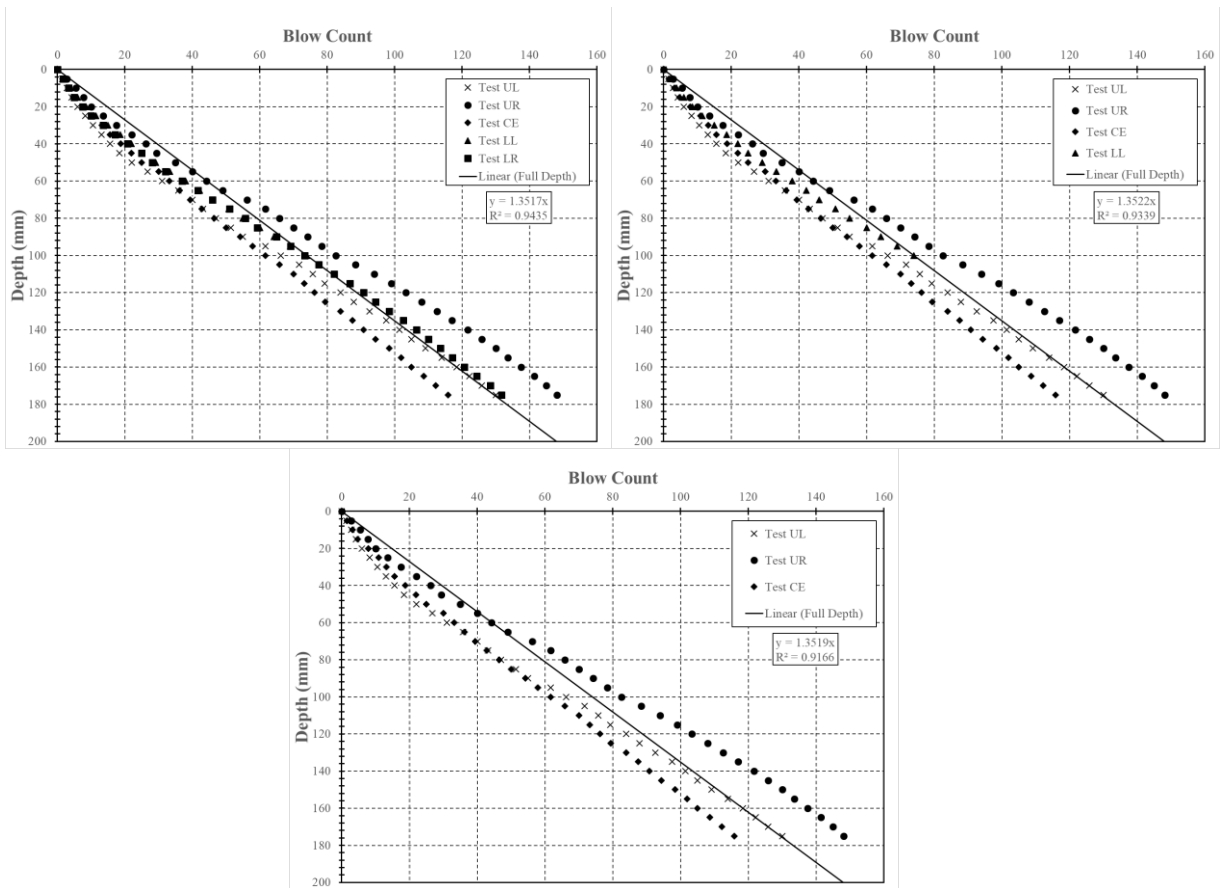


Figure N.22: Test performed on July 18, 2019, Location 28 (top left = 5 tests, top right = 4 tests, bottom = 3 tests)

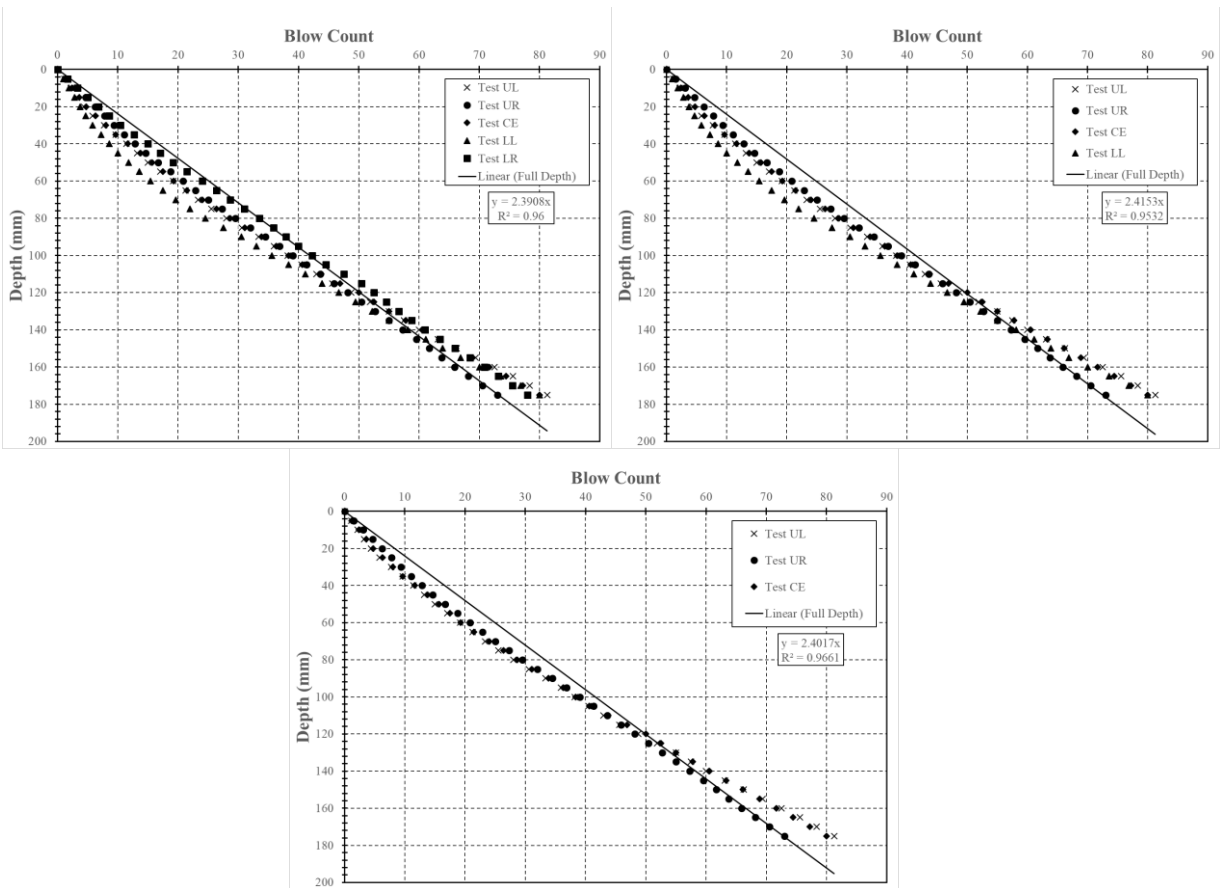


Figure N.23: Test performed on July 19, 2019, Location 30 (top left = 5 tests, top right = 4 tests, bottom = 3 tests)

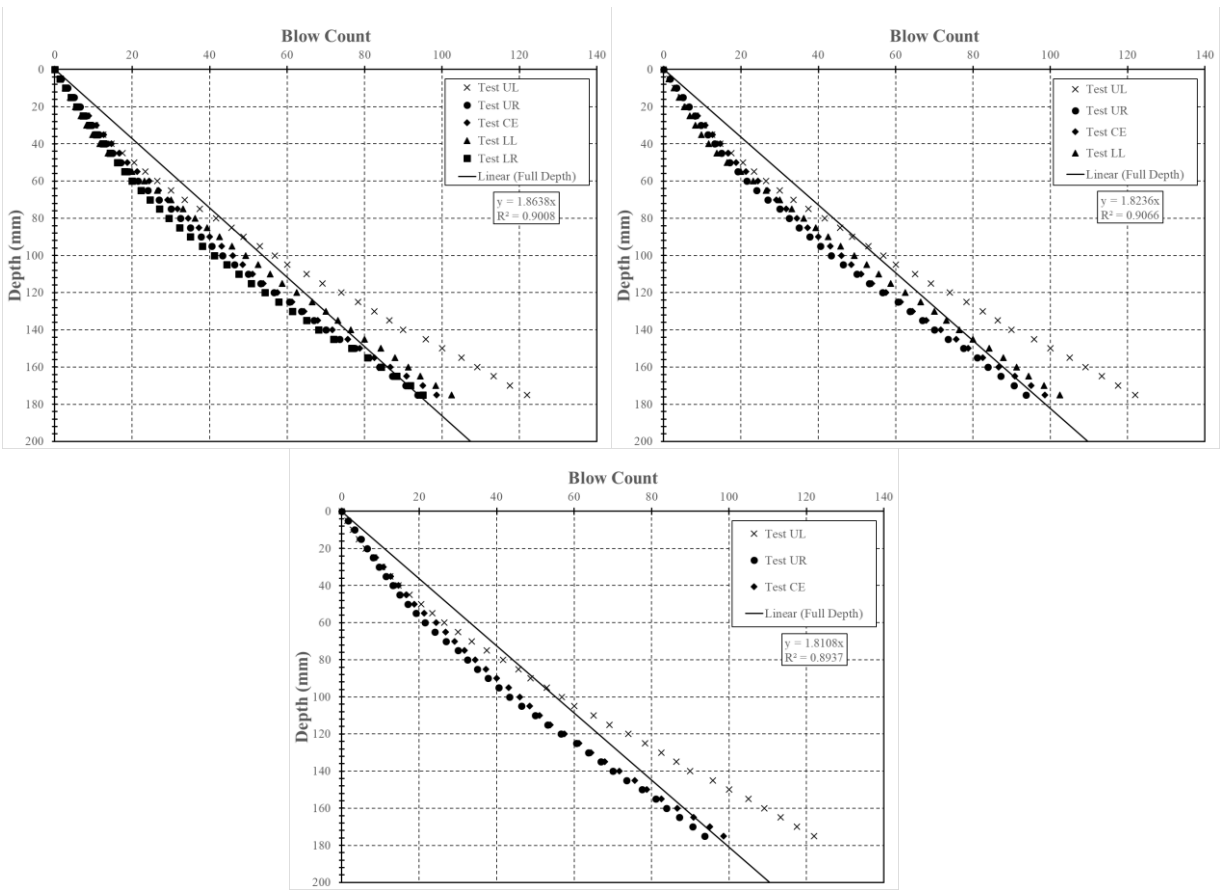


Figure N.24: Test performed on July 19, 2019, Location 31 (top left = 5 tests, top right = 4 tests, bottom = 3 tests)

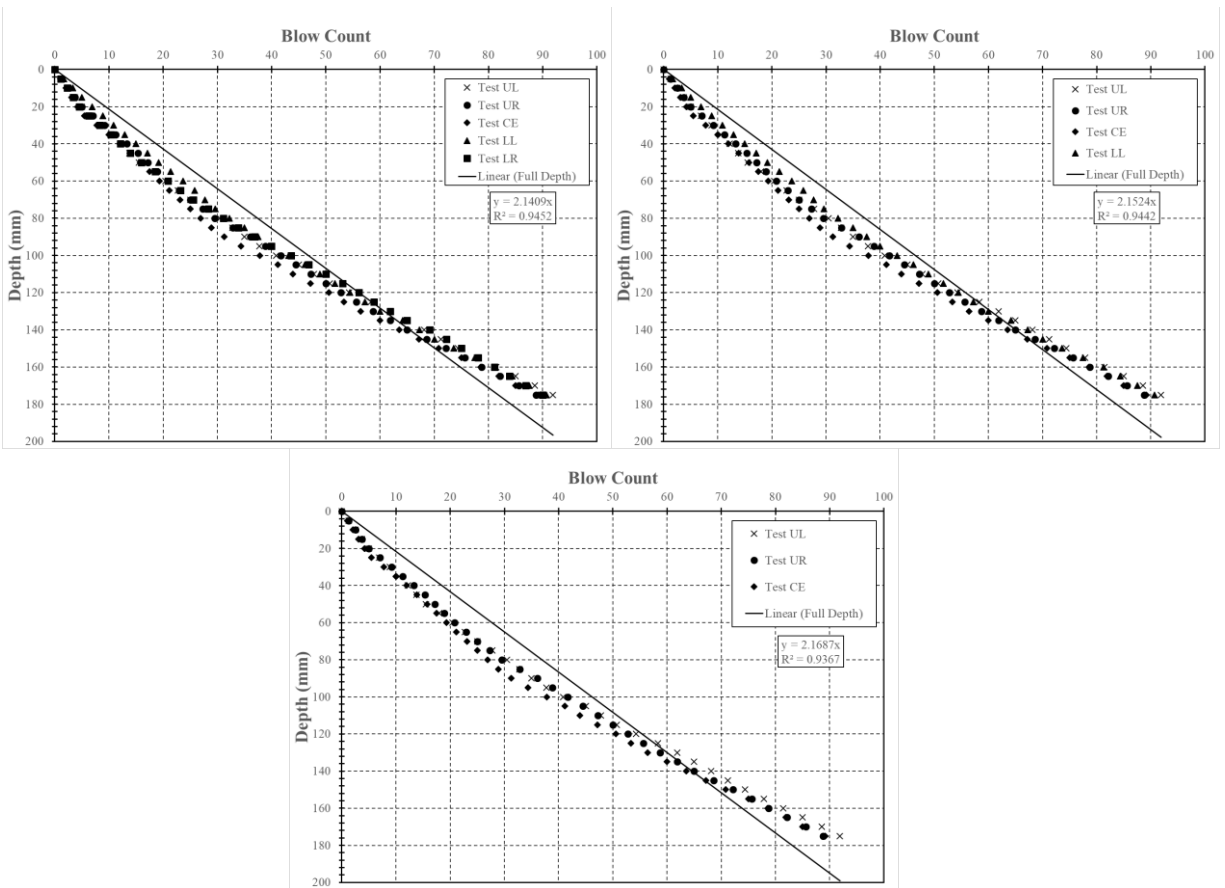


Figure N.25: Test performed on July 19, 2019, Location 32 (top left = 5 tests, top right = 4 tests, bottom = 3 tests)

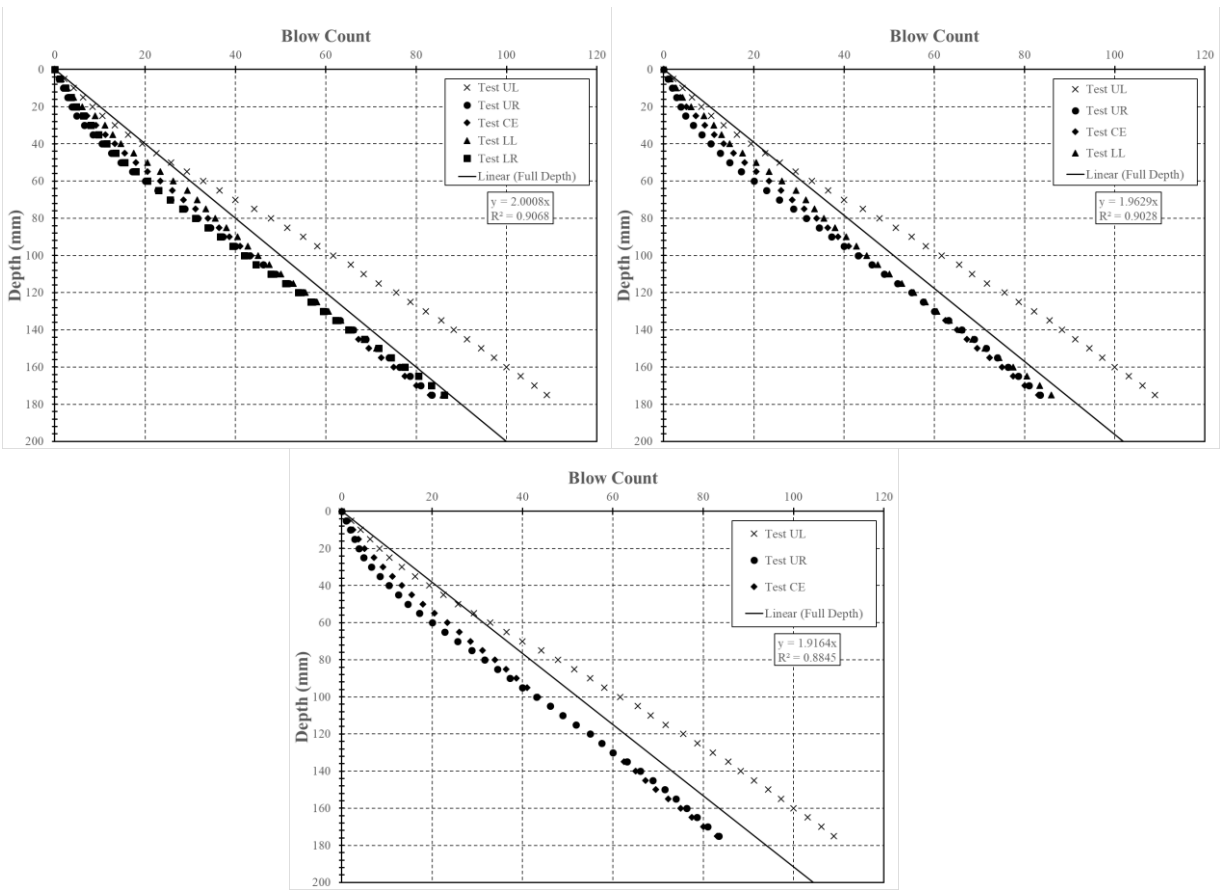


Figure N.26: Test performed on July 19, 2019, Location 33 (top left = 5 tests, top right = 4 tests, bottom = 3 tests)

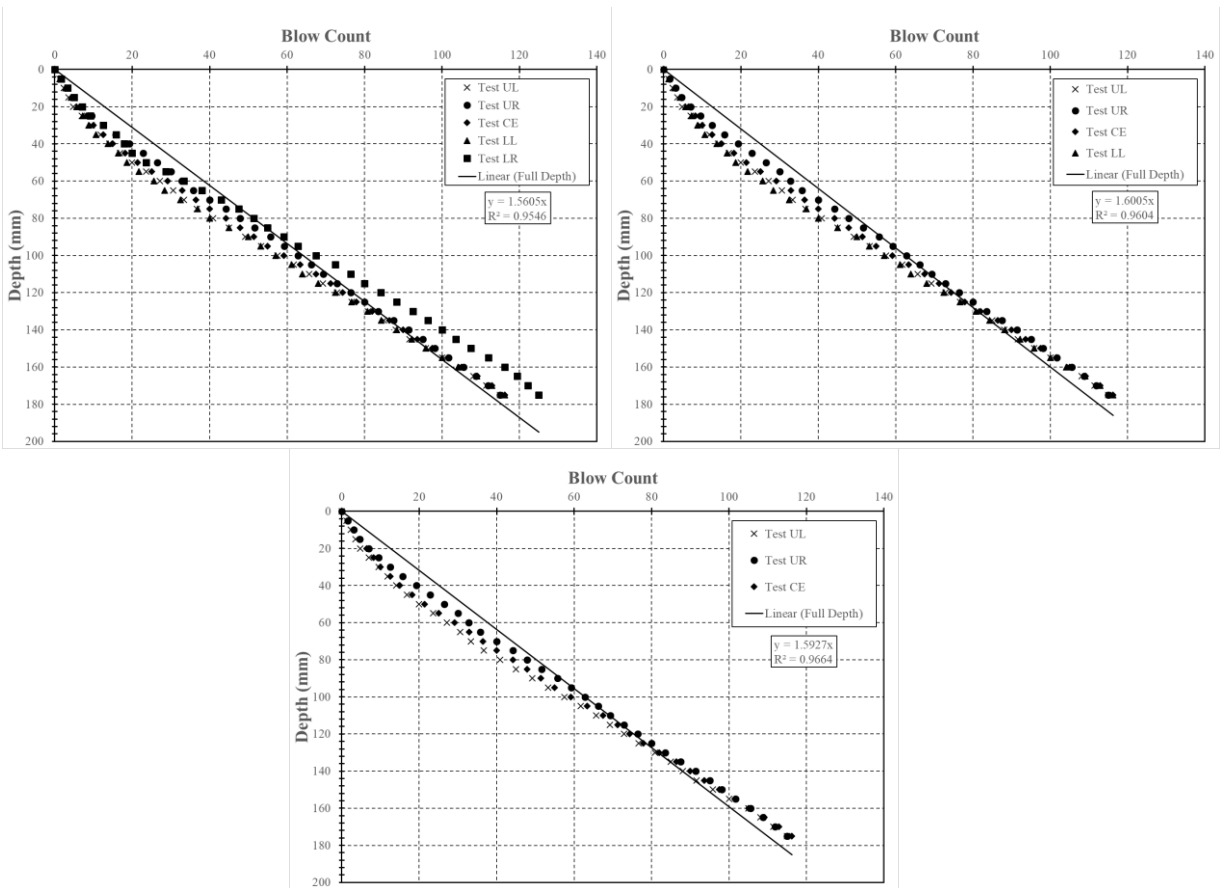


Figure N.27: Test performed on July 19, 2019, Location 34 (top left = 5 tests, top right = 4 tests, bottom = 3 tests)

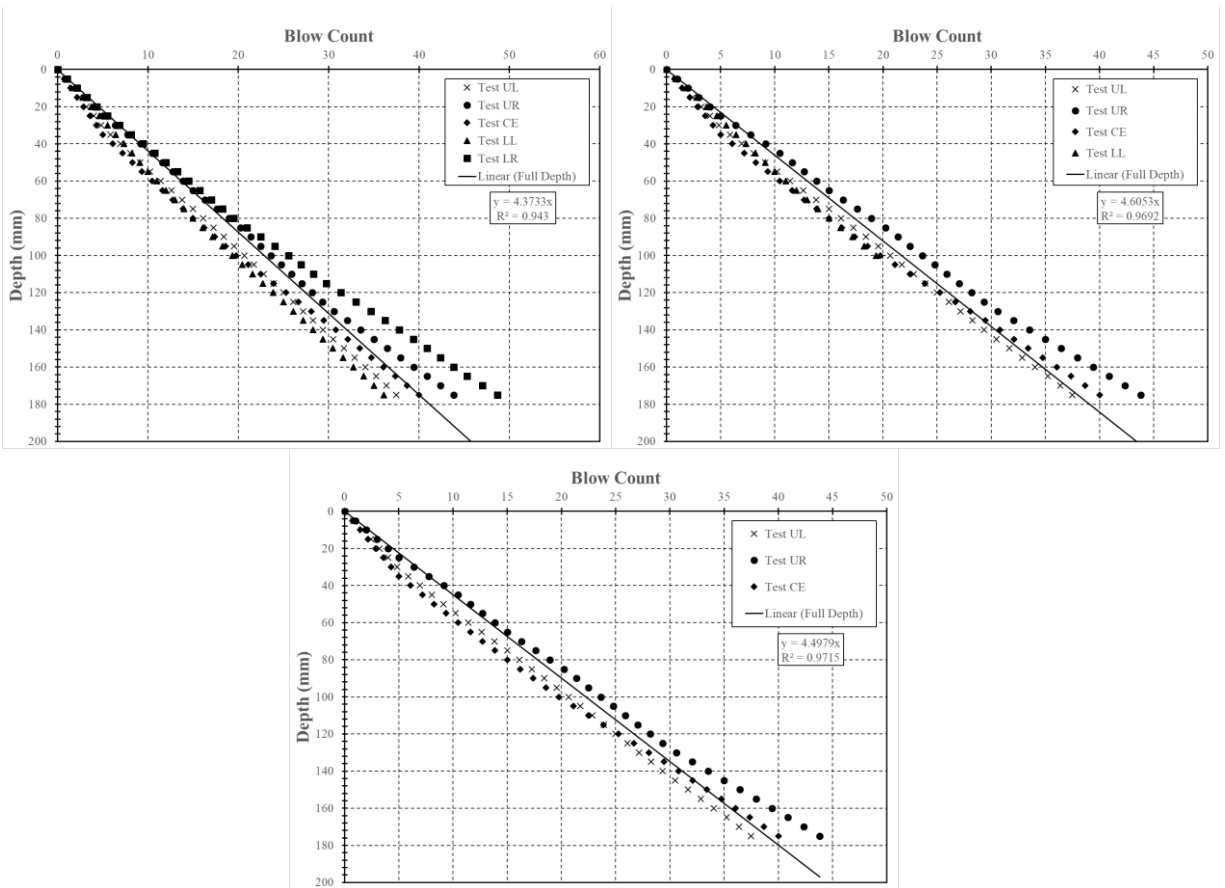


Figure N.28: Test performed on July 19, 2019, Location 35 (top left = 5 tests, top right = 4 tests, bottom = 3 tests)

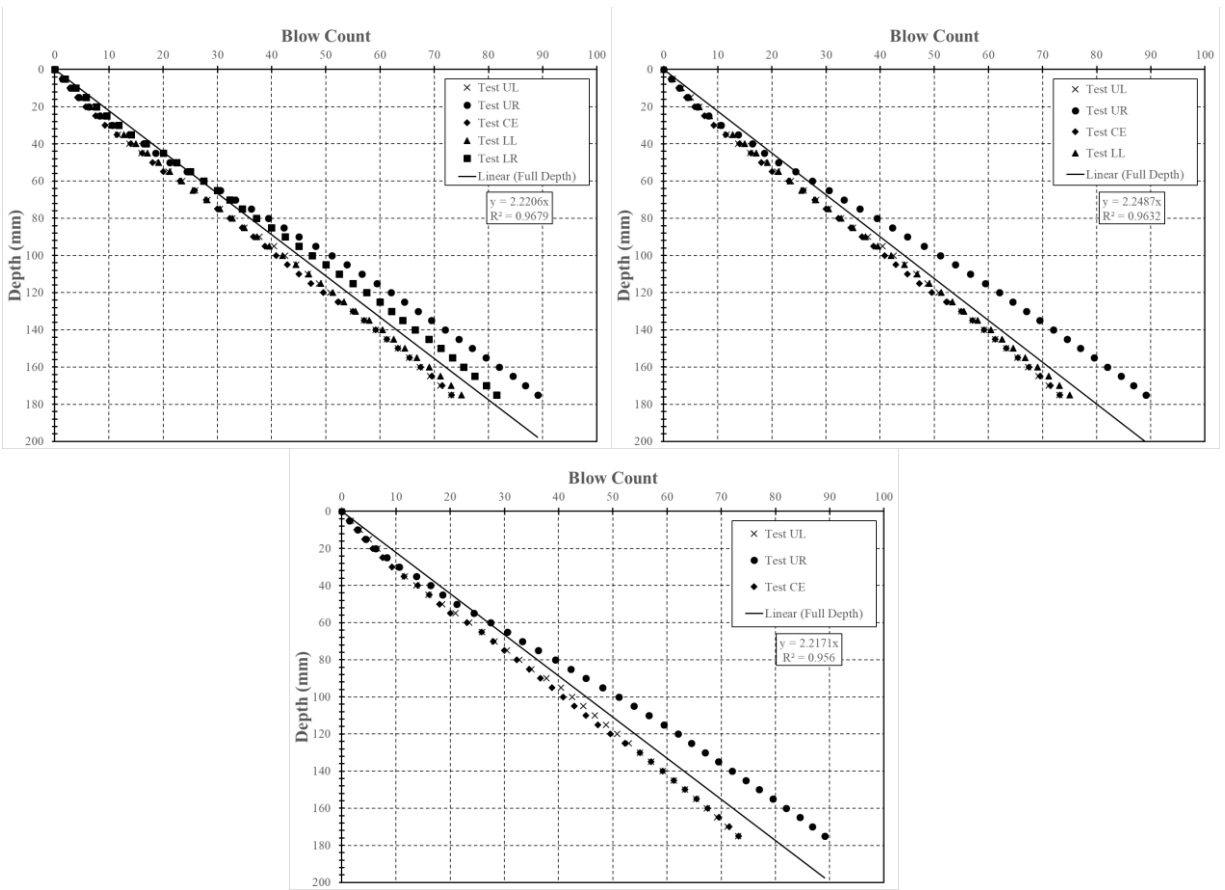


Figure N.29: Test performed on July 19, 2019, Location 36 (top left = 5 tests, top right = 4 tests, bottom = 3 tests)

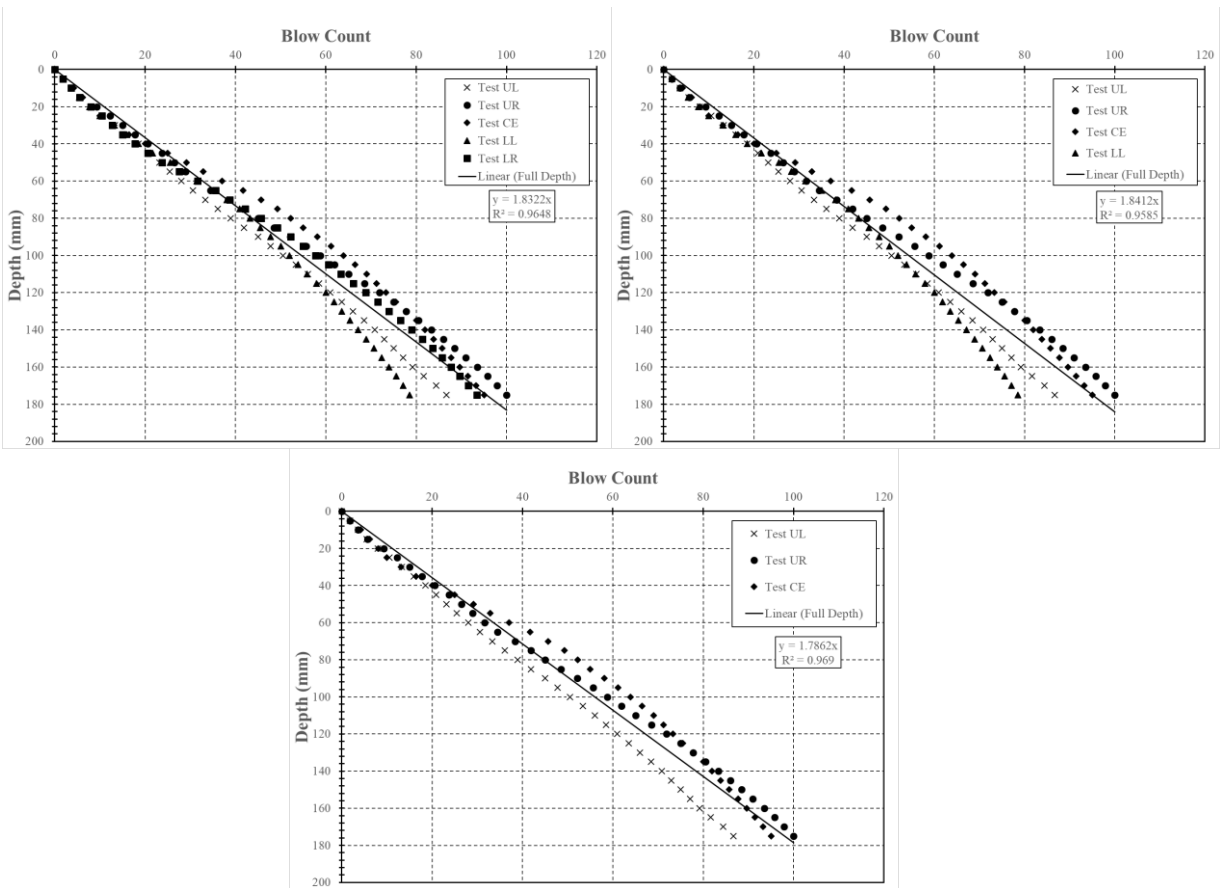


Figure N.30: Test performed on July 23, 2019, Location 37 (top left = 5 tests, top right = 4 tests, bottom = 3 tests)

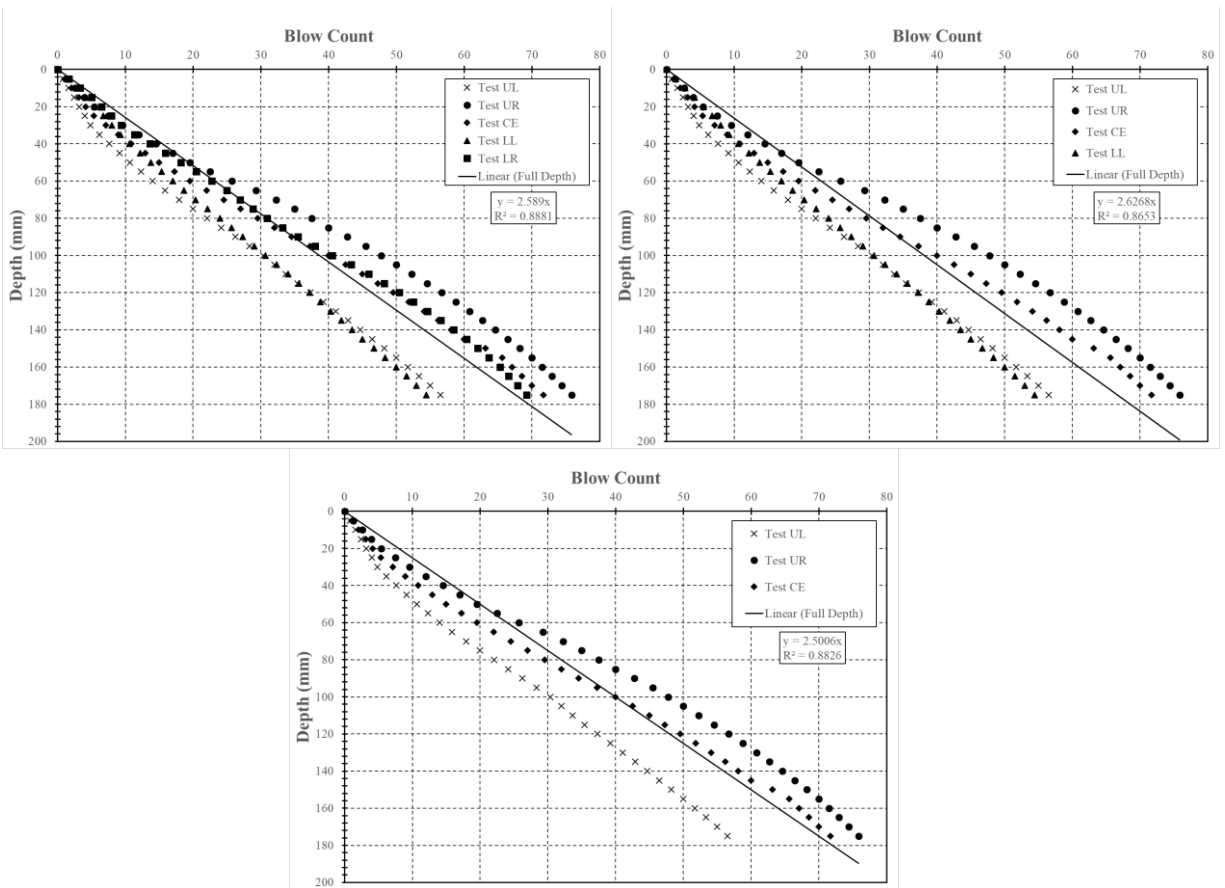


Figure N.31: Test performed on July 23, 2019, Location 38 (top left = 5 tests, top right = 4 tests, bottom = 3 tests)

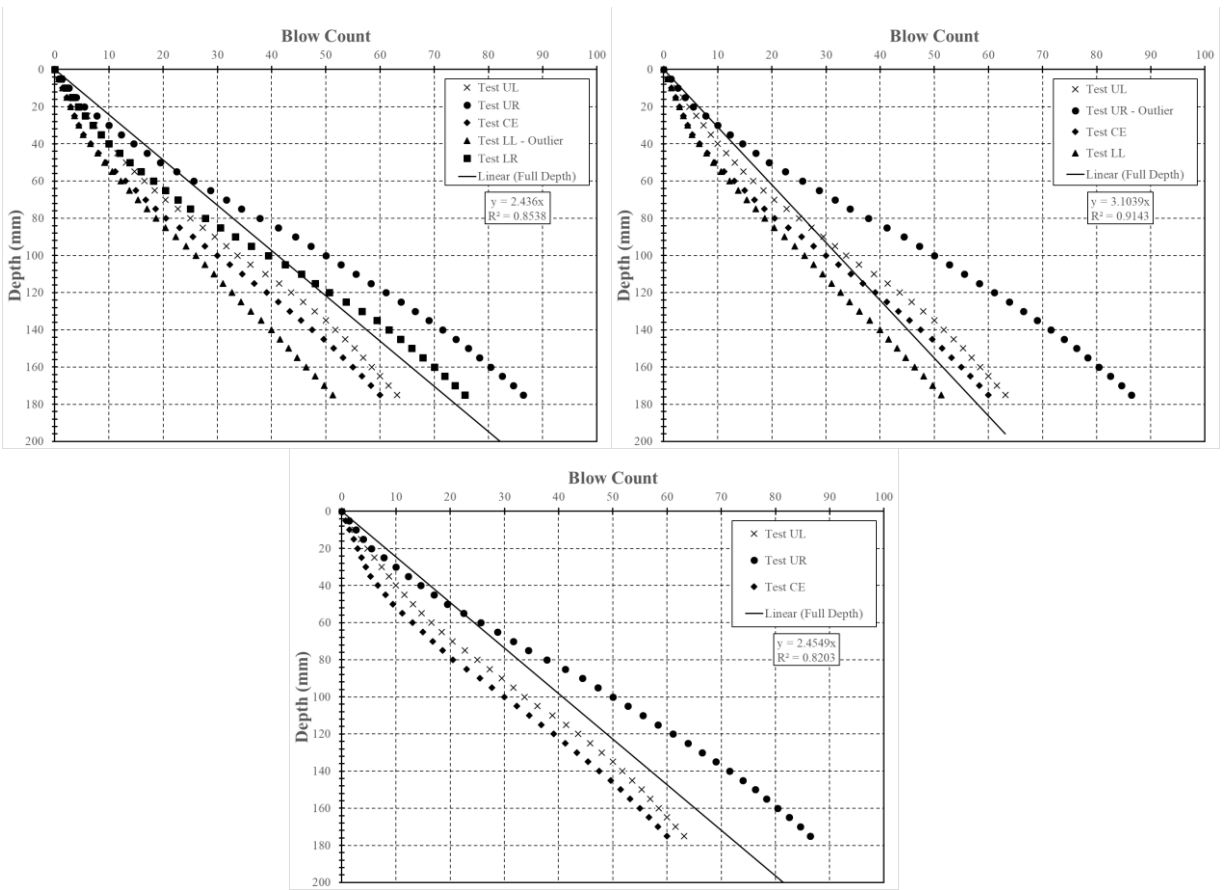


Figure N.32: Test performed on July 23, 2019, Location 39 (top left = 5 tests, top right = 4 tests, bottom = 3 tests)

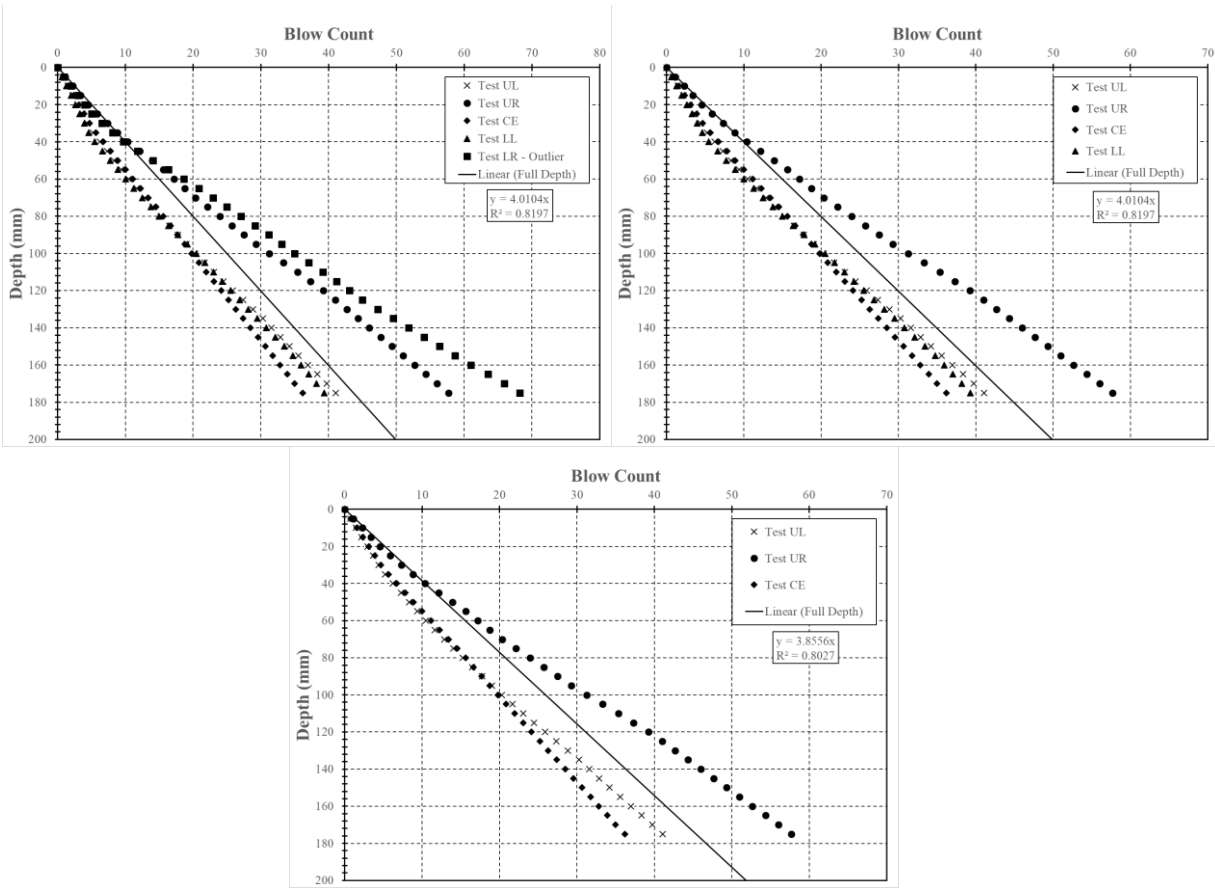


Figure N.33: Test performed on July 23, 2019, Location 40 (top left = 5 tests, top right = 4 tests, bottom = 3 tests)

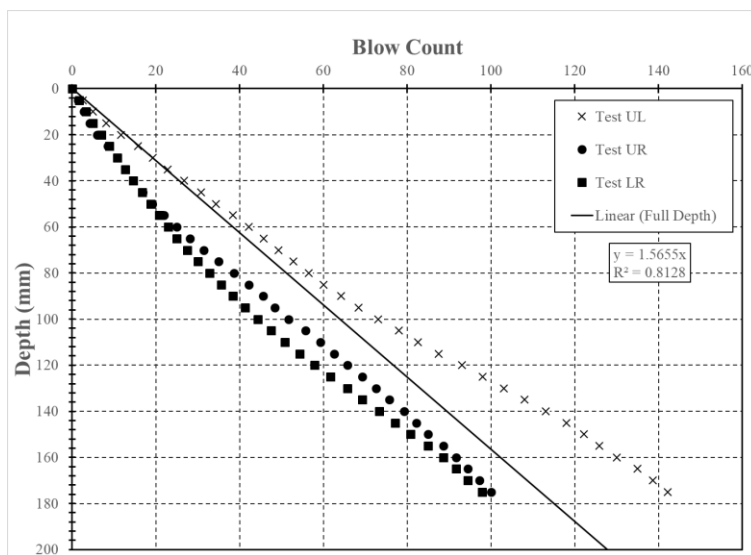


Figure N.34: Test performed on July 23, 2019, Location 41 (only 3 tests completed)

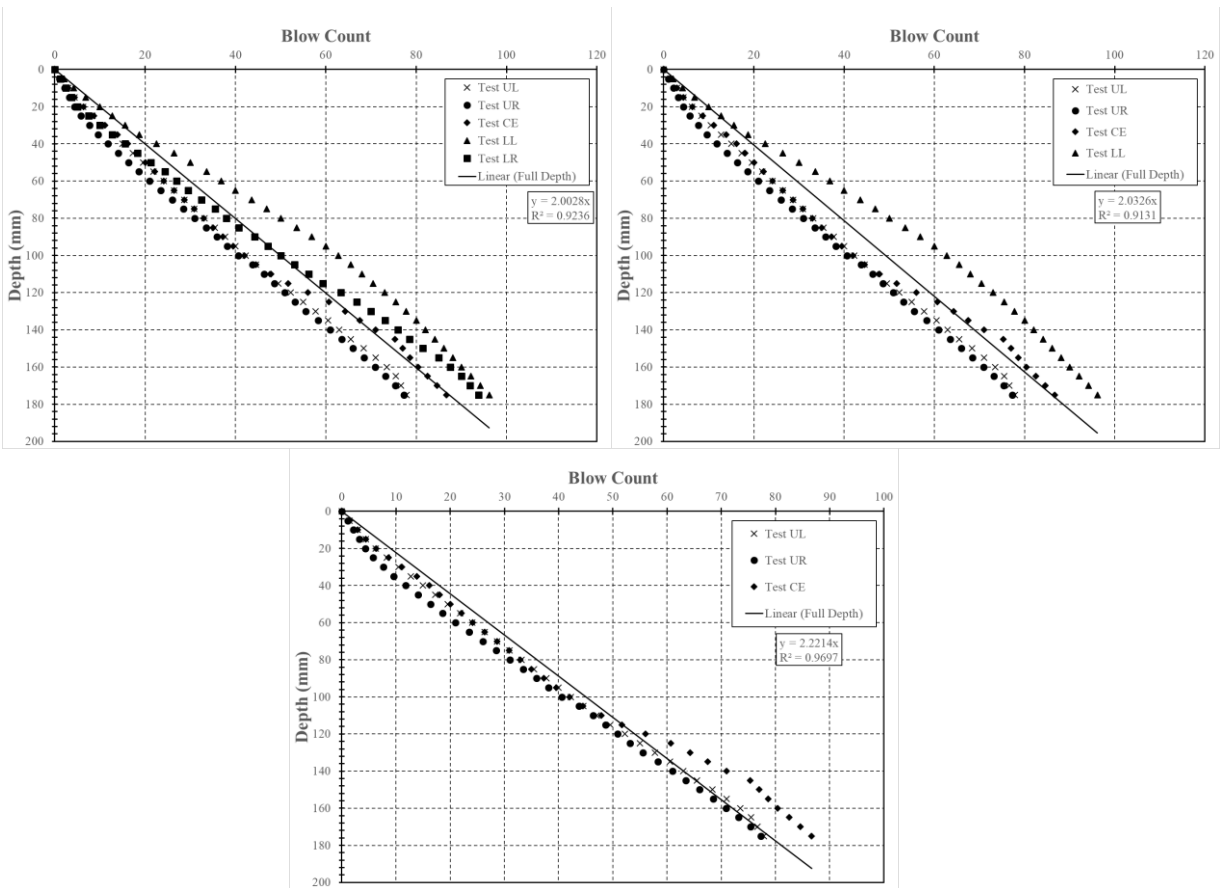


Figure N.35: Test performed on July 23, 2019, Location 42 (top left = 5 tests, top right = 4 tests, bottom = 3 tests)

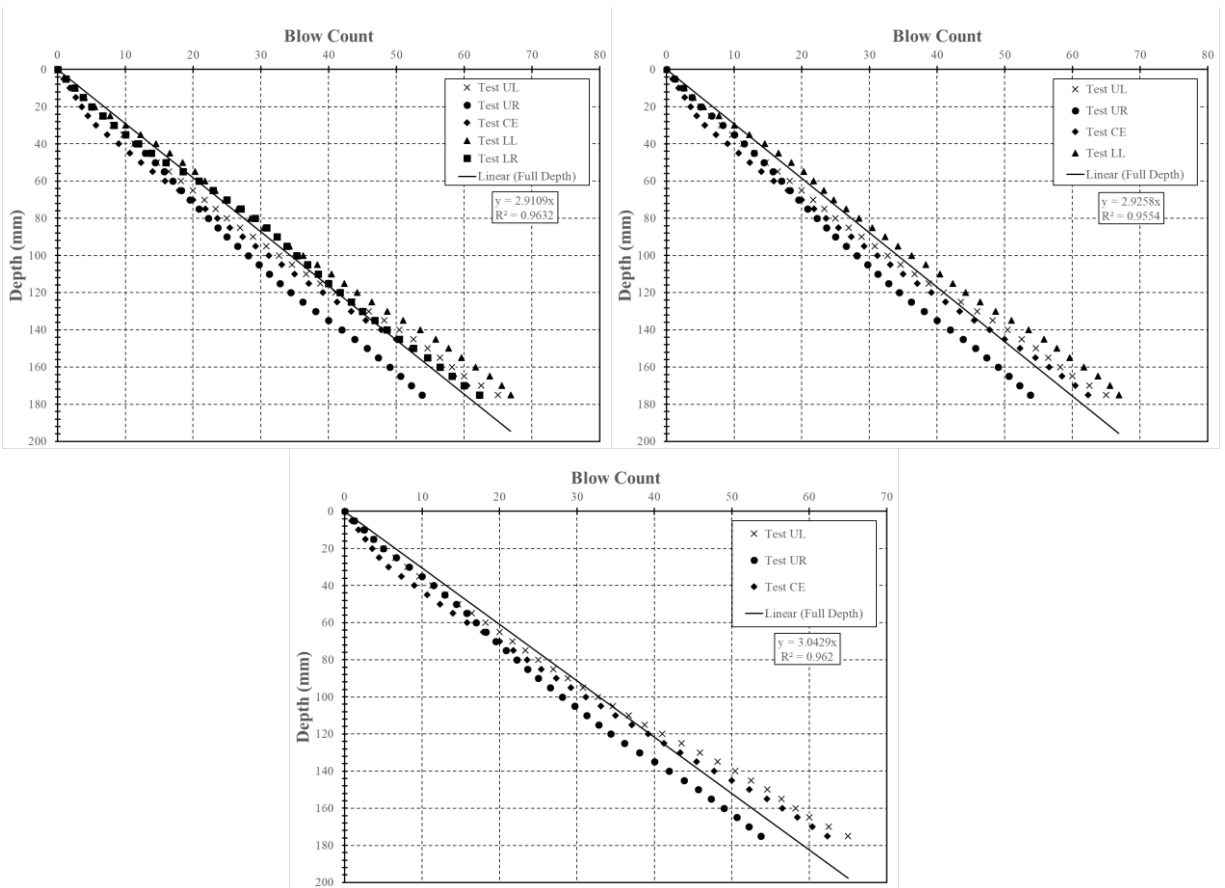


Figure N.36: Test performed on July 23, 2019, Location 43 (top left = 5 tests, top right = 4 tests, bottom = 3 tests)

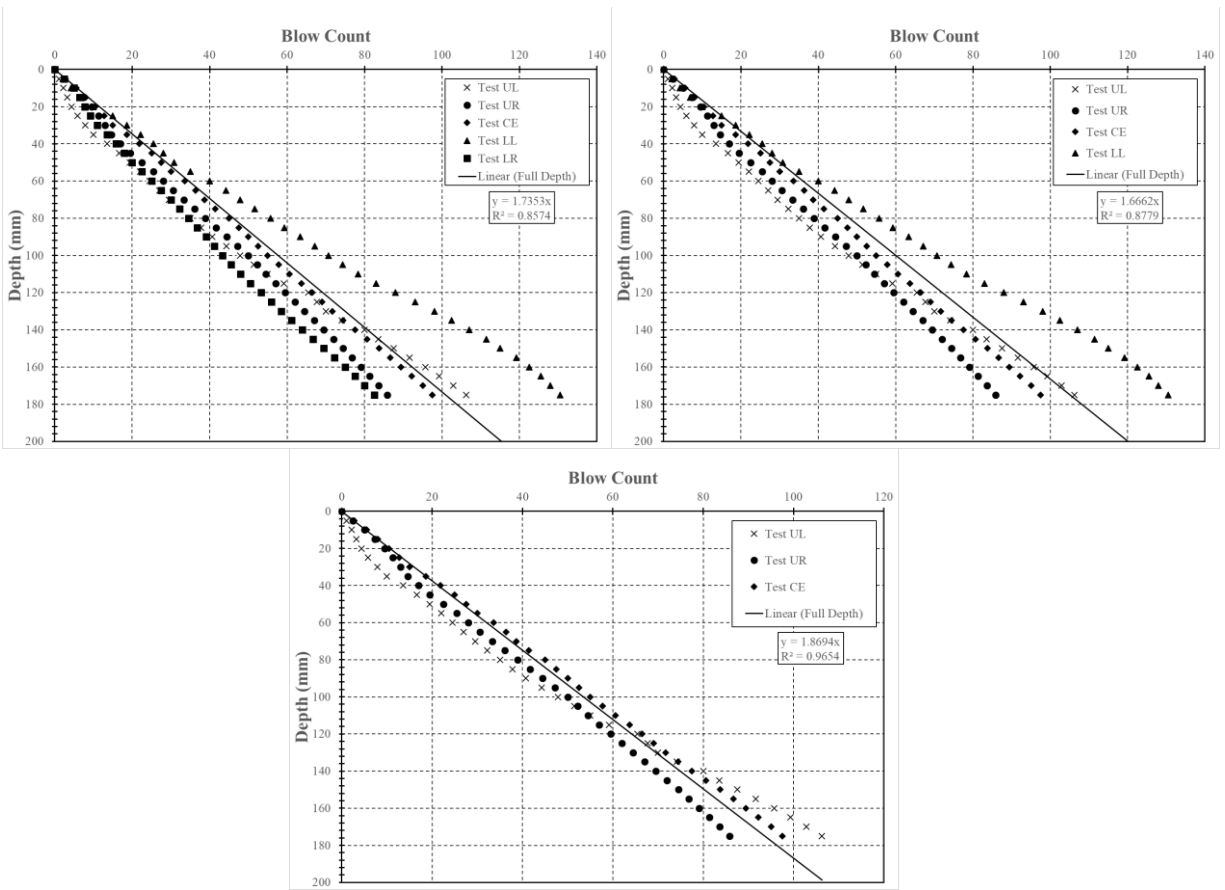


Figure N.37: Test performed on July 24, 2019, Location 44 (top left = 5 tests, top right = 4 tests, bottom = 3 tests)

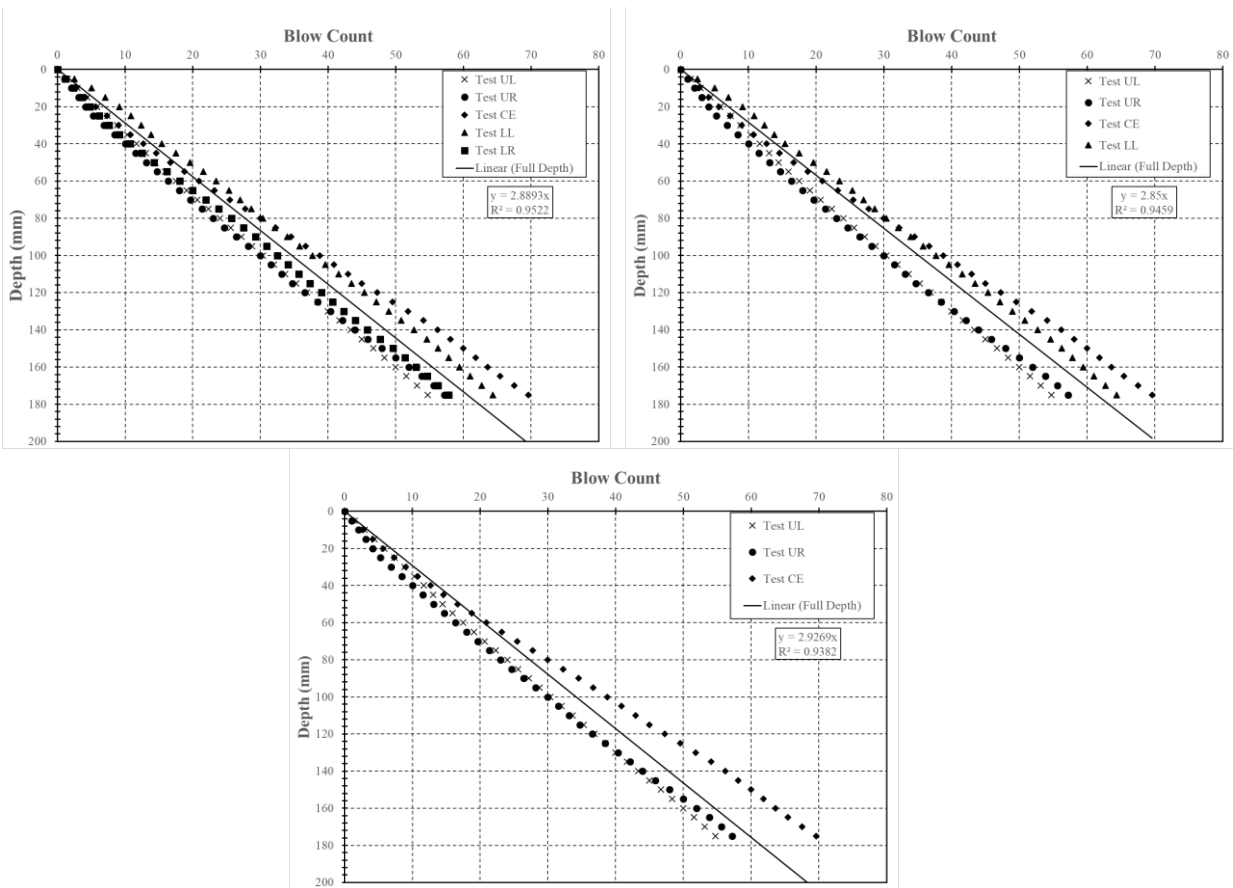


Figure N.38: Test performed on July 24, 2019, Location 45 (top left = 5 tests, top right = 4 tests, bottom = 3 tests)

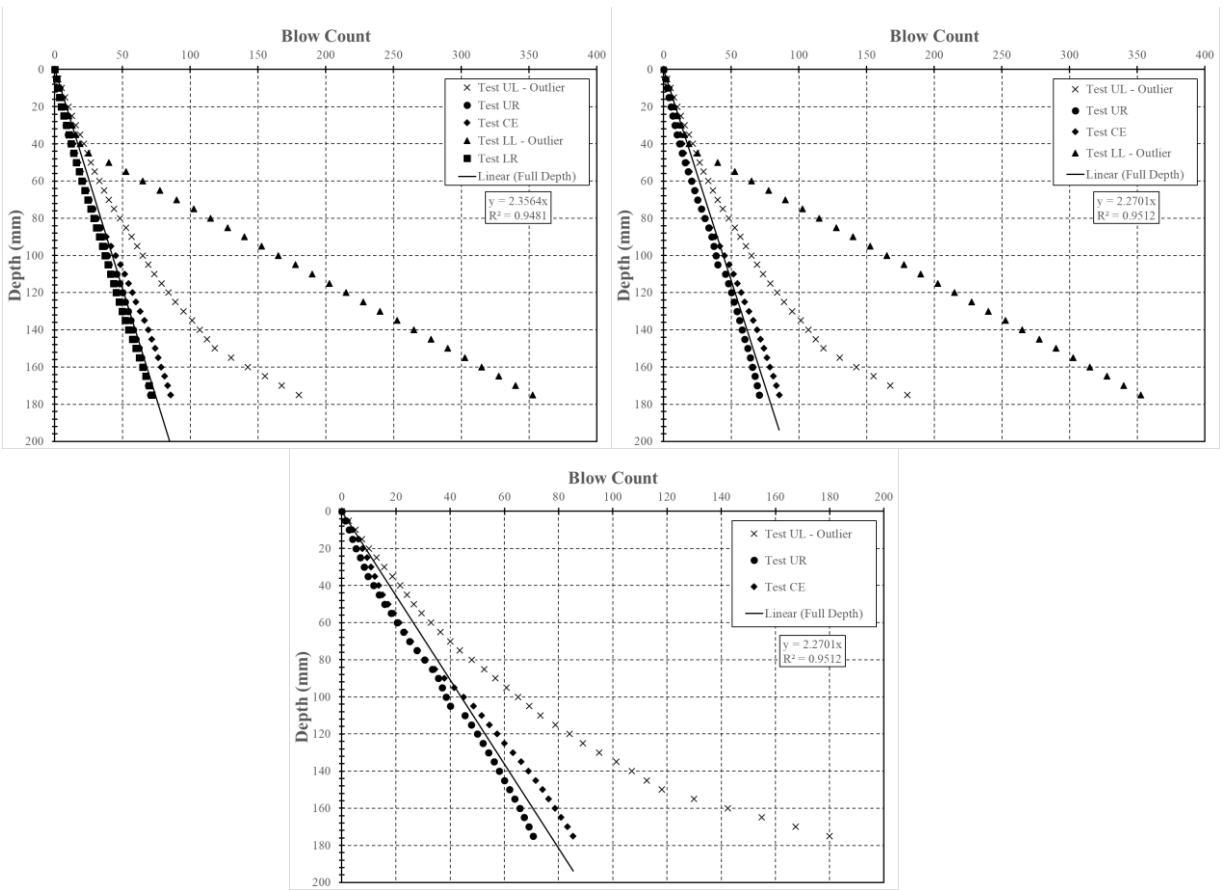


Figure N.39: Test performed on July 24, 2019, Location 46 (top left = 5 tests, top right = 4 tests, bottom = 3 tests)

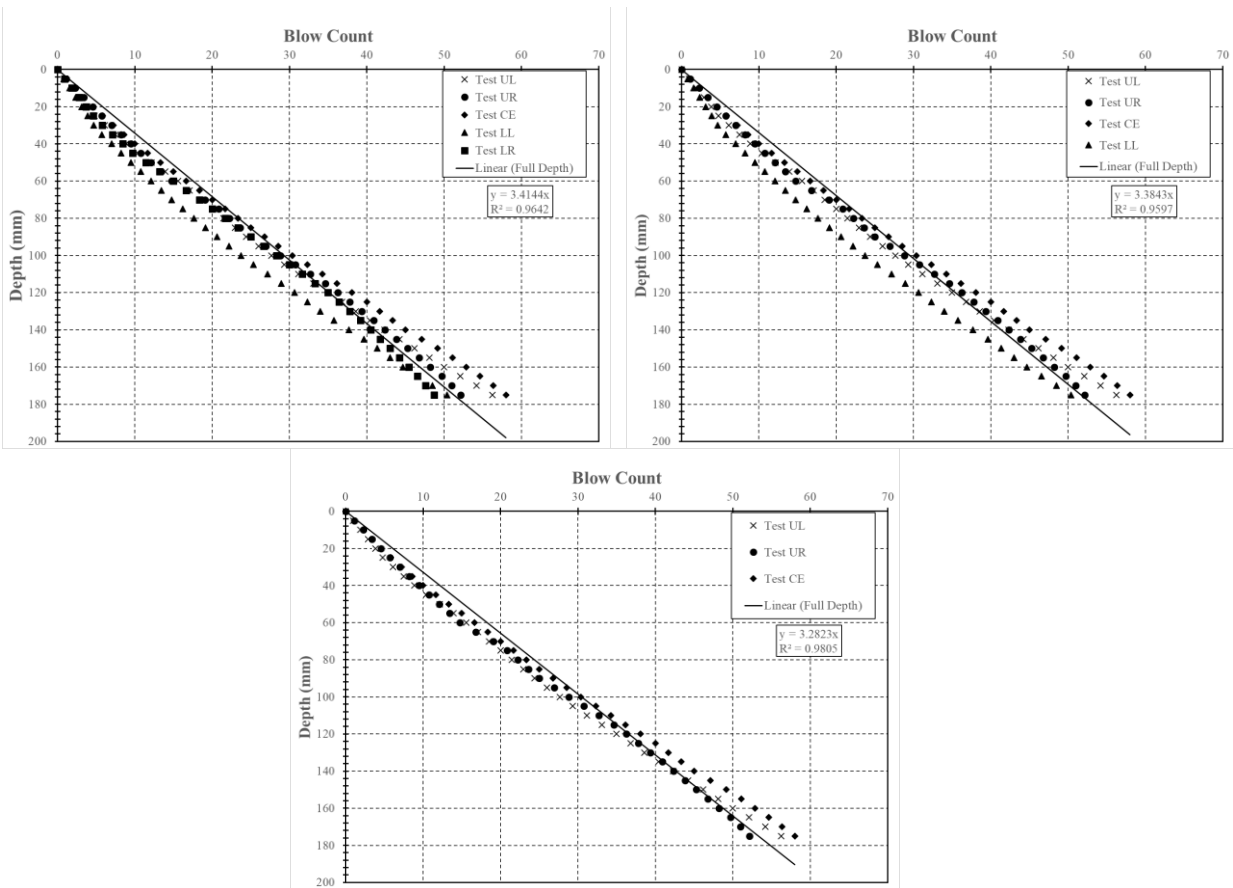


Figure N.40: Test performed on July 24, 2019, Location 47 (top left = 5 tests, top right = 4 tests, bottom = 3 tests)

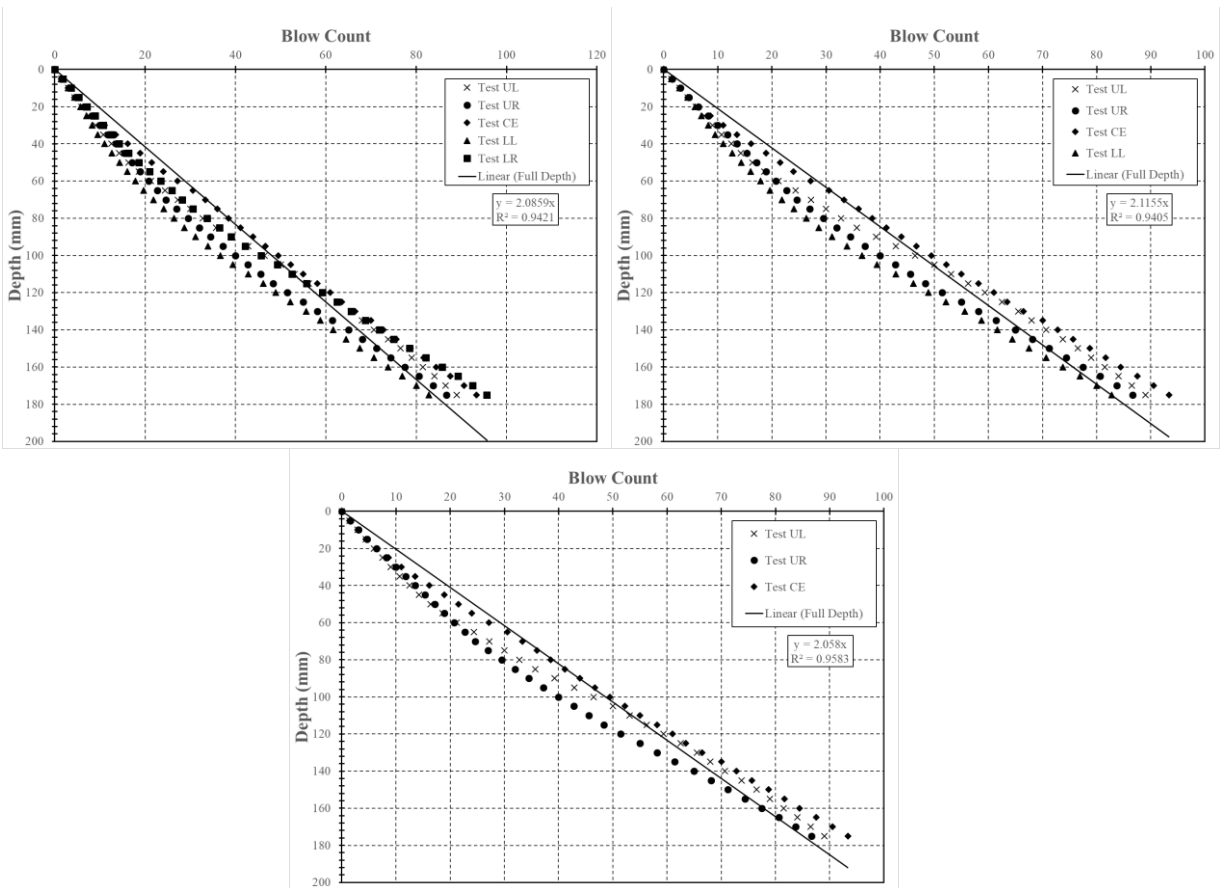


Figure N.41: Test performed on July 24, 2019, Location 48 (top left = 5 tests, top right = 4 tests, bottom = 3 tests)

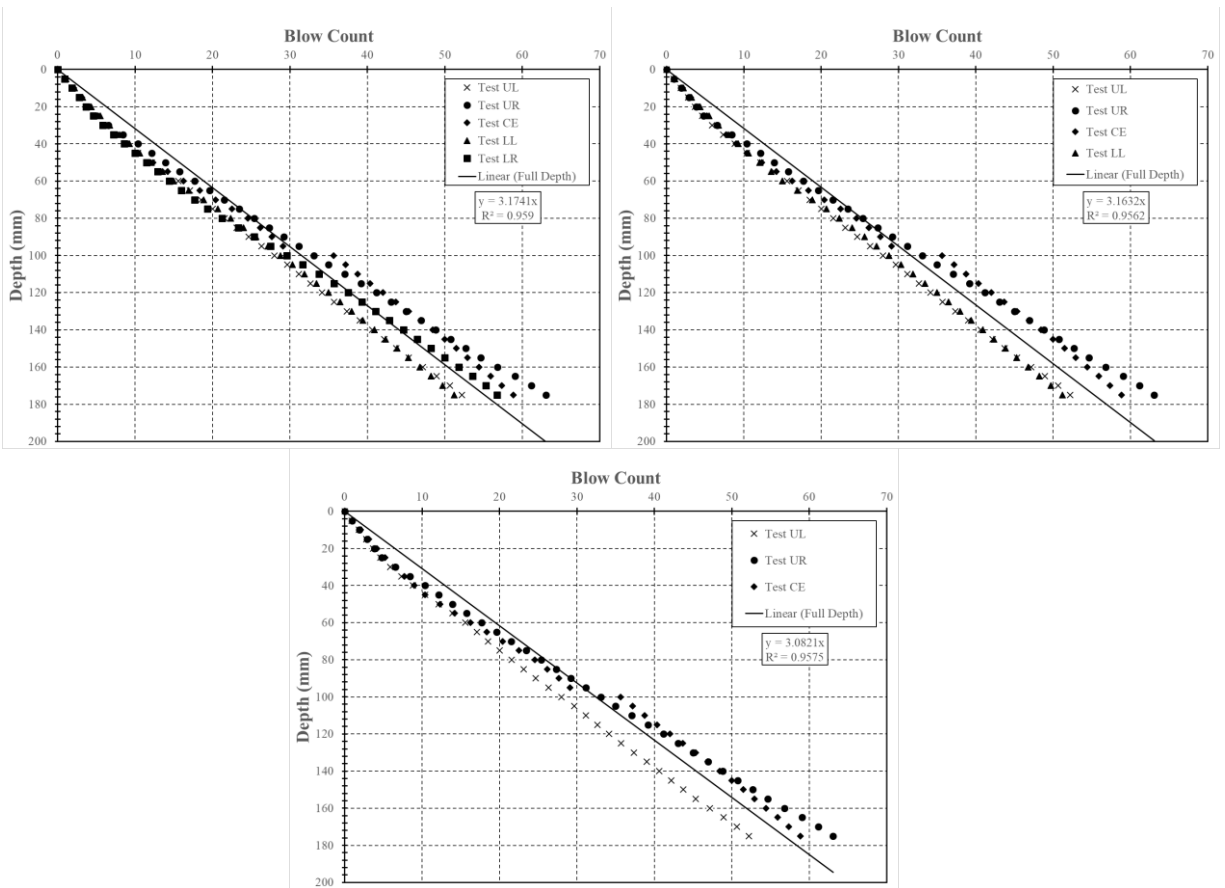


Figure N.42: Test performed on July 24, 2019, Location 49 (top left = 5 tests, top right = 4 tests, bottom = 3 tests)

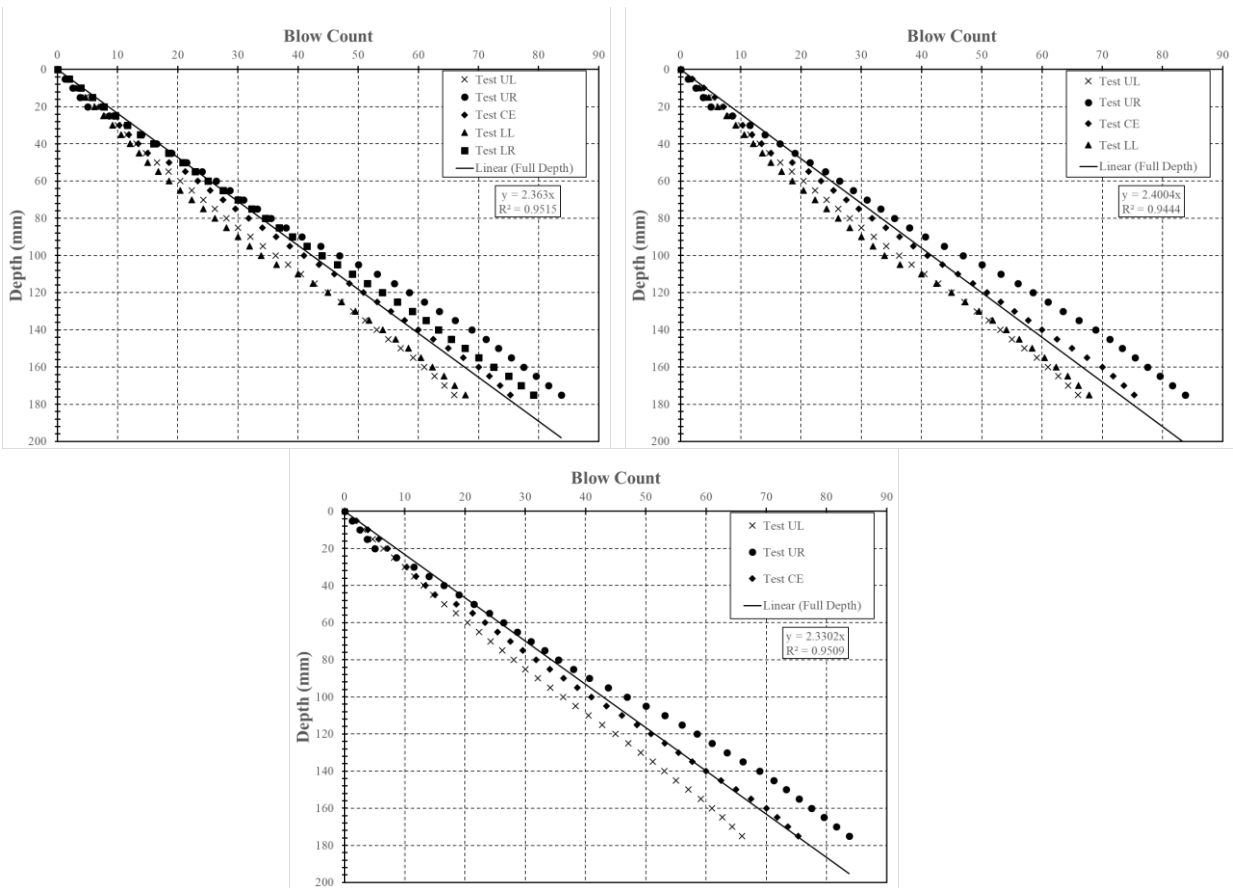


Figure N.43: Test performed on July 24, 2019, Location 50 (top left = 5 tests, top right = 4 tests, bottom = 3 tests)

Appendix N

Summary of Sections, Subsections, and Locations

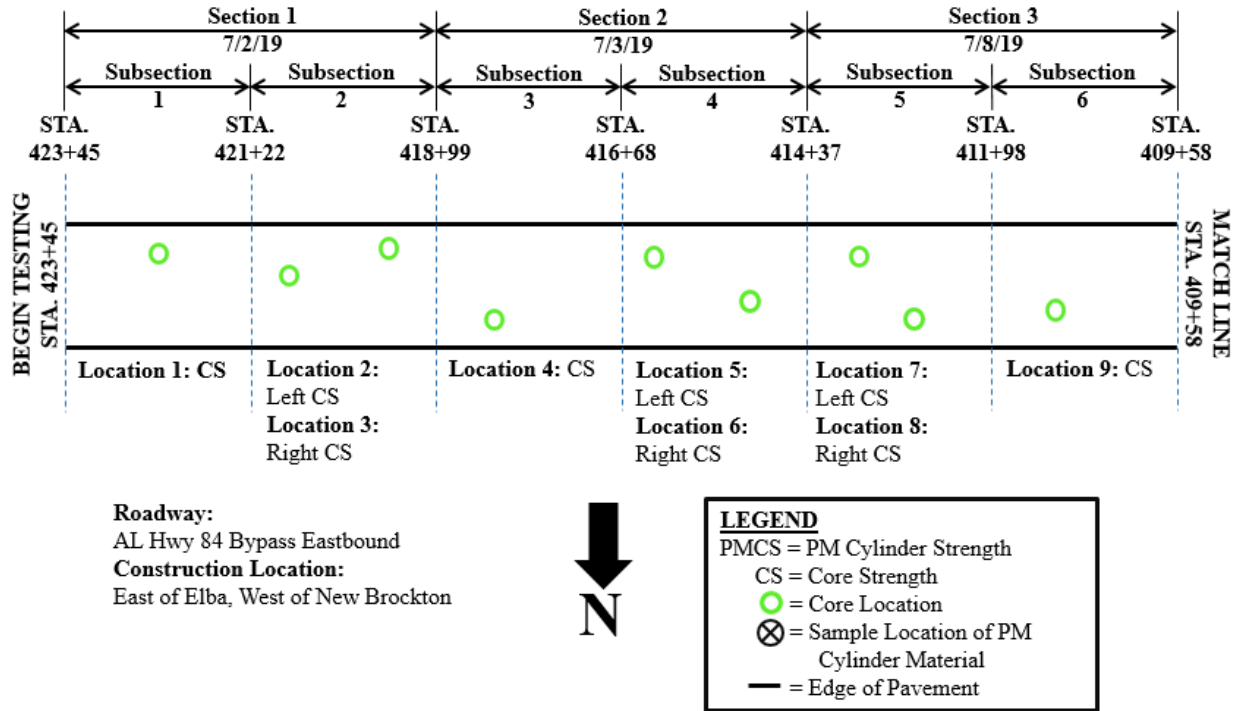


Figure O.1: Subsection layout for Station 423+45 to Station 409+58

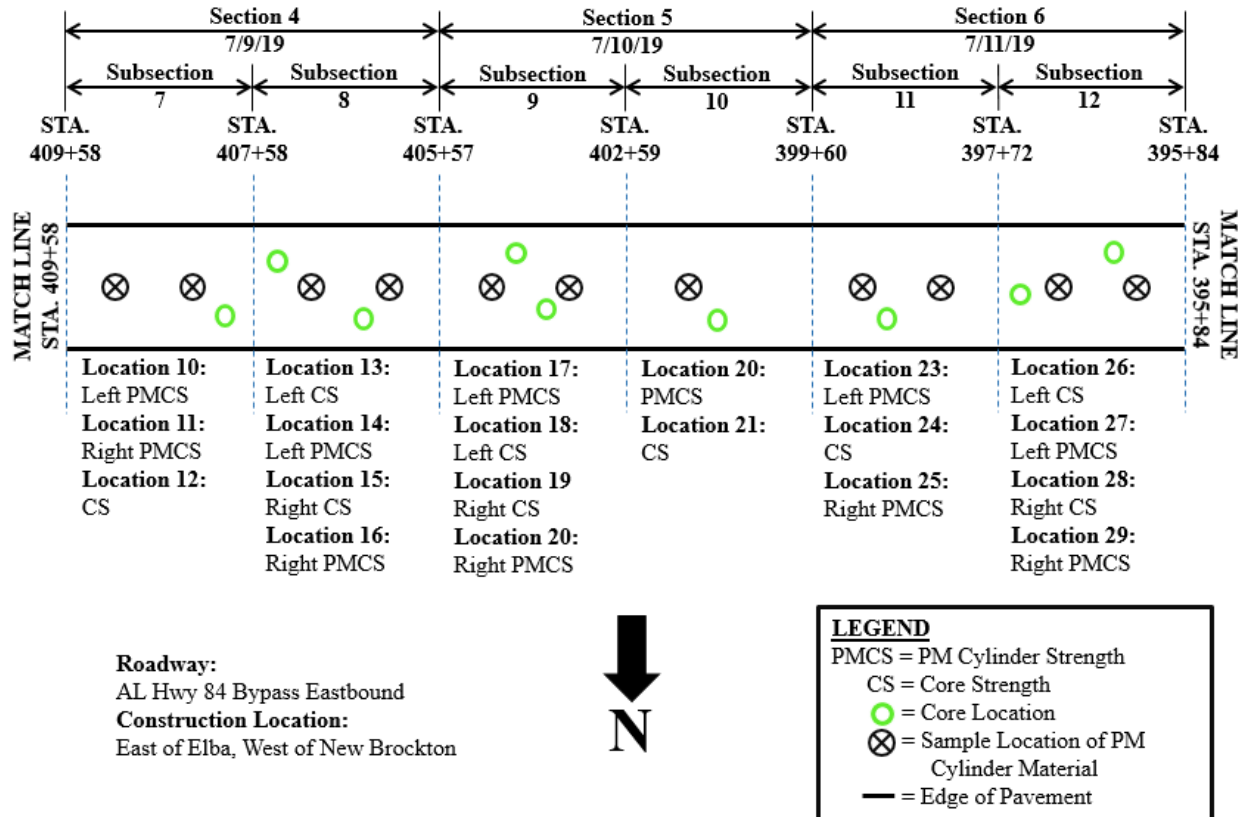


Figure O.2: Subsection layout for Station 409+58 to Station 395+84

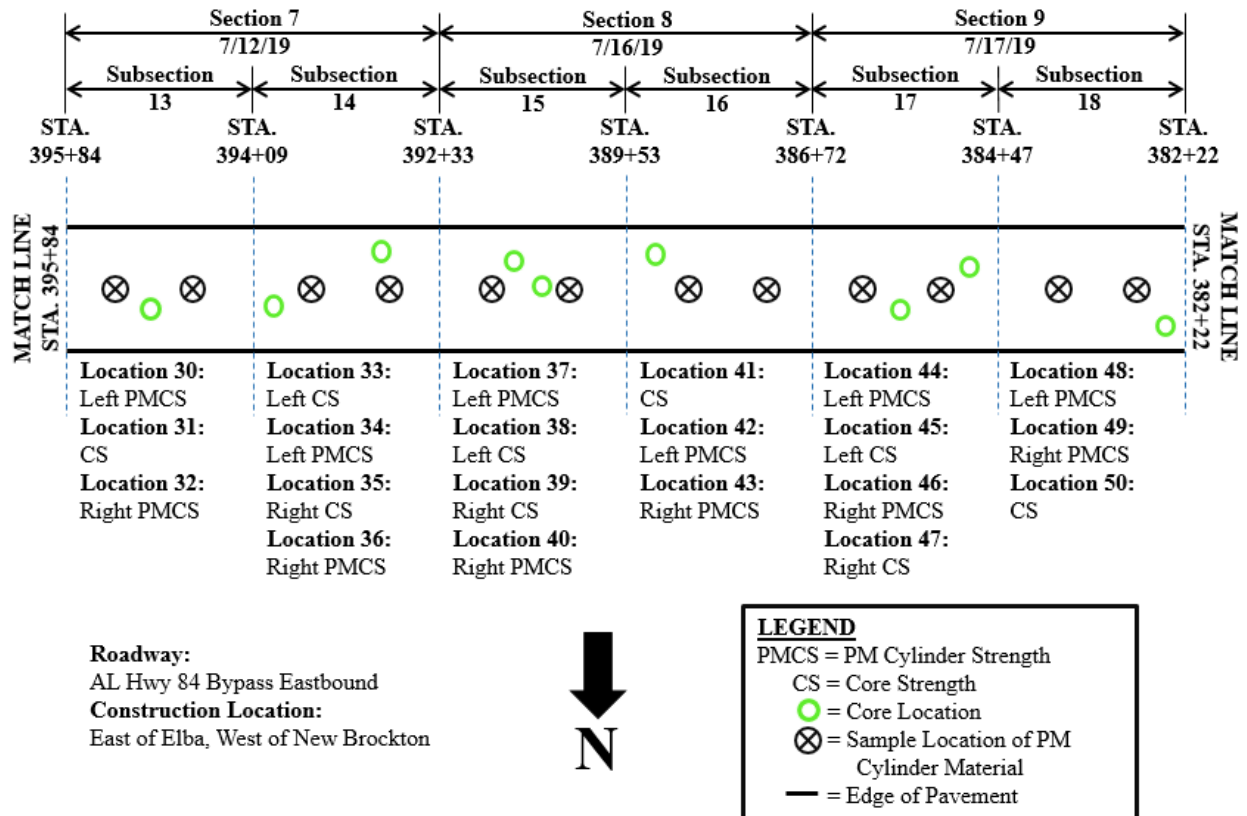
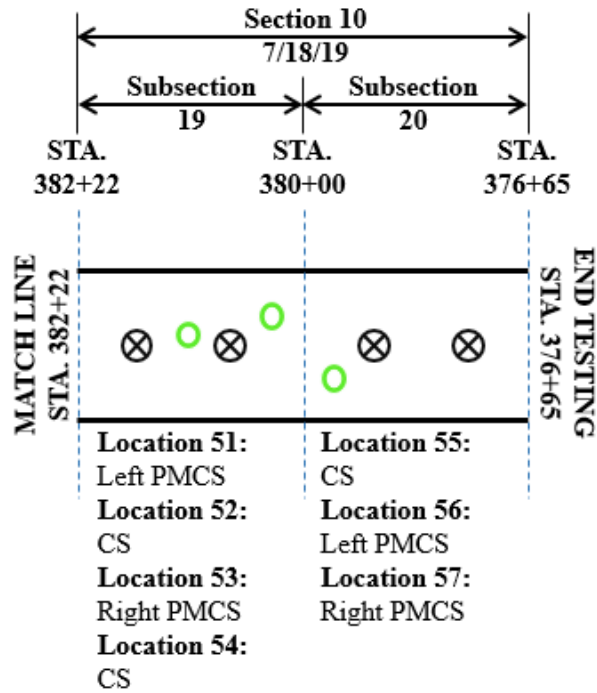


Figure O.3: Subsection layout for Station 395+84 to Station 382+22



Roadway:
AL Hwy 84 Bypass Eastbound
Construction Location:
East of Elba, West of New Brockton



LEGEND	
PMCS = PM Cylinder Strength	
CS = Core Strength	
○ = Core Location	
⊗ = Sample Location of PM Cylinder Material	
— = Edge of Pavement	

Figure O.4: Subsection layout for Station 382+22 to Station 376+65